Edited by

Bouke P. C. Hazenberg

Johan Bijzet

XIIIth International Symposium on Amyloidosis

From Misfolded Proteins to Well-designed Treatment

XIIIth International Symposium on Amyloidosis

XIIIth International Symposium on Amyloidosis

"From Misfolded Proteins to Well-Designed Treatment"

The Proceedings of the XIIIth International Symposium on Amyloidosis, May 6-10, 2012, Groningen, The Netherlands

Edited by

Bouke P.C. Hazenberg
Johan Bijzet

GUARD (Groningen Unit for Amyloidosis Research & Development)
UMC Groningen, The Netherlands

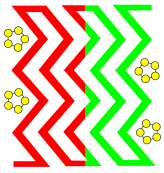

Published by
GUARD (Groningen Unit for Amyloidosis Research & Development)
Department of Rheumatology & Clinical Immunology AA21
University Medical Center Groningen
P.O. Box 30.001, 9700 RB, Groningen
The Netherlands

ISBN 978-90-821593-0-1 (hardback)
ISBN 978-90-821593-1-8 (e-book)

Printed and bound by Zalsman Groningen B.V., Groningen, The Netherlands
Photography: Niels van der Geest
Cover Design: Douwe Buiter and Johan Bijzet

Table of Contents

SECTION II – CELL TOXICITY AND AMYLOID TISSUE TARGETING

SECTION III – ANIMAL MODELS AND CELL CULTURE SYSTEMS

SECTION IV – DIAGNOSIS, TYPING AND IMAGING

SECTION V – AL AMYLOIDOSIS

SECTION VI – ATTR AMYLOIDOSIS

SECTION VIII – DESIGN OF TARGETED MOLECULES AND INNOVATIVE DRUGS

Acknowledgements

The Organizing Committee of the XIIIth International Symposium on Amyloidosis is grateful to the following sponsors whose generous contributions made this Symposium possible:

Platinum sponsor:

Pfizer

Silver sponsors:

Millennium

The Binding Site

Celgene

Celtic

Bronze sponsor:

Spectral Imaging

Alnylam

Regular sponsors:

GSK

Proteotech

Isis

Amyloidosis Support Groups Inc.

Amyloid Foundation

Preface

In September 1967 Dr. Enno Mandema hosted the first Symposium on Amyloidosis in Groningen, The Netherlands. Almost 45 years later, the XIIIth International Symposium on Amyloidosis was held again in Groningen, in the University Medical Center, on May 6-10, 2012. In 1967 only 46 participants from 11 countries attended the meeting and 41 papers were presented. In 2012 there were 417 participants from 33 countries who attended the Symposium and had the opportunity to listen to 90 oral presentations and to visit 197 poster presentations. The scientific program included presentations on fibril formation, cell and tissue toxicity, animal models, cell culture systems, diagnosis and typing, imaging techniques, AL- , ATTR- , and AA- amyloidosis, treatment, design of targeted molecules, and innovative drugs.

The Symposium was opened with a short introduction by Dr. Martin van Rijswijk, being one of the first amyloid researchers in Groningen, who enthusiastically supported clinical amyloid research by younger investigators for many years. Dr. Van Rijswijk specially and warmly welcomed Dr. Luuk Ruinen, one of the organizers of the first Symposium in 1967 (Figure 1). Despite serious physical disabilities that precluded him to attend later Symposia, Dr. Ruinen remained interested in the field of amyloidosis and was actively involved in the first International Course on Amyloidosis that was organized by Dr. Jan Marrink and Dr. Van Rijswijk in Groningen in 1986 (Figure 2). We felt it a special privilege having Dr. Ruinen with us this meeting.

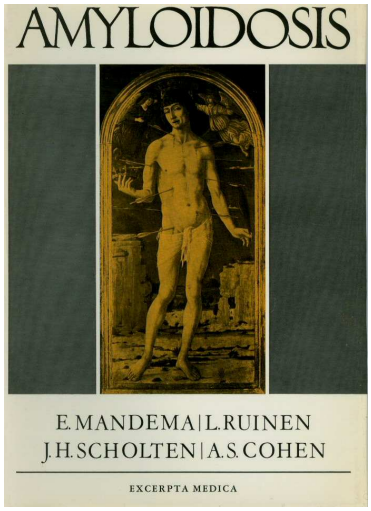

Figure 1. Proceedings of the 1st Symposium.

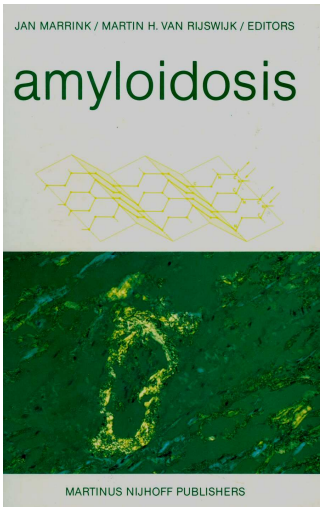

Figure 2. 1st Course on Amyloidosis.

The first speaker was Dr. Arminda Magalhaes, who personally experienced the frightening situation of having familial ATTR amyloidosis and the need to decide on liver transplantation. She soberly analyzed her current situation, now 15 years after liver transplantation, and made it obvious to all of us that much more still needs to be done to treat this disease and that finding an effective treatment is the real purpose of our work. The Opening Lecture was given by Dr. Bob Kyle, our first President of the Society. Dr. Kyle described the surprising history of amyloidosis, starting with the observation made by the Amsterdam doctor Nicolaes Fontijn, who was

in his time a well-known poet and writer. It was fascinating to learn from Dr. Kyle how scientific knowledge of amyloid and amyloidosis developed and accumulated during almost four centuries.

The Keynote Lecture of the Symposium was given by Dr. Jan Münch who described the augmenting role on HIV-1 transmission of amyloid formation of prostatic acid phosphatase in semen. Dr. Münch showed that the possible role of amyloid formation in other virus infections might have therapeutic consequences. The next day Sir Mark Pepys started with the Enno Mandema Memorial Lecture. Sir Mark received his knighthood from Queen Elizabeth because of his outstanding scientific work, most of it related to the field of amyloidosis. In his lecture he shortly described a couple of developments of the last decennia lively illustrated with some personal memories of Dr. Mandema and other key players.

The International Society of Amyloidosis formally thanked Dr. Martha Skinner for her dedicated work as President of the Society. Dr. Skinner successfully negotiated with the publisher of AMYLOID about contract renewal for the next years. Dr. Merrill Benson succeeded Dr. Skinner as President of the Society until the next Symposium that will be held in his home town Indianapolis, in April 2014.

Before the meeting 24 travel awards were given to young researchers. At the last evening nine awards were given to young researchers (<35 years) for the best oral presentation, best poster presentation, and most promising research of each of the three days. Thursday afternoon, after closure, Dutch patients suffering from systemic amyloidosis met for the first time. Dr. Martha Skinner and Dr. Giampaolo Merlini stayed to attend this meeting to give lectures and to address questions.

We specially want to thank the members of the International and National Organizing Committees for choosing speakers, reviewing abstracts, and their full support of the meeting. It is merely impossible to organize such a meeting without such heartwarming support of so many people. In particular Mr. Harry Gubbels and his collaborators of the Wenckebach Institute were essential. We also thank the many companies that supported the meeting financially, such as Pfizer, our Platinum sponsor. Last, but not least, we want to thank all the participants of the symposium (many of them young researchers) who made this symposium a success because of their presentations and critical discussions. We hope to meet each other again in Indianapolis!

Bouke P.C. Hazenberg
Johan Bijzet

The editors: Bouke Hazenberg (left) and Johan Bijzet (right).

OPENING SECTION

DISTINGUISHED LECTURES


Registration
&
Opening ceremony

OPENING LECTURE - Amyloidosis: A Brief History

Robert A. Kyle, Division of Hematology, Mayo Clinic, Rochester, MN, USA

In 1639 Nicolaus Fontanus reported the autopsy of a young man with ascites, jaundice, epistaxis and an abscess in the liver with a large spleen filled with white stones. This may have been the first description of the sago spleen of amyloidosis. Thomas Bartholin, discoverer of the lymphatic system in humans, described in his Historiarum Anatomicarum Rariorum the autopsy of a female whose spleen was so hard that it could scarcely be cut with a knife. He stated that incision of the spleen produced a sound like that of the cutting of spongy timbers. These two autopsy reports were included among the 3000 collected in Theophili Boneti's Sepulchretum Sive Anatomia Practica which was published in 1679 (1). (Figure 1)

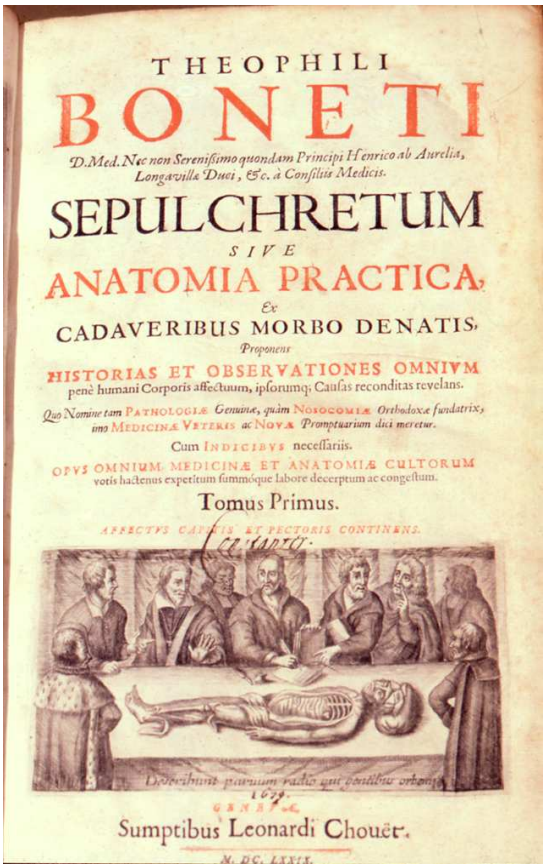
THEOPHILI
BONETI
D. Med. Nec non Serenissimo quondam Principi Henrico ab Aurelia, Longavillæ Duci, &c. à Consiliis Medicis.
SEPULCHRETUM
SIVE
ANATOMIA PRACTICA,
Ex
CADAVERIBUS MORBO DENATIS,
Proponens
HISTORIAS ET OBSERVATIONES OMNIVM
penè humani Corporis affectuum, ipsorumq; Causas reconditas revelans.
Quo Nomine tam PATHOLOGIÆ Genuinæ, quàm NOSOCOMIÆ Orthodoxæ fundatrix, imo MEDICINÆ VETERIS ac NOVÆ Promptuarium dici meretur.
Cum INDICIBVS necessariis.
OPVS OMNIUM MEDICINÆ ET ANATOMIÆ CULTORUM
votis hactenus expetitum summóque labore decerptum ac congestum.
Tomus Primus.
AFFECTVS CAPITIS ET PECTORIS CONTINENS.
Sumptibus Leonardi Chouët.

Figure 1. Sepulchretum sive Anatomia Practica, Theophili Boneti.

Boneti was born in Geneva in 1620 and received his medical degree from the University of Bologna at age 23. Deafness forced him to retire from practice at age 55 and he decided to devote the rest of his life to the collection of medical knowledge. This resulted in his Sepulchretum which contained 1700 pages and began with a dedication, lengthy preface and an impressive list of authors that began with Hippocrates and extended to the current time. The cases were categorized on the basis of anatomy, but he made few comments or deductions and arrived at no conclusions. He described many cases of pulmonary tuberculosis with accurate clinical histories and good postmortem studies. The section on neoplasms emphasized tumors in bones. The Sepulchretum contains a large collection of cases but is marred by the lack of judgment in grouping and separating lesions and the absence of critical review of the cited author's opinion. Some feel that a patient described by Wainewright in 1722 who had hepatomegaly and swellings in the neck and a "clay-coloured pituitous substance" in the liver had amyloid deposition.

Antoine Portal described a substance similar to lard in the liver of an elderly person in 1789. He later described the markedly enlarged liver of an 8-year-old boy with scrofula and stated that when exposed to heat that it hardened like albumin.

Figure 2. George Budd (1808-1882).
By courtesy of the Wellcome Trustees

F. V. Raspail (1794-1878) froze tissues for microscopic investigation and used alcohol to firm up the tissues and the iodine test for detection of starch. Some feel that Raspail was the founder of histochemistry. Carl Rokitasnky noted liver enlargement from infiltration by a grey albuminous, gelatinous substance in patients with tuberculosis or syphilis. He believed that the lardarceous or waxy livers were a type of fatty liver. However, George Budd analyzed the liver of a patient with lardaceous changes and found that it contained 16% albumin and only 5.75% fat (2). (Figure 2). He reported that the infiltration was albuminous and not fatty. He stated that the kidneys of

two of his patients showed the same infiltration as in the liver. Both patients had tuberculosis involving bone. Gairdner also reported that the fat content of the liver was not increased.

The term “amyloid” was coined in 1838 by Matthias Schleiden, a German botanist, to describe a normal amylaceous constituent of plants. The term was used by Rudolph Virchow in 1854 because of the peculiar reaction of the corpora amylacea of the nervous system with iodine. Virchow preferred the term amyloid to the commonly used “lardaceous” or “waxy” changes. Virchow made the statement “only when we have discovered the means of isolating the amyloid substance, shall we be able to come to any definite conclusion with regard to its nature." He also described cases with involvement of the glomeruli and the afferent arteries of the kidney as well as the digestive tract. Johann Meckel emphasized that the lardaceous changes were present not only in the liver and kidneys but also in the aorta, arteries and intestinal wall.

Samuel Wilks very likely reported the first case of primary amyloidosis in 1856 when he described a 52-year-old man with lardaceous viscera in whom there was no evidence of syphilis, tuberculosis, osteomyelitis or other osseous disease (3). (Figure 3). Albuminuria was found and the patient was felt to have dropsy. The autopsy showed hypertrophy of the heart and lardaceous changes in the spleen and kidneys. However, the patient had had episodes of dropsy for eight years, which is much longer than one would expect in a patient with nephrotic syndrome from primary amyloidosis. Wilks subsequently reported that five of 96 patients with lardaceous disease had no evidence of an underlying disease and thus appears to have been AL amyloidosis.

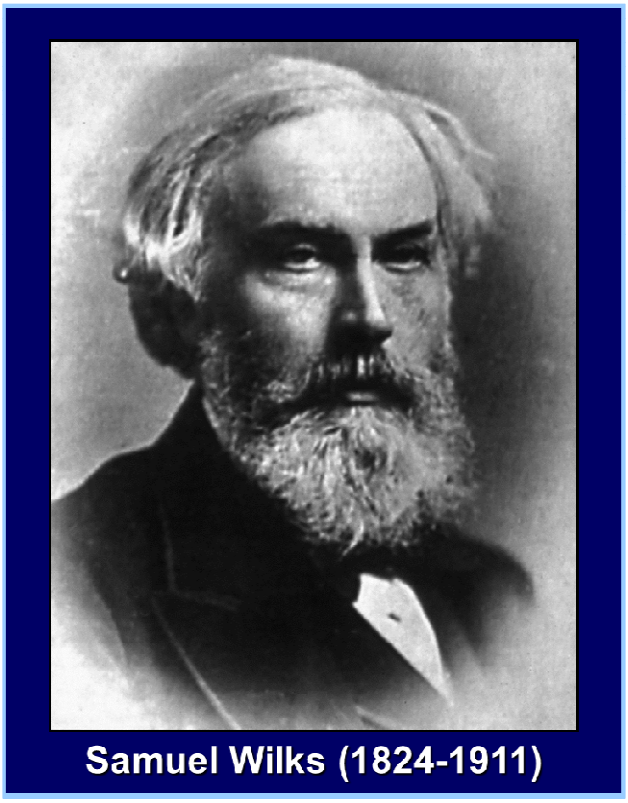

Figure 3. Samuel Wilks.
By courtesy of the Wellcome Trustees

The Royal Society of London appointed a Committee to report “on the nature of the so-called lardaceous disease and as to the name by which it should be recognized.” The Committee which included Wilks believed that the tissue was nitrogenous with 13-14% nitrogen and thus of albuminous origin. Strangely, the Committee recommended that the term “lardaceous” could be adopted because it was widely used and well understood.

The first case of amyloidosis associated with multiple myeloma was reported by Weber in 1867. Spontaneous fractures of the sternum with replacement by a grayish, red substance containing many small nucleated cells were seen at autopsy. Hypertrophy of the left ventricle of the heart was noted. A 60-year-old woman with lardaceous changes in the heart and spleen and multiple pathologic fractures was reported by Adams in 1872. He also noted that the bone marrow was infiltrated with plasma cells and a pink gelatinous material.

AMYLOID STAINS AND FIBRIL FORMATION

André-Victor Cornil of Paris, Richard Heschl of Vienna and Rudolph Jürgens of Berlin independently reported the use of aniline dyes for the recognition of amyloid. William Ackroyd introduced the term “metachromasia” and this term was used by Paul Ehrlich to describe the staining reaction of amyloid. Everyone agreed that the metachromatic stains, particularly methyl violet, were superior to the iodine sulphuric acid test. Virchow, however, rejected the metachromatic stains for amyloid for a decade after their discovery. Congo red eventually replaced the metachromatic stains. This is an aniline dye that was used initially for staining textiles. In 1884-1885, a major diplomatic conference was held in Berlin to mediate trade disputes between several European colonial powers concerning the Congo River Basin. This conference coincided with the introduction of a new aniline dye. Because Congo was on the tip of every tongue and represented an exotic place to Europeans, it is not surprising that the dye was given the name Congo red. However, it was not until 1922 that it was found to bind avidly to amyloid. Five years later Divry and Florkin at the University of Liege, Belgium, described the green birefringence of amyloid when stained with Congo red and viewed under polarizing light. A non-branching fibrillar structure was noted under the electron microscope by Cohen and Calkins in 1959.

Amyloid deposits stained with Congo red when viewed under the electron microscope reveal fibrils. The amyloid fibrils consist of protein A in patients with secondary amyloidosis, monoclonal kappa or lambda light chains in AL amyloidosis, and mutated transthyretin in hereditary amyloidosis.

ORIGIN OF PRIMARY (AL) AMYLOIDOSIS

In 1931, Magnus-Levy felt that Bence Jones protein was the “mother substance” of amyloidosis (4). He subsequently described 31 cases of multiple myeloma in which amyloid was present in the bone marrow and 18 had amyloid in other organs. He thought that the myeloma cells produced amyloid, but that it could not be removed from the area. Consequently, amyloid together with myeloma cells broke through the bone and involved the muscles and fatty tissue. He concluded that increased production and decreased metabolism of Bence Jones protein was responsible for the accumulation of amyloid in various organs. Magnus-Levy predicted that amyloid would be isolated as a pure substance and then its relationship to other proteins would be established. Apitz in 1940 emphasized the presence of amyloid in the heart, tongue, periarticular tissues and subcutaneous tissue in multiple myeloma in contrast to its presence in the liver, spleen and kidneys in secondary amyloidosis. He also believed that there was a chemical difference between the amyloid associated with chronic infection and that associated with Bence Jones proteinuria.

The association of primary amyloidosis with multiple myeloma or a plasma cell proliferative disorder was reported by Kyle and Bayrd in 1961 (5). Osserman et al., in 1964 suggested that Bence Jones protein played a major role in primary amyloidosis (6). In 1971, Glenner et al., reported that the amino acid sequence of a patient's Bence Jones protein was virtually identical to the sequence of his amyloid protein (7).

HEREDITARY AMYLOIDOSIS

In 1929, a 52-year-old man was reported with pain and numbness of his extremities, loss of energy and diarrhea. Three siblings had died of a similar illness. Masses of a non-nucleated, homogeneous substance were found in the peripheral nerves at autopsy. However, familial amyloidosis was not recognized until Andrade's monumental report of 74 patients from multiple families in Portugal was described in 1952 (8). Thirteen years later, Rune Andersson of Umea University, Sweden, saw a patient who had had peripheral neuropathy for 15 years whose cousin was also found to have peripheral neuropathy, vitreous opacities and amyloidosis. Systemic amyloidosis was subsequently reported in more than 60 cases from northern Sweden. These patients did not develop the disease until the fifth decade of life in contrast to the occurrence in the second or third decade in the Portuguese patients. Familial amyloidosis, often in elderly patients, was reported from Kumamoto and Nagano prefectures in Japan. The amyloid fibrils of the Portuguese, Swedish and Japanese patients consisted of transthyretin with a methionine substituted for valine at position 30. Since then, more than 100 mutations of transthyretin have been reported. Liver transplantation has been of benefit for many patients with familial polyneuropathy but late deposition of wild type transthyretin is a major problem.

OTHER TYPES

Senile cardiac amyloidosis often presents with congestive heart failure. In these patients the amyloid consists of normal transthyretin. These patients usually present with congestive heart failure, but the survival is much longer than in patients with AL amyloidosis who present with congestive heart failure.

SECONDARY AMYLOIDOSIS

Secondary (AA) amyloidosis consists of fibrils composed of protein A. This is a non-immunoglobulin protein that is a cleavage product of normal SAA. The most common cause has been chronic infections such as tuberculosis, leprosy or chronic osteomyelitis. Familial Mediterranean fever (FMF) is characterized by attacks of fever and pain in the abdomen, chest or joints. More than half of patients have more than one affected family member. The major features are proteinuria, nephrotic syndrome and renal failure. Colchicine is effective in preventing attacks of fever and pain in patients with FMF.

REFERENCES

1. Kyle RA. Historical review. Amyloidosis: a convoluted story. British Journal of Haematology. 2001;114(3):529-38.
2. Budd G. On diseases of the liver. 2nd ed. London, UK: J. Churchill; 1852, pp 301-329.
3. Wilks S. Cases of lardaceous disease and some allied affections, with remarks. Guy's Hosp Rep 1856;2:103-132.

4. Magnus-Levy A. Bence-Jones-Eiweiss and amyloid. Zeitschrift fur Klinische Medizinische 1931;116:510-531.
5. Kyle RA, Bayrd ED. "Primary" systemic amyloidosis and myeloma. Discussion of relationship and review of 81 cases. Arch Intern Med. 1961 Mar;107:344-53.
6. Osserman EF, Takatsuki K, Talal N. Multiple myeloma I. The pathogenesis of 'amyloidosis.' Semin Hematol 1964;1:3-85.
7. Glenner GG, Terry W, Harada M, Isersky C, Page D. Amyloid fibril proteins: proof of homology with immunoglobulin light chains by sequence analyses. Science 1971a;172:1150-1151.
8. Andrade C. A peculiar form of peripheral neuropathy. Familiar atypical generalized amyloidosis with special involvement of the peripheral nerves. Brain 1952;75:408-427.

KEYNOTE LECTURE - Amyloid in semen boosts HIV-1 transmission

Jan Münch

Institute of Molecular Virology, Ulm University Medical Center, Meyerhofstrasse 1, 89081 Ulm, Germany, phone: +49 731 500 65154, fax: +49 731 500 65167, e-mail: jan.muench@uni-ulm.de

IDENTIFICATION OF AN EFFECTIVE HIV ENHANCER IN HUMAN SEMEN

Since its introduction into the human population in the first half of the 20th century by zoonotic transmission of simian immunodeficiency viruses (SIVs) found in chimpanzees, HIV-1 has caused one of the most devastating pandemics of modern times. To date, HIV-1 has infected more than 60 million people and caused about 20 million deaths. The great majority of all HIV-1 transmissions results from unprotected sexual intercourse and genital exposure to semen contaminated with HIV-1 accounts for most transmissions worldwide. Thus, semen represents the major vector for the dissemination of HIV-1 in the human population. To identify natural agents that might play a role in sexual transmission of HIV/AIDS, we generated and screened a complex peptide/protein library derived from human semen for novel inhibitors and enhancers of HIV infection. We found that fragments of prostatic acidic phosphatase (PAP) drastically enhance HIV infection. The predominant form, PAP248-286, is present in pooled semen in concentrations of ≥35 µg/ml, which is within the concentration range in which we observed the strongest effects on infectivity enhancement. ThT and Congo Red staining, transmission electron microscopy and X-ray powder diffraction then showed that these peptides form amyloid fibrils, which were termed SEVI (Semen derived Enhancer of Viral Infection). In contrast to the inactive monomeric peptide, SEVI fibrils capture HIV-1 particles and strongly enhance the number of productively infected cells by promoting virion-cell attachment and fusion (Fig. 1) (1). Further tests revealed that semen also enhances the infectivity of HIV-1, HIV-2, and SIVs independently of the viral genotype and coreceptor tropism as well as the virus producer and target cell type (2). Semen-mediated enhancement of HIV-1 infection was also observed under acidic pH conditions which occur in the female's genital tract, and in the presence of vaginal fluid (2). Interestingly, we found that the potency of semen in boosting HIV-1 infection is to some extent donor dependent and correlates with the levels of SEVI in the individual semen samples (2). Thus, semen, the main vehicle for HIV-1 transmission contains factors which increase the infectivity of the virus. Inhibition of this enhancing activity may substantially reduce the rates of sexual transmission of HIV/AIDS.

MECHANISM OF SEVI MEDIATED INFECTIVITY ENHANCEMENT

Only SEVI fibrils but not the monomeric peptides enhance HIV-1 infection (1). We found that the SEVI fibrils display a positive surface charge (3, 4) which facilitates the interaction with negatively charged membranes of

virions and cells. A mutant form of SEVI in which lysines and arginines were replaced with alanines retains the ability to form amyloid fibrils but is largely defective in binding virions and enhancing infection (3). In addition, the interaction of wild-type SEVI with virions and the ability of these fibrils to increase infection are abrogated in the presence of various polyanionic compounds. Anionic polymers also decrease the enhancement of HIV infection mediated by semen. These findings suggest that SEVI and other amyloid fibrils identified in semen enhance viral infection by serving as a polycationic bridge that neutralizes the negative charge repulsion that exists between the viral and host cell membranes.

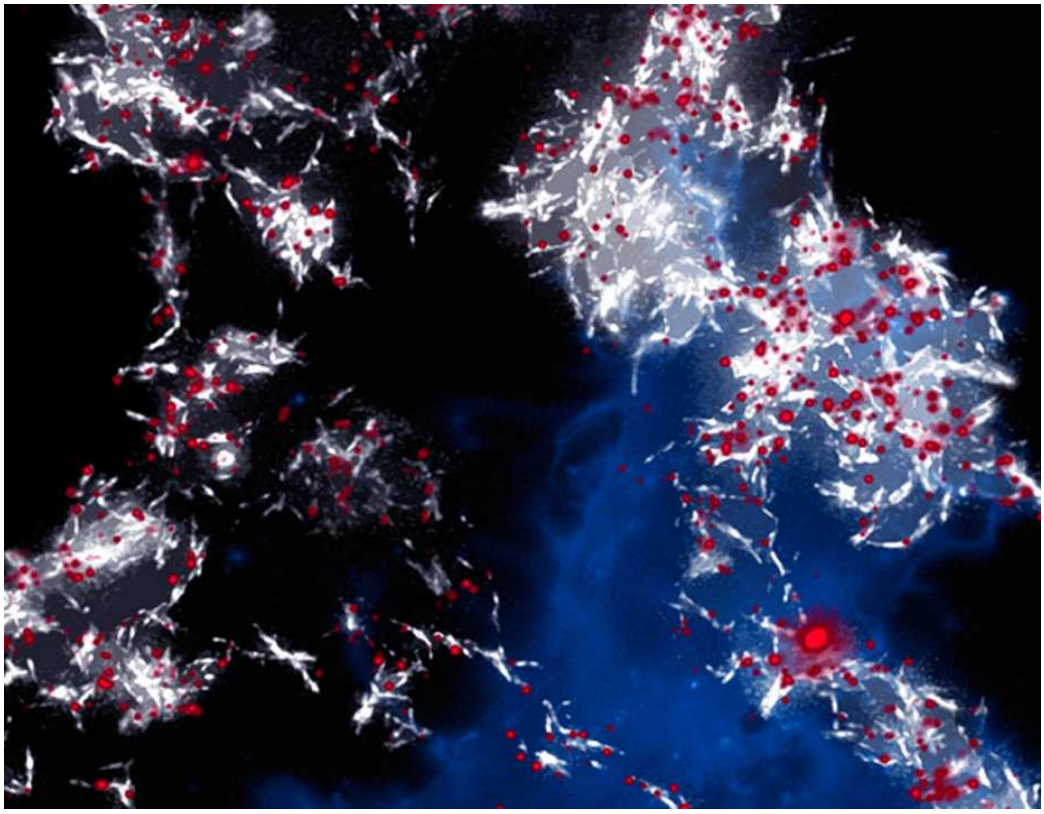

Figure 1. SEVI fibrils capture viral particles and increase virion attachment. Confocal microscopy image showing SEVI fibrils (white), viral particles (red) and one target cell (blue). Note that all virions are bound to fibrils which in turn bind to the membrane of the target cell thereby increasing viral attachment and infection rates. Kindly provided by Walther Mothes, Yale University.

SEMEN CONTAINS DIFFERENT AMYLOIDOGENIC PEPTIDES ENHANCING HIV INFECTION

In our initial screen of a semen-derived peptide library which resulted in the identification of SEVI (1), we also identified a second independent fraction with HIV-1 enhancing activity (4). Surprisingly, this fraction contained an N-proximal fragment of PAP (PAP85-120). Similar to PAP248-286, this peptide forms positively charged amyloid fibrils which increase virion attachment to cells. These results provide a first example for amyloid

formation by fragments of distinct regions of the same precursor protein (4). Another type of fibril was identified by depleting amyloid from semen using the conformation-dependent antibodies WO1 and WO2 and subsequent mass spectrometry analysis (5). The depleted peptides mainly consisted out of a subset of semenogelin I and II fragments. Again, the synthesized peptides formed amyloid fibrils with cationic surface charge that boost HIV-1 infection. Whereas semen samples from healthy individuals greatly enhance HIV infection, semenogelin-deficient semen samples from patients with ejaculatory duct obstruction are completely deficient in boosting virus infection (5). Semen thus harbors distinct amyloidogenic peptides derived from different precursor proteins that promote HIV infection and thus most contribute to the spread of the AIDS pandemic.

COUNTERACTING SEMEN'S ABILITY TO ENHANCE HIV INFECTION

Compounds that inhibit amyloid formation in semen or block the ability of fibrils to promote virus infection may represent a novel class of agents inhibiting sexual HIV-1 transmission (1). Indeed, we and others identified and developed first "SEVI amyloid inhibitors" with different mechanisms of action that also abrogate semen mediated infectivity enhancement (6-12). For example, a structure-based design approach using the atomic structures of segments of amyloid as templates resulted in the generation of a non-natural amino-acid inhibitor which blocked the formation of SEVI (6). Another compound shown to counteract SEVI-mediated enhancement of HIV infection is the green tea polyphenol epigallocatechin-3-gallate which binds to and precipitates SEVI fibrils (7, 8). However, its use as microbicide seems to be limited because of its variable activity against semen-mediated infectivity enhancement (9). The aminoquinoline "surfen" (10) and certain Thioflavin derivatives (11, 12) bind SEVI fibrils and prevent their interaction with the membranes of virions and/or cells thus abrogating SEVI's and also semen`s ability to increase HIV infection. In conclusion, microbicides incorporating inhibitors against naturally occurring amyloidogenic viral enhancement factors in semen may prove useful in limiting the spread of HIV-1 in the human population.

SUMMARY AND PERSPECTIVES

We and others have shown that human semen contains multiple amyloidogenic peptides derived from abundant proteins which greatly increase HIV-1 infection and most likely promote sexual transmission of the virus. First inhibitors of amyloid- and semen-mediated infectivity enhancement have been identified and represent a promising novel class of microbicides. However, we are still just at the beginning to understand why these fibrils form, what the endogenous amyloids look like and – most importantly – which physiological role they may have. Further research in this field is highly warranted because we may not only gain new insights into the mechanism of virus transmission but also in reproduction – which is the real purpose of semen.

REFERENCES

1. Münch J, Rücker E, Ständker L, Adermann K, Goffinet C, Schindler M, Wildum S, Chinnadurai R, Rajan D, Specht A, Giménez-Gallego G, Sánchez PC, Fowler DM, Koulov A, Kelly JW, Mothes W, Grivel JC, Margolis L, Keppler OT, Forssmann WG, Kirchhoff F. Semen-derived amyloid fibrils drastically enhance HIV infection. Cell. 2007 Dec 14;131(6):1059-71.

2. Kim KA, Yolamanova M, Zirafi O, Roan NR, Staendker L, Forssmann WG, Burgener A, Dejucq-Rainsford N, Hahn BH, Shaw GM, Greene WC, Kirchhoff F, Münch J. Semen-mediated enhancement of HIV infection is donor-dependent and correlates with the levels of SEVI. Retrovirology. 2010 Jun 23;7:55.
3. Roan NR, Münch J, Arhel N, Mothes W, Neidleman J, Kobayashi A, Smith-McCune K, Kirchhoff F, Greene WC. The cationic properties of SEVI underlie its ability to enhance human immunodeficiency virus infection. J Virol. 2009 Jan; 83(1):73-80. Epub 2008 Oct 22.
4. Arnold F, Schnell J, Zirafi O, Stürzel C, Meier C, Weil T, Ständker L, Forssmann WG, Roan NR, Greene WC, Kirchhoff F, Münch J. Naturally occurring fragments from two distinct regions of the prostatic acid phosphatase form amyloidogenic enhancers of HIV infection. J Virol. 2012 Jan; 86(2):1244-9. Epub 2011 Nov 16.
5. Roan NR, Müller JA, Liu H, Chu S, Arnold F, Stürzel CM, Walther P, Dong M, Witkowska HE, Kirchhoff F, Münch J, Greene WC. Peptides released by physiological cleavage of semen coagulum proteins form amyloids that enhance HIV infection. Cell Host Microbe. 2011 Dec 15;10(6):541-50.
6. Sievers SA, Karanicolas J, Chang HW, Zhao A, Jiang L, Zirafi O, Stevens JT, Münch J, Baker D, Eisenberg D. Structure-based design of non-natural amino-acid inhibitors of amyloid fibril formation. Nature. 2011 Jun 15;475(7354):96-100. doi: 10.1038/nature10154.
7. Hauber I, Hohenberg H, Holstermann B, Hunstein W, Hauber J. The main green tea polyphenol epigallocatechin-3-gallate counteracts semen-mediated enhancement of HIV infection. Proc Natl Acad Sci U S A. 2009 Jun 2;106(22):9033-8. Epub 2009 May 18.
8. Popovych N, Brender JR, Soong R, Vivekanandan S, Hartman K, Basrur V, Macdonald PM, Ramamoorthy A. Site specific interaction of the polyphenol EGCG with the SEVI amyloid precursor peptide PAP(248-286). J Phys Chem B. 2012 Mar 22;116(11):3650-8. Epub 2012 Mar 7.
9. Hartjen P, Frerk S, Hauber I, Matzat V, Thomssen A, Holstermann B, Hohenberg H, Schulze W, Schulze Zur Wiesch J, van Lunzen J. Assessment of the range of the HIV-1 infectivity enhancing effect of individual human semen specimen and the range of inhibition by EGCG. AIDS Res Ther. 2012 Jan 19;9(1):2.
10. Roan NR, Sowinski S, Münch J, Kirchhoff F, Greene WC. Aminoquinoline surfen inhibits the action of SEVI (semen-derived enhancer of viral infection). J Biol Chem. 2010 Jan 15;285(3):1861-9. Epub 2009 Nov 6.
11. Olsen JS, Brown C, Capule CC, Rubinshtein M, Doran TM, Srivastava RK, Feng C, Nilsson BL, Yang J, Dewhurst S. Amyloid-binding small molecules efficiently block SEVI (semen-derived enhancer of virus infection)- and semen-mediated enhancement of HIV-1 infection. J Biol Chem. 2010 Nov 12;285(46):35488-96. Epub 2010 Sep 10.
12. Capule CC, Brown C, Olsen JS, Dewhurst S, Yang J. Oligovalent amyloid-binding agents reduce SEVI-mediated enhancement of HIV-1 infection. J Am Chem Soc. 2012 Jan 18;134(2):905-8. Epub 2012 Jan 3.

ENNO MANDEMA MEMORIAL LECTURE - Amyloidosis 1979-2012

Sir Mark B. Pepys

Wolfson Drug Discovery Unit, Centre for Amyloidosis and Acute Phase Proteins, and UK NHS National Amyloidosis Centre, University College London.

Figure 1. Professor Enno Mandema MD (1921-2010).

It is a pleasure and a privilege to commemorate Professor Enno Mandema, especially at this International Symposium on Amyloidosis in his academic home of Groningen. Enno Mandema was a wonderfully charming, intelligent and friendly colleague, a pioneering figure in the field internationally and the founder of the modern study of amyloidosis in the Netherlands. He undertook his medical studies in Groningen between 1939 and 1948, becoming a specialist internist in 1954 and graduating PhD *summa cum laude* in 1956. He was a visiting post-doctoral researcher with Professor Robert M Kark in Chicago in 1959 and in 1963, together with Nienhuis, Mandema discovered the so-called anti-perinuclear factor, the important autoantibody now known as anti-CCP. Mandema's distinguished career as an internist and a world leader in amyloidosis was widely recognised. In 1975 he became an Honorary Fellow of the American College of Physicians and in 1979 a member of the Royal

Netherlands Academy of Arts & Sciences. An outstanding international meeting on amyloidosis was held in Groningen on his retirement in 1986 and from 1986-1993 he was the first President of the Dutch Council for Health Research. The honour of Knighthood in the Nederlanse Leeuw was conferred on him by Queen Beatrix and she made him the Queen's Chamberlain for Groningen Province. In 2009 the University Medical Centre of Groningen created a prestigious post-doctoral fellowship, the 'Mandema Stipendium', in his honour.

Enno Mandema's contributions to amyloidosis comprised both his enormous enthusiasm for the subject, he participated in all the significant meetings in the field throughout his senior career, and his invaluable legacy of Dutch amyloidologists. He created the specialty in the Netherlands by inspiring his own students and they in turn inspiring theirs. All have made seminal contributions to knowledge of the disease and patient care. Mandema's 'personnel legacy' comprises Martin van Rijswijk, Jan Marrink, Sijtze Meijer, Sven Janssen, Piet Limburg, Bouke Hazenberg, Johan Bijzet and Miek van Leeuwen (Groningen); and, Erik Gruys, Paul Hol, Adriaan Andel, Theo Niewold, Yves Goffin, Wil Landman, Bereket Zekarias, Narin Upgarin, Jaime Rofina, S Alsemgeest and Mathilda Toussaint (Utrecht).

I first met Enno Mandema and his charming wife Atie at the International Amyloidosis Symposium in Póvoa de Varzim and we continued to meet at many large and small amyloid gatherings thereafter. He was always exceptionally friendly, well informed and a thoroughly delightful colleague with whom those of us in the field shared not only exciting science and medicine but also entertaining social activities.

Figure 2. European Society of Internal Medicine, Vienna 1984. Left to right: Martin van Rijswijk, Gunnar Husby, Mark Pepys, Enno Mandema, Otto Wegelius, Hans Falck, Christina Wegelius, Atie Mandema, Ragnhilde Husby.

IAS PÓVOA DE VARZIM 1979 AND BEFORE

I first saw amyloid as a rare histological finding during my pre-clinical pathology studies at Cambridge in 1963 and then as a rare, obscure differential diagnosis during clinical studies in 1965-8. The field was transformed in 1968-71 by Osserman's elegant association of amyloidosis with the plasma cell dyscrasias and then by Glenner's seminal identification of monoclonal immunoglobulin light chains as amyloid fibril proteins. In 1974 I started to work on C-reactive protein and discovered the close relationship with serum amyloid P component (SAP), leading in 1979 to the demonstration with Cohen & Skinner of the calcium dependent binding of SAP to all amyloid fibrils. I first attended an amyloidosis meeting at Póvoa de Varzim that year, where the crucial scientific breakthrough was Costa's discovery of transthyretin as the amyloid fibril protein in familial amyloid polyneuropathy, but most of the meeting comprised clinical and histopathological descriptions. The only therapies were prednisone, melphelan and colchicine and the prognosis of amyloidosis was terrible. However the rational nomenclature based on the fibril protein type was created, which has since made a massive contribution to understanding and managing amyloidosis patients. The nomenclature focus at the Portugal meeting inspired Keith McAdam and I to establish a humorous 'Alternative Nomenclature Committee' which reported regularly at several subsequent IAS Symposia.

IAS GRONINGEN 2012

33 years later there has been enormous progress. The clinical phenotypes and natural history are known for almost all forms of amyloidosis. National centres of excellence in amyloidosis and international networks for instant communication and sharing of expertise have been established. In conjunction with rapidly advancing diagnostics and monitoring, and novel pharmaceutical and other interventions, current management provides greatly improved survival for many patients. However many AL patients still die soon after diagnosis, there is no effective therapy for much hereditary amyloidosis, and systemic amyloidosis remains fatal in most cases. Key advances include identification of fibril proteins and other amyloid constituents, understanding instability, misfolding and aggregation in amyloidogenicity, precursor product relationships and their clinical significance in AA and AL amyloidosis especially with serial free light chain (FLC) and SAA assays, and recognition of the variety and prevalence of hereditary amyloidosis. Diagnosis and monitoring have been and are being revolutionised by SAP scintigraphy including CT-SPECT, cardiac MRI including new modalities such as EQ-MRI, DPD scintigraphy, advanced immunohistochemistry, laser capture proteomic analysis and new biomarkers of organ dysfunction such as NT pro-BNP and troponin. Therapy of AA and AL amyloidosis has been rationalized and transformed by serial SAA and FLC monitoring, the potent biological anti-inflammatories and improved cytotoxic chemotherapy, including the new generation of myeloma drugs. Organ transplantation can be curative in AFib but complicated by early renal recurrence, in contrast to long graft survival in AapoAI, while progressive cardiac amyloidosis has been disappointing after the early promise of liver transplantation for ATTR. On the other hand elucidation of the genetics and molecular pathogenesis of the auto-inflammatory diseases (FMF, CAPS) has led to remarkable, rational specific anti-cytokine therapy which abolishes all symptoms and completely prevents amyloidosis.

THE FUTURE, 2012…….

Despite all these advances, critical fundamental questions remain, the www of amyloidosis: Who? Where? When? Little or nothing is yet known about the mechanisms of individual susceptibility, anatomical localisation or the timing of amyloid initiation, progression and regression, nor indeed about exactly how amyloid deposition causes disease. Nevertheless the therapeutic goals for the future are clear: early diagnosis; maintenance/replacement of organ function; reduction of fibril precursor protein abundance and/or fibrillogenesis; and, crucially, elimination of existing deposits. Encouragingly there is now greater interest and much more therapeutic R&D activity in amyloidosis then ever before with many exciting and promising approaches, including: stabilisers of amyloidogenic precursors; competition with proteoglycans/GAGs; siRNA and ASO inhibition of precursor production; depletion of SAP and fibril proteins precursors; and antibody therapies. Our own strategy, administration of anti-SAP antibodies after depletion of circulating SAP by CPHPC, safely eliminates visceral amyloid deposits in mice (1) and will shortly be tested in patients. A single 'magic bullet' therapy for all types of amyloidosis is very unlikely but nonetheless the future is bright and there are genuine grounds for cautious optimism. At the same time the complexity and enormous variety of the disease means that we should not be overconfident.

REFERENCES

1. Bodin K, Ellmerich S, Kahan MC, Tennent GA, Loesch A, Gilbertson JA, Hutchinson WL, Mangione PP, Gallimore JR, Millar DJ, Minogue S, Dhillon AP, Taylor GW, Bradwell AR, Petrie A, Gillmore JD, Bellotti V, Botto M, Hawkins PN, Pepys MB. Antibodies to human serum amyloid P component eliminate visceral amyloid deposits. Nature 2010; 468: 93-97.

SECTION I

MECHANISMS OF FIBRIL AND AMYLOID FORMATION


Welcome party

STATE OF THE ART AND PERSPECTIVES FOR THE FUTURE: Fibril and Amyloid Formation

M. Fändrich, Max-Planck Research Unit for Enzymology of Protein Folding & Martin-Luther University Halle-Wittenberg, Weinbergweg 22, 06120 Halle (Saale), Germany, Email: fandrich@enzyme-halle.mpg.de

Vittorio Bellotti Department of Molecular Medicine-Institute of Biochemistry University of Pavia Italy (http://www.amyloidresearch.it) National Amyloidosis Center, Center for Amyloidosis and Acute Phase Proteins, University College London (UCL), London UK (v.bellotti@ucl.ac.uk)

STATE OF THE ART

Structure of amyloid fibrils: For more than 50 years it is now known that amyloid tissue deposits primarily consist of fibrils. These fibrils can be viewed by electron microscopy (1) and X-ray diffraction additionally revealed that they encompass a characteristic β-sheet structure that is termed cross-β (2). This β-sheet conformation forms the structural spine of amyloid protofilaments, while one or several of these protofilaments together shape up a mature fibril (3). Mature fibrils are usually long and straight particles that are characteristically twisted and give rise to discernible crossovers in electron micrographs. Atomic force microscopy or transmission electron microscopy coupled with metal side shadowing demonstrated that this twist is for most, but not all, amyloid-like fibrils left-handed (4). *In vitro* prepared fibrils typically show considerable heterogeneity regarding the individual fibril morphologies present in this sample (4). Different fibril polymorphs can arise from differences in the number or shape of the underlying protofilaments or in their relative orientation (5). Atomic views of cross-β structures could be provided with X-ray crystallography of peptide microcrystals (6, 7). This research revealed an assembly of two cross-β sheets with closely interdigitating side chains. This arrangement was termed a steric zipper (6), and analysis of different peptide microcrystals revealed steric zipper structures, which varied in β-sheet architecture (parallel or anti-parallel β-sheet) and relative packing of the two cross-β sheets (7). Electron cryo microscopy and three-dimensional image reconstruction enabled insights how the cross-β structure composes the protofilament core (8), but it has not so far enabled analysis of residue-specific details. To obtain such information and to identify the amino acid residues forming the fibril β-strand structure, hydrogen exchange coupled with solution state nuclear magnetic resonance (NMR) spectroscopy (9) as well as solid-state NMR can be used (10, 11). The latter technique even provided atomic structures (10, 11). The most detailed biophysical data is currently available on fibrils that were formed inside the test tube. Further research will be necessary to clarify whether fibrils occurring in diseased tissues share all the properties that could so far be clarified for these *in vitro* fibrils.

Mechanism of fibril formation: When fibril formation is monitored with light scattering or thioflavin T fluorescence two phases become evident, termed lag phase and growth phase (12). This biphasic behavior was initially identified to occur with fibrils forming from pure peptides inside the test tube, but more recent evidence reports similar growth kinetics for the formation of single amyloid plaques in a cell culture model (13). The observation of biphasic growth was initially explained with a nucleation-polymerization mechanism, where monomers initially assembly to form a fibrillation nucleus (lag phase). This nucleus then sparks of the rapid formation of large quantities of fibrils (growth phase) (12). Indeed, addition of preformed fibrils to monomeric peptide was shown to be able to seed the formation of fibrils and to eliminate any observable lag phase (12). Careful biophysical analysis of fibril growth reactions carried out under systematically varied growth conditions revealed that nucleation and growth do not suffice in explaining the observable data and that secondary events, such as fibril fragmentation reactions or branching events must be involved (14). The extension of fibrils from such seeds could be visualized at a single particle level and in real time with fluorescence microscopy (15). Atomic force microscopy and other techniques additionally revealed the morphology of structural intermediates preceding mature fibrils, such as oligomers and protofibrils (16). Recently, even atomic resolution data of toxic oligomers prepared from a peptide fragment from αB crystallin could be provided, revealing a β-barrel architecture (17).

PERSPECTIVES

In the recent years, several laboratories, all around the world were intensively occupied in identifying folding and misfolding intermediate that prime the formation of fibrils. The theory that assigns to folding instability a key pathogenic role in many amyloid diseases is largely confirmed. This paradigm is strengthen by results obtained by innovative real time spectroscopy that, in some cases, can reveal structural details of the partially folded state of a globular protein in amyloidogenic conformation (18). Many efforts are now focused in providing, for a large variety of amyloidogenic proteins, conditions of fibrillogenesis compatible with the physiologic environment. However so far a deep gap still exists between a detailed knowledge of the molecular events occurring in vitro in non-physiological conditions under the relatively short time frame of hours and days and what happen *in vivo*, in the interstitial space of the target organs, where the amyloid proteins make the amyloid deposits on a time frame of a few decades. An important link between the theory that assigns a pathogenic role to folding instability and the mechanism of the disease *in vivo* could be provided by the identification of the forces capable to perturbate *in vivo* the folding state of protein and overcome the energetic barrier normally protecting the protein native state from its dragging into the fibrillogenic pathway. Conditions of fibrillogenesis requiring a very high temperature, a very low pH of the presence of organic solvents are probably too far from the physiologic conditions, but a source of energy sufficient to locally break the native conformation could be derived by the combination of the shear forces of the fluid dynamics in the interstitial space and the denaturing forces at the interface of hydrophobic and hydrophilic surfaces. The efficacy of the combination of shear forces and hydrophobic interactions in promoting structural perturbation and consequently priming the amyloid conversion is well demonstrated in the case of the new amyloidogenic variant of β2-m D76N (19). In other cases it has been shown that shear forces compatible with in vivo environment can significantly accelerate the amyloid fibrils formation (20). In the near future we expect and intensive work in reproducing in vitro a certain level of complexity of the architecture and fluid dynamics of the interstitial space where amyloidogenesis occurs in vivo. The formation of amyloid fibrils in vivo is most likely in equilibrium with oligomeric conformers whose formation is a prerequisite for fibrils formation. We have hypothesized that once the fibrils are formed in the interstitial

space, the amyloid material can favour the oligomerization of soluble amyloidogenic protein precursors (21). In fact the occupancy of the interstitial space by the net of the amyloid fibres could dramatically modify the architecture, the composition and the parameters of the fluid dynamics typical of the normal interstitial space. In particular, the increased molecular crowding can affect the colloidal stability of the amyloid precursors and can increase the area occupied by hydrophobic surfaces and finally could increase the turbulence and shear forces of the fluid. Such a concatenation of events and the strict interconnection between amyloid fibrils and pre-fibrillar species could provide reconciliation between theories assigning a prevalent pathogenic role to the amyloid fibrils or to the oligomeric pre-fibrillar species. The hypothesis that important pathologic aspects of disease are based on the catastrophic interplay between different protein conformers urgently needs an experimental validation. We can be cautiously optimistic on our possibility to shed light on this crucial issue of the molecular mechanism of the disease. This heterogeneous scientific community has already proved the peculiar capacity of successful multidisciplinary approach in which different disciplines provide basic analytical tools, consistent biological models of the disease and essential clinical and molecular information on the patients.

REFERENCES

1. Cohen & Calkins Nature 183, 1202 - 1203 (1959)
2. Eanes & Glenner J Histochem Cytochem 16, 673-677 (1968)
3. Serpell Biochim. Biophys. Acta 1502, 16-30 (2000)
4. Goldsbury et al. J. Struct. Biol. 130, 217–231 (2000)
5. Fändrich et al. Prion 3, 89-93 (2009)
6. Nelson et al Nature 435, 773-778 (2005)
7. Sawaya et al Nature 447, 453-457 (2007)
8. Jimenez et al. EMBO J. 18, 815–821 (1999)
9. Lührs et al. PNAS 102, 17342-17347 (2005)
10. Jaroniec et al. PNAS 101, 711-717 (2004)
11. Wasmer et al. Science 319, 1523-1526 (2008)
12. Harper & Lansbury Annu. Rev. Biochem. 66, 385-407 (1997)
13. Friedrich et al. PNAS 107, 1942–1947 (2010)
14. Xue et al. PNAS 105, 8926-8931 (2008)
15. Ban et al. J. Biol. Chem. 281, 33677-33683 (2006)
16. Morgado & Fändrich Curr. Opin. Colloid. Interface Chem. 16, 508–514 (2011)
17. Laganowsky et al. Science 335, 1228 (2012)
18. Neudecker et al. Science 336,362-6 (2012)
19. Valleix et al. N. Engl. J. Med. 24:2276-83 (2012)
20. Webster et al. J. Phys. Chem.B. 11, 2617-2626 (2011)
21. Bellotti & Chiti Curr. Opin. Struct. Biol. 6,771-779 (2008)

Structure of mature Aβ fibrils investigated by electron cryo-microscopy

M. Schmidt, A.Schmidt, N. Grigorieff, M. Fändrich

Max-Planck Research Unit for Enzymology of Protein Folding & Martin-Luther University Halle-Wittenberg, Weinbergweg 22, 01620 Halle (Saale), Germany
Rosenstiel Basic Medical Sciences Research Center and Howard Hughes Medical Institute, Brandeis University, MS 029, Waltham, MA 02454-9110, USA

ABSTRACT

Electron-cryo microscopy (cryo EM) represents a powerful tool to investigate the structure of Aβ fibrils. Based on this methodology, we have achieved structural resolutions of 1-2 nm for several Aβ fibril morphologies. In a few cases, even sub-nm resolution was possible. Our analysis illuminated the shape of the Aβ protofilament and the way how it is assembled from amyloid cross-β sheets. This assembly was also found to be conserved within a range of different Aβ fibril morphologies, which were derived from either Aβ(1-40) or Aβ(1-42) peptides. Their comparison provided new information on the structural basis of amyloid fibril polymorphism.

INTRODUCTION

Fibril formation from Aβ peptide is thought to act as the key trigger of Alzheimer`s disease (AD) [1]. It involves the formation of many different peptide assemblies [2] with mature fibrils representing the terminal end products of the reaction. These fibrils can occur in multiple fibril morphologies, but for none the atomic structure could so far be provided [3]. Different biophysical methodologies produced different structural models, often assuming a U-shaped conformation of the peptide [4].

To further analyze the structure of mature Aβ fibrils, we have used cryo EM combined with three-dimensional (3D) image reconstruction. This methodology combination involves the freezing of particles into a thin layer of ice to retain the native fibril 3D shape. Previous work where cryo EM was used to analyze highly symmetrical viral capsids yielded spatial resolutions of close to 0.3 nm [5]. In the case of amyloid-like fibrils derived from insulin and SH3 domain the principle feasibility of the technique was demonstrated and first 3D reconstructions could be provided [6,7]. During the past 10 years, we have obtained improved methods of helical particle reconstruction to investigate the global fibril structure of Aβ(1-40) fibrils as well as Aβ(1-42) filaments. This article provides an overview on the most important results obtained throughout this work.

METHODS

To obtain a 3D density map from amyloid fibril micrographs we used an improved helical reconstruction based on single particle methods [8]. For this reconstruction the fibrils were divided into segments and each was treated as independent single particle. Derived from the helical amyloid fibril structure additional constraints for each segment were applied. This improved the alignment of the segments by controlling the degrees of freedom. Further improvement was achieved by correcting for the contrast transfer function of the electron microscope (amplitude and phase correction), and by optimizing the helical symmetrization of the particle.

RESULTS

Cryo-EM was used to reconstruct the 3D architecture of different Aβ(1-40) fibril polymorphs. We found that most analyzed fibrils (11 out of 12) display two-fold symmetry [9]. Only one of these fibrils was not compatible with a two-fold symmetry and had to be reconstructed without symmetry assumption. All reconstructed fibrils varied considerably in their crossover distances, widths and cross-sectional shapes. The fibrils could not be readily clustered into a few well-resolvable morphology types. Instead, they represented an almost continuous spectrum of many different fibril morphologies.

These data were obtained by reconstructing individual fibrils, limiting the resolution to 2 nm or lower. To improve resolution, we averaged over a large number of morphologically similar filaments, resulting in a structural resolution of better than 1 nm. The feasibility of this approach was first demonstrated for a sample of Aβ(1-40) fibrils [10, 11]. The examined fibril morphology consisted of two equally shaped protofilaments, while each protofilament was constructed from two sandwiched cross-β sheets. The cross-sectional dimensions of the protofilament sandwich were ~2.5 x 9 nm [11], incompatible with previous models of Aβ fibril structures, which assumed a U-shaped peptide fold.

The basic substructure of this Aβ protofilament is conserved for different Aβ fibril morphologies, suggesting that they arose from different combinations of similarly structured protofilaments [12]. Therefore, different fibril morphologies may either differ in the number, relative orientation or substructure of the underlying protofilaments. This notion was supported by data showing that structurally analogous protofilaments occur with fibrils formed from either Aβ(1-40) and Aβ(1-42) peptide [13]. Hence, the C-terminal extension of Aβ peptide by two residues has only small effects on the protofilament assembly. Cryo-EM finally enabled analysis of the nanoscale flexibility parameters of Aβ fibrils [14]. This analysis revealed the significant bending rigidity of Aβ fibrils, which might be important in diseased tissues, where the deposition of rigid fibrils impairs naturally flexible and elastic tissue functions.

CONCLUSIONS

The structure of Aβ fibrils is more complex than anticipated from previous studies, and our analyses clearly reveal a structural assembly that differs from earlier proposals. However, further work will be required to establish the structural details of this assembly and whether Aβ peptide might not be able to adopt fundamentally different fibril types.

ACKNOWLEDGEMENTS

We are grateful to our previous co-workers Dr. Carsten Sachse and Dr. Jessica Meinhardt for their contributions to the recording, processing and interpretation of the data described here. This work has supported by grants from Deutsche Forschungsgemeinschaft, the Sonderforschungsbereich 610 and the Bundesministerium für Bildung und Forschung (BioFuture). N.G. gratefully acknowledges financial support by National Institutes of Health Grant 1 P01 GM-62580.

REFERENCES

1. Jakob-Roetne, R. and H. Jacobsen (2009). "Alzheimer's disease: from pathology to therapeutic approaches." Angew Chem Int Ed Engl **48**(17): 3030-3059.
2. Morgado, I. and M. Fandrich (2011). "Assembly of Alzheimer's Aβ peptide into nanostructured amyloid fibrils." Current Opinion in Colloid & Interface Science **16**(6): 508-514.
3. Wetzel, R., S. Shivaprasad, et al. (2007). "Plasticity of amyloid fibrils." Biochemistry **46**(1): 1-10.
4. Fandrich, M., M. Schmidt, et al. (2011). "Recent progress in understanding Alzheimer's β-amyloid structures." Trends Biochem Sci **36**(6): 338-345.
5. Yu, X., P. Ge, et al. (2011). "Atomic model of CPV reveals the mechanism used by this single-shelled virus to economically carry out functions conserved in multishelled reoviruses." Structure **19**(5): 652-661.
6. Jimenez, J. L., E. J. Nettleton, et al. (2002). "The protofilament structure of insulin amyloid fibrils." Proc Natl Acad Sci U S A **99**(14): 9196-9201.
7. Jimenez, J. L., J. I. Guijarro, et al. (1999). "Cryo-electron microscopy structure of an SH3 amyloid fibril and model of the molecular packing." EMBO J **18**(4): 815-821.
8. Sachse, C., J. Z. Chen, et al. (2007). "High-resolution electron microscopy of helical specimens: a fresh look at tobacco mosaic virus." J Mol Biol 371(3): 812-835.
9. Meinhardt JMB x Meinhardt, J., C. Sachse, et al. (2009). "Aβ(1-40) fibril polymorphism implies diverse interaction patterns in amyloid fibrils." J Mol Biol **386**(3): 869-877.
10. Sachse, C., C. Xu, et al. (2006). "Quaternary structure of a mature amyloid fibril from Alzheimer's Aβ(1-40) peptide." J Mol Biol **362**(2): 347-354.
11. Sachse, C., M. Fandrich, et al. (2008). "Paired β-sheet structure of an Aβ(1-40) amyloid fibril revealed by electron microscopy." Proc Natl Acad Sci U S A **105**(21): 7462-7466.
12. Fandrich, M., J. Meinhardt, et al. (2009). "Structural polymorphism of Alzheimer Aβ and other amyloid fibrils." Prion **3**(2): 89-93.
13. Schmidt, M., C. Sachse, et al. (2009). "Comparison of Alzheimer Aβ(1-40) and Aβ(1-42) amyloid fibrils reveals similar protofilament structures." Proc Natl Acad Sci U S A **106**(47): 19813-19818.
14. Sachse, C., N. Grigorieff, et al. (2010). "Nanoscale flexibility parameters of Alzheimer amyloid fibrils determined by electron cryo-microscopy." Angew Chem Int Ed Engl **49**(7): 1321-1323.

Molecular basis of amyloid fibril recognition by the conformation-sensitive B10 antibody fragment

Christian Haupt [1], Liesa Heinrich [1], Isabel Morgado [2], Peter Hortschansky [3], Magdalena Bereza [1], Marcus Fändrich [4], Uwe Horn [1]

[1]Bio Pilot Plant, Hans-Knöll-Institute, Jena, Germany
[2]Institute for Biochemistry and Biotechnology, Martin-Luther-University Halle-Wittenberg, Halle, Germany
[3]Molecular and Apllied Microbiology, Hans-Knöll-Institute, Jena, Germany
[4]Protein Folding and Aggregation, Max-Planck Research Unit for Enzymology of Protein Folding, Halle, Germany

The unifying structural feature of amyloid fibrils is the cross-β conformation, differentiating this structure from natively folded polypeptide chains. While diagnosis of amyloid diseases and development of therapeutic strategies critically rely on the recognition of this conformation with specific molecules such as Congo red, the molecular basis by which amyloid fibrils are recognized is only partially understood. This is specifically the case for the recently emerging group of conformation-specific antibodies.

Here, we address this question by biophysical analysis of the B10 antibody fragment, which was recently shown by dot blotting to recognize a large panel of different amyloid and amyloid-like fibrils in a conformation-specific manner. Hence, it differentiates Aβ fibrils from soluble Aβ oligomers or disaggregated Aβ peptide.

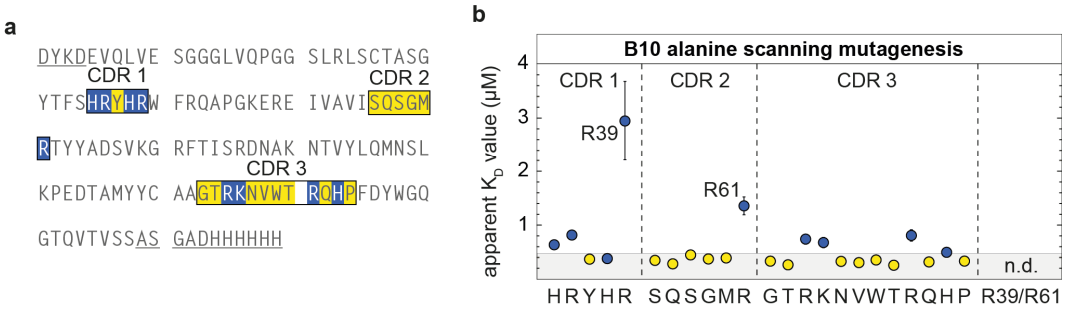

Figure 1. a) B10 sequence. Blue: positive charge, yellow: uncharged, underlined: not visible in crystal structure. **b)** Alanine scanning mutagenesis of B10. Apparent K_D values of single B10 mutants to to Aβ(1-40) fibrils were determined with surface plasmon resonance. Gray region: apparent K_D value of unmodified B10.

BASIC B10-CDR RESIDUES INTERACT WITH ACIDIC RESIDUES IN FIBRILS

Analyzing the complementarity determining regions (CDRs) of B10 we assumed that this conformational specificity depends on positively charged residue within the B10 antigen binding site. Alanine scanning mutagenesis of these positively charged amino acids results in significant increase of the apparent K_D value measured by surface plasmon resonance (SPR) whereas mutation of uncharged residues has no influence (Fig. 1).

To confirm the influence of electrostatic interactions on amyloid fibril binding by B10 we measured SPR under different running buffer conditions. Additives inhibiting ionic interactions had the strongest effect compared to 2 M urea or 20% ethanol. Moreover, we carboxyl-modified or amino-modified different fibrils. Measuring the B10AP binding by dot blot we find that masking of negatively charged groups in amyloid fibrils strongly abrogate B10-fibril interaction. Due to these findings we assume that ionic interactions between positively charged residues of B10 and negatively charged residues of amyloid fibrils are crucial.

B10 SHOWS CLOSE PROPERTIES TO A PATTERN RECOGNITION RECEPTOR

Furthermore B10 also recognizes the highly regular and polyanionic biopolymers heparin and DNA. This specificity is also conserved in natural amyloid receptors from the innate immune system, the pattern recognition receptors. Such a receptor is the receptor for advanced glycation end products (RAGE). Therefore we mapped out the extent of similarity between B10 and RAGE.

Using SPR analysis we measured strong binding affinity of RAGE-VC1 fragment to Aβ(1-40) fibrils whereas no interaction occurs with disaggregated Aβ(1-40) peptide (Fig. 2a). Dot blot experiments with RAGE-VC1 show binding to all B10-positive fibrils, while B10-negative fibrils were not detected by RAGE-VC1. RAGE further relates to B10, as it binds its ligands through basic residues and displays also a strongly positive electrostatic surface potential, closely matching that of B10 (Fig. 2b). Moreover binding of the RAGE-VC1 fragment to Aβ(1–40) amyloid fibrils can compete with B10AP. These data establish that the binding mechanism of B10 is effectively the same as the one that is characteristic of a typical and naturally occurring pattern recognition receptor.

These data imply that the antigen specificity of B10 is based on a pattern recognition mechanism. This mechanism involves the binding of a highly regular and anionic surface pattern which is presented by many but not all amyloid fibrils and reflects the highly ordered and regular structure of these biopolymers. These results enable a broad range of further studies on the molecular mechanism of amyloid fibril formation, their structure and the targeting of amyloid fibrils by conformation sensitive antibodies.

PROPOSED MODEL OF B10 BINDING TO AMYLOID FIBRILS

B10 binding depends on a pattern recognition mechanism, that involves specific electrostatic interactions with a highly ordered and regular arrangement of negatively charged chemical groups on the surface of amyloid fibrils. Such an anionic pattern characterizes the surface of some, though not all, amyloid fibrils and is a consequence of the specific conformational architecture of these proteinaceous filaments.

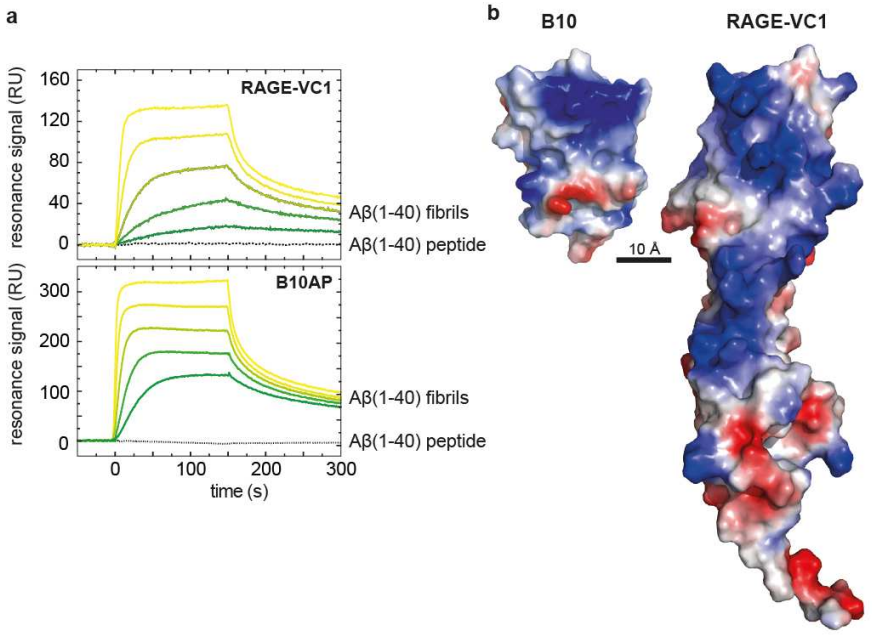

Figure 2. a) Surface plasmon resonance curves of RAGE-VC1 and B10AP binding to Aβ(1-40) peptide (black) or Aβ(1-40) fibrils (green-yellow). **b)** Electrostatic surface representation of B10 and RAGE-VC1. Blue: positive charge, red: negative charge.

REFERENCES

1. Habicht et al. (2007) Proc. Natl. Acad. Sci. U.S.A. 104, 19232-19237
2. Haupt et al. (2011) J Mol Biol 408, 529-540.
3. Haupt et al. (2011) J Mol Biol 405, 341-348.

Sensitive Histochemical Staining of Different Polysaccharide Complexes Associated with Amyloid fibrils

Levente Csóka[a], Thomas R. Appel[b], Anett Eitner[c], Josef Makovitzky[d,x]

a) University of West Hungary, Institute of Wood and Paper Technology, Sopron,Hungary
b) Niedersächsisches Internatsgymnasium, Bad Bederkesa, Germany
c) Friedrich Schiller University, Institute of Anatomy II, Jena, Germany
d) Heidelberg, Dep of Neurpathology,University Heidelberg and Inst for Legal Medicine, University Freiburg, Germany

BACKGROUND

Biomolecules, cells and tissues are complex structures, built from chemically different subunits. Biological structures are not regular, and they are not inherently birefringent. Thus, biologically complex structures have a weak or latent optical anisotropy (birefringence) in the native or fixed unstained state. To investigate their ultrastructure, various topo-optical staining reactions can intensify the weak birefringence of ordered subunits of complex biological structures. On the other hand insoluble fibrillar deposits in different tissues are thought to be a final consequence of systemic amyloidosis. The unstable monoclonal immunoglobulin light chains are responsible for the primary amyloidosis. To examine the complex fibrillar structure of amyloid in human brain, bacterial cellulose, chitosan and alginic acid polysaccharide materials were selected and comparative investigated.

MATERIAL AND METHODS

Three samples polysaccharides (microbial cellulose, chitosan and alginic acid) were chosen as well-characterized control for structural components of amyloid fibrils. The specimens were subjected to the following topo-optical staining reactions: staining with the toluidine blue with post precipitation (Romhányi 1963), 1,9 dimethyl methylene blue staining reaction acc. Módis 1974 (Makovitzky 1984). The aldehyde-bisulfite toluidine blue (ABT-)reaction (Romhányi et al., 1975) or, aldehyde-bisulfite-dimethyl-methylene blue eaction (ABD-r, Makovitzky 1984, Makovitzky and Richter 2009) are a specific reaction for the linear ordered OH groups of the sugar molecules. Also in its glycosaminoglycan (GAG)-specific variant “chemically intensified basophilic reaction”, the two steps anisotropic PAS-reaction (CIBR, Módis 1991), is specific for linearly ordered vicinal OH groups in the C2 and C3 position of uronic acid. The “critical electrolyte concentration” method is selective (CEC) for acidic groups like carboxyl and sulphate in GAGs (Módis 1991, Richter 2005). Congo red and Rivanol staining reaction has been applied acc. to Romhányi (1).

RESULTS

The 3 unstained samples of bacterial cellulose, chitosan and alginic acid in water or gum Arabic medium gave low anisotropic effect and the sign of the birefringence respect to the length is linear positive.

Table 1 summarizes the signs of topo-optical reactions in stained form and in native, unstained form.

sample	*Topo-optical staining reactions*				
	Unstained	ABT-r	ABD-r	Congo red	Rivanol
	Sign of birefringence / linear positive + or linear negative -				
Bacterial cellulose	+	-	-	+	No staining
Chitosan	+	-	-	+	+
Alginic acid	+	-	-	+	+

Table 1. Differences between bacterial cellulose, chitosan and alginic acid with topooptical staining reactions.

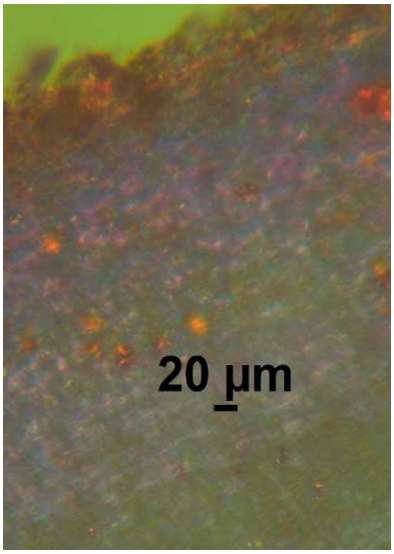

Bacterial cellulose ABT staining reaction

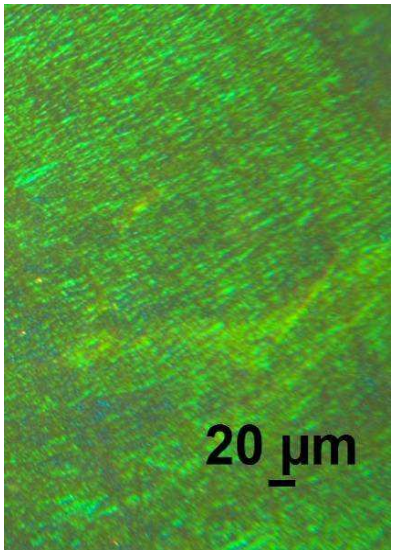

Bacterial cellulose ABD staining reaction at pH 1.2

The bacterial cellulose, chitosan and alginic acid (from brown algae) give with ABT/ABD- reaction an inversive topo-optical reaction.(Csóka et al., 2012).

Human amyloid deposits, which were thought to have a similar structure and staining behavior as cellulose, also have a positive ABT-or ABD- reaction based on examination (Makovitzky 2003; Richter 2005; Appel et al., 2003, 2005). The amyloid fibrils are not homogeneous but heterogeneous, and have a highly ordered structure in oriented fashion: the center is formed by a glycoprotein core (AP), helical structures of chrondroitin and heparin sulphate surround this core and a filament network of protein (AA or AL and others) constitute the

surface of the fibril (Inoue et al. 2002, Makovitzky, 2005). Prolonged methylation of amyloid fibrils causes conversion of hydroxyl radicals to methyl ether and thus these OH groups are responsible for the toluidine blue binding in orthochromatic staining. Hydroxyl groups of carbohydrates bound to protein and glycoproteins of amyloid fibrils.

Since chitin is a highly insoluble molecule (chitosan is soluble) and a substrate for glycan-protein interactions, chitin-like polysaccharides within the Alzheimer disease (AD) brain could provide a scaffolding for amyloid-β deposition. As such, glucosamine, which is part of the structure of the polysaccharides chitosan and chitin, may facilitate the process of amyloidosis, and/or provide neuroprotection in the AD brain (Castellani et al. 2007; Sotgiu 2008).

CONCLUSIONS

These data indicate that the presented polysaccharide complexes, glycosaminoglycans and sulphate groups by histochemical methods can be used for further amyloid research on *in vitro* fibrils prepared with and without GAGs and on *ex vivo* fibrils. Glucosamine, which is part of the structure of the selected polysaccharides chitosan and chitin, may facilitate the process of amyloidosis, and/or provide neuroprotection in the Alzheimer disease brain.

REFERENCES

1. Romhányi Über die submikroskopische Grundlage der metachromatischen Reaktion. Acta Histochem 1963;15: 201-33
2. Módis L: Topo-optical investigations of mucopolysaccharides (acid glycosaminoglycans). In: Hdb. der Histochemie. Ed.: Graumann, W. – Neumann, K. Vol. II/4. G. Fischer 1974, Stuttgart
3. Makovitzky J: Polarization optical analysis of amyloid deposits with various topo-optical reaction. Acta histochem 2003: 105;369-370.
4. Romhányi G, Deák G, Fischer : Aldehyde-bisulfite-toluidine blue (ABT) staining as a topo-optical reaction for the demonstration of linear order of vicinal OH groups in biological structures. Histochemistry 1975: 43; 333-348.
5. Makovitzky J, Richter S. The relevance of the aldehyde bisulfite toluidine blue reaction and its variants in the submicroscopic carbohydrate research. Acta Histochem 2009;111: 274-92.
6. Módis L: Organization of the extracellular matrix: a polarization microscopic approach. Boca Raton, FL, USA: CRC Press; Boca Raton. 1991 pp 35-37.
7. Csóka L, Appel TR, Eitner A, Jirikowski G, Makovitzky: Polarization optical histochemical characterization and supramolecular structure of carbohydrate fibrils Acta Histochemi 2012:Apr 10 (Epub ahead of print)
8. Appel TR, Makovitzky J: Romhányi's staining methods applied to tissue-isolated amyloid fibrils Acta histochem 2003:105; 371-372.
9. Appel TR, Richter S, Linke RP, Makovitzky J: Histochemical and topo-optical investigations on tissue-isolated and in vitro amyloid fibrils. Amyloid 2005:12; 174-183.
10. Makovitzky J: Polarization optical analysis of amyloid deposits with various topo-optical reaction. Acta histochem 2003: 105;369-370.

11. Richter S. Amyloidose des Respirationstraktes. Eine polarisationsoptich-histochemische Untersuchung mit klinischem Bezug. MD thesis, Rostock 2005, Germany
12. Inonue S, Kuroiwa M, Kisilevsky R : AA protein in experimental murine AA amyloid fibrils: a high resolution ultrastructural and immunohistochemical study comparing aldehydfixed and cryofixed tissues. Amyloid 2002: 9;115-125.
13. Makovitzky J: The submicroscopic structure of amyloid deposits and ex vivo isolated amyloid fibrils. Romhányi Memorial Lecture at the Hungarian Academy of Sciences in Budapest 2005, on 15 September.
14. Castellani RJ, Perry G, Smith MA:The Role of Novel Chitin-like Polysaccharides in Alzheimer Disease. Neurotox Res 2007;12(4): 269-74.
15. Sotgiu S, Musumeci S, Marconi S, Gini B, Bonetti B: Different content of chitin-like polysaccharides in multiple sclerosis and Alzheimer's disease brains. J Neuroimmunol 2008;197(1):70-3.

Polarization optical and histochemical analysis of amyloid samples from various animal species

M. Kröger, B.M. Kovács ,T.R. Appel, E. Gruys, J. Makovitzky[X]

Maria Kröger, Tierärztliche Praxis, Gelbesande ,Germany
Bea Marianna Kovács, Szent István University, Faculty of Veterinary Science, Dept of Physiology and Biochemistry, Budapest, Hungary
Thomas R. Appel, Niedersächsisches Internatsgymnasium, Bad Bederkesa, Germany
Erik Gruys, Dept of Veterinary Pathology, Faculty of Veterinary Medicine, Utrecht University, Netherlands
Josef Makovitzky, Dept of Neuropathology, University Heidelberg and Inst for Legal Medicine of University Freiburg Germany ([X] sponsored by NAR (Heidelberg, Germany))

BACKGROUND

Former results on *post mortem* tissue-isolated human amyloid fibrils showed a protein fibril co-localised with strong acidic groups, interpreted as chondroitine and/or heparan sulphate attached to the amyloid fibrils (1, 2).

In the three dimensional amyloid model of Inoue et al. (2002), amyloid has a highly ordered structure in an oriented fashion: the center is formed by a glycoprotein core (AP), helically structures of chondroitin and heparan sulfate surround this core, a filament network of protein (AL or others) constitutes the surface of the fibril (cited in 3, 4, 5, 6).

The aim of this study was to compare the occurrence of different chemical components in a variety of animal amyloid deposits: derived from dog, cat, cow, mouse, goose, chicken and marten.

METHODS

Tissue samples from seven different species were fixed with 4% formalin in PBS pH 7.4 and paraffin-embedded. Sections (2-5 µm) of the following amyloidotic tissues were investigated: dog - kidney, spleen, liver; cat – pancreas; marten - kidney, spleen; cow – kidney; mouse - liver, intestine, spleen, heart, lung (AA and AapoA II); goose – liver, intestine (7).

We have demonstrated sugar moieties in all amyloid deposits selectively with the ABT-reaction (8). Sialic acid and O-acyl sialic acid were demonstrated with a specific reaction (9). The glycosaminoglycan components have been visualized in the amyloid deposits by the chemically intensified basophilic reaction (CIBR, 10, 5) and by the critical electrolyte concentration (CEC) method (10). The protein core was demonstrated with 0.1% aqueous solution of Congo red, Thiazin red, Eosin, Pinacyanol, Pinacyanol chloride, N,N´-Diethylspeudoisocyanine-chloride (PSI), Toluidine blue, 1,9-Dimethyl-methylene blue and Rivanol.

RESULTS

The unstained amyloid deposits show – embedded in water or in gum Arabic – an anisotropy,the sign is linear positive to the length.

After Congo red, Thiazin red, Eosin, Pinacyanol, Pinacyanol chloride and N,N´-Diethylspeudoisocyanine chloride (PSI) we registered an additive topo-optical staining reaction, i.e. the original sign is not changed but the intensity increased. The dyestuff molecules are oriented parallel to the surface. After Toluidine blue, 1,9-Dimethyl methylene blue and Rivanol staining, the sign of the anisotropy becomes linear negative, the dye molecules are oriented perpendicular to the surface. The latter is an inversive topo-optical staining reaction.

In the mammalian amyloid of cat (AIAPP), cattle (AL), dog (AA), marten (fibrinogen) and mouse (AA and AapoAII) we found strong acidic groups in linear order, but only weak acidic groups in avian amyloid (both AA). Our observation differs from those of Peperkamp (1997), who demonstrated highly sulphated GAGs (heparin/heparan sulphate) in joint amyloid fibrils of chicken with the Alcian blue CEC method (11).

Furthermore, we observed a gradation of the topo-optical reaction intensity in murine and canine amyloid with changing polarization colour from strong red orange at 0.1 M $MgCl_2$ to hardly noticeable pink at 1.0 and 1.8 M $MgCl_2$. However, the topo-optical staining reaction appeared with stable strong positive results in the cases of cat, marten and cow, as well as in the above mentioned human amyloid (Kroeger et al., 2006).

After diegestion with hyaluronidase, chondroitinase AC and B we found an optimally oriented Congo red binding and more intensity compared to the controls (12).

The amyloid deposits from AA type (dog, mouse, goose and chicken) are sensitive to potassium permanganate or performiate treatment followed by pronase or trypsin (4-8 h), the Congo red, Thiazin red and Eosin induced anisotropy is abolished. However, the cat, cattle, marten and mouse (AapoAII) amyloid is resistent to this treatment.

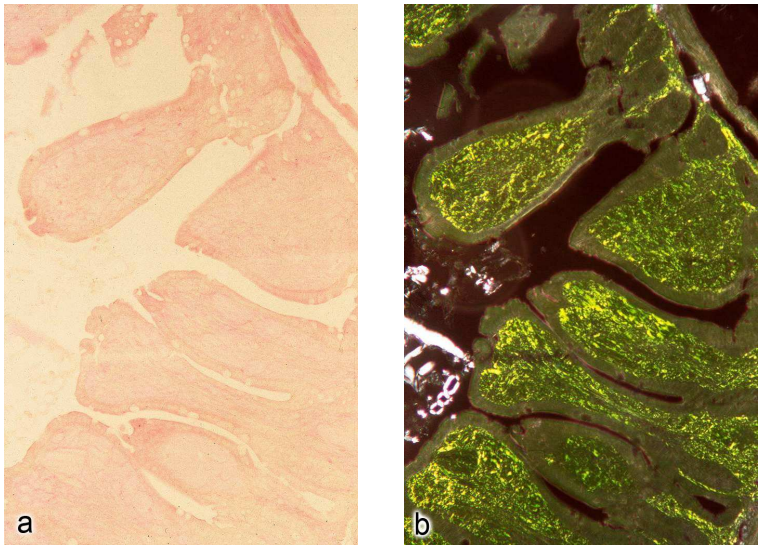

Picture 1. Mouse jejunum Amyloid staining: Eosin. a) light microscopic picture 80X, b) polarization optical picture 80X

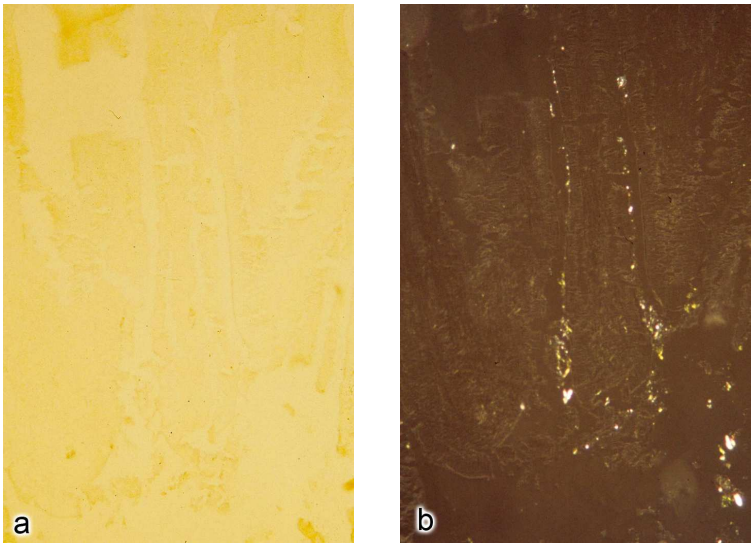

Picture 2. Goose jejunum amyloid after KMnO4 -Trypsin digestion 8 h, staining with Congo red. a) light microscopic picture 80X, b) polarization optical picture 80X

Table 1. Results of $KMnO_4$/trypsin or HCOOOH/trypsin pretreatment followed by Congo red staining

animal	*amyloid type*	*$KMnO_4$/trypsin*	*HCOOOH/trypsin*
Cow	AL	resistant	resistant
Dog	AA	sensitive	sensitive
Cat	AIAPP	resistant	resistant
Marten	Afibrinogen	resistant	resistant
Mouse	AA	sensitive	sensitive
	AapoAII	resistant	resistant
Goose	AA	sensitive	sensitive
Chicken	AA	sensitive	sensitive

In the amyloid deposits of all cases the linearly ordered OH groups of the sugar and sialic acid / or O-acyl sialic acid molecules are perpendicularly ordered to the surface of the amyloid fibrils. The sugar chains are oriented parallel to the surface.

With the CIBR we found similar positive topo-optical reactions in all species including human, with intensive violet metachromasy in light optic. The linear negative sign of anisotropy indicates a perpendicular orientation of the toluidine blue or 1,9-Dimethyl methylene blue dye molecules.

CONCLUSIONS

There are differences in quality and quantity of linearly ordered acidic groups which are interpreted as GAG components: heparan and keratan sulphate (strong acidic group SO_4^{2-}) are missing in goose and chicken amyloid. Mouse and dog exhibit all four components but with less intensity than cow, marten, cat and human amyloid.

The polysaccharide chains are orientated parallel to the length of the amyloid fibrils, their vicinal OH groups are orientated perpendicularly to the length of the fibril. In all species sialic acid and O-acyl sialic acid are detectable with a perpendicular orientation of their vicinal OH groups.

The sensitivity of AA amyloid for $KMnO_4$ oxidation, and/or performiate oxidation combined with trypsin or pronase digestion varies between species. In order to identify secondary AA amyloidosis by sensitivity to pretreatment, the most reliable method is performiate trypsin or performiate pronase digestion.

REFERENCES

1. Appel TR, Makovitzky J: Romhányi's staining methods applied to tissue-isolated amyloid fibrils Acta histochem 2003: 105; 371-372.
2. Appel TR, Richter S, Linke RP, Makovitzky J: Histochemical and topo-optical investigations on tissue-isolated and in vitro amyloid fibrils. Amyloid 2005: 12; 174-183.
3. Inonue S ,Kuroiwa M, Kisilevsky R: AA protein in experimental murine AA amyloid fibrils: a high resolution ultrastructural and immunohistochemical study comparing aldehydfixed and cryofixed tissues. Amyloid 2002: 9;115-125
4. Makovitzky J: Polarization optical analysis of amyloid deposits with various topo-optical reaction. Acta histochem 2003;105:369-370.
5. Richter S: Amyloidose des Respirationstraktes. Eine polarisationsoptisch-histochemische Untersuchung mit klinischem Bezug MD Thesis Rostock, Germany, 2005.
6. Makovitzky J, Richter, S.: The relevance of Aldehyde-bisulfite toluidine blue reaction and its variants in the submicroscopic carbohydrate research. In: acta histochem. Fischer,s special issue 2009: 111; 273-291
7. Kröger M, Richter S, Gruys E, Makovitzky J: Topo-optical investigations of AA-amyloid deposits from various species. In: János Fischer Memorial Symposium, Sept 15. 2006 Szeged, Hungary. Abstract 8.
8. Romhányi G, Deák G, Fischer J.: Aldehyde-bisulfite-toluidine blue (ABT) staining as a topo-optical reaction for the demon- stration of linear order of vicinal OH groups in biological structures. Histochemistry 1975:43;333-348
9. Makovitzky J: Polarization optical analysis of blood cell membranes. In: Progress in Histo- and Cytochemistry. Vol 15 No.3, G Fischer Verlag Stuttgart New York, 1984
10. Módis L: Organization of the extracellular matrix: a polarization microscopic approach. Boca Raton, FL, USA:CRC Press; Boca Raton. 1991 pp 35-37.
11. Peperkamp NHMT, Landman WJM, Tooten PCJ, Ultee A, Voorhout WF, Gruys E: Light microscopic, immunohistochemical and electron microscopical features of amyloid arthropathy in chickens, Vet Pathol 1997;34:271-278
12. Makovitzky J, Richter S, Appel TR: Topo-optical investigation and enzymatic digestions on tissue- isolated amyloid fibrils. Acta histochem 2006; 108:193-196.

The polarization optical-histochemical analysis of the amyloid deposits in Alzheimer's, Creutzfeldt-Jakob diseases and Down syndrome

J. Makovitzky[x], G.G. Kovács, E. Gömöri, L. Csóka

Josef Makovitzky, Dep of Neuropathology, University Heidelberg and Inst for Legal Medicine, University Freiburg Germany
Gábor G. Kovács, Medical University of Vienna, Institute of Neurology, Austria
Éva Gömöri, Institute of Pathology, University of Pécs, Hungary
Levente Csóka, University of West Hungary, Inst of Wood and Paper Technology, Sopron, Hungary

BACKGROUND

Former results on *post mortem* tissue-isolated human amyloid fibrils and on human amyloid deposits showed a protein fibril co-localised with strong acidic groups, interpreted as chondroitine and/or heparan sulphate attached to the amyloid fibrils (1,2,3).

In the three dimensional amyloid model of Inoue et al. (2002), amyloid has a highly ordered structure in an oriented fashion: the center is formed by a glycoprotein core (AP), helically structures of chondroitin- and heparan sulfate surround this core, a filament network of protein (AA, AL or others) constitutes the surface of the fibril (4, 5, 6, 7).

AIM

Our aim was to evaluate whether the fibril constituents discussed above can be demonstrated in brain amyloid deposits in Alzheimer`s, Creutzfeldt-Jakob diseases and Down syndrome. Furthermore, we were interested whether additional topo-optical reactions provide more information or not.

METHODS

Formalin-fixed (4% formaldehyde in PBS pH 7.4) and paraffin-embedded brain sections (2-5 µm) of Alzheimer, Morbus Down and Creutzfeld-Jakob were investigated with various topo-optical staining reactions. Synthetic amyloid ß (1-40 and 1-42) fibrils served as control. Our topo-optical staining reactions are an indicative method of linearly ordered functional groups. The aldehyde bisulfite toluidine blue reaction (ABT-r acc. Romhányi et al., 1975) is specific for linearly ordered vicinal OH groups in carbohydrates. Also its glycosaminoglycan (GAG)-specific variant "chemically intensified basophilic reaction", the two step anisotropic PAS-reaction (CIBR, Módis 1991), is specific for linearly ordered vicinal OH groups in the C2 and C3 position of uronic acid. The sialic acid

specific reaction indicates sialic acid (Makovitzky 1984) and the “critical electrolyte concentration” method (CEC) denotes acidic groups like carboxyl and sulphate in GAGs (Módis 1991, Richter 2005).

RESULTS

The sign of the anisotropy on unstained sections with amyloid (amyloid deposits, amyloid plaques and blood vessels affected by amyloid angiopathy) in water or gum arabicum is linear positive to the length.

The stained brain sections showed amyloid fibrils (deposits), Aβ amyloid plaques and blood vessels affected by amyloid angiopathy. Brain sections and controls were stained with Congo red, Thiazine red, N,N´-diethyl pseudoisocyanine chloride (PSI), pinacyanol, pinacyanol chloride, toluidine blue, 1,9-dimethyl methylene blue and rivanol for protein core. All samples including controls were positive in all cases. Depending on whether the dye molecules aggregated parallel or perpendicular to the longitudinal axis, the angle of the polarised light was affected positively (Congo red, PSI, pinacyanol, pinacyanol chloride) or negatively (toluidine blue, 1,9-dimethyl methylene blue and rivanol).

The sugar-specific ABT and sialic acid reactions were positive for amyloid plaques and blood vessels. Based on our analysis the linearly ordered OH–groups were perpendicularly oriented to the longitudinal fibril axis.

The CEC and CIBR reactions were positive on amyloid plaques and blood vessels at all ionic strengths pointing to strong acidic groups like sulphate or phosphate. Synthetic Aβ fibrils (control) were negative.

All amyloid fibrils, amyloid plaques (primitive and diffuse) and blood vessels affected by amyloid angiopathy were resistant to potassium permanganate/trypsin, permanganate/pronase, performic acid/trypsin and performic acid/pronase digestion (24-48 hours).

Table 1. Results of anisotropic (topo-optical) staining reactions

	linearly ordered protein (Congo red and others)	*Linearly ordered sugars / vicinal OH-groups (ABT-reaction i.e. anisotropic PAS)*	*linearly ordered vicinal OH-groups in C2-C3 position of uronic acid (CIBR i.e. for GAGs)*	*linearly ordered OH-groups of sialic acid (sialic acid specific reaction)*	*linearly ordered acidic groups (Critical electrolyte concentration,CEC, 0.1M, 0.5M, 1M, 1.8M)*
Amyloid plaques	+	+	+	+	+
Amyloid fibrils	+	-	+	-	+
Blood vessel by Amyloid angiopathy	+	+	+	+	+

In amyloid plaques the CEC and CIBR induced birefringence disappeared after 6-8 h digestion with heparinase I, II, III and/or hyaluronidase, chondroitinase AC and B. Only the birefringence of the protein core remained behind showing a linear positive sign after CEC reaction embedded in gum arabic or water. After enzyme digestions and staining with Congo red, the intensity of birefringence increased, and the measured retardation differences were increased, too.

DISCUSSION

Allsop et al. investigated isolated senile amyloid plaques with Congo red and observed birefringence, moreover amino acid compositions of isolated plaque cores were assigned (10). Wisniewski et al. described the morphological spectrum of amyloid deposits in Alzheimer's disease (11). Amyloid fibrils were found as large areas of diffuse depositions in the neuropil, ribbon-like infiltration in the subpial layer of the cerebral cortex, furthermore, as granular deposits in the white matter, as diffuse deposits in the molecular layer of the cerebellum and the basal ganglia and as star-shaped deposits in the cerebellar Purkinje cell layer. In our investigations hippocampus tissue was used.

In their investigations Yamada et al., Snow et al., Castillo et al. and McLaurin et al. unambiguously proved that in Alzheimer type amyloid deposits the protein core is surrounded by GAGs and the GAGs have an important role in amyloid synthesis (12-16). Snow reported the presence of GAGs by alcian blue CEC reaction (13). We think that the CEC reaction from Módis, Appel et al. and Richter is a more selective method to investigate GaG components, since by polarisation the CEC reaction gives information about the linearly ordered structure of GAGs (8,1,5).

Our results with toluidine blue and 1,9 dimethyl methylene blue under light microscopy show metachromasy. At pH 7.4 the sign of birefringence is linear negative to the length, an inversive topo-optical reaction. At pH 3.6 the sign of birefringence is linear positive, which is an additive type topo-optial reaction. Congo red, Thiazine red, PSI, pinacyanol and pinacyanol chloride stained amyloid with linear positive sign of birefringence; the binding dye molecules are parallel oriented to the surface. Toluidine blue, 1,9 dimethyl methylene blue and rivanol stained amyloid with linear negative sign of birefringence, the binding dye molecules are oriented perpendicular to the surface.

The pretreatments (potassium permanganate or performic acid) of trypsin and pronase digestion show no effect in Alzheimer brain samples. This indicates that the amyloid deposits are solid and structurally highly ordered. The resistance to oxidative pretreatment is common to all "primary" amyloid deposits that do not contain serum amyloid A protein (17). Snow suggested that brain Aβ amyloid was resistant to potassium permanganat/performiate trypsin/pronase digestion because of the stabilizing effect of GAGs (18).

Our results show that after Heparinase, Hyaluronidase and Chondroitinase digestions the CEC and CIBR induced anisotropy disappeared. We only found the original protein's core birefringence. The sign is linear positive to the length, which is the same as in synthetic pure Aβ fibrils. A similar phenomenon was observed on collagen and described by Németh - after enzymatic removal of GAG components from collagen fibers (19). According to his assumption, GAG components possess a stabilizing effect on collagen fibers. Bruinsma et al. characterized the pathological lesions as Aβ plaques consisting mainly of aggregated Aβ protein, whose aggregation is affected by heparin sulphate proteoglycans (20).

Ariga et al. emphasised the role of proteoglycans and GAGs in Alzheimer disease and in other similar clinical cases (21). According to Ariga et al. the Aβ protein binds to many biomolecules, including lipids, proteins and proteoglycans. Proteoglycans play an important role in amyloid formation, increasing the neurotoxicity of Aβ protein. The proteoglycan binding site in the 13-16 amino-acid region (His-His-Gln-Lys) of amyloid ß represents a unique target for inhibition of amyloid fibril formation. GAG binding accelerates fibril formation and maintains the fibril stability.

The results of our various reactions are in accordance with the amyloid model of Snow et al. (13,18). Zschiesche and Jakob reported the PAS positivity of amyloid plaques in the brain of various animals (22). We have shown the sialic acid positivity of human brain Aβ plaques. Asn-linked carbohydrates (sialic acid specific reaction) were demonstrated in brain amyloid plaques and blood vessels with amyloid angiopathy, but not in synthetic amyloid β fibrils. This is somehow surprising, since Aß should not be glycosylated. It shows that brain amyloid deposits are composed of multiple constituents, not restricted to Aβ only.

REFERENCES

1. Appel TR, Makovitzky J.: Romhányi's staining methods applied to tissue-isolated amyloid fibrils Acta histochem 2003: 105; 371-372.
2. Appel TR, Richter S, Linke RP, Makovitzky J: Histochemical and topo-optical investigations on tissue-isolated and in vitro amyloid fibrils. Amyloid 2005: 12; 174-183.
3. Makovitzky J.: Polarization optical analysis of amyloid deposits with various topo-optical reaction. Acta histochem 2003;105:369-370.
4. Inonue S, Kuroiwa M, Kisilevsky R.:AA protein in experimental murine AA amyloid fibrils: a high resolution ultrastructural and immunohistochemical study comparing aldehydfixed and cryofixed tissues. Amyloid 2002: 9:115-125.
5. Richter S: Amyloidose des Respirationstraktes. Eine polarisationsoptisch-histochemische Untersuchung mit klinischem Bezug MD Thesis Rostock, Germany, 2005.
6. Makovitzky J, Richter, S.: The relevance of Aldehyde-bisulfite toluidine blue reaction and its variants in the submicroscopic carbohydrate research. In: acta histochem. Fischer,s special issue 2009: 111; 273-291
7. Romhányi G, Deák G, Fischer J.: Aldehyde-bisulfite-toluidine blue (ABT) staining as a topo-optical reaction for the demonstration of linear order of vicinal OH groups in biological structures. Histochemistry 1975: 43; 333-348.
8. Módis L. Organization of the extracellular matrix: a polarization microscopic approach. Boca Raton, FL, USA: CRC Press; Boca Raton. 1991 pp 35-37.
9. Makovitzky J: Polarization optical analysis of blood cell membranes. In: Progress in Histo- and Cytochemistry. Vol 15 No.3, G Fischer Verlag Stuttgart New York, 1984 .
10. Allsop D, Landon M, Kidd M The isolation and aminoacid composition of senile plaque core protein. Brain Res 1983: 259: 348-352.
11. Wisniewski HM, Bancher C, Barcikowska M, Wen GY, Currie J Spectrum of morphological appearance of amyloid deposits in Alzheimer's disease Acta Neupathol 989: 78: 337-347.
12. Yamaguchi H, Hirai S, Morimatsu M, Shoji M, Ihara Y A variety of cerebral amyloid deposits in the brains of the Alzheimer type dementia demonstrated by B protein immunostaining. Acta Neuropathol 1988: 76: 541-449.
13. Snow AD, Sekiguchi RT, Nochlin D, Kalaria RN, Kimata K Heparan sulfate proteoglycan in diffuse plaques of hippocampus but not of cerebellum in Alzheimer's disease brain. Am J Pathol 1994: 144: 337-347.

14. Castillo GM, Ngo C, Cummings J, Wight TN, Snow AD Perlecan binds to the beta-amyloid proteins (A beta) of Alzheimer's disease, accelerates A beta fibrilformation, and maintains A beta fibril stability. J Neurochem 1987: 69: 2452-65.
15. Castillo GM, Lukito W, Wight TN, Snow AD The sulfate moieties of glycosaminogly- cans are critical for the enhancement of ß-Amyloid Protein Fibril Formation: J of Neurochemistry 1999: 72:1681-1687.
16. McLaurin JA, Franklin Tr., Kunhs WJ., Frase PE. A sulfated proteoglycan aggregation factor mediates amyloid-ß peptide fibril formation and neurotoxicity Amyloid: Int J Exp Clin Invest 1999: 6: 233-243.
17. Romhányi G Differences in ultrastructural organization of amyloid as revealed by sensitivity or resistance to induced proteolysis. Virchows Arch A Pathol Anat 1972: 357: 29-52.
18. Snow AD, Kinsella MG, Parks E, Sekiguchi RT, Miller JD, Kimata K, Wight TN: Differential binding of vascular Cell –derived Proteoglycans (Perlecan, Biglycan, Decorin and Versican) to the Beta-Amyloid Protein of Alzheimer`s Disease Arch of Biochem and Biophysics 1995: 320: 84-95.
19. Németh P. Age dependency of the enzyme-resistance of collagen fibres. Student research thesis Pécs 1972.
20. Bruinsma IB, te Riet L, Gevers T, ten Dam GB, van Kuppevelt TH, David G, Küsters B, de Waal RM, Verbeek MM Sulfation of heparan sulfate associated with amyloid-beta plaques in patients with Alzheimer's disease Acta Neuropathol 2010: 119: 211-220.
21. Ariga T, Miyatake T, Yu RK Role of proteoglycans and glycosaminoglycans in the pathogenesis of Alzheimer's disease and related disorders: amyloidogenesis and therapeutic strategies - a review J Neurosci Res 2010: 88: 2303-15.
22. Zschiesche W, Jakob W Pathology of animal amyloidosis Pharmacology and Therapeutics 1989: 41: 49-83.

[X] J. Makovitzky sponsored by NAR (Heidelberg)

Two types of fibril compositions in ATTR amyloidosis and their correlation to clinical phenotype

E. Ihse[1], O.B. Suhr[2], C. Rapezzi[3], G. Merlini[4], M.D. Benson[5], Y. Ando[6], S-I Ikeda[7], O. Leone[8], C.C. Quarta[3], M. Lorenzini[3], L. Obici[4], F. Lavatelli[4], J. Liepnieks[5], H. Jono[6], T. Ohshima[9], M. Tasaki[6], M. Ueda[5], P. Westermark[1].

[1]Dept of Immunology, Genetics and Pathology, Uppsala University, Sweden, [2]Dept of Public Health and Clinical Medicine, Umeå University, Sweden, [3]Cardiovascular Dept, University of Bologna, Italy, [4]Amyloid Research and Treatment Center, Scientific Institute Policlinico San Matteo, University of Pavia, Italy, [5]Dept of Pathology and Laboratory Medicine, Indiana University School of Medicine and Roudebush VA medical Center, Indianapolis, IN, USA, [6]Dept of Diagnostic Medicine, Graduate School of Medical Sciences, Kumamoto University, Japan, [7]Dept of Medicine, Shinshu University, School of Medicine, Matsumoto, Japan, [8]Pathology Department, S.Orsola-Malpighi Hospital, Bologna, Italy, [9]Dept of Neurology, Graduate School of Medical Sciences, Kumamoto University, Japan

ABSTRACT

We have previously shown that amyloid fibrils in ATTRVal30Met amyloidosis can have either of two compositions, with or without truncated ATTR, and that the fibril composition type seems to be intra-individual consistent. We have also demonstrated that the fibril types are correlated to phenotypic differences found among these patients. We have now investigated the fibril composition in patients with other mutations than Val30Met in the TTR gene. The fibril type was determined by western blot for 56 patients having one of 26 different mutations. All patients, except two with TTRY114C, had fibrils with fragments. We thereby show that ATTR amyloid fibrils containing fragmented ATTR species are very common, and probably even the rule, while fibrils composed of only full-length ATTR likely is an exception. More studies focusing on the fragments and their possible role in pathogenesis are therefore needed.

INTRODUCTION

Familial ATTR amyloidosis is caused by a mutation in the transthyretin (TTR) gene. So far over a hundred different TTR mutations have been reported, and most of these render the protein more amyloidogenic [1]. The main tissue sites affected are the sensorimotor and autonomic nervous system as well as the heart, but dysfunction of other organs, like kidneys and eyes may also occur [2]. The clinical phenotype varies depending on the specific mutation, but interestingly, large variations are also found between patients carrying the same mutation [1, 3].

For most mutations, only one or a few patients or families are known, and they are scattered around the world. In contrast, relatively large amount of patients carrying the Val30Met mutation are known, and many of these patients, but not all, are found in endemic areas in Japan, Portugal and Sweden. Thus, most studies on familial ATTR amyloidosis has been carried out on this group of patients.

It has been noted that the Val30Met patients can roughly be divided into two phenotypic groups [3]. In the endemic areas in Portugal and Japan, most patients have an early onset, while many of the patients in the endemic area in Sweden, as well as patients found outside the endemic areas, have a late onset. Detailed clinicopathological investigations of the two groups have shown numerous differences in amyloid deposition sites as well as symptoms. The late onset group is for example characterized by massive myocardial amyloid deposition, leading to increased ventricular wall thickness and restrictive cardiomyopathy, while the cardiac deposits in the early onset group mainly are limited to the subendocardial layer, thereby causing conduction disturbances.

We have earlier shown that two different compositions are seen for amyloid fibrils in ATTRVal30Met amyloidosis patients; in some individuals the tissue contained large amounts of N-terminally truncated ATTR in addition to the full-length protein (denominated fibril type A) while in others only full-length ATTR were found (denominated fibril type B) (Figure 1A) [4]. From our study, as well as a recent report from Japan [T. Oshima, unpublished], it seems likely that the fibril type is intra-individual, so that the same fibril type is consistently found in different organs for each patient. We have also shown that the presence of two fibril compositions offers an explanation for the two phenotypic groups, as they are strongly correlated, with fibril type A found in patients with late onset and cardiac enlargement and fibril type B found in early onset patients without cardiac enlargement (Figure 1B) [5]. The fibril types also seem to differ in propensity to incorporate wtTTR, which likely is important for the outcome after liver transplantation [6, 7].

We have now continued by investigating the fibril composition in patients suffering from ATTR amyloidosis caused by other mutations than the Val30Met mutation.

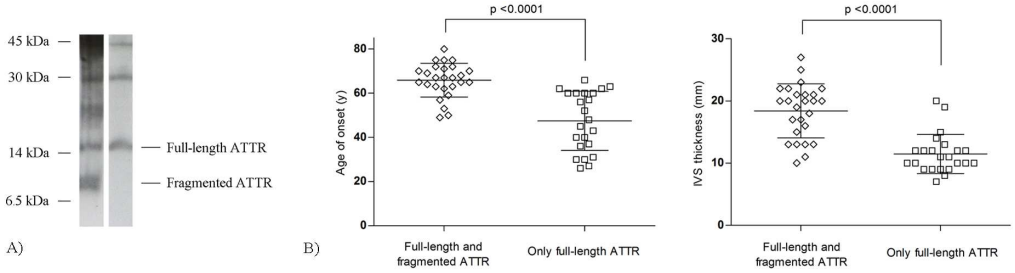

Figure 1. A) The two fibril composition types shown by western blot analysis. Left lane shows a fibril composition of type A, right lane shows type B. **B)** Correlation between fibril composition and age of onset (left graph) and thickness of the interventricular septum of the heart (right graph) in Val30Met patients.

METHODS

Fifty-six patients carrying one of 26 different mutations in the TTR gene were included. Fibril composition was determined by western blot using an in-house produced antiserum that detects C-terminal fragments. Adipose or cardiac tissue was used for the analysis.

RESULTS

All patients had a fibril composition with fragmented ATTR, except two patients, both of whom carried the TTRTyr114Cys mutation.

DISCUSSION

The fact that fragmented ATTR species can be found in large amounts in, and even be the main constituent of, amyloid fibrils in both sporadic and familial ATTR amyloidosis have been known for many years [8, 9]. Nevertheless, in most studies of today, the fragments are not considered. This is especially evident for *in vitro* studies, where almost all studies are investigating only full-length TTR. This situation is probably a consequence of a combination of two factors. Firstly, the most commonly used commercial antibodies do not recognize the fragmented ATTR species in western blot [5]. Secondly, as mentioned above, the by far most studied group of patients are those carrying the Val30Met mutation and living in endemic areas, and these patients do indeed have fibrils composed of only full-length ATTR.

From the present study, it can be concluded that a fibril composition consisting of not only full-length but also fragmented ATTR is very commonly occurring and may even be the general rule in familial ATTR amyloidosis. In a previous study, we have also shown that amyloid fibrils from patients with senile systemic amyloidosis (in which wild-type TTR is forming the deposits), have a composition with fragmented ATTR [4]. Therefore, it seems as if most studies on ATTR amyloidosis have been carried out on a patient group that may not be very representative of ATTR amyloidosis in general. It is now time to start paying attention to the fragmented species. Even though we do not know yet if they are part of the pathogenesis, we do know that they have diagnostic value, as they are correlated to clinical phenotype.

REFERENCES

1. Connors LH, Lim A, Prokaeva T, Roskens VA, Costello CE. Tabulation of human transthyretin (TTR) variants, 2003. Amyloid. 2003; 10: 160-84
2. Ando Y, Nakamura M, Araki S. Transthyretin-related familial amyloidotic polyneuropathy. Arch Neurol. 2005; 62: 1057-62
3. Koike H, Misu K, Ikeda S, Ando Y, Nakazato M, Ando E*, et al.* Type I (transthyretin Met30) familial amyloid polyneuropathy in Japan: early- vs late-onset form. Arch Neurol. 2002; 59: 1771-6
4. Bergström J, Gustavsson Å, Hellman U, Sletten K, Murphy CL, Weiss DT*, et al.* Amyloid deposits in transthyretin-derived amyloidosis: cleaved transthyretin is associated with distinct amyloid morphology. J Pathol. 2005; 206: 224-32
5. Ihse E, Ybo A, Suhr O, Lindqvist P, Backman C, Westermark P. Amyloid fibril composition is related to the phenotype of hereditary transthyretin V30M amyloidosis. J Pathol. 2008; 216: 253-61

6. Ihse E, Suhr OB, Hellman U, Westermark P. Variation in amount of wild-type transthyretin in different fibril and tissue types in ATTR amyloidosis. J Mol Med. 2011; 89: 171-80
7. Gustafsson S, Ihse E, Henein MY, Westermark P, Lindqvist P, Suhr OB. Amyloid fibril composition as a predictor of development of cardiomyopathy after liver transplantation for hereditary transthyretin amyloidosis. Transplantation. 2012; 93: 1017-23
8. Westermark P, Sletten K, Johansson B, Cornwell III GG. Fibril in senile systemic amyloidosis is derived from normal transthyretin. Proc Natl Acad Sci USA. 1990; 87: 2843-5
9. Pras M, Prelli F, Franklin EC, Frangione B. Primary structure of an amyloid prealbumin variant in familial polyneuropathy of Jewish origin. Proc Natl Acad Sci USA. 1983; 80: 539-42

Molecular Mechanisms of β_2-Microglobulin Amyloid Fibril Formation

D. Ozawa, K. Hasegawa, T. Ookoshi, H. Naiki

Department of Pathological Sciences, Faculty of Medical Sciences, University of Fukui, Japan

Recently, the relationship between various amyloidoses and chaperones is gathering attention. In patients with dialysis-related amyloidosis, α_2-macroglobulin (α2M), an extracellular chaperone found in β_2-microglobulin (β2-m) amyloid deposits, forms a complex with β2-m in the blood, but the molecular mechanisms and biological implications of the complex formation remain unclear. Here, we found that α2M inhibited the β2-m fibril formation at a neutral pH in the presence of sodium dodecyl sulfate (SDS), a model for anionic lipids. Intriguingly, SDS dissociated tetrameric α2M into dimers with increased surface hydrophobicity and both tetrameric and dimeric α2M interacted with SDS-denatured β2-m. At a physiologically relevant acidic pH and in the presence of heparin, α2M was also dissociated into dimers, and both tetrameric and dimeric α2M interacted with β2-m, resulting in the fibril growth inhibition. These results suggest that both tetrameric and dimeric α2M may play an important role in controlling β2-m amyloid fibril formation.

INTRODUCTION

We previously developed the thioflavine-T (ThT) method (1) and established a nucleation-dependent polymerization model of amyloid fibril formation (2). β2-m is a major component of amyloid fibrils deposited in dialysis-related amyloidosis. The β2-m amyloid fibril formation is thought to be induced by partial unfolding of β2-m. We found that β2-m amyloid fibrils are formed at a neutral pH in the presence of SDS (3). Moreover, we proposed that in β2-m-related amyloidosis, many amyloid-associated molecules including glycosaminoglycans, proteoglycans and lipids partially unfold β2-m, catalyze its subsequent nucleus formation and stabilize the β2-m fibrils formed (2). Although many groups have proposed the mechanisms by which β2-m amyloid fibrils are formed under physiological conditions, the biological machineries to inhibit the β2-m amyloid fibril formation are poorly understood.

α2M is an abundantly secreted glycoprotein present in human plasma and is a homotetramer that is formed by non-covalent association of two disulfide-bonded dimers. α2M has been found to be associated with extracellular amyloid deposits in various amyloidoses (4). Recently, α2M has been shown to inhibit the amyloid fibril formation and amorphous aggregation of various proteins and has been described as an extracellular chaperone (5). In patients with dialysis-related amyloidosis, α2M is identified in the amyloid deposits (6) and forms a complex with β2-m in the blood (7). However, it is unclear whether α2M affects the β2-m amyloid fibril

formation. In this study, we first examined the effect of α2M on the formation of β2-m amyloid fibrils. We next assessed the interaction of α2M with β2-m. Our results provide new insights into the effect of α2M on β2-m amyloid fibril formation and the mechanism of α2M-β2-m interaction.

METHODS

Seed β2-m amyloid fibrils used for the growth reaction were prepared from the patient-derived β2-m amyloid fibrils by the repeated growth reaction at pH 7.5 with recombinant human β2-m. Seeds were prepared by sonication of the amyloid fibrils. The seed-dependent growth reaction mixture containing 30 μg/ml seeds, 25 μM β2-m, 0-25 μM α2M or bovine serum albumin, 50 mM phosphate buffer (pH 6.3 or 7.5), 100 mM NaCl, 0.5 mM SDS or 100 μg/ml heparin, and 0.05% NaN_3 was incubated at 37 °C with or without agitation. Amyloid fibril formation was monitored by ThT method and transmission electron microscopy (8). α2M-β2-m interaction was monitored by enzyme-linked immunosorbent assay, analytical ultracentrifugation and Western blotting (8).

RESULTS

First, we examined the effect of α2M on the seed-dependent growth of β2-m amyloid fibrils at pH 7.5 monitored by ThT fluorescence assay (Figure 1). In the absence of α2M, ThT fluorescence increased without a lag phase. In the presence of α2M at molar ratios of 1:200-1:20 to β2-m, a concentration-dependent inhibitory effect was observed. Next, to assess quantitatively the binding of β2-m to α2M, we performed enzyme-linked immunosorbent assay. The binding affinity between α2M and β2-m in the presence of SDS was higher than that without SDS. Analytical ultracentrifugation and Western blotting revealed that SDS dissociated tetrameric α2M into dimers with increased surface hydrophobicity and both tetrameric and dimeric α2M interacted with SDS-denatured β2-m. At a physiologically relevant acidic pH and in the presence of heparin, α2M was also dissociated into dimers, and both tetrameric and dimeric α2M interacted with β2-m, resulting in the fibril growth inhibition.

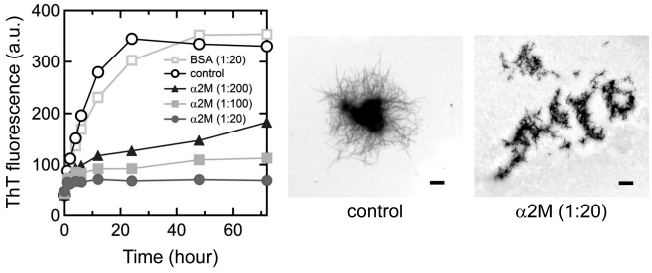

Figure 1. Effect of α2M on the seed-dependent growth of β2-m amyloid fibrils.

DISCUSSION

We revealed that α2M inhibits the β2-m amyloid fibril formation. Moreover, we demonstrated that tetrameric and dimeric α2M interact with SDS-denatured β2-m. Under conditions where native β2-m is denatured, tetrameric α2M is converted to dimers to favor the hydrophobic interaction with denatured β2-m with exposed hydrophobic

surfaces. These results suggest that α2M plays an important role in controlling the abnormal aggregation of unfolded proteins in the extracellular space (Figure 2). Further understanding of the function of α2M may help the development of the therapeutics and prophylaxis of dialysis-related amyloidosis and other protein deposition diseases.

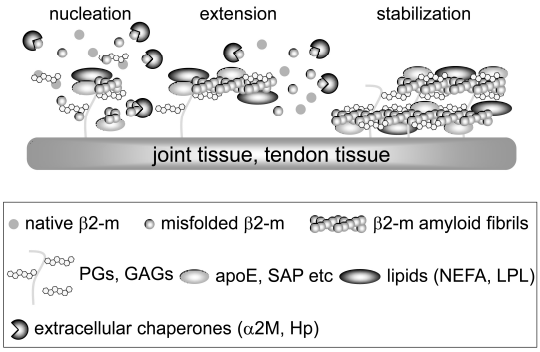

Figure 2. A model for the molecular mechanism of β2-m amyloid fibril formation *in vivo*.

ACKNOWLEDGEMENTS

We thank Professor Y. Goto, Osaka University for helpful discussion.

REFERENCES

1. Naiki H, Higuchi K, Hosokawa M, Takeda T. Fluorometric determination of amyloid fibrils in vitro using the fluorescent dye, thioflavin T1. Anal Biochem 1989;177:244-249.
2. Naiki H, Nagai Y. Molecular pathogenesis of protein misfolding diseases: pathological molecular environments versus quality control systems against misfolded proteins. J Biochem 2009;146:751-756.
3. Yamamoto S, Hasegawa K, Yamaguchi I, Tsutsumi S, Kardos J, Goto Y, Gejyo F, Naiki H. Low concentrations of sodium dodecyl sulfate induce the extension of β_2-microglobulin-related amyloid fibrils at a neutral pH. Biochemistry 2004;43:11075-11082.
4. Wilson MR, Yerbury JJ, Poon S. Potential roles of abundant extracellular chaperones in the control of amyloid formation and toxicity. Mol Biosyst 2008;4:42-52.
5. Yerbury JJ, Kumita JR, Meehan S, Dobson CM, Wilson MR. α_2-Macroglobulin and haptoglobin suppress amyloid formation by interacting with prefibrillar protein species. J Biol Chem 2009;284:4246-4254.
6. Argiles A, Mourad G, Axelrud-Cavadore C, Watrin A, Mion C, Cavadore JC. High-molecular-mass proteins in haemodialysis-associated amyloidosis. Clin Sci 1989;76:547-552.
7. Motomiya Y, Ando Y, Haraoka K, Sun X, Iwamoto H, Uchimura T, Maruyama I. Circulating level of α_2-macroglobulin-β_2-microglobulin complex in hemodialysis patients. Kidney Int 2003;64:2244-2252.
8. Ozawa D, Hasegawa K, Lee YH, Sakurai K, Yanagi K, Ookoshi T, Goto Y, Naiki H. Inhibition of β_2-microglobulin amyloid fibril formation by α_2-macroglobulin. J Biol Chem 2011;286:9668-9676.

Atomic Structure of a Nanobody Trapped Domain Swapped Dimer of an Amyloidogenic β2-microglobulin Variant

K. Domanska[1,2], S. Vanderhaegen[1,2], V. Srinivasan[1,2], E. Pardon[1,2], F. Dupeux[3], J.A. Marquez[3], R. Porcari[4], S. Gorgetti[4], M. Stoppini[4], L. Wyns [1,2], V. Bellotti[4,5] & J. Steyaert[1,2]

[1]Department of Molecular and Cellular Interactions, VIB, Pleinlaan 2, B-1050 Brussels, Belgium
[2]Department of Structural Biology Brussels, Vrije Universiteit Brussel, Pleinlaan 2, B-1050 Brussels, Belgium
[3]Grenoble Outstation, European Molecular Biology Laboratory and Unit of Virus Host-Cell Interactions, UJF-EMBL-CNRS, 6 rue Jules Horowitz, BP181, 38042 Grenoble Cedex 9, France
[4]Department of Molecular Medicine, Institute of Biochemistry, University of Pavia, via Taramelli 3b, Pavia, Italy;
[5]Centre for Amyloidosis & Acute Phase Proteins Division of Medicine, Royal Free Campus University College London Rowland Hill Street, London NW3 2PF, UK

Atomic-level structural investigation of the key conformational intermediates of amyloidogenesis remains a challenge. Here we demonstrate the utility of nanobodies to trap and characterize intermediates of β2-microglobulin (β2m) amyloidogenesis by X-ray crystallography. For this purpose, we selected five single domain antibodies that block the fibrillogenesis of a proteolytic amyloidogenic fragment of β2m (ΔN6β2m). The crystal structure of ΔN6β2m in complex with one of these nanobodies (Nb24) identifies domain swapping as a plausible mechanism of self-association of this amyloidogenic protein. In the swapped dimer, two extended hinge loops – corresponding to the heptapeptide NHVTLSQ that forms amyloid in isolation – are unmasked and fold into a new two-stranded antiparallel β-sheet. The β-strands of this sheet are prone to self-associate and stack perpendicular to the direction of the strands to build large intermolecular β-sheets that run parallel to the axis of growing oligomers, providing an elongation mechanism by self-templated growth.

INTRODUCTION

The autoaggregation process of amyloidogenic proteins may be described as a dynamic equilibrium between diverse structural species that occurs in very uneven amounts and time frames. Fibril formation *in vivo* usually takes several years, and the intermediate species are short living and highly unstable. The identification and characterization of oligomers preceding the formation of fibrils is of particular interest because of an increasing awareness that these species are likely to play a critical role in the pathogenesis of protein deposition diseases (1). Here we demonstrate the utility of camelid heavy chain antibodies (nanobodies/Nb) consisting of a single domain for the structural investigation of prefibrillar intermediates of β2-microglobulin (β2m) amyloidosis (2). In patients suffering from renal failure, the β2m concentration increases up to 60-fold leading to the formation of

insoluble amyloid fibrils causing dialysis-related amyloidosis (DRA) (3). In amyloid deposits extracted from DRA patients, up to 25–30% of the constituting β2m corresponds to a truncated isoform lacking the six N-terminal amino acids (ΔN6β2m). This isoform has a higher tendency to self-associate in vitro than the intact protein, and unlike wild-type β2m, is able to form amyloid fibrils at physiological pH.(4).. In this study, we selected nanobodies that block the fibrillogenesis of ΔN6β2m. We found that one nanobody traps a domain-swapped dimer of ΔN6β2m in the crystal, that shows several properties ascribable to prefibrillar intermediates of β2m fibrillogenesis, providing previously undescribed insights in this process with implications for DRA.

RESULTS

NANOBODIES EFFICIENTLY BLOCK β2m FIBRILLOGENESIS.

Camel and llamas immunized with β2m and ΔN6β2m in order to generate antibodies able to stabilize early intermediates along the pathway of β2m fibrillogenesis. We have then selected eight nanobodies with K_D in the nanomolar to micromolar range for β2m and ΔN6β2m variants. Nbs were tested as inhibitors of ΔN6β2m fibrillogenesis by incubating ΔN6β2m in the presence or absence of an equimolar amount of each nanobody. Fibrillogenesis was monitored by measuring the increase of the thioflavin T (ThT) fluorescence, by Electron Microscopy (EM) imaging, and by SDS-PAGE (Fig. 1).

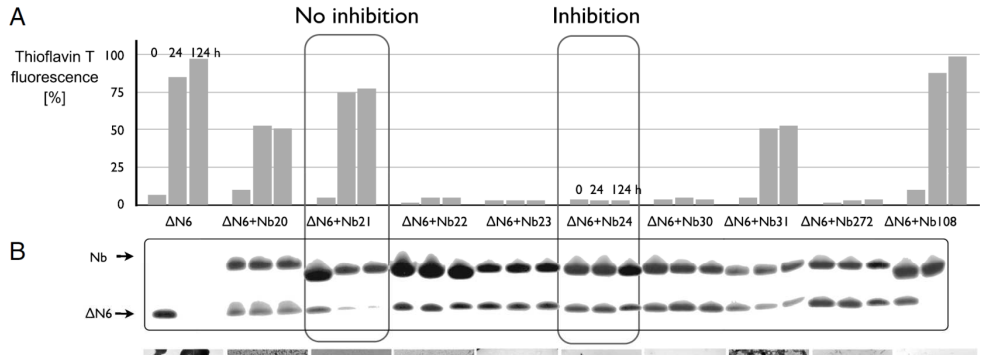

	Nb20	Nb21	Nb22	Nb23	Nb24	Nb30	Nb31	Nb272
K_D [nM] for β2m	24	130	269	50	58	1,6	6,8	129
K_D [nM] for ΔN6β2m	35	1500	330	54	44	6,7	8,4	72

Figure 1. The effect of Nbs on ΔN6ß2m fibrillogenesis. **(A):** Fibril growth kinetics were monitored by measuring the increase in ThT fluorescence. Nb108 is a β2m-unrelated nanobody used as negative control. **(B):** To visualize remaining soluble protein, samples were centrifuged and their supernatant was analyzed by SDS-PAGE. **(C):** EM images of the samples after 124 hours of incubation. **(D):** Affinities of nanobodies for β2m and ΔN6β2m as measured by Surface Plasmon Resonance.(5)

CHAPERONE-ASSISTED CRYSTALLIZATION OF ΔN6β2m

Five nanobodies, able to inhibit β2m fibrillogenesis, were tested as cocrystallization chaperones of prefibrillar intermediates. Despite extensive screening, diffracting crystals were obtained only from ΔN6β2m-Nb24 complex with the hanging drop vapor diffusion method. Low temperature X-ray diffraction data of the crystallized ΔN6β2m-Nb24 complex extended to 2.2Å resolution. The coordinates of full-length monomeric β2m (1BMG) were used as a search model to solve the crystal structure of ΔN6β2m by molecular replacement. The crystal structure of ΔN6β2m-Nb24 complex reveals that ΔN6β2m exchanged identical subdomains between two monomers to form a 3D swapped dimer (Fig 2A). Each domain is composed of six β-strands contributed by one subunit and one swapped C-terminal β-strand (strand G: residues 91–94, β2m numbering) contributed by the other (Fig. 2B). The short NHVTLSQ peptide (residues 83–89) serves as the hinge loop. In the monomer, the closed conformation of the hinge loop connects strands F and G. In the domain-swapped dimer the hinge adopts an extended conformation, lengthening the F strand by four amino acids (Fig. 2B).

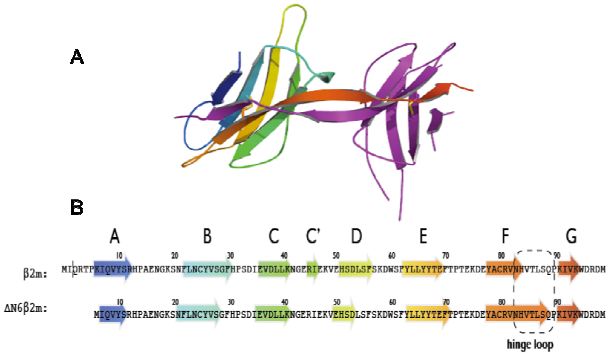

Figure 2. (A) Focus on the domain-swapped dimer of ΔN6β2m. **(B)** Sequences and topology diagrams of β2m and domain-swapped ΔN6β2m. The hinge loop is included in dashed boxes.(5)

DISCUSSION

In this study we have trapped and characterized the structure of the amyloidogenic β2m variant ΔN6β2m. Its crystal structure in complex with Nb24 identifies a swapped dimer as a plausible structural nucleus that may serve as a mold for the self-templated growth of β2m fibrils. We speculate that the self-association of two β2m monomers by domain swapping generates a dimeric intermediate with an exposed stacking prone antiparallel β-sheet. The domain-swapped dimer serves as a structural nucleus for intermolecular β-sheets that run parallel to the axis of the growing oligomer. Within the oligomer, a transition from stacked dimers to a runaway domain-swapped oligomer can lead to open ended protofibrils that grow by binding open monomers.

Our data demonstrate that Nbs are powerful tools able to inhibit the fibrillogenesis process and stabilize highly unstable protein like ΔN6β2m. These Nbs can be used as a medicament or in the prevention and/or treatment of DRA and result in being precious tools for the study of protein aggregation pathways (5).

REFERENCES

1. Chiti F, Dobson CM. Protein misfolding, functional amyloid, and human disease. Annu Rev Biochem 2006; 75:333–366.
2. Muyldermans S, Cambillau C, Wyns L. Recognition of antigens by single-domain antibody fragments: The superfluous luxury of paired domains. Trends Biochem Sci 2001; 26:230–235.
3. Floege J, Ehlerding G. Beta-2-microglobulin-associated amyloidosis. Nephron 1996;72:9–26.
4. Esposito G, et al. Removal of the N-terminal hexapeptide from human beta2-microglobulin facilitates protein aggregation and fibril formation. Protein Sci 2000;9:831–845.
5. Domanska, K., et al. Atomic Structure of a Nanobody-trapped Domain-swapped Dimer of an Amyloidogenic Beta2-microglobulin Variant. Proc Natl Acad Sci U S A. 2011;108:1314-9.

Identifying Fibrillogenic Regions of the λ6 Light Chains by Limited Proteolysis

L. Del Pozo-Yauner[1], B. Becerril-Luján[2], J. Meléndez-Zajgla[1], R. Sánchez-López[1], D. A. Fernández-Velasco[3], L. Güereca[2], M. González[1], C. Ferreira[2], E. Ortiz-Suri[2].

[1] Instituto Nacional de Medicina Genómica. México, D.F. C.P. 01900. México. ldelpozo@inmegen.gob.mx. [2] Instituto de Biotecnología, UNAM. Cuernavaca, Morelos. Apdo. Postal 510-3, México. [3] Facultad de Medicina, UNAM. Ciudad Universitaria, México, D.F., CP 04510. México.

ABSTRACT

We proposed that the abnormally high propensity of the λ6 light chains to aggregate as amyloid fibrils is driven by sequence elements that can be identified by their capacity to form amyloid-like fibril autonomously. To test this hypothesis we used limited proteolysis/MALDI-TOF analysis combined with site-directed mutagenesis and identified four fibril-forming fragments in the λ6 recombinant variable domain 6aJL2. The fibrillogenic fragments are located in CDR-1 and also in a number of β strands that are structural related to this loop in the native folding. Based on these data we propose a possible mechanism of fibrillogenesis for the variable domain of the light chains.

INTRODUCTION

Light chain derived (AL) amyloidosis is a misfolding disease characterized by the extracellular deposition of a monoclonal free light chain in form of insoluble fibrillar aggregates. Due to its systemic nature, the clinical picture of AL amyloidosis is dominated by the signs and symptoms of dysfunction of the organs targeted by the deposits, being the heart, kidneys, liver, digestive tract, and peripheral nervous system the most frequently affected. Despite the substantial advances in diagnosis and therapeutic management made during the last decade, AL amyloidosis remains as an incurable disease with a poor prognosis. Changing this tendency will require the development of more effective therapies based on new principles, a goal that will be greatly facilitated by deciphering the structural factors driving the mechanism of amyloidogenesis of the light chains. [1] The particular structural features that render λ6 light chains highly amyloidogenic remain unknown. We propose that the abnormally high propensity of this family of immunoglobulins to aggregate as amyloid is driven by discrete regions of the variable domain that can be recognized by their ability to aggregate as amyloid-like fibrils autonomously. To test this hypothesis we used limited proteolysis/MALDI-TOF analysis and site-directed mutagenesis to identify fibril-forming fragments of the recombinant protein 6aJL2, a recombinant λ6 variable domain with the germline sequence of the gene segments *6a* and *jl2*.

METHODS

Six pint mutants to Asp of 6aJL2 at positions A31, S31a, N31b, Y32, V33 and Q34 were generated by conventional PCR, using mutagenic synthetic oligonucleotides. The DNA segments encoding 6aJL2 proteins and the six point-mutants were cloned in pET27b vector (Novagen, Merck-Millipore) and expressed in *E*. coli BL21(DE3). Bacterial expression and purification of the recombinant proteins 6aJL2, 6aJL2-R25G and the above mentioned single mutants were performed as describe elsewhere. [2] Proteolysis was performed with Sequencing Grade Modified Trypsin (Promega, Madinson, WI) that was added to the protein solution (3.0 mg/ml in Tris-HCl 100mM pH 8.0) with a final trypsin:protein ratio at 1:200 (w/w). The sample was incubated overnight at 37 ^{0}C without shaking. After completion of proteolysis, the mixture was subsequently incubation at 37 ℃ with constant shaking (500 rpm-Thermomixer Eppendorf Confort). After completion of fibrillogenesis, the aggregates were examined under electron microscope (E.M.) and spectroscopically characterized (ThT fluorescence, intrinsic fluorescence, and circular dichroism). The aggregates were harvested by centrifugation, washed twice in PBS and resolubilized in GdnHCl 6.0 M. The fibrillogenic peptides were purified by reverse phase high-performance liquid chromatographic (RF-HPLC) using a Vydac 218TP54 C18 analytical column. The fractions were collected manually and the identity of each peptide fragment was determined by mass spectrometry (MALDI-TOF).

Cross-seeding experiments were performed by co-incubating 6aJL2 fibrils fragmented by sonication (seed) with soluble monomers of the six point-mutants to Asp mentioned above. The monomer to seed w/w ration was 10:1. The experiment was performed according was describe previously. [3] Computational analysis of the 6aJL2 sequence to predict fibril forming segments was performed with the structure-based algorithm ZipperDB (http://services.mbi.ucla.edu/zipperdb/). [4]

RESULTS AND DISCUSSION

Proteolysis of 6aJL2 with trypsin and the subsequent overnight incubation at 37 ℃ with constant shaking ended up with the formation of aggregates having both, fibrillar morphology under the electron microscopy, and the spectroscopic characteristics of amyloids. Four fragments were isolated and identified from the aggregates. (Fig. 1) One of them was composed of two peptides -Thr18-Arg25 and Thr80-Lys103- linked by the disulfide bridge Cys23-Cys88. The other three components were peptides Ser26-Arg39, Ser26-Arg54 and Phe62-Lys79. Kinetic experiments revealed that the fastest aggregating components were peptides Ser26-Arg39 and Ser26-Arg54. Fragment Thr18-Arg25-C23-C88-Thr80-Lys103 readily formed fibrils when incubated alone, but not if previously reduced with dithiothreitol. None of the two peptides composing this fragment aggregated as fibrils when incubated separately. Peptides Ser26-Arg39 and Phe62-Lys79 did not form fibrils when incubated independently, but did aggregate as fibrils when co-incubated.

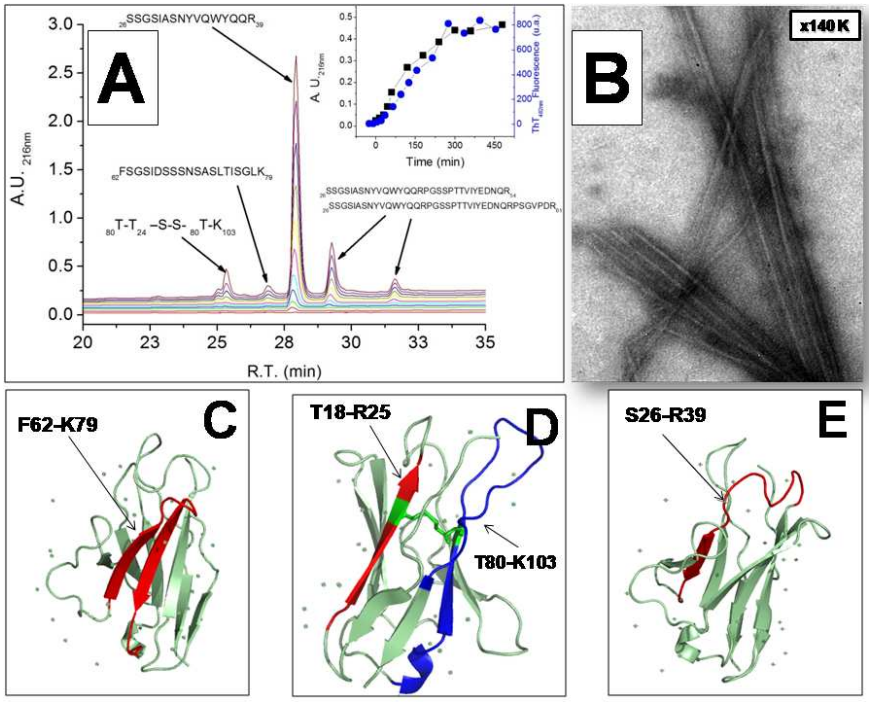

Figure 1. The extensive proteolysis of 6aJL2 protein with trypsin and the subsequent overnight incubation at 37 ℃ with constant shaking ended in fibrillar aggrega tes formation with the characteristics of amyloid. **A)** Reverse-Phase High Performance Liquid Chromatographic (RF-HPLC) analysis of the aggregates collected at different times of incubation. The inset represents the time course of: 1) ThT fluorescence intensity variation of the experimental sample [solid circles in blue color] and 2) $AU_{216\ nm}$ variation of the component with sequence $_{26}$SSGSIASNYVQWYQQR$_{39}$ [solid squares in black color]. **B)** Electron micrograph showing the fibrillar morphology of the aggregates collected at the end of the incubation. **Panels C-E.** Spatial location of the fibrillogenic fragments in the crystallographic structure of 6aJL2 (PDB ID 2W0K).

Proteolysis with trypsin of mutant 6aJL2-R25G –where Arg25 is substituted by Gly- and the subsequent incubation of the product in the conditions described above led to formation of fibrillar aggregates composed by three fragments. One of them was composed of two peptides -Thr18-Arg39 and Thr80-Lys103- linked by the disulfide bridge Cys23-Cys88. The second fragment represents a variant of the former, in which peptide Thr18-Arg54, instead of Thr18-Arg39, was the component disulfide bridged to peptide Thr80-Lys103. The third component was peptide Phe62-Lys79. When the same experiment was performed in the presence of 10 mM dithiothreitol, fibrillar aggregates with ThT-binding capacity were also recovered from the sample, being the peptides Thr18-Arg39, Thr18-Arg54 and Phe62-Lys79 the most abundant components of the aggregates. Co-incubation of the six single mutants to Asp with wild-type seed resulted in fibrillar aggregates formation, but in a quantity that varied depending of the mutated position. Proteins 6a-A31D and 6a-N31bD produced aggregates in a quantity equal to 30% and 40%, respectively, of that produced by the self-seeding of the wild-type (reference). Proteins 6a-S31aD and 6a-Q34D elongated the wild-type fibril seeds more efficiently, producing

60% and 70%, respectively, of the aggregates of the reference. Protein 6a-Y32D elongated the wild type fibril seeds as efficiently as the wild-type monomers, indicating that the Asp residue introduced at position 32 didn´t modify its fibril elongation capacity. Mutation V33D seems to have been highly destabilizing in 6aJL2, as it is suggested by the almost null bacterial expression of the mutant. The results of cross-seeding experiments suggest that some amino acids of the segment spanning from A31 to Q34 are part of the core of the 6aJL2 fibrils, or at least are structurally related to it.

The structure-based algorithm ZipperDB identified several small stretches of six amino acids in length with the suitable pattern to form steric zipper-type structures. The stretches overlap in such a way that give rise to three long hot spots. One of them spans along of edge strand B. A second hot-spot spans along the CDR-1 and the edge strand C. The third hot-spot spans from the beta strand E to the beta strand D, including the loop connecting both strands. A number of individual stretches are located dispersed along the beta strand F, CDR-3 and edge strand G.

CONCLUSION

We conclude that the lambda 6 light chains have discrete segments with the ability to form amyloid-like fibril aggregates in vitro autonomously. The experimental and theoretical data suggest the existence of at least two amyloidogenic hot-spots in the region comprising the beta strand B, the CDR1 loop and the beta strand C. Based on these data, we posit that the structural core of the AL fibril in formed mainly by the above mentioned regions of the variable domain, although other regions, as the β strand D and E could be also involved. Besides, we postulate that structural rearrangements of the N-terminal segment and the loop comprising the region Pro40-Asp60, with the subsequent solvent exposition of the amyloidogenic hot-spots identified in this study, are a key step of the mechanism of amyloid aggregation of the light chain variable domain. [3]

REFERENCES

1. Dispenzieri A, Gertz MA, Buadi F. What do I need to know about immunoglobulin light chain (AL) amyloidosis? Blood Rev. 2012; 26 (4): 137-154.
2. del Pozo Yauner L, Ortiz E, Sánchez R, Sánchez-López R, Güereca L, Murphy CL, Allen A, Wall JS, Fernández-Velasco DA, Solomon A, Becerril B. Influence of the germline sequence on the thermodynamic stability and fibrillogenicity of human lambda 6 light chains. Proteins. 2008 Aug; 72 (2): 684-689.
3. Hernández-Santoyo A, del Pozo Yauner L, Fuentes-Silva D, Ortiz E, Rudiño-Piñera E, Sánchez-López R, Horjales E, Becerril B, Rodríguez-Romero A. A single mutation at the sheet switch region results in conformational changes favoring lambda6 light-chain fibrillogenesis. J Mol Biol. 2010; 396 (2): 280-92.
4. Goldschmidt L, Teng PK, Riek R, Eisenberg D. Identifying the amylome, proteins capable of forming amyloid-like fibrils. Proc Natl Acad Sci U S A. 2010 Feb 23; 107 (8): 3487-3492.

High-resolution crystal structure of the C-terminal truncated human apoA-I sheds new light on the amyloid formation by the N-terminal fragment

O. Gursky, X. Mei, D. Atkinson

Department of Physiology & Biophysics Boston University School of Medicine, 700 Albany St. Boston MA USA

ABSTRACT

ApoA-I is the major protein of high-density lipoproteins (HDL) that remove excess cell cholesterol and prevent atherosclerosis. In hereditary amyloidosis, mutations in apoA-I residue segments 26-107 and 154-178 cause deposition of the 9-11 kDa N-terminal proteolytic fragments as fibrils in vital organs. The 2.2Å resolution X-ray crystal structure of the C-terminal-truncated human Δ(185-243)apoA-I suggests a novel mechanism for amyloidogenesis. All 19 known amyloidogenic mutations occupy key positions within the largely helical four-segment bundle (residues 1-120, 144-184). All mutations probably destabilize the bundle structure in free apoA-I, enhancing its proteolysis. Many mutations place a hydrophilic or Pro group in the hydrophobic lipid-binding α-helical face, promoting apoA-I dissociation and proteolysis. Importantly, segment L44-S55 adopts an extended β-strand-like conformation whose exposure upon bundle destabilization probably initiates α-helix-to-β-sheet conversion in amyloid. Hence, the amyloidogenic mutations probably destabilize lipid-free and HDL-bound apoA-I promoting its proteolysis, with segment L44-S55 forming a template for the cross-β-sheet conformation.

INTRODUCTION

HDL, a.k.a. “Good Cholesterol”, are nanoparticles comprised of lipids and specific proteins, mainly apolipo-protein A-I (apoA-I, 243 a. a.). HDL remove cholesterol from peripheral cells to the liver for excretion via the reverse cholesterol transport (RCT) pathway. Over 90% of plasma apoA-I circulates on HDL, yet ~5% is present in a transient monomeric lipid-poor / lipid-free form. Dissociation of lipid-poor / free apoA-I from HDL promotes HDL biogenesis and benefits RCT, yet overproduction of this labile species increases apoA-I cata-bolism. Moreover, dissociated apoA-I can misfold in amyloidosis. Hereditary apoA-I amyloidosis (AApoA-I) is an autosomal dominant disorder in which mutant apoA-I is cleaved between residues 80-110 and the N-terminal 9-11 kDa proteolytic fragments deposit as fibrils in vital organs (kidney, liver) causing organ failure (1). Little is known about the pathogenic pathway of apoA-I misfolding, from native ~80% α-helical to highly β-sheet structure in amyloid. Despite low levels of plasma HDL and apoA-I, AApoA-I patients show no increase in atherosclerosis. This suggests that: a) apoA-I and HDL remove cholesterol more efficiently in these patients which, we posit, results from HDL destabilization by apoA-I mutation; b) amyloid deposition is not due to protein

overproduction but results from the destabilization of the solution structure of mutant apoA-I (2). We take advantage of the 2.2Å resolution crystal structure of the C-terminal-truncated protein, Δ(185-243)apoA-I (3), to postulate a novel molecular mechanism of protein destabilization and misfolding in AApoA-I (4).

RESULTS AND DISCUSSION

All 19 AApoA-I mutations found in humans are clustered in two residue segments, 26-107 (inside the deposited 9-11 kDa fragment) and 154-178 (outside this fragment) (1, 2). The Δ(185-243)apoA-I crystal structure contains all 19 sites of these mutations, providing an excellent model for elucidating the structural basis for AApoA-I. By mapping the AApoA-I mutations on the crystal structure, we showed that they correspond to key positions within the four-segment bundle that was observed in the crystallographic dimer of Δ(185-243)apoA-I (Figure 1).

Each of the AApoA-I mutations disrupts the bundle packing and hence, is expected to destabilize lipid-free apoA-I monomer. Moreover, most mutations place a hydrophilic or Pro group in the hydrophobic lipid-binding face of the amphipathic α-helices in apoA-I; this is expected to destabilize HDL and shift the population distribution, from HDL-bound to lipid-poor / lipid-free apoA-I that is labile to proteolysis. The resulting 9-11 kDa N-terminal proteolytic fragments are unfolded in solution (5) since they lack at least 1.5 segments from the 4-segment bundle (Figure 2C). The unfolding of the bundle increases solvent exposure of L44-S55 groups. In the crystal structure, these groups adopt an extended β-strand-like conformation (Figure 1B, C), which is unique in this highly α-helical protein. We postulate that increased solvent exposure of L44-S55 upon destabilization of the four-segment bundle initiates α-helix to β-sheet conversion in amyloid (Figure 2C, D). This idea is further supported by the amino acid sequence analysis showing that L44-S55 is the only segment in apoA-I with high amyloidogenic propensity (http://services.mbi.ucla.edu/zipperdb/protein/21449, courtesy of Dr. Donald Puppione, UCLA) and by the recently demonstrated ability of the tryptic fragment apoA-I(46-59) to form amyloid fibrils (5).

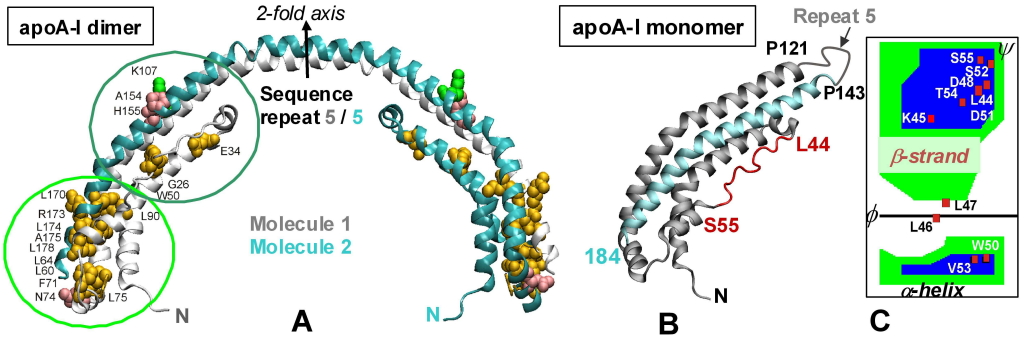

Figure 1. Crystal structure of the N-terminal-truncated human apoA-I (residues 1-184) (3) showing locations of 19 know amyloidogenic mutations (A) and L44-S55 extended segment with a β-strand-like geometry (B, C). (**A**) Amyloidogenic mutations (yellow spheres) mapped on the structure of the crystallographic dimer of Δ(185-243)apoA-I. The mutations cluster in two regions of the four-segment bundle (green circles): bottom cluster

(L60R; L64R; L60-F71 del/ 60V-61T ins; E70-W72 del; F71Y; N74K frame shift (fs); L75P; L90P; K107 del; L170P; R173P; L174S; A174S; L178H) and middle / top cluster (G26R; E34K; W50R; A145 fs; H155M fs). Based on the biochemical character and location in the structure, each mutation is expected to destabilize the four-segment bundle and thereby increase the solvent exposure of the L44-S55 segment. We postulate that a similar four-segment bundle is formed by monomeric lipid-free apoA-I in solution (**B**) via the domain swapping around the central repeat 5 (arrow) (3). L44-S55 (red) is the only extended segment in the crystal structure that adopts a non-helical conformation; its main chain ϕ / ψ angles are consistent with the β-strand-like geometry, as shown in the Ramachandran plot (**C**).

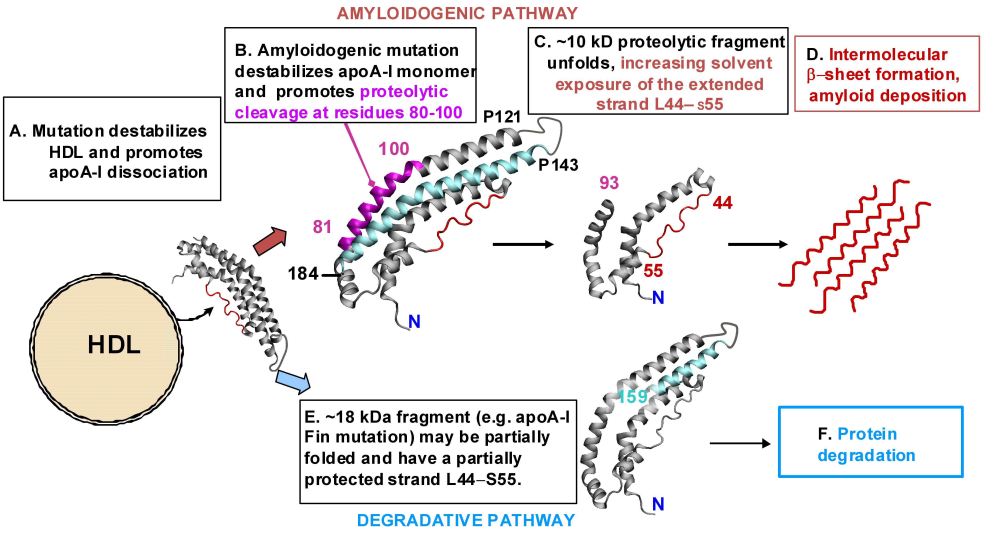

Figure 2. Hypothetical amyloidogenic and degradative pathways for *in vivo* processing of mutant apoA-I. **A**: Mutation reduces the apoA-I affinity for lipid and thereby shifts the population distribution from HDL-bound to lipid-poor / free apoA-I monomer. **B**: In the amyloidogenic pathway, the four-segment bundle in apoA-I in solution is destabilized by the mutation that disrupts the packing of repeats 2-4, including residues 81-120 (purple), rendering them labile to proteolysis. **C**: The resulting ~10 kDa proteolytic fragment is missing approximately 1.5 helical segments from the four-segment bundle and hence, is unfolded in solution (6); this increases solvent exposure of the extended strand L44-S55 (red) that is primed for the β-sheet formation. **D**: L44-S55 strands initiate intermolecular cross-β-sheet conformation in amyloid. **E**: In the degradative pathway, larger (~18 kDa) proteolytic fragment is probably at least partially folded in a bundle, which renders protection to the segment L44-S55 and thereby favors degradation (**F**) over intermolecular β-sheet formation.

REFERENCES

1. Rowczenio, D., Dogan, A., Theis, J. D., Vrana, J. A., Lachmann, H. J., Wechalekar, A. D, Gilbertson, J. A., Hunt, T., Gibbs, S. D., Sattianayagam, P. T., Pinney, J. H., Hawkins, P. N., and Gillmore, J. D. (2011)

Amyloidogenicity and clinical phenotype associated with five novel mutations in apolipoprotein A-I. *Am. J. Pathol. 179(4),* 1978-1987.

2. Obici, L., Franceschini, G., Calabresi, L., Giorgetti, S., Stoppini, M., Merlini, G., and Bellotti, V. (2006) Structure, function and amyloidogenic propensity of apolipoprotein A-I. *Amyloid 13(4),* 191-205.
3. Mei, X. and Atkinson, D. (2011) Crystal structure of C-terminal truncated apolipoprotein A-I reveals the assembly of HDL by dimerization. *J. Biol. Chem. 286(44),* 38570-38582.
4. Gursky O., Mei X., and Atkinson D. (2012) Crystal structure of the C-terminal truncated apolipoprotein A-I sheds new light on the amyloid formation by the N-terminal segment. *Biochemistry 51(1)*, 10-18.
5. Wong, Y. Q., Binger, K. J., Howlett, G. J., and Griffin, M. D. (2012) Identification of an amyloid fibril forming peptide comprising residues 46-59 of apolipoprotein A-I. *FEBS Lett. 586(13),* 1754-1758.
6. Raimondi, S., Guglielmi, F., Giorgetti, S., et al. (2011) Effects of the known pathogenic mutations on the aggregation pathway of the amyloidogenic peptide of apolipoprotein A-I. *J. Mol. Biol. 407(3),* 465-476.

Interaction studies of amyloid-β peptide with ionic fluorinated amphiphiles

Joana A. Loureiro, Sandra Rocha, Maria do Carmo Pereira

LEPAE, Department of Chemical Engineering, Faculty of Engineering, University of Porto
Rua Dr. Roberto Frias, 4200-465 Porto, Portugal

Amyloid-beta peptide (Aβ) is the major constituent of Alzheimer's disease plaques, which deposit in the brain extracellularly resulting in neuronal loss. The studies of Aβ interaction with different amphiphile molecules are important to better understand the alterations and aggregation process of the peptide. They will also contribute to screen for molecules that can inhibit amyloid fibril formation. Fluoroorganic compounds are of big interest in medical applications due to the unique properties of the fluorine atom. In this study, $A\beta_{(1-42)}$ was incubated with micelles of perfluorooctanoic acid (PFOA), an anionic fluorinated amphiphile. The results were compared with the study of $A\beta_{(1-42)}$ aggregation in the presence of anionic micelles and non-ionic micelles, sodium dodecyl sulfate (SDS) and octyl β-D-glucopyranoside (OG), respectively. The results demonstrated that the charge of the micelles can significantly influence the aggregation of $A\beta_{(1-42)}$.

INTRODUCTION

Aβ peptide forms a large amount of extracellular deposits and several scientists believe that the aggregation of this peptide is the primary cause driving Alzheimer's disease (1). The most abundant forms of the peptide have 40 and 42 amino acids (2). The sequence of 42 amino acids is the major component of amyloid plaque core deposits. The aggregation of Aβ can be affected by various factors as for example solvent hydrophobicity, pH, peptide concentration, temperature, ionic strength, metal ions and type of micelle interactions. Physiological Aβ in monomeric form is benign, but its aggregated forms, particularly the oligomeric species, are neurotoxic (3). The studies of Aβ interaction with different amphiphile molecules are important to better understand the aggregation process of Aβ. In this work, the interaction of the anionic fluorinated surfactant PFOA with $A\beta_{(1-42)}$ is described. This surfactant was chosen because fluoroorganic compounds have unique properties that make them suitable for biomedical applications. Fluor increases the chemical stability and the bioavailability of molecules, and modulates their physicochemical properties such as lipophilicity or basicity (4). Few fluorinated compounds have already been studied in regard to protein misfolding and organofluorine compounds were established as effective inhibitors of $A\beta_{(1-40)}$ fibrillogenesis (5).

METHODS

$A\beta_{42}$ (amyloid-β peptide 1-42, purity > 95%, MW 4514.14, Selleck Chemicals) was dissolved in HFIP

(1,1,1,3,3,3-hexafluoro-2-propanol, ≥ 99.8%, Sigma-Aldrich) at 1 mg/mL. The solvent was then evaporated and the peptide film was dissolved in DMSO (dimethyl sulfoxide for molecular biology, 99,9%, Sigma-Aldrich) at 9 mg/mL. PFOA (perfluorooctanoic acid, 96%, Sigma-Aldrich), SDS (sodium dodecyl sulfate, ≥ 98.5%, Sigma-Aldrich) and OG (octyl β-D-glucopyranoside, ≥ 98%, Sigma-Aldrich) were prepared in Hepes buffer 10 mM, pH 7.4 (HEPES hemisodium salt, ≥ 99%, Sigma-Aldrich). Aβ peptide (100 μM) was incubated at 37ºC with PFOA, SDS and OG for 6 days and the samples were analyzed by transmission electron microscopy (TEM), using uranyl acetate (2%) as negative staining, and by thioflavin T (ThT) binding assay. An aliquot of 25 μL of each sample was mixed with 175 μL of filtered ThT 50 μM solution and the fluorescence was measured using a Perkin Elmer LS 50B fluorescence spectrometer.

RESULTS

The aggregation of $A\beta_{(1-42)}$ was studied in the presence of PFOA above its critical micelle concentration (CMC). The CMC of PFOA in 10 mM Hepes buffer is 12.2 mM (6). TEM analysis demonstrated that $A\beta_{(1-42)}$ aggregates into amyloid fibrils in the presence of 18.8 mM of PFOA, similarly to what is observed for the peptide incubated alone (Figure 1).

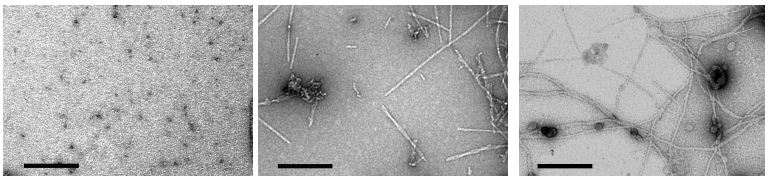

Figure 1. TEM images of $A\beta_{(1–42)}$ incubated at 37ºC. A) $A\beta_{(1–42)}$ alone at 0 hours; B) $A\beta_{(1–42)}$ alone after 6 days; C) $A\beta_{(1–42)}$ with PFOA (18.8 mM) after 6 days. The scale bar corresponds to 200 nm.

A significant binding to ThT is observed for $A\beta_{(1-42)}$ incubated alone at 37ºC for 6 days (Figure 2). The mixture of $A\beta_{(1-42)}$ and PFOA shows an increase of the ThT fluorescence intensity. This means that the presence of PFOA micelles accelerates the $A\beta_{(1-42)}$ aggregation (Figure 2).

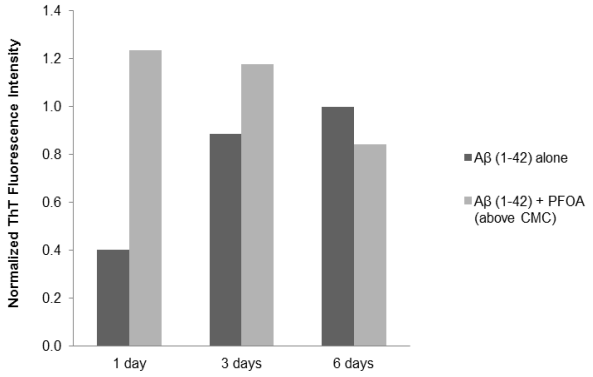

Figure 2. Effect of PFOA micelles on $A\beta_{(1–42)}$ fibril content as monitored by ThT fluorescence at 37ºC.

For comparison, the aggregation of $A\beta_{(1-42)}$ was also studied in solutions of other anionic micelles (SDS) and non-ionic micelles (OG). TEM analysis demonstrated that SDS retards or even inhibits the aggregation of the peptide. OG, on the other hand, leads to the formation of $A\beta_{(1-42)}$ amyloid fibrils (Figure 3).

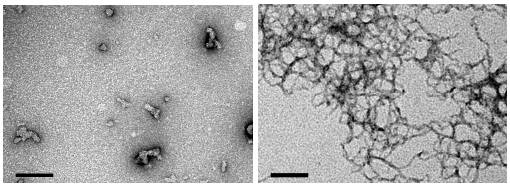

Figure 3. TEM images of $A\beta_{(1–42)}$ incubated with micelles at 37ºC for 6 days. A) $A\beta_{(1–42)}$ with SDS (14.0 mM); B) $A\beta_{(1–42)}$ with OG (28.8 mM). The scale bar corresponds to 200 nm.

DISCUSSION

Anionic SDS micelles inhibit the aggregation of $A\beta_{(1–42)}$ peptide. The surfactant micelles interact with $A\beta_{(1-42)}$ through electrostatic interactions and the surrounding micelles induce an electrostatic repulsion between the peptide molecules. OG and PFOA are not able of inhibiting the structural changes and aggregation of the peptide. Uncharged micelles cannot prevent the peptide-peptide ion-pairing interactions. In the case of the fluorinated anionic micelles, these interactions could also not be prevented, as PFOA is a weak acid. As in this study, a previous work with $A\beta_{(1-28)}$ and charged surfactants demonstrated that the inhibition of amyloid fibril formation is highly dependent on the surface charge of micelles (7).

ACKNOWLEDGMENTS

This work was financed by FCT Research Project PTDC/QUI-BIQ/102827/2008.

REFERENCES

1. Hardy J, Selkoe DJ. The amyloid hypothesis of Alzheimer's disease: progress and problems on the road to therapeutics. Science. 2002 Jul 19; 297 (5580): 353-6.
2. Barrow CJ, Zagorski MG. Solution structures of beta peptide and its constituent fragments: relation to amyloid deposition. Science. 1991 Jul 12; 253 (5016): 179-82.
3. Lorenzo A, Yankner BA. Beta-Amyloid Neurotoxicity Requires Fibril Formation and Is Inhibited by Congo Red. Proceedings of the National Academy of Sciences of the United States of America. 1994 Dec 6; 91 (25): 12243-7.
4. Bohm HJ, Banner D, Bendels S, Kansy M, Kuhn B, Muller K, et al. Fluorine in medicinal chemistry. Chembiochem. 2004 May 3; 5 (5): 637-43.
5. Saraiva AM, Cardoso I, Pereira MC, Coelho MA, Saraiva MJ, Mohwald H, et al. Controlling amyloid-beta peptide(1-42) oligomerization and toxicity by fluorinated nanoparticles. Chembiochem. 2010 Sep 3; 11 (13): 1905-13.
6. Rocha S, Loureiro JA, Brezesinski G, Pereira M C. Peptide-surfactant interactions: consequences for the amyloid-beta structure. Biochem Biophys Res Commun. 2012 Mar 30; 420 (1): 136-40.

7. Marcinowski KJ, Shao H, Clancy EL, Zagorski MG. Solution structure model of residues 1-28 of the amyloid beta peptide when bound to micelles. J Am Chem Soc. 1998 Nov 4; 120 (43): 11082-91.

The crystal structure of the calcium-free Serum Amyloid P-component decamer

Alun R. Coker[1], Shu-Fen Coker[1], Rebecca Coker[1], Valerie Pye[2], Mark B. Pepys[1] & Steve Wood[1]

[1] Wolfson Drug Discovery Unit, Centre for Amyloidosis and Acute Phase Proteins, UCL Medical School (Royal Free Campus), Roland Hill, Street, London, NW3 2PF.
[2] School of Biochemistry & Immunology, Trinity Biomedical Sciences Institute, Trinity College Dublin, Pearse Street, Dublin 2, IRELAND.

ABSTRACT

Amyloidosis is a protein misfolding disease characterised by the extracellular deposition of insoluble fibres. Serum amyloid P component (SAP) is a disc shaped plasma protein universally associated with amyloid deposits; it has a potent molecular chaperone activity and has been reported to both inhibit and promote fibrillogenesis depending upon its oligomeric state. *In vivo* – in the presence of calcium ions – SAP exists as a pentamer, but in the absence of calcium ions it forms a stable decamer. Here we report the X-ray structure of the SAP decamer which shows that the two pentamers stack B-face to B-face. This suggests that these two activities reside on opposing faces of the structure. Using an insulin fibrillation assay we have confirmed the previous observations that the SAP decamer inhibits fibrillogenesis and that the SAP pentamer promotes it.

INTRODUCTION

All amyloid deposits contain significant quantities of serum amyloid P-component (SAP); it stabilises amyloid fibres *in vitro* and contributes to amyloidogenesis *in vivo* (1). SAP is a homo-pentameric protein with five Mr 25,462 protomers assembled non-covalently with cyclic symmetry in a disc with two planar faces (2). The B (binding) face carries a double calcium binding-site on each subunit through which SAP interacts with amyloid fibres. The opposite, A-face, bears five prominent α-helices.

In the absence of calcium, human SAP forms stable decamers composed of pairs of SAP pentamers. This is not the *in vivo* form, but calcium-free SAP has often been used in *in vitro* experiments to circumvent the auto-aggregation of SAP that occurs *in vitro* in the presence of calcium ions. Janciauskiene demonstrated that calcium-free SAP could prevent the Alzheimer's peptide Aβ 1-42 forming fibers (3), whereas Hamazaki demonstrated that in the presence of calcium SAP promotes Aβ aggregation (4).

We have previously reported that SAP has molecular chaperone activity *in vitro*; enhancing the regain of enzymatic activity of chemically denatured LDH on dilution of the denaturant and protecting the native enzyme from agitation-induced denaturation (5). These effects were observed in both the presence and absence of calcium and were not inhibited by small molecule ligands for SAP that block the amyloid recognition site.

METHODS

SAP was purified by previously published procedures (6) and concentrated to 10mg/ml in 10mMTris/HCl buffer containing 140mM sodium chloride and 5mM EDTA. Crystals were grown at 4^{o}C by the hanging drop method in 50mM MES pH5.5, 12% PEG 4000 and 6% isopropyl alcohol. Crystals were vitrified by transfer to a 50:50 mixture of Paratone-N and paraffin oil prior to rapid immersion in liquid ethane. X-ray data was collected at the ESRF. The data were indexed, integrated and scaled with XDS and XSCALE (7). Structure determination was carried out using the CCP4 suite of programmes (8).

Insulin fibrillogenesis was initiated by continual inversion of zinc free insulin (1 mg/ml) solutions on a revolving tube mixer. Thioflavin-T fluorescence spectra were measured (excitation wavelength 442 nm) after six days to quantify the relative amounts of cross-β fibres according to published methods (9). Fibrillogenesis experiments in calcium free conditions were conducted in 20mM TRIS pH 8,150mM NaCl, 0.1% NaN_3. Fibrillogenesis experiments with calcium ions were conducted in 20mM TRIS pH 8, 600mM NaCl, 2mM $CaCl_2$, 0.1% NaN_3, in order to avoid auto-aggregation of SAP (0.2 mg/ml).

RESULTS

The crystal structure shows a decamer with two pentameric rings stacked B-face to B-face (figure 1.). No calcium ions are present and a loop comprising of residues 134-150, which is normally stabilised by calcium ions, is displaced and binds in the grove between two subunits on the opposite ring, stabilising the decamer.

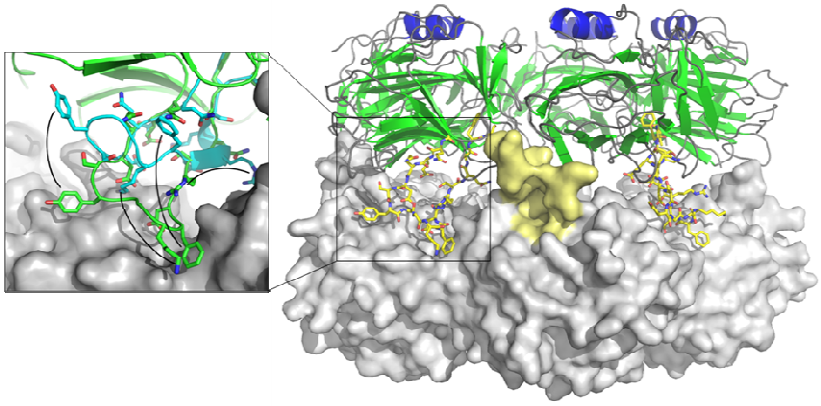

Figure 1. The calcium free SAP decamer viewed from the side to show the stacking of the two pentamers. The upper pentamer is shown as a cartoon illustrating the secondary structure elements; the molecular surface of the lower pentamer is shown in white. Residues 134-151 of each subunit (coloured yellow) are displaced from the B-face and bind in a grove between two subunits on the opposite ring. The inset shows the detail of the loop movement. The position of the loop in the native pentamer is shown in blue and its position in the calcium free decamer is shown in green. Curved black lines are drawn between equivalent residues in each loop.

Electron density for this loop is complete in four of the ten subunits and the two rings are slightly tilted with respect to each other, suggesting a high degree of conformational flexibility.

In the light of the decamer structure we have revisited the effect of SAP on amyloidogenesis. We used an insulin fibrillation assay that we have developed and monitored the quantity of fibres formed using Thioflavin-T fluorescence. In the presence of calcium, SAP pentamers increased fibrillation by 52%, but in the absence of calcium ions, the SAP decamer reduced fibrillation by 55%

DISCUSSION

The calcium-free SAP decamer was previously assumed to be an A-face to A-face decamer (10). This caused difficulty in the interpretation of our observation that the chaperone activity of SAP is independent of calcium. The crystal structure of calcium-free SAP presented here shows a B-face-to-B-face decamer with the protease sensitive loops from the calcium-binding site extended to clasp the opposite pentamer.

Although the calcium-free decamer is not physiological, it allows us to separate the chaperone activity from the pro-fibrillation and fibril binding activity on the B-face – which is obscured in the decamer. In its native pentameric form both activities will be present. SAP is therefore an extracellular chaperone with two distinct chaperone activities; the chaperone activity seen in the decamer and a pro-fibrillation activity associated with the calcium binding site.

ACKNOWLEDGEMENTS

This work was funded in part by a studentship for R. Coker from the British Heart Foundation.

REFERENCES

1. Pepys MB, Booth DR, Hutchinson WL, Gallimore JR, Collins IM, Hohenester E. Amyloid P component. A critical review. Amyloid. 1997;4(4):274–95.
2. Emsley J, White HE, O'Hara BP, Oliva G, Srinivasan N, Tickle IJ, et al. Structure of pentameric human serum amyloid P component. 1994;367(6461):338–45.
3. Janciauskiene S, de Frutos PG, Carlemalm E, Dahlbäck B, Eriksson S. Inhibition of Alzheimer-Peptide Fibril Formation by Serum Amyloid P Component. J. Biol. Chem. 1995;270(44):26041–4.
4. Hamazaki H. Amyloid P Component Promotes Aggregation of Alzheimer's [beta]-Amyloid Peptide. Biochem. Bhiophys. Res. Comm. 1995;211(2):349–53.
5. Coker AR, Purvis A, Baker D, Pepys MB, Wood SP. Molecular chaperone properties of serum amyloid P component. FEBS Letters. 2000;473(2):199–202.
6. De Beer FC, Pepys MB. Isolation of human C-reactive protein and serum amyloid P component. Journal of Immunological Methods. 1982;50(1):17–31.
7. Kabsch W. XDS. Acta Crystallographica Section D Biological Crystallography. 2010;66(2):125–32.
8. Collaborative Computational Project, Number 4. The CCP4 suite: programs for protein crystallography. Acta Cryst D. 1994;50(5):760–3.
9. LeVine III H. Quantification of β-sheet amyloid fibril structures with thioflavin T. Methods in Enzymology - Amyloid, Prions, and Other Protein Aggregates. 1999;308: 274–84.
10. Ashton A, Boehm M, Gallimore J, Pepys M, Perkins S. Pentameric and decameric structures in solution of serum amyloid P component by X-ray and neutron scattering and molecular modelling analyses. J. Mol. Biol. 1997;272(3):408–22.

SECTION II

CELL TOXICITY AND AMYLOID TISSUE TARGETING


Monday

STATE OF THE ART: Cell Toxicity and Amyloid Tissue Targeting

R. Kisilevsky

Department of Pathology and Molecular Medicine, Queen's University, Kingston, Ontario CANADA, K7L 3N6

HOW DOES AMYLOID CAUSE CELL INJURY?

To date two fundamental mechanisms have been proposed, and there may be others to be discovered in the future. One is based on the gross and microscopic appearance of amyloid as described at organ and tissue levels respectively [1]. The other is based on more recent work stemming primarily from observations in tissue culture.

Organs infiltrated with substantial quantities of amyloid, regardless of type, become firm and lose their flexibility which may affect their physiological function. An example is the heart whose ability to fill and propel blood may be significantly impaired by the rigidity imposed by the presence of amyloid. At a histological level amyloid is generally deposited along the stromal architecture in the extra-cellular matrix between blood vessels and parenchymal cells [1]. This may impair the transfer of nutrients to, and of metabolic and functional products from, these parenchymal cells affecting their physiological function. An example is adrenal insufficiency in cases of severe systemic AA amyloidosis. Histological observations also suggest that amyloid deposits surround parenchymal cells and constrict the space about these cells [1]. These ways by which amyloid potentially alters cell viability and function were first suggested many decades ago, long before we obtained some understanding of the fibrillary nature of amyloid and the potential mechanisms by which such fibrils are generated. Although these older perspectives are no longer in fashion there is little experimental evidence that rules them out.

Alternative proposals have arisen in the last 20 years based on tissue culture data. Attempts to determine whether large amyloid deposits, as seen histologically, had toxic properties vis a vis cells in cell culture proved disappointing. In contrast oligomeric units (small aggregates, not necessarily fibrillar) of amyloidogenic proteins did adversely influence cell viability [2,3]. It was therefore proposed that it was small fibrils/oligomers, rather than the large amyloid aggregates formed in vivo that were responsible for cell toxicity and altered cell viability and physiology in vivo. This conclusion is only partly true, and the exclusion of the effects of large deposits is premature. The anatomic relationship of large aggregates to cells in culture is in no way analogous to amyloid seen in the extra-cellular matrix between cells, and between cells and capillaries, in vivo. Nevertheless, there is ample evidence that oligomers do have an effect on cell viability in culture and in vivo. An interesting example is impaired cardiac function in AL amyloid and its positive correlation with the plasma level of free amyloidogenic light chains rather than the amyloid load in the heart [4]. When treatment reduces this free light chain load cardiac function tends to improve. More recent studies have revealed that amyloidogenic monomers can form

beta barrels and they, as well as oligomers, can insert themselves into cell membranes (plasma membranes and intracellularly) altering cell permeability, or creating membrane pores, and impairing mitochondrial and endoplasmic reticulum function with devastating consequences [2,3]. It may well be that both oligomers as well as large deposits are operative in vivo but only one can be demonstrated in culture. The in vivo roles of large deposits and oligomers are not mutually exclusive.

HOW DOES AMYLOID GET TO THE RELEVANT TISSUES AND CELLS?

Deposition of amyloid may occur at, or close to, the site where the amyloidogenic precursor is synthesized, or at a site remote from its site of synthesis.

1) At the site of synthesis fibrillogenesis may occur within the cell or extra-cellularly. Examples of the former are fibrils found within the light chain synthesizing cells in multiple myeloma, phosphorylated tau fibrils found in neurons containing neurofibrillary tangles and amyloid-like fibrils seen in various species of yeast. In all these situations the oligomers can adversely influence the cells as described above. Examples of the latter are AIAAP amyloid deposits found in the islets of Langerhans in type 2 diabetes and Aβ deposits in the central nervous system in Alzheimer's disease. The IAPP form of amyloid is also instructive for several additional reasons. IAPP fibrils may also be found in the β-cells of the islets [5], their site of synthesis, and throughout the islets though not beyond its confines. If the iapp protein, or its initial fibrils, can diffuse beyond its cell of origin in the islets why does it not also diffuse to and involve the immediately adjacent exocrine portions of the pancreas? What are the factors that restrict its deposition to the islets? This question also recurs in "extracellular amyloid deposition remote from the site of synthesis" but in a somewhat different but more important context.

2) Extracellular amyloid deposition remote from the site of synthesis of the protein precursors occurs in many forms of systemic amyloidoses such as AA, AL, ATTR and AApoAI. Though there are many examples that can be discussed only AA and ATTR will be considered, as together they identify a series of questions that are not being addressed in studies of in vitro fibril formation. Furthermore these questions raise concerns about some of the conclusions reached by such in vitro studies.

The precursor to AA amyloid, serum amyloid A (SAA), is synthesized primarily in the liver and during an inflammatory reaction its plasma concentration may increase 1000 fold. However, the deposition of SAA as AA amyloid occurs first in the spleen and specifically the perifollicular zone within this organ. This is the filtering zone within the spleen and one can argue that high concentrations of SAA may lead to the formation of oligomers in the plasma which are then cleared by the spleen. If it is true that oligomer formation is the common pathway of amyloid precursors to amyloid deposits then other amyloid precursors which exist in plasma should also follow this deposition pattern and be found in the perifollicular zone in the spleen. This however is not the case. Transthyretin (TTR), the precursor to ATTR, is also made primarily in the liver but its anatomic distribution as amyloid appears to be a related to particular mutations, or lack of mutations, involved. Wild-type TTR is seen mainly in the heart later in life, the peripheral nervous system is the preference of one mutation and in another it is the leptomeninges. The spleen is rarely involved in ATTR. If oligomers play the role proposed from in vitro studies they must then be generated not in the plasma but in the micro-locale where they are deposited. We know very little about these micro-environmental factors and how they may determine which organ is targeted by the different amyloidogenic proteins and in particular why single amino acid substitutions in a specific amyloidogenic protein changes the organs targeted.

POTENTIAL FACTORS INFLUENCING TISSUE TARGETING

The fact that single amino acid substitutions can change the tissue site of amyloid deposition suggests that some of the information determining this deposition resides in the amyloid protein itself. But, with what does the amyloidogenic protein interact? Though possible, it is unlikely that the ionic composition of interstitial fluid in the tissue stroma varies significantly from one anatomic locale to another which suggests that our attention should focus on larger molecular entities with which the amyloidogenic may interact. At least two possibilities come to mind. 1) Protein:Protein interactions in a ligand:receptor nature as one may see in antigen:antibody binding, and 2) Protein:Glycosaminoglycan, particularly heparan sulphate (HS) interactions for which there is a substantial literature in amyloid research [6]. Though HS has a common repeating disaccharide backbone there is ample variation in its pattern of sulphation and epimerization to account for differences between tissues. Furthermore, these structural variations also change with age and physiological states. Precisely how proteins bind/interact with HS and where the specificities lie awaits additional research.

TISSUE TARGETING AND THE MECHANISM OF AMYLOID FORMATION AND CELL INJURY

A consideration of the general determinants that govern which tissues are targeted by which amyloidogenic proteins is an aspect that, at present, is not being, or cannot be, assessed in vitro. Just as “large deposits” when assessed in culture lose their relationship to cells, capillaries and stroma as seen in vivo, the behaviour of oligomers in vitro do not necessarily indicate how and where these are formed in vivo. They are not likely to be formed in the blood stream as, being particulate, they would then all have a similar tissue distribution, which they do not. This suggests that oligomers are formed locally and are therefore subject to the same factors that determine specific tissue distribution of amyloids. If so is the process really different than the formation of large deposits, or are they just different stages of the same process?

REFERENCES

1. Kisilevsky R. The Amyloidoses. Chapter 23 In: Rubin E, Strayer D, Editors. Pathology, A Clinicopathological Approach. Philadelphia: Lippincott, Williams and Wilkins. 2007; pp 989-998.
2. Haass C, Steiner H. Protofibrils, the unifying toxic molecule of neurodegenerative disorders? *Nat.Neurosci.* 2001;4:859-860.
3. Glabe CG. Common mechanisms of amyloid oligomer pathogenesis in degenerative disease. *Neurobiol.Aging*. 2006.
4. Palladini G, Lavatelli F, Russo P, Perlini S, Perfetti V, Bosoni T, Obici L, Bradwell AR, D'Eril GM, Fogari R, Moratti R, Merlini G. Circulating amyloidogenic free light chains and serum N-terminal natriuretic peptide type B decrease simultaneously in association with improvement of survival in AL. *Blood.* 2006;107:3854-3858.
5. Paulsson JF, Andersson A, Westermark P, Westermark GT. Intracellular amyloid-like deposits contain unprocessed pro-islet amyloid polypeptide (proIAPP) in beta cells of transgenic mice overexpressing the gene for human IAPP and transplanted human islets. *Diabetologia.* 2006.
6. Kisilevsky R, Ancsin JB, Szarek WA, Petanceska S. Heparan sulfate as a therapeutic target in amyloidogenesis: prospects and possible complications. *Amyloid J.Prot.Folding Disorders.* 2007;14:21-32.

PERSPECTIVE: The Role of "Chaperoning at a Distance" in the Systemic Amyloidoses: molecular responses to the synthesis and deposition of transthyretin (TTR) aggregates

J. N. Buxbaum

Department of Molecular and Experimental Medicine, The Scripps Research Institute, LaJolla, CA, U.S.A

ABSTRACT

Responses of cells to newly synthesized misfolded proteins have been extensively studied in bacteria, yeast and mammalian cells. Cellular self-protection from the toxic effects of protein aggregates is an ancient process and has evolved to meet the needs of metazoans. It is easy to understand how extreme degrees of protein misfolding can exceed the cell's capacity for self-defense and result in cell damage and disease. With the acquisition of specialized systems for secretion and compartmentalization of cellular functions the mechanisms have become more differentiated. We now recognize cytoplasmic chaperones, chaperones of the endoplasmic reticulum and specific mitochondrial.chaperones. Yet in the systemic amyloidoses proteins that have the capacity to misfold and aggregate transit the synthesizing cell, circulate and do their damage at a distant tissue site. For TTR we propose that successful chaperoning in the synthesizing hepatocyte by an active unfolded protein response reduces the occurrence of deposition in the heart.

INTRODUCTION

Diseases associated with protein misfolding may be manifested by loss of normal function or a gain of toxic function. The loss of function states may be related to distortion of an active site or the inability of the misfolded molecule to transit the cell to reach its normal functional compartment or both. In contrast the amyloidoses are disorders characterized by a gain of toxic function, which may or may not be accompanied by actual diminished function of the substrate protein. In neurodegenerative disorders such as Parkinson's and Huntington's diseases the aggregated synuclein or huntingtin are visible as cellular inclusions, which makes sense since the proteins misfold and aggregate intracellularly presumably very close to the time of synthesis. It is possible to accelerate experimental models of these disorders by making elements of the intracellular chaperone system defective. The pathologic phenotype can be ameliorated by decreasing the abundance of aggregates by transfecting the synthesizing cells with genes encoding known chaperones (1;2). In the systemic amyloidoses, notably those related to TTR deposition, intracellular inclusions are never seen in the synthesizing hepatocytes (although that may not be true for choroid plexus epithelial cells), and the variants are secreted, circulate and deposit at a distance from the liver in the heart, gastrointestinal tract, peripheral nerves and connective tissue. It has been

shown in tissue culture studies, that the most unstable variants, TTR D18G, for example, are not secreted (3). However, patients producing D18G protein do not have hepatic inclusions (4). The tissue culture studies strongly indicate that much of the protein is degraded by endoplasmic reticulum associated degradation (ERAD). All these patients have a characteristic oculo-leptomeningeal clinical picture related to the in situ deposition of the mutant TTR in the leptomeninges where it is synthesized by choroid plexus epithelium and leptomeningeal cells of the same cell type (5). However some of these patients have peripheral deposits in the skin, kidneys, ovaries, heart, spinal ganglia and cutaneous lymphatics, suggesting either that the mutant proteins are synthesized and secreted locally (by kidney, skin or Schwann cells) or by the liver and reach the site of deposition through the circulation (4;6). The latter is consistent with studies showing that cultured hepatoma cells are more capable of secreting D18G than cultured BHK cells or choroid plexus epithelium in the absence of thyroxine (T_4) (3). These studies illustrate that the mechanisms engaged in defense against the toxicity of aggregated proteins may vary both qualitatively and quantitatively among various cell types.

We have previously described a mouse strain that is transgenic for 90 copies of the wild type human TTR gene that develops age dependent human TTR deposition in the heart and kidneys beginning at about one year of age (7). We have used the model to explore some aspects of the pathogenesis of human TTR deposition and performed the current studies in an attempt to determine if there is a significant hepatic protein homeostatic response to the extreme overproduction of an amyloidogenic protein and whether the response had any impact on the distal deposition of the TTR aggregates. We also wished to analyze the molecular response of a *bona fide* deposition target tissue for changes that enabled deposition or were associated with resistance to the process.

METHODS

We performed microarray transcriptional analyses of RNA pools from livers and hearts of male mice transgenic for approximately 90 copies of the wild type TTR gene that were 3 and 24 months old (8). Pools contained equal amounts of RNA for each experimental condition. Comparisons were made with age and gender matched control mice as well as between transgenic mice with and without histologically documented cardiac deposition of human TTR.

RESULTS

None of the mice had cardiac deposition at three months of age. At 24 months about half the animals showed cardiac TTR deposition. In most instances the deposition was non-fibrillar but some animals showed classic Congophilic deposits with the characteristic birefringence under polarized light.

HEPATIC TRANSCRIPTION

Livers from 3 month old transgenic mice showed almost 400 genes that were more highly transcribed than in the non-transgenic mice and 258 genes that were in lower abundance. Thirty-two genes involved in some aspect of inflammation were increased, while ten were decreased. There was no evidence of a specific antibody or T-cell response. Genes encoding an anti-oxidant response as well as genes encoding mitochondrial proteins were increased. There was a small increase in genes involved in apoptosis but a considerable increase in genes encoding matrix proteins such as extracellular matrix protein 1, biglycan, secreted acidic cysteine rich

protein and procollagen XIV, alpha 1 among others. Several p38 associated Map kinases were also more highly expressed including ERK1. Most interesting from our perspective was the increased transcription of genes regulated by Xbp1s, the initiator of the unfolded protein response. These included Derlins 1 and 2 and the secretory transporters SEC24c, SSr2 and Spcs2. In addition the HSP40 homolog Dnajb1, the cytoplasmic chaperone Cct3 and a number of components of the proteasome-ubiquitin system.

More striking were the differences in liver transcript abundance between mice in which there were documented cardiac deposits and those in which such deposits could not be detected. In the mice showing cardiac deposition there was almost no evidence of activation of any of the elements of protein homeostasis, except for an increase in Tribbles 3 a protein thought to be a negative feedback inhibitor of the ATF4 pathway. There was a small relative increase in the number of inflammatory genes transcribed all of which appeared to be interferon driven. In the livers of the mice without cardiac deposition there was increased expression of Xbp1, which on qtPCR analysis was the spliced form, there were increases in cytoplasm chaperone associated molecules including Dnajb1 and Dnaja4, AHA1 a co-chaperone of HSP90. Interestingly the mice without cardiac deposition also had lower levels of both human and murine TTR mRNA, lower levels of hepatic transcription in general and lower serum TTR levels, all of which have been reported in the context of the unfolded protein response in simpler experimental systems.

CARDIAC TRANSCRIPTION

In the hearts of the young transgenics approximately 250 genes were increased and 300 were decreased relative to the age matched wild type mice. The most striking difference was in the number of inflammation associated genes showing an increase relative to the non-transgenic mice (40 increased, 4 decreased). In contrast to the liver there was a suggestion of a specific immune response in these mice with increases in both Ig and some T-cell receptor genes. There were decreases in genes encoding mitochondrial proteins, cardiac structural genes and surprisingly genes encoding proteasome components and three genes involved in autophagy LC3, Rab1b and cathepsin D.

In the hearts of the two year old mice there were striking differences between the transcripts in the presence of TTR deposits and those transgenics in which there was no cardiac deposition. In the hearts with deposition more than 500 transcripts were increased relative to the hearts without deposition while only one hundred and thirty were decreased. In the hearts without deposition only 140 genes showed a relative increase but 60 of them were inflammation associated with no evidence for specificity of the response. There was no evidence of a stress or anti-oxidant response in those hearts. In the hearts with deposition there was a profound oxidative stress response with increases in cytosolic chaperones, proteins regulated by HSF1, ER-associated FK506 binding proteins, peptidylprolyl isomerases, proteasome element encoding genes, many elements of the ubiquitin system and some autophagy related proteins. Genes involved in apoptosis were increased as were a set of genes involved in glutathione metabolism. Twenty three genes involved in inflammation were more highly expressed in these hearts including genes encoding Ig heavy chains, light chain and J-chain, suggesting an adaptive immune response perhaps diminished from that seen in the hearts from the younger transgenics prior to deposition. Ribosomal and mitochondrial gene transcripts were highly increased with substantial representation of genes involved in fatty acid metabolism and energy generation. There was also a collection of transcripts that are related to the response to hypoxia including Hif2 alpha, and Vegf A.

DISCUSSION

The experiments reported here represent a concerted attempt to systematically apply molecular techniques to an organismal model of systemic amyloidosis. Prior studies have examined the expression of particular proteins as either amyloid precursors or responders to the process of amyloidogenesis *in vivo* (9;10). More detailed studies have generally been performed in isolated cell culture systems, which are easier to manipulate but may not be entirely relevant to what takes place *in vivo*. We have been able to examine the systems biology of both the TTR synthesizing tissue and that of the major target tissue for TTR deposition. While our analyses may be compromised by the fact that we have examined mixed cell populations the experimental design and the strength of the signals obtain allow us to draw some tentative conclusions. We must express the additional caveat that it is not clear that the response to over-expression of the relatively stable wild type TTR molecule is necessarily the same as that seen in the presence of an unstable mutant TTR, particularly as unstable molecule as TTR D18G, which has been studied by two groups and shown to be subject to ERAD activity in cultured BHK and CHO cells (3;11). Importantly the prior studies clearly showed differences in the proteostatic capacity of cells of different origins.

That being said we believe that our experiments reveal several interesting features of the response to over-expression of a protein that has a tendency to dissociate to yield an amyloidogenic subunit. Prior to the time there is any tissue deposition the synthesizing cells display transcriptional evidence of an inflammatory and anti-oxidant response, increased transcription of extracellular matrix genes and clear evidence of activation of genes involved in the unfolded protein response. With aging maintenance of the UPR, as defined by increased abundance of Xbp1s, decreased transcription and lower serum TTR concentration, appears to be associated with the absence of cardiac TTR deposition. The mice with cardiac TTR deposition show no evidence of a sustained UPR or ERAD response, transcription of a set of interferon responsive genes and some evidence of an anti-oxidant response. It is not clear if the apparent lack of response represents active suppression (via Tribbles 3) or a diminished capacity to maintain an effective UPR because of the effects of aging or oxidative damage secondary to lifelong exposure to over-production of a potentially amyloidogenic protein.

The cardiac response to the over-expressed TTR transgene is manifested early by a robust inflammatory response, which is largely non-specific. In the mice that do not develop deposition the inflammatory transcriptome persists however in the presence of TTR deposits the nature of the inflammatory response is narrowed with more evidence of specificity. There is evidence of an HSF1 driven stress responses with increases in both cytoplasmic and ER-associated chaperones. Xbp1 transcription is increased but there is no apparent increase in the spliced form that drives the UPR. Mitochondrial gene transcriptional activity is increased reflecting increased energy demands associated with in increase in transcription of genes associated with the response to hypoxia.

In summary we believe that “chaperoning at a distance” in which the quality control system of the liver prevents the secretion of the misfolded or potentially misfolded TTR is at least partially responsible for protecting the heart from TTR deposition. While we cannot discern what determine which livers will be able to perform the function throughout life we can detect the response. However that does not appear to be the only factor involved. It is clear that the transcription pattern of the hearts of the young transgenics differs from that of mice not expressing the transgene in a very profound way. Surprisingly the response is inflammatory and reflects either an intrinsic anti-inflammatory capacity of the cardiac transcriptome or a population of inflammatory cells that is either resident in or traversing the heart. In any case it must be a response to something in the circulation

most likely some form of TTR in a partially misfolded state or complexed to some other molecule. We have not yet identified the entity. It is possible that a similar molecule circulates in humans with TTR tissue deposition.

REFERENCES

1. Gidalevitz T, Ben Zvi A, Ho KH, Brignull HR, Morimoto RI. Progressive disruption of cellular protein folding in models of polyglutamine diseases. Science 2006 Mar 10;311(5766):1471-4.
2. Muchowski PJ, Schaffar G, Sittler A, Wanker EE, Hayer-Hartl MK, Hartl FU. Hsp70 and hsp40 chaperones can inhibit self-assembly of polyglutamine proteins into amyloid-like fibrils. Proc Natl Acad Sci USA 2000 Jul 5;97(14):7841-6.
3. Sekijima Y, Wiseman RL, Matteson J, Hammarstrom P, Miller SR, Sawkar AR, et al. The biological and chemical basis for tissue-selective amyloid disease. Cell 2005 Apr 8;121(1):73-85.
4. Garzuly F, Vidal R, Wisniewski T, Brittig F, Budka H. Familial meningocerebrovascular amyloidosis, Hungarian type, with mutant transthyretin (TTR Asp18Gly). Neurol 1996 Dec;47(6):1562-7.
5. Vidal R, Garzuly F, Budka H, Lalowski M, Linke R, Brittig F, et al. Meningocerebrovascular amyloidosis associated with a novel transthyretin (TTR) mis-sense mutation at codon 18 (TTRD18G). Am J Pathol 1996;148:361-6.
6. Harkany T, Garzuly F, Csanaky G, Luiten PG, Nyakas C, Linke RP, et al. Cutaneous lymphatic amyloid deposits in "Hungarian-type" familial transthyretin amyloidosis: a case report. Br J Dermatol 2002 Apr;146(4):674-9.
7. Teng MH, Yin JY, Vidal R, Ghiso J, Kumar A, Rabenou R, et al. Amyloid and nonfibrillar deposits in mice transgenic for wild-type human transthyretin: a possible model for senile systemic amyloidosis. Lab Invest 2001 Mar;81(3):385-96.
8. Buxbaum JN, Tagoe C, Gallo G, Walker JR, Kurian S, Salomon DR. Why are some amyloidoses systemic? Does hepatic "chaperoning at a distance" prevent cardiac deposition in a transgenic model of human senile systemic (transthyretin) amyloidosis? FASEB journal : official publication of the Federation of American Societies for Experimental Biology 2012 Feb 23;26:1-11.
9. Ailles L, Kisilevsky R, Young ID. Induction of perlecan gene expression precedes amyloid formation during experimental murine AA amyloidogenesis. Lab Invest 1993 Oct;69(4):443-8.
10. Page LJ, Suk JY, Bazhenova L, Fleming SM, Wood M, Jiang Y, et al. Secretion of amyloidogenic gelsolin progressively compromises protein homeostasis leading to the intracellular aggregation of proteins. Proc Natl Acad Sci USA 2009 Jul 7;106(27):11125-30.
11. Sato T, Susuki S, Suico MA, Miyata M, Ando Y, Mizuguchi M, et al. Endoplasmic reticulum quality control regulates the fate of transthyretin variants in the cell. EMBO J 2007 May 16;26(10):2501-12.

Transthyretin binding to heparan sulfate proteoglycan: differences between a commercial transthyretin and a senile amyloidogenic transthyretin: a biochromatographic study

A. Geneste[1], N. Magy-Bertrand[1,2], C. André[1], M.D. Benson[3], Y.C. Guillaume[1]

[1] Université de Franche-Comté, UFR SMP, EA 4662 "Equipe nanomédecine, imagerie et thérapeutique ", 25030 Besançon, cedex France

[2] Université de Franche-Comté, UFR SMP, Internal Medicine Department, University Hospital, 25030 Besançon, cedex France

[3] Department of Pathology and Laboratory Medicine, Indiana University School of Medicine, Indianapolis, IN, USA

ABSTRACT

Transthyretin (TTR) is an amyloidogenic protein involved in senile systemic amyloidosis. The interaction between heparan sulfate proteoglycan (HSPG) and TTR is a key-phase for the development of amyloid deposits. A novel biochromatographic approach was developed to measure the thermodynamical data for the binding of a commercial TTR (TTRc) and a senile TTR (TTRs) to HSPG in a wide temperature range and at different pH of the medium. The TTRc (or TTRs)-HSPG binding was enthalpically driven. The negative values of thermodynamic data showed that van der Walls and hydrogen bonds were preponderant in the association mechanism. At pH= 6, the strongest value obtained for TTRs (ΔHTTRc= - 11.9 kJ.mol^{-1}, ΔHTTRs= -8.1 kJ.mol^{-1}) suggested a conformational change between TTRc and TTRs in the binding mechanism. This conformational change may enhance more favorable electrostatic interactions between the sulfate groups of HSPG and the basic amino acids of TTRs.

INTRODUCTION

Human transthyretins (TTR) is a plasmatic protein transports the thyroxin (T4) and the retinol binding protein carrier. TTR is a tetrameric β-sheeted structure and TTR misfolding and aggregation is known to be associated with amyloid diseases (ATTR) [1] as senile systemic amyloidosis (SSA). SSA is constituted by insoluble fibrils made of proteins and other constituents as heparan sulfate proteoglycan (HSPG). HSPG is a major component of extracellular matrices and interacts with a multitude of proteins. HSPG has been found in almost all amyloid deposits [2] and is known to accelerate fibril formation *in vitro*. Little is known about the *in vivo* TTR-HSPG interactions. In order to better understand the association mechanism TTR-HSPG, a novel biochromatographic column was developed to evaluate the thermodynamlc data of this binding.

METHODS

A novel stationary phase based on HSPG was developed for HPLC. HSPG was immobilized on NH2-silica spherical particles (3 µm) into a 50 mm*4,6mm column. The mobile phase consisted of a phosphate buffer pH=7.4 (0.01 M) [3, 4]. TTRs was obtained by extraction from cardiac tissue [5] provided by an American patient with senile cardiac amyloid. TTRc was provided by Sigma Aldrich France. The phosphate buffer was prepared by mixing equimolar solutions of mono- and dibasic sodium phosphate to produce the desired eluent pH adjusted to values equal to 7.4, 7, 6.5, 6 and 5.5. The experiments were carried out over the temperature range 5-35℃ and at 214 nm detection wavelength. For each pH value, 20 µL of TTR in PBS pH 7.4 was injected and the retention factors *k'* were determined.

RESULTS

The association constant TTR-HSPG represented by the retention factor *k'* (Figure 1.) was calculated. The corresponding Van't Hoff plots were all linear suggesting no temperature dependence in the association mechanism. The TTRc (or TTRs)-HSPG binding was enthalpy driven. The negative values of the thermodynamic data (Table 1.) demonstrated that van der Walls and hydrogen bonds were preponderant in the association mechanism. At pH= 6, the highest value for TTRs (ΔHTTRc= - 11.9 kJ.mol^{-1}, ΔHTTRs= -8.1 kJ.mol^{-1}) suggested a conformational change between TTRc and TTRs. This difference was explained by more favorable electrostatic interactions due to protonation of a histidine residue (p*K*a = 6.04) which interacted with the sulfate groups of HSPG.

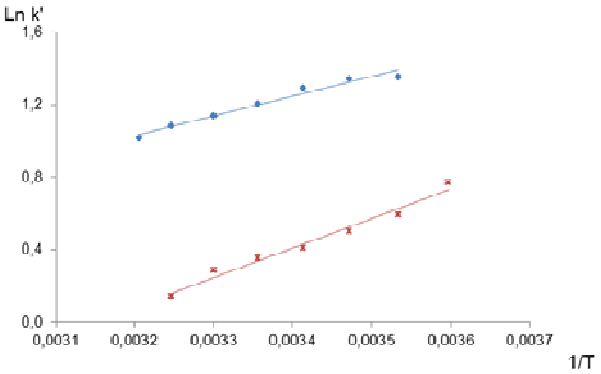

Figure 1. Temperature dependence of the ln k' values of TTR (a: TTRc, b: TTRs) at pH=7.4

DISCUSSION AND CONCLUSION

This biochromatographIc approach allowed us to study interactions between heparan sulfate proteoglycan and transthyretin. Van der Waals and hydrogen bonds governed this association mechanism. Differences observed between TTRs and TTRc at pH= 6 were due to a histidine residue protonation which enhanced more favorable electrostatic interactions for TTRs.

Table 1. Thermodynamic parameters for the binding of TTRs or TTRc to HSPG (ΔH° (kJ/mol); ΔS* (no unit))

pH	ΔH°(TTRs)	ΔS*(TTRs)	ΔH°(TTRc)	ΔS*(TTRc)
7.4	-9	-2.4	-13.5	-5.1
7	-11.2	-3.5	-13	-4.6
6.5	-12.4	-4	-12.3	-4
6	-8.2	-2.5	-11.9	-3.4
5.5	-9.7	-2.5	-9	-1.7

AKNOWLEDGEMENTS

I would like to thank all Dr. Benson's lab team for teaching me amyloidosis and extraction.

REFERENCES

1. Magy-Bertrand N. La Revue de Médecine Interne. 2007; 28 :306-13.
2. Kisilevsky R, Ancsin J.B, Szarek W.A, Petanceska S, Amyloid. 2007; 14 (1): 21-32.
3. Excoffon L, Andre C, Magy-Bertrand N, Limat S, Guillaume Y.C. Chromatographia. 2009; 70:1569-73.
4. Andre C, Excoffon L, Magy-Bertrand N, Limat S, Guillaume Y.C. Chromatographia. 2010; 72:1035-41.
5. Liepnieks J.J, Kluve-Beckerman B, Benson M.D. B. B. A. 1995; 1270 (1): 81-86.

Biochemical Characterization of Leptomeningeal Amyloid in Hereditary Transthyretin Amyloidosis

Juris J. Liepnieks[1], Merrill D. Benson[1,2]

[1]Department of Pathology and Laboratory Medicine, Indiana University School of Medicine, Indianapolis, IN USA

[2]Richard L Roudebush–Veterans Affairs Medical Center, Indianapolis, IN USA

ABSTRACT

The majority of the mutations in the transthyretin (TTR) gene associated with hereditary TTR amyloidosis result in cardiac and peripheral nervous system involvement. About a dozen TTR gene mutations, however, result in amyloid deposition in the leptomeninges. Plasma TTR synthesized by the liver is the source for cardiac and peripheral nerve TTR amyloid, and TTR synthesized by the choroid plexus is the source for leptomeningeal amyloid. Amyloid protein was isolated from the leptomeninges of heterozygous Val30Gly, Gly53Arg, and Tyr114Cys TTR patients and biochemically characterized to determine if differences exist in the leptomeningeal TTR deposits compared to other organs. In all three cases, essentially all of the leptomeningeal amyloid TTR was derived from variant TTR. In contrast, cardiac and peripheral nerve TTR amyloid usually contain 50-70% variant and 30-50% wild-type TTR. These results suggest that differences may exist in the processing pathway of TTR to amyloid deposits in heart and leptomeninges.

INTRODUCTION

Over 100 mutations in the transthyretin (TTR) gene are associated with hereditary TTR amyloidosis (1). The majority result in peripheral nervous system and cardiac involvement. However, about a dozen TTR gene mutations are characterized by amyloid deposition in the leptomeninges with little, if any, deposition in visceral organs. What determines the differences in organ targeting by the various TTR mutations is unknown. TTR is synthesized by the liver, choroid plexus, and retinal pigment epithelium. Plasma TTR synthesized by the liver is the source for peripheral nerve and cardiac amyloid. TTR synthesized by the choroid plexus is the source for leptomeningeal amyloid. To elucidate whether differences exist in the leptomeningeal TTR amyloid deposits compared to other organs such as nerve and heart, we have biochemically characterized the amyloid protein in the leptomeninges of TTR patients.

METHODS

Isolation of Amyloid Protein: Brain tissues were obtained at autopsy from three patients heterozygous for the Val30Gly, Gly53Arg, or Tyr114Cys TTR mutation and stored at -80° C. Amyloid protein was isolated as previously described (2). Leptomeninges were dissected from brain tissue, and amyloid fibrils were isolated by repeated homogenization in 0.1 M sodium citrate, 0.15 M sodium chloride and centrifugation. Isolated fibrils were solubilized in 6 M or 8 M guanidine hydrochloride, 0.5 M Tris, pH 8.3 containing 1 mg EDTA/ml and 10 mg dithiothreitol/ml, alkylated with iodoacetic acid, and centrifuged. The supernatant was fractionated on a Sepharose CL6B column equilibrated and eluted with 4 M guanidine hydrochloride, 25 mM Tris pH 8.3. Pooled fractions were exhaustively dialyzed against water and lyophilized.

Characterization of Amyloid Protein: Sepharose CL6B pools were analyzed by SDS-PAGE using a Tris-Tricine system, and were electrophoretically transferred to polyvinylidene difluoride membrane (3). Samples were digested with trypsin in 0.1 M ammonium bicarbonate, and the resulting peptides were fractionated by reverse-phase HPLC on a Synchropak RP8 column eluted with an acetonitrile gradient in 0.1% trifluoroacetic acid in water. Samples were analyzed by Edman degradation analysis on an Applied Biosystems Procise 491 cLC protein sequencer using the manufacturer's standard cycles.

RESULTS

SDS-PAGE analysis of the Sepharose CL6B pools of the amyloid protein from the Val30Gly and Gly53Arg leptomeninges showed several prominent bands in the 7-12 kDa region and a weak band at 15 kDa corresponding to intact TTR. Edman analysis of the 7-12 kDa bands after transfer to PVDF indicated major sequences starting with residues 49 and 52 of TTR suggesting that the amyloid TTR was highly proteolyzed around the residue 49 region. Edman analysis of the 15 kDa band indicated sequences starting with residues 1, 3, and 5 of TTR. SDS-PAGE analysis of the pools from the Tyr114Cys leptomeninges showed a prominent band at 15 kDa and weak bands in the 8-11 kDa area. Edman analysis of the 15 kDa band showed sequence starting with residues 1,3, and 5 of TTR, while the 8-11 kDa bands showed major sequences starting with residues 49 and 52 of TTR. These results indicate that the Tyr114Cys leptomeningeal amyloid is composed mainly of intact TTR with minor amounts of proteolysis in the residue 49 region.

The relative amount of wild-type and variant TTR in the leptomeningeal amyloid was estimated from the recovery of tryptic peptides containing residues 22-34 of TTR with wild-type Val30 or variant Gly30 from trypsin digests of the pools from the Val30Gly TTR patient, from the recovery of tryptic peptides containing residues 104-127 of TTR with wild-type Tyr114 or variant Cys114 from trypsin digests of the pools from the Tyr114Cys TTR patient, and from the recovery of tryptic peptides containing residues 49-70 of TTR with wild-type Gly53 or variant Arg53 from trypsin digests of the pools from the Gly53Arg TTR patient. For the Val30Gly and Tyr114Cys TTR patients, no tryptic peptides containing the wild-type residue were found, only peptides with the variant residue. For the Gly53Arg patient a very minor amount of peptide with wild-type Gly53 was found besides the peptides with variant Arg53 (≤ 3% wild-type Gly53 and ≥ 97% variant Arg53). These results indicate that the leptomeningeal TTR amyloid in these three patients was derived exclusively or almost exclusively from variant TTR.

DISCUSSION

Leptomeningeal amyloidosis is a rare central nervous system manifestation of hereditary TTR amyloidosis. Clinical manifestations include ataxia, spasticity, seizures, dementia, subarachnoid hemorrhage, and impaired consciousness. TTR mutations in exons 2, 3, and 4 have been reported associated with leptomeningeal amyloid. Our previous studies of cardiac and peripheral nerve tissues from hereditary TTR amyloid patients heterozygous for the TTR mutation have shown that the amyloid TTR is significantly proteolyzed in the area around residue 49 in both tissues (4-6). The Val30Gly and Gly53Arg TTR amyloid in the leptomeninges showed similar extensive proteolysis in this region while the Tyr114Cys TTR amyloid showed minor proteolysis. Cardiac TTR amyloid contained both wild-type and variant TTR with the variant predominating, 50-70% variant and 30-50% wild-type TTR (4,5). Similarly nerve TTR amyloid contained both wild-type and variant TTR with the variant predominating, 60-65% variant and 35-40% wild-type TTR (6). In contrast, the leptomeningeal amyloid was composed entirely or almost entirely of variant TTR, 97-100% variant and 0-3% wild-type TTR. These results suggest that differences may exist in the processing pathway of TTR synthesized by the liver to cardiac and peripheral nerve amyloid deposits, and of TTR synthesized by the choroid plexus to leptomeningeal amyloid deposits.

REFERENCES

1. Connors LH, Lim A, Prokaeva T, Roskens VA, Costello CE. Tabulation of human transthyretin (TTR) variants, 3003. Amyloid J Protein Folding Disord 2003;10:160-184.
2. Liepnieks JJ, Dickson DW, Benson MD. A new transthyretin mutation associated with leptomeningeal amyloidosis. Amyloid 2011;18:(Supplement 1);160-162
3. Schagger H, Von Jagow G. Tricine-sodium dodecyl sulfate-polyacrylamide gel electrophoresis for the separation of proteins in the range from 1-100 kDa. Anal Biochem 1987;166:368-379.
4. Liepnieks JJ, Wilson DL, Benson MD. Biochemical characterization of vitreous and cardiac amyloid in Ile84Ser transthyretin amyloidosis. Amyloid 2006;13:170-177.
5. Liepnieks JJ, Benson MD. Progression of cardiac amyloid deposition in hereditary transthyretin amyloidosis patients after liver transplantation. Amyloid 2007;14:277-282.
6. Liepnieks JJ, Zhang LQ, Benson MD. Progression of transthyretin amyloid neuropathy after liver transplantation. Neurology 2010;75:324-327.

Differences of histopathological features and amyloid components among various tissue sites of FAP patients after liver transplantation

T. Ohshima[1], S. Kawahara[2], M. Ueda[2], Y. Kawakami[2], R. Tanaka[2], Y. Misumi[1], M. Tasaki[1], H. Jono[5], S. Shinriki[4], K. Obayashi[4], T. Yamashita[1], Y. Ohya[3], K. Asonuma[3], Y. Inomata[3], P. Westermark[6] and Y. Ando[1]

[1]Department of Neurology, [2]Department of Diagnostic Medicine, [3]Department of Transplantation and Pediatric Surgery, Graduate School of Medical Sciences, Kumamoto University, [4]Diagnostic Unit for Amyloidosis, Department of Laboratory Medicine, [5]Department of Pharmacy, Kumamoto University Hospital, Japan, [6] Department of Genetics and Pathology, Uppsala University, Sweden

ABSTRACT

To evaluate the pathological circumstances among various tissues of familial amyloidotic polyneuropathy (FAP) patients with liver transplantation (LT), we investigated histopathological features and wild-type (WT) transthyretin (TTR) proportions of amyloid deposition in various tissues of 11 autopsied FAP ATTR V30M patients (4 patients died over 10 years after LT and 7 without LT). Patients with LT showed severe amyloid deposition in heart and tongue and WT TTR ratios of amyloid deposition were over 90% in most tissue sites. WT TTR ratios of amyloid in heart and tongue were higher than those in other tissue sites of the patients without LT. Pathological features of FAP after LT may be different from those of the patients without LT.

INTRODUCTION

It has been widely accepted that liver transplantation (LT) halts the symptoms of familial amyloidotic polyneuropathy (FAP) patients who had been carefully selected for LT (1, 2), while in some FAP patients, LT reportedly failed to prevent progression of cardiac amyloidosis (2). However, pathological features of FAP patients with LT are still unknown (3). In this study, to evaluate the pathological features of FAP patients with LT, we investigated histopathological features and amyloid components in autopsied FAP patients with and without LT.

METHODS

We evaluated 4 autopsied FAP ATTR V30M patients who had survived more than 10 years after LT. The other 33 patients who had undergone LT were still living. We also studied 7 non-LT FAP ATTR V30M patients who were autopsied at Kumamoto University Hospital (4, 5). Tissue samples were embedded in paraffin, serially sectioned at a thickness of 4 µm, and placed on microscope slides. Amyloid deposition was assessed by

alkaline Congo-red staining, and examined under polarized light to detect the presence of green birefringence. In addition, we examined amyloid fibrils in heart by electron microscopy. Post-morten heart samples were fixed with 4% paraformaldehyde and 1% glutaraldehyde solution, and then fixed with 1% OsO_4 and embedded in Epon. Ultrathin sections were stained with 4% uranyl acetate and lead citrate, and examined with transmission election microscope.

Transthyretin (TTR) composition of amyloid deposits (ratio of WT to mutated TTR) was examined in frozen tissue specimens. In order to remove soluble component from frozen specimens (100 mg wet weight), we homogenized the tissues in phosphate-buffered saline (PBS) and centrifuged at 14,000 *g* for 10 min repeatedly. This process was repeated until the supernatant value of A280 by optical density method was 0.2 or less. Remaining pellet and 20% acetonitrile containing 0.1% trifluoroacetic acid incubated for 5 hours at room temperature and centrifuged. Supernatants were lyophilized. Lyophilized proteins were analyzed by 12.5% polyacrylamide gel and stained by silver staining method. A band at 15 kDa (TTR monomer) was cut from gels and digested with trypsin. The peptides were examined by surface-enhanced laser desorption/ionization time-of-flight mass spectrometry. The relative amounts of WT and mutated TTR were estimated from the height of peaks derived from tryptic peptides of amino acid residue 22-34, which contained the mutated amino acid position 30.

Table 1. Information of 11 autopsied FAP ATTRV30M patients

	Patient 1	Patient 2 With LT	Patient 3	Patient 4	Average of 7 patients Without LT
Sex	M	M	F	M	M (4 patients)/ F (3 patients)
Age of onset (years old)	26	27	41	47	42
Duration from onset to LT (years)	3	1	6	2	NA
Age of death (years old)	42	44	57	59	52
Duration from LT to death (years)	13	16	10	10	NA
From onset to death (years)	16	17	16	12	10
Main causes of death	Arrhythmia, alcohol-induced malnutrition and electrolyte abnormality	Hepatic failure (rejection), Sepsis	Cardiac failure	Cardiac failure	

M: male, F: female, NA: not available.

RESULTS

Patients with LT showed severe amyloid deposition in several tissue sites, such as heart, tongue and spinal code, while, less amyloid deposition was observed in other tissue sites, such as thyroid gland, glomerulus of kidney, peripheral nerve and gastrointestinal tract. On the other hand, amyloid deposits were severe in most tissue sites of the patients without LT. Electron microscopic examination revealed differences in morphology of cardiac amyloid fibrils in greater detail: long, straight fibrils were arranged in parallel in the patients without LT, whereas short, rigid fibrils were haphazardly arranged in the patients with LT.

WT TTR ratios of amyloid deposition were over 90% in most of tissue sites of the patients with LT, except for the spinal cord (below 25%), while WT TTR ratios of amyloid deposition were below 50% in the patients without LT.

DISCUSSION

Histopathological and morphological features of amyloid deposits in the FAP patients long after LT were different from those in the patients without LT, and were similar to senile systemic amyloidosis (SSA) (6). Mass spectrometric analyses revealed that the patients long after LT suffer from amyloid deposits mostly derived from WT TTR, which was secreted from the normal liver graft, in systemic tissue sites except for the spinal cord. Those results agree with several other studies (7, 8).

Amyloid formation in FAP patients with LT might differ from those in the patients without LT. Although FAP patients without LT develop amyloid deposits are mainly derived from mutated TTR, amyloid deposits in the patients after LT are mainly derived from WT TTR. This amyloid formation pathway may be similar to SSA and may also associate with old mutated TTR amyloid deposits before LT.

REFERENCES

1. Yamashita T, Ando Y, Okamoto S, Misumi Y, Hirahara T, Ueda M, et al. Long-term survival after liver transplantation in patients with familial amyloid polyneuropathy. Neurology 2012; 78: 637–643.
2. Ericzon G, Lundgren E, Suhr O. Liver transplantation for transthyretin amyloidosis. In: Richardson S, Cody V, editors. Recent advances in transthyretin evolution, structure and biological functions. Heidelberg: Springer-Verlag; 2009: 239–260.
3. Gustafsson S, Ihse E, Henein MY, Westermark P, Lindqvist P, Suhr OB. Amyloid fibril composition as a predictor of development of cardiomyopathy after liver transplantation for hereditary transthyretin amyloidosis. Transplantation 2012; 93: 1017-23.
4. Sakashita N, Ando Y, Haraoka K, Terazaki H, Yamashita T, Nakamura M, Takeya M. Sever congestive heart failure with cardiac liver cirrhosis 10 years after orthotopic liver transplantation for familial amyloidotic polyneuropathy. Pathol Int 2006; 56: 408-12
5. Obayashi K, Ueda M, Misumi Y, Yamashita T, Ando Y, et al. Pathologic changes long after liver transplantation in a familial amyloidotic polyneuropathy patient. BMJ Case Rep 2012; in press
6. Ueda M, Misumi Y, Tasaki M, Obayashi K, Ando Y, et al. Clinicopathological features of senile systemic amyloidosis: an ante- and post- mortem study. Mod Pathol 2011; 24: 1533-44.
7. Liepnieks JJ, Benson MD. Progression of cardiac amyloid deposition in hereditary transthyretin amyloidosis patients after liver transplantation. Amyloid 2007; 14: 277–282.
8. Tsuchiya-Suzuki A, Yazaki M, Kametani F, Sekijima Y, Ikeda S. Wild-type transthyretin significantly contributes to the formation of amyloid fibrils in familial amyloid polyneuropathy patients with amyloidogenic transthyretin Val30Met. Hum Pathol 2011; 42: 236–243.

Fighting familial amyloidosis using an impaired ER-stress response yeast strain

Cátia Rodrigues, Joana Branco, Marta Cerejo, Patrícia Calado, Helena Vieira

BIOALVO S.A., Edificio ICAT – Campus da FCUL, Campo Grande, 1749-016 Lisbon, Portugal.

Hereditary amyloidosis are rare and lethal disorders mostly caused by mutations in transthyretin (TTR), a plasma protein associated with an autosomal dominant neurodegenerative disorder called Familial Amyloidotic Polyneuropathy (FAP).The aim of this study was to develop a yeast model of TTR expression in conditions of impaired endoplasmic reticulum (ER) stress response. Although expression of TTR variants in a wild type yeast strain did not affect cell growth, expression of TTR L12P in Δ*hac1* and Δ*ire1*knock-out strains caused total growth arrest. To validate the sensitivity of Δ*hac1* and Δ*ire1* to ER stress response, a reporter vector expressing GFP under the control of the yeast ER stress promoter *KAR2* was used. GFP signal was decreased in these two strains as compared to the wild type strain, indicating that ER stress response machinery is impaired. This yeast model provides the basis of a screening tool for the identification of compounds able to modulate ER stress response pathway in FAP.

INTRODUCTION

Amyloidosis are a group of diseases caused by the deposition of insoluble and toxic proteins in tissues (1). Hereditary amyloidosis are mostly caused by the extracellular accumulation of a mutated plasma protein, TTR that causes deposits specially in peripheral nervous system (PNS), being FAP the most common disease (2). The Portuguese form of FAP is associated with the mutation Val30Met. It has been reported that extracellular accumulation of nonfibrillar TTR aggregates resulting in cell dysfunction and death triggers calcium homeostasis, inflammatory and apoptotic pathways and ER stress. These molecular mechanisms appear to be involved in various neurodegenerative diseases including FAP (3). ER stress is generally caused by the expression and accumulation of misfolded proteins in the ER lumen and this process is termed ER quality control. In order to respond to the ER stress caused by the accumulation of misfolded proteins, cells activate a mechanism known as unfolded protein response (UPR). It is known that TTR can pass the quality control of the ER; however the molecular mechanism involved remains to be elucidated (4). In this work yeast was used as a model organism, which has been already validated for neurodegenerative diseases such as Alzheimer's and Parkinson's. Moreover, BIOALVO detains a patented technology based on yeast named GPS D^2 platform (5). In yeast, the *IRE1* pathway is the only UPR mechanism. Focusing on ER stress molecular mechanisms and *IRE1* pathway genes, knock-out (KO) deletion strains for ER stress associated genes were selected (Δ*ire1*, Δ*hac1*, Δ*gcn2*and Δ*mnl1*) to express TTR (WT, Val30Met and Leu12Pro) and were used to evaluate their potential to become a

yeast-based platform for the screening of compounds that modulate TTR toxicity with therapeutic application in FAP disease, the main goal of this work.

METHODS

The TTR Leu12Pro and TTR Thr119Met cDNA were kindly provided by Prof. Maria João Saraiva. These two TTR mutants together with three other TTR variants (wild type, Val30Met and Leu55Pro) were cloned in an episomal yeast vector under the control of galactose promoter. All variants were cloned without the signal peptide in order to keep the protein inside the cell. To evaluate the toxic effect caused by the expression of TTR variants in an ER stress response impaired system, ER stress associated genes in yeast cells were selected through the *Saccharomyces* Genome Database (SGD). These selected genes were: *HAC1*, *IRE1*, *GCN2* and *MNL1*. The wild type BY4741 strain and the ER stress response KO strains were transformed with the TTR variants. All strains were grown overnight in synthetic complete media (SC) supplemented with necessary carbon sources and until the $OD_{600\ nm}$ reached the mid-log exponential phase. The media used included rafinose, glucose or galactose, depending on the experiments. Yeast cell viability assays in solid and liquid media were performed. Growth and fluorescence were monitored for 40h, measuring the OD and GFP signal every 4 hours on Victor 3V microplate reader (Perkin Elmer). Protein extraction was performed using a SDS sample buffer. TTR protein was detected by immunoblotting with anti-pre albumin antibody (DAKO) and GAPDH antibody was used as loading control.

RESULTS

In order to study the yeast growth effect caused by the expression of different TTR variants, cell viability assays in solid and liquid media were performed. The results obtained showed that expression of all TTR variants in the wild type yeast strain BY4741 did not affect cell growth; however TTR Leu12Pro expression in Δ*hac1* and Δ*ire1* deleted strains caused total growth impairment, both in solid and liquid media (Figure 1). Interestingly, immunoblotting analysis revealed that this TTR variant was the least expressed, suggesting a toxic effect of the TTR Leu12Pro even at low protein levels.

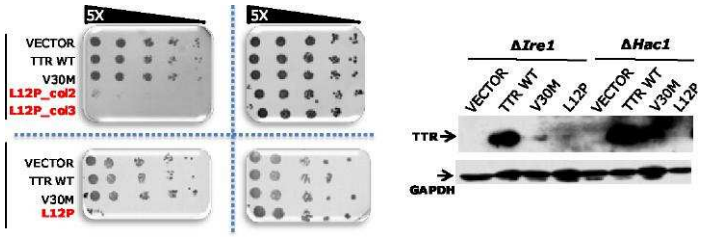

Figure 1. Expression of TTR Leu12Pro causes growth impairment in Δ*Ire1* and Δ*Hac1*deleted strains. Immunoblotting result showed that this TTR variant is the least expressed in both yeast strains.

The ER stress response sensitivity in the yeast strains deleted for ER stress genes was then evaluated. KO strains were transformed with an ER stress-responsive vector containing an EGFP reporter gene under the control of *KAR2* promoter, inducible by tunicamycin, a compound that prompts ER stress. Cell viability assays

in liquid media revealed that the wild type BY4741 and deleted (Δ*ire1*, Δ*hac1*, Δ*gcn2* and Δ*mnl1*) yeast strains have the same growth in media without tunicamycin. However, in the presence of tunicamycin the deleted strains Δ*ire1* and Δ*hac1* show minimal growth when compared with the wild type. The normalized GFP curves showed that BY4741 strain responds to tunicamycin, as the GFP level increased compared to the basal level GPDH (without tunicamycin). Conversely, for the deleted strains Δ*ire1* and Δ*hac1* the basal level of normalized GFP is much lower than the basal level of wild type strain. Moreover, both deleted strains show that the presence of tunicamycin does not affect the normalized GFP level.

DISCUSSION

The choice of evaluating ER stress mechanism upon expression of TTR in yeast cells is based on strong evidence showing that this mechanism underlies the neurotoxicity observed in FAP (3). This work describes a cellular model based on *Saccharomyces cerevisiae* for screening compounds that modulate TTR toxicity in an ER stress response impaired system. We started by expressing all TTR variants (WT, Val30Met, Leu55Pro, Leu12Pro and Thr119Met) in wild type BY4741 yeast strain and evaluating the resulting phenotype by cell viability assays. TTR expression of all variants did not affect cell growth and immunoblotting results showed that all variants are detected at different protein levels. Focusing on ER stress molecular mechanisms, knock-out deletion strains for ER stress associated genes were selected (Δ*ire1*, Δ*hac1*, Δ*gcn2*and Δ*mnl1*) to express TTR (WT, Val30Met and Leu12Pro) and cell viability in solid and liquid media were evaluated in these strains. TTR expression in Δ*gcn2* and Δ*mnl1* KO strains induced no growth alterations, but TTR Leu12Pro expression in Δ*ire1* and Δ*hac1* KO strains caused total growth arrest (Figure 1). As observed for the wild type BY4741 strain, all TTR variants were expressed at different levels in the four KO strains, being Leu12Pro the least expressed variant, suggesting a toxic effect even at low protein levels. To validate the ER stress sensitivity of these strains, an ER stress vector containing a GFP reporter gene under the control of the yeast ER stress promoter *KAR2* was used. In the Δ*ire1* and Δ*hac1* KO strains the presence of the ER stress inducer tunicamycin did not affect the normalized GFP level compared to the wild type strain, suggesting that both deleted strains are ER stress response impaired. These Δ*ire1* and Δ*hac1* yeast strains expressing TTR Leu12Pro will be used as a screening tool for the identification of compounds that modulate ER stress response pathway in FAP disease.

ACKNOWLEDGEMENTS

We thank Prof. Maria João Saraiva (IBMC) for the reagents and the helpful discussions. This work was supported by the Portuguese Funding Program QREN “Sistema de Incentivos à Investigação & Desenvolvimento Tecnológico”, contract 2010/013107 – LUSOEXTRACT.

REFERENCES

1. Merlini, G. and Belloti, V. Review: Molecular Mechanisms of Amyloidosis; 2003, N Engl J Med, 349, 583-96.
2. Pepys, M. B. Amyloidosis; 2006, Annu. Rev. Med., 57:223-41.
3. Macedo, B., Batista, A. R., Amaral, J. B., Saraiva, M. J. Biomarkers in the Assessment of Therapies for

Familial Amyloidotic Polyneuropathy; 2007, Mol. Med., 13: 584-591.

4. Sato, T., Susuki, S., Suico, M. A., *et al*. Endoplasmic reticulum quality control regulates the fate of transthyretin variants in the cell; 2007, The EMBO Journal, 26, 2501 – 2512.
5. Patent “A screening method for compounds that reduce ER stress: WO2008/150186 A1”.

TTRV30M oligomeric aggregates inhibit proliferation of renal progenitor cells but maintain their capacity to differentiate into podocytes *in vitro*

L. Moreira[1,2,3], L. Ballerini[2], A. Peired[2], C. Sagrinati[2], E. Parente[2], M.L. Angelotti[2], E. Ronconi[2], E. Lazzeri[2], B. Mazzinghi[2], P. Lacerda[1], I. Beirão[4], L. Lasagni[2], P.P. Costa[1,3], P. Romagnani[2]

1 Medical Genetics Center Doutor Jacinto de Magalhães, INSA, I.P., Porto, Portugal ; 2 Excellence Centre for Research, Transfer and High Education for the Development of DE NOVO Therapies (DENOTHE); University of Florence; 3 UMIB - Abel Salazar Biomedical Sciences Institute; 4 Nephrology, Santo António Hospital, CHP.

In Familial Amyloidotic Polyneuropathy, the amyloid deposition of mutant transthyretin TTR V30M can lead to renal complications. An unexplored mechanism is the toxicity of oligomeric TTR aggregates. A subset of renal progenitor cells (RPC) in the adult human kidney can induce regeneration of podocytes and tubular structures of the nephron, which can be critical for preventing irreversible renal failure. We assessed whether RPC are vulnerable, *in vitro*, to TTRV30M oligomers. RPC proliferation was reduced by 16.3±9.7% and 32.6±6.3% after 48 and 72 hours, respectively, in the presence of the oligomers. However, oligomers did not induce apoptosis or alterations in cell cycle to any significant extent, and did not influence RPC differentiation into podocytes. From this first attempt, we can say that TTRV30M oligomers inhibit RPC proliferation but do not influence their capacity to differentiate into mature podocytes, and thus should not compromise tissue regeneration.

INTRODUCTION

Familial Amyloidotic Polyneuropathy Type I (FAP-I) is an autosomal dominant disease characterized by systemic extracellular amyloid deposition of a mutant transthyretin, TTR V30M [1], affecting particularly the peripheral nervous system. Renal complications can also occur, including nephrotic syndrome and end-stage kidney failure [2]. An unexplored mechanism is the toxicity of early oligomeric TTR aggregates [3].

A subset of renal progenitor cells (RPC) with self-renewal and multidifferentiation potential exist at the urinary pole of Bowman's capsule in the adult human kidney [4]. These resident progenitor cells can induce regeneration of podocytes and tubular structures of different portions of the nephron, which can be critical for preventing irreversible renal failure, and could be useful in cell therapies.

We intend to evaluate the influence of oligomeric TTRV30M aggregates on proliferation and differentiation of RPC in order to understand if their regenerative potential could be compromised.

METHODS

Recombinant human TTRV30M was produced using an *E. coli* expression system and purified by affinity, ion exchange and gel filtration chromatographies. Oligomerization was induced as described by Lindgren *et al*, and assessed by chemical cross-linking and thioflavin T assay.

Viability and proliferation of RPC were evaluated by MTT assay. RPC were treated with soluble and oligomeric TTRV30M for 24, 48 and 72 hours. The results were represented as the ratio: (ODsample – ODblank)/(ODcontrol –Odblank). Average values and SD were calculated from triplicate determinations.

Fluorescence-activated cell sorting (FACS) analysis of annexin V and propidium iodide was used to assess induction of apoptosis. Staining with propidium iodide was used for cell cycle analysis. RPC were tretated with 3 µM of oligomeric TTRV30M for 48 and 72 hours.

RPC differentiation into podocytes i*n vitro* was induced with VRAD medium: DMEM-F12, 0,5% FBS, vitamin D3 and all-trans retinoic acid. For the non differentiation controls, cells were treated with EBM 0,5% FBS. The oligomeric TTRV30M was diluted in the correspondent media at a final concentration of 3 µM. Cells were stimulated for 24 and 48 h. Relative expression levels of the nephrin gene were measured by real time pcr.

RESULTS

The proliferation of RPC treated with oligomeric and soluble TTRV30M for 24 hours was not significantly affected, except for the highest protein concentration (Figure 1A). The treatment with 3 µM oligomeric TTRV30M for 48 and 72 hours reduced RPC proliferation, respectively, 10 and 33%, when compared to the controls. Soluble TTRV30M reduced 25% the proliferation of RPC after 72 hours, what may reflect the natural instability of the tetramer caused by the V30M mutation.

RPC from different patients were treated with 3 µM TTRV30M. On average, the oligomeric TTR reduced RPC proliferation, respectively, 16.3±9.7% and 32.6±6.3% after 48 and 72 h (Figure 1B).

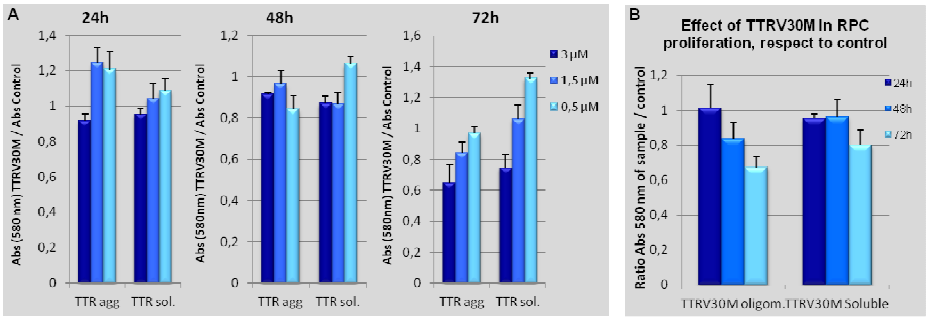

Figure 1. Viability of RPC exposed to TTRV30M, measured by MTT assay. A - RPC treated with 0,5 µM, 1,5 µM and 3 µM TTRV30M for 24, 48 and 72h; B - RPC treated with 3 µM TTRV30M for 24, 48 and 72h; results are shown as mean with indicated standard deviation of triplicate samples from three independent assays.

FACS analysis showed no significant differences between the control and the cells exposed to the TTRV30M oligomers, either for apoptosis or cell cycle progression, either at 48 and 72h (data not shown).

Relative expression levels of the nephrin and the housekeeping gene GAPDH were measured by real time pcr. The results varied between experiments, but on average we obtained similar results between the controls and the cells exposed to TTRV30M aggregates (Figure 2).

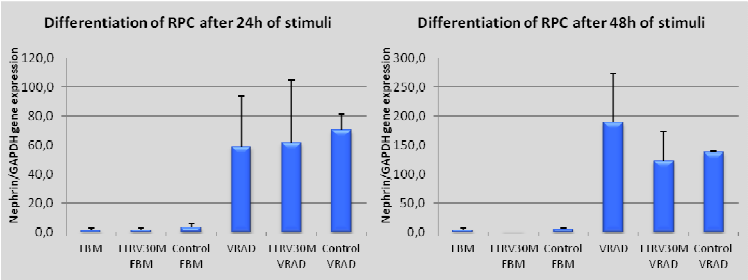

Figure 2. Differentiation of renal progenitor cells into podocytes. Assessment by quantitative RT-PCR of fold increase mRNA levels for the podocyte marker nephrin and the housekeeping gene GAPDH.

DISCUSSION

The mutant TTRV30M reduced proliferation and metabolic viability of renal progenitor cells. However, the FACS analysis of annexin V and propidium iodide did not show induction of apoptosis or necrosis to any significant extent. Also, cell cycle progression was not significantly influenced by the oligomers. The expression level of the nephrin gene, a marker for podocytes, showed no alterations relatively to controls, so the inherent capacity of these progenitor cells to differentiate into podocytes was apparently not affected by the oligomers.

Further studies are needed to elucidate the mechanisms of toxicity in the kidney, particularly the role of oxidative stress. From this first attempt, we can say that TTRV30M oligomers inhibit the proliferation of renal progenitor cells but do not influence their capacity to differentiate into functionally mature podocytes, and thus should not compromise tissue regeneration.

ACKNOWLEDGEMENTS:

This study was supported by Fundação para a Ciência e Tecnologia (FCT) through fellowship SFRH/BD/46441/2008 and co-financed by European Social Fund and POPH program.

REFERENCES

1. Andrade C. A peculiar form of peripheral neuropathy; familiar atypical generalized amyloidosis with special involvement of the peripheral nerves. Brain. 1952; 75(3):408-27.
2. Lobato L, Beirao I, Guimaraes SM, Droz D, Guimaraes S, Grunfeld J, et al. Familial amyloid polyneuropathy type I (Portuguese): Distribution and characterization of renal amyloid deposits. Am J Kidney Dis 1998; 31:940–6.

3. Reixach N, Deechongkit S, Jiang X, Kelly JW, Buxbaum JN. Tissue damage in the amyloidoses: Transthyretin monomers and nonnative oligomers are the major cytotoxic species in tissue culture. PNAS. 2004; 101(9):2817–2822.
4. Sagrinati C, Netti GS, Mazzinghi B, Lazzeri E, Liotta F, Frosali F, et al.Isolation and characterization of multipotent Progenitor Cells from the Bowman's Capsule of Adult Human Kidneys. J Am Soc Nephrol. 2006; 17:2443-6.
5. Lindgren M, Sörgjerd K, Hammarström P. Detection and Characterization of Aggregates, Prefibrillar Amyloidogenic Oligomers, and Protofibrils Using Fluorescence Spectroscopy. Biophysical Journal. 2005; 88:4200–4212

Cardiotoxicity of pre-fibrillar transthyretin oligomers and attenuation by doxycycline

C.M. Koch[1,3], E. Klimtchuk[3], D.C. Seldin[2,3], L.H. Connors[1,3]

Departments of Pathology and Laboratory Medicine[1], and Medicine[2], and Amyloid Treatment and Research Program[3], Boston University School of Medicine, Boston, MA, USA

ABSTRACT

Pre-fibrillar, oligomeric forms of transthyretin (TTR) may be important in TTR cardiac amyloid pathology. We investigated the response of cardiac cells to TTR oligomers and the effect of doxycycline on observed changes. Rat cardiomyocyte (H9C2) cells were treated with native and oligomeric TTR; wild-type and mutant forms (TTR-V30A, -L55P, or -V122I) associated with amyloidotic cardiomyopathy were tested. To generate oligomeric TTR, proteins were incubated at 80 ℃ for 4 hours. Cell viability, assessed after 48 h treatment, was significantly decreased in cells treated with aggregated (4 hours) forms of TTR-V30A and -L55P. Cells treated with mutant TTR heated for 4 hours in the presence of doxycycline at 50:1(dox:TTR) showed significantly increased viability compared to cells treated with oligomers/no drug. These data suggest that aggregated forms of TTR-L55P and -V30A have a potent effect on cardiac cell viability and provide evidence that doxycycline may inhibit formation of amyloidogenic TTR oligomers.

INTRODUCTION

Aggregation of transthyretin (TTR) can lead to amyloid fibril formation and deposition, which frequently occurs in the myocardium. Pre-fibrilllar, oligomeric forms of TTR may be important in TTR cardiac amyloid pathology. It has previously been shown that doxycycline disrupts TTR amyloid fibrils in an FAP mouse model (1,2). Furthermore, Ward *et al*. have recently reported that doxycycline blocks immunoglobulin light chain (LC) amyloid formation *in vitro*, disrupts the structure of *ex vivo* LC fibrils, and inhibits amyloid deposition *in vivo* in a transgenic mouse model of AL amyloidosis (3). Based on this evidence, we investigated the ability of doxycycline to modulate cardiotoxicity in cells treated with cardiac-associated, amyloidogenic forms of TTR including wild-type, L55P, V30A, and V122I.

METHODS

Oligomer formation assay. Recombinant TTR (rTTR) proteins were solubilized in PBS at 0.4 mg/mL and incubated in presence or absence of doxycycline (1:50 molar excess). Mixtures were incubated at 80 ℃ for 4 hours. Aliquots were removed at timed intervals (0 - 4 hours) for cell studies and electrophoretic analysis.

Congo red binding analysis. Solutions of 0.4 mg/mL rTTR in PBS were incubated at 80 ℃ for 1 week. Following incubation, samples were centrifuged at 25000 x g for 10 minutes. Each pellet was reconstituted in 10 μM Congo red. Absorbance was monitored in a wavelength scan from 350 to 700 nm.

Electrophoretic analysis. Oligomer formation samples were cross-linked with 25% glutaraldehyde and electrophoresed on 10% SDS-PAGE reducing gels and stained with GelCode Blue Stain (Pierce).

Cell culture studies. Rat cardiomyocyte (H9C2) cells were treated with native and oligomeric forms of rTTR. TTR proteins tested included wild-type, L55P, V30A, and V122I. The rTTR solution (0.2 mg/mL) was heated for 0 or 4 hours in the presence or absence of doxycycline at 50 molar excess of drug. Cell viability was assessed after 48 hour treatment using an ApoToxGlo kit (Promega). Data was analyzed using ANOVA and unpaired two-tailed t-test; statistical significance was $p < 0.05$.

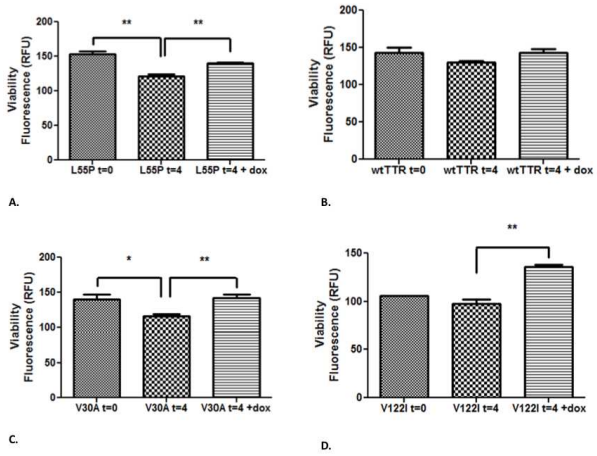

Figure 1. (A) Cells treated with TTR-L55P oligomers from 4 hours (t=4) at 80 ℃ have significantly decreased viability ($p<0.01$), which is recovered when doxycycline is present ($p<0.01$) **(B)** No significant decrease in viability in cells treated with wild-type TTR **(C)** Cells treated with TTR-V30A heated for 4 hours at 80 ℃ (t=4) were significantly less viable ($p<0.05$) than cells treated with native (t=0) TTR; this effect was significantly recovered when doxycycline was present **(D)** Cell viability was not significantly decreased with the TTR-V122I mutant. Viability was increased ($p<0.01$) in the heated sample when doxycycline was present.

RESULTS

As is shown in Figure 1, cardiac cell viability was significantly lowered when cells were treated with TTR-L55P and -V30A oligomers (t=4 hours). TTR-V122I and wild-type showed minimal effects. Moreover, cells treated with TTR-L55P, -V30A, or -V122I samples heated in the presence of doxycycline showed significantly increased cell viability compared to those treated with TTR oligomers ($p<0.01$). As is shown in figure 2, SDS-PAGE analysis revealed that doxycycline inhibited TTR oligomer formation in the heat-mediated amyloid oligomer formation assay. A decreased presence of TTR high molecular weight species, as well as, an increased amount of monomeric TTR was noted in the presence of doxycycline. Moreover, we showed by surface plasmon

resonance (SPR) that there is a concentration-dependent interaction between doxycycline and wild-type, as well as L55P-TTR (data not shown).

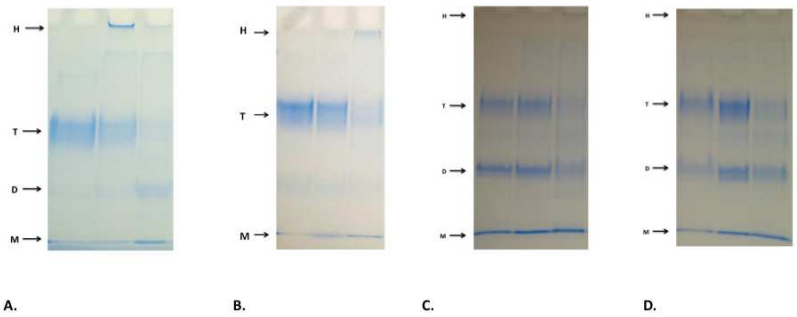

Figure 2. SDS-PAGE analysis of the TTR samples. Compared to 0 hour timepoints (left lane), after 4 hours at 80 ºC (middle lane), there are HMW (H) species present in the **(A)** TTR-L55P, **(B)** -wt, **(C)** –V30A and **(D)** –V122I samples; these species are much less abundant when TTR proteins are heated in the presence of doxycycline (right lane). In addition, an increased amount of monomeric forms (M) of TTR is observed when doxycycline was present in –L55P and –wt samples, as well decreased tetrameric (T) and dimeric (D) forms of the TTR-V30A and -V122I

DISCUSSION

These results provide evidence that TTR oligomers generated by thermal denaturation are toxic to cardiomyocytes and cause a decrease in viability. Interestingly, the aggregated forms showing the strongest effect on viability were the mutants with earlier disease onsets in the patient population (L55P and V30A). In addition, our data suggests that doxycycline prevents the formation of amyloidogenic, pre-fibrillar forms of TTR. It is possible that doxycycline promotes the formation of amorphous TTR aggregates or dissociation of aggregated forms of TTR, driving the equilibrium back toward monomeric forms. Alternatively, the drug may act by directly preventing monomeric forms to self-associate into TTR oligomeric species.

ACKNOWLEDGEMENTS

Support for this work provided by the Young Family Amyloid Research Fund and the NIH grant R01AG031804 (LHC). Many thanks to the Amyloidosis Foundation for granting me a Travel Award which allowed me to attend and present my work at the ISA conference.

REFERENCES

1. Cardoso I, et al. Synergy of combined doxycycline/TUDCA treatment in lowering Transthyretin deposition and associated biomarkers: studies in FAP mouse models. J Transl Med 2010; 30(8):74
2. Cardoso I, Saraiva MJ. Doxycycline disrupts transthyretin amyloid: evidence from studies in a FAP transgenic mice model. FASEB J. 2006; 20(2):234-9

3. Ward JE. Doxycyline reduces fibril formation in a transgenic mouse model of AL amyloidosis. Blood. 2011; 118(25):6610-7
4. Connors LH, et al. Tabulation of human transthyretin (TTR) variants. Amyloid. 2003:10(3);160-84

Investigation on the functional consequences of amyloidogenic light chains on *Caenorhabditis elegans*

Paola Rognoni[1], Luisa Diomede[2], Margherita Romeo[2], Francesca Lavatelli[1], Veronica Valentini[1], Giovanni Palladini[1], Vittorio Perfetti[1], Mario Nuvolone[1], Mario Salmona[2] and Giampaolo Merlini[1]

[1]Amyloid Research and Treatment Center, Foundation IRCCS Policlinico San Matteo, Pavia, Italy,
[2]Department of Molecular Biochemistry and Pharmacology, Instituto di Ricerche Farmacologiche "Mario Negri", Milan, Italy

ABSTRACT

In AL amyloidosis, cardiac involvement is common and is the leading cause of death (1). Using the nematode *Caenorhabditis elegans*, whose pharynx is considered an orthologous of the vertebrate heart (2), we developed a behavioral test to assess the cardiotoxic potential of amyloidogenic LC. This test was based on the evaluation of the ability of LC to reduce the muscular pumping contractility of the nematode's pharynx. Results indicate that the pumping rate was significantly impaired only in nematodes fed with cardiotoxic amyloidogenic LC, whereas LC with different organ tropism had no effect. The *C. elegans* was here used, for the first time, as a model to investigate the tissue-specific toxicity of LC.

INTRODUCTION

Systemic amyloidoses are protein misfolding diseases characterized by the widespread interstitial deposition of proteins as amyloid fibrils, which leads to alteration of organ architecture and cellular toxicity. Cardiac involvement is common and is the leading cause of death (1). In vitro evidence indicate that soluble, prefibrillar amyloidogenic LC, rather than fibrils themselves, may be directly cardiotoxic (3-5). In order to investigate the tissue-specific toxicity of LC, we designed a new in vivo assay in the model organism *Caenorhabditis elegans.* The pharynx of this invertebrate nematode is considered to be evolutionarily related to the vertebrate heart because its muscles cells have autonomous contractile activity reminiscent of cardiac myocytes. Besides, both organs rhythmically and continuously contract for all the life of the organism and their contraction relies on similar electrical circuitry which can continue in the absence of neuronal input (2,6).

Our *Caenorhabditis elegans*-based behavioural test evaluates the cardiotoxic potential of amyloidogenic LC, on the basis of their ability to reduce the muscular pumping motions of the nematode's pharynx.

METHODS

Monoclonal LC were isolated from patients' 24 hours urine collection. In parallel to cardiotoxic amyloidogenic LC, non-cardiotoxic amyloidogenic LC and non-amyloidogenic LC were purified, as controls. The cardiotoxicity of LC was assessed in each patient from clinical, biochemical and instrumental parameters (7). Urine proteins were purified by ion-exchange chromatography, the homogeneity of the isolated species was assessed by SDS-PAGE and immunoblotting. N2 ancestral nematodes were fed with soluble LC (100 μg/mL) for 2 hours, transferred onto fresh NGM agar seeded with *E. coli* and the pharyngeal motion was measured (in terms of beats per minute) 20 hours after exposition.

Table 1. Clinical and laboratory characteristics of patients with AL amyloidosis and controls included in the study. MM1 and MM2 patients were affected by multiple myeloma without amyloidosis. Subcutaneous abdominal fat biopsy was performed in all cases; negativity to Congo red staining was assessed only in MM1 and MM2 patients.

Patient code	Gender, age	Main organ involved	iFLC (mg/L)	BNP (ng/L)	cTnI (ng/mL)	IVS (mm)
H1	M, 73	Heart	λ, 683	866	0.20	15
H2	M, 47	Heart	λ, 477	707	0.16	19
H3	M, 54	Heart	λ, 839	411	0.22	17
H4	M, 72	Heart	λ, 383	1926	1.19	15
K	F, 69	Kidney	λ, 228	36	< 0.04	10
ST	F, 55	Soft tissues	λ, 1220	43	< 0.04	12
MM1	F, 72	Myeloma	λ, 6130	42	< 0.04	9
MM2	M, 64	Myeloma	λ, 5410	60	< 0.04	9

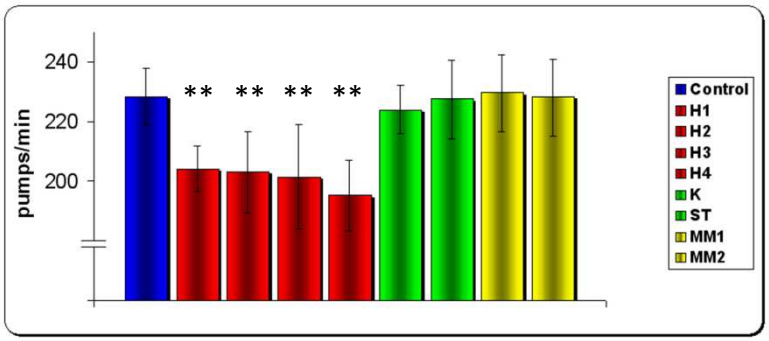

Figure 1. The pumping rate measured in N2 worms after exposure to the different light chains. Values are the means±s.d., n=10. **p<0.01 vs control, Student's T-test.

RESULTS

Eight different LC with different organ tropism were tested (Table 1).

The pumping rate was significantly impaired of 15-20% ($p<0.05$, Student's t-test) only in nematodes fed with the cardiotoxic amyloidogenic LC, whereas solutions containing non-cardiotoxic amyloidogenic LC and non-amyloidogenic LC had no effect (Figure 1).

CONCLUSIONS

The *C. elegans* was here used, for the first time, to investigate the tissue-specific toxicity of LC. This nematode-based assay is a promising surrogate model for investigating the heart-specific toxicity of amyloidogenic light chains, and could be used for assessing the mechanisms of disease and for a rapid screening of the biological effects of LC.

REFERENCES

1. **Biochim Biophys Acta** 2005;1753:11-22.
2. **WormBook** 2007; 22:1-26.
3. **Circulation** 2001;104:1594-7.
4. **Circ Res** 2004;94:1008-10.
5. **PNAS** 2010;107:4188-93
6. **J Exp Biol** 2003;206:2441-57.
7. **Circulation** 2003;107:2440-5.

Ataxin 3 amyloid aggregates interacting with rat cerebellar granule cells induce dysregulation of calcium homeostasis

F. Pellistri[1], A. Relini[1], E. Gatta[1], G. Invernizzi[2], P. Tortora[2], M. Stefani[3], A. Gliozzi[1] and M. Robello[1]

[1]Department of Physics, University of Genoa, Italy, [2]Department of Biotechnology and Biosciences, University of Milano-Bicocca, Italy, [3]Department of Biochemical Sciences, University of Florence, Italy

ABSTRACT

Several human neurodegenerative diseases are associated to the expansion over a defined threshold of a polyglutamine (poly Q) encoding triplet in the relative genes. Affected individuals have repeats in the 36-180 range, while normal individuals have between 6 to 39 glutamine repeats. Aggregates of the proteins with expanded poly(Q) display amyloid-like morphological and biophysical properties. Actually, early oligomers have been identified as the primary species responsible for the events associated to deregulation of biochemical homeostasis and in particular to the damage arising from abnormal neuronal Ca^{2+} signaling. We studied the correlation between the Ca^{2+}signaling, due to the interaction between neurons and aggregates and the properties of the aggregates. So we investigated the changes in the intracellular Ca^{2+} levels produced by oligomers formed by variants of Ataxin 3 in cerebellar granule cells. We used two expanded forms of ataxin 3: a pathological protein variant, a non pathological protein and a truncated variant to compare the effects produced by aggregates with different morphological features,

INTRODUCTION

Ataxin 3 (ATX3) is a 43 kD cytosolic protein containing an N-terminal Josephin domain (JD) and a poly(Q) expansion in the C-terminal region. In the present work we used a non-pathological ATX3 form (ATXQ26), a pathological expanded form (ATXQ55), and a variant truncated at residue 291 lacking the poly(Q) expansion (ATX/291Δ). While all these forms aggregate into soluble amyloid assemblies which persist under aggregating conditions at 37 ℃, only ATXQ55 aggregates into bu ndles of elongated mature fibrils after 48 h of incubation (1).

In this work we analyzed the relation between the morphological properties of ATX aggregates containing normal or pathological poly(Q) expansions and the abnormal Ca^{2+}signaling resulting from the interaction of these aggregates with neuronal cells. In particular, we investigated the changes in the intracellular Ca^{2+} levels following their interaction with rat cerebellar granule cells. Morphologically different aggregates of ATXQ55 were characterized at various incubation times by AFM analysis, whereas ATXQ26 and ATX/291Δ aggregates displayed a similar morphology over the entire aggregation time. The reported results suggest that ATXQ26,

ATXQ55 and ATX/291Δ oligomers elicited qualitatively similar time-dependent intracellular Ca2+ responses, however with dissimilar"efficacy", the latter being remarkably reduced in cells exposed to ATXQ26. At longer times of ATXQ55 aggregation preceding full fibril presence a quite different time-dependent response was observed. Furthermore, while cell interaction with ATXQ55, ATXQ26 and ATX/291Δ oligomers involved both glutamatergic receptors and GM1 monosialoganglioside-rich membrane domains, the interaction with ATXQ55 pre-fibrillar aggregates resulted in membrane disassembly by a mechanism involving only the GM1 ganglioside. Interestingly, we found that neural cell apoptosis resulted from cell exposure to ATXQ55 and ATX/291Δ aggregates while ATXQ26 was substantially harmless to the cells. The importance of GM1 for ATX aggregate toxicity was confirmed by cell protection against ATXQ55 and ATX/291Δ toxicity upon ganglioside depletion.

METHODS

Full length ATX(Q55), ATX(Q26) and the truncated form. ATX /291Δ were purified as described previously (1) provided by the group of prof Paolo Tortora, University of Milano-Bicocca. togliere

Cell culture. Cerebellar granule neurons were prepared from 8-days-old Sprague-Dawley rats following the procedure of Levi and collaborators (2) In particular, the cells were studied from the 6th to the 10th day in vitro. By contrast, in the experiments on immature neurons, the granules were used after the 1st or the 2nd day.

Fluorescence Measurements. The neuronal cells were incubated with Oregon Green AM ester (Molecular Probes, Eugene, OR) observed with a Nikon Eclipse TE300 inverted microscope. The fluorescence signal, including real time changes of the internal calcium concentration in cells exposed to protein aggregates, was detected using a Hamamatsu digital CCD camera with appropriate filters (Nikon Italia, Florence, Italy). The images were acquired with the Simple PCI software (Compix Imaging Systems, Hamamatsu Corp., Sewickley, PA). Measurements in the presence of antagonists of glutamatergic receptors were performed using CNQX and APV (Sigma Chemical Co., St Louis, MO, USA).

Sialic acid cleavage from membrane GM1. Cerebellar granule cells were starved by incubation with DMEM serum-free media for 3.0 h at 37 ℃. Then cells wer e left for 2.0 h in the presence of a mixture composed of V. cholera (11,7 mU, Sigma Aldrich) and C. perfringens (100mU, Sigma Aldrich) neuraminidase.

Atomic force microscopy. ATX was aggregated at a 1.0 mg/ml-concentration in PBS at 37 ℃. Samples for AFM inspection were prepared as described previously (1). Tapping mode AFM images were acquired as described in (3).

RESULTS

Isolated globular particles, identified as protein oligomers, were imaged using tapping mode atomic force microscopy at early stages of ATXQ55 aggregation, whereas the first bundles of fibrils appeared after 24 h and became very abundant after 48 h. A different behavior was found for ATXQ26 and ATX291Δ, which did not form fibrils at our experimental aggregation times.

A fast increase, followed by a slower decrease, of the fluorescence intensity of cerebellar granule cells loaded with Oregon Green upon exposure to ATXQ55 oligomers was recorded, indicating a sudden rise, followed by a slower drop, of the intracellular free Ca^{2+} . The mean time associated to the fluorescence signal was 61±8 s and the signal reached its maximal value after about 20 s (Figure 1).

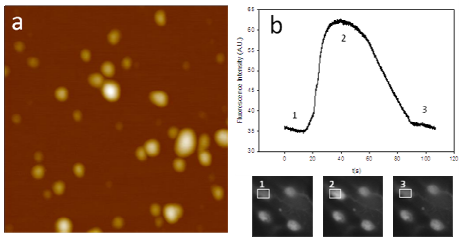

Figure 1

Figure 1a and 1b show a representative image of neuronal cells exposed to ATXQ55 oligomers aged 4 h and a typical time course of the average fluorescence intensity of the same exposed cells, respectively. We have indicated this behavior as type 1 response. The lower part of Figure 1b shows three time-dependent fluorescence images of granule cells loaded with Oregon Green.

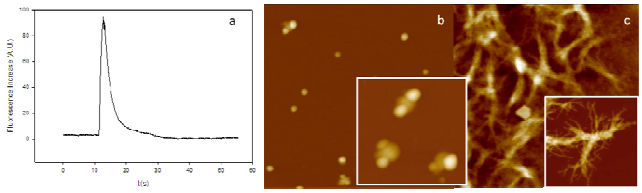

Figure 2

Beside type 1 response, we recorded another type of fluorescence response in the same cells exposed to ATQ55 aggregated for longer times (14, 24 or 48 h); in these cases, we also noticed a much shorter spike-like response (type 2 response) characterized by a mean time of 13 ± 1 s (Figure 2a). The occurrence of either response was dependent on the morphology of differently aged aggregates. In fact, after 14 h, AFM inspection showed a complex morphology of the aggregates: in addition to isolated globular oligomers, coalesced oligomers (Fig. 2b) and large clusters of aggregates (inset)were also found. Fig. 2c shows the fibrillar structures found after 48 h, while the inset shows the insoluble fibrillar fraction recovered by sample treatment with SDS and centrifugation. To check whether the type 2 fluorescence response was related to the presence of fibrils or to pre-fibrillar assemblies like those shown in Fig.2b, we separated the soluble and insoluble fraction of 24 h-aged aggregates by centrifugation. The results indicated that while the soluble fraction still elicited both type one and type two responses, the insoluble fraction, composed mainly by fibrillar aggregates, was completely inactive. This suggests that the soluble aggregates of ATXQ55 display a significant correlation between aggregate structure (oligomeric or pre-fibrillar) and the fluorescence signal.

To better elucidate the contribution of the poly(Q) tract to the modification of the membrane permeability to Ca^{2+} in aggregate-exposed cells, we also investigated the fluorescence response of neuronal cells exposed to ATXQ26 and to ATX/291Δ, aggregated at 37 ℃ for different lengths of time . Normal ATXQ26 and ATX/291Δ aggregates produced only type 1 response. These results suggest that type 2 response is related to the presence of pre-fibrillar assemblies representing a later aggregation stage than that of isolated oligomers.

We repeated the fluorescence experiments by exposing the cells to ATXQ55 aggregates in the presence of 10 μM CNQX, which hinders membrane depolarization thus maintaining the NMDA-R block by the Mg2+ ions. When the cells were exposed to 24 h aged ATXQ55 aggregates in the presence of CNQX, the efficacy of cell response W(F) value (defined as the product of % of responding cells and the relative intensity of the fluorescence response) decreased by about 80%. A minor decrease of W(F) (about 30%), was recorded in the presence of APV (an NMDA-R competitive antagonist). Effects qualitatively similar to type 1 response were obtained by exposing the cells to ATX/291Δ or ATXQ26 aggregates in the presence of APV or CNQX. No significant changes of W(F) were detected when the cells were exposed to ATX Q55 variants aged 24 h in the presence of Cd^{2+} , a Ca^{2+}voltage dependent (VDCCs) channel blocker, while an effect was observed when the cells were exposed to ATXQ55 aged 6h or to ATXQ26 aged 24h.These results are summarized in Table 1. In contrast with these results, no significant changes of type 2 response were detected in the presence of CNQX, APV or Cd^{2+} , suggesting that this response, due to pre-fibrillar aggregates, is not related to any interaction of ATXQ55 pre-fibrillar structures with glutamatergic receptors or VDCCs.

To further elucidate the mechanism of interaction of ATX aggregates with the cell membrane, we treated mature granule cells, with a mixture of neuraminidases to specifically cleave the GM1sialic acid component. We found that in neuraminidase-treated cells the aggregate-driven Ca^{2+} influx was noticeably reduced and type 2 response elicited by the pre-fibrillar ATXQ55aggregates was completely abolished (Table 1).

Table 1

Condition	AT3Q55 ΔW/W (%) Type 1	AT3Q55 ΔW/W (%) Type 2	AT3/291Δ ΔW/W (%)	AT3Q26 ΔW/W (%)
Cd^{2+}	0	0	0	-65± 5
APV	−41 ± 9	0	−49 ± 7	-56 ± 10
CNQX	−82 ± 14	0	−59 ± 7	-44 ± 11
Ganglioside-depleted cells	−41 ± 12	−100 ± 4	−75 ± 13	-33 ± 2

DISCUSSION

The results show that the ”efficacy” W(F) was almost independent of the aggregation time in the case of ATXQ26 and ATX/291Δ aggregates, in agreement with the persistence of the oligomeric aggregates of these variants over the investigated aggregation times. In contrast, ATXQ55 showed a more complex behavior, due to the the changes of aggregate morphology at different aggregation times. When large oligomeric assemblies were widespread in the sample the highest values of Ca2+ influx was observed, whereas when oligomers, prefibrillar and fibrillar structures co-existed with a parallel decrease of oligomer abundance, W(F) value declined. As the isolated fibrillar fraction did not produce any fluorescence response, the type 2 response is due to cell interaction with individual prefibrillar structures, imaged at longer aggregation times.

It is likely that the presence of the expanded poly(Q) tract of 55 consecutive glutamine residues dramatically favors irreversible aggregation and fibril growth.

Increasing evidence has shown that lipid rafts play a crucial role in amyloid associated neurodegenerative diseases (reviewed in 9). Our results indicate that GM1depletion significantly reduced type 1 response in cells exposed to ATX oligomers. Therefore, we conclude that interaction of amyloid oligomers with glutamatergic receptors requires that membrane rafts are integer. In particular, we confirm that GM1, and its sialic acid moiety are required for most favorable interaction of the cell membrane with amyloid oligomers, as previously reported for oligomers of other peptides/proteins.

REFERENCES

1. A. Natalello, et al. (2011) PLoS ONE 6, e18789.
2. Robello et al.(1993) Neuroscience 53(1):131-8.1993
3. S. Campioni, et al(2010) Nature Chem. Biol. 6, 140-147
4. Kayed R. et al. (2003) Science. 300(5618):486-9,;
5. Demuro A., et al. (2005) J. Biol. Chem. 280, 17294-17300
6. Bucciantini et al. (2002) Nature. 416(6880):507-11
7. S. Baglioni, et al.(2006) J. Neurosci., 26: 8160-8167
8. Pellistri et al. (2008) J Biol Chem. 283(44):29950-60
9. Malchiodi-Albedi, F. et al. Int. J. Alz. Dis.2011, 906964, 1-17

SECTION III

ANIMAL MODELS AND CELL CULTURE SYSTEMS


Spectral Imaging
Bringing Details to Light
THAOS:
Monday

STATE OF THE ART AND PERSPECTIVES: Animal models and cell culture systems

M.J. Saraiva[1] and B. Kluve-Beckerman[2]

[1]Institute for Molecular and Cellular Biology, IBMC, University of Porto, Portugal
[2]Indiana University School of Medicine, Department of Pathology and Laboratory Medicine, Indianapolis, Indiana, USA

Animal models have long been used to study amyloid pathogenesis, and cell culture systems are being used with increasing frequency. AA amyloidosis can be induced in laboratory animals via establishment of chronic inflammation and mimicked in macrophage cultures by providing cells with either SAA-enriched HDL or lipid-free recombinant SAA. Transthyretin amyloidosis (ATTR), however, does not occur naturally in species other than man and cannot be experimentally induced. Therefore, transgenic mice carrying human TTR genes, either wild-type or variant, have been developed and are actively being used in studies of ATTR. In addition to AA and ATTR amyloidoses, other types including AL and $A\beta_2M$ as reported in this session, are now being studied using a diversity of models, e.g., pluripotent stem cells, *Drosophila melanogaster,* and *C. elegans*. The State of the Art and Perspectives talks for this session focus on TTR and AA amyloidoses, respectively, as these two types have been the most extensively investigated in animal models and cell culture systems.

ANIMAL MODELS AND CELL CULTURE SYSTEMS OF ATTR AMYLOIDOSIS

Mice models: Transgenic TTR rodent models for human mutant TTR have been useful to address different questions related to: (i) formation and resolution of deposits; (ii) molecular mechanisms of pathogenesis; (iii) “in vivo” modulating factors which allow the development of novel therapies.

To study age related TTR deposition in the heart, a feature of senile systemic amyloidosis, transgenic mice was generated over- expressing human wild type TTR. Most animals older than 18 months presented TTR amyloid deposits in the heart and kidney. At early ages animals had diffuse non-fibrillar deposits in the same organs (1).

Several groups produced transgenic mice carrying the human *ttr* V30M gene with and without the endogenouse mouse TTR as models for familial amyloidotic polyneuropathy (FAP). Generally, amyloid was observed starting at age 6 months; at 24 months the pattern of amyloid was similar to that observed in human autopsy cases of FAP, with exception of amyloid presence in the choroid plexus and in peripheral and autonomic nervous systems (2). Other transgenic animals with constructs for different TTR mutants, such as TTR L55P (3) or I84S (4) were also generated. The L55P model presented early non-fibrillar TTR deposition starting at age 1-3 months, and later, at age 4-8 months; mice presented fibrillar deposits in the gastrointestinal

(GI) track and skin; however, no evidence for TTR deposits in the peripheral and autonomic nervous system was found.

In 2010, a new FAP mouse model (hTTR HSF1) was generated, carrying the human TTR V30M in a heat shock transcription factor 1 (HSF1) knock- out background (5). hTTR HSF1 transgenic mice presented early and extensive TTR deposition and for the first time non-fibrillar deposits were observed in the autonomic and peripheral nervous system. The TTR/HSF-1 model allows different studies not possible with previous models. Sural-nerve biopsies, on which most of the pathological analyses in FAP have been performed, represent a restricted portion of the peripheral nervous system, and it is clearly possible that TTR deposits in ganglia, or more proximally in nerve trunks could be responsible for distal nerve fiber loss. The possibility to analyze dorsal root ganglia (DRG) with deposition in the TTR/HSF-1 mouse model is invaluable, and permits a close evaluation of events occurring in sensory and autonomic neurons responsible for neurodegeneration and in the assessment of therapies. For instance, increased inflammatory stress in DRG and nerve, as studied by expression of interleukin 1- Beta and a reduction in unmyelinated nerve fibers were observed, as in human patients, indicating that HSF-1-regulated genes are involved in FAP, modulating TTR tissue deposition. MMP9 apparently is a good biomarker for the presence of TTR amyloid as suggested by gene arrays of amyloid ladden FAP tissues. Data from studies on TTR transgenic mice recapitulate the human situation as only mice with amyloid deposits displayed increased levels and activity of MMP-9 as compared to younger animals without fibrillar deposits (6).

Inhibition of aggregate formation and/or disruption of pre-formed TTR deposits has been sucessfuly approached in the V30M TTR transgenic mice. Thus, it was recently shown (7) that combined cyclic drug administration of doxycycline and taurodexocolic acid TUDCA, resulted in significant reduction in TTR deposition and associated tissue markers in the TTR V30M transgenic mouse model. The observed synergistic effect of doxycycline/TUDCA within the range of human-tolerable quantities prompted their application in FAP, particularly in the early stages of disease.

The above described mice models have not yet addressed how do organs/systems function, namely liver, heart, kidney, GI tract and the peripheral and autonomic nervous systems. Thus, there are some limitations to their use. Besides, intra and interspecies (with humans) variability occurs due to (i) differences in tissue composition, architecture and barriers; (ii) ligands, endogenous counterparts and metabolism; (iii) environment; (iv) genetic background; (v) diet.

Alternative models include Insects, Nematodes and cell culture methodologies, which have on their own important limitations, such as (i) the use of synthetic material; (ii) up-regulation/suppression of genes under culture conditions; (iii) intra vs extracellular aggregation; (iv) absence of normal ligands; (v) absence or primitive extracellular matrix; (vi) absence or significant differences of specialized systems as the immune and nervous systems (e.g., myelin).

Drosophila model: Transgenic flies, expressing the clinical amyloidogenic L55P TTR variant and the engineered variant TTR-A (TTRV14N/V16E) as well as the wild-type protein, were generated, all in secreted form. Within a few weeks, both mutants but not the wild-type TTR demonstrated a time-dependent aggregation of misfolded molecules. This was associated with neurodegeneration, change in wing posture, attenuation of locomotor activity including compromised flying ability and shortened life span. In contrast, expression of wild-type TTR had no discernible effect on either longevity or behavior (8). The TTR flies are amenable for drug screening purposes.

Cellular systems: A cellular system was created using transfected cells expressing L55P TTR, precluding isolation of the target protein and representing a more physiological in vitro approach to study inhibitors of amyloidogenesis (9). Aggregated L55P accumulates in conditioned media and is retained in a filter; quantification of the retained material is indicative of the anti-amyloidogenic properties of the drugs under study.

ANIMAL MODELS AND CELL CULTURE SYSTEMS OF AA AMYLOIDOSIS

Animal models: AA amyloidosis occurs naturally in many species and can be experimentally induced by establishing chronic inflammation via injection of such agents as casein, LPS, Freund's adjuvant, and silver nitrate plus amyloid-enhancing factor (AEF). Animals used for amyloid induction include rabbits, hamsters, mink, and most commonly mice. In addition, transgenic mice overexpressing IL-6 spontaneously develop AA amyloidosis, and transgenic mice in which mouse SAA1.1 production is controlled by doxycycline develop AA amyloidosis in the absence of predisposing inflammation. Amyloid pathogenesis in all of the animal models closely mimics the natural history of the human disease. Animals very reproducibly show amyloid deposition sequentially in spleen, liver, intestine, and kidneys. These models, especially the casein (classic) and silver nitrate plus AEF (accelerated) models, have contributed invaluably to our understanding of both AA amyloidosis and serum amyloid A (SAA), the precursor protein of AA fibrils. Seminal findings discovered and/or verified in the mouse model include: AA amyloidosis develops secondary to inflammation; SAA is the precursor to and constituent of AA fibrils; SAA is a hepatically-derived plasma protein carried on HDL; SAA production is stimulated by inflammatory cytokines TNF, IL-1, and IL-6; AA amyloid deposition is nucleation-dependent; and glycosaminoglycans (GAGs), heparan sulfate in particular, co-deposit with AA fibrils. The mouse model continues to serve as the gold standard in which to test new compounds for efficacy against amyloid development and progression.

Table 1. Cell culture systems in use for AA amyloid research

Cell type	SAA	AEF	Reference
Mouse peritoneal mφ, primary	Mouse rSAA1.1	+/−	11
Human fibroblast, primary	Mouse rSAA1.1	+	12
Mouse mφ, J774 cell line	Mouse SAA-HDL	+	13
Human PBMC	Mouse rSAA1.1	+/−	14
Human PBMC	Human rSAA1	−	This meeting
Human fibroblast, primary	Human rSAA1	−	This meeting

Cell culture systems: Cell culture systems offer an alternative approach for studying amyloid pathogenesis. Over ten years ago, Shirahama and colleagues showed that peritoneal macrophages from amyloidotic mice cultured in acute phase (SAA-rich) serum developed amyloid-like deposits associated with macrophage clusters (10). Since then, amyloid formation has been demonstrated in several types of cell culture systems maintained in SAA-supplemented medium (Table 1). Neither the addition of SAA to cultures nor the process of AA

amyloidogenesis is cytotoxic. The amount of amyloid, identified as Congo red-stained, green birefringent material, is directly proportional to SAA concentration and duration of incubation with SAA and is accelerated and augmented by AEF. The insoluble material extracted from cultures comprises both full-length SAA and N-terminally intact, C-terminally processed SAA fragments. Amyloid formation in cell cultures is accompanied by increased GAG production. Furthermore, SAA interaction with GAGs, heparan sulfate in particular, has been shown to be a critical step in amyloidogenesis (13). Until now, all culture systems have utilized highly amyloidogenic mouse SAA1.1. In this session, an all human cell culture system is presented for the first time. Conversion of human SAA 1.1, 1.3, and 1.5 into amyloid is demonstrated in human PBMC cultures maintained in serum-free medium without the use of AEF.

REFERENCES

1. Teng MH, Yin JY, Vidal R, Ghiso J, Kumar A, Rabenou R, Shah A, Jacobson DR, Tagoe C, Gallo G, Buxbaum J. Amyloid and nonfibrillar deposits in mice transgenic for wild-type human transthyretin: a possible model for senile systemic amyloidosis. Lab Invest. 81:385-396 (2001).
2. Kohno K, Palha JA, Miyakawa K, Saraiva MJ, Ito S, Mabuchu T, Blaner WS, Iijima H, Tsukahara S, Episkopou V, Gottesman ME, Shimada K, Takahashi K, Yamamura K, Maeda S. Analysis of amyloid deposition in a transgenic mouse model of homozygous familial amyloidotic polyneuropathy. Am J Pathol., 150: 1497-1508 (1997).
3. Sousa MM, Fernandes, R, Palha JA, Taboada A, Vieira P, Saraiva MJ. Evidence for early cytotoxic aggregates in transgenic mice for human transthyretin Leu55Pro. Am J Pathol 161:1935-1948 (2002).
4. Benson MD, Kluve-Beckerman B, Zeldenrust SR, Siesky AM, Bodenmiller DM, Showalter AD, Sloop KW. Targeted suppression of an amyloidogenic transthyretin with antisense oligonucleotides. Muscle Nerve 33:609-618 (2006).
5. Santos SD, Fernandes R, Saraiva MJ. The heat shock response modulates transthyretin deposition in the peripheral and autonomic nervous systems. Neurobiology of Aging. 31:280-289 (2010).
6. Cardoso I, Brito M, Saraiva MJ. Extracellular matrix markers for disease progression and follow-up of therapies in familial amyloid polyneuropathy V30M TTR-related. Dis Markers. 25:37-47 (2008).
7. Cardoso I, Martins D, Ribeiro T, Merlini G, Saraiva MJ. Synergy of combined Doxycycline/TUDCA treatment in lowering Transthyretin deposition and associated biomarkers: studies in FAP mouse models. J Translational Medicine. 8: 74-78 (2010).
8. Pokrzywa M, Dacklin I, Vestling M, Hultmark D, Lundgren E, Cantera R. Uptake of aggregating transthyretin by fat body in a Drosophila model for TTR-associated amyloidosis. PLoS One 5:e14343 (2010).
9. Cardoso I, Almeida MR, Ferreira N, Arsequell G, Valencia G, Saraiva MJ. Comparative *in vitro* and *ex vivo* activities of selected inhibitors of transthyretin aggregation – relevance in drug design. Biochem J. 408:131-138 (2007).
10. Shirahama T, Miura K, Ju S-T, Kisilevsky R, Gruys E, Cohen A. Amyloid enhancing factor-loaded macrophages in amyloid fibril formation. Lab Invest 62:61-68 (1990).

11. Kluve-Beckerman B, Liepnieks JJ, Wang L, Benson MD. A cell culture system for the study of amyloid pathogenesis. Amyloid formation by peritoneal macrophages cultured with recombinant serum amyloid A. Am J Pathol 155:123-133 (1999).
12. Magy N, Liepnieks, JJ, Benson MD, Kluve-Beckerman B. Amyloid-enhancing factor (AEF) mediates amyloid formation on fibroblasts via a nidus/template mechanism. Arthritis Rheum 48:1430-1437 (2003).
13. Elimova E, Kisilevsky R, Szarek WA, Ancsin JB. Amyloidogenesis recapitulated in cell culture: a peptide inhibitor provides direct evidence for the role of heparan sulfate and suggests a new treatment strategy. FASEB J 18:1749-1751 (2004).
14. Magy N, Benson MD, Liepnieks JJ, Kluve-Beckerman B. 2007. Cellular events associated with the initial phase of AA amyloidogenesis: insights from a human monocyte model. Amyloid 14:51-63 (2007).

Anti-amyloid drug development using Drosophila as a model

D. Segal[1], R. Scherzer-Attali[1], S. Peled[1], R. Shaltiel-Karyo[1], M. Frenkel-Pinter[1], D. Farfara[2], D. Frenkel[2], E. Gazit[1]

Dept. Molecular Microbiology & Biotechnology[1], Dept. Neurobiology[2], George S. Wise Faculty of Life Sciences, and Sagol School for Neurosciences, Tel Aviv University, Tel Aviv 69978, Israel

Drosophila offers an attractive model for drug development which can reduce the use of vertebrates and cut costs. In addition, the wealth of genetic information and tools available for the fruit fly are highly conducive for such endeavors. Our recent work on developing inhibitors of amyloid assembly exemplifies the power of using Drosophila. Recently, we and others have identified a key role of aromatic residues in the molecular recognition and self-assembly of various amyloidogenic proteins [1]. The interaction between molecules containing aromatic residues, referred to as aromatic (π–π) stacking, involves attractive non-covalent interactions, including electrostatic, hydrophobic and Van der Waals interactions between planar aromatic rings, which are believed to provide selectivity as well as stability to the interacting molecules. This notion has gained direct evidence from high-resolution structural studies and is supported by theoretical studies and molecular dynamics simulations. Indeed, the amyloidogenic potential of aromatic residues is significantly higher than that of aliphatic amino acids [2].

The concept of aromatic stacking suggested to us a new approach to control the self assembly of amyloidogenic proteins for therapeutic purposes. Specifically, novel small molecules could be designed to contain an aromatic core that would target and bind the aromatic residues in the amyloidogenic monomer, and a moiety that would confer steric hindrance and thus prevent, or suppress, the very early steps of the molecular recognition required for the assembly of the monomers into pathogenic amyloid species. To that end we rationally designed a library of small aromatic aggregation inhibitor molecules, based on naphthoquinon-tryptophan hybrids. Quinones were chosen as a steric hindrance motif, since previous work has shown their potential as anti-cancer, anti-viral and anti-amyloid agents. They are small, easy to synthesize and related compounds can cross the blood-brain barrier. Tryptophan was chosen as an aromatic recognition motif since, among the aromatic moieties it was ranked as the residue with highest amyloidogenic potential [2]. Our work has supported this conclusion via an un-biased analysis, using peptide array technology, that has clearly indicated a significantly higher affinity of tryptophan-modified recognition module in the molecular association of the islet amyloid polypeptide [3].

Two of the compounds from the library, 1,4-naphthoquinon-2-yl-L-tryptophan (hereafter termed NQTrp) and Cl-1,4-naphthoquinon-2-yl-L-tryptophan, hereafter termed Cl-NQTrp (MW 360-400; see [4]) were found to be most

effective using *in vitro*, *ex-vivo* and *in vivo* assays in their ability to inhibit the assembly of Aβ into oligomers and fibrils. The compounds inhibited efficiently, in a dose dependent manner, the assembly of synthetic Aβ1-42 monomers into either toxic oligomers Aβ species, even at a molar ratio as low as 5:1 of Aβ:inhibitor (IC50 = 50nM), or into fibrils, even at very low concentration of 1.25 μM [4]. Their affinity towards the smaller Aβ assemblies, measured by fluorescence anisotropy, was ca. 90 nM. It is noteworthy that this IC50 value is markedly lower than those for other aromatic Aβ inhibitors reported in the literature. NMR studies, CD spectroscopy and molecular modeling confirmed that the compounds bind the aromatic residues in Aβ [4, 5]. As an initial functional assay we showed that they protected cultured neuronal cells from the cytotoxic effect of Aβ oligomers, while having no toxic effect on these cells on their own [5].

To examine the effect of the compound in the intact organism we first tested it in transgenic Drosophila expressing Aβ throughout their nervous system, which serve as a canonical model for AD [6]. Feeding these transgenic flies with either compound in their culture medium throughout their life cycle resulted in a dramatic rectification of their behavioral defects (i.e. abnormal locomotion) and their reduced longevity, both of which have been amply shown to correlate well with other AD symptoms of these flies. This restoration was accompanied by a marked reduction in the level of Aβ assemblies in extracts and in histological preparations of their brains. The compounds had no effect on control normal flies nor did they have other adverse effects [4].

The encouraging results in flies, obtained in a relatively short period of time, provided an impetus for studies in mammals. In preparation for testing the compounds in rodents we examined their ability to cross the blood-brain-barrier (BBB). We employed an established ex-vivo model of BBB based on a co-culture of primary cultures of porcine brain endothelial cell in contact with rat brain glial cells. Passage of the compounds (measured by HPLC) was 3.3 times higher than that of the standard used - FITC-labeled dextran [5].

We next examined the effect of the compounds on an acute transgenic AD mouse model, carrying five familial AD mutations (5XFAD), which displays early plaque formation (at 2 months of age), impaired cognition and neuronal death as in human AD patients [8]. Two months old 5XFAD mice were injected, every other day, intraperitoneally, with 50 mg/kg by weight of either compound in PBS, or with PBS alone for a period of 4 months, after which their behavior and brain Aβ load were examined. Cognitive tests (New Object Recognition, Fear Conditioning) showed marked amelioration of their memory [5]. This was accompanied by 91% reduction of the toxic Aβ species (56*) in their brain extracts compared to vehicle-treated 5XFAD mice. A 40 % reduction of total non-soluble Aβ was also seen. Immunostaining of frontal hippocampus from these mice corroborated these results, showing a significant reduction in both β-sheet-specific Congo-Red staining (45% reduction) and in staining with an Aβ-specific, 6E10 antibody (39% reduction) of compound-treated vs. vehicle treated 5XFAD mice [5]. Formal toxicity assays remain to be done. Yet, casual inspection of the treated flies and mice indicated no adverse effects; Rotarod tests showed no decline in locomotion among treated mice compared to control. Initial toxicological studies showed that even at a dose of 350 mg/Kg, injected subcutaneous, every other day to 2-months old wild type mice for a period of four weeks had no harmful influence on their weight or mobility (manuscript in preparation).

We have further demonstrated that NQTrp and Cl-NQTrp have a more general anti-amyloid effect. Specifically, they are able to efficiently inhibit the in vitro aggregation of other amyloidogenic proteins including α-synuclein, islet amyloid polypeptide, lysozyme, calcitonin, and insulin [8]. We have begun to test them in Drosophila models available for some of these proteins.

Drosophila has also been useful for us for examining natural substances as candidate inhibitors of Aβ assembly. We identifed a natural substance, based on cinnamon extract (CEppt), which markedly inhibited the formation of toxic Aβ oligomers and prevented the toxicity of Aβ towards neuronal PC12 cells. When administered to AD model flies, the cinnamon extract rectified their reduced longevity, fully recovered their locomotion defects and totally abolished tetrameric species of Aβ in their brain. Based on these encouraging results we administered CEppt orally to the 5XFAD mice. This treatment resulted in marked decrease in 56 kDa Aβ oligomers, reduction of plaques and improvement in cognitive behavior [9].

Drosophila proved to be useful also for studying peptidomimetics as anti-amyloid agents. Our work on α-synuclein in Parkinson's disease (PD) exemplifies this [10]. Using unbiased systematic peptide array analysis, we identified molecular interaction domains within the β-synuclein polypeptide that specifically binds α-synuclein. When we added such peptide fragments to α-synuclein significantly reduced both amyloid fibrils and soluble oligomer formation in vitro. We next designed a retro-inverso analogue of the best peptide inhibitor with the goal of developing it into candidate drug. We found that this peptide shows indistinguishable activity as compared to the native peptide, yet, in contrast to the native peptide, it is stable in mouse serum and penetrates α-synuclein over-expressing cells. The interaction interface between the D-amino acid peptide and α-synuclein was mapped by Nuclear Magnetic Resonance spectroscopy. As a test in the intact organism we administered the retro-inverso peptide to an established Drosophila model of PD, expressing mutant A53T α-synuclein in the nervous system. This resulted in a significant recovery of the behavioral abnormalities of the treated flies and in a significant reduction in α-synuclein accumulation in the brains of the flies [10]. This paves now the way for testing this peptidomimetic in rodent models of PD.

Taken together, these studies and comparable reports by other labs call for expanding the use of Drosophila as a model for drug development, in particular for amyloid diseases.

Supported in part by the Israel Ministry of Health and the Alliance Foundation.

REFERENCES

1. Gazit, E. A possible role for pi-stacking in the self-assembly of amyloid fibrils. FASEB J. 2002;16:77-83.
2. Pawar, AP., Dubay, KF., Zurdo, J., Chiti, F., Vendruscolo, M., Dobson, CM. Prediction of "aggregation-prone" and "aggregation-susceptible" regions in proteins associated with neurodegenerative diseases. J Mol Biol. 2005; 350:379-392.
3. Porat, Y., Mazor, Y., Efrat, S., Gazit, E. Inhibition of islet amyloid polypeptide fibril formation: a potential role for heteroaromatic interactions. Biochemistry. 2004;43:14454-62.
4. Scherzer-Attali, R., Pellarin, R., Convertino, M., Frydman-Marom, A., Egoz-Matia, N., Peled, S., Levy-Sakin, M., Shalev, DE., Caflisch, A., Gazit, E., Segal, D. Complete phenotypic recovery of an Alzheimer's disease model by a quinone-tryptophan hybrid aggregation inhibitor. PLoS One. 2010; 5:e11101.
5. Scherzer-Attali, R., Farfara, D., Ben-Romano, T., Trudler, D., Vientrov, M., Shaltiel-Karyo, R., Shalev, D.E., Gazit, E., Segal, D., and Frenkel, D. (2012). Naphthoquinone-tryptophan reduces neurotoxic Aβ*56 level and improves cognition in Alzheimer's disease animal model. Neurobiology of Disease. 2012; 46: 663–672.
6. Moloney, A., Sattelle, DB., Lomas, DA., Crowther, DC. Alzheimer's disease: insights from *Drosophila melanogaster* models. Trends Biochem Sci. 2010; 35:228-35.

7. Oakley, H,, Cole, SL., Logan, S., Maus, E., Shao, P., Craft, J., Guillozet-Bongaarts, A., Ohno, M., Disterhoft, J., Van Eldik, L., Berry, R., Vassar, R. Intraneuronal beta-amyloid aggregates, neurodegeneration, and neuron loss in transgenic mice with five familial Alzheimer's disease mutations: potential factors in amyloid plaque formation. J Neurosci. 2006; 26:10129-40.
8. Scherzer-Attali, R., Shaltiel-Karyo, R., Adalist, Y., Segal, D., and Gazit, E.. Generic inhibition of amyloidogenic proteins by two naphthoquinone-tryptophan hybrid molecules. Proteins, 2012; 80:1962-73
9. Frydman-Marom, A., Levin, A., Farfara, D., Benromano, T., Scherzer-Attali, R., Peled, S., Vassar, R., Segal, D., Gazit, E., Frenkel, D., and Ovadia, M.. Orally administrated cinnamon extract reduces β-amyloid oligomerization and corrects cognitive impairment in Alzheimer's disease animal models. PLoS One, 2011; e16564.
10. Shaltiel-Karyo, R., Frenkel-Pinter, M., Frydman-Marom, A., Shalev, D.E., Segal, D. and Gazit, E. Inhibition of α-synuclein oligomerization by stable cell-penetrating β-synuclein fragments results in phenotypic recovery of Parkinson's disease model flies. PLoS One. 2010; 5:e13863.

Heparin/Chitosan nanoparticle delivery system for *in vivo* evaluation of glycosaminoglycans influence on transthyretin deposition

Nádia Pereira Gonçalves[1,2], Ana Paula Pêgo[3], Maria João Saraiva[1,2]

1. *Molecular Neurobiology Unit, IBMC – Instituto de Biologia Molecular e Celular, Portugal*
2. *Instituto de Ciências Biomédicas Abel Salazar, University of Porto, Portugal*
3. *New therapies Group, INEB - Instituto de Engenharia Biomédica, Portugal*

Recent studies stress the involvement of heparan sulfate as a modulator of transthyretin (TTR) amyloidogenesis. To study *in vivo* the role of glycosaminoglycans in TTR deposition, we created a novel local delivery system into mice sciatic nerve using heparin/chitosan (CH) nanoparticles. To address drug release and diffusion throughout nerve tissue, fluorescently labeled CH and heparin were used. Our results show maximal absorption throughout the nerve extracellular matrix (ECM) and minor inflammatory reaction. Using this system, heparin/CH nanoparticles were locally applied into sciatic nerve of TTR V30M transgenic mice, heterozygous for the heat shock factor 1 (HSF1). Fifteen days after nanoparticle application, both heparan sulfate and TTR deposition were significantly increased in treated nerves, indicating that proteoglycan enhanced TTR deposition.

INTRODUCTION

Familial amyloidotic polyneuropathy (FAP) is a human autosomal dominant neurodegenerative disorder characterized by extracellular deposition of mutant TTR aggregates and amyloid fibrils, particularly in the peripheral nervous system. It is well known that ECM remodeling contribute to the progress of this disease; some ECM-related genes are upregulated in human nerve biopsies of FAP patients carrying the most prevalent TTR mutation V30M [1]; and in tissues from FAP transgenic mice models [2]. One of those is biglycan that was found overexpressed at early stages before amyloid deposition, as compared to normal nerves [1,2]. Neutrophil gelatinase-associated lipocalin (NGAL), chondroitin sulfate and matrix metalloproteinase-9 (MMP-9) are upregulated only when TTR fibrils are already present, all colocalizing in later stages with amyloid deposits [1,2].

Heparan sulfate proteoglycans were identified as components of amyloid deposits in amyloid-related disorders [3], indicating that ECM remodeling occurs continuously until the later stages of disease. Moreover recent *in vitro* studies and *in vivo* studies in a Drosophila model indicate the potential involvement of heparin and heparan sulfate proteoglycans as enhancers of the amyloidogenic cascade, prompting TTR fibrillogenesis [4,5]. Therefore, in the present work we evaluate *in vivo* how changes in glycosaminoglycans type and distribution could alter the tissue metabolism promoting TTR fibrillogenesis and deposition in a mouse model, through the development of a novel local nanoparticle delivery system, based on CH.

METHODS

Heparin/CH nanoparticles were generated as previously described [6]. Nanoparticles characterization regarding size, polydispersity index and ζ potential was carried out using dynamic light scattering and its morphology assessed by transmission electron microscopy (TEM).

Fourteen months-old TTR V30M transgenic mice used lacked endogenous TTR and were heterozygous for the HSF1 [7]. Wild-type animals were also used to optimize the delivery system. Mice were anesthetized with a premixed solution containing ketamine and medetomidine and surgeries performed in aseptic conditions. Briefly, the sciatic nerve was exposed in the mid-thigh and dissected free from the surrounding tissue. Heparin/CH nanoparticles were applied under the left nerve and the right nerve served as the sham nerve, receiving uncoupled CH nanoparticles. Mice were sacrificed at different time points (5, 10, 15, 30, 45 days) and tissues were analyzed by confocal scanning microscopy, using fluorescein-labeled heparin and rhodamine-labeled CH (CHROX). Immunofluorescence was performed with frozen sciatic nerve sections, for collagen IV, PGP 9.5 and S-100. Immunohistochemistry to detect TTR deposition in nerve tissue, heparan sulfate levels and inflammatory mediators, such as activated macrophages, TNF-α and IL-1β, was performed using paraffin sections.

RESULTS

Heparin/CH nanoparticles characterization and release in time

Heparin/CH nanoparticles had in average 198 nm in size, a monomodal population was obtained and with a positive net charge of 28.7 mv. They were spherical in shape, as determined by TEM.

To study the release kinetics of heparin from CH we used CHROX mixed with fluorescein-labeled heparin and analyzed the unprocessed nerve with confocal scanning microscopy. Ten and 15 days after nanoparticles application, we found regions of heparin staining without CHROX colocalization suggesting continuous heparin release (Fig.1). Fifteen days after surgery was chosen for subsequent analysis since maximal intensity of fluorescence was detected. After 30 days only weak green staining was visible, while at day 45 no signal was identified.

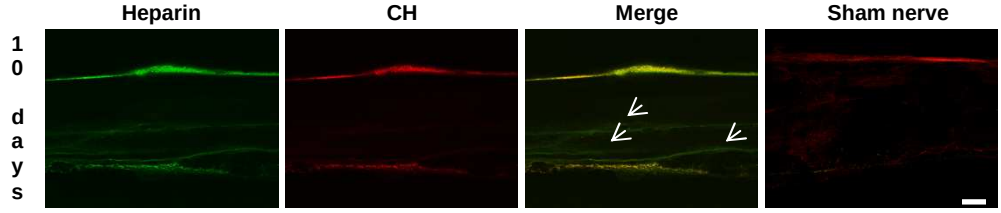

Figure 1. Heparin release to the ECM, as a function of time. Regions of heparin staining without colocalization with CH are shown by the arrows. Sham nerve received uncoupled CH. Scale bar 50 µm.

Heparin localization into the tissue and inflammatory response

Using fluorescein-labeled heparin and markers for nerve components, such as for ECM (collagen IV), axons (PGP 9.5) and Schwann cells (S-100), colocalization was found between heparin and collagen IV. This result indicates that heparin has been released to the ECM.

The inflammatory response was assessed by immunohistochemistry for proinflammatory markers, such as activated macrophages, TNF-α and IL-1β. Only a minor inflammatory reaction was detected and decreased with time, most likely related to CH, since it was also present in sham nerves.

Effect of heparin on TTR deposition

Heparin/CH nanoparticles were applied into the sciatic nerve of TTR transgenic mice to study the effect of heparin on TTR deposition, *in vivo*. After 15 days nerves were analyzed by immunohistochemistry and the levels of heparan sulfate and TTR were both significantly increased in heparin treated nerves as compared with sham (Fig.2).

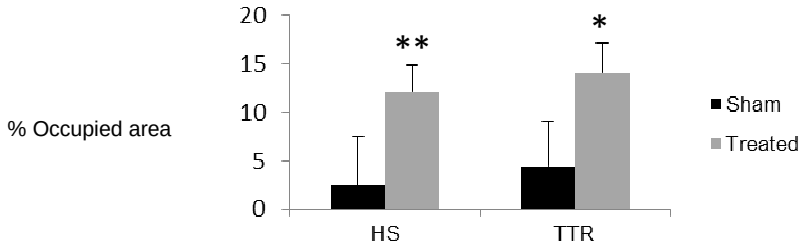

Figure 2. Heparin/CH nanoparticles application to sciatic nerve of TTR transgenic mice, increased TTR deposition.

DISCUSSION

Highly sulfated GAGs have been implicated as TTR fibrillogenesis promoters in some *in vitro* studies [4,5]. To evaluate the *in vivo* influence of heparin/heparan sulfate on TTR deposition, a novel local delivery system to the nerve tissue was developed. Some technical challenges must be satisfied as heparin needs to be efficiently absorbed by the tissue, the procedure must be minimally invasive and the release sustained in time. Therefore, a nanoparticle delivery system based on CH, as the vehicle material, was optimized. Heparin, due to its high negative charge, interacts strongly with CH forming stable nanoparticles by polyelectrolyte complexation, with slow release properties. Smaller size and positive zeta potential allows higher penetration into the tissues escaping from cellular barriers and increasing the resistance to degradation.

So, this optimized local delivery system allows the release of drugs that could prompt nerve regeneration, as previously described [6], can be a therapeutic strategy regarding neurodegeneration allowing the functional evaluation of the animals with tests for nociception, electrophysiology or walking tract analysis, and finally permits the delivery of components prompting or inhibiting TTR fibrillogenesis to animal models of disease. Moreover, this work demonstrates that changes in proteoglycan type and distribution could possibly account for alteration of the physical properties of tissues, increasing TTR deposition *in vivo*. This new and versatile nanoparticle delivery system opens novel avenues in the field of neuropathology, in the design of suitable animal models and therapeutic strategies targeting directly the nerve tissue.

ACKNOWLEDGMENTS

The authors would like to thank Paula Sampaio and Paula Gonçalves from IBMC for the help with confocal microscopy and paraffin tissue processing, respectively. We also thank Hugo Oliveira from INEB and Jin-Ping Li from Uppsala University for helping in nanoparticle characterization and for heparin source, respectively. Finally, we thank the Portuguese Foundation for Science and Technology (FCT), for funding the work and fellowship to NPG through project SFRH/BD/74304/2010.

REFERENCES

1. Sousa MM, do Amaral JB, Guimarães A, Saraiva MJ. Up-regulation of the extracellular matrix remodeling genes, biglycan, neutrophil gelatinase-associated lipocalin, and matrix metalloproteinase-9 in familial amyloid polyneuropathy; 2005. *FASEB J* 19(1): 124-6.
2. Cardoso I, Brito M, Saraiva MJ. Extracellular matrix markers for disease progression and follow-up of therapies in familial amyloid polyneuropathy V30M TTR-related; 2008. *Dis Markers* 25(1): 37-47.
3. Lyon AW, Narindrasorasak S, Young ID et al. Co-deposition of basement membrane components during the induction of murine splenic AA amyloid; 1991. *Lab. Invest.* 64, 785–790.
4. Bourgault S, Solomon JP, Reixach N, Kelly JW. Sulfated glycosaminoglycans accelerate transthyretin amyloidogenesis by quaternary structural conversion; 2011. *Biochemistry* 50(6): 1001-1015.
5. Noborn F, O'Callaghan P, Hermansson E et al. Heparan sulfate/heparin promotes transthyretin fibrillization through selective binding to a basic motif in the protein; 2011. *Proc Natl Acad Sci* 108(14): 5584-5589.
6. Gonçalves NP, Oliveira H, Pêgo AP, Saraiva MJ. A novel nanoparticle delivery system for *in vivo* targeting of the sciatic nerve: impact on regeneration; 2012. *Nanomedicine (Lond)* [Epub ahead of print].
7. Santos SD, Fernandes R, Saraiva MJ. The heat shock response modulates transthyretin deposition in the peripheral and autonomic nervous systems; 2010. *Neurobiol Aging* 31(2): 280-289.

Heat shock factor 1 (Hsf1) plays a key role in AApoAII cardiac amyloidosis in mice

J. Qian[1,2], M. Hirose[3], B. Zhang[1], Y. Wang[1], G. Tian[1], H. Luo[1], Y. Liu[1], X. Fu[1], F. Ge[1], J. Sawashita[1], M. Mori[1], M. Fujimoto[4], A. Nakai[4], and K. Higuchi[1]

[1]Department of Aging Biology, Institute of Pathogenesis and Disease Prevention, Shinshu University Graduate School of Medicine, Matsumoto, Japan. [2]Department of Pathology, Hebei Medical University, Shijiazhuang, China. [3]Department of Molecular and Cellular Pharmacology, Iwate Medical University, School of Pharmaceutical Sciences, Iwate, Japan. [4]Department of Biochemistry and Molecular Biology, Yamaguchi University School of Medicine, Japan

ABSTRACT

In mouse senile amyloidosis, apolipoprotein A-II (apoA-II) forms extracellular amyloid fibril deposits (AApoAII) throughout the entire body, excluding the brain. Heavy amyloid deposition in the heart is a characteristic feature of this disease. Heat shock factor 1 (HSF1) is known to regulate the expression of a set of heat shock proteins (Hsps) that suppress the formation of protein aggregates. We induced amyloidosis through injection of AApoAII fibrils. We found that extracellular deposition of AApoAII induces expression of Hsps, and HSF1 deficiency results in the insufficient induction of Hsps expression in the heart. Compared with wild-type mice, the degree of AApoAII amyloid deposition was significantly increased in the heart of HSF1-deficient mice. During the accelerated progression of cardiac amyloidosis, Hsf1 deficiency caused the deteriorating loss of the cytoskeletal protein α-actin, as well as cardiac contractile dysfunction associated with hypertrophic changes. Over-expression of human HSF1 reduced amyloid deposition in the heart.

INTRODUCTION

There are two evolutionarily conserved pathways, the heat shock response (HSR) and unfolded protein response in the endoplasmic reticulum, that maintain the protein-folding homeostasis or proteostasis. The HSR is characterized by induction of heat shock proteins (Hsps), which are known as molecular chaperones and play an important role in protein folding and degradation. Heat shock factor 1 (HSF1), which binds to DNA at a specific site of the Hsp gene promoter region called the heat shock element (HSE), is a major determinant in this pathway. This pathway is required for acquisition of thermotolerance and protection of cells from various pathological diseases, such as neurodegenerative and other degenerative diseases. We hypothesized that (1) extracellular deposition of amyloid fibrils might induce HSR; (2) defective HSF1 might accelerate the

extracellular fibril deposition by inhibiting the expressions of Hsps; and (3) enhancing HSR might decelerate amyloid deposition.

MATERIALS AND METHODS

To test this hypothesis, we crossed mice lacking the Hsf1 gene (Hsf1$^{-/-}$)[1] or transgenic mice expressing an activated form of human HSF1 (h*HSF1*Δ*RD*Tg) with R1.P1-*Apoa2^{c}* mice with amyloidogenic *Apoa2^{c}* for the present study[2]. AApoAII fibrils were isolated from the liver of an R1.P1-*Apoa2^{c}* mouse with severe amyloidosis induced by injection of AApoAII fibrils, using Pras' method with some modifications[3]. A single dose of 1 μg of sonicated AApoAII fibrils were injected into the tail veins of 2-month-old mice. After 2 or 4 months, the treated mice were sacrificed. Half of each tissue from the whole body was fixed in 10% neutral buffered formalin and the other half was stored at –80 ℃ for future use. Amyloid deposition was identified in Congo red-stained sections under polarizing microscopy and immunohistochemically with antiserum against AApoAII. The intensity of the amyloid deposition was determined semi-quantitatively using the amyloid index (AI) as a parameter[3]. Amyloid fibrils in cardiac tissue were identified by transmission and immunolabeled electron microscopy. Cardiac function was assessed with echocardiography (GE Yokogawa Medical System, Tokyo, Japan) as previously described[4]. Hearts were viewed at the level of the papillary muscles in the short axis. In M-mode tracings, the average of three consecutive beats was used to measure the following parameters: interventricular septum thickness, left ventricular end-diastolic dimension (LVEDd), end-systolic dimension (LVESd) and fractional shortening (LVFS), which was calculated as follows: (LVEDd - LVESd)/LVEDd x 100%.

RESULTS

We induced amyloidosis through injection of AApoAII amyloid fibrils. After 2 and 4 months, we found that extracellular deposition of amyloid fibrils induces expression of Hsps (Hsp70, Hsp40 and Hsp27), and HSF1 deficiency results in the insufficient induction of Hsps expression, especially in the heart. Compared with wild-type mice, the degree of AApoAII amyloid deposition was significantly increased in the heart of HSF1-deficient mice (Figure1).

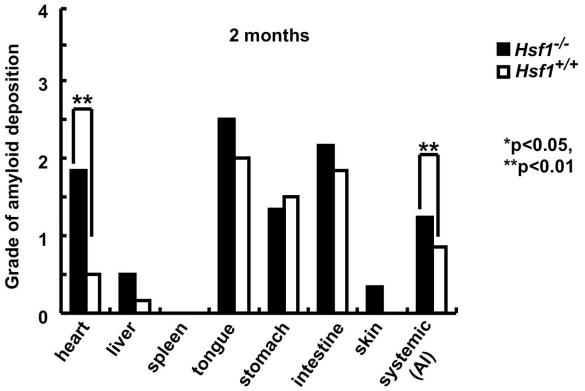

Figure 1. Comparison of amyloid deposition in *Hsf1$^{-/-}$* and *Hsf1$^{+/+}$* mice.

Bundles of amyloid fibrils deposited in the endomysiums and capillaries of cardiac muscles were observed in transmission electron micrographs. Abundant gold particles labeling AApoAII fibrils were seen at endomysiums of cardiac muscles by immuno-electronmicroscopy. Two-month-old *Hsf1*$^{-/-}$ (n=6) and wild-type (n=6) mice were injected with 1 µg AApoAII fibrils and euthanized at 2 months after injection. The grade of amyloid deposition was determined in 7 major organs (heart, liver, spleen, tongue, stomach, intestine, skin) and AI was determined[3].

During the accelerated progression of cardiac amyloidosis, Hsf1 deficiency caused the deteriorating loss of the cytoskeletal protein α-actin in the heart, as well as cardiac contractile dysfunction associated with hypertrophic changes (Table 1). Transgenic mice express an active form of human HSF1 (h*HSF1*Δ*RD*) only in the heart. There was a significant difference in the degree of amyloid deposition in the heart between the transgenic mice and the wild-type mice.

Table 1. Echocardiographic analysis in Hsf1$^{+/+}$ and Hsf1$^{-/-}$ mice with/without AApoAII-injection

Mouse Strain	Hsf1$^{-/-}$ (n=8)	Hsf1$^{-/-}$ (n=8)	Hsf1$^{+/+}$ (n=8)	Hsf1$^{+/+}$(n=7)
AApoAII injection	-	+	-	+
IVS (mm)	0.73 ± 0.05 [a, c]	0.95 ± 0.09 [b]	0.75 ± 0.02 [d]	0.75 ± 0.04
LVEDd (mm)	2.8 ± 0.1 [e, g]	2.5 ± 0.1 [f]	3.4 ± 0.2 [h]	3.3 ± 0.1
LVFS (%)	45 ± 2 [i, k]	32 ± 3 [j]	49 ± 1 [l]	47 ± 1

Each value represents the mean ± S.E. IVS, interventricular septum; LVEDD, left ventricular end-diastolic dimension; LVFS, left ventricular fractional shortening
a vs. b, p< 0.01; c vs. d, p< 0.01; e vs. f, p< 0.05; g vs. , p< 0.001; i vs. j, p< 0.001; k vs. l, p< 0.001.

DISCUSSION

Many studies have pointed out the importance of Hsps and HSF1 as protective effectors during neurodegenerative or other degenerative diseases with intracellular accumulation of misfolded proteins. Here, we studied the role of Hsf1 and Hsps in protection against deposition of systemic and extracellular amyloid fibrils using mouse AApoAII amyloidosis, in which heavy amyloid deposition in the heart is characteristic[5]. We can induce constant amyloidosis in a relatively short period in mice by “transmission” caused by injection of exogenous amyloid fibrils[6]. We show that absence of HSF1 induces severe extracellular cardiac AApoAII deposition and results in cardiomyocyte damage and cardiac dysfunction. But it is unclear how to activate HSF1 to stimulate the expression of Hsps or HSR by extracellular amyloid deposition. Our results demonstrate that HSF1 is a potential pharmacological target in amyloidosis, and its activation may be viewed as a novel therapeutic strategy for a variety of cardiac amyloidoses.

REFERENCES

1. Inouye S, Katsuki K, Izu H, et al. (2003) Activation of heat shock genes is not necessary for protection by heat shock transcription factor 1 against cell death due to a single exposure to high temperatures. *Mol Cell Biol*, 23: 5882–5895
2. Nakai A, Suzuki M, Tanabe M. (2000) Arrest of spermatogenesis in mice expressing an active heat shock transcription factor 1. *EMBO J,* 19: 1545–1554.

3. Xing Y, Nakamura A, Korenaga T, et al. (2002) Induction of protein conformational change in mouse senile amyloidosis. *J Biol Chem,* 277: 33164–33169.
4. Kamiyoshi Y, Takahashi M, Yokoseki O, et al. (2005) Mycophenolate mofetil prevents the development of experimental autoimmune myocarditis. *J Mol Cell Cardiol,* 39: 467–477..
5. Higuchi K, Yonezu T, Kogishi K, et al. (1986) Purification and characterization of a senile amyloid-related antigenic substance (apoSASSAM) from mouse serum. apoSASSAM is an apoA-II apolipoprotein of mouse high density lipoproteins. *J Biol Chem*, 261: 12834–12840.
6. Qian J, Yan J, Ge F, et al. (2010) Mouse senile amyloid fibrils deposited in skeletal muscle exhibit amyloidosis-enhancing activity. *PLoS Pathogens* 6: e1000914.

The C-terminal sequence of type F apolipoprotein A-II inhibits the polymerization of apolipoprotein A-II into amyloid fibrils in mice

Jinko Sawashita[1], Beiru Zhang[1], Kazuhiro Hasegawa[2], Masayuki Mori[1], Hironobu Naiki[2], Fuyuki Kametani[3], and Keiichi Higuchi[1]

[1]Department of Aging Biology, Institute of Pathogenesis and Disease Prevention, Shinshu University Graduate School of Medicine, Matsumoto, Japan, [2]Division of Molecular Pathology, Department of Pathological Sciences, Faculty of Medical Science, University of Fukui, Fukui, Japan, [3]Department of Dementia and Higher Brain Function, Tokyo Metropolitan Institute of Medical Science, Tokyo, Japan.

In murine senile amyloidosis, misfolded serum apolipoprotein A-II (apoA-II) deposits as amyloid fibrils in a process associated with aging, and type C apoA-II (APOA2C) is known as an amyloidogenic protein. Previously, we showed that N- and C-terminal sequences of apoA-II are critical for polymerization into amyloid fibrils. Here, we demonstrated that congenic mouse strains carrying type F apoA-II (APOA2F), which contains 4 amino acid substitutions in the amyloidogenic regions of APOA2C, were absolutely resistant to amyloidosis, and that N- and C-terminal peptides of APOA2F did not polymerize into amyloid fibrils *in vitro*. Thus, we have succeeded in suppressing amyloid deposition in amyloid-susceptible mice by treatment with the APOA2F C-terminal peptide. APOA2F C-terminal peptide might inhibit the conformational changes required for polymerization of amyloidogenic N- and C-terminal apoA-II sequences into amyloid fibrils. We provide a new model system for investigating inhibitory mechanisms against amyloidosis *in vivo* and *in vitro*.

INTRODUCTION

Apolipoprotein A-II (ApoA-II) is the most important protein associated with murine senile amyloidosis, as it is the precursor of amyloid fibrils (AApoAII) (1-3). Seven alleles of the apoA-II gene have been found among inbred strains of mice (4), each inbred laboratory mouse strain has a single type apoA-II protein and the pathological findings of senile amyloidosis in strains with type A, B, or C apoA-II (APOA2A, APOA2B, and APOA2C) have been investigated (2, 5-8). For example, C57BL/6J strain has APOA2A and exhibits a moderate incidence of mild amyloid deposition with aging, and BALB/c strain has APOA2B and exhibits a low incidence of slight amyloid deposition. In contrast, the SAMP1 strain has APOA2C and spontaneously exhibits a high incidence of severe systemic amyloid deposition with aging. We previously reported a unique mechanism in which N- and C-terminal peptides of apoA-II associated into amyloid fibrils *in vitro* (9). The N-terminal sequence from positions 6 to 16 of apoA-II is critical for polymerization into amyloid fibrils. The C-terminal sequence from positions 48 to 65

of ApoA-II is also necessary for nucleation, but not for the extension phase. Interestingly, both sequences are common and there is no substitution in them among APOA2A, APOA2B and APOA2C.

We hypothesized that some amino acid substitutions in these amyloidogenic sequences of apoA-II might inhibit the polymerization of apoA-II into amyloid fibrils. Type F apoA-II (APOA2F) contains 4 substitutions in the N- and C-terminal peptides relative to APOA2C (4). So, we evaluated the incidence of amyloidosis in mice having APOA2F, and compared it with those in mice having APOA2A or APOA2C *in vivo*. We analyzed the ability of N- and C-terminal peptides of APOA2F to polymerize into amyloid fibrils *in vitro*. Then, we investigated whether the C-terminal sequence of APOA2F had inhibitory effects on senile amyloidosis *in vivo*.

METHODS

Experiment 1 - We developed two strains of congenic mice that have type F apoA-II originating from *Mus Spretus* in the genetic backgrounds of C57BL/6J and R1.P1-*Apoa2*^{c} using standard procedures. Two-month-old mice were injected intravenously with 100 µg of sonicated AApoAII prepared by using methods described previously (3). The mice were sacrificed at arbitrary intervals until 11-month-old. Several organs were collected from these mice and used to detect amyloid deposition. Plasma was collected from 2-month-old mice that had fasted for 12-16 h and was used the levels of apoA-I and apoA-II in HDL, HDL particle size, and total- and HDL-cholesterol levels (3, 8).

Experiment 2 - We investigated that the polymerization of synthetic partial peptides of APOA2F into amyloid fibrils using methods described previously (9). The reaction mixtures, which contained 50 µM peptides, 100 mM NaCl in 50 mM buffer (pH 2.5), were incubated with agitation at 300 rpm at 37˚C, and were used for several analyses as ThT binding assay, microscopic analyses using TEM and LM, CD analysis, and LC-MS/MS. For CD analysis, the solvent for peptides used hexafluoroisopropanol instead of DMSO.

Experiment 3 - We used *Apoa2*^{c} transgenic mice, which were developed as an amyloidosis-susceptible strain in our laboratory (8). The C-terminal peptide in 5% DMSO (1 mM) or 5% DMSO were filled in sterile osmotic pumps. Two-month-old transgenic mice were anesthetized and were implanted osmotic pumps into their abdominal cavities. One day after the implantation, mice were injected intravenously with 5 µg of sonicated AApoAII fibrils. After 27 days, several organs were collected and used to detect amyloid deposition.

Ethics statement - All *in vivo* experiments were carried out in accordance with the Regulations for Animal Experimentation of Shinshu University.

Statistical analysis - The Mann-Whitney *U*-test was used to analyze the amyloid index for AApoAII deposition. The Tukey-Kramer method for a multiple comparison was performed to test for any significant differences in various pair-wise comparisons in blood biochemical parameters.

RESULTS AND DISCUSSION

We detected amyloid depositions in mice with the either *Apoa2*^{a} or *Apoa2*^{c} alleles, but none of the homozygous *Apoa2*$^{f/f}$ mice showed amyloid depositions anywhere in the body (**Figure 1**). In addition, none of the homozygous *Apoa2*$^{f/f}$ mice showed spontaneous amyloid deposition until 13 month-old, even though heterozygous *Apoa2*$^{c/f}$ mice had amyloid deposition in several organs at the same period and homozygous *Apoa2*$^{c/c}$ mice had severe amyloid deposition. From those findings, we found that mice with homozygous

Apoa2$^{f/f}$ were absolutely amyloidosis-resistant. And, the APOA2F did not affect the contents of apoA-I and apoA-II proteins and the plasma lipid profiles.

We examined the polymerization of APOA2F into amyloid fibrils by using partial synthetic peptides *in vitro*. APOA2F peptides could not polymerize into amyloid fibrils, and C-terminal peptide of APOA2F was a strong inhibitor against the polymerization of amyloidogenic APOA2C peptides. And, the single amino acid substitution at position 62 of APOA2C (c48/65(N62K)) did not polymerize into amyloid fibrils. From those findings, we hypothesized that APOA2F C-terminal peptide might inhibit the onset of amyloidosis on mice. Interestingly, amyloidosis-susceptible mice treated with the c48/65(N62K) showed the onset of amyloidosis, but their amyloid depositions were lower than those in mice treated with the others (**Figure 2**). We cannot explain the molecular inhibitory mechanism in detail, but C-terminal peptides of APOA2F might inhibit the conformational changes required for polymerization into amyloid fibrils from our CD-spectra data using several partial peptides of apoA-II.

We provide a new model system for investigating inhibitory mechanisms against amyloidosis *in vivo* and *in vitro*, and believe that this system will be useful for the development of novel therapies.

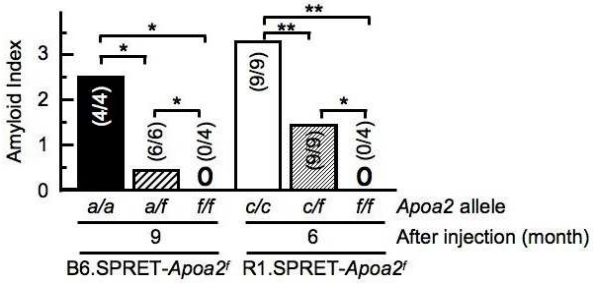

Figure 1. Mice with homozygous *Apoa2*$^{f/f}$ were absolutely amyloidosis-resistant**.** Each bar shows the mean. Numbers in parentheses represent amyloid positive mice/total mice examined.

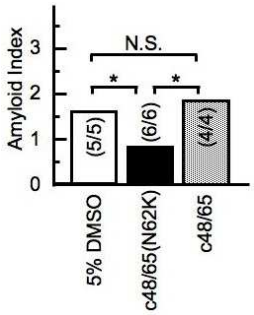

Figure 2. A single substitution C-terminal peptide of APOA2C (c48/65(N62K)) suppressed amyloid deposition *in vivo*.

ACKNOWLEDGEMENTS

This research was supported in part by a Grant-in-Aid for Young Scientists (B) (15790199) from the Japan Society for the Promotion of Science, by Grants-in-Aid for Priority Areas (22020015) and Scientific Research (B)

(20300144 and 23390093) from the Ministry of Education, Culture, Sports, Science and Technology, and by grants for the Amyloidosis Research Committee and the Amyloidosis Research Committee for the Research on Intractable Disease from the Ministry of Health, Labour and Welfare, Japan.

REFERENCES

1. K. Higuchi, T. Yonezu, K. Kogishi, *et al.* (1986) *J. Biol. Chem.* 261: 12834-12840.
2. Y. Xing, A. Nakamura, T. Korenaga, *et al.* (2002) *J. Biol. Chem.* 277: 33164-33169.
3. H. Zhang, J. Sawashita, X. Fu, *et al.* (2006) *FASEB J.* 20:1012-1014 (*Full-length ver.* E211-E221).
4. K. Kitagawa, J. Wang, T. Matsushita, *et al.* (2003) *Amyloid* 10: 207-214.
5. K. Higuchi, T. Yonezu, S. Tsunasawa, *et al.* (1986) *FEBS Lett.* 207: 23-27.
6. X. Fu, T. Korenaga, L. Fu, *et al.* (2004) *FEBS Lett.* 563: 179-184.
7. K. Higuchi, K. Kitagawa, H. Naiki, *et al.* (1991) *Biochem. J.* 279: 427-433.
8. F. Ge, J. Yao, X. Fu, *et al.* (2007) *Lab. Inves*t. 87: 633-643.
9. J. Sawashita, F. Kametani, K. Hasegawa, *et al.* (2009) *Biochim. Biophys. Acta* 1794: 1517-1529.

Potential induction of vaccine-associated amyloid A amyloidosis in white young hens

Tomoaki Murakami[1], Yasuo Inoshima[1], Masakazu Inagaki[2], Eigo Sakamoto[2], Syouzou Sakamoto[3], Tokuma Yanai[4], Naotaka Ishiguro[1]

[1]Laboratory of Food and Environmental Hygiene, Department of Veterinary Medicine, Gifu University, Gifu, Japan. [2]Department of research and technical, Chubu Shiryo co., LTD, Aichi, Japan. [3]Sakamoto Sangyo Co., Ltd, Okayama, Japan. [4]Laboratory of Veterinary Pathology, Department of Veterinary Medicine, Gifu University, Gifu, Japan

ABSTRACT

Avian amyloidosis is a type of systemic amyloid-A (AA) amyloidosis, and occurs most frequently in waterfowl such as Pekin ducks. In chickens, AA amyloidosis is observed in relatively older birds. However, outbreaks of systemic amyloidosis in flocks of young layers are known to be induced by repeated inflammatory stimulations, such as those resulting from multiple vaccinations with oil-emulsified bacterins. We found irregular fatal disease outbreaks of AA amyloidosis in growing white hens in a large scale poultry farm. The outbreak in the farm was observed within three weeks after vaccination. Therefore, we histologically examined the many young white hens with AA amyloidosis in the poultry farm and characterized etiological factors of chicken AA amyloidosis. Outbreak of chicken AA amyloidosis in the poultry farm seems to be potentially associated with administration of multiple vaccines.

INTRODUCTION

Avian amyloidosis, also referred to as systemic AA amyloidosis, is observed in older birds, where the condition develops secondarily to inflammatory disorders such as tuberculosis. Avian amyloidosis occurs most frequently in waterfowl, particularly Pekin ducks. A similar condition in chickens, where the disease is known as amyloid arthropathy, is associated with infection by Enterococcus faecalis. Several reports suggest that outbreaks of systemic amyloidosis in young layer flocks are induced by repeated inflammatory stimulations, such as injections with casein or vaccinations with oil-emulsified bacterins.

We encountered irregular outbreaks of fatal disease in growing hens in a large-scale poultry farm. Postmortem examinations revealed the presence of AA amyloidosis in the carcasses of these young chickens. AA outbreaks in this farm occurred after administration of a combined vaccine. Therefore, we investigated the possible relationship between avian AA amyloidosis and the vaccination program, including characterizing etiological factors of the disease and possible treatments, the use of antibiotics, and/or varying the vaccine components.

CASE HISTORY & METHODS

The poultry farm T is a large-scale farm, which raises a total of about 200,000 white growing hens per year. In each farming term, 44,000 chickens were farmed. Chickens were introduced in farm T at the age of about 70 days, subcutaneously or intramuscularly inoculated with the multiple vaccines in pectoral muscle at 90-days and shipped to an egg-laying farm at about 130 days. From February 2010, the mortality of chickens increased in farm T (about 2.0%). The chickens deceased from February 2010 to June 2011 were examined in the following ways.

- Historical analysis in farm T
- Analysis of pathological condition of chicken amyloidosis
- Verification of the treatment effect of antibiotics

RESULTS

Chicken amyloidosis was observed within 20 to 30 days after one-time co-administration of vaccines. In group No.7, the total number of deceased animals was 711 out of 44,000 chickens (1.6%). Of these deceased animals, 130 carcasses were examined macroscopically, histologically, and immunohistochemically. Treatment with antibiotics reduced the number of chicken deaths.

Table 1. *Surveillance of mortality, vaccine inoculation, and experimental treatment at poultry farm T*

Group No.	Nos. of chickens	Month-year starting of farming	Medication by antibiotic	Overall mortality in a group	Incidence of chickens with amyloidosis in dissected group
1	32,000	Feb. 2010	-	1.1	-
2	32,000	Apr. 2010	-	1.2	-
3	32,000	Jun. 2010	-	2.0	-
4	32,000	Aug. 2010	-	1.7	-
5	32,000	Aug. 2010	-	1.4	-
6	44,000	Dec. 2010	-	1.8	-
7	44,000	Feb. 2011	-	1.6	22/25 (88%)
8	44,000	Apr. 2011	+	0.7	3/40 (7.5%)

To estimate the relationship between occurrence of chicken amyloidosis and vaccination, 25 chickens were inoculated with the vaccines according to vaccination program as the monitoring group, while 5 chickens were kept as the control group without vaccination. The histopathological observation revealed the development of AA amyloidosis in 22 of the 25 animals inoculated with vaccines, while AA amyloidosis was not observed in 5 control chickens. In 22 chickens with AA amyloidosis, inflammatory lesions in the pectoral muscles were more severe than those seen in chickens without amyloidosis

DISCUSSION

Outbreaks of chicken amyloidosis previously have been reported primarily in colored chickens. However, in this study, the outbreak developed in growing hens of the Julia-Lite (white) breed. Furthermore, these chickens developed AA amyloidosis within 20 days after a single vaccine injection, even though young Sonia and Boris-

Brown (colored) hens raised at the same poultry farm didn't develop AA amyloidosis (data not shown). In most previous reports, AA amyloidosis was observed in chickens or other animals over a month after the administration of multiple (repeated) inflammatory stimulations. Our results suggest that the Julia-Lite breed may have greater susceptibility to AA amyloidosis following inflammatory stimulation.

Chickens administered antibiotics exhibited decreased mortality, suggesting that prophylactic administration of antibiotics after vaccination is effective in reducing mortality due to AA amyloidosis. Generally, amyloidosis is a disease caused by chronic inflammation, as seen in rheumatoid arthritis and various bacterial infections. In this study, chicken amyloidosis presumably was enhanced by inflammation from purulent myositis with bacterial infection at the pectoral muscle site of injection. Administration of antibiotics is assumed to have reduced bacterial infection and thereby weakened inflammatory stimulation, leading to a reduction in the incidence of amyloidosis.

In the monitoring group, three of 40 chickens (7.5%) exhibited AA amyloidosis. This percentage is higher than mean mortality in group No. 8. The result suggests that some of the chickens that survived to harvest (i.e., were not found dead) may have been harboring AA amyloidosis. Furthermore, in the three necropsied chickens that exhibited amyloidosis, amyloid deposits were observed in each lesion-containing pectoral muscle. These observations suggest that chickens with systemic amyloid deposits may have been shipped to egg farms as layers. Given recent reports of cross-species transmission of AA amyloidosis (by ingestion of amyloid in edible meat), further surveys of chicken AA amyloidosis in laying hens are recommended.

REFERENCES

1. Cowan, D.F. (1968). Avian amyloidosis. I. General incidence in zoo birds. *Pathologia veterinaria*, 5, 51-58.
2. Landman, W.J., Gruys, E. & Dwars, R.M. (1994). A syndrome associated with growth depression and amyloid arthropathy in layers: a preliminary report. *Avian pathology : journal of the W.V.P.A*, 23, 461-470.
3. Landman, W.J., Gruys, E. & Gielkens, A.L. (1998). Avian amyloidosis. *Avian pathology : journal of the W.V.P.A*, 27, 437-449.
4. Ling, Y. (1992). Experimental production of amyloidosis in ducks. *Avian pathology : journal of the W.V.P.A*, 21, 141-145.
5. Ram, J.S., Glener, G.G. & DeLellis, R.A. (1968). Amyloid. I. Use of Freund's adjuvant in experimental amyloidosis. *Proceedings of the Society for Experimental Biology and Medicine. Society for Experimental Biology and Medicine (New York, N.Y.)*, 127, 854-856.
6. Rampin, T., Sironi, G. & Gallazzi, D. (1989). Episodes of amyloidosis in young hens after repeated use of antibacterial oil emulsion vaccines. *Deutsche tierärztliche Wochenschrift*, 96, 168-172.
7. Sato, K., Yasuda, J., Katagiri, S., Nakamura, K., Yamada, M., Asahi, S., et al. (2003). Pathology of amyloidosis collectively occurring in a commercial layer chicken flock. *Journal of the Japanese Society of Poultry Diseases*, 39, 38-42. [in Japanese with English abstract].
8. Shibatani, M., Imoto, H., Suzuki, T., Hasegawa, I. & Itakura, T. (1984). Amyloidosis in a layer chicken flock. *Journal of the Japan Veterinary Medical Association*, 37, 787-792. [in Japanese with English abstract].
9. Solomon, A., Richey, T., Murphy, C.L., Weiss, D.T., Wall, J.S., Westermark, G.T., et al. (2007). Amyloidogenic potential of foie gras. P*roceedings of the National Academy of Sciences of the United States of America*, 104, 10998-11001.

Heparan sulfate induced dissociation of serum amyloid A from acute-phase HDL requires a minimum length of the polysaccharide

F. Noborn[1], J.B Ancsin[1], W. Ubhayasekera[1], R. Kisilevsky[2], J.P. Li[1]

[1]Department of Medical Biochemistry and Microbiology, The Biomedical Center, Husargatan 3, Box 582, 751 23 Uppsala University, Uppsala, Sweden. [2]Department of Pathology and Molecular Medicine, Richardson Laboratory, 88 Stuart Street, Queen's University, Kingston, Ontario K7L3N6, Canada.

Serum amyloid A (SAA) is an acute-phase reactant associated with high-density lipoproteins (HDLs) in plasma (1). SAA is produced by the liver where its synthesis is under the control of inflammatory cytokines, including interleukin-1, interleukin 6 and tumor necrosis factor. During episodes of inflammation the SAA levels become substantially elevated due to an increased hepatic production (0.001 – 1mg/ml), thus increasing the SAA content of HDL (HDL-SAA) (2). The amount of other protein constituents of HDL, such as apolipoprotein A-I (ApoA-I), is concomitantly reduced. This altered, but physiological relevant lipoprotein, has an increased binding affinity for macrophages that is dependent on heparan sulfate (HS), a sulfate polysaccharide expressed on cell surfaces and in the extracellular matrix (3).

During longstanding inflammatory conditions, SAA can accumulate and deposits in organs, primarily in the spleen, liver and kidneys, causing AA-amyloidosis (4). The development of the disease is a progressive process, often associated with persistent or reoccurring acute inflammation such as rheumatoid arthritis and familial Mediterranean fever (5). AA-amyloidosis is relatively rare compared to other types of amyloid disorders, but often severe due to functional failure of affected organs. Although a sustained increase in circulating SAA is a prerequisite for the disease, only a proportion of the patients with persistent inflammatory conditions develop this form of amyloidosis. Thus, factors other than circulating SAA concentration must be critical for the generation of AA-amyloid.

AA-amyloidosis can be induced in mice by intravenous injection of amyloid fibrils (also known as amyloid enhancing factor, AEF) in combination with an inflammatory stimulation by subcutaneous injection of silver nitrate. This causes AA-amyloid within 24 hours in affected organs (6). Experiments with this model have revealed an intimate structural and temporal relationship between AA-amyloid and HS *in situ*, suggesting a role for HS in the pathogenic process (7).

Our lab previously showed that transgenic mice overexpressing heparanase, an HS degrading enzyme, are resistant to experimental induction of AA-amyloid. Organs of the transgenic mice with high heparanase expression selectively escaped amyloid deposition, demonstrating a decisive role for HS in the pathogenic process. Gel chromatographic analysis of isolated HS revealed a pronounced reduction in the average chain

length of the heparanase-overexpressing organs (i.e. liver and kidney) (8). Taken together, this study indicates that the HS chain-length is critical for the aggregation of SAA and its subsequent deposition as AA-amyloid. The present study aimed to investigate the molecular basis of this finding.

THE POLYSACCHARIDE LENGTH IS CRITICAL FOR THE BINDING ACTIVITY TO ACUTE-PHASE HDL

HDL particles were isolated from normal (HDL) and inflamed mouse plasma (HDL-SAA) by sequential density flotation. The apolipoprotein content in respective HDLs was analyzed with SDS-Urea PAGE and, as expected, the HDL-SAA contained high amount of SAA whereas it was essentially absent in regular HDL. We found that heparin (a commonly used analogue of HS) efficiently promoted the formation of amyloid fibrils when incubated with HDL-SAA at mildly acidic conditions; an effect that is likely exerted through a pH-sensitive motif on SAA (9). This conversion of SAA, from a lipid-associated protein to an amyloid structure, is considered to be a central issue in the pathogenesis of AA-amyloidosis.

To examine the binding of HS/heparin to HDL-SAA we employed surface plasmon resonance (SPR) spectroscopy. HDL-SAA was immobilized onto a Biacore CM5 sensor chip and heparin was injected over the surface at different pH-conditions. As observed for the aggregation experiment, the heparin and HDL-SAA interaction required mild acidic condition (pH 5.0). Unexpectedly, the heparin binding generated a negative cure, which is rarely observed in SPR-analysis. Characterization of the interaction revealed that the polysaccharide influenced the stability of HDL-SAA, and that the negative binding curve represented a direct dissociation of SAA from the lipoprotein.

To further investigate the molecular basis of this finding, we examined the binding of short heparin fragments (e.g. 6-mers) with HDL-SAA. Shorter heparin fragments interacted transiently with the lipoprotein and did not induce SAA dissociation. Further, injection of oligosaccharides with different chain-lengths revealed that only structures exceeding 12-14 sugar units in length were capable of inducing SAA dissociation. This size-dependent effect was further illustrated by examination of HDL-SAA aggregation; heparin efficiently promoted aggregation, while 6-mers failed to induce aggregation.

HS INDUCED DISSOCIATION LIKELY INVOLVES TWO BINDING SITES ON ACUTE-PHASE HDL

Inspection of the SPR-data suggested that an additional HDL-associated component, to which HS/heparin binds, is involved in the SAA dissociation process. Since ApoA-I is the other major protein constituent of HDL-SAA, we considered whether simultaneous binding of HS/heparin to ApoA-I and SAA would be required for SAA dissociation. Accordingly, HS was found to bind normal HDL abundant in ApoA-I. This interaction was only observed at mild acidic pH, consistent with the condition at which HS/heparin-mediated SAA displacement occurred. Furthermore, molecular modeling revealed that the putative binding motifs of SAA and ApoA-I each correspond to that of a heparin 6-mer (31.8 Å). Thus, a heparin structure of 12-14-mer provides two such sites, enabling simultaneous binding to the two HDL-SAA components. In comparison, a fragment of 6-mers can only accommodate one motif. Notably our study does not exclude the possibility that the HS/heparin-mediated displacement of SAA occurs through co-binding of HS/heparin to SAA and other HDL-associated apolipoproteins (e.g. ApoE, ApoC). Such an interpretation warrants consideration since HS/heparin binding sites have been identified on ApoE.

Taken together, this study suggests that HS structures that exceeding a certain minimal length induces separation of SAA from the lipoprotein. Our results point to a novel role of HS in AA-amyloidosis, in which an optimal chain length of the polysaccharide is required for separation of SAA from HDL-SAA. This concept is consistent with earlier *in vivo* findings (8) and introduces a novel mechanistic concept in inflammatory (AA) amyloidosis.

REFERENCES

1. Benditt, E.P and Eriksen N. (1977) *Proc Natl Acad Sci* U S A **74**, 4025-4038
2. Gabay C., and Kushner, I. (1999) *N Engl J Med* **340**, 448-454
3. Tam SP, Kisilevsky R, Ancsin J.B. (2008) *PLoS One* 3(12):e3867
4. Westermark G.T., and Westermark P. (2009) *FEBS Lett* **583**, 2685-2690
5. Gillmore J.D., Lovat L.B, Persey M.R, Pepys M.B, and Hawkins P.N. (2001) *Lancet* **358**, 24-29
6. Axelrad M.A, Kisilevsky R., Willmer J., Chen S.J. and Skinner M. (1982) *Lab Invest* **47**, 139-146
7. Snow A.D., Willmer J., and Kisilevsky R. (1987) A close ultrastructural relationship between sulfated glycosaminoglycans and AA amyloid fibril. *Lab Invest* **57**, 687-698.
8. Li J.P, Galvis M.L., Gong F., Zhang X., Zcharia E., Metzger S., Vlodavsky I., Kisilevsky R., and Lindahl U. (2005) *Proc Natl Acad Sci* **77**, 6551-6555
9. Elimova E., Kisilevsky R., and Ancsin J.B. (2009) *Faseb J* **23**, 3436-3448

Transthyretin deposition in cultured cells

M. Ueda,[1,2] B. Kluve-Beckerman,[1] J.J. Liepnieks,[1] M. Mizuguchi,[3] Y. Ando,[2] and M.D. Benson[1]

[1]Department of Pathology and Laboratory Medicine, Indiana University School of Medicine, Indianapolis, Indiana, USA. [2]Department of Diagnostic Medicine, Graduate School of Medical Sciences, Kumamoto University, Kumamoto, Japan. [3]Faculty of Pharmaceutical Sciences, University of Toyama, Toyama, Japan.

ABSTRACT

It remains to be fully elucidated how transthyretin (TTR) makes amyloid in tissues and causes organ damage. The aim of this study is to investigate TTR deposition on cell morphology and viability. Recombinant TTR were expressed in E. coli and purified. TTR aggregates were formed in vitro by pretreating TTR in 100 mM acetate buffer, pH 4.0. Aggregate preparations were centrifuged to generate pellet and supernatant fractions or used without fractionation. Smooth muscle cells were cultured with the various TTR preparations. TTR aggregates in non-fractionated pretreated preparations, as well as resuspended pelleted material, deposited on the surface of cells. The deposits stained weakly with Congo red but were not birefringent. Western analyses of cell lysates revealed that both non-treated TTR and TTR pretreated at pH 4.0 bound to cells. No decrease in viability was noted for cells incubated with nontreated and treated TTR.

INTRODUCTION

Background. Mutant (MT) forms of transthyretin (TTR) cause autosomal dominant hereditary systemic amyloidosis.[1,2] In addition, wild-type (WT) TTR causes senile systemic amyloidosis, a sporadic disease seen in the elderly.[3] Although destabilization of TTR tetramers is widely believed to be a critical step in TTR amyloid formation, it remains to be fully elucidated how TTR makes amyloid in tissues and causes organ damage. The aim of the study is to investigate TTR deposition in cell culture and examine effects of deposition on cell morphology and viability.

METHODS

Recombinant wild-type and mutant (Val30Met) TTR were expressed in E. coli and purified by ammonium sulfate precipitation and DEAE and Sephacryl S-100 chromatography. TTR aggregates were formed in vitro by pretreating TTR in 100 mM acetate buffer, pH 4.0, for 30 min. Aggregate preparations were centrifuged to generate pellet and supernatant fractions or used without fractionation (Figure 1). Cultures of smooth muscle cells (glomotel cells) were incubated with the various TTR preparations for 6 days. Congo red staining and

immnohistochemical staining using an anti-TTR antibody (DAKO, Glostrup, Denmark) were performed. Cell lysates were examined by western analysis using the anti-TTR antibody. Cell viability was measured by MTS assay.

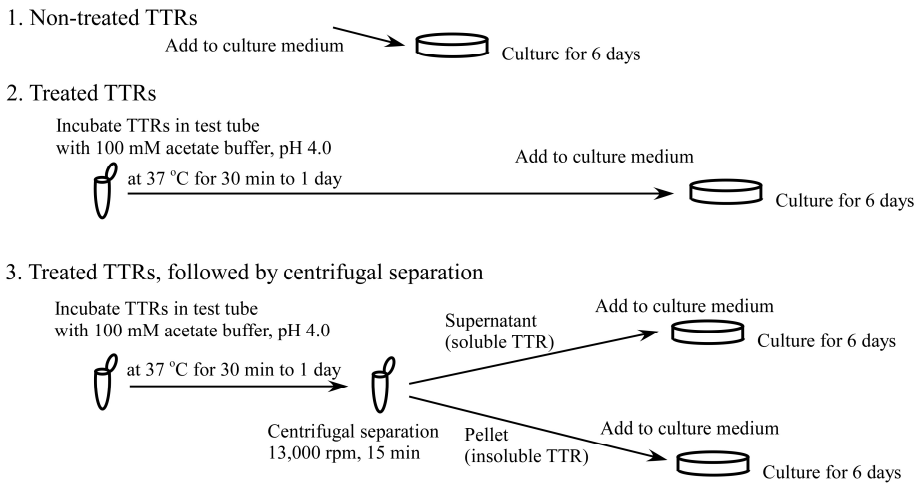

Figure 1. Preparations of TTR for cell culture studies.

RESULTS

TTR aggregates in non-fractionated pretreated preparations, as well as resuspended pelleted material, deposited on the surface of cells (Figure 2A). The deposits stained weakly with Congo red (Figure 2B) but were not birefringent (Figure 2C). Western analyses of cell lysates revealed that both non-treated TTR and TTR pretreated at pH 4.0 for 30 min bound to cells.

MTS assay revealed that viability of cells cultured with pretreated TTR was almost same as cells cultured with non-treated TTR in both wild-type and Val30Met TTR.

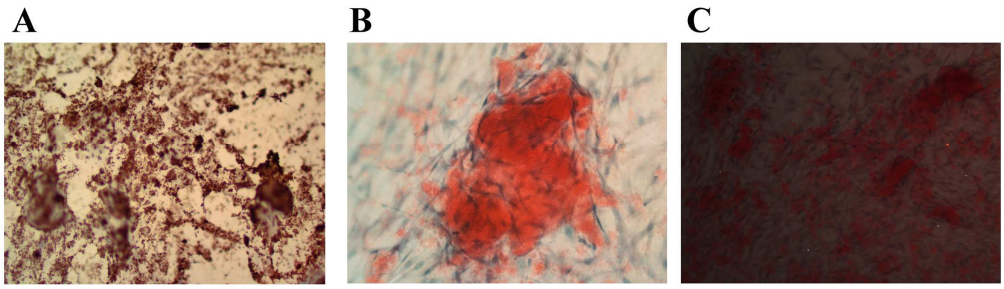

Figure 2. Congo red staining and immnohistochemical staining

(A) Immunohistochemical staining using the anti-TTR antibody in glomotel cells cultured with the pretreated TTR Val30Met. (B) Congo red staining in glomotel cells cultured with the pretreated TTR Val30Met. (C) Congo-red staining under polarized light.

DISCUSSION

TTR pretreated with acidic buffer in a test tube made deposits of TTR aggregates on the cells, while it is still unclear how TTR binds to cell surface. Those aggregates did not show birefringent under polarized light. This result suggests that TTR aggregates on the cells are different from amyloid deposits in the patients. To determine how TTR makes amyloid on the cells, further investigations should be performed.

REFERENCES

1. Zeldenrust S, Benson MD. Familial and senile amyloidosis caused by transthyretin. In Protein Misfolding Diseases: Current and Emerging Principles and Therapies. Edited by Alvarado M, Kelly JW, Dobson CM. Hoboken, NJ: John Wiley & Sons; 2010:795–815.
2. Ando Y, Nakamura M, Araki S. Transthyretin-related familial amyloidotic polyneuropathy. Arch Neurol 2005;62:1057–1062.
3. Westermark P, Bergström J, Solomon A, Murphy C, Sletten K. Transthyretin-derived senile systemic amyloidosis: clinicopathologic and structural considerations. Amyloid. 2003;10 Suppl 1:48–54.

Multi-system disease-specific induced pluripotent stem cell modeling of familial amyloidosis

Amy Leung[1,5], Shirley Nah[1,5], Clarissa Koch[2], Stefano Monti, John Berk[2], Lawreen Connors[2], David Seldin[1,2], Darrell Kotton[3,5], Gustavo Mostoslavsky[4,5], George Murphy[1,5].

*1. Section of Hematology and Medical Oncology. 2. Amyloid Treatment and Research Program. 3. Boston University Pulmonary Center and Department of Medicine. 4. Section of Gastroenterology. 5. Center for Regenerative Medicine (CReM). *All sections affiliated with the Department of Medicine, Boston University School of Medicine, Boston, Massachusetts, USA.*

ABSTRACT

Induced pluripotent stem cells (iPSCs) provide an unprecedented opportunity to model and to develop therapies for human genetic diseases in the genetic context of the patient. We have generated iPSC lines from a hereditary transthyretin amyloidosis (ATTR) patient heterozygous for the leucine-55-proline mutation. We demonstrate the successful modeling of this multi-systemic disease through the directed differentiation of ATTR-iPSC into both disease effector cells (hepatocytes) and peripheral target cells (cardiomyocytes, neurons). ATTR-iPSC derived target cells display oxidative stress and increased apoptosis when exposed to aberrant TTR protein produced by ATTR-iPSC hepatocytes, thus recapitulating aspects of the disease *in vitro*. Furthermore, the deleterious effects of ATTR hepatic supernatants were negated in the presence of known small molecule stabilizers of TTR such as diflunisal, thus validating the iPSC-based system as a suitable platform for small molecule drug testing.

INTRODUCTION

Induced pluripotent stem cell (iPSC) technology was first discovered in 2006 by the group of Shinya Yamanaka, who elucidated the combination of four factors, Oct4, Sox2, Klf4 and C-Myc whose overexpression was sufficient to reprogram somatic cells to pluripotency [1]. The generation of iPSC from patients with inherited diseases provides an unprecedented opportunity to study the effects of genetic abnormalities and disease progression. The derivation of unlimited quantities of the genetically relevant cell types targeted and affected in patients allows investigation of the cellular, molecular, and epigenetic events involved in multi-systemic genetic disease such as hereditary TTR amyloidosis (ATTR). Although most cases of ATTR are due to the autosomal dominant presence of a single base-pair mutation in hepatic serum protein transthyretin [2], the damage is seen extrinsically in the peripheral nervous system and heart [3], highlighting the need for a model that can recapitulate the multi-system complexity of the disease.

We have generated ATTR patient-specific iPSCs and used directed differentiation protocols to generate cells of hepatic, neuronal and cardiac lineages, modeling the three major tissue types involved in this lethal disease. Our data recapitulate clinical trial findings that certain small molecule TTR stabilizers can inhibit TTR fibril formation *in vivo*, validating this system as a platform for the testing of therapeutics.

RESULTS

Creation of disease-specific iPSCs; A lentiviral vector containing the four genes in a single "stem cell cassette" -known as STEMCCA- has been created and characterized by our group [4,5], and has been shown to be able to be highly efficient at generating "fully reprogrammed" iPSCs from transduced patient skin fibroblasts and peripheral blood cells. Using the STEMCCA system, we have generated multiple iPSC lines from an ATTR patient dermal fibroblast sample heterozygous for the L55P mutation, the most clinically aggressive disease-causing variant of the TTR gene [6] which targets the heart and the peripheral nerves in addition to other tissues.

The resultant ATTR-iPSCs were karyotypically normal and expressed a panel of associated pluripotency markers including Oct4, SSEA-4, Tra1-60 and Tra1-81. Importantly, the ATTR-iPSC clones were able to give rise to tissue derivatives of all three germ layers in teratoma formation assays in immunocompromised mice, indicating that the cells were functionally pluripotent**.**

Directed differentiation of ATTR-iPSCs to cellular lineages affected in ATTR; Using growth factor dependent, directed differentiation methodologies, ATTR-iPSCs were pushed towards the hepatic, cardiac and neuronal cell lineages for utilization in downstream disease modeling experiments.

Hepatic-lineage cells derived from ATTR-iPSCs were capable of glycogen storage, a property of *bona fide* hepatic cells, and they expressed a panel of hepatic markers such as alpha-fetoprotein, albumin and also the disease-affected gene transthyretin. Importantly, for the use of these cells in downstream experiments, western blot analysis of hepatic supernatants revealed that these cells produced and secreted TTR protein.

Cardiac and neuronal lineage cells derived from the ATTR-iPSCs also displayed hallmarks of their respective lineages as assessed by immunofluorescence and gene expression analysis, displaying upregulation of genes such as Tbx5 and cardiac troponin for the cardiac cells and neuronal class III β-Tubulin (Tuj1) and homeobox protein HB9 for neuronal cells. Functionally, ATTR-iPSC derived cardiac cells were capable of spontaneous contraction while neuronal cells were capable of labeled TTR uptake, a property of neuronal cells *in vivo* [7].

Assessment of damage to ATTR-target tissues; Having successfully derived the cellular lineages involved in ATTR, we then focused on the modeling of the disease in an *in vitro* setting, by dosing the "ATTR target" cells with supernatants from iPSC-derived hepatic cells (both control and ATTR). Flow cytometry of viability dye-stained cells revealed that compared to control, both neuronal and cardiac cells reacted adversely to ATTR hepatic supernatants (ATTR-hs), with an overall decrease in the number of live cells. Preliminary gene expression analysis of dosed ATTR-neuronal cells also revealed that cells exposed to ATTR-hs had comparatively higher levels of genes typically upregulated in response to aberrant protein folding and cellular stress, such as heat-shock 70 family proteins and heme oxygenase 1.

Amelioration of damage with TTR stabilizing molecules; Having ascertained that hepatic supernatants containing the L55P variant of TTR had a deleterious effect on cell survival, we next investigated whether it was possible to rescue this effect through the addition of known small molecule stabilisers of aberrant tetrameric TTR; diflunisal and flufenamic acid [8,9]. The addition of either of these compounds to ATTR-hs had a protective

effect on both neuronal and cardiac cell survival compared to cells exposed to ATTR-hs alone, indicating that the stabilization of aberrant TTR in the supernatant was sufficient to prevent the toxic effects observed with ATTR-hs.

DISCUSSION

Pluripotent stem cells are a useful tool for disease modeling as it is possible, through directed differentiation, to study the lineages of interest *in vitro*. iPSCs, which are derived from patient-specific cells, further this by allowing the study of genetic diseases in the context of the genetic background of the patients. For a disease such as ATTR, in which a degree of clinical variability has been observed in patients with the same genetic variants in the TTR gene, it may provide insights into the underlying causes of disease manifestation. Using our versatile iPSC system, we have recapitulated aspects of ATTR *in vitro* through the exposure of directed-differentiated tissues to hepatic supernatants containing aberrant TTR. We have also demonstrated that known small molecule stabilizers of the TTR tetrameric structure can overcome the deleterious effects of aberrant TTR in this system, therefore validating this system as a potential platform in which to study the effects of novel therapeutics for the disease.

REFERENCES

1. Takahashi K, Yamanaka S. Induction of pluripotent stem cells from mouse embryonic and adult fibroblast cultures by defined factors. Cell. 2006 Aug 25;126(4):663–76.
2. Connors LH, Lim A, Prokaeva T, Roskens VA, Costello CE. Tabulation of human transthyretin (TTR) variants, 2003. Amyloid. 2003 Sep;10(3):160–84.
3. Falk RH, Comenzo RL, Skinner M. The systemic amyloidoses. N. Engl. J. Med. 1997 Sep 25;337(13):898–909.
4. Sommer CA, Stadtfeld M, Murphy GJ, Hochedlinger K, Kotton DN, Mostoslavsky G. Induced pluripotent stem cell generation using a single lentiviral stem cell cassette. Stem Cells. 2009 Mar;27(3):543–9.
5. Somers A, Jean J-C, Sommer CA, Omari A, Ford CC, Mills JA, et al. Generation of transgene-free lung disease-specific human induced pluripotent stem cells using a single excisable lentiviral stem cell cassette. Stem Cells. 2010 Oct;28(10):1728–40.
6. Jacobson DR, McFarlin DE, Kane I, Buxbaum JN. Transthyretin Pro55, a variant associated with early-onset, aggressive, diffuse amyloidosis with cardiac and neurologic involvement. Hum. Genet. 1992 May;89(3):353–6.
7. Fleming CE, Mar FM, Franquinho F, Saraiva MJ, Sousa MM. Transthyretin internalization by sensory neurons is megalin mediated and necessary for its neuritogenic activity. J. Neurosci. 2009 Mar 11;29(10):3220–32.
8. Peterson SA, Klabunde T, Lashuel HA, Purkey H, Sacchettini JC, Kelly JW. Inhibiting transthyretin conformational changes that lead to amyloid fibril formation. Proc. Natl. Acad. Sci. U.S.A. 1998 Oct 27;95(22):12956–60.
9. Miller SR, Sekijima Y, Kelly JW. Native state stabilization by NSAIDs inhibits transthyretin amyloidogenesis from the most common familial disease variants. Lab. Invest. 2004 May;84(5):545–52.

SECTION IV

DIAGNOSIS, TYPING AND IMAGING


Tuesday

STATE OF THE ART: Diagnosis and typing of amyloid in the Amyloid Registry Kiel

C. Röcken

Department of Pathology, Christian-Albrechts-University, Kiel, Germany.

Amyloid is a pathologic fibrillar aggregation of polypeptides in a cross-β-sheet conformation. Amyloidoses are caused by the deposition of amyloid and may occur as cerebal and extracerebral diseases. More than 29 different amyloid proteins have been identified. Inspection of a Congo red-stained tissue section by polarization microscopy is the gold standard for diagnosing amyloid. Subsequent classification of the amyloid is mandatory and is increasingly supported by molecular biological analyses. This led to the discovery of several hereditary amyloid diseases in Germany. The correct classification of amyloid is of paramount importance. This helps to assess the prognosis and tailors patient treatment.

DIAGNOSING AMYLOID HISTOLOGICALLY

Amyloid can only be diagnosed by the inspection of a tissue specimen either by light microscopy or electron microscopy. Even 150 years after the first description of amyloid by Rudolf Virchow, no clinical, laboratory or imaging technology has replaced the analysis of a tissue sample, putting the histopathologist in a central position for recognizing and diagnosing amyloid. While *amyloid* is defined by the presence of proteinaceous deposits with specific tinctorial properties, *amyloidosis* denotes the disease state caused by the deposition of amyloid. Amyloid can be unapparent without clinical and/or histological evidence of a resulting disease.

On an H&E-stained tissue specimen, amyloid appears as a homogeneous eosinophilic mass. Following Congo red staining, amyloid shows a typical apple green birefringence when viewed in polarized light between crossed polars. Electron microscopically, amyloid consists of non-branching linear fibrils with an average diameter of 10 nm. Several alterations in human tissue can mimic amyloid, including various forms of scaring, which are far more common than amyloid in the routine surgical pathology service. Thus, prior to diagnosing amyloid, it is necessary to consider this differential diagnosis, and I strongly recommend to constantly remind clinicians and surgical pathologists of this orphan disease.

When amyloid is suspected, Congo red staining in conjunction with polarization microscopy is the gold standard. The light source of the microscope has to be set at maximum power and the crossed polarization filters should darken the field almost completely. Amyloid then shows the characteristic and diagnostic apple green birefringence. However, there is ample evidence that the intensity of the birefringence varies between different types of amyloid, commonly being weaker in AL and certain forms of ATTR amyloid. In these settings, amyloid can be missed when the Congo red staining and polarization microscopy are not properly applied.

Recognizing tiny deposits can be difficult at times and are prone to sampling errors. Application of step sections and/or fluorescence microscopy to the Congo red-stained sections may increase the sensitivity.

CLASSIFICATION OF AMYLOID IMMUNOHISTOLOGICALLY

Once a diagnosis has been reached, amyloid has to be classified. The vast majority of tissue specimens studied in surgical pathology have been fixed in formalin and embedded in paraffin (FFPE). Thus, classification technologies should be applicable to these specimens. Immunohistochemistry is a standard technique, which, in general, can be applied robustly to FFPE-tissue specimens (1). It is available in almost any Department of Pathology (University Hospital, Community Hospital, Private Practice) and as such has the broadest distribution. However, while immunodetection of common cellular and tissue antigens, such as cytokeratin or vimentin, is straight forward, classification of amyloid is more sophisticated for the following reasons:

1) Many amyloid proteins have undergone conformational and post-translational modifications. Therefore, antibodies raised with the cognate native, physiologically folded precursor proteins may not yield antibodies suitable for the recognition of amyloid proteins.
2) All amyloid proteins derive from physiological, autologous precursor proteins, which may still be present in the test tissue bearing the risk of “false positive”, although specific, immmunolabeling not identical with the amyloid protein.
3) Amyloid is deposited loosely in the tissue and serum proteins regularly diffuse into the amyloid deposits further corroborating immunohistochemical classification.
4) Amyloid is a rare disease of diverse origin and classification requires a large battery of different antibodies (Table 1), which will only be used rarely making classification of amyloid in a routine diagnostic laboratory uneconomical.

Thus, advanced immunohistochemical classification of amyloid should be carried out in specialized units, which have special expertise with the classification of amyloid and are able to make classification economical (1). This also applies to more advanced proteomics based classification systems of amyloid (see A. Dogan, this *Proceedings book*).

THE AMYLOID REGISTRY KIEL

The Amyloid Registry Kiel is a central pathology service unit for the diagnosis and classification of amyloid in Germany. We receive samples from clinicians and referring surgical pathologists from all over Germany. Mostly FFPE-tissue samples are submitted to the registry after the referring surgical pathologist has diagnosed amyloid. On a routine basis, we apply nine different antibodies to every specimen using serial sections of which one is stained with Congo red. Immunolabelling is done with fully automated immunostainers using also on slide positive and negative controls (Figure 1). In addition to that many more mostly non-commercially available antibodies are kept on stock and are applied to the tissue specimens depending on the origin and type of amyloid to be considered (Table 1). The Amyloid Registry Kiel now houses more than 2000 cases of amyloid with an annual increment of about 450 new cases. This unique collection has enabled a new sort of systematic studies investigating the prevalence and histoanatomical distribution of the diverse types of amyloid in tissue biopsies. This ultimately improves recognition and classification of amyloid, since the deposition patterns vary among the different types of amyloid improving significantly clinico-pathological diagnosis.

Table 1. Antibodies used by the Amyloid Registry Kiel for the classification of amyloid

Antibody	Commercial / non commercial	mono- / polyclonal	Manufacturer / peptide sequence used for immunisation
Amyloid-P Komponent	C	P	DakoCytomation, Glostrup, Denmark
AA-Amyloid	C	M (clone mc_1)	DakoCytomation, Glostrup, Denmark
Aβ-Amyloid	C	M (clone 6F/3D)	DakoCytomation, Glostrup, Denmark
β2-Mikroglobulin	C	P	Novocastra, Newcastle upon Tyne, England
Calcitonin	C	M (clone SP17)	Thermo Fisher Scientific, U.S.A.
hDYSF5a (Dysferlin)	C	P	NH_2-CTTPRKLPSRPPPHY-$CONH_2$
hDYSF-5b (Dysferlin)	C	P	NH_2-CRKRSAPTSRKLLSDK-$CONH_2$
hDYSF-6 (Dysferlin)	C	P	NH_2-AGQTKRTRIHKGNSC-$CONH_2$
Gelsolin	C	M (clone GS-2C4)	Sigma-Aldirch, Deisenhofen
Insulin	C	M (HB125)	BioGenex, U.S.A.
Lactoferrin	C	P	DakoCytomation, Glostrup, Denmark
λ-Leichtkette	C	P	DakoCytomation, Glostrup, Denmark
AL1 (λ-Leichtkette)	N	P	Native $AL_{V\lambda VI}$ Amyloidproteine (10)
AL3 (λ-Leichtkette)	N	P	NH_2-ISCSGSSSNIGSNTV-$CONH_2$ and NH_2-QRPSGVPDRFSGSKSGTS-$CONH_2$ (11)
AL7 (λ-Leichtkette)	N	P	NH_2 – CLFPPSSEELQANKATLV – $CONH_2$
κ-Leichtkette	C	P	DakoCytomation, Glostrup, Denmark
AK1 + AK2 (κ-light chain)	N	P	NH_2-CQMTQSPSSLSASVGD-$CONH_2$
AK3 + AK4 (κ-light chain)	N	P	NH_2-CFIFPPSDEQLKSGTA-$CONH_2$
Fibrinogen	C	P	DakoCytomation, Glostrup, Denmark
Fib1 (Fibrinogen)	N	P	NH_2-EKVTSGSTTTTRRSC-$CONH_2$
Fib2 (Fibrinogen)	N	P	NH_2-CQNLASSQIQRNPVLIT-$CONH_2$
Fib3 (Fibrinogen)	N	P	NH_2-EKVTSGSTTTTRRSC-$CONH_2$ and NH_2-CQNLASSQIQRNPVLIT-$CONH_2$
Apolipoprotein A-I	N	P	NH_2-DEPPQSPWDRVKDLAC-$CONH_2$ and NH_2-CVLKDSGRDYVSQFEG-$CONH_2$ (12)
Apolipoprotein A-II	C	P	Biodesign International, U.S.A.
Transthyretin	C	P	DakoCytomation, Glostrup, Denmark
Transthyretin (TTR3)	N	P	NH_2-FHEHAEVVFTANDSGPRRYT-$CONH_2$
Lysozyme	C	P	DakoCytomation, Glostrup, Denmark

C: commercial; N: non commercial; P: polyclonal; M: monoclonal

HEREDITARY AND RARE LOCAL AMYLOIDOSES IN GERMANY

Although the first medical report on hereditary amyloidosis by Ostertag stems from Germany (2), most types of hereditary amylodoses were subsequently identified in Japan, North America, Portugal, Sweden and the United Kingdom. Except for hereditary ATTR amyloidosis, other forms of extracerebral hereditary amyloidoses did not seem to occur in Germany. Therefore we carried out a systematic search for hereditary type amyloidoses in Germany and since then discovered hereditary forms of amyloid caused by mutations of the apolipoprotein AI- (3), dysferlin- (4), fibrinogen- (5), lysyozme- (6), and oncostatin M receptor-gene (7). We also studied the

prevalence of *TTR*-gene mutations in a consecutive series of surgical pathology specimens (8). The central collection and classification of amyloid also led to the re-discovery of the local AIns amyloid caused by the injection of recombinant insulin in insulin-dependent diabetics (9), which was thought to have disappeared. These studies elegantly demonstrate the fundamental problem of orphan diseases in our health care systems: These rare diseases need to be specifically sought by specialized health care professionals, otherwise they will be missed.

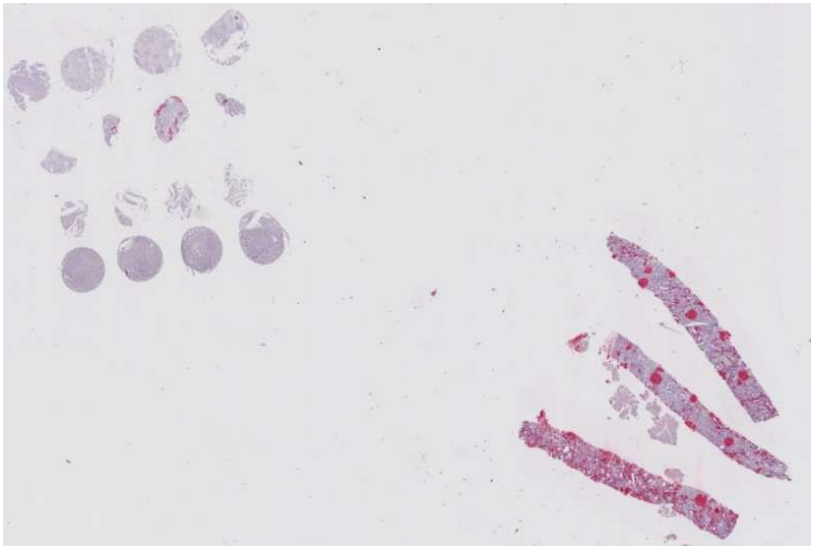

Figure 1. Renal AA amyloidosis (note the on slide positive control in the left upper corner consisting of a tissue micro array with AA-, AL-, and ATTR amyloid, and liver without amyloid).

AMYLOID IN ORGAN BIOPSIES

The Amyloid Registry Kiel and its predecessor at the Charité Berlin (2006-2009) allowed the systematic investigation of the prevalence of amyloid types in different organ biopsies. While these studies do not reflect the true prevalence of the diverse amyloidoses and their respective organ distributions, it mirrors the clinico-pathological background in which amyloid is diagnosed. This is influenced by the clinical presentation of the disease and the subsequent diagnostic procedures undertaken to reach a diagnosis. Amyloid is often not the first differential diagnosis considered by either the general practitioner or the specialized physician. We explored systematically the prevalence of the diverse types of amyloid in large patient series of kidney biopsies (233 patients) (13), liver biopsies (46 patients) (14), heart biopsies (283 patients) (15) and in biopsies of the respiratory tract (144 patients). Interestingly and as expected, the pattern of amyloid types varies among the different organ biopsies. In kidney biopsies, AL and AA amyloidosis are most prevalent and in addition to that almost any systemic hereditary type of amyloidosis affects in the kidney. In liver biopsies almost 90% of the cases harbor AL amyloidosis, whilst cardiac biopsies obtained from the ventricles enclose either AL (53%) or ATTR (45%) type. Biopsies obtained from the airways and lung show AL amyloid in 78% of the cases (Figure 2).

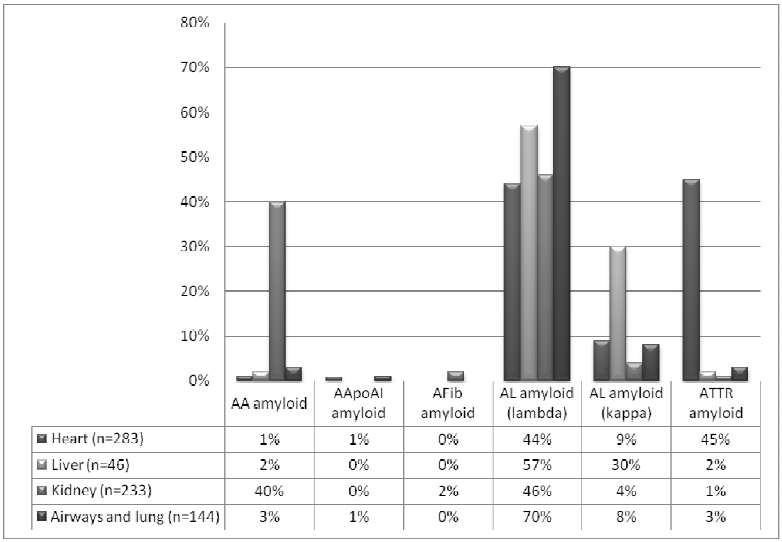

	AA amyloid	AApoAI amyloid	AFib amyloid	AL amyloid (lambda)	AL amyloid (kappa)	ATTR amyloid
Heart (n=283)	1%	1%	0%	44%	9%	45%
Liver (n=46)	2%	0%	0%	57%	30%	2%
Kidney (n=233)	40%	0%	2%	46%	4%	1%
Airways and lung (n=144)	3%	1%	0%	70%	8%	3%

Figure 2. Prevalence of amyloid types in biopsy specimens

SUMMARY (BULLET POINTS)

- Amyloid is a rare disease and considering it in the differential is half way.
- Novel detection technologies for amyloid should be broadly applicable without necessitating specific technology.
- Combination of clinical information, histology, immunhistochemical classification and molecular typing is mandatory and state of the art.
- Protein biochemistry (mass spectrometry) is evolving and will improve diagnosis.

REFERENCES

1. Schönland SO, Hegenbart U, Bochtler T, Mangatter A, Hansberg M, Ho AD, et al. Immunohistochemistry in the classification of systemic forms of amyloidosis: a systematic investigation of 117 patients. Blood 2012; 119(2): 488-93.
2. Ostertag B. Demonstration einer eigenartigen familiären Paramyloidose. Zbl Pathol 1932; 56: 253-4.
3. Eriksson M, Schönland S, Yumlu S, Hegenbart U, von HH, Gioeva Z, et al. Hereditary apolipoprotein AI-associated amyloidosis in surgical pathology specimens: identification of three novel mutations in the APOA1 gene. J Mol Diagn 2009; 11(3): 257-62.
4. Spuler S, Carl M, Zabojszcza J, Straub V, Bushby K, Moore SA, et al. Dysferlin-deficient muscular dystrophy features amyloidosis. Ann Neurol 2008; 63(3): 323-8.
5. Eriksson M, Schönland S, Bergner R, Hegenbart U, Lohse P, Schmidt H, et al. Three German fibrinogen Aalpha-chain amyloidosis patients with the p.Glu526Val mutation. Virchows Arch 2008; 453(1): 25-31.

6. Röcken C, Becker K, Fändrich M, Schroeckh V, Stix B, Rath T, et al. ALys amyloidosis caused by compound heterozygosity in exon 2 (Thr70Asn) and exon 4 (Trp112Arg) of the lysozyme gene. Hum Mutat 2006; 27(1): 119-20.
7. Babilas P, Fiebig BS, Aslanidis C, Hansen J, Röcken C, Schroeder J, et al. Identification of an oncostatin M receptor mutation associated with familial primary cutaneous amyloidosis. Br J Dermatol 2009; 161(4): 944-7.
8. Eriksson M, Büttner J, Todorov T, Yumlu S, Schönland S, Hegenbart U, et al. Prevalence of germline mutations in the TTR gene in a consecutive series of surgical pathology specimens with ATTR amyloid. Am J Surg Pathol 2009; 33(1): 58-65.
9. Yumlu S, Barany R, Eriksson M, Röcken C. Localized insulin-derived amyloidosis in patients with diabetes mellitus: a case report. Hum Pathol 2009; 40(11): 1655-60.
10. Bohne S, Sletten K, Menard R, Bühling F, Vockler S, Wrenger E, et al. Cleavage of AL amyloid proteins and AL amyloid deposits by cathepsins B, K, and L. J Pathol 2004; 203(1): 528-37.
11. Kuci H, Ebert MP, Röcken C. Anti-lambda-light chain-peptide antibodies are suitable for the immunohistochemical classification of AL amyloid. Histol Histopathol 2007; 22(4): 379-87.
12. Gregorini G, Izzi C, Obici L, Tardanico R, Röcken C, Viola BF, et al. Renal apolipoprotein A-I amyloidosis: a rare and usually ignored cause of hereditary tubulointerstitial nephritis. J Am Soc Nephrol 2005; 16(12): 3680-6.
13. Hutten Hv, Mihatsch M, Lobeck H, Rudolph B, Eriksson M, Röcken C. Prevalence and origin of amyloid in kidney biopsies. Am J Surg Pathol 2009; 33(8): 1198-205.
14. Gioeva Z, Kieninger B, Röcken C. Amyloidosis in liver biopsies. Pathologe 2009; 30(3): 240-5.
15. Kieninger B, Eriksson M, Kandolf R, Schnabel PA, Schönland S, Kristen AV, et al. Amyloid in endomyocardial biopsies. Virchows Arch 2010; 456(5): 523-32.

Digitally reinforced Hematoxylin-eosin slides: First clue in detection of amyloid depositions

B. Pehlivanoglu, B. Doganavsargil, B. Sarsik, M. Sezak, S. Sen

Ege University Faculty of Medicine, Department of Pathology, Bornova, Izmir, Turkey

Amyloid has an amorphous, eosinophilic appearance on Hematoxylin-eosin and Congo-red is the gold standard for diagnosis. In this study, we searched the potential power of digitalized Hematoxylin-eosin slides to detect amyloid depositions. Ninety-one upper gastrointestinal endoscopic biopsy specimens of 75 patients with amyloidosis and 20 consecutive control cases without gastric amyloidosis were reevaluated blindly using Olympus BX51 polarising microscope equipped with DP21 camera with stand alone system. Depositions which show green birefringence on HE with digitalized microscopy were considered as positive and results were confirmed using Congo-red. The sensitivity, specificity, positive and negative predictive values were estimated as 85%, 96%, 99% and 65%, respectively. We concluded that digitalized HE sections can be used as a fast search method for diagnosis of amyloidosis. Further investigation is needed on this matter. However, as the technique improves, it may predict the positivity of Congo-red.

INTRODUCTION

Various stains have been used for detection of amyloid fibrils in histologic specimens to date and Congo red has been established as the gold standard for diagnosis (1, 2). Currently, Hematoxylin-eosin (HE) is the most widely used stain in pathology practice and amyloid has an amorphous, eosinophilic appearance on HE, giving the pathologist the first clue to suspect amyloidosis. We recently realized that the Toluidine-blue stained amyloid deposits show birefringence in digitally photographed (digitally reinforced) sections. In this study, we searched the potential power of this technique to detect amyloid depositions in HE stained slides.

METHODS

Ninety-one upper GI endoscopic biopsy specimens of 75 patients (41 male and 34 female) with amyloidosis and 20 control cases without gastric amyloidosis were reevaluated blindly using Olympus BX51 polarising microscope equipped with DP21 camera with stand alone system. Average age was 47.5 ± 14, 8 (range 10-79 years-old). Depositions which show green birefringence on HE with digitalized microscopy were considered as positive and results were correlated with Congo-red staining results and distribution of amyloid deposition by nonparametric tests.

RESULTS

Amyloid deposition was seen on HE in 67 specimens (Figures 1 and 2) and confirmed by Congo red except for one “false positive” case. In 12 cases no depositions were distinguished on HE although they were visible in Congo red stained sections (False negative). Ten biopsies were excluded as they were unqualified for evaluation of amyloidosis. A total of 22 specimens including the control group did not show birefringence either on HE or Congo red (true negative). The sensitivity, specificity, positive and negative predictive values were estimated as 85%, 96%, 99% and 65%, respectively.

Amyloid deposition was most frequently encountered in vasculary walls (73,6%) followed by muscularis mucosa (65,3%) and lamina propria (41,3%).Thirty cases (40%), 36.6% of which also had renal involvement, showed extensive *vascular*, *muscular* and *stromal* amyloid deposition. Four patients had rheumatoid arthritis, seven had ankylosing spondylitis, five had familial Mediterranean fever (FMF), one had Behcet’s disease and one patient had Reiter syndrome. Stromal involvement was only seen in widely distributed cases.

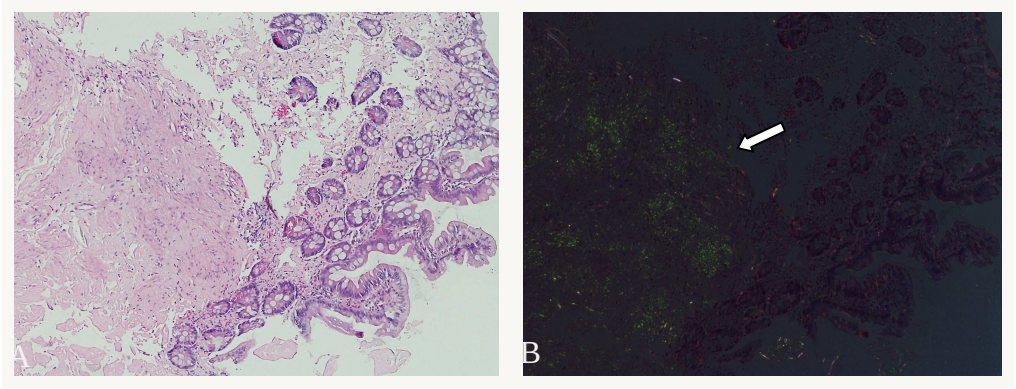

Figure 1. Amyloid depositions in duodenum

A) Ordinary Hematoxylin-eosin section (x10), B) digitally reinforced polarized Hematoxylin-eosin**.**

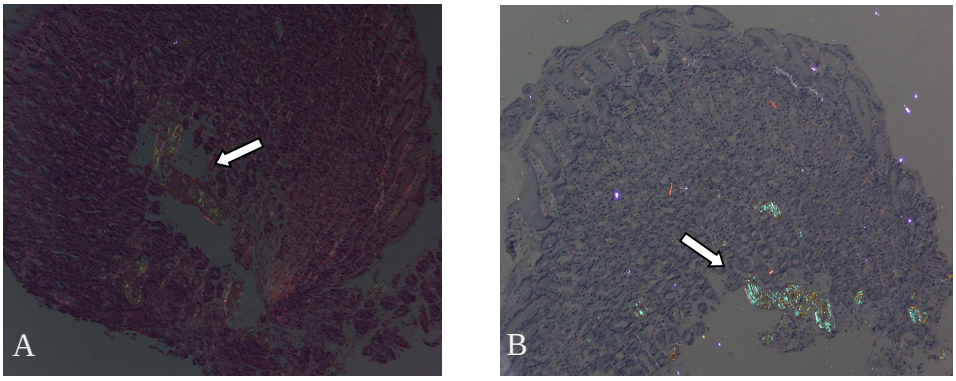

Figure 2. Vascular amyloid depositions. A) Ordinary Hematoxylin-eosin section, B) digitally reinforced polarized hematoxylin-eosin

DISCUSSION

Various stains have been used to detect amyloid in tissues however, detection of Congo red stained deposits that show green birefringence under polarized light has become the gold standard for diagnosis of amyloidosis (1, 2). But, staining method may change the sensitivity and specificity of Congo red staining (3) and pathologists may require ancillary studies such as histochemistry and immunohistochemistry for definitive diagnosis and histotyping of amyloidosis. However HE stained section maintains its value as the first step of evaluation and amorphous, eosinophilic appearance of amyloid must be differentiated from other changes as sclerosis or hyalinization. It has been reported that unstained amyloid fibrils may show birefringence (4). We realized that HE stained deposits show the very same green birefringence under polarized light (5). The camera system attached to the polarizing microscope allows more powerful polarization, providing a polarization degree that one could not see through binoculars but only on the monitor. It is also noteworthy that collagen and smooth muscle fibers displayed birefringence of white yellow tint that is different from amyloid depositions in some cases which is of help in evaluating especially muscular deposits. This technique gives the pathologists the opportunity to confirm their preliminary diagnosis to preserve tissue and reduce the laboratory workload by eliminating the need for additional sectioning

In conclusion, digitalized HE sections can be used as a fast search method for diagnosis of amyloidosis. To our knowledge, there is no other study reported in the literature on HE polarization of amyloid fibrils but further investigation is needed to prove its value in prediction of Congo-red positivity.

REFERENCES

1. Sipe JD, Benson MD, Buxbaum JN, Ikeda S, Merlini G, Saraiva MJ, Westermark P. Amyloid fibril protein nomenclature: 2010 recommendations from the nomenclature committee of the International Society of Amyloidosis. Amyloid. 2010;17:101-4. DOI:10.3109/13506129.2010.526812.
2. Westermark GT, Johnson KH, Westermark P. Staining methods for identification of amyloid in tissue. Methods Enzymol 1999;309:3-25. DOI: 10.1016/S0076-6879(99)09003-5.
3. Bély M, Makovitzky J. Sensitivity and specificity of Congo red staining according to Romhanyi. Comparison with Puchtler's or Bennhold's. Acta histochemica 108 (2006) 175—180.
4. Appel TR, Richter S, Linke RP, Makovitzky J. Histochemical and topo-optical investigations on tissue-isolated and in vitro amyloid fibrils. Amyloid. 2005;12:174-8. DOI:10.1080/13506120500221906.
5. Sen S, Sarsık B. Digitally reinforced polarization of hematoxylin eosin diagnosing of renal amyloidosis. Turk Patoloji Derg. 2012;28(3): in press. DOI: 10.5146/tjpath.2012.01126

Digitally reinforced Toluidine blue can safely be used for detection of amyloid depositions

S. Sen, B. Sarsik, B. Pehlivanoglu, M. Sezak, B. Doganavsargil

Ege University, School of Medicine, Department of Pathology, Izmir, Turkey

Gastrointestinal (GI) amyloidosis is not infrequent however; GI endoscopic biopsies can be too small for additional stains such as Congo red. In our center, a metachromatic dye, Toluidine-blue, is used as a reflex stain for *H.pylori* detection. We searched its potential value in detection of amyloidosis, applying a recently introduced technique “Digitally reinforced polarization” for visualization of amyloid deposits. Ninety-one upper GI biopsy specimens of 75 patients were blind-reviewed by using polarising microscope equipped with a digital camera. Of the 91 biopsies, 70 showed typical birefringence with Toluidine-blue in digital images. One case was considered as false positive and the number of false negative cases was 8. The sensitivity, specificity, positive and negative predictive values were estimated as 90%, 96%, 99% and 74%, respectively. We concluded that digitally reinforced Toluidine-blue can be used safely in diagnosis of amyloidosis, particularly in laboratories which use Toluidine-blue routinely.

INTRODUCTION

The term amyloidosis refers to a heterogeneous group of diseases characterized by the deposits of amyloid protein fibrils and Congo red is required for definitive diagnosis. Gastrointestinal (GI) amyloidosis is a universal finding in systemic amyloidosis and characterised by extracellular deposition of amyloid proteins in the mucosa, submucosa, and muscularis propria. However, GI endoscopic biopsies can be too small in size for additional stains. In our center, Toluidine-blue, is used as a routine reflex stain for *H.pylori* detection. Toluidine blue is a metachromatic dye producing orthochromatic blue staining of most amyloid deposits and stained amyloid deposits also show a specific birefringence (1).

In this study, we evaluated Toluidine-blue stained amyloid deposits showing birefringence in digitally photographed (digitally reinforced) sections in addition to expected metachromasia and we searched its potential value in detecting amyloid depositions in upper GI biopsies.

METHODS

Ninety-one upper GI (oesophagus, stomach and duodenum) endoscopic biopsy specimens of 75 patients with known amyloidosis, proven by Congo red stain and twenty consecutive patients without gastric amyloidosis (control group) were included the study. All Toluidine-blue stained sections were evaluated and photographed

by using Olympus BX51 polarising microscope equipped with DP21 camera with stand alone system and blind-reviewed. Details of the digital photography and evaluation technique were described elsewhere (2). Depositions which show magenta-red green birefringence with Toluidine blue were considered as amyloid positive (Figure 1). Results were confirmed using Congo red staining according to Pucthler (3) with evaluation in polarized light (Figure 2).

RESULTS

Seventy of the 91 biopsies showed metachromasia and green birefringence with Toluidine blue. Ten Toluidine blue sections were unqualified for diagnosis of amyloid deposits. Collagen and smooth muscle fibers also displayed birefringence, however they showed yellow white tint, which was different from amyloid depositions.

One biopsy was considered as false positive and the number of false negative biopsies was 8. No positivity was found in the control group. The sensitivity, specificity, positive and negative predictive values were estimated as 90%, 96%, 99% and 74%, respectively.

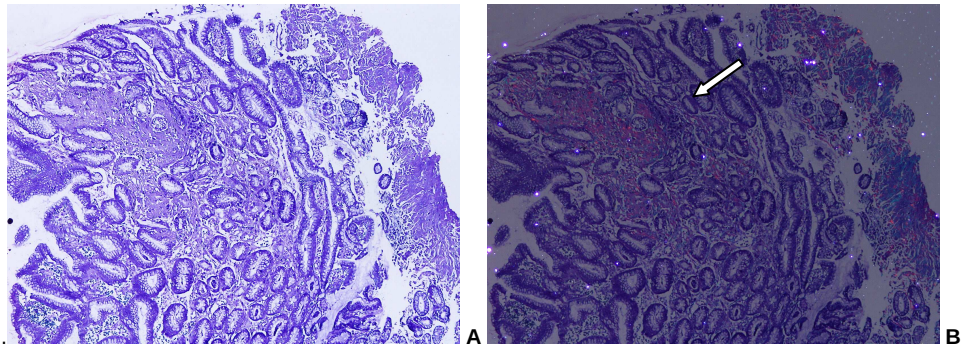

Figure 1. A: Ordinary bright field illumination of Toluidine Blue stained sections. Amyloid depositions shows metachromasia (pale violet - blue in colour) (x10). B: Polarized view of the same section. When polariser was rotated until the background gets dark, amyloid deposited places showed magenta-red-green tint ion (anomalous colours) while other parts were dark (x10).

DISCUSSION

Most pathologists identify amyloid depositions with Congo red and make the definitive diagnosis based on green birefringence with anomalous color changes (4). Although Congo red is the golden standard for visualization of amyloid deposits it can be affected from the type of fixative, fixation time, section thickness, age of the patients' slides or even age of amyloid deposits (5). Amyloid can also be demonstrated by metachromatic or polychromatic dyes. However these extra stains require serial sections and have the risk of losing area of interest especially in small biopsies as we have seen in some cases of our series. Recently we showed that Hematoxylin-eosin and/or other metachromatic stains may also show amyloid depositions under polarized light (2, 6). This polarization can efficiently be reinforced by a digitalized camera and easily be detected in those captured images. Anomalous color changes with Toluidine-blue polarization exhibit a wide spectrum between red and green which is different from collagen and smooth muscles polarization tint. In this study, we evaluated

reflex Toluidine-blue stained sections for H.Pylori detection to reveal amyloidosis. High values of sensitivity, specificity, positive and negative predictive were found, suggesting that it may predict amyloidosis when Congo red cannot be performed.

CONCLUSION

We concluded that digitally reinforced Toluidine-blue can be used safely in diagnosis of amyloidosis, particularly in laboratories which use Toluidine-blue routinely, by eliminating the need for extra Congo red stain, thus providing opportunity to conserve tissue samples.

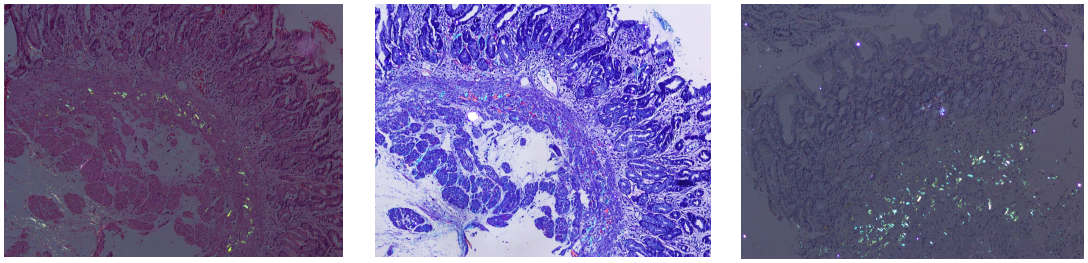

A B C

Figure 2: Comparison of digitally reinforced polarized amyloid depositions, A) Hematoxylin eosin, B) Toluidine blue, C) Congo red X10

Table 1. Patients' characteristics in the upper gastrointestinal tract amyloidosis

Type of Amyloidosis	**Number of cases**	**Antecedent disease**	
AA (secondary) Amyloidosis	**56**		
		Chronic Rheumatic Disease	23
		FMF and periodic fever	16
		Inflammatory bowel disease (Crohn's disease.)	2
		Chronic Infection	5
		Malignancy	1
		Undefined	9
AL Amyloidosis	**6**		
		Multiple Myeloma	5
		Plasma Cell Dyscrasia	1
Hereditary Amyloidosis	**1**		
Unknown	**12**		
Total	**75**		

REFERENCES

1. Elghetany MT, Saleem A. Methods for staining amyloid in tissues: a review. Stain Technol. 1988 Jul;63:201-12. PMID: 2464206
2. Sen S, Sarsık B. Digitally reinforced polarization of hematoxyline eosin diagnosing of renal amyloidosis. Turk Patoloji Derg. 2012;28(3): will be published. DOI: 10.5146/tjpath.2012.01126.
3. Putchler Puchtler H, Sweat F, Levine M. On the binding of Congo red by amyloid. J Histochem Cytochem 1962;10:355-64. DOI: 10.1177/10.3.355.

4. Howie AJ, Brewer DB, Howell D, Jones AP. Physical basis of colors seen in Congo red-stained amyloid in polarized light. Lab Invest. 2008;88:232-42. DOI:10.1038/labinvest.3700714.
5. Wenk PA. Troubleshooting the Congo red stain for amyloid. http://www.mihisto.org/Resources/Documents/tp.3904%5Bfa10%5Damyloid.pdf accessed on 20.08.2012.
6. Pehlivanoglu B, Doganavsargil B, Sarsik B, Sezak M, Sen S. Digitalized Hematoxylin-eosine slides: First clue in detection of amyloid depositions. XIII International Symposium on Amyloidosis, May 6-10, 2012, Groningen. PA57, Congress book, pages 119-120.

Diagnosis of amyloid in frozen sections

Maria M. Picken

Department of Pathology, Loyola University Medical Center, Chicago, USA.

Amyloidosis is perceived as being rarely seen in surgical pathology and there is a paucity of data regarding its diagnosis on frozen sections.

This report presents 7 patients with unsuspected amyloidosis who were diagnosed at the time of frozen section. There were 4 females and 3 males, with ages ranging from 52 to 72. Two patients presented with laryngeal mass, one with ocular mass, two other patients with hematuria and two patients with intractable gastrointestinal bleeding. Four patients underwent surgical exploration with frozen section evaluation and planned immediate staging procedure based on frozen section diagnosis; three patients underwent a biopsy evaluated with frozen section for sample adequacy. Frozen sections demonstrated acellular deposits of amorphous material. Congo red stain performed on frozen and paraffin sections confirmed the presence of amyloid. Subsequent studies demonstrated localized amyloid in 5 patients and systemic amyloidosis (AL x 1 and senile ATTR x 1) in 2 patients.

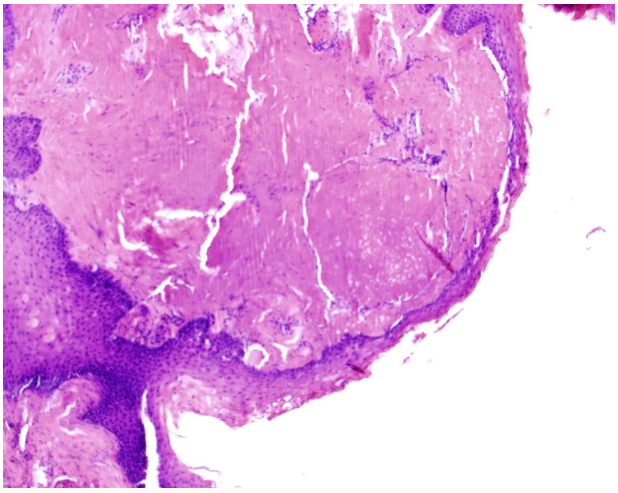

Figure 1. Laryngeal localized amyloid, H&E stained section; Congo red stained section confirmed the presence of amyloid (not shown). Subsequent abdominal fat biopsy was negative for amyloid and bone marrow biopsy was negative for plasma cell dyscrasia; serum free light chains levels and the ratio were within normal limits. There was no evidence of systemic amyloidosis and there was no recurrence after local treatment (follow-up 12 months).

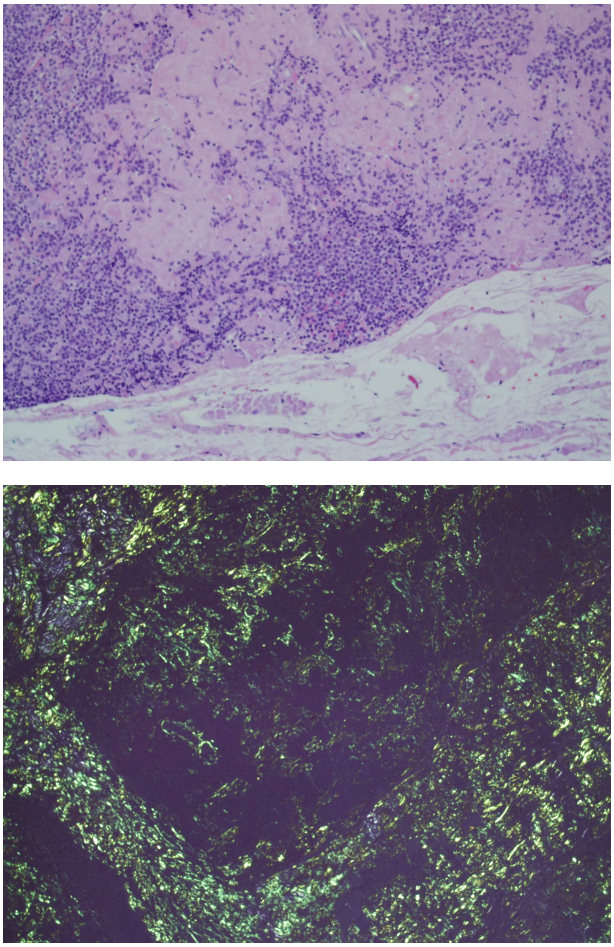

Figure 2. Ocular localized amyloid (AL-lambda). H & E stained section (upper figure) and Congo red stained section viewed under polarized light (lower figure). Subsequent abdominal fat biopsy was negative for amyloid and there was no evidence of systemic amyloidosis. There was no evidence of plasma cell dyscrasia in bone marrow biopsy and serum free light chain levels and ratio were within normal limits.

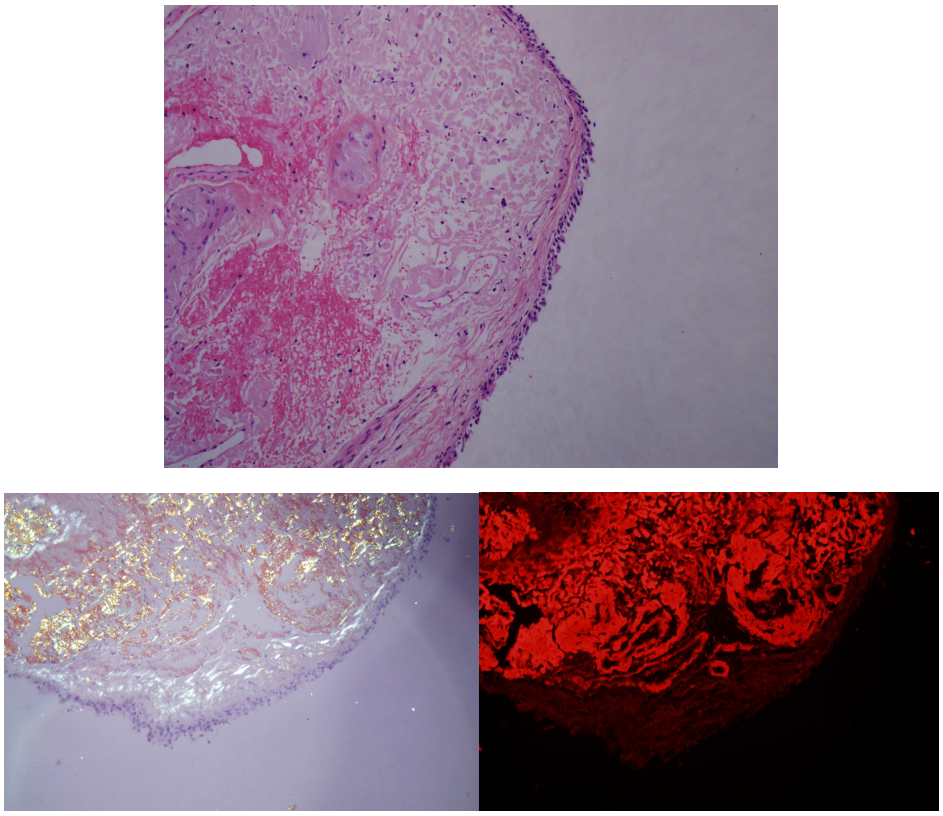

Figure 3. Urinary bladder biopsy with amyloid in the lamina propria (H&E stained section, upper figure). Lower panel - Congo red stained slide viewed under polarized light (left) and Congo red stain under fluorescence light (Texas red filter, right). Amyloid typing demonstrated AL-lambda (not shown). There was a local recurrence 14 months after initial local treatment. There was no evidence of systemic amyloidosis.

CONCLUSION

Diagnosis of amyloid at the time of frozen section evaluation allowed the avoidance of unnecessary extended surgery and, hence, had a significant impact on patient management.

REFERENCES

1. Picken MM. Amyloidoses of the kidney and genitourinary tract. In: Amyloid and related disorders. Surgical pathology and clinical correlations. Ed: MM Picken, A Dogan, GA Herrera, Springer 2012, pp.305-318.

Diagnosis of amyloid in urine cytology specimens

Maria M. Picken

Department of Pathology, Loyola University Medical Center, Chicago, USA..

Amyloidosis is perceived as being rarely seen in surgical pathology and there is a paucity of data regarding its diagnosis in cytology preparations. This report presents the detection of unsuspected amyloid in cytology specimens.

Patient 1. A 51 year old male presented with hematuria and underwent cystoscopy with bladder barbotage for cytology and a bladder biopsy. Thinprep cytology slides demonstrated benign urothelial cells and small clumps of amorphous material, which was subsequently shown to be amyloid by Congo red stain. Subsequently-available biopsy slides confirmed the presence of vascular and interstitial amyloid in the lamina propria; no amyloid was seen in the deep muscle. Amyloid typing demonstrated the presence of amyloid derived from the lambda light chain – AL-lambda. There was no evidence of systemic amyloidosis or underlying plasma cell dyscrasia. Figure 1 below demonstrates a pauci-cellular specimen with Congo red positive and birefringent material diagnostic of amyloid.

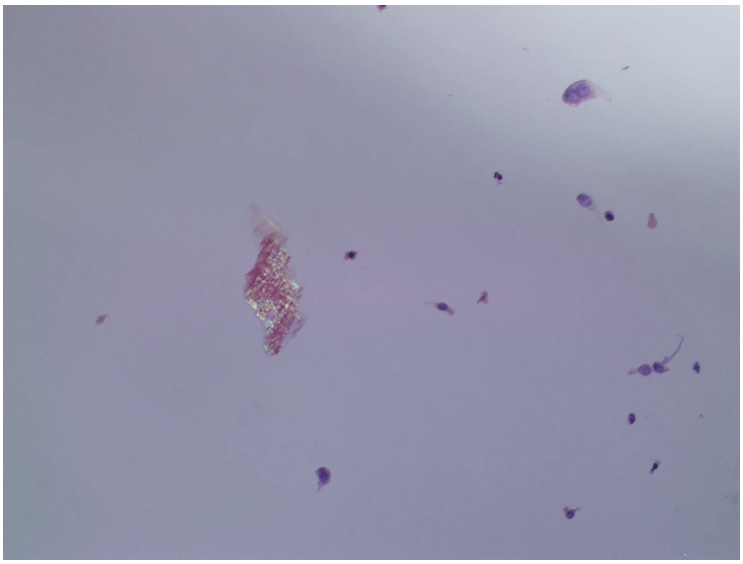

Figure 1. Amyloid seen in urine cytology. Thinprep, Congo red stain viewed under polarized light.

Patient 2. A 54 year old female with systemic AL-lambda amyloidosis presented with difficulty voiding and urine retention. Urine cytology and a urinary bladder biopsy were submitted to Surgical Pathology. Urine cytology showed a pauci-cellular specimen and small clumps of amorphous material, which was subsequently shown to be amyloid by Congo red stain. Urinary bladder biopsy showed amyloid deposits in the lamina propria and in the deep muscle. Amyloid typing of the bladder biopsy confirmed the deposits to be of the AL-lambda type.

CONCLUSION

This report illustrates the feasibility of amyloid detection in cytology thinprep preparations.

REFERENCES

1. Picken MM. Amyloidoses of the kidney and genitourinary tract. In: Amyloid and related disorders. Surgical pathology and clinical correlations. Ed: MM Picken, A Dogan, GA Herrera, Springer 2012, pp.305-318.

Diagnosing and typing early amyloidosis using Congo red fluorescence and immunohistochemistry - Preconditions for its success; a short review

H. Michels[1)], H. Maier-Boetzel[2)] and R.P. Linke[2)]

[1)] German Center of Pediatric and Adolescent Rheumatology, Garmisch-Partenkirchen, Germany

[2)] Reference Center of Amyloid Diseases, Martinsried, Germany

Diagnosing amyloid needs the expertise of special laboratories since amyloidosis is not a single disease. It has been separated into approximately 30 different classes based on the different proteins deposited in patients in diverse varieties of the amyloidoses. Among each of the amyloid classes identified by the presence of a single amyloidotic protein a large variety of clinical pictures and genetic variants can occur. These additional clinical variants within one amyloid class lead to a total of by far more than 500 different amyloid diseases with many clinical overlaps between the classes (1). Due to the heterogeneity of this amyloid complex, diagnosing of amyloid is not of minor importance. Since each amyloid class needs a different therapy, precise amyloid classification is indispensible for therapeutic reasons. In addition, diagnosis and classification has to be performed very early in the course of the diseases since the majority of the amyloidoses follow a relentless, progressive course without intervention. Therefore, the full diagnosis of amyloidosis should be made only in an expert laboratory. Here, some of the major facts for achieving a reliable diagnosis and routine classification of amyloid will be reviewed shortly. This article is restricted to immunohistochemical (IHC) classification applying appropriate antibodies (2, 3), although mass spectrometry (MS) in two variants is also in use (4, 5). The first results of a blinded comparison of the two methods (IHC versus MS) have been published (3).

The **very early full diagnosis of amyloidosis** is the most important factor in many amyloid diseases for initiating and achieving a most successful therapy (6). The full diagnosis includes the detecting of amyloid, its typing and staging. As the first step the awareness of an experienced clinician is crucial. The second step represents the performance of appropriate biopsies very early during the onset of the disease. The third step for succeeding in diagnosing early amyloid includes the very careful microscopic examination of Congo red stained (Puchtler et al., cited in 1) tissue sections in an expert laboratory experienced in the diagnosis of amyloid. This evaluation includes the microscopic inspection in bright light, in polarized light and in fluorescent light, the latter operates with increased sensitivity using Congo red as a fluorochrome. Congo red fluorescence is mandatory when no amyloid had been detected by the classical Congo red staining method (1). Since the case of negativity for amyloid in a single tissue section does not exclude the presence of amyloidosis in the patient, a fourth step is needed. It will include the examination of 10 – 20 more sections cut from the same tissue block

and examined likewise in order to exclude or minimize the sampling error (1) When amyloid has been detected, the fifth step includes routine amyloid typing using IHC employing amyloid antibodies (2-4) which have been proven to be appropriate for this purpose (www.amymed.net). In case of unclear results, in a sixth step, the double staining with the Congo red pre-staining followed by an immunohistochemical overlay is the method of choice. For evaluation and recognition of the diagnostic reaction on such double stained sections, the switching of the light source between bright and fluorescent light is crucial for recognition of the precise congruence of the fluorescent and the immunohistochemical marker stain at the same site (1-3).

The **time lag between the clinical awareness and the bioptic proof** is still a major drawback for initiating a timely therapy. The delay of bioptic diagnoses by missing the microscopic identification, in spite of the clinician's suspicion, has been documented and can indeed become serious. In AA amyloidoses the lag between the awareness of the clinician and the morphologic proof of amyloid on tissue sections was measured in retrospect on eight patients with an average of 2.9 years delay in retrieved tissue blocks from children with juvenile rheumatoid arthritis and related juvenile inflammatory diseases. As a consequence of this delay most of the young patients developed a fatal disease (Michels and Linke, cited in 6). Today, AA-amyloidosis in rheumatoid arthritis has almost vanished due to cytostatics (7) and the very efficient modern anti-inflammatory therapeutics. In AL amyloidosis, this gap between suspicion by the clinician and the morphologic proof was reported as being 1.5 years (9) and, in ATTR amyloidoses (with point mutation), this gap was reported as being on the average of 3.5 years (9). However, in our own experience, this gap can sometimes double in cases without point mutations (unpublished). We also diagnosed by IHC a non-amyloidotic immunoglobulin deposit disease in a patient that had progressed over the past 5 years, since no diagnosis could be made in spite of many tests in different medical specialities and no treatment was therefore indicated until our final bioptic diagnosis (unpublished).

The bioptic amyloid diagnosis is indispensible for all amyloid types. Other markers such as blood constituents, preceding diseases or genetic traits can be regarded as risk factors. While they can indicate that a special amyloid type is more or less likely, they can never be a substitute for a full diagnosis. This full diagnosis can only be obtained from a biopsy since whether a risk factor had caused a given amyloidosis or not can only be identified by the amyloidotic protein deposited in tissures of the patient (1).

Classification of amyloidosis in order to identify the chemical nature of the amyloidotic protein causing the given amyloid disease is most often performed by way of IHC (8). However, this method demands some considerations concerning the antibodies used and some practical experience in order to provide a reliable diagnosis. For this achievement, some decisive points need to be considered for getting a reliable IHC diagnosis.

The first point relates to reliability of an available antibody which must detect all members of a given amyloid class. A "cross-over" to other amyloid classes must be minimal. Antibodies of this quality have been published (1-3) and are available (www.amymed.net).

The second point is that amyloid is never a clean substance in chemical terms, since, as an extracellular substance, it is perfused by the extracellular fluid containing various constituents which can stick to the amyloid and obscure the true nature of the underlying amyloidotic protein (10). This fact haunts all routine methods by which amyloid is being classified today including in particular also MS as derived in our Ringstudies I and II (3).

Therefore, amyloid has been called “Schlammfang” (meaning sewage trap) in the old German literature. Extracting the amyloid fibrils first circumvents largely these impurities but is too laborious as a routine method in most laboratories. Very helpful for suppressing unspecificity in IHC was the discovery that epitopes of amyloidogenic proteins are resistant towards formalin-fixation while the epitopes of the adsorbed proteins are much less resistant (3). This blockage of unspecificiy is even more pronounced by plastic embedding used for immunoelectron microscopy and has lead to the term “differential fixation” (3).

The third point relates to the optimal ratio of the signal-to-background staining as defined by the optimal dilution of the first antibody and the of the secondary amplification system. Every antibody used for amyloid typing needs to be tested separately on its respective prototype tissue section before it can be employed for typing of amyloid. (This standardization has already been performed on the available set of 10 individual standard antibodies which are included in the “amY-kit” of amYmed.)

The fourth point relates to the validation of immunohistochemical results when the IHC typing of amyloid had been performed correctly. One should be aware of the fact that amyloid is not a clean substance (see above) and that various reactivities of the background can show up. With a single antibody it is difficult to proof the correct amyloid type as the diagnostic one since the reactivity can also be related to an impurity. In order to evaluate the reactivity as the diagnostic one, one needs to compare the different reactivities in order to be able to distinguish the diagnostic from the unspecific one (2, 3).

The fifth point is experience. This is a decisive point for success since there is not always a single reactivity. With time and practice the distinction between the diagnostic reactivity and the unspecific one will become clear and published illustrations in reference 3 (Fig. 1-16) may assist. To start with IHC, prototype amyloids are useful in order to adjust the particular IHC system in an institution. In case of any question, one could ask experienced laboratories for assistance (10).

Comparison of IHC and MS during an international blinded study (Ringstudy I) has shown that both methods used for typing of amyloid today have a similar specificity but that IHC has a significantly higher sensitivity (3, see Linke, Westermark, Solomon in this issue) and that both methods have to be used for precise typing of amyloid in tissue sections. To overcome some unreactivities of IHC, MS can be applied. To overcome the insensitivity of MS (when a tissue sample is described as “inappropriate for MS”), IHC can be used. The insensitivity of MS is found particularly in biopsies prone to sampling error, i.e. those involving small biopsies or biopsies with very little amyloid. Such biopsies are also taken during the initial phases of amyloidosis with the clinician’s first awareness. These biopsies with marginal amounts of amyloid can get an immediate full diagnosis by IHC. Other differences between the two methods IHC and MS will be presented elsewhere.

TAKE HOME LESSONS

1. Amyloid detection demands an expert examiner for arriving at the correct conclusions when problems arise, since lack of experience is the most severe pitfall (10).
2. The Congo red staining method is not an easy one. Its execution and evaluation requires training in an expert laboratory. In any case, a tissue section with amyloid should be stained in parallel to demonstrate the validity of the test.
3. A negative amyloid diagnosis derived from one tissue section is always inconclusive. The sampling error has to be considered and it needs to be made unlikely or even excluded by examining more tissue sections (1).

4. The green anisotropy (green polarization color) of amyloid is only a special case. In thicker sections the amyloid can turn yellow, orange or even red and, in thinner sections, the color can become light bluish. All of these different colors between bluish and red are “specific for amyloid” (J.H. Cooper, cited in 1).
5. The Congo red fluorescence is more sensitive than the classical Congo red staining and needs to be used in cases with very little amyloid.
6. The IHC amyloid typing is easy, fast, very sensitive and precise when performed in an expert laboratory. It requires a series of positive controls in order to validate the performance of the antibodies applied.
7. The IHC amyloid typing needs an appropriate set of special antibodies.
8. The evaluation needs some training since one amyloid – one antibody is insufficient for a precise diagnosis because IHC typing includes the diagnostic reaction which reveals the amyloid type and the exclusion of all other amyloids. This “dual proof” is unique to IHC, it increases the precision considerably, and identifies amyloid double types.
9. The antibody set “amY-kit” of amYmed does not only recognize the amyloid type, but it can also stain non-amyloidotic constituents and can diagnose non-amyloidotic protein storage diseases.
10. An unclear IHC reactivity can be overcome by a double staining with Congo red first followed an IHC overlay. The congruence between the Congo red signal and strong IHC signal defines the diagnostic reactivity when reactivities against the other amyloids are unreactive or inconsistently reactive.
11. The blinded comparisons with MS have reliably proven the precision of the cited IHC method for amyloid typing (1-3).

REFERENCES

1. Linke R. Congo red staining of amyloid: Improvements and practical guide for a more precise diagnosis of amyloid and the different amyloidoses. In: "Protein Misfolding, Aggregation and Conformational Diseases (V.N. Uversky and A.L. Fink; eds.), Protein Reviews, Volume 4, (M.Z. Atassi, ed.); Chapter 11.1, pp. 239-276; Springer 2006.
2. Linke RP. Routine use of amyloid typing on formalin-fixed paraffin sections from 626 patients by immunohistochemistry. In: Amyloid and related disorders: surgical pathology and clinical correlations, current clinical pathology. Picken MM, et al. editors. Springer Science & Business Media. 2012;17:219-229.
3. Linke RP. On typing amyloidosis using immunohistochemistry. Detailed illustrations, review and a note on mass spectrometry. Progr Histochem Cytochem 2012; 47:61-132.
4. Murphy CL, Wang S, Williams T, Weiss DT, Solomon A. Characterization of systemic amyloid deposits by mass spectrometry. Methods Enzymol. 2006; 412: 48-62.
5. Vrana JA, Gamez JD, Madden BJ, Theis JD, Bergen HR 3rd, Dogan A. Classification of amyloidosis by laser microdissection and mass spectrometry based proteomic analysis in clinical biopsy specimens. Blood. 2009; 114:4957-4959.
6. Linke RP. Diagnosis of minimal amyloid deposits using the Congo red fluorescent method: a review. In: Amyloid and Related Disorders: Surgical Pathology and Clinical Correlations; Current Clinical Pathology. Picken MM, et al (eds.) Chapter 13, pp 175-185; Springer Science & Business Media. 2012.

7. Savolainen HA, Isomäki HA. Decrease in the number of deaths from secondary amyloidosis in patients with juvenile rheumatoid arthritis. J. Rheumatol 1993; 20:1201-1203.
8. Picken MM, Westermark P. Amyloid detection and typing: summary of current practice and recommendations of the consensus group, Amyloid 2011; 18, Suppl 1, 48-50.
9. Di Girolamo M, Mono, D, Pirro MR, Novakowski M. Approach to diagnosis in systemic amyloidosis: initial findings and time from symptoms onset to diagnosis (light chain amyloidosis vs. transthyretin). Problems and observations. Amyloid, 2011; 18, Suppl 1, 183-85.
10. Picken MM, Herrera GA. The burden of “sticky” amyloid: typing challenges. Arch Pathol Lab Med. 2997; 131:850-851.

An indirect ELISA for transthyretin quantification in fat tissue of patients with ATTR amyloidosis

Johan Bijzet (1), Lammie de Boer (1), Elizabeth B. Haagsma (2), and Bouke P. Hazenberg (1)

Departments of (1) Rheumatology & Clinical Immunology and (2) Gastroenterology & Hepatology, University of Groningen, University Medical Center Groningen, Groningen, The Netherlands

BACKGROUND

Detection of Congo red positive amyloid deposits in tissue is still the gold standard to detect amyloidosis in the routine setting. However, it heavily depends on quality of staining, the microscope, and experience of observers. Quantification of ATTR in fat tissue may be diagnostic for detection of ATTR amyloidosis similar to AA amyloidosis [1, 2]. Besides the diagnostiv value, the tissue concentration of ATTR amyloid may also be useful as a measurent of the amyloid load of fat tissue, in this way possibly reflecting the severity of amyloid deposition during the course of the disease in a patient with systemic ATTR amyloidosis.

The diagnostic performance was studied of an indirect transthyretin (TTR) ELISA for detection and characterization of transthyretin-derived (ATTR) amyloid in subcutaneous fat tissue.

METHODS

Fat tissue specimens were analyzed of 49 consecutive patients (29 men and 20 women) with ATTR amyloidosis, 204 controls (21 AA, 46 AL, 22 localized amyloidosis, and 115 non-amyloidosis controls), and 20 carriers of 6 TTR mutations (M30V, G47E, V71A, C114T, V94A, and E89K).

The amount of amyloid was graded semi-quantitatively in Congo red-stained specimens (0-4+) [2]. A minimum of 30 mg fat tissue was used for the quantification of amyloid. Fat tissue was washed 3x with PBS and amyloid was extracted from tissue in 1 ml TRIS pH 8 + 6 M guanidine overnight at room temperature. The solution was centrifuged at 10,000 g for 10 min, and the supernatant was collected.

The TTR concentration was measured using a newly developed indirect TTR-ELISA. In short: Microtitre plates (Corning) were coated with samples, diluted 1:100 – 1:6400. Rabbit anti-human TTR antibodies (Dako, 1:4000) were used in combination with goat anti-rabbit Ig-HRP (SBT, 1:4000), followed by a color reaction with TMB.

RESULTS

Intra-assay variability coefficient was 4.1% and the interassay variability coefficient 7.7%. The lowest level of detection was 0.01 ng/mg. The mean TTR concentration in controls was 0.10 ng/mg fat tissue with a 98%

interval (mean ± 2.33 SD) ranging from 0.01 to 4.0 ng/mg fat tissue. The TTR concentration of patients with ATTR amyloidosis (mean 16.2 ng/mg fat tissue; 95% interval 0.04 - 7180 ng/mg fat tissue) was higher than controls (p <0.0001). See Figure 1. The TTR concentration of 4.38 ng/mg fat tissue was chosen as cut-off value (upper limit of 99% of the controls) and 36 of all 49 ATTR patients were identified resulting in overall sensitivity for finding patients with ATTR amyloidosis of 73% (95% CI, 59-85%). If the six ATTR patients without any amyloid detected by Congo red staining in fat aspirates were excluded, 36 of 43 ATTR patients having amyloid in fat tissue were identified resulting in sensitivity for this Congo red positive group of 84% (95% CI, 69-93%). See Figure 2. All but one of the 204 controls had TTR values below the cut-off value resulting in specificity 99% (95% CI, 97-100%). All 20 carriers had values below the cut-off value. ANOVA showed a linear trend between TTR and amyloid grades (Figure 3). All ATTR patients with grade 3+ and 4+ were identified.

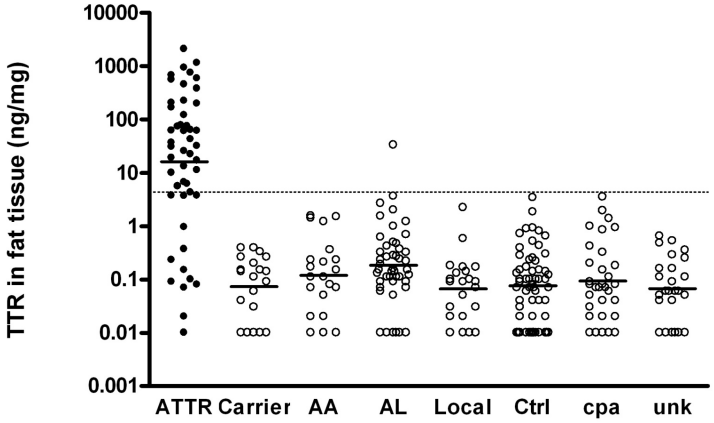

Figure 1. TTR concentrations in fat tissue of patients with ATTR amyloidosis, of carriers of a TTR mutation,of controls with AA, AL, and localized amyloidosis, of disease controls (neuropathy and cardiomyopathy), of patients with chronic polyarthritis (cpa) and of patients with other diseases (unk).

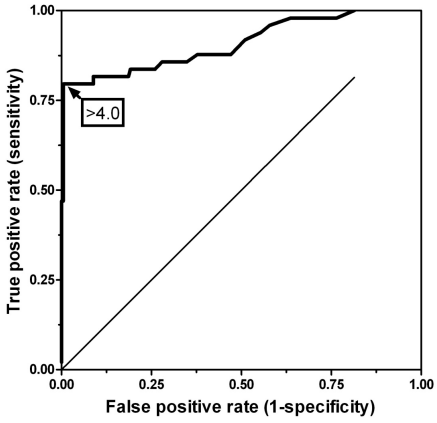

Figure 2. ROC curve of the TTR ELISA with the cut-off value of 4.0 ng/mg fat tissue and AUC 0.91.

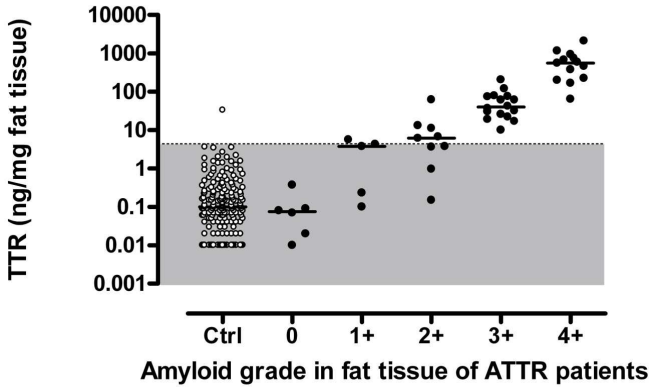

Figure 3. TTR concentration in fat tissue of controls and of patients with ATTR amyloidosis, subdivided by the severity of amyloid deposition in fat tissue as recognized in the Congo red stain.

CONCLUSIONS

Measuring the TTR concentration in fat tissue appears to be useful for detecting ATTR patients. In patients with 3+ or 4+ amyloid in fat tissue, the TTR concentration of fat tissue is a highly sensitive method for characterizing the amyloid as ATTR-type.

REFERENCES

1. Hazenberg BP, Limburg PC, Bijzet J, van Rijswijk MH. A quantitative method for detecting deposits of amyloid A protein in aspirated fat tissue of patients with arthritis. Ann Rheum Dis 1999; 58:96-102.
2. Hazenberg BP, Bijzet J, Limburg PC, et al. Diagnostic performance of amyloid A protein quantification in fat tissue of patients with clinical AA amyloidosis. Amyloid 2007; 14:133-40.

AA Protein in AL amyloidosis

F. Barros [1], J. Frazão [1], I.Tavares [1], P. Salamanca [2], C. Paulo[3], M. Alvelos[3], R. Neto[1], R. Vaz [1], M. Pestana[1]

[1]Department of Nephrology, Hospital São João, Porto, Portugal , [2]Department of Medical Oncology, Instituto Português de Oncologia, Porto, Portugal, [3]Department of Internal Medicine, Hospital São João, Porto,

INTRODUCTION

Renal amyloidosis is a detrimental disease caused by the deposition of amyloid fibrils, in which renal impairment may follow. Clinically evident renal involvement occurs mainly in AL, AA and some hereditary amyloidosis. It presents usually as proteinuria or nephrotic syndrome and renal failure. We report a case of a patient whose kidney biopsy disclosed the coexistence of protein AA and immunoglobulin light-chain derived protein in amyloid deposits.

CASE REPORT

A 73-year-old male, sculptor, complaining of asthenia, peripheral oedema, decreased urine output and foamy urine was admitted to our hospital. Previous history of hypertension, dyslipidemia, arrhythmia and hyperuricemia was present. Twenty years ago he was treated for boutonneuse fever (*Rickettsia conorii*) and was asymptomatic thereafter. He denied past medical history of rheumatoid disease, inflammatory bowel disease or chronic infections like tuberculosis. On admission he had nephrotic syndrome and severe renal failure, beginning of haemodialysis on admission. Analytical evaluation disclosed hypoalbuminemia 1.6 g/dL, proteinuria 20.19 g/24h, negative VDRL, TPPA reactive, β2-microglobulin 42908 mcg/L (1090-2530), increased free light chain lambda 157 mg/dL (0.57-2.63), serum ratio free kappa / free lambda <0.01 (N 0.26-1.65) and immunoelectrophoresis with incomplete lambda monoclonal gammopathy. Renal ultrasound showed preserved renal size and morphology, with a diffuse slight increase of parenchymal echogenicity bilaterally. Chest X-ray had no significant changes. Echocardiography had no signs compatible with infiltrative miocardiopathy Bone marrow biopsy revealed interstitial marrow infiltration by plasmacytoma / multiple myeloma, without amyloid infiltration. Immunophenotyping showed 1.3% plasma cells. Kidney biopsy was performed. Green birefringence was observed with Congo red staining under polarized light. The immunohistochemistry staining was extensively positive for lambda immunoglobulin light chains in glomerular and intersticial regions, and in some points, also for AA amyloid (minor expression in glomeruli and intersticium). The patient was treated with 4 cycles of chemotherapy (bortezomib and dexamethasone), with normalization of serum free light chains. There was no recovery of renal function despite treatment. Eight months after diagnosis he is alive and there's no evidence of progression of monoclonal gammopathy, in periodic surveillance.

DISCUSSION

In the present case we report the finding of AA amyloid as a minor constituent of amyloid deposits in a patient with AL amyloidosis. One possible explanation is that AA amyloid deposition was already present before the development of plasma cell disease, but we didn't depict a cause although we can't exclude professional exposure or a previous treated infectious disease. As far as we know, the significance of protein AA in AL amyloidosis is unknown. In 1983 Falck and Westermark reported protein AA in kidney sections from five out of 14 cases of primary and myeloma associated amyloidosis, all having an immunoglobulin light chain derived protein as a major subunit(1). They discussed that there might be some common pathogenetic mechanism working in both AL and AA type of systemic amyloidosis(1).

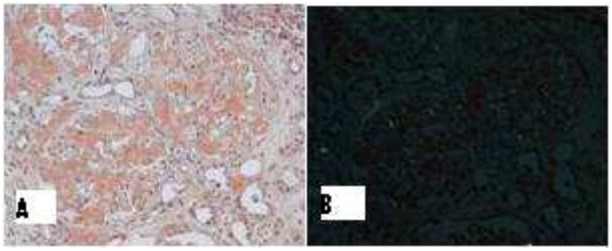

Figure 1. Glomerulus from renal biopsy stained with congo red showing orange red amyloid in the glomeruli (A). The characteristic "apple-green" birefringence of amyloid is apparent when examined by polarization microscopy (B).

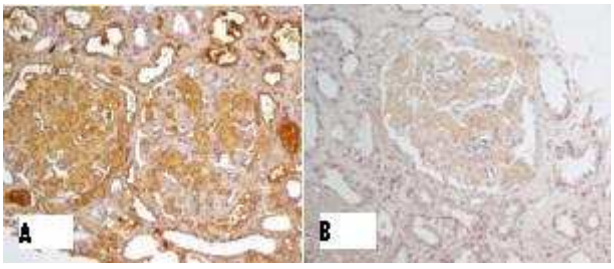

Figure 2. Immunohistochemistry staining showing positivity for lambda immunoglobulin light chains in glomerular and interstitial regions (A). Immunohistochemistry staining showing positivity for AA amyloid (minor expression in glomeruli and intersticium) (B).

REFERENCES

1. Falck HM, Westermark P. Protein AA in primary and myeloma associated amyloidosis. Clin Exp Immunol 1983;54(1):259-264

Antibodies specific to AA76, the common species of AA

Toshiyuki Yamada, Jyunji Sato

Department of Clinical Laboratory Medicine, Jichi Medical University. Japan.

ABSTRACT

In order to specifically detect the AA amyloid, antibodies specific to AA76, the common species of AAs, were developed. Two established monoclonal antibodies reacted with AA6 solely, not with intact SAA. In immunohistochemistry, the antibodies stained AA deposits well, not with SAA leaked from vessels. Reactivity of the antibodies to AA fibrils were reduced largely by degenerative treatments, suggested that the antibodies might react with a fibril-specific structure. The antibodies should seek usefulness for diagnosis and investigative studies.

INTRODUCTION

AA amyloidosis occurs in patients with chronic inflammatory disease such as rheumatoid arthritis. In this disorder, the degradation products of SAA, a representative acute phase reactant, deposits in several organs. Degradation take place in plenty sites of SAA molecule. The most common site is between 76 and 77 residue of SAA[1]. The carboxyl-terminal part disappears and the remaining amino-terminal part, named AA76, constitutes the amyloid fibrils. Detection of this specific peptide would be useful for both investigative and clinical examinations for AA amyloidosis. In this study, we established the monoclonal antibodies specifically recognizing AA76.

METHODS

Rat was immunized with the peptide corresponding to carboxyl terminus of AA76 and lymphocytes from the rat were fused with mouse myeloma cell line. Hybridoma was grown in the selective medium and clones producing designated monoclonal antibodies were established. Designated reactivity of monoclonal antibodies was positive for the immunized peptide and negative for peptides shorter or longer than the immunized one. The obtained antibodies were compared in immunohistochemistry mainly with already established antibody, SAA30, which reacts with intact SAA[2].

RESULTS

Two clones were obtained by the initial screening. Basically, the characteristics of both was not different. The new antibodies reacted with AA amyloid deposits in tissues from AA amyloid patients well, not with SAA leaked

from vessels (Fig.1). Reactivity of the new antibodies to AA fibrils were reduced largely by degenerative treatments, those were, SDS, urea, guanidine. One of the new antibodies lost reactivity by trypsin treatment of specimens.

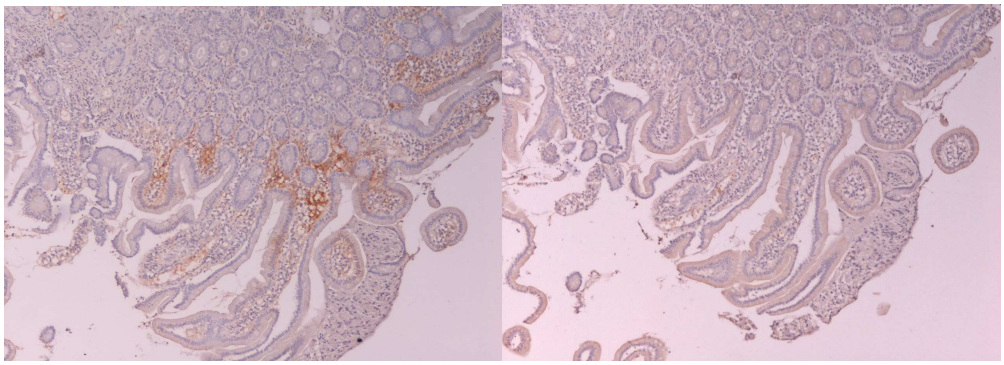

Figure 1. Gastric mucosa, which was denied AA amyloidosis, from patients with rheumatoid arthritis was immunohistochemically stained with the clone SAA30 (left) and the new antibody (right). The new antibody did not react with SAA leaked from the vessels.

DISCUSSION

The new antibodies may recognize the structures specific to fibril formation. Anyway, AA76 may be a species appeared specifically during amyloidogenesis. The present new antibodies can specifically detect, though in the limited, AA76. The antibodies should seek usefulness for diagnosis and investigative studies.

ACKNOWLEDGMENTS

This work was supported by a grant to the Amyloidosis Research Committee for Research on Intractable Diseases from the Ministry of Health, Labor and Welfare, Japan.

REFERENCES

1. Husby G, Marhaug G, Dowton B, Sletten K, Sipe JD. Serum amyloid A (SAA): biochemistry, genetics and the pathogenesis of AA amyloidosis. Amyloid:Int J Exp Clin Invest 1994;1:119-37.
2. Yamada T, Hirano N, Kuroda T, Okuda Y, Itoh Y: Generation and characterization of rat monoclonal antibodies against human serum amyloid A. Scand J Immunol 1997;46:175-9.

Amyloid fibrils possess characteristic electronegative fingerprints that can be distinguished by poly-basic peptides

J.S. Wall[1,2], A. Williams[1], Y. Huang[2], S. Macy[1], E.B. Martin[1], T. Richey[1] and S.J. Kennel[1,2]

Departments of [1]Medicine or [2]Radiology, University of Tennessee Graduate School of Medicine, Knoxville, TN. USA

ABSTRACT

Amyloid deposits are heterogeneous matrices composed principally of protein fibrils, amyloid P component, and heparan sulfate proteoglycans (HSPG). We have identified a series of heparin-binding, polybasic peptides that specifically co-localize with amyloid deposits in tissue sections and *in vivo* using the murine models of AA and ApoA2c amyloidosis. We originally hypothesized that amyloid binding was mediated by the amyloid-associated HSPG, but now we have demonstrated that certain of these peptides bound synthetic amyloid fibrils in the absence of HSPG.

Our data demonstrate that the peptides bound to synthetic fibrils via ionic interactions of the lysine or arginine side chains. Furthermore, the avidity of the reactivity was dependent on the fibril type suggesting that each fibril might possess a distinct “electrostatic fingerprint”. This fingerprint is defined by the density and juxtaposition of electronegative side chains exposed on the fibril surface.

INTRODUCTION

Small (31-mer) heparin-reactive peptides, such as p5 and p5R, have been shown to bind specifically to murine AA amyloid deposits *in vivo* by using single photon emission computed tomographic (SPECT) imaging and micro-autoradiography (1) presumably due to the presence of bio- or electrochemically distinct heparan sulfate proteoglycans associated with the amyloid (2). In contrast, the peptides did not bind to healthy tissues or organs that were devoid of amyloid. Other reagents such as the camelid antibody, B10, have been shown to bind to synthetic amyloid fibrils via electrostatic interactions in the absence of HSPG (3). We, therefore, hypothesized that the polybasic peptides p5 and p5R might bind synthetic fibrils in a similar fashion. This would likely require a linear array of acidic side chains spaced favorably along the length of the fibril, similar to the pattern of charge distribution seen in heparin. Based on these requirements and the fact that different fibrils have different structures and thus charge signatures, we posited that certain fibrils would possess optimal binding characteristics for the p5 peptides and others would be less favorable. Thus, binding of the peptides defines an amyloid-specific phenotypic characteristic represented as a distinct “electrostatic fingerprint” associated with each fibril.

METHODS

Synthetic biotinylated polybasic peptides designated p5 and p5R, Aβ(1-40) and islet amyloid polypeptide were synthesized by FMOC chemistry (Yale School of Medicine). The λ6Wil light chain variable domain (V) was prepared as a recombinant protein and purified as previously described (4).

Peptide p5 – GGGYS KAQKA QAKQA KQAQK AQKAQ AKQAK Q

Peptide p5R – GGGYS RAQRA QARQA RQAQR AQRAQ ARQAR Q

The sequence integrity of the peptides was confirmed by mass spectrometry. Peptides p5 and p5R were also purchased with a biotinylated-glycine residue at position 1. The secondary structure of peptide p5 was predicted using the web-based prediction algorithm iTASSER (5)

Binding to tissue amyloid was assessed using formalin-fixed, paraffin-embedded (FFPE) tissue sections obtained at autopsy (with informed consent) from patients with light chain (AL) amyloidosis. Biotinylated peptide was added to the tissue at ~10 µg/mL and visualized by addition of streptavidin-conjugated horseradish peroxidase and diaminobenzidene. Synthetic fibrils were prepared from Aβ(1-40), IAPP or Vλ6Wil proteins as previously described (1). Reactivity of the biotinylated p5R with synthetic fibrils was assessed by using increasing concentrations (100 µL of peptide at 1 µM – 0.1 nM) of peptide. Binding was measured by the addition of europium-conjugated streptavidin followed by enhancing solution and measuring time-resolved fluorescence emission (Wallac)

RESULTS

The secondary structure of peptide p5 (and p5R) was predicted to be α-helical with the 8 basic lysine side chains arranged linearly in 2 discrete “rows” along the length of the peptide (Fig. 1A). The mean charge spacing of lysine residues at positions 6, 9, 16, 23, and 30 was found to be 11 Å which is less than the linear spacing of sulfate moieties in the crystal structure of heparin (~ 17 Å; PDB# 1HPN).

The biotinylated peptides p5 and p5R were found to bind specifically to many forms of tissue amyloid in FFPE tissue samples including the most common visceral forms of amyloid diseases – TTR, AA, and AL (e.g. Fig. 1B).

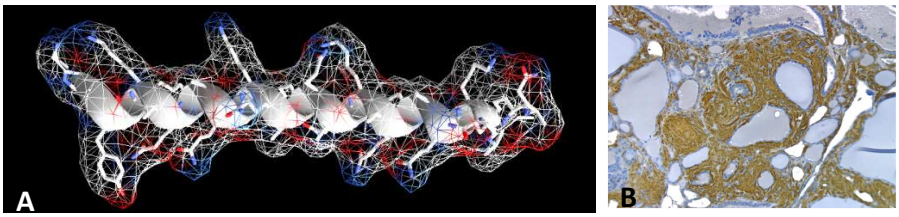

Figure 1. The heparin-binding peptide p5 adopts an α-helical configuration and binds tissue amyloid. (A) The secondary structure of p5 was predicted to be α-helical with 2 linear arrays of charged lysine residues (blue). (B) Histochemical detection of ALλ amyloid in FFPE using biotinyl-p5.

Based on these data, we assessed the reactivity of p5R with a panel of synthetic fibrils composed of Aβ(1-40), IAPP or λ6Wil. The p5R bound with relatively high affinity to each of the synthetic fibrils with estimated concentration at 50% binding (EC_{50}) of 50 nM, ~125 nM and ~190 nM for the Aβ(1-40), λ6Wil and IAPP fibrils, respectively (Fig. 2).

In contrast, p5 peptides in which the basic arginine or lysine residues had been substituted with glycine or leucine were completely unreactive with the synthetic fibrils and tissue amyloid (data not shown).

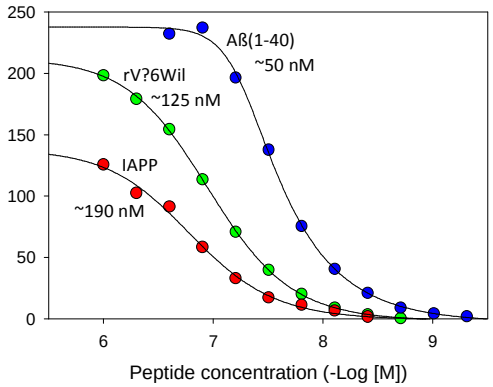

Figure 2. Biotinylated peptide p5R binds synthetic amyloid fibrils with varying relative affinity.

DISCUSSION

The poly-basic peptides p5 and p5R bound certain synthetic amyloid fibrils due to the presence of an electronegative “fingerprint” on the fibril. It has been shown that the reactivity of the camelid mAb B10 with some fibrils (but notably not AL) resulted mainly from electrostatic interactions. We posit that many ligands with an appropriate poly-basic motif will bind amyloid fibrils and that there may be an optimal charge distribution for each fibril type of ligand-fibril interaction. Custom peptides could be optimized for fibril reactivity based on the aforementioned determinants.

ACKNOWLEDGEMENTS

This work was supported a PHS grant R01DK079984 from the NIDDK

REFERENCES

1. Wall JS, Richey T, Stuckey A, Donnell R, Macy S, Martin EB, et al. In vivo molecular imaging of peripheral amyloidosis using heparin-binding peptides. *Proceedings of the National Academy of Sciences of the United States of America*. 2011;**108**(34):E586-94.
2. Smits NC, Kurup S, Rops AL, ten Dam GB, Massuger LF, Hafmans T, et al. The heparan sulfate motif (GlcNS6S-IdoA2S)3, common in heparin, has a strict topography and is involved in cell behavior and disease. *The Journal of biological chemistry*. 2010;**285**(52):41143-51.
3. Haupt C, Bereza M, Kumar ST, Kieninger B, Morgado I, Hortschansky P, et al. Pattern recognition with a fibril-specific antibody fragment reveals the surface variability of natural amyloid fibrils. *Journal of molecular biology*. 2011;**408**(3):529-40. Epub 2011/03/08.

4. Wall J, Schell M, Murphy C, Hrncic R, Stevens FJ, Solomon A. Thermodynamic instability of human lambda 6 light chains: correlation with fibrillogenicity. *Biochemistry*. 1999;**38**(42):14101-8.
5. Roy A, Kucukural A, Zhang Y. I-TASSER: a unified platform for automated protein structure and function prediction. *Nature protocols*. 2010;**5**(4):725-38. Epub 2010/04/03.

Luminescent conjugated oligothiophenes: A novel dye for amyloid diagnostics

D. Sjölander[1], J.J. Mason[1], G.T. Westermark[2], P. Westermark[3], P. Hammarström[1], K.P.R. Nilsson[1]

[1]Department of Physics, Chemistry & Biology (IFM), Linköping University, Linköping, Sweden
[2]Department of Medical Cell Biology, Uppsala University, Uppsala, Sweden
[3]Department of Immunology, Genetics and Pathology, Uppsala University, Uppsala, Sweden

ABSTRACT

The alkaline Congo red staining method has, for almost half a century, been the gold standard of amyloid diagnosis. Unfortunately, the method is both laborious and requires great skill to achieve proper diagnosis. In this study we are presenting an alternative method that is compatible with immunofluorescence typing. We used a novel dye, h-FTAA, designed and synthesized by us. The dye belongs to the novel class of conformation sensitive dyes known as Luminescent conjugated oligothiophenes (LCOs). We examined 37 different cases of systemic amyloidoses from various tissues. It was found that h-FTAA binds to amyloid with higher sensitivity and greater selectivity than Congo red, as was determined by both fluorescence- and light polarization microscopy. Due to the methods ease of use and performance compared to Congo red, it is concluded that h-FTAA is a better first choice for screening of systemic amyloidoses.

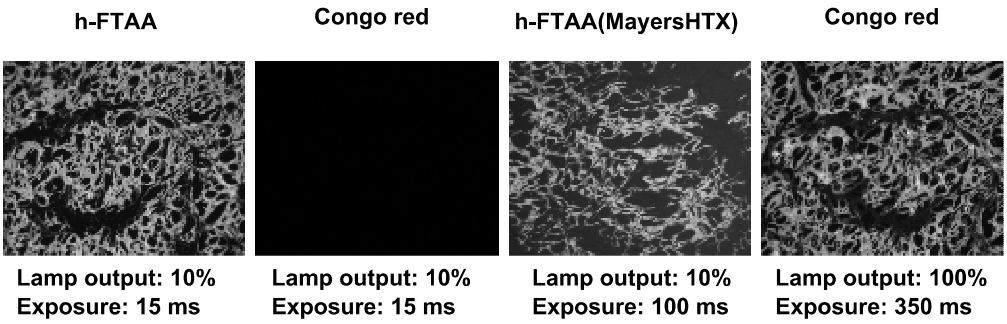

Figure 1. Fluorescence intensity comparison of h-FTAA and Congo red. The immense intensity of h-FTAA compared to Congo red allows for usage of cheaper optical components in the microscope setup.

INTRODUCTION

Presently Congo red staining is the gold standard for screening and diagnosis of amyloidoses. Under ideal conditions amyloid stained with Congo red, viewed with linearly polarized light between crossed polarizers, will

display a green (anomalous) color. However due to inherent drawbacks of both the dye and the microscope technique – a laborious staining process and following microscopy diagnosis of the amyloid calls for a highly skilled and experienced pathologist (1).

Previously the luminescent conjugated polythiophenes/oligothiophenes (LCPs/LCOs) PTAA and p-FTAA have successfully been utilized for the detection and typing of systemic amyloidoses as well as the localized amyloidoses and prion proteinopathies, both ex vivo and in vivo (2-4). The LCOs constitute a novel set of fluorophores that selectively binds to amyloidotic deposits and upon doing so changes its spectral signature, hence the color of the dye (5)

METHODS

In this study we have limited ourselves to a simple setup of equipment common to most histolabs. We employed wide-field fluorescence and bright-field polarization microscopy for detection of amyloid deposits in immunohistochemically confirmed systemic amyloidoses cases. 37 cases in total, comprising ATTR, AA, AL-λ, AL-κ systemic amyloidoses from various tissues were used to benchmark the LCO dye h-FTAA against Congo red using only 5x and 10x objective lenses. After deparaffinization and rehydration of FFPE-sections; consecutive sections were stained with either Congo red according to the modified Puchtler method (1); or h-FTAA (2mg/L solution in PBS for 30 min). Also the compatibility of h-FTAA to concomitant immunofluorescence labeling was assed.

RESULTS

Wide-field fluorescence imaging of systemic amyloidosis deposits stained with h-FTAA and Congo red showed that h-FTAA was immensely brighter than Congo red even though stained at 1000-fold lower concentration (Figure 1). In contrast to Congo red whose sensitivity in fluorescence mode is compromised by the lack of selectivity, h-FTAA showed unrivalled selectivity and sensitivity towards amyloidotic deposits. Also, due to the conformation sensitive properties of the dye, different morphologies of the amyloid deposits could be uncovered (Figure 2.a) AA–Spleen). However Congo red staining of amyloid can achieve acceptable selectivity if polarization microscopy is used, usually at the price of reduced sensitivity. Polarization microscopy examination of ATTR diagnosed heart tissue stained with either Congo red or h-FTAA confirmed once again that h-FTAA was the more sensitive of the two as well as having similar or better selectivity. It was also found that h-FTAA is compatible with immunofluorescence allowing immuno sub-typing as diagnostic tool.

DISCUSSION

There is a great need of a novel class of amyloid specific ligands that can address both fundamental scientific as well as clinical diagnostic needs. The unique properties and versatility of the LCOs has allowed them entering the correlative multimodal domain of biomedical imaging, such as the intrinsic LCO-fluorescence (Intensity, Hyperspectral, and Lifetime) in conjunction with LCO-PET, -MRI, -EPR and -EM ligands.

However, the aforementioned techniques require access to well equipped core facilities and is thus not easily available. Therefore, with the limitation of a standard fluorescence and light polarization microscope, we wanted to investigate whether the new LCO dye, h-FTAA, could be used as an alternative to Congo red – the present, but cumbersome, standard for amyloid diagnosis. In this study we have demonstrated that the very easy to use

dye, h-FTAA, can detect amyloid deposits with outmost sensitivity and selectivity. It is our belief that h-FTAA is a better first screen alternative for suspected cases of amyloidosis than Congo red.

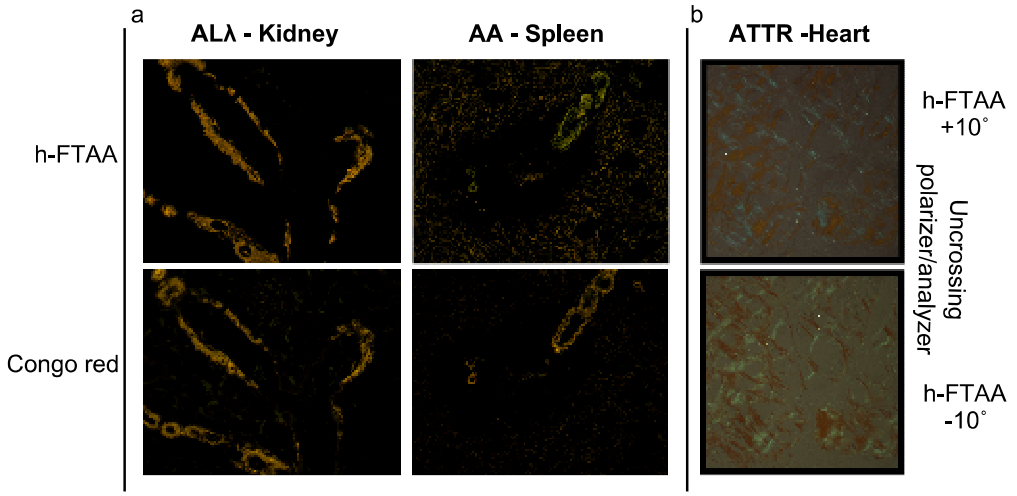

Figure 2. a) Fluorescence comparison of h-FTAA and Congo red selectivity and sensitivity toward systemic amyloid deposits, revealing favorable outcome for h-FTAA. Also due to the conformational sensitive properties of h-FTAA, the dye reports on the underlying structural heterogeneity of the amyloid deposits. b) Polarization light micrographs of h-FTAA bound to ATTR in heart tissue. Partial uncrossing of the polarizer & analyzer yields characteristic colors.

ACKNOWLEDGEMENT

Our work is supported by Linköping university, the Swedish research council, the Swedish strategic research foundation, Astrid and Georg Olsson, and the EU-FP7 Health programme through the project LUPAS

REFERENCES

1. Westermark GT, Johnson KH, Westermark P. Staining methods for identification of amyloid in tissue. Methods Enzymol. 1999;309:3-25.
2. Åslund A, Nilsson KP, Konradsson P. Fluorescent oligo and poly-thiophenes and their utilization for recording biological events of diverse origin-when organic chemistry meets biology. J Chem Biol. 2009 Nov;2(4):161-75.
3. Nilsson KP, Ikenberg K, Åslund A, Fransson S, Konradsson P, Röcken C, Moch H, Aguzzi A. Structural typing of systemic amyloidoses by luminescent-conjugated polymer spectroscopy. Am J Pathol. 2010 Feb;176(2):563-74.
4. Lord A, Philipson O, Klingstedt T, Westermark G, Hammarström P, Nilsson KP, Nilsson LN. Observations in APP bitransgenic mice suggest that diffuse and compact plaques form via independent processes in Alzheimer's disease. Am J Pathol. 2011 May;178(5):2286-98.

5. Klingstedt T, Åslund A, Simon RA, Johansson LB, Mason JJ, Nyström S, Hammarström P, Nilsson KP. Synthesis of a library of oligothiophenes and their utilization as fluorescent ligands for spectral assignment of protein aggregates. Org Biomol Chem. 2011 Dec 21;9(24):8356-70.

A comparison of immunohistochemistry and mass spectrometry for determining the amyloid fibril protein from formalin fixed biopsy tissue

[1] Janet A. Gilbertson, [2] Jason D. Theis, [1] Toby Hunt, [2] Julie A. Vrana, [1] Philip N. Hawkins, [2] Ahmet Dogan, [1] Julian D. Gillmore

[1] National Amyloidosis Centre, Division of Medicine, Royal Free Campus, UCL Medical School, Rowland Hill Street, London, NW3 2PF, UK.
[2] Dept of Laboratory Medicine & Pathology, Mayo Clinic, Rochester, MN 55905. USA.

ABSTRACT

There are many types of amyloid, which are classified according to the protein precursor from which the fibrils are derived. Accurate identification of amyloid type is critical in every case since therapy is type-specific. At the UK National Amyloidosis Centre (NAC), all biopsy specimens containing amyloid, the vast majority of which are formalin fixed, are routinely stained with a panel of 11 antibodies to determine the amyloid fibril protein. In ~20-25% cases however, immunohistochemistry (IHC) fails to prove the amyloid type and further tests are required. Laser capture microdissection and mass spectrometry (LDMS) is a powerful tool for identifying proteins from formalin-fixed, paraffin embedded tissues. We undertook a blinded comparison of IHC (NAC) and LDMS (Mayo Clinic) in 142 consecutive biopsy specimens from 38 different tissue types.

INTRODUCTION

When a patient is referred to the NAC their diagnostic tissue block is re-stained with Congo red and a panel of antibodies to confirm amyloid and determine the fibril type before the patients attends clinic. Histology and immunohistochemistry is widely available for determining the amyloid type. It is fairly quick and is the preferred method in clinical practice.[1] However it has variable sensitivity and specificity (figure 1). Other methods for identifying the amyloid fibril protein include electron microscopy (EM) with immunogold and proteomic analysis. EM and Immunogold, although used in some centres, is not widely available in the UK and is a specialised technique requiring expert knowledge and equipment. Using proteomic analysis (LDMS) the amyloid fibril protein can be identified in only a small quantity of formalin fixed tissue, making it an attractive diagnostic tool.[2] However, it is relatively novel and until now, has been used mainly as a research tool.

Our aim was to compare IHC carried out at the NAC and LDMS performed at Mayo Clinic to evaluate the potential role of LDMS in routine clinical practice.

METHODS

One hundred and forty two consecutive formalin fixed paraffin wax embedded biopsies received as part of routine clinical practice at the NAC were processed in the usual way but, in addition, an extra 10 µm section was cut onto a Director Slide™ and sent to the Mayo Clinic without any associated clinical information. The standard protocol at the NAC consists of cutting 22 serial sections from a single block, of both 2µm and 6µm thickness, for Congo red and IHC staining. IHC was performed with a panel of 11 antibodies (table 1) using the Shandon Sequenza™ system, without antigen retrieval, the exception being 6M Guanidine for TTR staining. Primary antibodies were incubated overnight at 4℃, identified with IMMPRESS™ (Vector Laboratories) polymer detection kit and metal enhanced DAB. Interpretation was carried out initially without any clincial information by two people idnependently. Data obtained from proteomic analysis at the Mayo Clinic was compared with IHC from the NAC.

Table 1. Antibodies used routinely at the NAC

Antibody	Raised in	Dilution	Cat No	Source	Absorbed by
P- component	Rabbit	1:200	A0302	DAKO	Human SAP
AA (REU 86.2)	Mouse	1:100	2232MREU	Euro Diagnostica	Human SAA
Kappa	Rabbit	1:20000	A0191	DAKO	human serum
Lambda	Rabbit	1:20000	A0193	DAKO	human serum
Lyzozyme	Rabbit	1:1000	A099	DAKO	Pure antigen
Fibrinogenα chain	Sheep	1:300	CA1023	Cambiochem	human plasma
TTR	Rabbit	1:4000	A002	DAKO	Pre-albumin
Insulin	Mouse	1:20	NCL-insulin	Novocastra	
apoA1	Goat	1:4000	PBA0313	Genzyme	HD Lipo-Protein
β 2 Microglobulin	Rabbit	1:500	A0072	Dako	
Lect2	Goat	1:600	AF722	R&D Systems	

All human serum is from a normal pool

RESULTS

Thirty-eight different tissues were biopsied, most commonly kidney (30%). There was 100% concordance between IHC and LDMS with respect to identification of the amyloid fibril protein among 108 biopsies in which there was diagnostic IHC staining. Thirty-four of 142 (24%) cases did not stain immunospecifically such that the amyloid type was not confirmed by IHC alone. LDMS was diagnostic in 25 of these 34 cases (74%), confirming AL (lambda) and AL (kappa) type amyloid in 7 and 10 cases respectively. The amyloid fibril protein was heavy chain (AH) in 3 cases, apolipoprotein A4 in 3 cases and atrial natriuretic factor (ANF) in 2 cases. Reasons for failure to identify the amyloid fibril protein in 9 cases were s follows: insufficient amyloid remaining in the specimen (2 cases), technical failure (1 case), and interpretation not conclusive (6 cases; although fibril protein ‘suggested’ in 3).

DISCUSSION

IHC is available in any laboratory, it is easy to adapt, can be performed on the bench without any specialist housing and is relatively low cost but expertise is required for interpretation. In this study we found that when IHC was definitive, there was 100% concordance with LDMS findings. However, only 76% of cases gave definitive results by IHC. LDMS requires specialist accommodation for two large pieces of equipment, both

purchase and running costs are high, and availability is limited to specialist centres. As with IHC, expertise is required to analyse and interpret the data. In this study we found that running both IHC and LDMS simultaneously resulted in positive identification of the amyloid fibril protein in 94% of biopsies compared to 76% by IHC alone (18% additional pick-up rate).

Although LDMS is labour intensive and expensive, it is an excellent diagnostic tool which should be considered whenever the IHC is not conclusive.

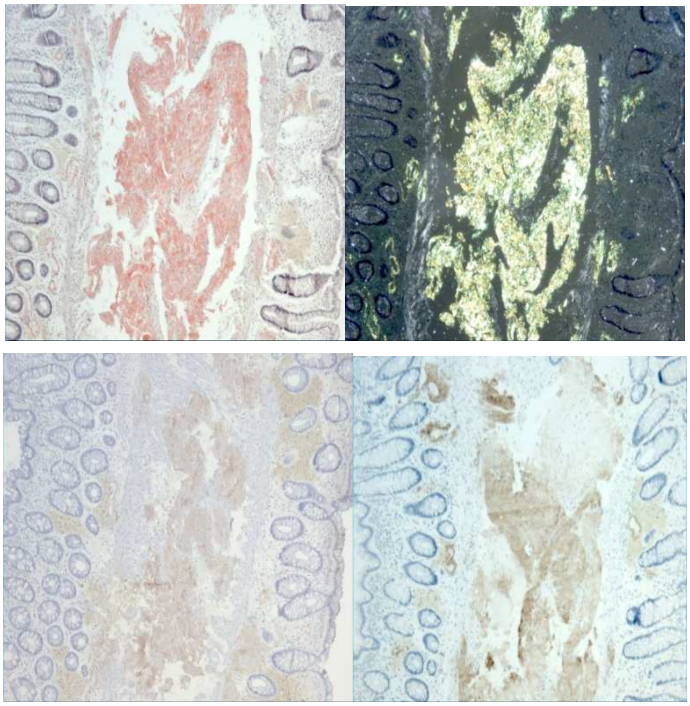

Figure 1. An example of non diagnostic IHC.
Showing Congo red staining, green birefringence and weak patchy IHC staining with AA and lambda.

ACKNOWLEDGEMENTS

Thank you to all colleagues at the National Amyloidosis Centre. With special thanks to Rose Coughlan, George Chennell, Ania Baginska, Graham Taylor and Nigel Rendell.

REFERENCES

1. Puchtler, H., Sweat, F., Levine, M., on the binding of Congo red by amyloid. Journal of Histochemisrty and Cytochemistry 1962. 10:355
2. Vrana JA., Gamez JD., Madden BJ., Theis JD., Bergen HR 3rd., Dogan A. Classification of amyloidosis by lasser dissection and mass spectrometry based proteomic analysis in clinical biopsy specimens. Blood 2009,114:4957-4959

Classification of Amyloidosis, Comparison of Two Leading Routine Methods: Immunohistochemistry and Mass spectrometry - Procedure and First Results

R.P. Linke [1)], P. Westermark [2)], A. Solomon [3)]

[1)] Reference Center of Amyloid Diseases amYmed, Martinsried, Germany

[2)] Dept. of Immunology, Genetics and Pathology, Uppsala University, Uppsala, Sweden

[3)]Human Immunology and Cancer Program ,University of Tennessee Graduate School of Medicine, Knoxville, TN 37920

ABSTRACT

Amyloid typing can be achieved in different ways. The two leading procedures for routine typing of amyloidosis are immunohistochemistry (IHC) using amyloid antibodies and mass spectroscopy (MS).These two methods have been compared here in a blinded fashion (Ringstudy I). The largely unselected fixed paraffin sections from three laboratories were coded. This study encompassed 14 rounds of exchanges during the years 2002-2009. The codes were broken at stages when a block of these studies had been concluded until the final code was broken in 2009. A total of 145 samples were exchanged, including repetitions. The overall comparison of IHC versus MS reveals a definitely higher sensitivity of IHC with approximately 90% versus MS with approximately 50%, but a similar specificity. This study documents the strength and the failures of both methods and reveals that both methods are needed for classifying amyloidosis correctly.

INTRODUCTION

The amyloid diseases are pathogenically very diverse among the different patients. This variety is based mainly on the different chemical nature of the amyloidogenic proteins deposited. Therefore, every individual amyloidosis which has been identified first using Congo red needs to be classified using tissue sections in order to provide reliable information to the clinician concerning the chemical amyloid type as a solid fundament for therapeutic decisions (1). Amyloid typing can be performed in different ways, including immunochemistry (IHC), amino acid sequence or by mass spectrometric (MS/MS) analysis (2). For routine immunohistochemical amyloid typing on formalin-fixed paraffin tissue sections, commercial and in house-made anti-amyloid antibodies are used (3). Since an independent comparison of IHC and MS/MS has never been done, scientists at three institutions have agreed in 2002 to perform such a comparison: the origins of samples are abbreviated here with the first letter of the authors' names (L, W, S, see Table 1). Here, we describe the procedure and the first results. An abstract had been presented in Kumamoto in 2011 (4).

MATERIAL AND METHODS

In the early agreement: Two authors (S and L) meeting at the FASEB-Conference on Protein Folding in Snowmass/CO in 2002 agreed to compare the immunohistochemical method using homologous antibodies directed against amyloidogenic proteins (5-7) with the (at this time) newly published method using MS (2). In order to conduct such a collaboration sufficient amyloid prototype samples were needed and W, who also attended the same conference, could be interested in joining this collaboration and later could provide needed amyloid prototypes. At this conference this project was initiated by defining the mode of exchange, the blinding of the study and the distribution of work which needed to be carried out.

Exchange of samples: The samples were not selected by any criterion such as the kind of preceding disease, amyloid type, size, type of organ, biopsy or autopsy. From autoptic paraffin blocks 4 mm broad rims or 6 mm broad triangles were sawed using a small hand saw with a fine blade as shown in Figure 1. Other samples were large autoptic samples or small standard biopsies. The contributions of samples were as follows: W contributed 43 samples (all were amino acid sequenced), S contributed 11 samples (the typing was performed using amino acid sequencing and/or MS/MS), and L contributed 48 samples (some were amino acid sequenced, others typed after micro-extraction and immunochemical identification, and others using immunohistochemistry followed by genetic analysis and/or clinical evaluation (see prototypes in 7) as summarized in Table 1.

Processing of coded samples and typing: All sample fragments from W (see Fig. 1) were re-imbedded in paraffin. Paraffin sections were prepared of all samples on charged glass slides. For IHC, approximately 4 µm thick sections were prepared. The sections for MS were of approximately 8-10 µm thickness. The number of paraffin sections per patient for MS was dependent on the size of the tissue. So, from autoptic samples usually 10 paraffin sections per paraffin block were prepared for MS while from tissue fragments and from routine biopsies 15-30 sections were provided. The number of sections for IHC amyloid typing was 11 sections per patient, whereby one section was used for the diagnosis of amyloid using Congo red and the other 10 sections for classifying the amyloid by a panel of 10 commercial standard antibodies ("amY-kit", www. amymed.net).
The two methods for typing the various amyloids used for comparison have been described in detail before that is IHC (3, 5-7, including the review 7) and MS/MS (2).

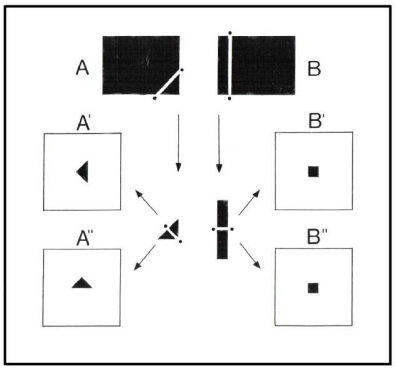

Figure 1. The procedure by which tissue fragments have been generated from larger tissue blocks, schematically. Black (A, B), formalin-fixed and paraffin-embedded tissues. Small black dots indicate the primary direction of motion of the sawing blade with the result of generating two kinds of fragments with dimensions of approximately 6x6/2 mm^2 (A) and 4x4mm^2 (B). The arrows indicate the subsequent processing of the tissue fragments up to the final tissue sections as shown in A'/A'' and B'/B''.

Breaking the code: Decoding of the blinded samples after the typing had been executed on three different occasions that was the time when a block of experiments had been completed. We used two varieties of breaking the code that is by crossing the data either in person (twice) or by letter. The first decoding was done at the X^{th} International Symposium on amyloidosis in Tours/France in 2004 in person by crossing a closed

envelope containing the data obtained by either of the two partners (L and S) in the presence of a trusted witness. The last decoding was performed by letter in the fall of 2009 by sending each of the closed envelopes with the data for being crossed to a person trusted by the examiners in this study.

FIRST RESULTS AND DISCUSSION

Evaluation of the results: For a summary of the samples employed, see Table 1. The *first step* was to diagnose amyloid using Bennhold's Congo red method as modified by Puchtler et al. (cited in 1). When no amyloid could be microscopically detected including the green birefringence in polarized light (in some samples of S or W), more sections (5-20) were examined likewise in order to exclude the sampling error. When no amyloid could be found in a larger number of sections a new specimen of the same patient was requested from the supplier and, in some cases, amyloid could be detected. Therefore, more than one specimen was examined for some patients. The *second step* represented the typing of amyloid by either of the two methods followed by a comparison of the data. The results of this study were placed schematically into two categories: a: data "as expected" from the known amyloid type; b: data "different from the expected ones" including a variety of statements which will be not discussed here. These inconsistent data and statements will not fulfil clinical standards for a specific therapy anyway. The *third step* was the comparison of the two methods IHC and MS. In some cases more than one amyloid was present while each amyloid was counted separately.

Table 1. Typing of amyloid: Samples exchanged in Ringstudy I by S, Solomon; W, Westermark; and L, Linke

Project	Provider	Examiner-Method*	Number of samples**	Number of samples with amyloid
A	L	S - MS	48	48
B	S	L - IHC	11	10
C	W	L - IHC	43	38
D	W	S - MS	43	38
		Total	145	134

* Methods of amyloid typing: MS, mass spectrometry; IHC, immunohistochemistry using appropriate antibodies

The 38 prototype samples with amyloid of W were typed in agreement with the known chemical type in 14 cases (36.8%) by MS and in 34 cases (89.5%) by IHC. Laboratory S provided 10 samples with amyloid which were typed in line with the known amyloid type in 9 cases (90%) by IHC. Laboratory L provided 48 samples containing 53 amyloids which had been typed in all (100%) by IHC in agreement with in part chemical and/or clinical data (5-7), and the amyloids were typed as expected in 29 cases (54%) by MS. In general, most failing MS examinations did not produce any definitive data thus indicating a lower sensitivity. The overall specificity between of the two methods is statistical not different. This will be discussed in detail elsewhere since the severity of the unexpected amyloid types is of a different calibre between the methods IHC and MS. It should be noted, however, that the MS studies were performed without prior laser dissection, known to increase the sensitivity (8). In summary: The advantage of IHC in these series is not only the ease of its performance, but

mainly its higher sensitivity and the utilization of the crucial morphologic dimension (7, 9), which allows the identification of the different amyloidogenic proteins *in situ directly* and by this avoiding very severe misdiagnoses. The advantage of MS is the presentation of amyloidogenic proteins as a guide for their identification which cannot be typed by IHC since antibodies may not be available yet. So, during this Ringstudy I, MS was crucial in the discovery of Semenogelin I amyloid (10). Therefore, both methods seem to be indispensible and can complete one another for amyloid typing, with IHC for the known amyloids and those which cannot be typed by MS, and MS for the novel amyloids and those which cannot be typed by IHC (4).

REFERENCES

1. Linke R. Congo red staining of amyloid: Improvements and practical guide for a more precise diagnosis of amyloid and the different amyloidoses. In: "Protein Misfolding, Aggregation and Conformational Diseases (V.N. Uversky and A.L. Fink; eds.), Protein Reviews, Volume 4, (M.Z. Atassi, ed.); Chapter 11.1, pp. 239-276; Springer 2006.
2. Murphy CL, Wang S, Williams T, Weiss DT, Solomon A. Characterization of systemic amyloid deposits by mass spectrometry. Methods Enzymol. 2006; 412: 48-62.
3. Schröder R, Deckert M, Linke RP. Novel isolated cerebral ALλ amyloid angiopathy with widespread subcortical distribution and leukoencephalopathy due to atypical monoclonal plasma cell proliferation, and terminal systemic gammopathy. J Neuropath Exp Neurol. 2009; 68, No.3: 286-299.
4. Linke RP, Meinel A, Westermark P, Murphy C, Solomon A. Amyloid typing: Comparison of immunohistochemistry and mass spectrometry (Ringstudy I). VIIIth International Symposium on Familial Amyloidotic Polyneuropathy. Kumamoto, Japan. 20th-22nd Nov. 2011; Abstract No. O 1-16.
5. Linke RP. Classification of amyloid on fixed tissue sections for routine use by validated immunohistochemistry. Amyloid. 2011; 18, Supp. 1:74-76.
6. Linke RP. Routine use of amyloid typing on formalin-fixed paraffin sections from 626 patients by immunohistochemistry. In: Amyloid and related disorders: surgical pathology and clinical correlations, current clinical pathology. Picken MM, et al. editors. Springer Science & Business Media. 2012;17:219-229.
7. Linke RP. On typing amyloidosis using immunohistochemistry. Detailed illustrations, review and a note on mass spectrometry. Progr Histochem Cytochem 2012; 47:61-132.
8. Vrana JA, Gamez JD, Madden BJ, Theis JD, Bergen HR 3rd, Dogan A. Classification of amyloidosis by laser micro dissection and mass spectrometry based proteomic analysis in clinical biopsy specimens. Blood. 2009; 114:4957-4959.
9. Linke RP. Diagnosis of minimal amyloid deposits using the Congo red fluorescent method: a review. In: Amyloid and Related Disorders: Surgical Pathology and Clinical Correlations; Current Clinical Pathology. Picken MM, et al (eds.) Chapter 13, pp 175-185; Springer Science & Business Media. 2012.
10. Linke RP, Joswig R, Murphy CL, Wang S, Zhou H, Gross U, Röcken C, Westermark P, Weiss, D, Solomon, AS. Senile seminal vesicle amyloid is derived from semenogelin I. J. Lab. Clin. Med. 2005; 145:187-193.

A Simple Amyloid Typing Procedure Based on a Proteomic Approach

B. Kaplan[1], T. Ziv[2], A. Livneh[1]

[1] Heller Institute of Medical Research, Sheba Medical Center, Tel-Hashomer, Israel
[2]Smoler Proteomics Center, Department of Biology, Technion - Israel Institute of Technology, Israel

Correct determination of amyloid type is crucial for diagnosis, treatment and prognosis of amyloid disease. Current antibody-based amyloid typing methods have restricted capability to check a long list of different amyloid proteins. In this respect, proteomic identification of amyloid proteins by mass spectrometry seems to be promising. However, this approach is used in a few amyloid research centers, partially due to complex and time-consuming sample preparation procedures. In this study we present a new, simple procedure for proteomic-based amyloid typing. In contrast to the previously reported amyloid recovery from tissue methods, amyloid proteins were extracted using volatile solvent which might be easily removed by lyophilization, thus allowing efficient concentration of the extracted material. The extracted proteins were separated using one-dimensional SDS-electrophoresis and identified by mass spectrometry. The applied methodology allowed a successful determination of amyloid type, shown here in five tested biopsy samples.

INTRODUCTION

The well recognized drawbacks of antibody-based amyloid typing techniques prompted the development of new antibody-free chemical methods. During the last decade several proteomic approaches involving protein identification by mass spectrometry were developed and found to be promising for the unbiased classification of amyloid proteins in biopsy specimens. In these techniques, selection of an appropriate sample preparation mode is critical. Some reports describe amyloid protein extraction and purification using HPLC (1) or two-dimensional electrophoresis (2). Of special interest is a capture of amyloid deposits from tissue by a laser microdissection technique with a following mass spectrometry-based proteomic analysis (3). At present this method is considered as a gold standard for amyloid typing. These methods, however, are complex and expensive and still not available for clinical laboratories. The aim of our study was the development and application of a more simple and available procedure for amyloid typing by using proteomic technologies.

METHODS

Amyloid protein containing tissue components were extracted from a few milligrams of fresh-frozen biopsy specimens with 20% acetonitrile - 0.1% trifluoroacetic acid solution (4). The extracted proteins were lyophilized and run on 10-20% polyacrylamide gels.The electrophoretically separated proteins were electroblotted onto

PVDF membranes and stained with Commassie Blue. Alternatively, gels were directly stained with Coomassie blue. Since all major amyloid subunits are proteins smaller than 30 kDa, the revealed protein bands of the MW<30 kDa were excised for further analysis.

The proteins in each gel/membrane slice were reduced with 2.8 mM DTT (60ºC for 30 min), modified with 8.8 mM iodoacetamide in 100 mM ammonium bicarbonate (in the dark, room temperature for 30 min) and digested in 10% acetonitrile and 10 mM ammonium bicarbonate with modified trypsin (Promega) overnight at 37°C. The resulting tryptic peptides were resolved by reverse-phase chromatography on 0.075 X 200-mm fused silica capillaries (J&W Scientific, USA) packed with Reprosil reversed phase material (Dr Maisch GmbH, Germany). The peptides were eluted with linear 95 minutes gradients of 7 to 40% and 8 minutes at 95% acetonitrile with 0.1% formic acid in water at flow rates of 0.25 µl/min. Mass spectrometry was performed by an ion-trap mass spectrometer (Orbitrap, Thermo) in a positive mode using repetitively full MS scan followed by collision induced dissociation (CID) of the 7 most dominant ion selected from the first MS scan. The mass spectrometry data was analyzed using the Sequest 3.31 software (J. Eng and J.Yates, University of Washington and Finnigan, San Jose) searching against the human section Uniprot database.

RESULTS

Figure 1 demonstrates the typical electrophoretic profiles of the amyloid-containing tissue extracts. The prominent protein bands of MW<30kDa (indicated by arrows) were excised for protein identification by mass spectrometry. The identified sequences belonged not only to amyloid proteins, but also to other tissue components and contaminating serum substances of a similar molecular weight. Proteins identified in the excised band were checked for the presence of sequences matching the particular amyloid protein type and its characteristic molecular weight. The amyloidogenic sequences detected in 5 patients with amyloidosis (samples #1 - 5) are shown in Box 1. The identified sequences indicated to AA amyloidosis in the samples #1 and #2, AL-lambda amyloidosis (#3), AL-kappa amyloidosis (#4), and transthyretin amyloidosis (#5). These results were in concordance with the previous typing of the same cases using Western blotting and N-terminal microsequencing (5).

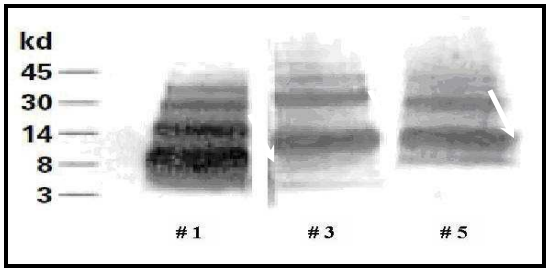

Figure 1. Electrophoretic profiles of amyloid-containing tissue extracts (patients ## 1, 3, 5)

Box 1. Samples #1 – 5: amyloidogenic sequences

Sample #1, 8 kDa (liver): Human Serum amyloid A protein (SAA1)
EANYIGSDK
EANYIGSDK
EANYIGSDKYFHAR
GPGGVWAAEAISDAR
RGPGGVWAAEAISDAR
GPGGVWAAEAISDAR

Sample #2, 8 kDa (thyroid): Human Serum amyloid A protein (SAA1)
EANYIGSDK
EANYIGSDKYFHAR
GPGGVWAAEAISDAR
SFFSFLGEAFDGAR

Sample #3, 14 kDa (spleen): Human Immunoglobin lambda-like polypeptide 5
VTVLGQPK

Sample #4, 15 kDa (fat): Human Immunoglobulin kappa light chains
SGTASVVC(+57.021)LLNNFYPR
DSTYSLSSYLTLSK
VDNALQSGNSQESVTEQDSKDST
TVAAPSVFIFPPSDEQLESGTASV
ASQIGSYLNWYQQEPGKAPK
LLIYAASNLLSGVPSR
DIQM(+15.996)AQSPSSLSASVGD
ASQIGSYLNWYQQEPGK
FSGSGSGTDFTLTISSLQPEDFAT

Sample #5, 14 kDa (heart): Human Transthyretin
AADDTWEPFASGK
TSESGELHGLTTEEEFVEGIYK

DISCUSSION

In this study, we have demonstrated the utility of a new procedure for typing of amyloid proteins by proteomic approach. In contrast to the previously reported amyloid extraction methods (1, 2), we employed volatile extraction solvent which might be easily removed by lyophilization, thus allowing efficient concentration of the extracted material. For separation and purification of the extracted proteins, we applied a widely used SDS-electrophoresis technique, while the reported amyloid protein purification methods were more complex and included HLPC (1) or 2-dimensional electrophoresis (2).

The procedure we have used to extract and separate the amyloid proteins, is also applicable for amyloid typing by Western blotting and N-terminal sequence analysis, which enables the amyloid typing by different biochemical techniques. Such comprehensive examination of biopsy specimens may be particularly useful when solving “difficult” cases.

In conclusion, we present here a new proteomic-based amyloid typing method by employing a simple and inexpensive sample preparation procedure applicable in most clinical laboratories.

REFERENCES

1. Murphy CL, Wang S, Williams T, Weiss DT, Solomon A. Characterization of systemic amyloid deposits by mass spectrometry. Methods Enzymol. 2006;412:48-62.
2. Lavatelli F, Vrana JA. Proteomic typing of amyloid deposits in systemic amyloidoses, Amyloid. 2011:8(4):177-82.
3. Vrana JA, Gamez JD, Madden BJ, Theis JD, Bergen HR 3rd, Dogan A. Classification of amyloidosis by laser microdissection and mass spectrometry-based proteomic analysis in clinical biopsy specimens. Blood. 2009; Dec 3;114(24):4957-9.
4. Kaplan B, Hrncic R, Murphy CL, Gallo G, Weiss DT, Solomon A. Microextraction and purification techniques applicable to chemical characterization of amyloid proteins in minute amounts of tissue. Methods Enzymol. 1999;309:67-81.
5. Kaplan B, Martin BM, Livneh A, Pras M, Gallo GR. Biochemical subtyping of amyloid in formalin-fixed tissue samples confirms and supplements immunohistologic data. Am J Clin Pathol. 2004;121:794-800.

Diagnosis of Amyloidosis Subtype by Laser-Capture Microdissection (LCM) and Tandem Mass Spectrometry (MS) Proteomic Analysis

P. Renaut[1], P. Mollee[2], S. Boros[1], D. Loo[3], M. Hill[3]

[1]Anatomical Pathology Dept, Pathology Queensland, Princess Alexandra Hospital, Brisbane, QLD, Australia
[2]Haematology Dept, Pathology Queensland, Princess Alexandra Hospital, Brisbane, QLD, Australia
[3]The University of Queensland Diamantina Institute, Brisbane, QLD, Australia

ABSTRACT

Correct identification of the protein that is causing amyloidosis is crucial for clinical management. We assessed combining specific sampling of amyloid deposits by LCM and analysis of tryptic digests by tandem MS proteomic analysis in 23 cases of amyloid deposition. LCM was performed on 10µm sections of formalin-fixed paraffin embedded tissue stained with Congo Red. Proteins were digested with trypsin and peptides were analysed using a Chip CUBE-QTOF. Database searching utilized the NCBInr human protein database. The amyloid subtype was able to be determined in all 23 cases. Proteins identified included immunoglobulin light chain (localised amyloid n=3, systemic AL n=8), transthyretin (senile amyloid n=5, hereditary ATTR n=2), serum amyloid A2 (AA n=2), fibrinogen alpha chain (AFib n=1), TGFβ (corneal lattice amyloid n=1) and semenogelin (seminal vesicle amyloid n=1). In conclusion, LCM and tandem MS allows correct typing of amyloid deposits in clinical biopsy samples.

INTRODUCTION

Amyloid deposits comprise extracellular aggregates of amyloid fibrils embedded in a matrix containing other proteins such as serum amyloid P protein and other proteoglycans and apolipoproteins. Over 20 amyloidogenic precursor proteins have been identified and correct identification of the amyloidogenic protein is crucial for clinical management. Amyloid subtyping by immunohistochemistry is limited outside of centres of expertise. Immunohistochemistry can suffer from both low sensitivity and specificity, but perhaps the greatest factor is lack of pathologist expertise with the various immunostains due to the rarity of this disease.

Direct chemical identification of the protein composition of the amyloid deposits has previously been limited due to limited protein biochemistry sequencing methods, complex protein extraction, contaminating proteins from surrounding normal tissues and limited informatics and databases. Many of these limitations have now been overcome with tandem mass spectrometric techniques. We aimed to improve the diagnosis of amyloidosis subtype by combining specific sampling of amyloid deposits by LCM and analysis of tryptic digests by tandem MS proteomic analysis.

METHODS

Ten micron sections were cut from formalin fixed paraffin embedded tissue onto Arcturus PEN membrane glass slides. Tissue sections were deparaffinised and stained with Congo red. The stained sections were rinsed and thoroughly air-dried. Congo red positive areas were dissected using an Arcturus LCM system.

Amyloid regions were processed according to the Stratagene FFPE protein extraction protocol. Briefly, LCM samples were incubated with FFPE solution, at 90^{o}C for 10mins, followed by 60^{o}C for 120mins and alkylation with 200mM of IAA for 30mins. Samples were diluted 10 times with 50mM ammonium bicarbonate and 10% acetonitrile for overnight digestion with 0.1ug/ul trypsin at 37^{o}C. Trypsin inactivation was achieved by acidifying samples with 0.1% formic acid.

Amyloidogenic peptides were analysed with HPLC coupled Chip-cube 6250 QTOF (Agilent). Samples were desalted on the enrichment column of G4240-62010 HPLC chip for 12sec prior to a 20 minute gradient from 5% to 50%B. Solvent A composition was 0.1% formic acid, solvent B was 0.1% formic acid, 90% acetonitrile. HPLC loading pump was set to 2.5% B, flow rate of 3ul/min while analytical pump was set to 5%B and flow rate of 0.3ul/min. Mass spectrometer was programmed to acquire 8 MS and 4MS/MS spectra/sec with dynamic exclusion after 2 MS/MS and released after 0.2min.

Mass spec data was analysed using Spectrum Mill search engine against NCBInr human database with carbamidomethylation cysteine as fixed modification, and oxidized methionine, pyroglutamic acid N-term, and deamidated asparagine as variable modifications. Protein identification cut-offs were protein score > 11, peptide score > 10 and % scored peak intensity >60.

RESULTS

Twenty-three clinical biopsy samples were analysed. Nineteen cases had a well characterised amyloid subtype and in 4 cases the diagnosis was not definitive. Biopsy sites included gastrointestinal tract (n=6), heart (n=5), renal (n=3), liver (n=1), bladder (n=1) and various other sites (foot, breast, tongue, mesentery, orbit, cornea, seminal vesicle). While LCM was successful in all cases, use of an ultraviolet laser and mounting of tissue on membrane coated slides provided the cleanest and most consistent capture of targeted tissue. The amyloid subtype was able to be determined in all cases. An example of the tandem MS readout is given in Table 1 (senile cardiac amyloidosis) and the various amyloid fibrils identified are listed in Table 2.

Table 1. Example of tandem mass spectrometry readout

Sample	Size	Protein score	% coverage	Species	Database	Entry name
Heart	600000	49.59	20	Human	NCBInr	transthyretin
Heart	600000	38.99	8	Human	NCBInr	vitronectin
Heart	600000	29.59	8	Human	NCBInr	pre-SAP component
Heart	600000	15.05	2	Human	NCBInr	apolipoprotein A-IV
Heart	600000	12.51	2	Human	NCBInr	apolipoprotein E
Heart	600000	11.78	5	Human	NCBInr	beta-globin

Various other proteins are identified by tandem MS in amyloid extracts. Of particular interest is the presence of proteins typically known to be co-located in amyloid deposits which helps confirm that the microdissected tissue is amyloid. Typical amyloid-associated proteins were identified in the following number of cases: SAP (n=14),

apolipoprotein A4 (n=13), vitronectin (n=16), apolipoprotein E (n=14) and clusterin (n=11). Various types of collagen were frequently present (n=12) and various, presumably contaminating, keratins were identified (n=15).

Table 2. Amyloid fibril type identified by LAM and tandem MS

Amyloid type	Protein identified	N
AL	immunoglobulin light chain	11
Systemic		(8)
Localised		(3)
AA	SAA	2
ATTR	transthyretin	7
Senile		(5)
Hereditary		(2)
AFib	fibrinogen alpha chain	1
Corneal	TGFb	1
Seminal vesicle	semenogelin	1

One of the diagnostically challenging cases had: extensive gastrointestinal amyloidosis and no evidence of clonal light chain disease; negative kappa, lambda, SAA and transthyretin immunohistochemistry; and negative genetic studies. Tandem MS revealed immunoglobulin lambda light chain type. The second diagnostically challenging case had: isolated renal amyloidosis with a positive SAA stain, an IgG kappa paraprotein and kappa restricted serum free light chains. Tandem MS revealed serum amyloid A2 protein but no immunoglobulin. The third case had: cardiac, neurological and gastrointestinal involvement; and equivocal immunohistochemistry. Tandem MS demonstrated transthyretin and genetic studies showed an A97S ATTR mutation. The final case of interest had: isolated renal amyloidosis and no evidence of clonal light chain disease; negative kappa, lambda and SAA immunohistochemistry. Tandem MS demonstrated fibrinogen alpha chain and genetic studies showed a Val526 mutation.

DISCUSSION

This study illustrates the usefulness of tandem MS based approaches for subtyping of amyloid deposits. Our series adds to the pioneering work of the Mayo Clinic pathology department where nearly all cases of amyloidosis can be correctly classified by a combination of laser microdissection and mass spectrometry–based proteomic analysis (1). Other groups have successfully examined amyloid typing without LCM, either through proteomic analysis of subcutaneous adipose tissue (2) or via novel sample preparative techniques (3). We plan to pursue further method optimisation including improved definition of co-locating proteins in amyloid deposits, additional database and bioinformatic interrogation and defining formal analysis and reporting methodology.

In conclusion, we have demonstrated that LCM and tandem MS can successfully identify the fibril composition of amyloid deposits in clinical biopsy samples. Tandem MS based analysis is likely to become the new gold standard in the diagnosis of amyloid subtype.

REFERENCES

1. Vrana et al. Classification of amyloidosis by laser microdissection and mass spectrometry–based proteomic analysis in clinical biopsy specimens. Blood 2009;114:4957.

2. Merlini et al. Reliable typing of systemic amyloidoses through proteomic analysis of subcutaneous adipose tissue. Blood 2012;119:1844.
3. Jullig et al. A unique case of neural amyloidoma diagnosed by mass spectometry of formalin-fixed tissue using a novel preparative technique. Amyloid 2011;18:147.

Identification and characterization of TTR amyloid associated molecules in FAP

G. Suenaga[1], M. Tasaki[1], M. Ueda[1], C. Ogawa[1], A. Hirata[1], S. Mikami[2], M. Ying[3], S. Kawahara[1], T. Oshima[1], A. Yanagisawa[1], S. Shinriki[1], M. Shono[1], H. Jono[1], T. Yamashita[1], K. Obayashi[1], H. Koike[4], Y. Ando[1]

[1]Department of Diagnostic Medicine, Faculty of Life Sciences, Kumamoto University, Japan, [2]AMR INCORPORATED, Japan, [3]Thermo Fisher SCIENTIFIC, USA, [4]Department of Neurology, Nagoya University Graduate School of Medicine, Japan

ABSTRACT

Recently, it has been shown that some of amyloid associated molecules are co-localized with transthyretin (TTR) amyloid deposit and may play important roles in TTR amyloidosis. However, the role of these molecules is still largely unknown. In this study, we attempted to identify key molecules in TTR amyloid-laden tissues by using liquid chromatography tandem mass spectrometry (LC-MS/ MS).

Congo red-positive areas in autopsy tissue specimens from familial amyloid polyneuropathy (FAP) patients were analyzed by LC-MS/ MS. In addition, serum samples of FAP patients were also analyzed to determine the existence of identified molecules.

LC-MS/ MS analysis revealed that clusterin was co-localized with TTR amyloid deposit. Moreover, serum clusterin levels of FAP patients was significantly higher than that of healthy volunteers. In present study, LC-MS/ MS analysis identified clusterin as an amyloid associated molecule in FAP, and it was shown that clusterin may play important roles in the pathogenesis of FAP.

INTRODUCTION

Familial amyloidotic polyneuropathy (FAP) induced by amyloidotic transthyretin (TTR), is characterized by systemic accumulation of amyloid fibrils [1]. Despite a number of *in vitro* studies of TTR-related amyloidosis, many questions, including where and how amyloid fibrils form *in vivo* and what is the impact of amyloid deposition on tissues, remain unanswered. Recently, it has been shown that some of amyloid associated molecules, such as serum amyloid P component, apolipoprotein E, and proteoglycans, are co-localized with TTR amyloid fibrils and may play important roles in TTR amyloid fibril formation [2]. However, the role of those co-localized molecules with TTR amyloid deposition is still largely unknown. In this study, we focused on the amyloid associated molecules and attempted to identify key molecules in TTR amyloid-laden tissues from FAP patients by using liquid chromatography tandem mass spectrometry (LC-MS/ MS) [3].

MATERIALS AND METHODS

Autopsy tissue specimens from FAP patients were analyzed in this study. Four micro-meters formalin-fixed paraffin embedded (FFPE) sections were deparaffinized and stained by Congo red. Positive areas were collected by needle dissection and digested with Liquid Tissue (Expression Pathology, Inc., Gaithersburg, MD, USA) and trypsin. The digests were analyzed by LC-MS/ MS (LCQ DECA XP plus; Thermo Fisher scientific, Sunnyvale, CA 94085, USA) [3]. To evaluate the existence of molecules co-localized with TTR amyloid deposits in heart, lung, stomach, tongue, kidney and bladder from FAP patients, immunohistochemical staining was performed with anti clusterin antibody.

Serum samples of 25 FAP patients (18 of early onset cases and 7 of late onset cases; 16 males and 9 females) were collected. We measured serum clusterin levels in each sample by enzyme-linked immunosorbent assay kit (Biovendor Laboratory Medicine Inc), and the mean levels was compared with those of 32 healthy volunteers. Moreover, we assessed the correlation between each serum clustetrin level and the clinical indices, such as age of the onset, duration of the disease, and the severity of sensory and autonomic neuropathies.

RESULTS

As the result of LC-MS/ MS analysis of the site positive for Congo red in peripheral nerves collected from FFPE sections, various proteins were identified. These protein lists showed that only known amyloid associated molecules, including apolipoprotein E, apolipoprotein A-IV, but also many unknown amyloid associated molecules. In those amyloid associated molecules, we focused on clusterin.

First, in heart, lung, stomach, tongue, kidney and bladder from FAP patients, Congo red-positive site, the staining site of TTR and the staining site of clusterin were clearly matched.

Next, we evaluated serum clusterin concentrations in FAP patients, carriers and healthy volunteers. Mean serum clusterin level of all 25 FAP patients was significantly higher than that of 32 healthy volunteers ($P<0.05$). Whereas, serum clusterin concentrations did not correlate with sex or age.

Furthermore, no significant correllation was found between clusterin concentrations and duration of the disease, however, lower serum level of clusterin tended to be associated with more severe autonomic dysfunction in FAP patients.

DISCUSSION

In this study, we have demonstrated that clusterin was co-localized with TTR amyloid deposition. Clusterin is extracellular molecular chaperone, and recently reported that clusterin related to amyloid fibril formation and increased plasma clusterin concentrations are associated with severity of Alzheimer's disease [4,5]. Therefore, clusterin also may associate with TTR amyloidosis.

To test this possibility, we investigated localization of clusterin in various targeted tissues and serum clusterin concentrations in FAP. Clusterin was co-localized with TTR amyloid deposits in systemic organs of FAP patients.

LC-MS/ MS analysis identified clusterin as an amyloid associated molecule in FAP. Clusterin may play important roles in the pathogenesis of FAP. Therefore, LC-MS/ MS may be a useful system to identify novel amyloid associated molecules.

REFERENCES

1. Ando Y, Nakamura M, Araki S. Transthyretin-related familial amyloidotic polyneuropathy. Arch Neurol 2005;62:1057-1062.
2. Botto M, Hawkins PN, Bickerstaff MC, Herbert J, Bygrave AE, McBride A, Hutchinson WL, Tennent GA, Walport MJ, Pepys MB. Amyloid deposition is delayed in mice with targeted deletion of the serum amyloid P component gene. Nat Med 1997;3:855-859
3. Hood BL, Darfler MM, Guiel TG, Furusato B, Lucas DA, Ringeisen BR, Sesterhenn IA, Conrads TP, Veenstra TD, Krizman DB. Proteomic analysis of formalin-fixed prostate cancer tissue. Mol Cell Proteomics 2005;11:1741-1753.
4. Lee KW, Lee DH, Son H, Kim YS, Park JY, Roh GS, Kim HJ, Kang SS, Cho GJ, Choi WS.Clusterin regulates transthyretin amyloidosis. Biochem Biophys Res Commun 2009;2:256-260.
5. Schrijvers EM, Koudstaal PJ, Hofman A, Breteler MMM. Plasma clusterin and the risk of Alzheimer disease. JAMA 2011;13:1322-1326

Subtyping of amyloidosis by direct proteomic analysis of fixed biopsy samples

Sophie Liuu[1], Emmanuelle Demey[1], Emie Durighello[1], Magali Colombat[2], Gilles Grateau[3], Joëlle Vinh[1]

[1]Spectrométrie de Masse Biologique et Protéomique, CNRS USR 3149, ESPCI PARISTech, Paris, France
[2]Service d'anatomie pathologique, AP-HP Hopital Tenon, Paris, France
[3]Service de médecine interne, Hôpital Tenon, UPMC, INSERM U933, Paris, France

ABSTRACT

Diagnosis and subtyping of amyloidosis are critical for prognostic and treatment. Subtyping has been recently demonstrated combining laser capture microdissection (LCM) and mass spectrometry. Here we show that ultrasonic treatment could help for the completion of enzymatic proteolysis followed by mass spectrometry analysis which is an emerging proteomic technique, directly on raw biopsy samples even without LCM and to get closer to the clinical routine application for amyloidosis.

INTRODUCTION

Amyloidosis is a disease where insoluble deposits of specific proteins occur in tissues. Different classes of amyloidosis have been reported and their diagnostic relies on the identification of the associated proteins: up to 10 proteins can be targeted using histochemical approaches. Currently, Congo red staining is the golden standard for the diagnosis of amyloidosis based on apple-green birefringence follow-up by subtyping using antibodies. However they can be inconclusive on certain cases due to the competence of the pathologist and the quality and availability of the dye, antibody and microscopy, leading to a lack of information about the underlying etiology. Subtyping has been recently demonstrated combining laser capture microdissection (LCM) and mass spectrometry (1). However, the LCM is not available in every clinical department, requires a specialist and can be time-consuming. Here we report a new sample treatment directly on paraformaldehydefixed slices using an ultrasonic probe to complete the enzymatic proteolysis in 60s instead of 15 hours incubation (2). Ultrasonic treatment combined to our data processing allows performing diagnosis and subtyping of different type of tissues: kidney, accessory gland salivary, lung, testicle, spleen.

METHOD

Paraformaldehyde-immobilized tissues (Bouin/AFA) from patients and controls were directly proteolyzed with an ultrasonic probe. Proteolytic peptide mixtures were analyzed by nanoLC-MS/MS (LTQ-FT Ultra, ThermoFisher equipped with TriVersa NanoMate chip-based nanosource, Advion) after nanoLC optimization (U3000 Dionex).

RESULTS

Ultrasonic tryptic treatment on fixed raw tissues allowed performing subtyping of amyloidosis. The results were compared with data obtained with immunohistopathology using the whole series of antibodies for amyloidosis diagnosis.

It is a non targeted approach. Abundance of the protein were evaluated according to (3) taking into account the area of the three most intense peptides. Only biopsies containing Apolipoprotein E (named ApoE) and Serum amyloid P component (named SAMP) which are common to all amyloid deposits, were considered as potential amyloid candidate. Finally amyloidosis were classified according to the relative intensity of amyloidogen protein. Some significant examples from kidney tissues illustrate our results. The results are visualized with sector diagrams representing the relative intensities of amyloid proteins.

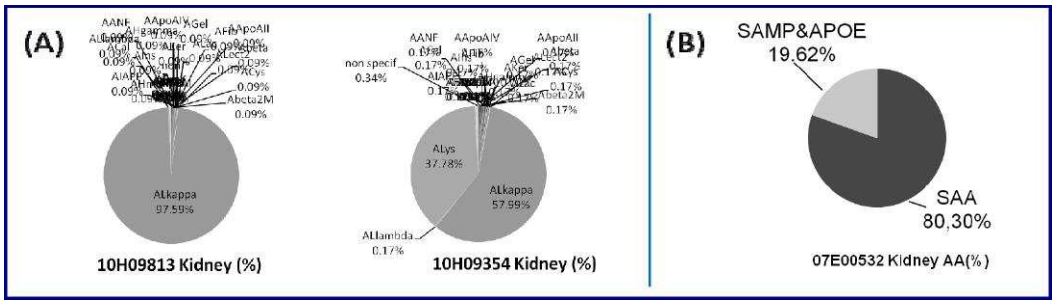

Figure 1. Biopsies of (A) negative controls, (A) AA amyloid patient.

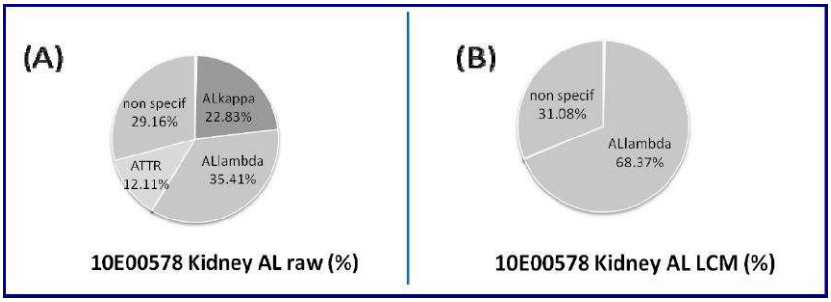

Figure 2. Biopsy of amyloid AL (A) raw tissue (50% amyloid), (B) Laser Capture Microdissected LCM tissue (95% amyloid)

No pure negative controls could be assayed because biopies come always from patients and are aimed to identify a pathology. Non amyloid diseased kidney does not present SAMP and ApoE (fibrils biomarkers), even if amyloidogen protein could be detected (Igκ and LysC) (1A). Their presence could be explained by inflammatory phenomenon or tissue dammage (eg. minor glomerular lesions). The controls are non amyloid pathologies. As shown in this example when amyloid deposits represents more than 80% of the tissue the diagnostic and the classification are clear (Figure 1B). When the percentage goes below 50%, amyloid diagnostic is clear but classification lacks some robustness (Figures 2A) even if the amyloid type is correct: here we analyzed a raw

biopsy without focalising on amyloid fibrils and without slicing. On the opposite LCM treatment on the same sample could offer preparation above 95% where the classification is unambiguous (Figure 2B).

DISCUSSION

This strategy opens the way for a rapid and accurate amyloidosis subtyping directly from raw clinical samples and allows to avoid at the most the laser capture microdissection step which is highly time-consuming. This is of particular interest for classes that could not be distinguished by the classical histochemical analysis. Our next step will be to validate our approach to different amyloidoses and tissues with clinicians.

The whole analysis lasts 1 day for enzymatic treatment and roughly 10 slices are required and lasts 1 day for triplicate LC-MS/MS and roughly 1 slice of 10µm is required. In order to increase cohorts for a realistic clinical application we intend to automatize the first step. Miniaturization is required to decrease sample consumption of the first treatment (only 10% of the sample is actually analyzed).

We want to characterize specificaly the isofoms of protein involved. One example is ATTR addressed either by bottom-up (4) or top-down (5) strategies, where the transthyretin isoform can discriminate between senile systemic amyloidosis and familial thranthyretin amyloidosis.

ACKNOWLEDGEMENTS

Sophie Liuu and Emie Durighello received a grant from SAESPCI.
This work was supported by CNRS, AP-HP, Ville de Paris and the Association Française contre l'Amylose

REFERENCES

1. Sethi S, Theis JD, Leung N, Dispenzieri A, Nasr SH, Fidler ME, et al. Mass spectrometry-based proteomic diagnosis of renal immunoglobulin heavy chain amyloidosis. *Clinical Journal of the American Society of Nephrology*. 2010 déc;5(12):2180-7.
2. Fernandez L, Santos HM, Nunes-Miranda JD, Lodeiro C, Capelo Martínez JL. Ultrasonic Enhanced Applications in Proteomics Workflows: single probe versus multiprobe. *Journal of Integrated OMICS*. 2011 feb;1(1):144-50.
3. Silva JC, Gorenstein MV, Li GZ, Vissers JPC, Geromanos SJ. Absolute quantification of proteins by LCMSE. *Molecular & Cellular Proteomics*. 2006;5(1):144-150.
4. Kingsbury JS, Théberge R, Karbassi JA, Lim A, Costello CE, Connors LH. Detailed Structural Analysis of Amyloidogenic Wild-Type Transthyretin Using a Novel Purification Strategy and Mass Spectrometry. *Analytical. Chemistry*. 2007 mar 1;79(5):1990-8.
5. Théberge R, Infusini G, Tong W, McComb ME, Costello CE. Top-down analysis of small plasma proteins using an LTQ-Orbitrap. Potential for mass spectrometry-based clinical assays for transthyretin and hemoglobin. *International Journal of Mass Spectrometry*. 2011 mar 1;300(2–3):130-42.

Amyloidosis of lymph nodes: a proteomic analysis using mass spectrometry to differentiate between localized and systemic forms

Anita D'Souza[1], Jason Theis[2], Patrick Quint[2], Julie Vrana[2], Steven Zeldenrust[1], Robert Kyle[1,2], Morie Gertz[1], Ahmet Dogan[2], Angela Dispenzieri[1,2]

[1]Division of Hematology, Department of Internal Medicine, [2]Department of Laboratory Medicine and Pathology Mayo Clinic, Rochester, MN, USA

Amyloidosis affecting lymph nodes is uncommon. Lymph node involvement with amyloid may occur in the setting of systemic amyloidosis or as a condition localized to the lymph nodes. Why some amyloid remains localized is yet unknown. We speculated that the composition of the amyloid with these two presentations may differ. Therefore, we undertook this study to detect differences in the lymph node amyloid proteome in localized and systemic amyloidosis using a mass spectrometric-based proteomic analysis. We identified all patients with lymph node biopsy proven amyloidosis seen at the Mayo Clinic, Rochester between May 1971 and October 2011. Clinical and laboratory data of these patients was abstracted. Using laser microdissection/tandem mass spectrometry, we analyzed the composition of amyloid in lymph nodes where the block was available. Fourty four patients with lymph node biopsy proven amyloidosis were identified. Table 1 shows the clinical and laboratory features of these patients. We were able to obtain mass spectrometric analysis in 30 of the 44 patients. Preliminary analysis demonstrated the presence of heavy chain amyloid (AH) in all localized cases where as only 9 of the systemic cases had AH deposits (p 0.004). Other significant differences were also seen in vimentin and clusterin deposits although this did not meet statistical significance. Mass spectrometry has made a definitive discrimination between amyloid precursor proteins possible. Further exploration of the amyloid proteome may allow for differentiation between localized and systemic presentations with important clinical implications.

INTRODUCTION

Amyloidosis involving lymph nodes (LN) is uncommon but may be seen in association with IgM monoclonal protein[1,2] and low grade lymphoproliferative disease, especially lymphoplasmacytic lymphoma and extranodal marginal zone lymphoma.[3-5] The clinical pattern in LN immunoglobulin-derived amyloidosis (AID) may be restricted to LN alone (site of amyloid production) or may be disseminated to cause classic amyloid syndromes, or systemic amyloidosis.[6] Why some amyloid remains localized to the site of production where as others disseminate is yet unknown. We speculated that differences in the amyloid proteome between these two forms and attempted to find these using mass spectrometry (MS)-based proteomic analysis.

METHODS

44 cases of LN amyloidosis were identified using the Dysproteinemia database. Each case was defined as follows; Localized- amyloidosis restricted to LN, single or multiple groups; Systemic- LN amyloid with associated classic amyloid syndromes, or involvement of organs or bone marrow.

The methods for MS have been previously published.[7] Laser microdissection was performed in Congo-red areas of formalin-fixed paraffin-embedded lymph node blocks. Two samples were analyzed per case. The dissected tissue was digested into tryptic peptides and analyzed using nano-flow liquid chromatography electrospray tandem mass spectrometer. The results were queried using the Swiss-Protein database and assigned peptide and protein probability scores in Scaffold (Proteome Software, Portland, OR).

Protein identifications were accepted if they could be established with a ≥90% probability, at a 90% confidence interval. The spectral count indicates the total number of spectra assigned to each protein and may be utilized as an indicator of relative abundance. A spectral count greater than 8 was considered clinically significant.

RESULTS

Figure 1 shows a representative scaffold overview of the 30 cases where mass spectrometric analysis was available.

Tables 1 and 2 show the clinical and laboratory features of the 44 cases of lymph node amyloidosis. Forty ones cases had immunoglobulin-derived amyloidosis (AID) with 1 each of AA, ACalcitonin and ATTR. One patient had AID + ATTR (Systemic #1).

Localized AID; 1 had AH (localized #4, fig 1) and 5 had AH/AL Systemic AID; 11/22 had AL, 11/22 had AH/AL.

Finding AH deposits was significantly associated with localized AID (6/6) versus systemic AID (11/22); p-value 0.03.

Patients with localized AID had better clinical outcomes with less treatment, including observation (fig 2).

Table 1. Features of Lymph node amyloidosis

	Localized , N=14	Systemic, N=27	p-value
Gender, male (%)	10 (71)	14 (52)	0.2
Age at diagnosis, years	63	62	0.8
Fatigue (%)	2 (14)	18 (67)	0.002
Weight loss (%)	2 (14)	11 (41)	0.08
Lower extremity edema (%)	1 (7)	8 (30)	0.1
Paresthesia (%)	2 (14)	8 (30)	0.3
Dyspnea on exertion (%)	3 (21)	14 (52)	0.06
Hemoglobin, g/dl	14.2	12.6	0.1
Creatinine, mg/dl	1	1	0.8
Albumin, g/dl	3.7	3	0.004
Beta2 microglobulin, mcg/ml	1.9	2	0.3
Circulating monoclonal protein	N=8 (of 13)	N=24	0.04
Urine protein, g/24h	0.09 (0.005-0.4)	0.2 (0.04-8.7)	0.01
Treatment			NS
None	6	6	
Surgery	2	1	
Chemotherapy	6	16	
Autologous stem cell transplant	0	4	
Number dead at last follow up	5	16	0.02
Median overall survival, years	10.6	4.3	0.04

Table 2.

Protein	# of cases where protein found	
	Localized, N=6 (%)	Systemic, N=22(%)
Apolipoprotein A1	6 (100)	20 (91)
Apolipoprotein A4	6 (100)	21 (95)
Apolipoprotein E	6 (100)	22 (100)
Serum Amyloid P	6 (100)	21 (95)
Ig light chain		
κ	3 (50)	7 (32)
λ	4 (66)	17 (77)
Ig heavy chain		
α	2 (33)	2 (9)
γ	5 (83)	10 (45)
μ	3 (50)	4 (18)
Clusterin	4 (66)	16 (73)
Vimentin	2 (33)	16 (73)
Vitronectin	6 (100)	22 (100)

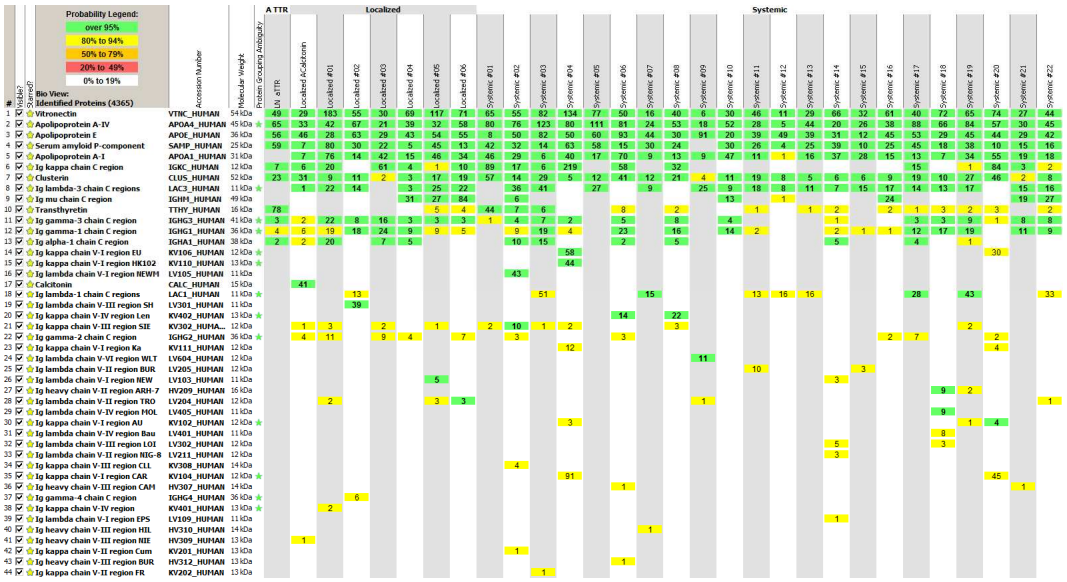

Figure 1. Scaffold overview of 30 cases of lymph node amyloidosis

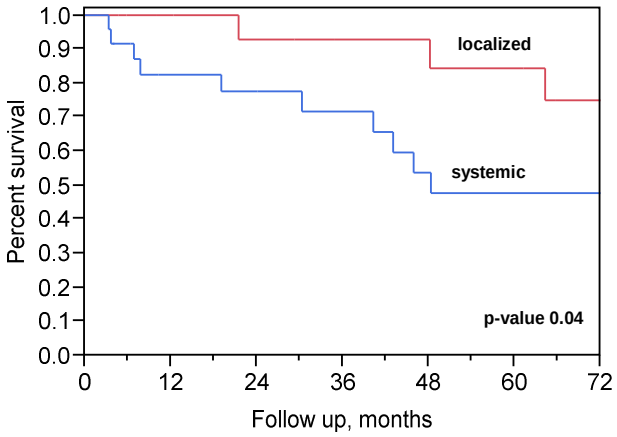

Figure 2. Kaplan-Meier analysis of the localized and systemic LN amyloidosis

CONCLUSIONS

We found that 61% of lymph node immunoglobulin-derived amyloidosis involving lymph nodes have AH amyloid deposits. Localized cases with lymph node AID appear to have higher quantities of AH amyloid.

Other proteins such as the apolipoproteins A-I, A-IV, E, serum amyloid P, clusterin, vimentin and vitronectin are also consistently seen in cases of lymph node AID. Further exploration of patients with AH and AH/AL amyloidosis in terms of their natural history and prognosis is warranted.

REFERENCES

1. Palladini G, Russo P, Bossoni T, et al. AL amyloidosis associated with IgM monoclonal protein: a distinct clinical entity. Clin Lymphoma Myeloma 2009;9:80-3.
2. Wechalkar A, Lachmann H, Goodman H, et al. AL amyloidosis associated with IgM paraproteinemia: clinical profile and treatment outcome. Blood 2008;112:4009-16.
3. Sanchorawala V, Blanchard E, Seldin D, et al. AL amyloidosis associated with B-cell lymphoproliferative disorders: frequency and treatment outcomes. Am J Hematol. 2006;81:692-5.
4. Cohen A, Zhou P, Xiao Q, et al. Systemic AL amyloidosis due to non-Hodgkin's lymphoma: an unusual clinicopathologic association. Br J Haematol. 2004;124:309-14.
5. Ryan RJ, Sloan J, Collins A, et al. Extranodal marginal zone lymphoma of mucosa-associated lymphoid tissue with amyloid deposition: a clinicopathologic case series. Am J Clin Pathol. 2012;137:51-64.
6. Telio D, Bailey D, Chen C, et al. Two distinct syndromes of lymphoma-associated AL amyloidosis: a case series and review of literature. Am J Hematol. 2010;85:805-8.
7. Vrana J, Gamez J, Madden B, et al. Classification of amyloidosis by laser microdissection and mass spectrometry-based proteomic analysis in clinical biopsy samples. Blood 2009;114:4957-9.

Tandem Mass Spectrometry Analysis of Protein Deposits in Human Subcutaneous Fat Tissues of a Patient with Immunoglobulin Light Chain Amyloidosis: *De novo* Sequencing and Post-translational Modifications

Y. Lu, R. Théberge, T. Prokaeva, N. Leymarie, B.H. Spencer, P.T. Soo Hoo, L.H. Connors, C.E. Costello

Departments of Biochemistry and Pathology, and Amyloid Treatment & Research Program, Boston University School of Medicine, Boston, Massachusetts, USA

ABSTRACT

Tandem MS methods, including LTQ-CID, LTQ-HCD-Orbitrap and TOF/TOF, provide information on both the amino acid sequences and the post-translational modifications (PTMs) of proteins extracted from small amounts of human fat tissues. In this report, we present our analyses of a fat sample from a patient with AL amyloidois demonstrating immunoglobulin light chain (LC) proteins with extensive C-terminal truncation. Even without access to the cDNA-derived sequence of Ig LCs, it was still possible to perform *de novo* sequencing and PTM analysis with TOF/TOF MS/MS and with HCD fragmentation followed by detection in the Orbitrap.

INTRODUCTION

For the systemic amyloidoses of immunoglobulin (Ig) light chains (LCs), we have found that deposited LCs are extensively processed, especially at the C-terminus, leading to fragment patterns that differ from patient to patient (1, 2). We are presently using high performance primary mass spectrometry (MS) and tandem (MS/MS) methods to compare LC fragments in amyloid deposits from fat biopsies.

METHODS

The fat biopsy described herein (F10-118) was obtained from a 59-year old male and showed extensive deposition of Ig lambda (λ) LC by Congo red staining. No amyloidogenic LC gene sequence information was available.

Protein extraction from the fat tissue was performed according to published protocols (1). Extracted proteins were subjected to 2D-gel electrophoresis. Isoelectric focusing (IEF) was performed on 17-cm strips in the pH range from 3 to 10. Finally, the PAGE gel was stained with GelCode® Blue (Pierce). Immunoblot analysis with anti-human Ig λLC antibodies was used to detect LC proteins and protein fragments that retained the constant region. In-gel digestion of immunoreactive gel spots was performed with trypsin Promega Gold (Promega) (3). Dried peptides were sequentially analyzed with 1) a Reflex IV™ MALDI-TOF MS (Bruker Daltonics) operated in

the positive ion, reflectron mode, 2) a MALDI-TOF/TOF ultrafleXtreme™ MS (Bruker Daltonics) and 3) LC/MS/MS (both CID and HCD) in an LTQ-Orbitrap™ MS (Thermo Fisher Scientific) with a TriVersa NanoMate™ system (Advion Biosciences). The MS/MS data was deconvoluted using Xtract™. Data sets were analyzed with MASCOT™ and the results were checked manually.

RESULTS

The fat biopsy obtained from a 59-year-old male showed extensive amyloid deposition (3+ score by Congo red staining) and Ig λLC proteins by immunohistochemistry. In patients with AL amyloidosis, each amyloid LC protein sequence is unique, especially in the variable region; lack of the LC gene and deduced protein sequences presented a significant obstacle in this work. Mass fingerprinting search on the MALDI-TOF MS data (Fig. 1) of a gel spot 18 (observed at 30 kDa) indicated a strong score for Ig λLC constant region. LC/MS/MS and MALDI-TOF/TOF MS data confirmed the peak assignments. Sequences for some variable region peptides were also assigned and aligned with germline gene IGLV1-51. MALDI-TOF/TOF MS revealed the oxidation of Trp (W) to kynurenine and *N*-formylkynurenine (1, 4).

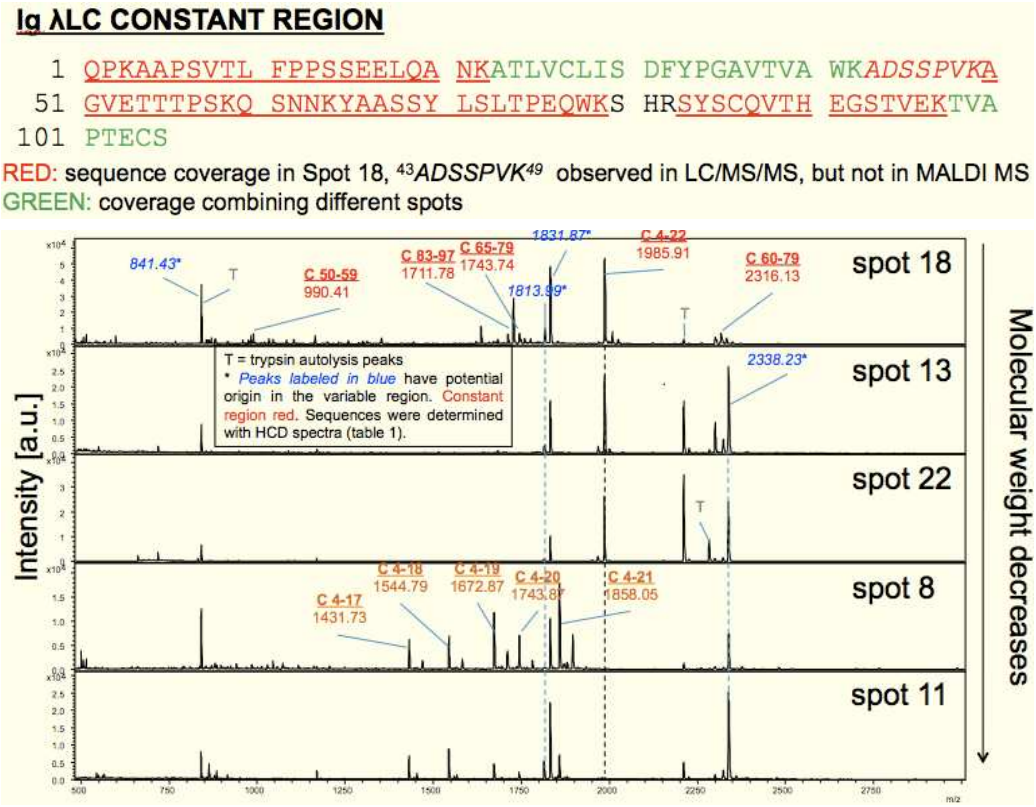

Figure 1. MALDI-TOF MS characterization of Ig LC species in AL fat sample

DISCUSSION

Spots 18 (observed at 30 kD), 13 (at 27 kD) and 22 (at 23 kD) were detected by immunoblot assay against Ig λLC; spots 8 and 11 were not. Full-length LC protein usually has MW *ca.* 25 kD. Considering PTMs and the unique primary sequence of this full-length LC, spot 18 appears to be the full-length amyloid deposited LC protein.

As the MW decreased, the abundances of the peaks for constant region (C) peptides, *e.g.*, C 4-22 *m/z* 1985.91, diminished. The serially truncated products from this peptide appear at *m/z* 1431.73 [4-17], 1544.79 [4-18], 1672.87 [4-19], 1743.87 [4-20] and 1858.05 [4-21], in the spectra of spots 8 and 11. These assignments were confirmed by tandem MS data.

HCD dissociation in the LTQ-Orbitrap of spot 11 provided sequence assignments for some variable region peptides found at, *e.g. m/z* 841.42, 1813.99 and 2338.23.

Unassigned peaks may originate from the variable region, or may be constant region peptides that have PTMs, including truncations. Digestion with additional proteases and/or acquisition of more tandem MS data should facilitate their analysis.

ACKNOWLEDGEMENTS

This research is supported by NIH grants P41 RR10888/GM 104603, S10 RR15942 and S10 RR20946 and the BUMC Amyloid Treatment and Research Program. We thank Bruker Daltonics for access to the Bruker ultrafleXtreme™. YL thanks a Finkielsztein Travel Grant for funding her conference participation.

REFERENCES

1. F Lavatelli, DH Perlman, B Spencer, T Prokaeva, ME McComb, R Théberge, LH Connors, V Bellotti, DC Seldin, G Merlini, M Skinner, CE Costello. Mol. Cell. Proteomics 2008, 7, 1570-1583.
2. LH Connors, Y Jiang, M Budnik, R Théberge, T Prokaeva, K Bodi, DC Seldin, CE Costello, M Skinner. Biochemistry, 2007, 46, 14259-14271.
3. DH Perlman, EA Berg, PB O'Connor, CE Costello, J Hu. Proc. Natl. Acad. Sci. U. S. A. 2005, 102, 9020-9025.
4. F Lavatelli, F Brambilla, V Valentini, P Rognoni, S Casarini, DD Silvestre, V Perfetti, G Palladini, G Sarais. Biochim. Biophys. Acta. 2011, 1814, 409-419.

Iodine-123 metaiodobenzylguanidine (^{123}I-MIBG) for the evaluation of cardiac sympathetic denervation in early stage amyloidosis

W. Noordzij[1], A.W.J.M. Glaudemans[1], B.P.C. Hazenberg[2], R.A. Tio[3], R.A.J.O. Dierckx[1], R.H.J.A. Slart[1]

[1] Department of Nuclear Medicine and Molecular Imaging,[2] Department of Rheumatology and Clinical Immunology, [3] Department of Cardiology. University Medical Center Groningen, University of Groningen PO Box 30.001, 9700 RB Groningen, The Netherlands

ABSTRACT

Cardiac amyloidosis is rare and may lead to potentially life-threatening restrictive cardiomyopathy. Amyloid depositions impair the function of sympathetic nerve endings. Iodine-123 metaiodobenzylguanidine (^{123}I-MIBG) can detect innervation changes. Sixty one patients with biopsy proven amyloidosis underwent general work-up, echocardiography and ^{123}I-MIBG scintigraphy. Early (15 min) and late (4 hrs) heart-to-mediastinum ratio (HMR) and wash-out rate were determined. Mean late HMR of all patients was 2.3 ± 0.75, mean wash-out rate was 8.6 ± 14%,. Late HMR was lower (2.0 ± 0.70 versus 2.8 ± 0.58, $p<0.001$) and wash-out rates were higher (-3.3 ± 9.9% vs 17 ± 10%, $p<0.001$) in patients with echocardiographic parameters for amyloidosis. In ATTR patients without echocardiographic parameters of amyloidosis, HMR was lower than in other types (2.0 ± 0.59 vs 2.9 ± 0.50, $p=0.007$). So, MIBG and echocardiography are complementary. Also, ^{123}I-MIBG scintigraphy can detect cardiac denervation in ATTR patients before echocardiographic parameters are present.

INTRODUCTION

Cardiac involvement of amyloidosis eventually leads to a type of cardiomyopathy in which ventricular filling is restricted, resulting in symptoms and signs of heart failure. Amyloidosis is the most common cause of this co-called ‘restrictive cardiomyopathy’ (1). Transthoracic echocardiography plays an important role in the evaluation of cardiac manifestation of amyloidosis. Nowadays it is the modality of choice for the evaluation of amyloid deposition in the heart (2). However, with this technique, the diagnosis of cardiac amyloidosis is often established at a late time point. Disturbance of myocardial sympathetic innervation may play an important role in this remodelling process, and may even lead to sudden death due to fatal arrhythmia (2). Amyloid deposits impair the function of myocardial sympathetic nerve endings.

A scintigraphic imaging modality using iodine-123 labelled metaiodobenzylguanidine (^{123}I-MIBG) is a validated method to evaluate sympathetic innervation in the heart and has also been used in patients with amyloidosis (3-5). ^{123}I-MIBG, an analogue of norepinephrine (NE), enters the sympathetic nerve terminals through a specific

"uptake-1 mechanism". Unlike NE, ^{123}I-MIBG is stored in granules in the nerve terminals and not catabolised. So, ^{123}I-MIBG indirectly visualises the effect of amyloid deposition in the myocardium (6).

The purpose of this study was to evaluate if ^{123}I-MIBG scintigraphy is able to identify cardiac sympathetic denervation in patients with different types of early stage amyloidosis.

METHODS

A total of 61 consecutive patients (30 women, 31 men) with systemic amyloidosis underwent ^{123}I-MIBG scintigraphy between June 2007 and August 2011. Diagnosis of amyloidosis was based on detection of amyloid in a biopsy site typically involved in systemic amyloidosis, such as the abdominal fat tissue, kidney or nerve. History and physical examination were used to determine the presence of polyneuropathy. All patients underwent the usual tests including 12-lead electrocardiogram (ECG), dynamic electrocardiogram (Holter investigation), radionuclide multiple gated acquisition (MUGA) for left ventricular ejection fraction (LVEF), autonomic function testing using bedside manoeuvres, heart rate variability analysis, echocardiographic examination before the ^{123}I-MIBG scintigraphy. At 15 min (early image) and 4 h (late image) after administration of 185 MBq ^{123}I-MIBG, a 10-min static acquisition was performed in anterior view of the chest. Heart-to-mediastinum activity ratio (HMR) was measured three times, and the average of measurements was taken into account. Cardiac ^{123}I-MIBG wash-out rate was defined as percentage change in activity from the early to the late images within the LV ROI as follows: $((H_{early}-H_{late})/H_{early}) \times 100\%$.

For ^{123}I-MIBG imaging, 9 age-matched consecutive normal volunteers were scanned to form a healthy control database. All subjects were in good health and did not take medication, especially no tricyclic antidepressants or other sympathicomimetics that can interfere with ^{123}I-MIBG uptake.

RESULTS

The mean age of all patients was 62 ± 8.8 years. For the 9 healthy controls (6 women and 3 men), the age was not significantly different: 52 ± 17 years. Of all 61 patients, 39 were diagnosed with AL type amyloidosis, 11 with AA type, and 11 with ATTR type. Table 1 summarizes the results of the ^{123}I-MIBG scans in the different patient subgroups and the healthy control subjects. In all patients the late HMR was significantly lower (mean 2.3 ± 0.75 versus 2.9 ± 0.58, $p<0.005$) and the wash-out rate was significantly higher (mean 8.6 ± 14% vs. -2.1 ± 10%, $p<0.05$) than in healthy controls. The HMR was significantly lower in patients with ATTR type amyloidosis (1.7 ± 0.52) than in the other subgroups ((2.5 ± 0.75 in AL and 2.4 ± 0.75 in AA, $p< 0.05$). In ATTR patients the HMR was significantly lower than in healthy controls ($p< 0.001$).

The late HMR was significantly different between patients with (2.0 ± 0.70) and without (2.8 ± 0.58) echocardiographic parameters for amyloidosis, defined as sparkling and LV wall thickness > 11 mm, $p<0.001$. Also, the wash-out rate was significantly higher in these patients, -3.3 ± 9.9% versus 17 ± 10% $p<0.001$.

In ATTR patients without echocardiographic parameters of amyloidosis, HMR was lower than those patients with other types (2.0 ± 0.59 vs 2.9 ± 0.50, $p=0.007$). Furthermore, wash-out rates were higher in these patients: 11 ± 1.4% vs -4.6 ± 9.3%, $p=0.03$

Table 1. ^{123}I-MIBG findings

	Frequency, mean ± SD			
	Healthy controls	AL	AA	ATTR
Late HMR	2.9 ± 0.58	2.5 ± 0.75	2.4 ± 0.75	1.7 ± 0.52
Wash-out rate	-2.1 ± 10	7.0 ± 14	5.9 ± 14	18 ± 8.3
Wash-out rate > 20% (n)	0	7	2	6

DISCUSSION

The current study shows that the sympathetic denervation, determined by diminished late ^{123}I-MIBG uptake in HMR and elevated wash-out rate, is prominent in patients with echocardiographic parameters for amyloidosis. Furthermore, this study shows that HMR is lower and wash-out rates are higher in patients with amyloidosis compared to healthy control subjects. In ATTR patients cardiac denervation can be found even before echocardiographic parameters are present. So, ^{123}I-MIBG scintigraphy and echocardiography should be performed in a routinely matter.

The use of ^{123}I-MIBG is studied most intensively in patients with FAP. The ^{123}I-MIBG results in this study are generally less aberrant than those in prior studies (3-5, 7). Not only do the healthy controls have higher HMR than those in previous studies, our amyloidosis patients also show higher ^{123}I-MIBG uptake and less wash-out. The most important explanation of the large difference lies in the use of collimator type. The prior studies all used low-energy collimators (LE), whereas in this protocol a medium-energy collimator (ME) was used.

A point of interest is the role of ^{123}I-MIBG scintography in the predictive potential for sudden cardiac death in patients with heart failure and even the predictive value of appropriate implantable cardioverter-defibrillator (ICD) therapy.

REFERENCES

1. Dubrey SW, Cha K, Anderson J et al. The clinical features of immunoglobulin light-chain (AL) amyloidosis with heart involvement. QJM. 1998;91:141–157.
2. Falk RH, Plehn J, Deering T et al. Sensitivity and specificity of the echocardiographic features of cardiac amyloidosis. Am J Cardiol. 1987;59:418–422.
3. Nakata T, Shimamoto K, Yonekura S, et al. Cardiac sympathetic denervation in transthyretin-related familial amyloidotic polyneuropathy: detection with iodine-12-MIBG. J Nucl Med. 1995;36 :1040–2.
4. Tanaka M, Hongo M, Kinoshita O, et al. Iodine-123 metaiodobenzylguanidine scintigraphic assessment of myocardial sympathetic innervation in patients with familial amyloid polyneuropathy. J Am Coll Cardiol. 1997;29:168-74.
5. Delahaye N, Dinanian S, Slama MS, et al. Cardiac sympathetic denervation in familial amyloid polyneuropathy assessed by iodine- 123 metaiodobenzylguanidine scintigraphy and heart rate variability. Eur J Nucl Med. 1999;26:416-24.
6. Glaudemans AWJM, Slart RHJA, Zeebregts CJ, Veltman NC, Tio RA, Hazenberg BPC, Dierckx RAJO. Nuclear imaging in cardiac amyloidosis. Eur J Nucl Med Mol Imaging. 2009;36:702-714.
7. Delahaye N, Rouzet F, Sarda L, et al. Impact of liver transplantation on cardiac autonomic denervation in familial amyloid polyneuropathy. Medicine. 2006;85:229–38.

^{99m}Tc-3,3-Diphosphono-1,2-Propanodicarboxylic Acid (^{99m}Tc DPD) scintigraphy in 171 patients with suspected systemic amyloidosis

D.F. Hutt[1], J. Page[1], H.J. Lachmann[1], J.D. Gillmore[1], C.J. Whelan[1], S.D.J. Gibbs[1], J.H. Pinney[1], S. Banypersad[1], J. Dungu[1], C.P. Venner[1], D. Gopaul[1], A.M. Quigley[2], M.L. Hall[2], D. McCool[2], P.N. Hawkins[1], A.D. Wechalekar[1]

[1]*Centre for Amyloidosis and Acute Phase Proteins, University College London Medical School, UK*
[2]*Department of Nuclear Medicine, Royal Free Hospital, London, UK*

ABSTRACT

Cardiac involvement is a major clinical feature and determinant of outcome in AL and ATTR amyloidosis, for which better diagnostic methods are required. We report ^{99m}Tc-3,3-Diphosphono-1,2-Propanodicarboxylic Acid (^{99m}Tc DPD) scintigraphy in 171 patients with suspected cardiac amyloidosis. Patients received 700 MBq ^{99m}Tc DPD, and planar whole body images were acquired after 5 minutes and 3 hours, along with cardiac SPECT-CT. Myocardial uptake was scored as grade 0-3 based on the amount of cardiac uptake and proportionate reduction in bone signal. Cardiac uptake occurred in all 76 patients with ATTR amyloidosis who fulfilled consensus criteria for cardiac involvement, but in only 16 (55%) of those with AL ($p<0.0001$); myocardial uptake was also present in eight other ATTR patients who did not meet the consensus criteria. This study confirms the utility of ^{99m}Tc DPD scintigraphy in cardiac amyloid imaging, most specifically for amyloid of ATTR type.

INTRODUCTION

Diagnosis of cardiac amyloidosis has been defined by the international amyloidosis consensus criteria (1) and typically relies on echocardiography demonstrating increased wall thickness in the absence of another cause. Echocardiographic diagnosis of amyloidosis is characteristic in advanced disease but can be difficult in early stages and is unable to differentiate between the AL and TTR type (2).

Uptake of diphosphonate compounds by the heart in cardiac amyloidosis has been recognised anecdotally for over 30 years and has been confirmed by small studies using technetium-99m (^{99m}Tc) labelled phosphate derivatives including pyrophosphate (PYP), methylene diphosphonate (MDP) and hydroxy diphosphonate (HDP) (3-5). More recently, ^{99m}Tc labelled 3,3-diphosphono-1,2-propanodicarboxylic acid (DPD) has been reported to have a much greater and more reliable affinity for cardiac amyloid. In 2002 Puille et al (6) reported cardiac uptake of ^{99m}Tc-DPD in 8 patients with ATTR-FAP whilst more recently Rapezzi et al in 2011 (7) looked at 45 patients with TTR and 34 with AL related amyloid cardiomyopathy. Myocardial uptake was seen in all TTR patients but in only 11 (32%) of the AL patients. The aim of this study was to further evaluate the role of ^{99m}Tc-DPD scintigraphy in imaging TTR vs AL cardiac amyloidosis as well as other amyloid types.

METHODS

700 MBq of ^{99m}Tc-DPD was given to 171 patients with suspected cardiac amyloid involvement between June 2010 and December 2011. Whole body (WB) sweeps were performed at 5 minutes and 3 hours post injection followed by either a gated or non-gated single photon emission computed tomography (SPECT)-CT of the heart. The delayed 3 hour WB sweep images were scored as grade as 0-3 using a modified version of the grading system as described by Perugini et al (8) whereby grade 0 indicated no cardiac tracer uptake on planar or SPECT-CT, grade 1 was mild cardiac uptake (less intense than bone), grade 2 was moderate cardiac uptake (with some bone attenuation) and grade 3 was strong cardiac uptake (with little or no bone signal). Figure 1 illustrates the grading system used. Planar (heart/whole body ratio) and SPECT-CT (total heart counts /average sternum counts per voxel) quantitation was also performed. Final diagnosis of amyloidosis was supported where possible by biopsy histology, proteomics, SAP scintigraphy, cardiac MRI, and DNA analysis.

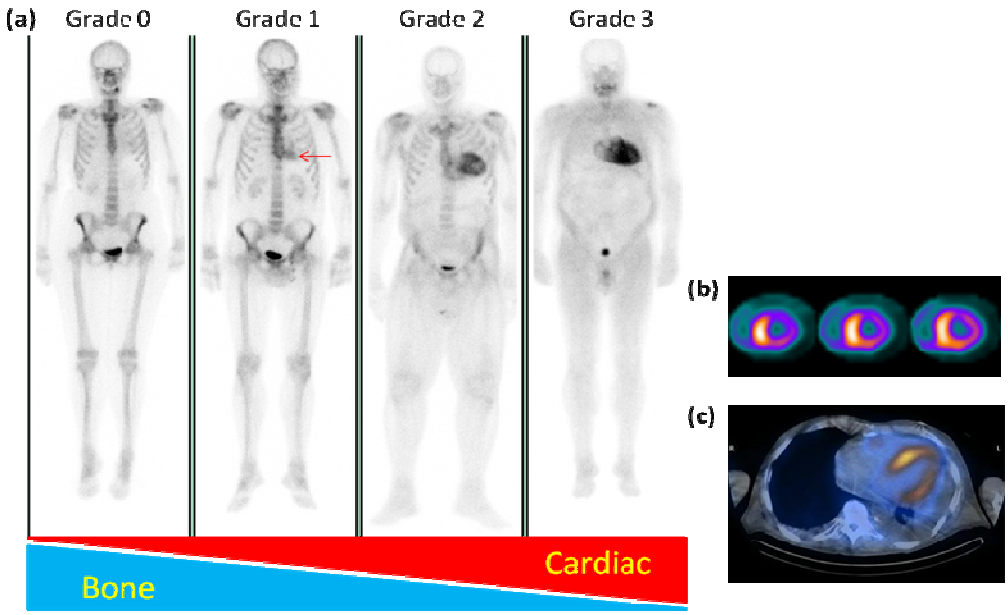

Figure 1. Demonstrating **(a)** grading system for cardiac tracer uptake on delayed whole body scans, **(b)** short axis view showing distribution of ^{99m}Tc-DPD within the myocardium and a **(c)** fused SPECT-CT image of the thorax confirming localisation of the tracer to the heart.

RESULTS

One hundred and seventy one patients were included in this study. The amyloid types were: TTR – 90 (53%), AL - 34 (20%), Apolipoprotein A1 - 4 (2%), AA – 3 (2%), Fibrinogen Aα-chain (Glu526Val) - 2 (1%), Lysozyme (Asp67His) - 1 (0.5%) and Gelsolin (Asp214Asn) – 1 (0.5%). Amyloid type could not be confirmed in 5 (3%) cases and 31 (18%) patients were subsequently found not to have systemic amyloidosis. Of the 90 patients with TTR amyloidosis, 38 (42%) patients had senile TTR amyloidosis and 52 (58%) had familial TTR amyloid.

ATTR mutations were as follows: Val122Ile (n=16), Thr60Ala (n=11), Val30Met (n=10), Gly47Val (n=4),

Glu54Gly (n=3), Ser77Tyr (n=2), Gly47Arg (n=1), Glu89Lys (n=1), Ile84Ser (n=1), Ile107Phe (n=1), Phe33Val (n=1) and Ser77Phe (n=1). Of the 4 Apolipoprotein A1 patients, mutations in Leu60Arg and Arg173Pro were present in 2 patients respectively.

Table 1 summarises the main ^{99m}Tc-DPD scintigraphic findings. Of those TTR (ATTR plus STTR) patients with a positive scan, 88% were grade 2 or above whilst 94% of positive AL patients were only grade 1. All patients (n=76) with TTR related cardiac involvement by consensus criteria had cardiac uptake of ^{99m}Tc-DPD compared to only 16/29 (55%) of AL patients ($p<0.0001$). Eight patients (one wild-type) with no cardiac involvement by current consensus criteria had cardiac uptake of ^{99m}Tc-DPD. One patient with cardiac AA and 3 with cardiac apolipoprotein AI amyloidosis had myocardial DPD uptake. Amyloidosis was ultimately excluded in 31 patients, all of whom had normal ^{99m}Tc-DPD scans. Abnormal ^{99m}Tc-DPD uptake into the liver and spleen each occurred in only 4% of cases, in contrast to the high frequency of visceral amyloidosis demonstrated on SAP scintigraphy. Using SPECT-CT imaging confirmed cardiac uptake that was not evident on planar scans in 6 patients.

Myocardial DPD uptake according to grade 1/2/3 was associated with median LV wall thickness of 14/16.5/17 mm, LV ejection fraction of 56/49.5/46%, and NT pro-BNP of 295/295/354 pMol/L respectively. Differentiation between AL and TTR types using SPECT-CT was better than the planar method mainly due to the fact that regions of interest drawn over the heart on whole body images will include counts from overlying structures such as the sternum, ribs and spine.

Table 1.

Amyloid type	***n* (%)**	**Grade of cardiac uptake (n)**				**Cardiac uptake / in pts with cardiac involvement ***	**Cardiac uptake / in pts without cardiac involvement ***
		0	**1**	**2**	**3**		
TTR (FAP + Wild Type)	90 (53)	6	10	59	15	76 / 76 (100%)	8 / 14 (57%)
AL	34 (20)	18	15	1	0	16 / 29 (55%)	0 / 5
Apolipoprotein AI	4 (2)	1	3	0	0	3 / 3 (100%)	0 / 1
AA	3 (2)	2	1	0	0	1 / 1 (100%)	0 / 2
Others (AFib, ALys, AGel)	4 (2)	0	0	0	0	0 / 0	0 / 4
Unknown	5 (3)	2	1	2	0	3 / 4 (75%)	0 / 1
No Amyloid	31 (18)	31	0	0	0	0 / 0	0 / 31

* As defined by International Consensus Criteria (Gertz et al 2005, Am. J. Hematol. 79: 319-328)

DISCUSSION

In our experience, ^{99m}Tc-DPD scintigraphy has 100% sensitivity for TTR cardiac amyloidosis of both senile and hereditary types compared to just 55% for AL cardiac amyloid thus confirming the utility of this imaging method.

The intensity of tracer uptake in the heart and soft tissue pattern can both support the diagnosis of TTR versus AL cardiac amyloidosis. Imaging using SPECT-CT not only allows for more accurate quantitation by eliminating counts from overlying bony structures but also demonstrated cardiac tracer uptake in 6 patients which was not evident on the planar scan. Myocardial uptake of ^{99m}Tc-DPD was also seen in one patient with cardiac AA and three with apolipoprotein AI amyloidosis which is a novel finding.

It would appear that ^{99m}Tc-DPD scintigraphy is the most sensitive method for detecting TTR cardiac amyloid and therefore we see its future role as a screening tool for both senile cardiac amyloidosis in the elderly and for asymptomatic carriers of TTR mutations.

ACKNOWLEDGEMENTS

We would like to thank the patients and their families, staff at the National Amyloidosis Centre (UK) and IBA Molecular UK Ltd who generously provided the TECEOS kits free of charge.

REFERENCES

1. Gertz, M. A., R. Comenzo, et al. (2005). "Definition of organ involvement and treatment response in immunoglobulin light chain amyloidosis (AL): A consensus opinion from the 10th International Symposium on Amyloid and Amyloidosis." Am. J. Hematol. 79: 319-328.
2. Selvanayagam, J. B., P. N. Hawkins, et al. (2007). "Evaluation and management of the cardiac amyloidosis." J. Am. Coll. Cardiol. 50: 2101-2110.
3. Falk, R. H., V. W. Lee, et al. (1983). "Sensitivity of technetium-99m-pyrophosphate scintigraphy in diagnosing cardiac amyloidosis." Am. J. Cardiol. 51(5): 826-830.
4. Lee, V. W., A. G. Caldarone, et al. (1983). "Amyloidosis of heart and liver: comparison of Tc-99m pyrophosphate and Tc-99m methylene diphosphonate for detection." Radiology 148(1): 239-242.
5. Kulhanek, J. and A. Movahed (2003). "Uptake of technetium 99m HDP in cardiac amyloidosis." Int.J. Cardiovasc. Imaging 19(3): 225-227.
6. Puille, M., K. Altland, et al. (2002). "99mTc-DPD scintigraphy in transthyretin-related familial amyloidotic polyneuropathy." Eur. J. Nucl. Med. Mol. Imaging 29(3): 376-379.
7. Rapezzi, C., C. C. Quarta, et al. (2011). "Usefulness and limitations of 99mTc-3,3-diphosphono-1,2-propanodicarboxylic acid scintigraphy in the aetiological diagnosis of amyloidotic cardiomyopathy." Eur. J. Nucl. Med. Mol. Imaging 38(3): 470-478.
8. Perugini, E., P. L. Guidalotti, et al. (2005). "Noninvasive etiologic diagnosis of cardiac amyloidosis using 99mTc-3,3-diphosphono-1,2-propanodicarboxylic acid scintigraphy." J. Am. Coll. Cardiol. 46(6): 1076-1084.

The non-invasive quantification of myocardial infiltration in AL Amyloidosis – an Equilibrium Contrast Cardiovascular Magnetic Resonance Study

S.M. Banypersad,[1,2] D.M. Sado,[1] A.S. Flett,[1] S.D.J. Gibbs,[2] J.H. Pinney,[2] M. Fontana,[1,2] V. Maestrini,[1] C.P. Venner,[2] J. Dungu,[2] L. Rannigan,[2] D. Foard,[2] T. Lane,[2] C.J. Whelan,[2] P.N. Hawkins,[2] J.C.C. Moon[1]

1. *The Heart Hospital, 16-18 Westmoreland Street, London, W1G 8PH.*
2. *The National Amyloidosis Centre, Royal Free Hospital, Pond Street, London, NW3 2QG*

ABSTRACT

Cardiac involvement predicts outcome in systemic AL amyloidosis and influences therapeutic options. Current methods of cardiac assessment do not quantify myocardial amyloid burden. We used Equilibrium Contrast Cardiovascular Magnetic Resonance (EQ-CMR) to quantify the cardiac interstitial compartment, measured as Extracellular Contrast Volume (ECV), hypothesising it would reflect amyloid burden.

Sixty patients with systemic AL amyloidosis (65% male, median age 65 years) underwent conventional clinical CMR including late enhancement, EQ-CMR, and clinical cardiac evaluation including ECG, echocardiography, assays of NT-proBNP and Troponin T, and functional assessment comprising the 6 minute walk test (6MWT) in ambulant individuals. Cardiac involvement in the amyloidosis patients was categorised as definite, probable or none suspected by conventional criteria. Findings were compared to 82 healthy controls.

ECV was significantly greater in patients than healthy controls (0.25 vs 0.40, $P < 0.001$), and correlated with conventional criteria for characterizing the presence of cardiac involvement, the categories of none, probable, definite corresponding to ECV of 0.276 vs 0.342 vs 0.488 respectively ($P<0.005$), ECV correlated with cardiac parameters by echocardiography (e.g. TDI S-wave R^2 0.27, $P<0.001$) and conventional CMR (e.g. indexed LV mass R^2 0.31, $P<0.001$). There was also significant correlations with NT-proBNP (R^2 0.47, $P<0.001$) and Troponin T (R^2 0.28, $P=0.006$). ECV was associated with smaller QRS voltages (R^2 0.33, $P<0.001$), and correlated with poorer performance in the 6MWT (R^2 0.13, $P=0.03$).

Myocardial ECV measurement appears to be the first non-invasive test to quantify cardiac amyloid burden.

INTRODUCTION

Cardiac involvement is frequent, a principal driver of prognosis, and can be the presenting feature of the disease [1]. Whilst a constellation of ECG, echocardiographic and biomarker findings becomes increasingly diagnostic and prognostic as cardiac amyloidosis progresses, evaluation of early stage cardiac involvement can be challenging. Confounding features are often present, commonly including left ventricular hypertrophy (LVH) and abnormal diastolic function associated with renal failure, diabetes or hypertension [2,3]. Definitive diagnosis

of cardiac amyloidosis, which has critical implications for choice of chemotherapy and management generally, requires cardiac biopsy which is invasive and prone to sampling error. There are currently no non-invasive tests that can quantify cardiac amyloid deposits. New imaging modalities such as DPD and CMR scans are showing promise but neither is quantitative. We have lately developed a new quantitative technique, Equilibrium Contrast Cardiovascular Magnetic Resonance (EQ-CMR) that measures the myocardial extracellular volume fraction i.e. the interstitial space within the heart. Here, we hypothesise that the technique would also be an effective method for quantifying cardiac amyloid burden, the proteotypic interstitial protein deposition disorder [4].

METHODS

EQ-CMR involves three steps: 1) a standard gadolinium bolus followed by constant infusion to eliminate contrast kinetic effects and achieve an equilibrium contrast state throughout the body; 2) signal intensity (T1) measurement pre and post contrast equilibrium using CMR; and 3) a direct measure of blood volume of contrast distribution, by taking a complete blood count, equating the blood volume of contrast distribution to one minus the hematocrit. The volume of distribution in the myocardium, also known as the extracellular volume, ECV, is then calculated as: ECV = (1-Hematocrit) x ($\Delta R1_{myocardium}$ / $\Delta R1_{blood}$) where $\Delta R1$ is ($1/T_1$ pre contrast - $1/T_1$ post contrast). EQ-CMR was performed on a 1.5T magnet (Avanto, Siemens, 16 channel coils) with T1 assessment as previously described [5].

Sixty consecutive consenting patients with systemic (primary) AL amyloidosis who were assessed between 2010-11 at the National Amyloidosis Centre (Royal Free Hospital, London UK) and in whom there no exclusions to CMR (GFR<30mls/minute; presence of non MR compatible devices, known atrial fibrillation) were recruited. Four patients who were found to have atrial fibrillation/flutter after they had consented were not excluded. The probability of cardiac involvement was categorised into definite or no cardiac involvement based on international consensus criteria published by Gertz et al [6]. An additional category of possible involvement was created for patients with cardiac abnormalities in whom there were confounding features.

Healthy subjects (n=82) were recruited through advertising in hospital, University and general practitioner surgeries. All had no history or symptoms of cardiovascular disease or diabetes, a normal 12-lead ECG and normal clinical CMR scan. All patients and healthy controls underwent 12 lead ECG. Patients additionally underwent assays of cardiac biomarkers (NT-proBNP and Troponin T), echocardiography, SAP scintigraphy including measurement of total body amyloid load, and a 6-minute walk test, although this was not possible in some patients(n=23, 38%) mainly due to other comorbid factors (e.g. arthritis, postural hypotension, peripheral neuropathy) and patient choice. NYHA class and ECOG status were also assessed using a standard questionnaire.

RESULTS

The mean ECV in patients with systemic amyloidosis was significantly elevated compared to healthy controls 0.400 (range 0.200-0.609) vs 0.254 (range 0.161-0.323), P<0.001. Mean ECV increased between groups from healthy controls to AL with no suspected cardiac involvement (ECV 0.276 (range 0.200-0.345), P<0.005), possible cardiac involvement (0.342 (range 0.239-0.479), P<0.005) and definite cardiac involvement (0.488 (range 0.423-0.609), P<0.005). There was no increase in ECV with age in the healthy controls. Other results are summarized in table 1.

Table 1. ECV correlations with cardiac structure and function, biomarkers and ECG changes

ECV compared against:	R^2	P-value
LV Structure		
LV mass	0.27	P<0.001
Indexed LV mass	0.31	P<0.001
Septal thickness	0.31	P<0.001
LA area	0.16	P=0.002
Indexed LA area	0.24	P<0.001
LV systolic Function		
Ejection Fraction	0.34	P<0.001
MAPSE	0.34	P<0.001
LV end-systolic volume	0.27	P<0.001
Indexed LV end-systolic volume	0.31	P<0.001
TDI-S wave	0.27	P<0.001
LV Diastolic Function		
E:E'	0.22	P<0.001
IVRT	0.13	P=0.03
E-Deceleration time	0.23	P<0.001
RV Structure & Function		
RV end-systolic thickness	0.16	P=0.005
TAPSE	0.25	P<0.001
Functional Assessment		
6-minute walk test	0.13	P=0.03
Biomarkers		
Serum NT-pro BNP (logBNP)	0.47	P<0.001
Troponin T	0.28	P=0.006
ECG		
ECG Limb Lead mean voltage	0.33	P<0.001
ECG chest lead mean voltage	0.09	P=0.02

DISCUSSION

Amyloidosis is the exemplar of an interstitial disease, the quantity of amyloid in the extracellular space amounting to kilograms in some patients. Cardiac involvement is a major cause of morbidity and mortality, particularly in AL type, but there are currently no non-invasive methods to quantify it. Here, the extracellular volume (ECV) was measured using EQ-CMR in systemic AL amyloidosis. ECV was massively elevated in the patients with definite cardiac involvement but also significantly higher in patients where conventional clinical testing suggested no cardiac involvement, and was significantly elevated in a quarter of patients with no LGE. ECV tracked a wide variety of markers of disease activity such as cardiac function and blood biomarkers, linked to patient's functional performance, and strongly correlated with limb lead ECG complex sizes. These data suggest that ECV measurement is picking up infiltration earlier than conventional testing and is a direct measure of the amyloid burden with potential utility in early diagnosis, disease monitoring, and, potentially, as a much needed cardiac surrogate endpoint for the various promising new therapies for amyloidosis currently in preclinical development and early phase clinical trials.

REFERENCES

1. Kyle RA, Gertz MA. Primary systemic amyloidosis: clinical and laboratory features in 474 cases. Semin Hematol. 1995;32(1):45-59.

2. Jacobson DR, Pastore RD, Yaghoubian R, Kane I, Gallo G, Buck FS, Buxbaum JM. Variant-sequence transthyretin (isoleucine 122) in late-onset cardiac amyloidosis in black Americans. N Engl J Med. 1997;336(7):466-73
3. Falk RH, Dubrey SW. Amyloid Heart Disease, Progress in Cardiovascular Diseases 2010 (52); 347, 361
4. White SK, Sado DM, Flett AS, Moon JC. Characterising the myocardial interstitial space: the clinical relevance of non-invasive imaging. Heart. 2012;98(10):773-9.
5. Flett AS, Hayward MP, Ashworth MT, Hansen MS, Taylor AM, Elliott PM, McGregor C, Moon JC. Equilibrium contrast cardiovascular magnetic resonance for the measurement of diffuse myocardial fibrosis: preliminary validation in humans. Circulation. 2010;122(2):138-44.
6. Gertz MA, Comenzo R, Falk RH, Fermand JP, Hazenberg BP, Hawkins PN, Merlini G, Moreau P, Ronco P, Sanchorawala V, Sezer O, Solomon A, Grateau G. Definition of organ involvement and treatment response in immunoglobulin light chain amyloidosis (AL): a consensus opinion from the 10th International Symposium on Amyloid and Amyloidosis, Tours, France, 18-22 April 2004. Am J Hematol. 2005;79(4):319-28.

Radioimmunoimaging of Patients with AL Amyloidosis

K.J. Wells,[1,2,3] J. Wall,[1,2] S. Kennel,[1,2] A. Solomon[1]

[1]Human Immunology and Cancer Program, Department of Medicine, University of Tennessee Graduate School of Medicine, Knoxville, TN, USA; [2]Molecular Imaging and Translational Research Program, University of Tennessee Graduate School of Medicine, Knoxville TN, USA; [3]Department of Radiology, University of Tennessee Graduate School of Medicine, Knoxville, TN, USA.

Heretofore, there has been no radiographic means in the USA to visualize AL amyloid deposits. In this regard, we have reported that our amyloidolytic fibril-specific mAb, 11-1F4, when labeled with I-124, could image by PET/CT hepatic, splenic, nodal, or bone marrow deposits in 11 of 18 subjects (1).

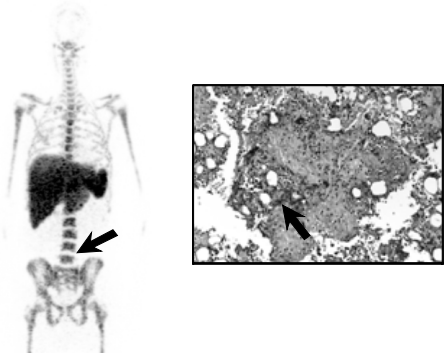

Figure 1. Left: MIP (maximum intensity projection) showing liver, spleen, and bone marrow (arrow) uptake of ^{124}I-11-1F4; Right: immunohistochemical analysis of amyloid-containing bone marrow from same patient using 11-1F4 as the primary reagent (ABC technique, original magnification, ×200)

METHODS

On the basis of these results, an additional 19 individuals, all of whom were tested and found to be HAMA negative, were placed on study (HAMA also was performed 30 and 60 days post imaging). Patients were pre-medicated with a saturated solution of potassium chloride (SSKI) 48 hrs prior to administration of the radiopharmaceutical and then, for another 8 days. Whole body PET/CT imaging was obtained 2 and 5 days post

^{124}I-11-1F4 infusion of 1 mg mAb 11-1F4 labeled with 2 mCi (74 MBq) ^{124}I using a Siemens mCT scanner (5 min per bed position) with low dose CT for attenuation correction. To increase the sensitivity of true count detection, the time of PET acquisition in the last 15 individuals was extended by 35 min for the kidneys and, additionally, a dedicated 35 min cardiac-gated acquisition was obtained. Organ–specific uptake was defined as that greater than mediastinal blood pool on day 5 and results were correlated with clinical evidence of organ involvement, as well as with Congo-red staining and immunohistochemical studies using mAb 11-1F4 of available biopsy materials (Figure 1) or fat aspirates.

Table 1. Results of Radioimmunoimaging using ^{124}I-mAb 11-1F4/PET/CT and Immunohistochemistry (IHC) with 11-1F4 as the Primary Reagent in Patients with AL Amyloidosis

Light Chain Isotype	Organ Affected*	PET/ CT*	IHC*	Light Chain Isotype	Organ Affected*	PET/ CT*	IHC*
κ	K	0	NT	λ	H,L,S	S,LN,ST	+ (Lu)
λ	LN	LN	+ (Lu)	λ	I	0	0 (I)
λ	K	0	+ (BM)	λ	H,L,S	0	+ (BM)
λ	Lu	0	+ (Lu)	κ	I,L,S,H	L,S,I,BM,A	+ (I)
λ	K	0	0 (K)	λ	H,L,K,BM,I	L,S,BM,A	+ (BM)
λ	F	0	NT	λ	H,K	S	NT
κ	H	I	+ (F)	λ	T,H,I	0	+ (T)
λ	K	0	+ (K)	λ	L,K,H	S	0 (K)
κ	H,I,L,S	L,S	NT	λ	K,H	H	0 (K)
λ	T,L,S	0	0 (T)	λ	K,H,S	H,S	0 (K)
λ	L,K,BM	L,S,BM	+ (BM)	λ	K,H,S	0	NT
κ	H,L,S	L,S	+ (GB)	κ	SC,PV,S	ST	+ (ST)
λ	K	L,S	0 (K)	λ	LN	0	+ (LN)
λ	K,L,LN	L,S,BM	0 (K)	κ	H,T,SC,I	K	0 (BM)
λ	H,K,L,S	S	+ (K)	λ	H,I,L	L,S,LN	+ (I)
λ	I	0	0 (I)	λ	H,K	K,S	+ (L,S)
λ	K	S,BM	+ (BM)	λ	H,S	S,I	0 (H)
λ	H,BM	I	+ (BM)	λ	H,K	0	NT
λ	K	0	0 (K)				

*NT, no tissue; BM, bone marrow; F, fat; GB, gall bladder; heart; I, intestine; K, kidney; L, liver; Lu, lung; LN, lymph node; PV, perivascular; S, spleen; SC, subcutaneous; ST, soft tissue; T, tongue

RESULTS

Of the 37 patients who have taken part in the study, organ- or tissue-specific uptake occurred in 22 (60%). In these cases, the spleen was visualized in 16 instances, the liver in 8, bone marrow in 5, lymph node in 3,

adrenals in 2, soft tissue in 2, intestine in 4, kidneys in 2, and heart in 2 (multiple positive sites were present in 13 subjects). A summary of the radioimmunoimaging results, light chain isotype, sites of organ involvement (as determined clinically), and immunohistochemical results are provided in Table 1. As shown, 14 subjects demonstrated radiotracer uptake in the same clinically-involved organ or tissue. Further, of the 16 patients with splenic uptake, none had evidence of hypersplenism (thrombocytopenia) and only 3 had splenomegaly in the absence of right heart failure, thus suggesting detection of subclinical amyloid involvement of the spleen. No liver uptake was seen in 8 of these 16.

Imaging results also were compared to immunohistochemical studies of Congo-red positive, amyloid-containing tissue biopsies or fat aspirates (when available) using the 11-1F4 mAb (Table 1). In 13 subjects, there was correlation between positive visualization and immunohistochemistry (in 6 instances, in the same organ [e.g., intestine, soft tissue, bone marrow, and spleen]). One patient, who had focal splenic uptake more intense than that seen in the liver, died 6 mo post-imaging. In this case, post-mortem quantification of congophilic material present in the spleen and liver revealed the former to contain 8.9% amyloid compared to 7.0% in hepatic tissue, findings that correlated proportionally with the degree of radiotracer uptake seen in these organs in the imaging studies.

Amyloid-containing kidney biopsy specimens were available for immunohistochemical analyses in 9 of the 18 patients with renal amyloid deposits (as demonstrated by biopsy or clinically by the presence of significant proteinuria). These studies revealed that in only 2 instances did 11-1F4 react with the pathologic material present in the biopsy tissue. Interestingly, in 5 of the remaining 7 that were negative using this methodology, organs other than kidney (i.e., liver, spleen, bone marrow, heart) were visualized by ^{124}I-11-1F4 PET/CT. We posit that the lack of the antibody's reactivity in the kidney resulted from proteolysis or inaccessibility of the antibody's N-terminal epitope or, possibly, that its concentration was too low for immunodetection.

Fifteen subjects, 12 of whom had clinical evidence of cardiac involvement, had 35 min cardiac-gated acquisitions. Visualization of the myocardium by PET/CT was demonstrated in 2 cases and in 1 of these, positive uptake of the antibody corresponded to areas of abnormal late gadolinium enhancement seen in the left vertricular wall on cardiac MRI.

Using the earlier described protocol, 3 individuals underwent repeat ^{124}I-11-1F4 PET/CT imaging after an interval of at least 12 mo. Semi-quantitative analyses using Siemen's software were performed whereby liver and spleen contours were defined and organ volume, as well as mean radiotracer activity in the organ of interest, calculated, thus leading to determination of total amyloid burden. One patient exhibited, respectively, 20% and 58% increases in splenic and hepatic amyloid loads (13 mo post initial study with treatment limited to only 2 mo during this time due to drug intolerance), a finding that correlated with clinical evidence of disease progression. In the second subject, 50% decreases in both hepatic and splenic amyloid loads were seen (26 mo post initial study), during which time the patient had excellent clinical response to bortezomib therapy with normalization of the free light-chain ratio and improvement in severity of congestive heart failure symptoms. As for the third individual, who (after the initial study) had undergone cardiac transplant with high dose melphalan therapy, followed by stem cell transplant resulting in a sustained and complete 13 mo serologic and bone marrow response, an 80% reduction in hepatic and splenic amyloid was seen on repeat imaging (33 mo post initial study). Interesting, in the follow-up study, there additionally was radiotracer uptake in the testes and kidneys. We posit that during the first imaging, the majority of ^{124}I-11-1F4 bound to the significant amount of amyloid present in the liver.

CONCLUSION

Our trial suggests that AL deposits, which are not yet evident clinically, may be identified using this sensitive technology. Further, amyloid burden may be assessed via visual and semi-quantitative methods and this information used to indicate therapeutic response. Most importantly, because this antibody can effect amyloidoysis, positive imaging results could be utilized to identify AL patients as candidates for passive immunotherapy using the chimeric version of 11-1F4, now under production for a Phase 1 clinical trial.

REFERENCES

1. Wall JS, Kennel SJ, Stuckey AC, Long MJ, Townsend DW, Smith GT, Wells KJ, Fu Y, Stabin MG, Weiss DT, Solomon A. Radioimmunodetection of amyloid deposits in patients with AL amyloidosis. Blood. 2010; 116 (13) : 2241-2244.

The amyloidophilic peptide p5 binds rapidly and stably to visceral amyloid *in vivo*: A potential radiotracer for PET/CT imaging

Emily B. Martin[1], Stephen J. Kennel[1,2], Tina Richey[1], Alan Stuckey[2], Dustin Osborne[2], and Jonathan S. Wall[1,2]

Departments of [1]Medicine or [2]Radiology, University of Tennessee Graduate School of Medicine, Knoxville, TN

ABSTRACT

Amyloid deposition in visceral organs contributes to the progression of clinical manifestations in a variety of diseases. We have developed a probe, designated p5, for non-invasive molecular imaging to monitor the organ distribution and extent of amyloid deposits. The purpose of this study was to determine the pharmacokinetics of radioiodinated-p5 in a murine model of AA amyloidosis. Dynamic PET/CT imaging with time activity data and static SPECT/CT scans were used to show the distribution, clearance and stability of p5 in diseased and healthy animals. Image analysis suggested that radioiodinated-p5 localized rapidly with amyloid-laden tissue and could be imaged for up to 72 hours. In healthy individuals, where the peptide did not encounter amyloid, the radiotracer was taken up in the kidney within 7 minutes of injection and was dehalogenated, freeing radioactive iodide to the circulation. The specific binding of amyloid and the accelerated loss of radioiodide from unbound peptide contribute to make p5 an excellent imaging agent for amyloidosis.

INTRODUCTION

Early detection of amyloid deposits can assist with prognostication and add value to the determination of each individual's course of treatment. Other than Congo red staining of biopsy-derived tissues, there is no method in the US to determine the distribution of amyloid *in vivo*. Since biopsies sample only localized areas, the extent of whole body amyloid burden generally remains undetermined. Molecular imaging has the potential to determine whole body distribution non-invasively.

To this end, we have developed a polybasic, synthetic peptide, designated p5 that specifically binds amyloid deposits *in vitro* and *in vivo* (1). We radiolabeled p5 with ^{124}I or ^{125}I and used the products in PET/CT or SPECT/CT studies. The gold standard for imaging amyloid deposition is planar scintigraphic imaging of ^{123}I-SAP (2). This method accurately visualizes the distribution of amyloid in many, but not all, visceral organs; however, it is not available to patients in the US. Herein, we use dynamic PET/CT scans to describe the uptake, distribution and dehalogenation of radioiodinated-p5 in a murine model of systemic AA amyloidosis and in healthy (WT) mice. The data suggest that p5 could be a valuable tool for imaging amyloidosis and monitoring response to therapy in patients.

METHODS

Animals: Three female H2-L^{d}-huIL-6 Tg BALB/c mice (AA) and 3 healthy (WT) female BALB/c mice were used for dynamic PET imaging, and 3 AA and 3 WT mice were also used at each time point in the extended SPECT study. AA was induced by iv injection of amyloid enhancement factor (100 µg) at 6 wk of age, and mice were imaged at 6-8 weeks post induction (3). This protocol was approved by the University of Tennessee Institutional Animal Care and Use Committee.

Procedure: The p5 peptide was radiolabeled with ^{124}I or ^{125}I and purified as previously described (1). Doses were formulated such that each mouse received a total volume of 200 µL (5 – 10 µg peptide; 200 µCi) iv in the tail vein. Dynamic PET imaging was performed using mice under isoflurane anesthesia, injected with ^{124}I-p5 iv 5 sec after the start of image acquisition to ensure that the initial uptake time points were captured. SPECT/CT scans on mice injected with ^{125}I p5 were acquired post mortem at various time points (2 h, 4 h, 8 h, 24 h, 48 h and 72 h) post injection. After acquiring images, organs were harvested for biodistribution measurements.

Analysis: Image analysis was performed on the 2D Inveon Research Workplace software (Siemens). Regions of interest (ROI) encompassing multiple slices of the CT image were drawn over the vena cava, heart, liver, spleen, kidneys, stomach and thyroid each mouse . Time activity curves were generated for each organ to show the uptake and clearance of ^{124}I-p5.

RESULTS

The dynamic behavior of ^{124}I-p5 was depicted via image analysis of PET/CT data acquired over a 2 h period. The time activity curves indicated that the radioiodinated peptide was quickly lost from the blood pool in both diseased and healthy mice. In diseased mice, ^{124}I-p5 bound rapidly to amyloid-laden organs, namely the liver and the spleen. In WT mice, the peptide was taken up by the kidneys (peak time ~ 7 min) and rapidly dehalogenated. The liberated radioiodide entered the blood stream and was sequestered by the thyroid and stomach (Fig. 1). Note that the blood pool is cleared rapidly for both diseased and healthy mice. It is also evident that the peptide accumulated in the amyloid-laden liver tissue and not in healthy liver tissue. Dehalogenation of the peptide in the WT animals was indicated by the rapid loss of activity from the kidney after ~7 min. The lack of renal uptake in the AA mice suggests that the peptide has been sequestered in organs afflicted with amyloid prior to its dehalogenation.

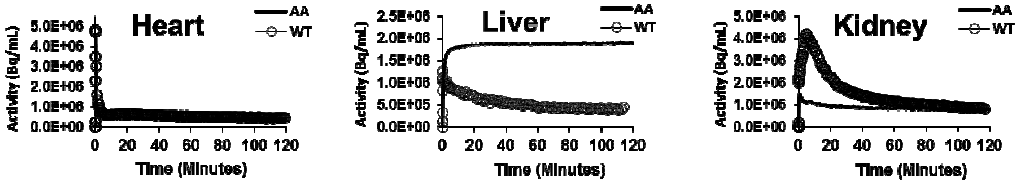

Figure 1. Time activity curves for both AA and WT mice. These representative curves demonstrate the blood pool clearance (heart), accumulation (liver) and dehalogenation (kidney) of ^{124}I-p5 *in vivo*.

Summed frames of the dynamic PET/CT scans through 120 min show the liberated radioiodide in only the stomach (St) and the thyroid (T) of WT mice (Figs. 2A and 2B). In contrast, the ^{124}I-p5 in AA mice was observed

mainly in the liver (L) and spleen (Sp). SPECT/CT imaging and biodistribution was used to determine longer term pharmacokinetics. The ^{125}I-p5 remained bound to amyloid deposits *in vivo* for up to 72 h post-injection (Fig. 2C). Micro-autoradiographs were acquired to ensure that ^{125}I-p5 was localized to amyloid deposits, and the presence of peptide correlated with Congophilic regions within the tissue samples (data not shown). These data indicate that the radioiodinated p5 remained stably bound to amyloid deposits which is an advantageous property for an imaging agent.

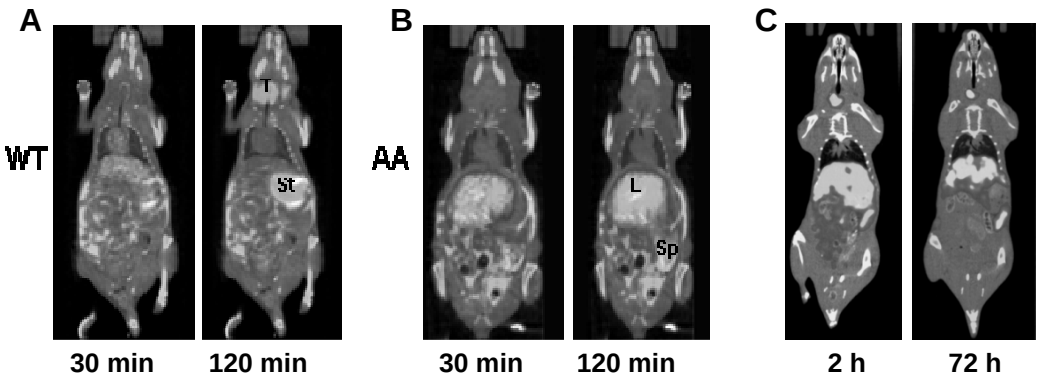

Figure 2. Representative images of p5 distribution in mice. (A & B) PET/CT images of ^{124}I-p5 at 30 and 120 min in AA and WT mice, respectively. (C) Static SPECT/CT images of ^{125}I-p5 indicate that there is preferential binding of ^{125}I-p5 to amyloid-laden liver and spleen at more than 72 h post injection.

DISCUSSION

In vivo dynamic molecular imaging studies indicate that p5 binds rapidly and stably to amyloid deposits. Kinetic analyses revealed that the peak renal uptake time of ^{124}I-p5 in WT mice was 7 min, where it was dehalogenated quickly. In contrast, the peptide bound to amyloid deposits in diseased mice was not significantly dehalogenated and was detectable for up to 72 h. The long target resident time is an advantage for the peptide as an imaging agent because it allows for clearance of free radiotracer from the blood pool before a scan is acquired. With less background activity, the presence of amyloid deposition can be detected more easily, and the level of certainty to the distribution of the radiotracer will be enhanced. These studies add value to peptide p5 as an imaging agent for the non-invasive detection of amyloidosis *in vivo*.

REFERENCES

1. Wall JS, Richey T, Stuckey A, Donnell R, Macy S, Martin EB, et al. In vivo molecular imaging of peripheral amyloidosis using heparin-binding peptides. *Proceedings of the National Academy of Sciences of the United States of America*. 2011;**108**(34):E586-94.
2. Hawkins PN, Pepys MB. Imaging amyloidosis with radiolabelled SAP. *European journal of nuclear medicine*. 1995;**22**(7):595-9.

3. Wall JS, Kennel SJ, Paulus MJ, Gleason S, Gregor J, Baba J, et al. Quantitative high-resolution microradiographic imaging of amyloid deposits in a novel murine model of AA amyloidosis. *Amyloid : the international journal of experimental and clinical investigation : the official journal of the International Society of Amyloidosis*. 2005;**12**(3):149-56.

SECTION V

AL AMYLOIDOSIS


Tuesday
Spectral Imaging
Bringing the Details to Light
Baseline Profile of Patients Undergoing Tafamidis Treatment in THAOS – the Transthyretin Amyloidosis Outcomes Survey
Exploratory case-control study of progression of AA Amyloidosis in rheumatic disease
AA Amyloid
Control

STATE OF THE ART AND PERSPECTIVES: Biology, clinical presentation and assessment of prognosis of AL amyloidosis: update from the XIII International Symposium on Amyloidosis

M.A. Gertz and G. Merlini

Division of Internal Medicine, Mayo Clinic, Rochester, MN, USA and Amyloidosis Research and Treatment Center, Foundation IRCCS Policlinico San Matteo, Department of Molecular Medicine University of Pavia, Italy

BIOLOGY OF THE CLONE

Light chain amyloidosis (AL) is caused by a small or modest, relatively indolent, plasma cell clone synthesizing misfolded light chains. These abnormal light chains display a pathologic conformation prone to aggregation and become toxic for cells and tissues, producing devastating systemic damage. Serum free light chains can be now measured also using a novel commercial nephelometry assay (1). Lambda light chains are more prone to misfold than are κ light chains, and certain subgroups have been reported to be preferentially associated with specific organ targeting (eg, IGVL1-44 with heart involvement). Several lines of evidence indicate that amyloid light chains can be directly cardiotoxic, although amyloid deposits may compress the microvasculature reducing the myocardial blood flow and coronary vasodilator reserve (2). Cytogenetic aberrations of the plasma cell clone and CCND1 overexpression may influence prognosis, or predict response to different chemotherapies. The analysis of the major cytogenetic aberrations in AL amyloidosis patients treated with melphalan-dexamethasone as first-line therapy showed that gain 1q21 is an independent predictor of poor survival (3). AL amyloidosis clone has fewer chromosomal aberrations compared with multiple myeloma, and the clone may be more manageable by chemotherapy. Increased sensitivity to proteasome inhibitors of amyloidogenic plasma cells compared to myeloma plasma cells has been reported (4) and may account for the high response rates observed with bortezomib-based regimens.

THE IMPORTANCE OF EARLY DIAGNOSIS

Early diagnosis is essential in AL amyloidosis in order to anticipate irreversible organ damage and restore the organ function, thus improving quality of life and extending survival. Heart involvement is the main determinant of survival. When heart failure becomes symptomatic the degree of the myocardial damage is already advanced and irreversible in more than half of the patients and the survival is restricted to less than 6 months (median). Advanced heart involvement at diagnosis is responsible for the persistently poor prognosis in a substantial proportion of patients enrolled in two prospective studies from UK and Italy reported at this Symposium (5, 6). It is therefore very important to exploit early “red flags” that may allow a timely detection of amyloid organ damage and to start chemotherapy promptly. Table 1 lists the most common early red flags that may direct the clinician toward the correct diagnosis. The cardiac biomarker, natriuretic peptide type B, is very sensitive to amyloid

heart damage, and the elevation of its serum levels can anticipate by several months the echocardiographic signs and clinical manifestations. This biomarker should be measured also during the follow-up of individuals with MGUS in order to detect early the development of AL amyloidosis cardiomyopathy. In patients who presents with advanced cardiac damage, cardiac transplantation may provide prolonged survival when performed in patients without other severe organ involvement, and when hematological response is obtained before or after cardiac transplantation, as reported by a French study reporting the outcome of 17 AL patients who underwent cardiac transplantation (7).

Table 1. Early "red flags" for suspecting AL amyloidosis

Organ or syndrome	**Present in**	**Early "red flags"**
Heart	70%	NT-proBNP >332 ng/L (100% sensitivity) BNP >73 ng/L (89% sensitivity)
Kidney	70%	Urinary alb./creat. >300 mg/g eGFR <50 mL/min per 1.73 m^2
Liver	22%	Elevation of ALP or γGT
PNS **ANS**	14%	Neuropathic pain and loss of sensitivity to temperature Erectile dysfunction
Soft tissues	13%	Carpal tunnel syndrome

PROGNOSIS

One should ask why refined measures of prognosis in light chain amyloidosis are needed. The amyloid community owes it to our patients that we are able to counsel realistic expectations of outcome. The amyloidosis community owes it to themselves since it is impossible to compare outcomes across phase II trials because of the heterogeneity of patients being entered at different centers. In amyloidosis phase III trials are expensive and difficult to complete. The majority of therapeutic trials have been single-arm phase II; and investigators still are unable to weigh the relative merits of the most commonly used regimens including: melphalan-dexamethasone, cyclophosphamide-thalidomide-dexamethasone, melphalan-dexamethasone-lenalidomide, cyclophosphamide-bortezomib-dexamethasone, bortezomib-dexamethasone, and stem cell transplantation. It would be important to identify those patients who are destined to do poorly and would be expected to fail all forms of therapy. These patients should be excluded from clinical trials because they have the potential to obscure a therapeutic signal associated with an active regimen. Survival for 40% of patients has not improved since 1960, with one-third dying within 6 months of diagnosis. Appropriately designed clinical trials would do well to exclude such patients.

The most common cause of death in amyloidosis is cardiac failure or sudden death. Predictors that refine the extent of cardiac involvement are quite useful. Cardiac biomarkers in the last 5 years have rapidly become the prognostic measures of choice for monitoring amyloidosis. Independent predictors of death include gender, BNP, troponin T, the presence of pleural effusion, E/A ratio, RV systolic pressure, and RV strain rate of the middle segment. At the Groningen Symposium, mid-wall fractional shortening was shown to be prognostically important. In a multivariable model, mid-wall fractional shortening and NT-proBNP were the only factors that

predicted survival. Currently, the NT-proBNP and the troponin T referred to as the Mayo staging system separates patients into three independent groups based on troponin T $\geq$ 0.035 and NT-proBNP $\geq$ 332.

t(11;14) is an adverse prognostic factor in light chain amyloidosis patients. Patients who had a gain 1q21 (22% of patients) had a median overall survival of 9 months; t(11;14) and hyperdiploidy were mutually exclusive findings. Gains of 1q21 favored hyperdiploidy. A three-point staging system based on whether the dFLC was > or < 18 mg/dL, the troponin T was > or < 0.025, and the NT-proBNP was > or < 1800 has been developed. The 4 stages had median survivals of 94, 40, 14 and 6 mos. Systolic blood pressure is a powerful measure of early mortality in amyloidosis and patients can be further subdivided by their systolic blood pressure. BNP levels rise with renal failure; and when the BNP is elevated due to kidney failure, it no longer appears to be prognostic in predicting survival. One must separate those patients whose BNP is elevated due to cardiac failure from those in whom the level is elevated because of a decreased creatinine clearance. In this study, the median overall survival was 7.1 months; but patients without echocardiographic evidence of involvement with an elevated BNP had a 2-year overall survival of 80%. An NT-proBNP >8000 with a systolic blood pressure of <100 constituted high-risk disease and they separated Mayo stage 3 patients into 3 groups with median survivals of 25, 6, and 3 months, respectively. Using an NT-proBNP of >10,000 with an involved free light chain level of >50 mg/dL, predicted treatment-related mortality for non-transplanted patients.

In conclusion, a consensus does not yet exist as to the next-generation staging system for amyloidosis. Fluorescent in situ hybridization, free light chain assay, new echocardiographic parameters, systolic blood pressure, uric acid, extreme elevations of the NT-proBNP are all capable of refining the currently existing Mayo staging system. Further discussions among investigators to help refine our prognostic measures are warranted. It is possible that a multiple stepwise classification based on NT-proBNP rather than a single cutoff will need to be explored.

REFERENCES

1. Palladini G, Bosoni T, Lavatelli F, Pirolini L, Foli A, Sarais G, et al. Diagnostic performance of the novel monoclonal assay for the measurement of circulating free light chain (FLC) in 220 consecutive newly-diagnosed patients with AL amyloidosis. XIIIth International Symposium on Amyloidosis; Groningen, NL, 2012, Abstracts p. 49-50.
2. Dorbala S, Bruyere JJ, Hanley M, Kruger J, Foster C, Di Carli M, et al. Coronary microvascular function in cardiac amyloidosis. XIIIth International Symposium on Amyloidosis; Groningen, NL, 2012, Abstracts p. 50-1.
3. Bochtler T, Hegenbart U, Benner A, Kunz C, Hose D, Seckinger A, et al. Prognostic significance of cytogenetic aberrations in light chain amyloidosis patients treated with melphalan/dexamethasone as first-line therapy. XIII International Symposium on Amyloidosis; Groningen, NL, 2012., Abstracts p. 52-3.
4. Oliva L, Cerruti F, Palladini G, Orfanelli U, Pengo N, Cascio P, et al. Investigating vulnerability to proteasome inhibition in primary light chain amyloidosis. XIIIth International Symposium on Amyloidosis; Groningen, NL, 2012, Abstracts p. 31-2.
5. Gillmore JD, Lane T, Rannigan L, Foard D, Gibbs SDJ, Pinney JH, et al. ALchemy - A large prospective 'Real World' study of chemotherapy in AL amyloidosis. XIII International Symposium on Amyloidosis; Groningen, NL, 2012, Abstracts, p. 52.

6. Palladini G, Milani P, Foli A, Obici L, Lavatelli F, Nuvolone M, et al. An Italian single center prospective study on outcomes in AL amyloidosis. XIII International Symposium on Amyloidosis; Groningen, NL, 2012, Abstracts p. 54-5.
7. Pourreau F, Muller C, Thierry A, Desport E, Fermand J-P, Touchard G, et al. Solid organ transplantation in AL amyloidosis and monoclonal immunoglobulin deposition disease: the French experience. XIII International Symposium on Amyloidosis; Groningen, NL, 2012, Abstracts p. 56.

Acquired cutis laxa should be considered one of the cutaneous manifestations of plasma cell dyscrasia: a case report and review of the literature

Ravera S[1], Economo L[1], Jeannin G[1], Devoti E[1], Ungari M[2], Cancarini G[1], Gregorini G[1]

Department of Nephrology[1] and Pathology[2], Spedali Civili and University of Brescia, Brescia, Italy

ABSTRACT

The acquired form of cutis laxa has been associated to various conditions. We focused on the association between cutis laxa and plasma cell dyscrasias. We describe in details the case of a 39 years old woman who recently afferred to our Department and we review 31 cases described in the literature. From our experience and from the literature it's evident that being aware of this association is helpful either for the treatment of this devastating skin disease and for an earlier diagnosis and treatment of the underlying plasma cell disorder.

INTRODUCTION

Cutis laxa is a group of rare diseases all characterized by:

- clinically widespread laxity of the skin resulting in premature ageing appearance;
- histologically decreased number and/or absence of elastic fibers in the dermis.

It is usually a diffuse disease, the skin laxity begins on the face and neck and progresses in a cephalo-caudal direction. In rare cases it can be localized at the acral sites (fingers), at the eyelid (dermatochalasis) or as isolated plaques (anetoderma).

Cutis laxa can be inherited or acquired. Acquired cutis laxa has been associated to several medical conditions and medications. Half of the cases are associated with an inflammatory dermatosis. The association with plasma cell dyscrasias/B cells lymphomas producing monoclonal protein is frequently reported.

Two main hypothesis have been proposed to explain cutis laxa in these diseases:

1) monoclonal proteins deposition on elastic fibers may induce an inflammatory and macrophagic reaction that destroy elastic fibers;

2) structurated deposits of monoclonal component (amyloid, heavy and ligth chains deposits, fibrils) per sé may induce elastic fibers' destruction.

In regards to this hypothesis, it is interesting what has been observed in gelsolin-amyloidosis induced cutis laxa. Cutis laxa is a principal clinical manifestation of gelsolin amyloidosis and is dramatic in elderly. In this form it has been demonstrated that amyloid P protein associated to elastic fibres (as a microfibrillar sheath-associated protein) plays an important role as a matrix for amyloid deposition and elastic fibres distruction. This

pathogenetic mechanism could be shared by cutis laxa associated to other types of amyloidosis such as AL amyloidosis.

CASE REPORT

A 39 years old woman with a two years history of urticaria and angioedema (treated with different drug association) and one year history of cutis laxa (mainly involving face, neck, axillae, upper arms, groins and thighs) was admitted with nephrotic syndrome and rapidly progressive uremia. Monoclonal component was detected in serum and urine (SIFE: IgAκ; UIFE: κ; sFLCκ 1576 mg/l; κ/λ ratio 44.6). A renal biopsy revealed LCDD and cast nephropathy with segmental crescents and fibrinoid focal necrosis in > 50 % of the glomeruli. A bone marrow biopsy revealed 7% of monoclonal plasma cell with κ restriction. A skeleton X-ray did not reveal osteolytic lesions.

Histology of the involved skin showed normal epidermis and cutaneous appendages, a superficial perivascular lymphocytic infiltrate with histiocytes and foreign body giant cells. Orceina stain for elastic fibers demonstrated the lost of fine elastic fibers in the papillary dermis, fragmentation, shortening and a marked reduction in elastic fiber number in the reticular dermis. There was also prominent elastophagocytosis by histiocytes. These histologic findings were consistent with the diagnosis of cutis laxa. Immunohistochemistry studies were performed for κ, λ, IgG, IgM, IgD, and IgA. There was deposition of IgA, with slight deposition of IgM, around the elastic fibers in the reticular dermis. Stains for IgG, IgD, kappa, and lambda were negative.

After haematology treatment (PEX, BDex, and two subsequent HDM/SCT) the patient achieved complete haematologic remission; she partially recovered renal function (last eGFR 25 cc/m') and achieved complete remission of urticaria and angioedema and stabilization of cutis laxa lesions.

Figure 1: the 39 years old patient before (A), at time of the diagnosis (B) and after the end of the haematological treatment.

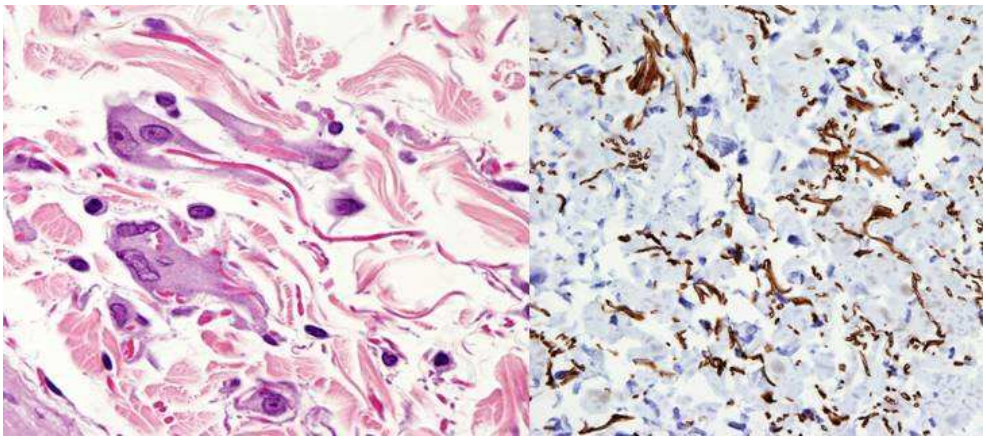

Figure 2: A: elastophagocytosis (Hematoxylin-Eosin stain); B: immunohistochemistry: deposition of IgA around the elastic fibers in the reticular dermis.

REVIEW OF THE LITERATURE

Since 1976, 31 cases of acquired cutis laxa associated with monoclonal gammopathy have been reported. Associated plasma cell disorders were multiple myeloma (12 pts), AL amyloidosis (6 pts), LCDD (1 pt), HCDD (3 pts), MGUS (4 pts), lymphocytic lymphoma (2 pts) and cutaneous lymphoplasmacytoid lymphoma (1 pt). Glomerulonephritis recently recognized as possibly associated with monoclonal gammopathy were present in 2 pts.

In 17 patients the M-protein was IgG, in 3 pts IgA, in 2 pts IgM (both with lymphocytic lymphoma), free κ in 1 pt and free λ in 2 pts. The M-protein light chain was κ in 12 pts and λ in 12 pts. In 7 pts urticaria/angioedema preceded or accompained cutis laxa. 25 pts underwent biopsies of the acquired cutis laxa involved areas: in 6 cases, all in AL amyloidosis group, biopsy revealed the presence of amyloid deposition.

In 14 cases skin histology revealed the presence of immunoglobulin of the same Ig class of the M-protein found in the serum.

CONCLUSION

Acquired cutis laxa should be considered one of the cutaneous manifestations of plasma cell dyscrasia and we suggest searching a possible underlying plasma cell dyscrasia in all the new cases of acquired cutis laxa.

Elastic fibers destruction in these patients could be induced directly by the M-protein, through the induction of an inflammatory and macrophagic reaction, or by AL amyloid or other monoclonal protein structured deposits.

It is important to be awared of this association in order to achieve two important goals:

1) to recognize and treat earlier the haematologic disease (cutis laxa may precede even of years the diagnosis of hematological disease);
2) to stop the progression of cutis laxa lesions through the treatment of the haematologic disease.

Table 1.

Authors, year	pt	clinical diagnosis of hematological disease	Monoclonal component	Skin biopsy features in addiction to diminution and fragmentation of elastic fibers	preciding urticaria/ angioedema
Hashimoto K et al, Arch Dermat, 1975		multiple myeloma	IgG		
Scott et al, Arch Dermat, 1976	F, 44	multiple myeloma	IgGκ	IF: negative	yes
Cho SY et al, Cutis, 1980	F, 46	multiple myeloma	IgG	IF: IgG on elastic fibers	yes
Hu H et al, Arch Dermat, 1984	2 pts	lymphocytic lymphoma	IgM λ; IgM κ	IF: negative	
Ting HC et al, Br J dermatol, 1984	F, 45	multiple myeloma	free λ	IF: negative	
Voigtlander V et al, Ann Dermatol Venereol, 1985		amyloidosis	IgGκ	amyloid	
Newton JA et al, Clin Exp Derm, 1986	M,31	amyloidosis	IgG in 1974 not confirmed later	amyloid	yes
Hunziker T et al, Hautarzt, 1986	M, 41	?; Gn with nephrotic syndrome	MC		
Gonnering RS et al, Ophthalmic Surg, 1987	M, 65	AL amyloidosis	IgGκ		no
Tsuji T et al, Arch Dermat, 1987	F, 41	low C3 MPGN			
Yoneda k et al, Arch Dermat, 1990	M,71; M,62	multiple myeloma	IgGκ; IgGλ	amyloid	
Niemi KM et al, Arch Dermat, 1993	M, 55	MGUS	IgGκ	immunotactoid	
Machet MC, 1995	M, 44	cutaneous lymphoplasmacytoid lymphoma			yes
McCarty MJ, Cutis, 1996	M, 62	multiple myeloma	IgGκ	IF: negative	
Krajnc I et al, Hautarzt, 1996	M, 49	MGUS	IgGλ	IF: IgGλ+C1q+C3 on elastic fibers	
Nikko A, Am J Dermatopathol, 1996	M, 40	MGUS	IgGλ	IF: IgG on elastic fibers	
Gupta A et al, Cutis, 2002	F, 62	multiple myeloma			
Dicker T et al, Austral Journ Dermat, 2002	F, 59	localized amyloidosis (tongue)	IgGκ	amyloid	
Tan S et al, J Cutan Med Surg, 2003	M,50	HCDD	IgGλ+λ	IF: IgG on elastic fibers	no
Fremont G et al, Ann Dermatol Venereol, 2007	F, 59	multiple myeloma	IgGλ	EM: elastho-phagocytosis	no
Appiah YE et al, J Am Acad Dermatol, 2008	F, 64	AL amyloidosis	free κ	amyloid	
Harrington C et al, J Am Acad Dermatol, 2008	F, 38	HCDD	negative	IF: IgG on elastic fibers; elastho-phagocytosis	yes
Fernandez de Larrea C et al, Eur J Haematol, 2009	M, 52	MGUS; Fibrillar Glomerulopathy	IgGλ	IF: IgG on elastic fibers	
Turner RB, J Am Acad Dermatol, 2009	M, 29	multiple myeloma, MPGN	IgAλ	leukocytoclastic vasculitis of small vessel in the superficial dermis	yes

Ferrandiz-Pulido C et al, Arch Dermat, 2010	*M, 63*	*AL amyloidosis*	*free λ*	*AL amyloidosis+λ light chain*	
Maruani A et ali, Acta Derm Venereol, 2010	*M, 34*	*MGUS, LCDD*	*IgGλ*	*Immunogold: Ab anti-λ on elastic fibers*	*no*
New HD et al, Arch Dermat, 2011	*M, 48*	*multiple myeloma*	*IgGλ and IgAκ*	*elastho-phagocytosis*	
Kim DP, Dermatol Online J, 2011	*F, 55*	*multiple myeloma,MIDD*	*IgGκ*	*interstitial foamy cells*	*no*
Alexander MP, Am J Kidney Dis, 2011	*F, 29*	*multiple myeloma,HCDD*	*IgAκ*	*α heavy chain on elastic fibers*	*yes*

REFERENCES

1. Nikko, Anthony B.A., Dunningan, et al. Acquired cutis laxa associated with a plasma cell Dyscrasia. Am J Dermatopathol. 1996; 18 (5): 533-537.
2. Maruani A., Arbeille B., Machalet M.C., et al. Ultrastructural demonstration of a relationship between acquired cutis laxa and monoclonal gammopathy. Acta Derm Venereol 2010; 90: 406-408.
3. Kiuru-Enari S, Keski-Oja J., Haltia M. Cutis laxa in hereditary gelsolin amyloidosis. British Journal of Dermatology 2005; 152: 250-257.
4. Hu C.H., Gottlieb M., Winkelmann R.K. Acquired elastolysis with lymphoproliferative disease and gammopathy: a new syndrome. Arch Dermatol 1984; 120: 1087.
5. Newton J. A., McKee P. H., Black M.M. Clinical adn Experimental Dermatology 1986; II: 87-91.
6. Niemi K.M., Lamprechet I.A., Virtanen I, et al. Arch Dermatol 1993; 129: 757-762.
7. Krajnc I., Rems D., Vizjak A., et al. Acquired generalized cutis laxa with monoclonal gammopathy (IgG-lambda). Clinical, histological and immunofluorescence evaluation and a review of the literature. Hautarzt 1996; 47: 545-549.
8. Joss N, Boulton-Jones J.M., More I. Premature ageing ang glomerulonephritis. Nephrol Dial Transplant 2001; 16: 615-618.
9. Alexander M. P., Nasr S. H., Watson D. C., et al. Am J Kidney Dis 2011; 58(4): 621-625.
10. New D.H., Callen J.P. Generalized acquired cutis laxa associated with multiple myeloma with biphenotypic IgG- λ and IgA- κ gammopathy following treatment of a nodal Plasmacytoma. Arch Dermatol 2011; 147: 323-328.

How can I understand? – A qualitative research study on the information needs of patients with AL Amyloidosis and their carers

Hamish Holewa [1], Pam McGrath[2], Peter Mollee[3], Pat Neely[4]

[1] Research Associate, Institute of Health and Social Science, CQ University, Brisbane Campus
[2] Senior Research Fellow, Centre of National Research on Disability and Rehabilitation Medicine Griffith Health Institute, Director International Program of Psycho-Social Health Research (IPP-SHR)
[3] Peter Mollee Director Amyloidosis and Myeloma Services, Princess Alexandra Hospital, Brisbane
[4] Pat Neely, Amyloidosis Patient and Family Advocate, Leukaemia Foundation Australia.

ABSTRACT / INTRODUCTION

No previous research has been undertaken in Australia into how AL amyloidosis patients gain information about their disease and treatment. This qualitative study was designed to identify: How patients and carers gained information at diagnosis and six months later. How useful that information was, how this information was used to make decisions about treatment. What information would have been useful at diagnosis? Suggestions from patients and carers about the most useful ways of delivering information.

PATIENTS AND METHODS

Patients and carers were recruited from participants on the Australasian Leukaemia and Lymphoma Group (ALLG) MM8 study (a prospective clinical trial of risk-adapted melphalan in patients with AL amyloidosis).

Patients and carers were offered the opportunity to take part separately in a 45-minute recorded interview by phone or in person at diagnosis and 6 months later. 11 patients (6 male and 5 female, aged 48 to 75) and 7 carers consented to be interviewed. 3 patients had no carers. 1 carer declined.

At 6 months 5 patients had died. 1 had dropped out of the trial, 5 patients and 5 carers were re-interviewed. In all 22 interviews were conducted. Because of the poor quality of 5 recordings these were not used making. 17 recordings were transcribed.

Longitudinal qualitative methodology using semi-structured interviews was used. Interview audio recordings were transcribed and analysed by SATURATE Qualitative Computer Aided Analysis software. Transcript coding was developed, driven by the exact words of the participants.

RESULTS

All patients and carers expressed feelings of relief at receiving a diagnosis but quickly gave way to feelings of shock, confusion, fear, bewilderment and loneliness on learning that they or their loved one was suffering from a very serious disease. Patients words at diagnosis, “Doctor did not give hope of a cure”, ”Decision to undergo treatment simplified to choosing life or death”. ”Living now with a lifetime illness”, “Not initially aware that I might go into remission”. “I did not want to know about the disease hoping I did not have it”.

Was the initial communication between you and your doctor useful? Majority of comments were favourable. Most doctors conveyed information verbally, occasionally accompanied by drawings or written notes and downloads from the web. Patients comments; “Information from haematologists useful”, “The doctor’s advice was down to earth and in layman’s terms”, ”Haematologist very direct and honest about seriousness of my disease”, “Specialist explained the disease could not be cured but could be managed”. “Doctor downloaded information from the web”, “The specialist drew a diagram so I could understand”, “Downloads from the Mayo Clinic and London were given to me”, “Information given was timely and incremental

Negative communication; The over worked doctor didn’t look up from the desk”, “Heart specialist was vague and not receptive to questions”, “I had trouble reading all the written materiel about the trial and Amyloidosis”, “Not given hope of a cure”, “Each member of the medical team communicated differently”. Carers made similar comments.

Where did patients gain information from other than their doctors? From various sources: other health professionals, The Web, Other patients, Support groups, Published information. Participant’s comments “Education from nursing staff more cancer orientated”, “Nurses administering chemotherapy offered information about Amyloidosis” “Hospital staff very good at explaining the procedures such as the Stem cell transplant”, "Some staff compared amyloidosis with myeloma".

Was Information from the web used? All participants used information from the web. Participants comments **“**Amyloidosis web sites very useful especially for communicating with patients in the USA and UK”, “Used information from the web to ask questions”, “Family and friends learnt from the internet”, “Internet information provided hope that treatments had improved”, “Good for researching treatments”, ”I received my first information from downloads my daughter got from the web”, ”The only information given by the doctor were downloads of information from London and the Mayo”, “The web sites did not give hope”, ”Information from the web only general and not particularly helpful”, “Have to sort the good from the bad”.

Information from pamphlets, written Information and support Groups. Participants comments**;** “At diagnosis I was not told about support groups”, “Not given any pamphlets on Amyloidosis”,” “No pamphlets seen around the hospitals”. Six months after diagnosis some patients were receiving the Leukaemia Foundation’s Amyloidosis News, other written information and attending support groups. Patient’s comments“, “Amyloidosis News useful as it was purely about Amyloidosis”, “Amyloidosis News offered hope”, ”I needed positive stories”, ”Became better informed by reading Amyloidosis News and attending Leukaemia Foundation Amyloidosis support groups”

How useful was information in assisting participants to make decisions about treatment at diagnosis? Patients found it was difficult to use information because of lack of information about their, shock and sometimes because they felt too unwell to read information.

Patient and carer comments “Treatment happened so quickly I had no time to dwell on illness”, “Many tests prior to staring the trail were tiring”, “ Some confusion with the trial materiel”, “Given information about the trial but nothing about Amyloidosis”, ”Information confusing”, “Printed information at hospital inadequate”.

By 6 months patients and carers had gained information from the web site, their doctors and other sources and were understanding their disease and treatment much better...

Patients comments. ”I have spoken to other patients and compared notes”, ”Relationship with the specialist had developed”, ”I learnt on the job by asking questions”, “Leukaemia Foundations Amyloidosis News was useful in explaining amyloidosis to others", "Information on the web useful post diagnosis”.

What did the participants feel was the most effective way of being offered information and receiving information? Patient and carer comments “Verbal communication with doctors should be accompanied by written notes about their own treatment”, “Great need for an Australian booklet giving general information about amyloidosis that can be read again and again”, “The need for honest information written with hope”, “Doctors need to encourage patients and carers to ask questions”. ”Talking with team of doctors together and not individually very beneficial”, “Patients need to be informed of support groups, information on ways of dealing with emotional problems”, “Loneliness and depression should be recognised and support or treatment offered.

CONCLUSION

This study provides the first systematic assessment of the information needs of Australian AL Amyloidosis Patients and their carers at diagnosis and 6 months later. It shows that the participants knew nothing about Amyloidosis at diagnosis in fact they had never heard the word. All patients felt shocked and frightened and were often feeling ill or exhausted because of the many tests and the emotional upset. Therefore any input into decision-making at diagnosis was difficult. Patients and carers felt that information about the their disease and treatment needed to delivered verbally accompanied by hand written notes and diagrams. They expressed the need for Australian booklets and videos about Amyloidosis written in simple language giving hope. Participants recommended that the emotional effects of diagnosis and treatment should be acknowledged and information on support services offered. By six months patients and their carers had obtained much more information allowing them to feel more in partnership with the treating team.

The Leukaemia Foundation Australia has used information from this study to produce the booklet Understanding Amyloidosis launched in December 2010.

Production of plasminogen activator and it's receptor in organs from AL amyloidosis

*H. Hata, **M. Uchiba, *Y. Kawano, *S. Fujiwara, *N. Wada, ***K. Obayashi, ***M. Ueda, *H.i Mitsuya, ***Y. Ando

*Department of Hematology, Kumamoto University
** Department of Blood Transfusion and Cell Therapy, Kumamoto University Hospital
*** Department of Diagnostic Medicine, Graduate School of Medical Sciences, Kumamoto University

ABSTRACT

We have been proposing that excessive fibrinolysis as a hallmark of AL amyloidosis. To elucidate mechnisms underlining fibrinolysis, expression of uPA was investigated in primary samples.

uPA was more abundantly expressed in organs in AL amyloidosis than those in familial amyloidosis 30 to 100 times. Moreover, uPA receptor (uPAR) expression was found more than 100 times in organs from AL amyloidosis comparing to familial amyloidosis. Expression of u-PA was induced by addition of amyloid fibrils in HepG2 cells. Abundant expression of uPA and uPAR at organs in AL amyloidosis cases suggests conversion of plasminogen to plasmin occurs at amyloid lesion. Induction of u-PA gene by amyloid fibrils may lead to vicious cycle leading to production of plasmin which may disrupt extracellular matrix at amyloid lesion thus possibly enhancing organ damage. Further analysis of fibrinolysis should elucidate unknown mechanisms regulating progression of amyloidosis and lead to development of unique therapeutic approach.

INTRODUCTION

Fibrinolysis is a phenomenon identified as degradation of fibrin clot subsequently happens from coagulation. Usually, fibrinolysis takes place after fibrin clot formation by conversion of plasminogen to plasmin which was followed by up-regulation of plasminogen activator. However, there have been some report showing excessive fibrinolysis in primary amyloidosis (1, 2). We also found that excessive fibrinolysis underwent in AL amyloidosis although no extensive coagulation was observed (Fig. 1) (3).

To understand the mechanisms regulating excessive fibrinolysis, we looked at expression of urokinase type plasminogen activator.

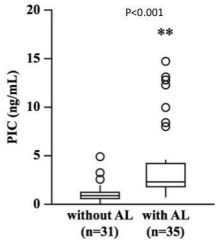

Figure 1. Concentration of PIC (plasmin/plasmin inhibitor complex) was elevated in AL amyloidosis comparing to myeloma cases without AL amyloidosis.

METHODS

Plasma cells were purified by using anti-CD138 antibody-coated immunomagnetic beads from bone marrow samples. Gene expressions were analyzed by real time PCR. In some experiments, mRNA was extracted from fresh frozen organs from amyloidosis cases. Paraffin embedded samples were utilized for immunostaining of uPA. Amyloid fibrils were extracted from tongue of AL amyloidosis case. Induction of uPA or uPAR was analyzed by incubating HepG2 cells with amyloid fibrils.

RESULTS

Expression of uPA was detected at low levels in plasma cells from both MGUS and Amyloid cases. Interestingly, uPA was more abundantly expressed in organs in AL amyloidosis than those in familial amyloidosis at 30 to 100 times. Moreover, uPAR-expression was found more than 100 times in organs from AL amyloidosis comparing to familial amyloidosis (Fig. 2). Expression of u-PA was slightly induced by addition of amyloid fibrils in HepG2 cells (approximately 1.5 tumes).

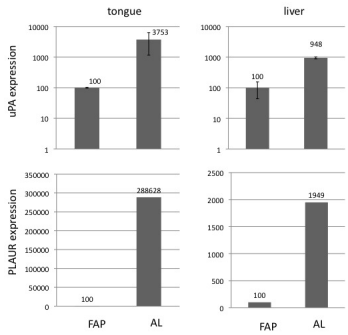

Figure 2. Expression of uPA and uPA-receptor (PLAUR) was higher in organs from AL amyloidosis comparing to FAP cases.

DISCUSSION

Abundant expression of uPA and uPAR at organs in AL amyloidosis cases suggests conversion of plasminogen to plasmin occurs at amyloid lesion. Induction of u-PA gene by amyloid fibrils may lead to vicious cycle leading to production of plasmin which may disrupt extracellular matrix at amyloid lesion thus possibly enhancing organ damage. Further analysis of fibrinolysis should elucidate unknown mechanisms regulating progression of amyloidosis and lead to development of unique therapeutic approach.

ACKNOWLEDGEMENT

This work was supported by grant in aid from Japanese ministry of health and welfare for amyloidosis.

REFERENCES

1. Liebman HA., et al. Excessive fibrinolysis in amyloidosis associated with elevated plasma single-chain urokinase. Am J Clin Pathol 98, 534-541 (1992)
2. Sane DC., Et al. Elevated urokinase-type plasminogen activator level and bleeding in amyloidosis: case report and literature review. Am J Hematol 31, 53-57 (1989)
3. Uchiba M., et al. Excessive fibrinolysis in AL-amyloidosis is induced by urokinae-type plasminogen activator from bone marrow plasma cells. Amyloid 16, 89-93 (2009)

Utility of the Heavy Light Chain (HLC) assay in patients with AL amyloidosis with a detectable serum monoclonal protein

Ashutosh D. Wechalekar[1], Philip Young[2], Nancy Wassef[1], Julian D. Gillmore[1], Simon D.J. Gibbs[1], Jennifer H. Pinney[1], Christopher P. Venner[1], Darren Foard[1], Lisa Rannigan[1], Thirusha Lane[1], Carol J. Whelan[1], Helen J. Lachmann[1], Arthur Bradwell[2], Stephen Harding[2] and Philip N. Hawkins[1]

[1] Centre for Amyloidosis and Acute Phase Proteins, University College London Medical School, UK, [2]The Binding Site Group Ltd, Birmingham, UK

ABSTRACT

The presence of a monoclonal immunoglobulin (M-Ig) in the serum is a common occurrence in AL amyloidosis patients. Standard serum protein electrophoresis (SPE) remains the gold-standard technique for detecting and measuring M-Ig. However, quantification of low level M-Ig (e.g., ≤2g/L) is inaccurate by SPE, making the technique unsuitable for serial monitoring. Specific immunoassays have been produced that quantify Ig'κ/Ig'λ (heavy/light chain, HLC) in serum. Here we report the use of the HLC assays as an aid in identifying and quantifying monoclonal proteins in AL amyloidosis patients.

INTRODUCTION

Patients with AL amyloidosis usually have subtle underlying clonal plasma cell dyscrasias that result in the presence of a monoclonal immunoglobulin (M-Ig) in the serum. The identification and quantification of monoclonal proteins is important for the diagnosis and monitoring of the disease. Standard electrophoresis techniques have traditionally been used for identifying and measuring monoclonal proteins. However, the expressed monoclonal proteins can be difficult to detect by SPE in up to 20% of AL amyloidosis patients because of low expression levels of the paraprotein (1). Immunofixation electrophoresis (IFE) is more sensitive than SPE but it is a non-quantitative approach and therefore not valid for measuring paraprotein levels.

Alternatively, new antibodies recognising epitopes spanning the junctional regions between bound kappa or lambda light chains and their respective heavy chain partner (HLC) allow accurate and specific quantification of serum IgGκ and IgGλ, IgAκ and IgAλ, and IgMκ and IgMλ. Furthermore, these molecules can be grouped in pairs (i.e., IgGκ/IgGλ, IgAκ/IgAλ and IgMκ/IgMλ) to calculate HLC ratios that provide indication of monoclonality (2).

METHODS

The study included 151 patients with AL amyloidosis in whom a serum M-Ig was detectable by SPE and/or IFE at time of diagnosis, as assessed at the UK National Amyloidosis Centre. HLC (IgG/IgA/IgM) ratios were measured retrospectively on a BN^{TM}II System nephelometer (Siemens, Munich, Germany) using stored sera from the above patients. HLC IgGκ/λ normal range: 0.98-2.75; IgAκ/λ normal range: 0.80-2.04; and IgMκ/λ normal range: 0.96-2.30. For sensitivity and specificity studies, all 151 AL amyloidosis patients were compared to 20 healthy control samples. Receiver operator characteristic (ROC) analysis was performed using SPSS 19.0 software for Windows.

Table 1. (**A**) Comparison of SPE and HLC measurements for the detection and quantification of monoclonal immunoglobulins (M-Ig). HLC ratio identified correctly the same number of IgG, and more IgA and IgM patients, than SPE. Further, in all three IgG, IgA and IgM monoclonalites, more patients had an abnormal HLC ratio than could be quantified by SPE densitometry. (**B**) Comparison of SPE and HLC sensitivity for the quantification of M-Ig in 151 AL amyloid patients.

A

	Number of Patients	Abnormal HLC ratio	SPE positive	Quantifiable by SPE
All	151	136 (90%)	129 (85%)	103 (70%)
IgG	101	91 (90%)	91 (90%)	71 (70%)
IgA	32	29 (91%)	23 (72%)	17 (53%)
IgM	18	16 (89%)	15 (83%)	15 (83%)

B

		HLC ratio		Total
		Normal	Abnormal	
SPE	Non-quantitative	13	35	48
	Quantitative	2	101	103
Total		15	136	151

RESULTS

The median age of patients was 70 years (range, 35-85 years) with 95 (63%) males. IFE analyses to characterise the serum M-Ig band showed that 101 patients displayed a monoclonal IgG, 32 patients had a monoclonal IgA, and in 18 patients the monoclonality was due to elevated IgM. Of the 101 IgG patients, 91 (90%) had an abnormal HLC ratio and positive band by SPE, but this was quantifiable by SPE densitometry in only 71 (70%) cases. Of the 32 IgA patients, 29 (91%) presented an abnormal HLC ratio and 23 (72%) had a positive band by SPE, which could be quantified in 17 (53%) patients. Of the 18 IgM patients, 16 (89%) had an abnormal HLC ratio, and 15 (83%) had a positive band by SPE that in all cases could be quantified using densitometry. Overall, 136/151 (90%) patients had an abnormal HLC ratio compared to 129/151 (85%) in whom monoclonal bands were detected by SPE (Table 1A), thus demonstrating the increased sensitivity of HLC versus SPE for the detection of monoclonal gammopathies in AL amyloidosis.

Next, we compared SPE and HLC sensitivities for the quantification of M-Ig in AL amyloid patients. 136/151(90%) patients had abnormal HLC ratios compared to 103/151 (70%) patients with quantifiable SPE. Cross-tabulation of normal and abnormal HLC ratios versus quantitative and non-quantitative SPE showed that out of 151 patients, 101 were correctly identified by both methods whereas 13 patients were missed by the two approaches. Importantly, 35 patients were identifiable by HLC alone and 2 patients were identifiable by SPE alone. The 2 patients detected by SPE and missed by HLC assays were: 1) an IgGλ patient with 3.6 g/L M-Ig.

Total IgG levels were 6.1 g/L, HLC IgGκ levels were 3.7 g/L and HLC IgGλ levels were 2.6 g/L; and 2) an IgGλ patient with 1 g/L M-Ig. Total IgA levels were not available, HLC IgAκ levels were 0.11 g/L and HLC IgAλ levels were 0.13 g/L.

The improved sensitivity of HLC measurements relative to SPE was further confirmed when both variables were compared using bioinformatics. Receiver operator characteristic (ROC) analysis including all 151 patients and 20 healthy controls showed that HLC ratios had a greater sensitivity than SPE for the detection and quantification of intact immunoglobulin in AL amyloidosis (area under curve (AUC): HLC ratio = 0.95 v quantifiable SPE=0.84) (Figure 1).

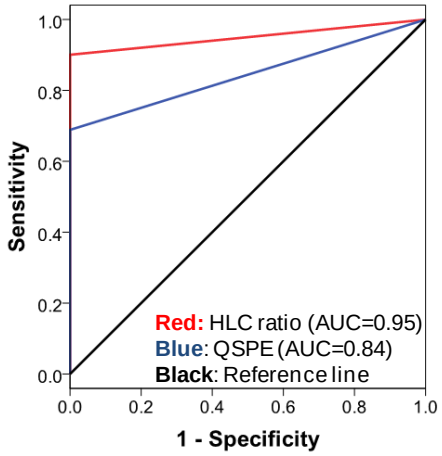

Figure 1. Receiver operator characteristic (ROC) analysis comparing the sensitivity and specificity of HLC ratios and quantifiable SPE (QSPE). Area under curve (AUC): HLC ratio = 0.95 v quantifiable SPE (QSPE) = 0.84.

DISCUSSION

The presence of a monoclonal protein in the serum and urine of patients is a common feature in the initial screening for AL amyloidosis patients. However, the underlying monoclonality can be missed in up to 20% of cases when assessed with standard electrophoretic methods, particularly when the protein is present al low concentrations. The introduction of the free light chain (FLC, Freelite™) assay has greatly improved the management of patients with AL amyloidosis, as recognised by its inclusion in international guidelines for monitoring the disease (3). However, patients with low levels of M-Ig and normal FLC cannot be properly monitored thus hindering assessment of treatment responses and preventing their inclusion in clinical trials (3, 4).

Our results demonstrate that HLC measurements have a greater than/equal to sensitivity for the detection and a greater sensitivity for the quantification of M-Ig's in AL amyloid patients compared to SPE / SPE densitometry. In all, 90% of patients were identified that had an abnormal HLC ratio versus 85% with a detectable monoclonal band by SPE, which was quantifiable in 70% of patients. Furthermore, while 35 patients with an abnormal HLC ratio were non-quantifiable by SPE densitometry, only 2 patients with quantifiable SPE displayed normal FLC ratios. These were an IgGλ patient with a below-normal IgGκ value by HLC, and an IgAλ patient with 1 g/L M-Ig as determined by SPE densitometry (i.e. expression below level of confidence necessary for accurate detection)

and below-normal IgAκ and IgAλ values that rendered a borderline normal ratio, which would undoubtedly have raised suspicion among clinicians.

In summary, HLC assays have greater sensitivity and quantitative potential than SPE in AL amyloidosis. Management of patients with AL amyloidosis relies on accurate assessment of patients' clonal disease responses to treatment. SPE is a relatively insensitive tool in this patient group and HLC may provide a more sensitive alternative. Further longitudinal studies are needed to determine the role of HLC analysis for this purpose.

REFERENCES

1 O'Connell, T.X., Horita, T.J, and Kasravi, B. Understanding and Interpreting Serum Protein Electrophoresis. (2005) *Am Fam Physician,* 71:105-112.

2 Bradwell, A.R., Harding, S.J., Fourrier, N.J., Wallis, G.L., Drayson, M.T., Carr-Smith, H.D., and Mead, G.P. Assessment of monoclonal gammopathies by nephelometric measurement of individual immunoglobulin kappa/lambda ratios. Clin Chem 2009;55:1646-1655.

3 Gertz, M. A., Comenzo, R., Falk, R. H., Fermand, J. P., Hazenberg, B. P., Hawkins, P. N., Merlini, G., Moreau, P., Roncon, P., Sanchorawala, V., Sezer, O., Solomon, A., and Grateau, G. Definition of organ involvement and treatment response in primary systemic amyloidosis (AL): A consensus opinion from the 10th International Symposium on Amyloid and Amyloidosis. (2005) *Amer J Hematology*, 79:319-328.

4 Dispenzieri, A., Kyle, R., Merlini, G., Miguel, J.S., Ludwig, H., Hajek, R. Et al. International Myeloma Working Groups guidelines for serum-free light chain analysis in multiple myeloma and related disorders. (2009) *Leukemia*, 23:215-224.

Normal heavy/light chain (HLC) and free light chain (FLC) ratios are associated with prolonged survival in patients with systemic AL amyloidosis

Ashutosh D. Wechalekar[1], Philip Young[2], Nancy Wassef[1], Julian D. Gillmore[1], Simon D.J. Gibbs[1], Jennifer H. Pinney[1], Christopher P. Venner[1], Darren Foard[1], Lisa Rannigan[1], Thirusha Lane[1], Carol J. Whelan[1], Helen J. Lachmann[1], Arthur Bradwell[2], Stephen Harding[2] and Philip N. Hawkins[1]

[1] Centre for Amyloidosis and Acute Phase Proteins, University College London Medical School, UK; [2]The Binding Site Group Ltd, Birmingham, UK

ABSTRACT

Here we report on the prognostic utility of heavy/light chain (HLC, measured using Hevylite™) measurements in AL amyloidosis patients with and without abnormal free light chain ratios (FLC, measured using the Freelite™ nephelometric assay). Normal FLC and HLC ratios were associated with improved overall survival (OS) compared to patients with an abnormal FLC or HLC ratios. Furthermore, patients with both an abnormal FLC and HLC ratio had the poorest outcome. We conclude that HLC measurements provide additional prognostic information in AL amyloidosis and may be useful in the design of strategies for patient management.

INTRODUCTION

Newly diagnosed AL amyloidosis patients usually present with abnormal serum FLC concentrations which have been shown to be predictive of survival outcome (1, 2). FLC measurements have been instrumental in improving detection and monitoring of AL amyloidosis patients, which has contributed to improvements in survival rates (3, 4). However, approximately 5-20% of patients present with normal FLC ratio. We have recently shown that novel nephelometric assays that are specific to junctional epitopes between the light chain (κ and λ) and their heavy partners (heavy/light chain; HLC) are of prognostic value in patients with normal FLC ratios (5). Here, we report a risk stratification model utilising HLC and FLC, and demonstrate this can be used to stratify patients in two independent populations.

METHODS

HLC (IgG, IgA and IgM) were measured in two series of patients with AL amyloidosis, population A: 147 unselected patients, and population B: 146 patients selected such that a higher-than-average percentage of patients within the population had normal FLC ratios (normal FLC / total number patients; population A: 46/147 (31%), population B: 105/146 (72%)). HLC ratios were measured on a BN^{TM}II System nephelometer (Siemens,

Munich, Germany) using stored sera from the above patients. HLC IgGκ/λ normal range: 0.98-2.75; IgAκ/λ normal range: 0.80-2.04; and IgMκ/λ normal range: 0.96-2.30. Statistical analyses were performed using SPSS v19.0 software for Windows.

RESULTS

In both populations, abnormal FLC ratios were associated with poorer overall survival (OS) at 36 months (population A: Hazard Ratio (HR)=2.2, p=0.037; population B: HR=2.1, p=0.006) (Figure 1). Individually, IgG, IgA or IgM HLC ratios were not associated with OS in either population. However, a model based on combining presence (or not) of abnormal HLC and FLC ratios as a risk factor (0=both normal, 1=either one abnormal and 2=both abnormal) showed significant discriminatory power. Population A: patients with no risk factors (normal FLC and HLC ratios, n=23) had significantly better OS than patients with 1 or 2 risk factors (abnormal FLC and/or HLC ratios, n=123, p=0.04). At 36 months, mortality was only 9% in patients with no risk factors compared to 47% in patients with 1 or 2 risk factors (Figure 2A). Population B: patients with no risk or 1 risk factor (n=127) had significantly better OS than those with both abnormal FLC and HLC ratios (n=21, p=0.007). At 36 months, the mortality was 34% in patients with 0 or 1 risk factors and 67% mortality in patients with 2 risk factors (Figure 2B).

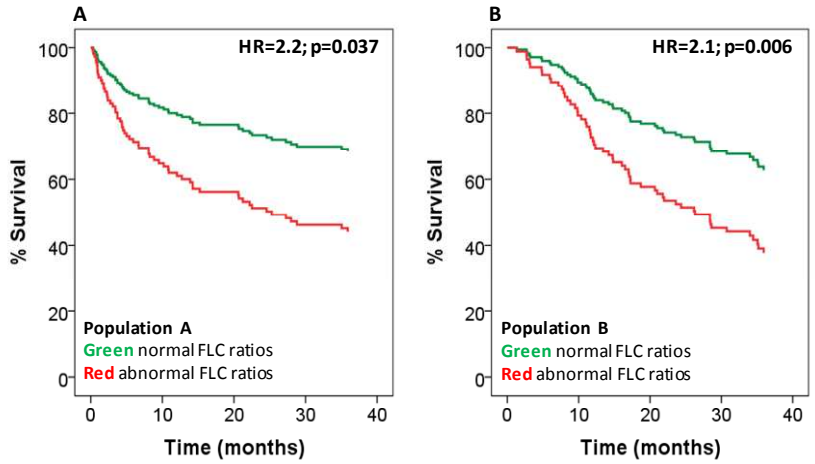

Figure 1. Cox regression survival analysis of (A) population A and (B) population B. FLC ratios were measured in presentation sera and overall survival (OS) of patients with normal FLC ratios (green lines) were compared to those with abnormal FLC ratios (red lines; A and B). Abnormal FLC ratios were significantly associated with shorter OS in both populations (population A, HR=2.2, p=0.037 and population B, HR=2.1, p=0.006).

DISCUSSION

Both baseline absolute FLC levels and abnormal FLC ratios are prognostic of overall long-term survival in AL amyloidosis patients (1, 2). Survival may be dependent on a number of factors such as type of treatment and

amount of dose, as well as the baseline FLC characteristics of the specific population under study (1, 6). Here, we have confirmed that an abnormal FLC ratio at presentation is predictive of a poorer outcome in two different cohorts, an unselected population of AL amyloidosis patients and a second, selected population with a higher-than-average percentage of patients with normal FLC ratios. Our results validate the importance of FLC measurements in newly diagnosed AL amyloidosis patients and demonstrate the robustness of FLC measurements as prognosticators of survival across heterogeneous populations of patients.

We also show that HLC ratios in combination with FLC measurements strengthen the evaluation of patients by allowing their better risk stratification. The observation that baseline HLC ratios are prognostic is novel. Whether its absolute levels also are, as demonstrated for FLCs, remains to be tested. However, when considering that the prognosis of the disease is currently determined by the levels of cardiac biomarkers and FLCs, and that over 30% of AL amyloidosis patients die within one year of diagnosis (7), the prognostic value of HLC measurements at presentation, as reported here, could represent an important additional tool to better predict survival outcomes in the AL amyloidosis population and, consequently, aid clinicians in adopting personalised treatment strategies.

In conclusion, a combination of HLC and FLC ratios provide useful prognostic information in patients with AL amyloidosis; those with both normal HLC and FLC ratios have excellent outcomes. The clinical utility of this model needs to be confirmed in larger unselected AL amyloidosis populations.

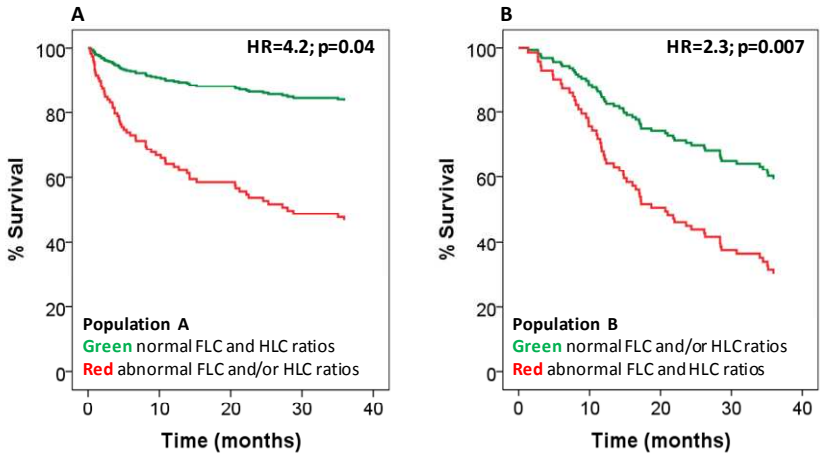

Figure 2. Risk stratification model based on abnormal free light chain (FLC) and heavy/light chain (HLC, Ig'κ/Ig'λ) ratios. **(A)** In a population of 147 unselected AL amyloidosis patients (population A), the patients with no risk factor (both FLC and HLC ratios normal, green line) had significantly longer overall survival (OS) compared to patients with 1 or 2 risk factors (abnormal FLC and/or HLC ratios, red line) (HR=4.2, p=0.04). **(B)** In population B, the patients with no risk or 1 risk factor (normal FLC and/or HLC ratios, green line) had significantly longer OS compared to patients with 2 risk factors (abnormal FLC and HLC ratios, red line) (HR=2.3, p=0.007).

REFERENCES

1. Dispenzieri, A., Lacy, M.Q., Katzmann, J.A., Rajkumar, S.V., Abraham, R.S., Hayman, S.R., et al. Absolute values of immunoglobulin free light chains are prognostic in patients with primary systemic amyloidosis undergoing peripheral blood stem cell transplantation. Blood 2006;107:3378-3383.
2. Kumar, S., Dispenzieri, A., Lacy, M.Q., Hayman, S.R., Buadi, F.K., Zeldenrust, S.R., et al. A novel staging system for light chain amyloidosis incorporating free light chain levels. Haematologica 2008;93:917a.
3. Gertz, M.A. Autologous attack on amyloidosis. Mayo Clinic Proceedings 2006;81:874-876.
4. Comenzo, R.L. Managing systemic light-chain amyloidosis. J Natl Compr Canc Netv 2007;5:179-187.
5. Wechalekar, A., Faint, J., Lachmann, H., Hawkins, P., Harding, S, and Bradwell, A. Significance of abnormal serum immunoglobulin heavy/light chain ratios (Hevylite) in 294 patients with systemic AL amyloidosis 2011. Haematologica 96(s1), P-392a.
6. Lachmann, H.J., Gallimore, R., Gillmore, J.D., Carr-Smith, H.D., Bradwell, A.R., Pepys, M.B., et al. Outcome in systemic AL amyloidosis in relation to changes in concentration of circulating free immunoglobulin light chains following chemotherapy. British J Haemat 2003;122:78-84.
7. Gertz, M.A., Dispenzieri, A. Immunoglobulin light-chain amyloidosis: growing recognition, new approaches to therapy, active clinical trials. Oncology (Williston Park) 2012;26:152-61.

Heavy/Light Chain Analysis Can Replace IFE in an Algorithm Utilizing Free Light Chain and Urinary Protein Electrophoresis for Identification of AL Amyloidosis Patients

J. Bijzet[1], I.I. van Gameren[1], A.C. Muller Kobold [2], J.G. van de Belt [2], A.R. Bradwell[3], and B.P.C. Hazenberg[1]

[1]Department of Rheumatology & Clinical Immunology and Pathology & Laboratory Medicine , [2]University Medical Center Groningen, University of Groningen, The Netherlands, [3]The Binding Site Group Ltd, Birmingham, UK.

ABSTRACT

Traditionally serum free light chain (FLC, Freelite™), serum protein electrophoresis (SPEP) and urinary electrophoresis (UPEP) with confirmation by immunofixation (IFE) have been used to identify monoclonal immunoglobulin (M-Ig) production in patients with AL amyloidosis. Here we report on the utility of Ig'κ/Ig'λ (HLC) assays for the detection of M-Ig in AL amyloidosis patients.

INTRODUCTION

International guidelines for the detection of monoclonal immunoglobulin (M-Ig) recommend a simple algorithm utilising serum protein electrophoresis (SPEP) and serum free light chains (FLC) quantified using the Freelite™ nephelometric immunoassay. Whilst this algorithm is sensitive enough to detect almost all monoclonal gammopathies, where AL amyloidosis is suspected 24hr urine analysis is required (1); highlighting the difficulty associated with the detection of clonality in this disease (2). In this study we evaluate the potential of novel nephelometric assays measuring intact immunoglobulin heavy and light chains in serum and their associated ratios as tools to identify monoclonal immuoglobulins alongside the Freelite assay (3).

METHODS

Serum from 92 AL amyloidosis patients (4 FLCκ, 15 FLCλ, 3 IgAκ, 8 IgAλ, 7 IgGκ, 21 IgGλ, 2 IgMκ, 2 IgMλ, 30 non-detectable M-Ig, 62/92 serum positive, 71/92 urine positive) were retrospectively analysed using IgGκ/IgGλ, IgAκ/IgAλ and IgMκ/IgMλ immunoassays. Results were compared to historic SPEP, immunofixation (IFE), Freelite and urine electrophoresis (UPEP) results.

RESULTS

Results for individual assays and various assay combinations are presented in table 1. M-Ig was identifiable by IFE in 62/92 patients (28 IgG, 11 IgA, 4 IgM, 19 FLC, and 30 patients with negative IFE), by FLC in 77/92 patients (23/28 IgG, 8/11 IgA, 2/4 IgM, 19/19 FLC, and 25/30 IFE negative patients), by HLC in 57/92 patients (25/28 IgG, 9/11 IgA, 4/4 IgM, 10/19 FLC, and 9/30 IFE negative patients), and by UPEP in 71/92 patients (26/28 IgG, 10/11 IgA, 2/4 IgM, 16/19 FLC, and 17/30 IFE negative patients). Of the 7 IgAλ patients positive by UPEP, 2 patients were positive for intact IgAλ and negative for BJP. Similarly 2/7 IgGκ and 3/19 IgGλ patients with positive UPEP, had intact IgGκ and IgGλ respectively and were negative for BJP (table 1).

A screening panel of UPEP and IFE identified 79/92 (86%) patients (28/28 IgG, 11/11 IgA, 4/4 IgM, 19/19 FLC, and 17/30 IFE negative patients). In comparison, UPEP, IFE and FLC detected 89/92 (97%) patients (28/28 IgG, 11/11 IgA, 4/4 IgM, 19/19 FLC, and 27/30 IFE negative patients). Similarly, a screening panel of UPEP, FLC and HLC identified 89/92 (97%) patients (27/28 IgG, 11/11 IgA, 4/4 IgM, 19/19 FLC, and 28/30 IFE negative patients) (table 1). Importantly, this analysis shows that HLC was able to assigned clonality in an IFE-negative sample that was missed by all other assays.

Table 1. Sensitivity of UPEP, FLC, HLC, and IFE screening panels for detection of M-Ig in 92 AL amyloidosis patients. An algorithm using the traditional and recommended tests (UPEP, FLC, and IFE) and a screening panel incorporating the newly developed immunoassays for the quantification of serum Ig'κ/Ig'λ (UPEP, FLC, and HLC) both identified 89/92 patients. There was concordance for 7/7 IgGκ, 3/3 IgAκ, 8/8 IgAλ, 2/2 IgMκ , 2/2 IgMλ, 4/4 FLCκ, and 15/15 FLCλ patients. UPEP, FLC, and IFE identified an additional IgGλ patient (highlighted with a green box), while UPEP, FLC, and HLC identified clonality in an IFE negative patient (highlighted with a red box).

IFE-Assigned Clonality	n	FLC	HLC	UPEP	IFE	FLC+IFE	UPEP+IFE	FLC+HLC	UPEP+FLC+IFE	UPEP+FLC+HLC
FLCκ	4	4	3	4	4	4	4	4	4	4
FLCλ	15	15	7	12	15	15	15	15	15	15
IgAκ	3	2	2	3	3	3	3	3	3	3
IgAλ	8	6	7	7[a]	8	8	8	8	8	8
IgGκ	7	5	6	7[b]	7	7	7	7[d]	7	7
IgGλ	21	18	19	19[c]	21	21	21	19[e]	21	20
IgMκ	2	1	2	1	2	2	2	2	2	2
IgMλ	2	1	2	1	2	2	2	2	2	2
IFE Negative	30	25	9	17	0	27	17	27	27	28
Total	92	77	57	71	62	89	79	87	89	89

[a] 2/7 positive for IgAλ and negative for BJP
[b] 2/7 positive for IgGκ and negative for BJP
[c] 3/19 positive for IgGλ and negative for BJP
[d] IFE identified IgGκ; FLC and UPEP identified a λ-clone, highlighting the difficulty in interpreting IFE when dealing with subtle clones
[e] Biclonal patient (IgGλ/IgAκ); IFE missed IgAκ clone; HLC identified both clones

DISCUSSION

SPEP and IFE are highly skilled techniques and require time and interpretation to determine clonality; this is particularly the case in diseases of subtle expression such as AL amyloidosis. A rapid automated addition to electrophoresis techniques would be a valuable tool and would obviate the need for interpretation. Here we report on a screening algorithm using automated nephelometric assays for the identification of intact immunoglobulin clones. The HLC measurements and the inferred ratios can identify and quantify low level M production in patients with AL amyloidosis, including those with multiple clones. Additionally, abnormal HLC ratio identified 1 patient in whom no clonal abnormality was detectable by traditional tests. An algorithm utilizing HLC, FLC, and UPEP achieved the same sensitivity as the traditional tests and may be a quantitative alternative. Further work is required to assess the utility of HLC assays compared to bone marrow assessments and in patient monitoring.

REFERENCES

1. Dispenzieri, A., Kyle, R., Merlini, G., Miguel, J.S., Ludwig, H., Hajek, R., *et al*. International Myeloma Working Groups guidelines for serum-free light chain analysis in multiple myeloma and related disorders. *Leukemia*, 2009;23:215-224.
2. Basic-Jukic, N., Kes, P., and Labar, B. Myeloma kidney: Pathogenesis and treatment. *Acta Med Croatica*, 2001;55:169-175.
3. Bradwell, A.R., Harding, S.J., Fourrier, N.J., Wallis, G.L., Drayson, M.T., Carr-Smith, H.D., and Mead, G.P. Assessment of monoclonal gammopathies by nephelometric measurement of individual immunoglobulin kappa/lambda ratios. *Clin Chem,* 2009;55:1646-1655.

Identification of factors contributing to poor outcomes in patients with AL amyloidosis with high serum free light chain concentration at diagnosis

C.D. Gunasekera, T.A. Ariyanayagam, J.D. Gillmore, S.D.J. Gibbs, J.H. Pinney, C.P. Venner, D. Foard, L. Rannigan, T. Lane, C.J. Whelan, H.J. Lachmann, P.N. Hawkins and A.D. Wechalekar

Centre for Amyloidosis and Acute Phase Proteins, University College London Medical School, London, UK

BACKGROUND

Systemic AL amyloidosis is caused by deposition of misfolded free immunoglobulin light chains. Most patients have an underlying plasma cell dyscrasia. Risk stratification of AL amyloidosis is difficult. Cardiac biomarkers, N-terminal fragment of brain natriuretic peptide (NT-proBNP) and cardiac troponin-T, form a valuable staging system for AL amyloidosis. Serum free light chain level at presentation is also an independent prognostic marker and the Mayo group have recently proposed a revised staging system which incorporates free light chains along with cardiac biomarkers. In patients with myeloma, the light chain level correlates, to a degree, with the plasma cell burden and in monoclonal gammopathy of uncertain significance, with a higher risk of disease transformation. In patients with systemic AL amyloidosis, although the free light chains are an independent prognostic marker, the mechanism by which the light chain burden contributes to the poor prognosis – rapid disease progression or poor response to therapy or other mechanisms – remains unclear.

We report the outcomes of patients with systemic AL amyloidosis presenting with high serum free light chains at the UK National Amyloidosis Centre.

PATIENTS AND METHODS

This retrospective study was done at the National Amyloidosis Centre (NAC), London, UK. It included all patients in the NAC database seen between July 2007 and December 2011 who had presenting involved serum free light chain (iFLC) > 500 mg/L. The presence of systemic amyloidosis was confirmed by characteristic Congo red staining and birefringence in a tissue biopsy. Amyloid of AL type was confirmed by immunohistochemistry with staining by appropriate antibodies and absence of mutation in genes for hereditary amyloidosis. The organ involvement was defined according to the 2005 amyloidosis consensus criteria, with the additional use of 123I-labeled serum amyloid P component (SAP) scintigraphy. Responses were defined as per 2010 revised consensus criteria. Patients were seen at the NAC for initial diagnostic evaluation and at then followed up at 6 monthly intervals. The treatment was given at the referring hospitals at the discretion of the referring haematologist.

RESULTS

A total of 95 patients were included in this study.

The median age of the patients at diagnosis was 65 years (range 59–90). The organ involvement was: cardiac in 61 (64.2%), renal in 68 (71.6%), and liver in 21 (22.1%). 20 out of 42 (47%) patients with baseline bone marrow data had >10% plasma cell infiltration. Baseline Mayo staging was: stage 1 – 7%, stage 2 – 35% and stage 3 - 58%, compared with stages 1/2/3 of 18%, 42% and 40% respectively in the ALchemy prospective cohort of patients with all levels of iFLC included.

Table 1. Organ Involvement

Organ Involved	**Cardiac**	**Kidney**	**Liver**
N (%)	61 (64.2%)	68 (71.6%)	21 (22.1%)

At diagnosis, the median NT-proBNP was 715 pMol/L (range 13 - 12945) and the median creatinine was 115 µmol/L (range 35 - 1124).

Table 2. Mayo Stage (1)

Mayo Stage	**1**	**2**	**3**
Current High iFLC Cohort	7%	35%	58%
Alchemy Cohort (2)	18%	42%	40%

81 patients were included in an intention to treat analysis, of whom 5 died or became too ill to proceed. On an intention to treat basis, 28 out of 81 (34%) patients achieved haematological response – 16 out of 81 (20%) with very good partial response (VGPR) or complete response (CR). This overall response rate and CR/VGPR rate was much less than we reported in our unselected Alchemy cohort where the overall response rate was 57% and VGPR/CR of 33%.

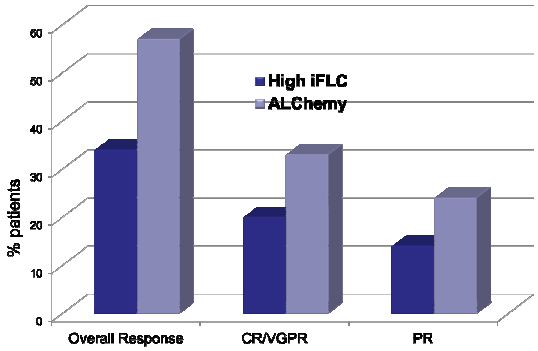

Figure 1. Haematological response to chemotherapy.

Patients with high presenting FLC have a double hit - greater abundance of the amyloid fibril precursor protein and inferior treatment responses – possibly contributing to poor outcomes in this group of patients. The median overall survival for all patients in our study group was 18 months (Figure 2A). Patients with cardiac involvement

had significantly worse outcomes (Figure 2B); the median survival time for patients with cardiac involvement was 12 months, and for patients without cardiac involvement, the median was not reached (Figure 2C). The two year survival for cardiac involvement and without cardiac involvement was 39% and 68% respectively (p=0.011). The median survival for patients who showed a haematological response to chemotherapy was 33 months, whereas non-responders had a median survival of 4.5 months (p<0.0001) (Figure 2D). Median survival for Mayo stage 1 and 2 versus Mayo stage 3 was 25 months and 8 months respectively (p=0.002)

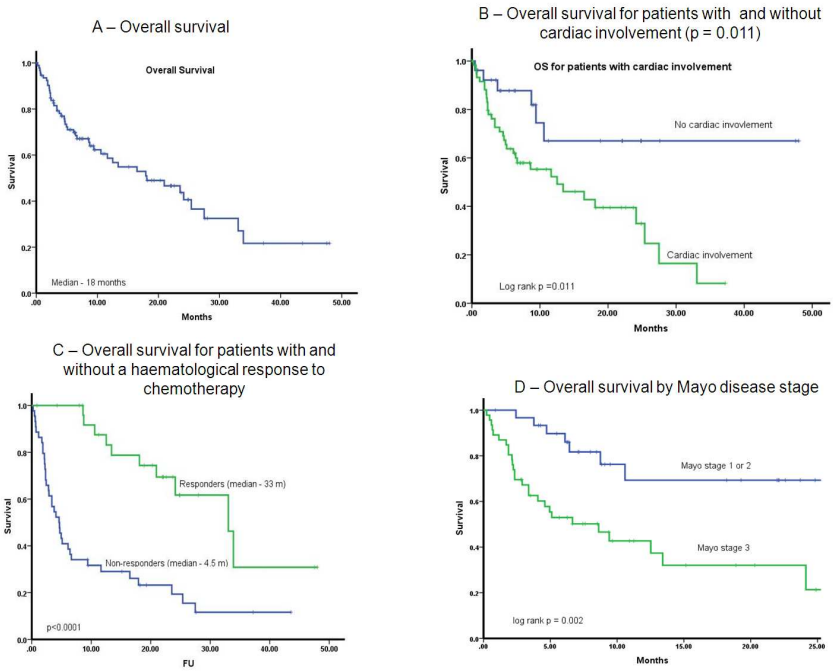

Figure 2. Survival Curves

CONCLUSION

A high proportion of patients presenting with iFLC >500 mg/L have stage 3 disease and higher bone marrow plasma cell burden. Compared to serial unselected AL patients, there is a 20% increase in stage III disease in those high iFLC and very few such patients present in early stage disease. The abundant precursor may lead to rapid amyloid accumulation accounting for quick progression to advanced disease. The higher clonal burden may be associated with resistance to treatment with only a third of the patients achieving a clonal response.

REFERENCES

1. Serum cardiac troponins and N-terminal pro-brain natriuretic peptide: a staging system for primary systemic amyloidosis. *Dispenzieri A, Gertz MA, Kyle RA, Lacy MQ, Burritt MF, Therneau TM, Greipp PR, Witzig TE, Lust JA, Rajkumar SV, Fonseca R, Zeldenrust SR, McGregor CG, Jaffe AS*. J Clin Oncol. (2004) 15;22
2. ALchemy - A Large Prospective 'Real World' Study of Chemotherapy in AL Amyloidosis. *Lane Thirusha; Rannigan Lisa; Foard Darren; et al.* BLOOD (2011*)* 118;21

Refinement in Patient Selection to Reduce Treatment-Related Mortality from Stem Cell Transplantation in Amyloidosis

M.A. Gertz, M.Q. Lacy, A. Dispenzieri, S.K. Kumar, D. Dingli, N. Leung, W.J. Hogan, F.K. Buadi, S.R. Hayman

Division of Hematology (Drs Gertz, Lacy, Dispenzieri, Kumar, Dingli, Leung, Hogan, Buadi, and Hayman), Division of Clinical Biochemistry and Immunology (Dr Dispenzieri), Department of Molecular Medicine (Drs Dispenzieri and Dingli), and Division of Nephrology and Hypertension (Dr Leung), Mayo Clinic, Rochester, Minnesota

ABSTRACT

We developed guidelines for patient selection for SCT in AL. Patients were reviewed in 2 cohorts: those who underwent transplantation before and after July 1, 2009. A second comparison was undertaken among patients who died before day 100. There were 410 in the earlier group and 89 in the later group. After July 1, 2009, fewer transplant recipients had Mayo stage III cardiac involvement. Mortality through day 100 was 10.5% (43/410) in the earlier group and 1.1% (1/89) in the later group. One-quarter of patients with NT-proBNP > 5,000 pg/mL, died by 10.3 months. When the serum troponin T level was > 0.06 ng/mL, 25% died at 3.7 months. Mayo staging is predictive for survival but not useful for selecting transplant recipients. Patients with serum troponin T levels > 0.06 ng/mL or NT-proBNP levels > 5,000 pg/mL (not on dialysis) should not be considered acceptable candidates for stem cell transplantation.

INTRODUCTION

Immunoglobulin light chain amyloidosis results from the deposition of immunoglobulin fragments in visceral organs. The deposition of amyloid fibrils leads to dysfunction of the organs and the death of the patients. When stem cell transplantation was introduced, few effective alternative treatments were available. At that time, combination therapy with melphalan and prednisone was the primary non transplant option, with median survival of only 18 months. In the single prospective randomized study, stem cell transplantation was not superior to conventional therapy with melphalan and dexamethasone. However, this study had serious patient selection issues insofar as the treatment-related mortality associated with transplant was 24%. A high mortality rate with stem cell transplantation is no longer acceptable because lower-risk alternatives, including lenalidomide-based and bortezomib-based therapies, have been introduced. Any attempt to advance the field of stem cell transplantation requires highly refined selection criteria so that patients can be offered stem cell transplantation safely. The purpose of this study was to determine the appropriate criteria for transplant centers

that see small numbers of these patients to identify those patients who can receive transplants without excessive risk.

PATIENTS & METHODS

The study performed 2 patient comparisons. Patients who received transplants between March 8, 1996, and June 30, 2009, were compared with those who received transplants between July 1, 2009, and December 31, 2011, to determine differences between the 2 groups. The second study compared all transplant recipients who died from any cause before posttransplant day 100 with those who survived beyond day 100 to determine features predictive of early death. The standard baseline evaluation of patients included immunofixation of serum and urine. An echocardiogram was performed in all. All transplant recipients received at least 1.98×10^6 CD34 cells/kg. Apheresis was performed by standard techniques. Patients were conditioned, infused, and monitored on an outpatient basis. Hospitalization occurred only in the event of a fever that could not be controlled with outpatient antibiotics, mucositis, or dehydration. Supportive care was standard for transplant after myeloablative. Growth factors were not administered after stem cell infusion. The criteria for hematologic and organ responses have been previously published. NT-proBNP and troponin levels were incorporated into organ response criteria, as defined by consensus, for patients for whom these values were available. Differences between groups were analyzed using the Kruskal-Wallis rank sum test for continuous variables and the Fisher exact test for discrete variables. All probabilities reported are 2-tailed. Significance was defined as $P<.05$. Survival was based on the Kaplan-Meier method.

RESULTS

Before July 1, 2009, 410 patients underwent autologous SCT. Forty-three of these patients died before posttransplant day 100 (10.5%). After July 1, 2009, 89 patients underwent transplantation, with 1 death before day 100 (1.1%). After July 1, 2009, there was a significant reduction in patients with Mayo stage III cardiac involvement, a slightly lower serum creatinine level, and a slightly lower pretreatment involved free light chain level. In the earlier group, the NT-proBNP level in the highest decile was > 6,537 pg/mL, whereas in the later group, the highest decile had an NT-proBNP level > 4,023 pg/mL, reflecting the increased reluctance of our group to perform transplants on patients with extreme elevations of NT-proBNP.

During this 30-month period, 6 patients with an NT-proBNP level higher than 5,000 pg/mL received transplants. Two of these patients, however, were on dialysis, which can have a profound effect on the level of NT-proBNP, and 1 of these 2 was not believed to have cardiac amyloidosis. Four of the 6 are alive, 1 having died 9.6 months after transplant of a severe upper gastrointestinal tract hemorrhage following dialysis, related to heparin administration. 43 patients who received their transplants before July 1, 2009, died before posttransplant day 100. These patients were compared with longer-term. The comparison revealed significant differences between the 2 groups in Mayo stage, clinically defined cardiac involvement, septal thickness, and levels of creatinine, troponin T, free light chain, albumin, and BNP. The NT-proBNP level was > 5,000 pg/mL in 41 patients. Their median survival was 27 months, but 10 (25%) of them had died by 10.3 months.

We reviewed the transplant recipients whose serum creatinine level was higher than 1.8 mg/dL and who were not on chronic stable dialysis at the time of transplantation. Thirty-four patients were identified, 5 of whom died

before posttransplant day 100. However, 21 of these patients are still alive. The median survival for the entire group has not been reached, and 60% were alive at 72 months, the longest now at 170 months.

Thirty-seven had troponin T levels higher than 0.06 ng/mL. Nine had died at 3.7 months, and at the time of this writing, 24 of 37 have died. The median survival of these patients with high troponin was 26.1 months. We identified 72 Mayo stage III patients in this study, and 31 (43%) survive at 5 years

DISCUSSION

The value of stem cell transplantation for the treatment of amyloidosis remains controversial. Its use is more common in the United States than in Great Britain, where only 1% of amyloidosis patients receive transplants. Investigators reviewed 421 patients and demonstrated a significant decline in treatment-related mortality over time. Mortality among 297 patients who received transplants between 1994 and 2003 was 13.8%. A similar group of 124 patients who received transplants from 2004 through 2008 had treatment-related mortality of 5.6%. This declining mortality is in accord with what we are currently seeing. They also noted that BNP levels were predictive of mortality at 100 days. To justify stem cell transplantation, criteria need to be established so that centers that see only a few of these patients annually can select those who can receive transplants. We believe that the criterion that would lead to exclusion of patients destined not to tolerate high-dose therapy is a serum troponin T level higher than 0.06 ng/mL. However, we now add the criterion of an NT-proBNP level higher than 5,000 pg/mL. We believe the mortality rates seen with an NT-proBNP level higher than 5,000 pg/mL make stem cell transplantation unacceptable. We do not believe the serum creatinine is a clear criterion for exclusion. The Mayo staging system is useful in predicting survival both in patients who receive high-dose therapy as well as standard-dose therapy at diagnosis. However, the cutoffs for the stages are serum troponin less than 0.035 ng/mL and NT-proBNP less than 332 pg/mL. Although these criteria clearly separate patients into 3 groups with very significant differences in survival, this does not mean that the Mayo amyloidosis staging system is a useful tool to select patients for stem cell transplantation. Patients with advanced cardiac amyloidosis are destined to do poorly. The early mortality rate for patients with amyloidosis seen at Mayo Clinic has not improved in nearly 40 years. Excluding patients with Mayo stage III from participation in clinical trial protocols or stem cell transplantation appears to be too stringent, and many patients who have moderate cardiac involvement may benefit stem cell transplantation. In this study, we identified 72 Mayo stage III patients, and 31 (43%) survive at 5 years. Clearly, the majority of patients that we would exclude from transplant selection would be Mayo stage III, but the converse is not true. The majority of patients with Mayo stage III disease can have a very good outcome after stem cell transplantation. Ten patients (11%) with Mayo stage III disease received transplants after July 1, 2009. Although the follow-up is short, the 1-year survival is 80% (8/10).

In conclusion, we believe the most rational approach is to exclude patients from transplantation based on their cardiac biomarker status, eliminating those patients whose troponin T is higher than 0.06 ng/mL or NT-proBNP level higher than 5,000 pg/mL. These patients should be considered for less toxic therapy.

REFERENCES

1. Dispenzieri A, Gertz MA, Kyle RA, et al: Prognostication of survival using cardiac troponins and N-terminal pro-brain natriuretic peptide in patients with primary systemic amyloidosis undergoing peripheral blood

stem cell transplantation. Blood 104:1881-7, 2004.

2. Reece DE, Hegenbart U, Sanchorawala V, et al: Efficacy and safety of once-weekly and twice-weekly bortezomib in patients with relapsed systemic AL amyloidosis: results of a phase 1/2 study. Blood 118:865-73, 2011.

Treatment And Outcome of 150 Patients With IgM-related AL Amyloidosis

M. Roussel[1,2], S. Gibbs [1], C. Venner [1], J. Pinney[1], S. Banypersad[1], J. Dungu[1], C. Whelan[1], H. Lachmann[1], J. Gillmore[1], P. Hawkins[1] and A. Wechalekar[1]

[1] Center for Amyloidosis and Acute Phase Proteins, University College London Medical School, UK.
[2] Haematology Department, CHU Purpan, Toulouse, France.

INTRODUCTION

Light chain amyloidosis is the commonest form of amyloidosis in the western world. Most patients with AL amyloidosis have an underlying clonal plasma cell dyscrasia. AL amyloidosis associated with IgM paraprotein is rare (5%) and is usually associated with Waldenström's macroglobulinaemia (WM) or low grade non-Hodgkin lymphoma (NHL) and only rarely with a plasma cell dyscrasia.

Response to alkylating agents is poor and there is no established standard of treatment. We report here the treatment and outcome of 150 patients with IgM-associated AL amyloidosis.

METHODS

This retrospective study was done at the National Amyloidosis Centre (NAC), London, UK. It included all patients in the NAC database who had a detectable IgM paraprotein. The presence of systemic amyloidosis was confirmed by characteristic Congo red staining and birefringence in a tissue biopsy. The organ involvement was defined according to the amyloidosis consensus criteria (1) with the additional use of 123I-labeled serum amyloid P component (SAP) scintigraphy (2). Responses were defined as per 2010 revised consensus criteria including dFLC response.

Patients were seen at the NAC for initial diagnostic evaluation and at then followed up at 6 monthly intervals. The treatment was given at the referring hospitals at the discretion of the referring haematologist.

RESULTS

A total of 150 consecutive patients were evaluated between 1988 and 2011, accounting for nearly 6 % of all patients with confirmed AL amyloidosis on the NAC database. There were 98 males and 52 females with a median age 66 yrs (range 46-89). The median number of organs involved was 2 (range 1-6). Amyloid was localized only to lymph nodes in 7 (5%) patients. Systemic AL amyloidosis requiring therapy was present in 137 (91%) patients. Underlying diseases and organ involvement are resumed in figure and table 1, respectively.

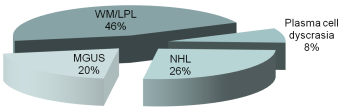

Figure 1. Underlying disorders

In the treated patients' cohort, all except 1 were evaluable for survival and 125 had available frontline regimen data. Six patients did not have time to receive any treatment. More than 90% were evaluable for haematological response. sFLC ratio was abnormal in 83/119 evaluable patients with baseline dFLC>50 in 66 (48%) cases. A variety of frontline chemotherapy regimen were used: oral Chlorambucil/Melphalan in 57 patients (46%), Rituximab-based chemotherapy in 28 (22%) including R-CVP in 9, FCR in 7, RCD in 5, R-CHOP in 3, Purine Analogs- based chemotherapy in 9 (7%) including Fludarabine in 5, FC in 4, CTD in 8 (6%), VAD in 8 (6%), CHOP or CVP in 5 (4%), High Dose Melphalan (HDM) with ASCT in 2 (2%) and CVD (bortezomib) in 2 (2%). Only 44 (35%) patients achieved hematologic response (≥PR); 41 (33%) had a PR, 1 (<1%) had a VGPR and 2 (<2%) had a CR. The 2 patients with CR were treated with CVD. Median time to next treatment was 10 months with a better outcome for frontline HDM.

Table 1. Organ involvement (%)

Renal	59
Heart	31
Liver (on SAP)	41
Lymph nodes	27%
Lung	5%

Considering all lines of therapy (>2 regimens in 60 patients), 47 patients received at some stage during their disease course Rituximab (R, R-CHOP, RCVP, RFC, RCD), 36 Purine Analogs (FC, RFC), 6 Bortezomib (CVD) and 5 HDM. 39 patients were mainly exposed to Multiple Myeloma (MM) like regimen (oral or IV Melphalan, CTD, VAD). Main treatment regimen exposure were: MM like chemotherapy in 39 patients (29%), R-CHOP or R-CVP in 23 (17%), FC in 16 (12%), FCR in 15 (11%), oral chlorambucil in 10 (7%), CVD (Bortezomib) in 6 (4%), HDM/ASCT in 5 (4%), and CHOP or CVP in 3 (2%).

Regarding response rates, 45 % of patients achieved hematologic and dFLC >PR including CR in 3 patients (2%; 2 CVD, 1 HDM), dFLC-VGPR in 6 (4%), PR in 48 (38%), and dFLC-PR in 27 (22%). Median follow-up from date of referral was 24 months.

Median OS (for the 150 patients) was 37 months (Fig. 2) with a survival advantage for patients receiving HDM, CVD (median OS not reached) and FCR (78 mo) compared to (R)CHOP/CVP, FC or MM like regimens (median OS 42, 31 and 32 months, respectively). The responders had a better survival with a median OS of 69 vs. 21 months for non responders (Fig. 3). There were too few patients in each chemotherapy group to further subgroup analysis.

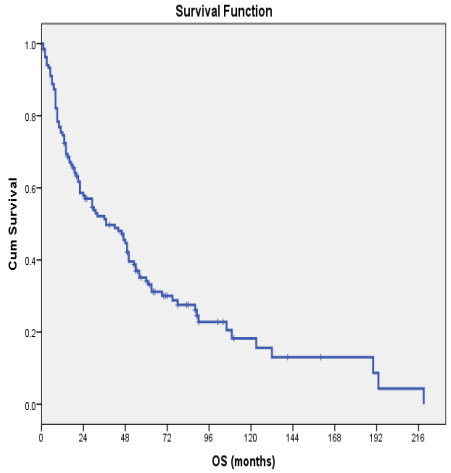

Figure 2. Overall survival

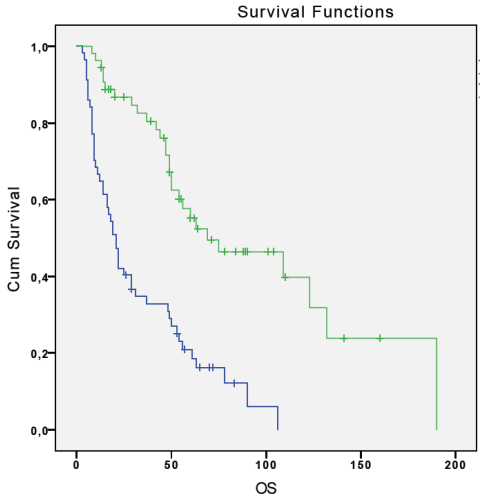

Figure 3. Overall Survival according to response

SUMMARY AND CONCLUSIONS

The presenting features of IgM associated amyloidosis are similar to amyloidosis with non-IgM paraprotein, though lymph node and lung involvement are more common. The response to “conventional” treatment used to be poor. There is no consensus about the best chemotherapy regimen, though patients treated at some stage during the disease course with bortezomib, HDM and FCR appear to have a survival advantage. New and novel combinations need to be studied into prospective studies to improve responses and survival.

REFERENCES

1. Gertz, M. A. *et al.* Definition of organ involvement and treatment response in immunoglobulin light chain amyloidosis (AL): a consensus opinion from the 10th International Symposium on Amyloid and Amyloidosis, Tours, France, 18-22 April 2004. *Am J Hematol* **79**, 319-328, (2005).
2. Hawkins, P. N., Lavender, J. P. & Pepys, M. B. Evaluation of systemic amyloidosis by scintigraphy with 123I-labeled serum amyloid P component. *N Engl J Med* **323**, 508-513, (1990).

Immunoglobulin D amyloidosis – a rare entity with a common phenotype

M. Roussel[1,2], S. Gibbs [1], C. Venner [1], J. Pinney[1], S. Banypersad[1], J. Dungu[1], C. Whelan[1], H. Lachmann[1], J. Gillmore[1], P. Hawkins[1] and A. Wechalekar[1]

[1] Center for Amyloidosis and Acute Phase Proteins, University College London Medical School, UK.
[2] Haematology Department, CHU Purpan, Toulouse, France.

INTRODUCTION

AL amyloidosis is caused by misfolding and deposition of particular monoclonal immunoglobulin (Ig) light chains as extracellular insoluble fibrillar deposits. The most common involved organs are the kidney, liver, heart and nervous system (1). AL amyloidosis is usually associated with clonal B-cell disorders (2). Many patients with AL have only a lambda light chain in the serum (27%). When a whole serum monoclonal component can be identified, it is much more commonly either IgG or IgA than IgM or IgD (3). Indeed, remarkably few patients with AL amyloidosis consequent on serum IgD paraprotein have been reported. Only 53 such patients were identified among the very large experience of AL amyloidosis at the Mayo Clinic over a 41-year period (4). In their series, IgD AL amyloidosis patients seem to have a distinct disease phenotype, with lower incidence of cardiac and renal involvement. Their overall survival does not appear to be different from other AL amyloidosis patients. The purpose of this review is to corroborate, within our experience, this particular phenotype.

METHODS

This retrospective study was done at the National Amyloidosis Centre (NAC), London, UK. It included all patients in the NAC database who had a detectable IgD paraprotein by electrophoresis and immunofixation. Although the recognition of IgD monoclonal component may be challenging, it is roughly a systematic assay, in our institution, in case of isolated FLC on immunofixation. The organ involvement was defined according to the amyloidosis consensus criteria (5) and Cardiac Mayo Clinic staging (6) with the additional use of 123I-labeled serum amyloid P component (SAP) scintigraphy (7). Responses were defined as per new amyloidosis criteria with dFLC evaluation. dFLC-VGPR was defined as a reduction of involved dFLC from baseline greater than 90%. Patients were seen at the NAC for initial evaluation and then followed up at 6 monthly intervals for evaluation of clonal disease and organ responses whenever possible.

RESULTS

Among 2861 patients with AL amyloidosis seen between 2000 and 2012, serum IgD monoclonal protein was isolated in 20 (0.7 %) patients with a majority of IgD lambda isotype (90%). There were 11 males and 9 females

with a median age of 64 years (51-84). Nine patients (45%) had underlying multiple myeloma of who 2 required specific therapy. Disease characteristics and laboratory findings are described in table 1.

A variety of frontline chemotherapy regimen were used: CTD in 7 patients (35%), VAD in 4 (20%), oral /IV melphalan in 3 (15%), high dose melphalan followed by ASCT in 3 (15%), and CVD (bortezomib) in 1 (5%). Four patients (20%) did not receive any treatment.

Overall haematological response rate was 56% in the 16 patients who received treatment with complete (CR) and partial (PR) responses reported in 5 (31%) and 4 (25%) patients, respectively.

Overall dFLC response rate was **63%** including dFLC-CR in 3 (19%) patients and dFLC-VGPR in 4 (25%) patients. Six (32%) patients needed further therapies for progressive disease.

Table 1. Disease characteristics and laboratory findings

ORGAN INVOLVEMENT	n, (%)
Renal	15, (75)
Heart	12, (60)
Mayo stage II/III	5/4, (25/20)
Liver (on SAP)	4, (20)
Peripheral Nerve	4, (20)
Autonomic Nerve	3, (15)
LABORATORY FINDINGS	Median, (range)
Serum IgD levels	1.5 g/L (1-3.5)
Serum lambda light chains levels	540 mg/L (53-6000)
Serum kappa light chains levels	387 mg/L (122-651)
24-hour proteinuria	2.8 g (0.5-14.8)
Albumin levels	33 g/L (19-47)
NT-proBNP levels	405 pMol/L (131-3558)
Troponin T levels	0.04 µg/l (0.01-0.19)
ALP levels	110 UI/L (44-203)

At data cut-off (10/01/2012), 14 over 20 (70%) patients are dead, of whom 7 (35%) died within 12 months of diagnosis. Median follow-up from referral was 22 months (2-93).

Although the estimated median overall survival (OS) was not significantly different between IgD and non-IgD patients (see Figure 1), the OS at 2 years was 39%, and 26% at 4 years for IgD patients compared to 46% and 37%, respectively for all non-IgD patients seen over the same time period.

Of note, 3 patients died at 30, 56 and 67 months from diagnosis, respectively, because of multiple myeloma progression for 2 of them and prostatic cancer for 1.

SUMMARY AND CONCLUSIONS

IgD associated AL amyloidosis is a rare occurrence, predominantly of the lambda subtype, that causes the typical amyloidosis disease. Compared to the Mayo Clinic cohort, higher proportion of patients presented with renal and cardiac involvement which, in our experience, is similar to non-IgD associated AL amyloidosis.

The haematological responses appear similar to non-IgD patients (8).

Early survival of IgD patients appears similar to that of non-IgD patients, probably related to the light chain, and not the complete M-protein, driving both the disease and prognosis as previously reported in AL amyloidosis (9).

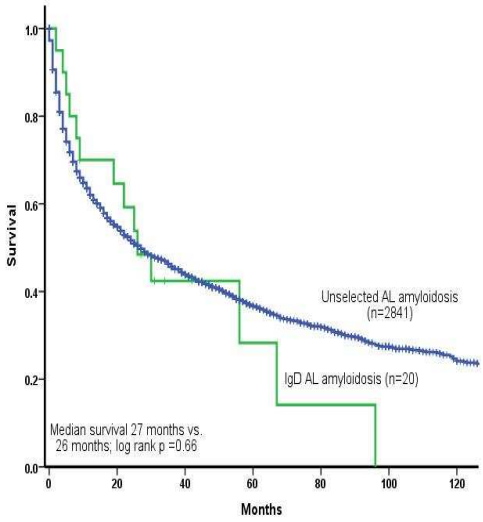

Figure 1. Overall survival

REFERENCES

1. Comenzo, R. L. How I treat amyloidosis. *Blood* **114**, 3147-3157 (2009).
2. Swan, N., Skinner, M. & O'Hara, C. J. Bone marrow core biopsy specimens in AL (primary) amyloidosis. A morphologic and immunohistochemical study of 100 cases. *Am J Clin Pathol* **120**, 610-616, (2003).
3. Kyle, R. A. & Gertz, M. A. Primary systemic amyloidosis: clinical and laboratory features in 474 cases. *Semin Hematol* **32**, 45-59 (1995).
4. Gertz, M. A. *et al.* Immunoglobulin D amyloidosis: a distinct entity. *Blood* **119**, 44-48, (2012).
5. Gertz, M. A. *et al.* Definition of organ involvement and treatment response in immunoglobulin light chain amyloidosis (AL): a consensus opinion from the 10th International Symposium on Amyloid and Amyloidosis, Tours, France, 18-22 April 2004. *Am J Hematol* **79**, 319-328, (2005).
6. Dispenzieri, A. *et al.* Serum cardiac troponins and N-terminal pro-brain natriuretic peptide: a staging system for primary systemic amyloidosis. *J Clin Oncol* **22**, 3751-3757, (2004).
7. Hawkins, P. N., Lavender, J. P. & Pepys, M. B. Evaluation of systemic amyloidosis by scintigraphy with 123I-labeled serum amyloid P component. *N Engl J Med* **323**, 508-513, (1990).
8. Wechalekar, A. D., Hawkins, P. N. & Gillmore, J. D. Perspectives in treatment of AL amyloidosis. *Br J Haematol* **140**, 365-377, (2008).
9. Kumar, S. *et al.* Serum immunoglobulin free light-chain measurement in primary amyloidosis: prognostic value and correlations with clinical features. *Blood* **116**, 5126-5129, (2010).

Stringent Patient Selection Improves Outcomes in Patients with AL Amyloidosis Undergoing Autologous Stem Cell Transplantation

Christopher P. Venner[1], Thirusha Lane[1], Darren Foard[1], Lisa Rannigan[1], Simon D.J. Gibbs[1], Jennifer H. Pinney[1], Carol J. Whelan[1], Helen J. Lachmann[1], Julian D. Gillmore[1], Murial Roussel[2], Philip N. Hawkins[1], Ashutosh D. Wechalekar[1]

[1]Centre for Amyloidosis and Acute Phase Proteins, University College London Medical School, UK
[2] Hématologie Clinique, CHU Purpan, Toulouse, France

ABSTRACT

Autologous stem cell transplantation (ASCT) in AL amyloidosis leads to both complete and durable responses. We report our experience with patients seen at the UK National Amyloidosis Centre who underwent transplantation after modern risks stratification. Median OS from time of ASCT was not reached. Median PFS was 27.6m. By intention-to-treat hematologic response rate was 80% (CR=28% and dFLC-VGPR=54%). CR and dFLC-VGPR correlated with superior PFS and OS. TRM was 6.8% (non-nephrotic patients=3.7%, nephrotic patients=12%). 2 patients become dialysis dependent both of whom had nephrotic syndrome. In patients whose baseline GFR was >45mL/min 11% had a post-ASCT GFR<45mL/min, one of whom required dialysis. One patient (13%) with baseline GFR<45mL/min required dialysis. ASCT remains an effective treatment option in AL amyloidosis. TRM has improved with more stringent patient selection. Depth of response positively impacts survival. Kidney injury remains a source of morbidity and should be considered when discussing high-dose therapy.

INTRODUCTION

Autologus stem cell transplantation (ASCT) is an effective treatment of AL amyloidosis leading to both complete and durable responses. Updated series have shown that a substantial proportion of patients may survive relapse free for greater than 8 years (1). Importantly, a significant improvement in transplant related mortality (TRM) has been observed with the advent of more stringent selection criteria and a better understanding of the intricacies involved in transplanting patients with amyloidosis. In properly selected patients who undergo the procedure at an experienced centre the TRM may be as low as 5-10%. Transplant related morbidity remains an area of concern. Of particular interest is the incidence of clinically significant renal impairment post-ASCT. Patients with amyloid, especially those with renal involvement are thought to possibly be at greater risk of renal injury both due to the organ involvement and increased sensitivity to the transplant procedure (2). Here we

report our experience with a cohort of patients with AL amyloidosis seen at the UK National Amyloidosis Centre who underwent risks stratification and transplantation in the modern era.

METHODS

We defined the modern era of transplantation from 2003-present and identified 88 patients who had undergone ASCT. > 2 organ involvement, ECOG > 1, eGFR ≤ 45mL/min, significant cardiac involvement, autonomic neuropathy, gastrointestinal involvement and TnT ≥ 0.05 ng/mL were considered relative contraindications to transplant. Organ involvement was as per the 2005 criteria (3). 24% had cardiac involvement by echo criteria (mean ejection fraction = 61%). 93% of patients were ≤ Mayo stage II (4). 70% had renal involvement (10% pre-ASCT GFR<45mL/min) with 39% having nephrotic range proteinuria. 38% underwent transplantation upfront.

We aimed to assess the maximal response by 6 months (m). Haematologic and organ responses were defined as per the 2005 consensus criteria (3). The dFLC response (difference between the involved and uninvolved free light chain) was defined as the percent difference in the dFLC at the start of therapy and at response assessment and was considered assessable if the baseline dFLC was >50mg/L. A dFLC of 50-90% defined a partial response, and a dFLC of >90% defined a VGPR(5). Renal outcome as defined by the eGFR (by MDRD) at 12 m was also examined. Progression free survival (PFS) was determined from the date of ASCT. Overall survival (OS) was calculated from both diagnosis and time of ASCT. TRM was defined as death within 100 days of transplant. Statistical analysis was performed using SPSS version 19. Approval for analysis and publication was obtained from the institutional review board at the University College London, and written consent was obtained from all patients.

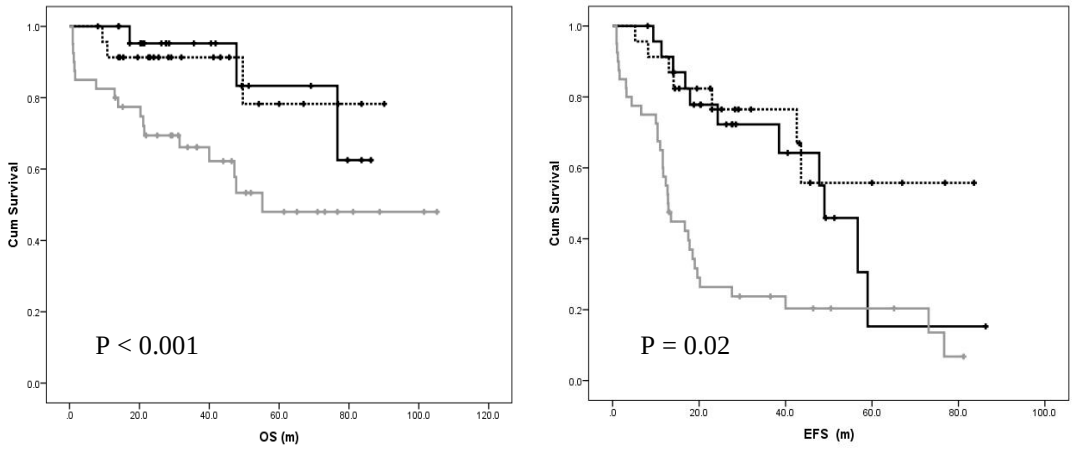

A. B.

Figure 1. Overall and event free survival in patients post-ASCT based on response. OS is shown in (A) and PFS in (B). Curves are separated based on CR (solid line), dFLC-VGPR (dashed line) and ≤ PR (grey line).

RESULTS

Median follow-up was 31.8 months (m). Median OS from time of ASCT was not reached and was 131.5m from diagnosis. Median PFS was 27.6m. There was no significant difference in PFS between upfront transplants and

those done at relapse (40.0m vs 27.6m respectively, p = 0.9). By intention-to-treat the overall hematologic response rate was 80% (CR=28% and dFLC-VGPR=54%). CR and dFLC-VGPR correlated with superior PFS and OS (figure 1). TRM was 6.8% (non-nephrotic patients=3.7%, nephrotic patients=12%). Renal responses were observed in 30%. 2 patients become dialysis dependent both of whom had nephrotic syndrome. In patients whose baseline GFR was >45mL/min 11% had a post-ASCT GFR<45mL/min, one of whom required dialysis. One patient (13%) with baseline GFR<45mL/min required dialysis.

DISCUSSION

ASCT remains an effective treatment option in AL amyloidosis. TRM has improved with more stringent patient selection. The response rates were comparable to what has been described previously and depth of response correlated with improved survival outcomes. In this highly selected group of patients the TRM was < 10%. Only 7 % of patients in this series would be classified as having Mayo stage III disease. There is a suggestion that pre-ASCT nephrotic syndrome and GFR < 45 ml/min may predispose patients to worse outcomes. These factors may decrease a patients reserve in dealing with known transplant related complications. That said the number of these patients in our series is small and thus these results should be interpreted with caution. However, given the more stringent patient selection criteria at most centres the likelihood of a large serried of such patients being compiled in the future is low. Irrespective, given the improved TRM, discussions regarding treatment related morbidity should be incorporated into the decision making process surrounding ASCT. Further trials are needed to assess the role of high-dose therapy in the modern era.

REFERENCES

1. Cibeira MT, Sanchorawala V, Seldin DC, Quillen K, Berk JL, Dember LM, et al. Outcome of AL amyloidosis after high-dose melphalan and autologous stem cell transplantation: long-term results in a series of 421 patients. Blood. 2011;118(16):4346-52.
2. Bird JM, Fuge R, Sirohi B, Apperley JF, Hunter A, Snowden J, et al. The clinical outcome and toxicity of high-dose chemotherapy and autologous stem cell transplantation in patients with myeloma or amyloid and severe renal impairment: a British Society of Blood and Marrow Transplantation study. British journal of haematology. 2006;134(4):385-90.
3. Gertz MA, Comenzo R, Falk RH, Fermand JP, Hazenberg BP, Hawkins PN, et al. Definition of organ involvement and treatment response in immunoglobulin light chain amyloidosis (AL): a consensus opinion from the 10th International Symposium on Amyloid and Amyloidosis, Tours, France, 18-22 April 2004. American journal of hematology. 2005;79(4):319-28.
4. Dispenzieri A, Gertz MA, Kyle RA, Lacy MQ, Burritt MF, Therneau TM, et al. Prognostication of survival using cardiac troponins and N-terminal pro-brain natriuretic peptide in patients with primary systemic amyloidosis undergoing peripheral blood stem cell transplantation. Blood. 2004;104(6):1881-7.
5. Pinney JH, Lachmann HJ, Bansi L, Wechalekar AD, Gilbertson JA, Rowczenio D, et al. Outcome in renal Al amyloidosis after chemotherapy. Journal of clinical oncology : official journal of the American Society of Clinical Oncology. 2011;29(6):674-81.

Ten Year Survival Following Autologous Stem Cell Transplantation for Immunoglobulin Light Chain Amyloidosis

S. Cordes[1], A. Dispenzieri[1,2], M.Q. Lacy[1,2], S. R. Hayman[1,2], F. K. Buadi[1,2], D. Dingli[1,2], S. K. Kumar[1,2], W. J. Hogan[1,2] and M. A. Gertz[1,2]

[1]Division of Internal Medicine Mayo Clinic, Rochester, MN 55904; [2]Division of Hematology, Mayo Clinic, Rochester, MN 55905.

ABSTRACT

To determine characteristics distinguishing the ten-year survivor group in patients with light chain amyloidosis (AL) who underwent autologous transplantation. The study group included all 74 AL patients who underwent high dose melphalan supported by autologous stem cell transplantation prior to August 2001. 32 (44%) patients survived for longer than 10 years. Statistically significant baseline differences in the ten-year survivor group include: (1) Number of Organs Involved, (2) Septal Thickness, (3) Total cholesterol, and (4) Urine total protein. The numbers of organs involved is the only predictor in multivariable analysis. Depth of the response to therapy, as measured by the lowest post-transplant serum free light chain, is the most significant indicator of durability of response. Autologous stem cell transplantation can offer durable benefit for AL patients. The number of organs involved offers the greatest pre-treatment prognostic value; lowest post-transplant serum free light chain offers the best post-treatment prognostic value.

INTRODUCTION

Systemic immunoglobulin (Ig) light chain (AL) amyloidosis is a plasma cell dyscrasia in which monoclonal light chain protein aggregates and deposits in tissue as amyloid fibrils. Only a relatively small proportion of immunoglobulin light chains are amyloidogenic, as is evidenced by the fact that amyloidosis occurs only in about 6 to 15% of patients with multiple myeloma

Treatments for amyloidosis have been targeted at reducing the concentration of the amyloidogenic light chain and have paralleled those used for multiple myeloma. Patients with amyloidosis differ from patients with other hematological malignancies in that they have impaired organ function with relatively normal bone marrow, which tends to be the reverse of what is found in patients with other hematological malignancies. This has implications in terms of the therapeutic window of many interventions. Since 1994 high-dose intravenous melphalan and autologous stem cell transplantation have joined the armamentarium in the treatment of amyloidosis[1]. The role of autologous stem cell transplants in the management of the Ig light chain amyloidosis remains controversial in part because of the fragility of the patient population. The objective of the current study is to highlight (a) the

validity of the transplant selection criteria and (b) the durability and long-term results of treatment.

.

MATERIALS & METHODS

All patients with AL amyloidosis who underwent autologous stem cell transplantation at the Mayo Clinic over the five-year interval from the beginning of our transplant program in July 1996 to July 2001 were included in this study (n=74). All patients underwent baseline evaluation, which included bone marrow biopsy, serum and urine electrophoresis and immunofixation, and serum light chain measurement. Amyloidosis was identified in biopsy specimens by positive Congo red staining. Eligibility criteria for autologous SCT were: (1) “physiological” age 70 years or younger; (2) ECOG performance score of 2 or less; (3) creatinine clearance of 30 mL/min or greater (unless on chronic dialysis); and (4) New York Heart Association classes I or II (unless on chronic dialysis). Prior to 2001 cardiac biomarkers were not routinely available as part of the eligibility criteria, but were performed on frozen sera when available[2].

Stem cell mobilization was accomplished with Sargramostim (GM-CSF) or Filgrastim (G-CSF). Apheresis was performed until a minimum of $2 \times 10(6)$ CD34+ cells/kg were collected. All patients underwent conditioning with high-dose melphalan prior to the autologous stem cell transplant. Hematological response to therapy was assessed by criteria from the consensus opinion of the 10th International symposium on Amyloid and Amyloidosis[3]. Statistical analyses were carried out with the R (version 2.13.0) and S-Plus (version 6.2) statistical software packages. The characteristics of the long-term survivor (LTS) and non-long-term survivor (NLTS) groups were compared using the Wilcoxon rank sum test. All probabilities reported are two-tailed; p-values < 0.05 were considered significant.

RESULTS

A total of 74 patients with AL who underwent autologous stem cell transplantation were included in the study. Forty-one patients (55%) were men; thirty-three patients (45%) were women. Patients were retrospectively divided into two groups: those surviving longer than 10 years, termed the long-term survivor (LTS) group (n=32); and those who did not, termed the non-long-term survivor (NLTS) group (n=42). The median (range) ages in the LTS and NLTS groups were 52.8 (37.4, 67.4) years and 55.2 (31.0, 69.9) years, respectively.

Four baseline characteristics were determined to be statistically different between the LTS and NLTS groups: (1) number of organs involved, (2) interventricular septal thickness, (3) total cholesterol, and (4) urine total protein.

Table 2 demonstrates the *post-therapy* characteristics of the study population. Only one characteristic was determined to be statistically different between the LTS and NLTS groups: the lowest post-SCT free light chain. To assess the importance of the four characteristics on survival, we fit the survival data to Cox proportional hazards models. On the basis of the criteria described in the methods section, the best fit to the survival data was found to be a Cox proportional hazards model with *number of organs involved* as the single covariate (predictor).

We computed the hazard ratios in the multivariate Cox proportional hazards model for all four characteristics. In the over-fit model, only the number of organs involved rises to the level of statistical significance.

DISCUSSION

This study demonstrates that response can be durable for AL patients who undergo HDM/SCT. Of the 74 patients who underwent HDM/SCT, 32 (44%) survived longer than 10 years.

Kidneys were the most commonly involved organs in AL patients who underwent SCT; renal involvement was present in 24 (67%) patients of the LTS group and 42 (62%) of patients of the NTLS group. The median serum cholesterol levels of the LTS group (329 mg/dL) were *higher* than those of the NLTS group (213 mg/dL), as were the total urine protein levels: 6.24 g/dL for the LTS group versus 3.07 g/dL for the NLTS group.

Cardiac involvement was the second most common organ involvement in AL, present in 9 (32%) patients of the LTS group and 11 (28%) patients of the NLTS group. The extent of cardiac infiltration as measured by septal thickness was lower in the LTS group (median 10 mm) relative to the NLTS group (median 13 mm). Systolic function is preserved in AL at least in the early stages of the disease. The median (range) number of organs involved in the LTS and NLTS groups were 1 and 2 , respectively.

In this study we have identified 4 baseline characteristics with statistically significant differences between the LTS and NLTS groups (ordered by statistical significance): (1) Number of Organs Involved, (2) Septal Thickness, (3) Total cholesterol, and (4) Urine total protein. The numbers of organ systems involved is the key prognostic characteristic: the median number of organ systems involved in the LTS group was 1, while that in the NLTS group was 2. Cardiac involvement, as assessed by septal thickness, possesses significant prognostic value that is however *subordinate* to numbers of organ systems involved. It should be noted that three of the patients in this study underwent kidney transplantation; two of these ended up as members of the LTS group; one patient ended up in the NLTS groups and was the recipient of both a cardiac and a renal transplant.

Depth of the response to therapy, as measured by the lowest post-transplant free light chain is the most significant leading indicator of *durability* of treatment. Unfortunately, since this cannot be assessed before therapy it has no predictive value in terms of selecting patients. It should be noted that NT pro BNP was available only in 34 of the 74 patients and therefore could not be systematically assessed for impact in this model even though the medians for the LTS and NLTS groups appear to be quite different.

The impact of serum and urine M proteins to survival was examined; no statistically significant differences were found.

REFERENCES

1. Gertz MA, Lacy MQ, Dispenzieri A, et al: Trends in day 100 and 2-year survival after auto-SCT for AL amyloidosis: outcomes before and after 2006. Bone Marrow Transplantation 46:970-975, 2011
2. Dispenzieri A, Kyle RA, Gertz MA, et al: Survival in patients with primary systemic amyloidosis and raised serum cardiac troponins. Lancet 361:1787-1789, 2003.
3. Palladini G, Dispenzieri A, Gertz MAA, et al: Validation of the Criteria of Response to Treatment In AL Amyloidosis. Blood 116:586-587, 2010

Updated Experience with Upfront Cyclophosphamide, Bortezomib and Dexamethasone (CVD) in the Treatment of AL Amyloidosis

Christopher P. Venner[1], Thirusha Lane[1], Darren Foard[1], Lisa Rannigan[1], Simon D.J. Gibbs[1], Jennifer H. Pinney[1], Carol J. Whelan[1], Helen J. Lachmann[1], Julian D. Gillmore[1], Murial Roussel[2], Philip N. Hawkins[1], Ashutosh D. Wechalekar[1]

[1]Centre for Amyloidosis and Acute Phase Proteins, University College London Medical School, UK
[2] Hématologie Clinique, CHU Purpan, Toulouse, France

ABSTRACT

Bortezomib combinations have shown great promise in the treatment of AL amyloidosis. Here we present an updated series of patients from the UK National Amyloidosis Centre treated with CVD in the upfront setting. The primary cohort comprises 30 patients referred between 2006-2011. Overall and progression free survival were examined as were haematologic, dFLC and organ responses. Overall hematologic response rate was 87% (CR = 63% and dFLC-VGPR = 68%). BNP responses were seen 38%. 3 deaths have been reported all in Mayo stage III patients. The estimated 1-year OS and PFS were 90% and 79% respectively. The 1-year PFS and OS for the Mayo stage III patients was 75% and 82% respectively. Attaining both a CR and dFLC-VGPR correlated with a improved PFS and OS. Upfront CVD is an effective treatment in AL amyloidosis.

INTRODUCTION

Bortezomib combinations have shown great promise in the treatment of AL amyloidosis. Prospective phase I/II data in relapsed patients has demonstrated high rates of response with or without dexamethasone(1). A number of retrospective series have shown unprecedented response rates with the addition of alkylating agents especially when the combination is used on the upfront setting(2, 3). Here we present an updated series of patients from the UK National Amyloidosis Centre treated with CVD as upfront therapy. We present data for response as well as progression free and overall survival.

METHODS

The primary cohort is a series of 30 patients referred to the National Amyloidosis Centre in London from January 2006 to March 2011. Organ involvement, hematologic and organ responses were defined as per the 2005 consensus criteria(4). The dFLC response was also examined as described previously(5). Median number of organs involved was 2.4 (1-6). 73% of patients had cardiac involvement by echo criteria. 77% had renal

involvement. Complete information for staging by the Mayo clinic criteria was available in 28 patients of which 57% were stage III.

The recommended CVD regimen was as follows: bortezomib 1.0 mg/m^2 IV days 1, 4, 8, 11 (increase to 1.3 mg/m^2 if well tolerated) cyclophosphamide 350 mg/m^2 po days 1, 8, 15 dexamethasone 20 mg po days 1, 4, 8, 11 (increase to 40 mg if well tolerated) with an aim to deliver 6 cycles of treatment. Dose modifications were at the discretion of the treating haematologist. We examined maximal response by 6 months (m).

RESULTS

Median follow-up was 12.2m. Median number of cycles given was 4.5 (1-8). All 30 patients were assessable by haematologic response criteria, 28 of whom were assessable for dFLC response. The time to maximal response was 3.5m. Overall hematologic response rate (RR) was 87% (CR = 63% and dFLC-VGPR = 68%). 23 patients were assessable for a BNP response based on a pre-treatment NT-proBNP > 660 ng/L. BNP responses were seen in 16 patients (38%). Organ responses were seen in 46% of patients (12% - cardiac, 41% - renal and 50 - liver).

3 deaths were reported. All had Mayo stage III disease and the deaths occurred within 6 months. The estimated 1-year OS was 90%. The median PFS has not been reached. The estimated 1-year PFS was 79%. Median PFS has not been reached. The estimated 1-year PFS was 79%. Attaining both a CR and dFLC-VGPR correlated with a significant improvement in PFS and OS (figure 1). The 1-year PFS and OS for the Mayo stage III patients was 75% and 82% respectively.

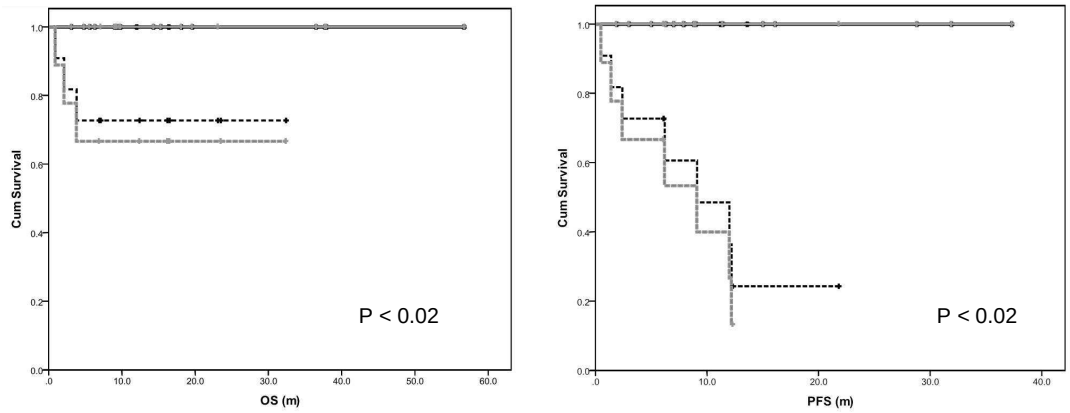

A. B.

Figure 1. Overall and event free survival post-upfront CVD based on response. OS is shown in (A) and PFS in (B). Curves are seperated based on CR (black solid line) vs non-CR (black dashed line), dFLC-VGPR (grey solid line) vs non-dFLC-VGPR (grey dashed line).

DISCUSSION

This retrospective series lends further support to the use of bortezomib containing regimens in the treatment of AL amyloidosis, especially in the upfront setting. CVD is a safe and effective treatment option supporting previous findings presented by our own group as well as others. In addition, it emphasizes the importance of attaining deep clonal responses to maximize outcome. Larger phase III studies are warranted and are underway.

REFERENCES

1. Reece DE, Sanchorawala V, Hegenbart U, Merlini G, Palladini G, Fermand JP, et al. Weekly and twice-weekly bortezomib in patients with systemic AL amyloidosis: results of a phase 1 dose-escalation study. Blood. 2009;114(8):1489-97.
2. Mikhael JR, Schuster SR, Jimenez-Zepeda VH, Bello N, Spong J, Reeder CB, et al. Cyclophosphamide-bortezomib-dexamethasone (CyBorD) produces rapid and complete hematologic response in patients with AL amyloidosis. Blood. 2012;119(19):4391-4.
3. Venner CP, Lane T, Foard D, Rannigan L, Gibbs SD, Pinney JH, et al. Cyclophosphamide, bortezomib, and dexamethasone therapy in AL amyloidosis is associated with high clonal response rates and prolonged progression-free survival. Blood. 2012;119(19):4387-90.
4. Gertz MA, Comenzo R, Falk RH, Fermand JP, Hazenberg BP, Hawkins PN, et al. Definition of organ involvement and treatment response in immunoglobulin light chain amyloidosis (AL): a consensus opinion from the 10th International Symposium on Amyloid and Amyloidosis, Tours, France, 18-22 April 2004. American journal of hematology. 2005;79(4):319-28.
5. Pinney JH, Lachmann HJ, Bansi L, Wechalekar AD, Gilbertson JA, Rowczenio D, et al. Outcome in renal Al amyloidosis after chemotherapy. Journal of clinical oncology : official journal of the American Society of Clinical Oncology. 2011;29(6):674-81.

Lenalidomide-dexamethasone in patients with relapsed light chain amyloidosis: previous high-dose chemotherapy does not impair response and survival

S. Dietrich, U. Hegenbart, T. Bochtler, AV. Kristen, H. Goldschmidt, AD. Ho, S. Schönland

University Hospital Heidelberg, Amyloidosis Centre, Heidelberg, Germany

Light chain amyloidosis (AL) is a lethal disorder that is caused by widespread deposition of amyloid fibrils derived from a malignant plasma cell clone. Survival of untreated patients is poor but could be successfully prolonged during recent years by conventional therapies such melphalan and Dexamethasone (M-Dex) and high dose melphalan (HDM) followed by autologous stem cell transplantation for eligible patients.(1-3) However, no plateaus of event free survival (EFS) and overall survival (OS) curves could be observed suggesting that relapses occur consciously.

The immunmodulatory drugs Thalidomide and its derivative Lenalidomide have been used with great success in multiple myeloma and were consequently evaluated in AL and have proven activity. However, tolerance of thalidomide in AL patients was inferior to that seen in patients with multiple myeloma (MM). Grade III–IV toxicity occurred in half of the AL patients and therapy with thalidomide could therefore not continued in more than 25% of patients.(4,5) Lenalidomide was evaluated with and without high dose dexamethsone.(6,7) In a first phase 2 trial lenalidomide was given at a dose of 25 mg/d, which was poorly tolerated.(7) The dose of lenalidomide was therefore reduced to 15 mg/d. Hematologic responses (HemeResp) were achieved in 67% of patients including 38% of patients with complete remission (CR).

We report a retrospective single center study of 62 patients who had relapsed after prior therapy and were therefore uniformly treated with lenalidomide and dexamethasone (LD).

PATIENT'S CHARACTERISTICS

The median age of 62 included patients was 61 (range 42-67) years. 14 patients were on hemodialysis at start of LD and 47 patients had heart involvement. Median Mayo Stage was 2. Twenty-nine patients had received previous high dose melphalan (HDM) and the number of previous therapy lines was 2 (range: 1-5).

TREATMENT

Lenalidomide treatment was initiated with 15 mg/d for 21 days of a 28-day cycle. The lenalidomide dose had to be reduced in 16 patients. Dosing of dexamethasone was determined by the treating physician based upon age and upon prior tolerance of dexamethasone (rage: 8 – 40 mg). Response was evaluated every 3 months. Therapy was stopped upon progressive disease. In total patients received a median of 5 cycles (range, 1-15).

RESULTS

Median overall survival (OS) for the entire group was 31 months (Figure 1) and median follow up was 39 months. Overall, 13 of 47 (27%) patients. responded already after 3 cycles and 18 of 36 (50%) responded after 6 cycles of LD leading to a significantly prolonged OS (p=0.04, HR 0.3).

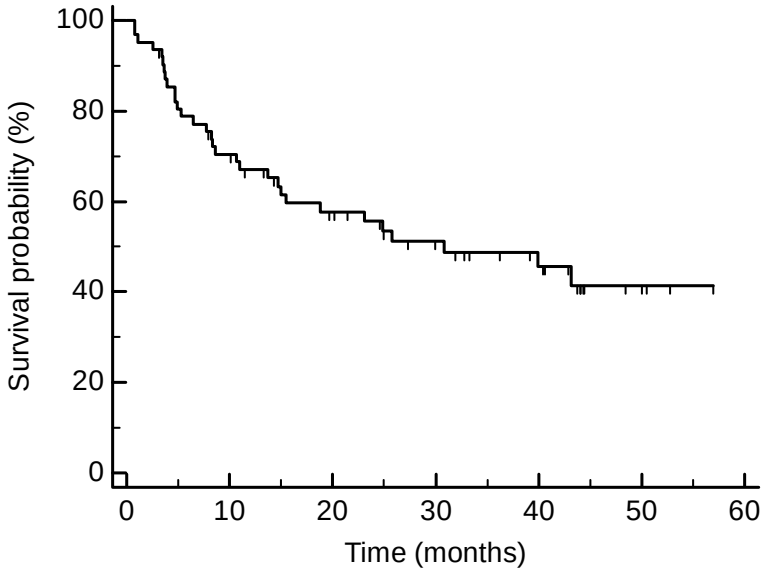

Figure 1. Overall survival

A multivariable logistic regression analysis for HR including the covariates: age, deltaFLC, previous HDM, number of previous therapy lines and creatinine clearance revealed by backward selection only dFLC as a borderline significant predictor for HR (p=0.13, OR 1.2). Therefore, previous HDM or number of previous therapy lines did not impair HR. Multivariable cox regression analysis revealed elevated NT-ProBNP levels, Karnofsky Index (KI), advanced age and high dFLC levels as significant predictors for OS (Table 1). In line with the results obtained for HR previous HDM as well number of previous therapy lines did not impact on OS.

Table 1. Multivaribale cox regression analysis for OS (n=56)

Covariates	P	HR	95% CI of HR
NT-ProBNP (>4400 ng/dl)	**0.0048**	**4.2005**	**1.5583 to 11.3223**
CreaCl (ml/min)	0.3193	0.9937	0.9815 to 1.0061
Age (years)	**0.0008**	**1.107**	**1.0491 to 1.2955**
Previous HDM	0.9169	0.9498	0.3627 to 2.4872
Number of previuos regimens (<2)	0.2573	0.5518	0.1983 to 1.5356
KI (increase of 10%)	**0.0010**	**0.9274**	**0.8871 to 0.9696**
deltaFLC (decrease of 100)	**0.0046**	**0.9120**	**0.9007 to 0.9852**

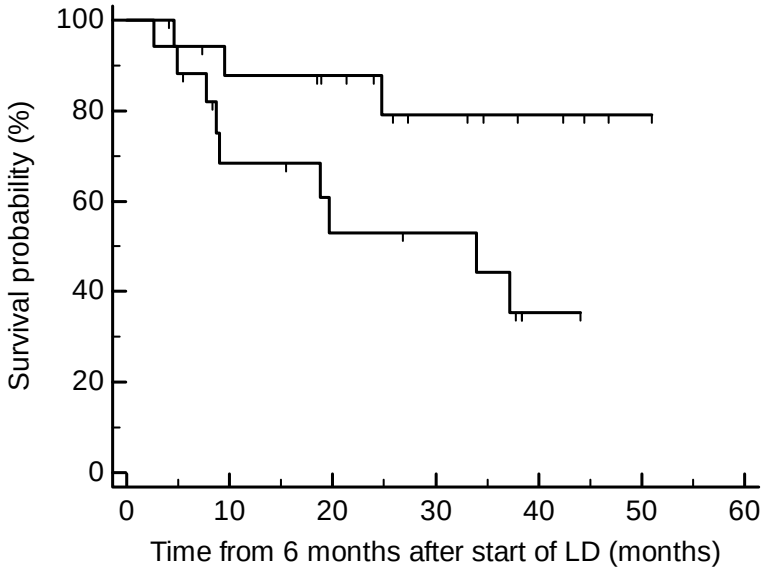

Figure 2. Responding patients have an improved OS (p=0.04, HR 0.3)

We observed that NT-ProBNP levels rose during therapy with LD (p=0.01). Among patients who received at least 3 cycles of LD an increase of NT-ProBNP was associated with a significantly reduced OS (p=0.03, HR 1.9).

SUMMARY

We could confirm that LD induces responses in a significant number of AL patients. Previous HDM seems not to impair response and survival after LD.

LITERATURE

1. Palladini G, Russo P, Nuvolone M, et al. Treatment with oral melphalan plus dexamethasone produces long-term remissions in AL amyloidosis. Blood. 2007;110(2):787-788.
2. Dietrich S, Schonland SO, Benner A, et al. Treatment with intravenous melphalan and dexamethasone is not able to overcome the poor prognosis of patients with newly diagnosed systemic light chain amyloidosis and severe cardiac involvement. Blood. 2010;116(4):522-528.
3. Skinner M, Sanchorawala V, Seldin DC, et al. High-dose melphalan and autologous stem-cell transplantation in patients with AL amyloidosis: an 8-year study. Ann Intern Med. 2004;140(2):85-93.
4. Palladini G, Perfetti V, Perlini S, et al. The combination of thalidomide and intermediate-dose dexamethasone is an effective but toxic treatment for patients with primary amyloidosis (AL). Blood. 2005;105(7):2949-2951.

5. Dispenzieri A, Lacy MQ, Rajkumar SV, et al. Poor tolerance to high doses of thalidomide in patients with primary systemic amyloidosis. Amyloid. 2003;10(4):257-261.
6. Moreau P, Jaccard A, Benboubker L, et al. Lenalidomide in combination with melphalan and dexamethasone in patients with newly diagnosed AL amyloidosis: a multicenter phase 1/2 dose-escalation study. Blood. 2010;116(23):4777-4782.
7. Sanchorawala V, Wright DG, Rosenzweig M, et al. Lenalidomide and dexamethasone in the treatment of AL amyloidosis: results of a phase 2 trial. Blood. 2007;109(2):492-496.

Early treatment has a significant impact on renal survival in light chain deposition disease (LCDD)

Econimo L[1], Gaggiotti M[1], Ravera S[1], Re A[2], Peli A[2], Tardanico R[3], Rossi G[2], Cancarini G[1], Gregorini G[1]

Dpt of Nephrology[1], Hematology[2], Pathology[3], Spedali Civili and University of Brescia.,Brescia, Italy

INTRODUCTION

Monoclonal immunoglobulin deposition diseases (MIDD) is a relatively new definition recently introduced in literature to collect , in the setting of the diseases related to monoclonal components, those that are caused by the deposition of monoclonal immunoglobulin in basement membranes. MIDD can be differentiated from AL amyloidosis, by the Congo negative and non-fibrillary nature of the deposits. MIDD include three subtypes, the light chain deposition disease (LCDD),the light and heavy chain deposition disease (LHCDD) and the heavy chain deposition (HCDD); LCDD is the most common subtype (1-6).

Renal involvement is almost always present in all the MIDD. Patients present with proteinuria (very often in nephrotic range), hematuria, hypertension (sometimes severe and difficult to treat) and renal insufficiency, often with a rapidly progressive course. Renal presentation strongly mimics primary glomerulonephritis. The high risk that MIDD rapidly lead to ESRD, if not rapidly recognized and treated, explains why the renal involvement should be considered the dominant factor in the prognosis of this group of diseases (1-6).

AIM, PATIENTS AND METHODS

Retrospective analysis of 15 cases of LCDD diagnosed and treated in our Center between August 2004 and December 2011: evaluation of renal survival in relation to the severity of renal involvement at the diagnosis and at the beginning of the treatment.

RESULTS

The study includes 15 pts (7 male; 8 female); the median age was 61.8 years (range 39.4-76.7 years). Four patients had severe extrarenal involvement: heart (3 patients, one of them with AL amyloidosis), liver (1 patient), skin (1 patient with cutis laxa). Three patients received a hematology diagnosis of multiple myeloma; only one had a symptomatic MM. All the 15 patients had a detectable monoclonal gammopathy (11 k, 4 λ).

Serum electrophoresis (SPEP) alone failed in revealing M-protein spike in 5/15 patients, urine electrophoresis (UPEP) alone in 8/15 patients, SPEP combined with UPEP did not reveal monoclonal component in 4/15 patients. Serum immunofissation (SIFE) failed in detecting monoclonal component in 3/15 patients, urine

immunofissatione (UIFE) in 1/15 patients, SIFE combined with UIFE in 1 patient. Serum free light chain assay, always performed since it was available, revealed a pathologic k/λ ratio in all the cases. A bone marrow biopsy was obtained in 13/15 patients: in two cases there was no evidence of monoclonal plasma cells.

At presentation all the patients had renal failure (median s-Creatinine 3.68 mg/dl; range 1.04-9.8 mg/dl) and proteinuria (median 4.15 g/24h; range 0.37-10 g/24h), 14 patients had significant microhematuria and 10 patients severe hypertension (HTA) (Table 1). A kidney biopsy was obtained in 14/15 cases (1 patient was diagnosed by a liver biopsy).

Table 1. General features of all the patients at presentation.

N°	*Diagnosis*	*Sex*	*Age at the diagnosis*	*Time from urine analysis alterations and diagnosis (months)*	*Cr/ClCr (mg/dl;ml/min)*	*Proteinuria (g/die)*	*Urine analysis*	*HTA*
1	*LCDD λ*	♀	*52,15*	*50,0*	*1,28/54*	*3,10*	*GR >20*	*yes*
2	*LCDD k*	♀	*61,30*	*1,9*	*5,4/ --*	*2,10*	*GR 5-10*	*yes*
3	*LCDD k*	♀	*40,49*	*2,0*	*1,4/42*	*3,80*	*10-20 GR*	*yes*
4	*LCDD k*	♂	*75,03*	*13,5*	*1,05/47*	*0,40*	*neg*	*yes*
5	*LCDD k*	♂	*76,72*	*12,2*	*3,9/14*	*10,00*	*GR rari*	*no*
6	*LCDD k*	♀	*61,97*	*1,8*	*1,14/--*	*6,00*	*GR rari*	*no*
7	*LCDD λ*	♀	*72,24*	*2,5*	*2,4/37*	*0,37*	*GR 10-20*	*no*
8	*cutis laxa+ LCDD λ*	♀	*39,44*	*0,8*	*9,8/5*	*4,09*	*GR>20*	*yes*
9	*LCDD k*	♂	*58,99*	*4,6*	*1,99/39*	*8,30*	*GR >20*	*yes*
10	*LCDD λ*	♂	*70,39*	*31,4*	*6,7/15*	*4,00*	*GR 5-10*	*yes*
11	*LCDD k*	♂	*63,58*	*1,2*	*5,9/10*	*0,80*	*GR 10-20*	*yes*
12	*AL+LCDD k*	♂	*57,16*	*4,6*	*1,04/88*	*8,60*	*GR>20*	*no*
13	*symptomatic MM+ LCDDk*	♀	*52,11*	*5,1*	*1,7/--*		*rare GR*	*no*
14	*asymptomatic MM+LCDD k*	♀	*70,24*	*2,8*	*4,2/10*	*6,00*	*5-10GR, rare GB*	*yes*
15	*asymptomatic MM+ LCDD k*	♂	*74,68*	*4,2*	*7,34/--*	*0,48*	*>20GR, 5-10 GB*	*yes*

Thirteen patients received hematology treatment (CyBorDex, MDex, Dex, VDex, VMDex, BDex, VAD, plasmapheresis); 4/13 patients underwent HDM/SCT. No patients experienced severe treatment related toxicities (Table 2).

Serum Creatinine at the diagnosis was <5 mg/dl (median 2.01; range 1.04-4.2 mg/dl) in 10/15 pts; nine of these patients received hematology treatment. Two patients died early as a consequence of severe extrarenal involvement, 1 patient achieved complete hematology response (CR) but renal disease progressed to ESRD, 6 patients improved or stabilized renal function (at the last follow-up visit median s-Creatinine 1.98 mg/dl; range 1-4.7 mg/dl) with normalization of urinalysis.

Serum Creatinine at the diagnosis was > 5 mg/dl (median 7.03; range 5.4-9.8) in 5/15 patients. Only one of the 4 treated patients recovered renal function and is off-dialysis. The other patients rapidly progressed to ESRD. Figure 1 shows the renal survival in patients with serum Creatinine > or < 5 mg/dl at presentation.

Table 2. Bone Marrow features at presentation, hematology treatment and relative response; follow-up features.

N°		*BMB biopsy at the diagnosis*	*hematologic therapy*	*HDM/ SCT*	*hematologic response*	*Follow-up*		
						months	*live yes/no*	*ESRD yes/no*
1	*LCDD λ*	*10-12% PC; λ restriction*	*CyBorDex (8 cycles)*		*PR*	*22,7*	*yes*	*no*
2	*LCDD k*	*8-10% PC; k restriction*	*MDex (6 cycles)*		*CR*	*51,9*	*yes*	*yes*
3	*LCDD k*	*15-20% PC*	*Dex (2 cycles)*	*yes (2)*	*CR*	*50,9*	*yes*	*no*
4	*LCDD k*	*5% PC; no restriction*	*Not done (severe comorbidity)*		*stable*	*9,7*	*no*	*no*
5	*LCDD k*	*3% PC; k restriction*	*MDex (3 cycles)*		*CR*	*44,7*	*yes*	*yes*
6	*LCDD k*	*nd*	*Dex*		*not evaluable**	*0,0*	*no*	*no*
7	*LCDD λ*	*10% PC; λ restriction*	*VMD (8 cycles)*		*CR*	*17,5*	*yes*	*no*
8	*cutis laxa+LCDD λ*	*6-7% PC; k restriction*	*PF+VDex (4 cycles)*	*yes (2)*	*CR*	*17,5*	*yes*	*no*
9	*LCDD k*	*25% PC; k restriction*	*VDex (4 cycles)*	*yes*	*CR*	*21,0*	*yes*	*no*
10	*LCDD λ*	*2-3% PC; no restriction*	*none*		*not evaluable**	*67,3*	*yes*	*yes*
11	*LCDD k*	*15-20% PC; k restriction*	*VDex (8 cycles)*		*relapse*	*21,2*	*yes*	*yes*
12	*AL+LCDD k*	*35-40% PC; λ restriction*	*yes*		*not evaluable**	*8,1*	*no*	*no*
13	*symptomatic MM+ LCDD k*	*>80% PC; k restriction*	*VAD (3 cycles)+ MDex (8 cycles) + VDex (8 cycles)*	*yes (2)*	*CR*	*89,4*	*yes*	*no*
14	*asymptomatic MM+ LCDD k*	*35-40% PC; K restriction*	*VDex (6 cycles)*		*PR*	*8,7*	*yes*	*no*
15	*asymptomatic MM+ LCDD k*	*nd (bone frailty). Myelocentesis:31%PC*	*VDex (0,5 cycles)*		*not evaluable**	*4,6*	*no*	*yes*

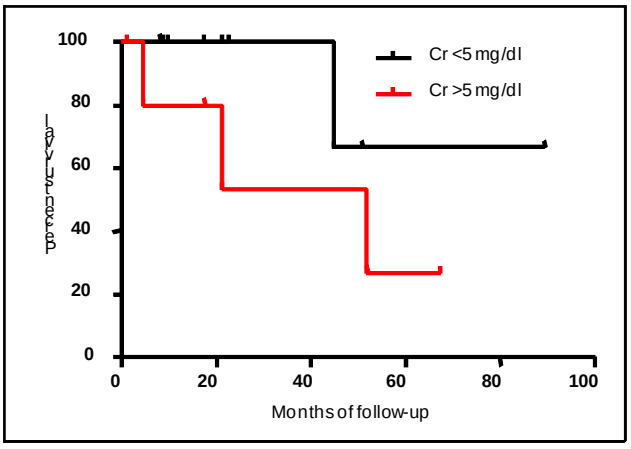

Figure 1. Renal survival in relation to serum Creatinine value at the diagnosis (red line: s-Cr > 5 mg/dl; black line: s-Cr < 5 mg/dl).

COMMENTS AND CONCLUSIONS

In LCDD patients serum Creatinine value at the diagnosis and immediately before the hematology treatment, is the main determinant of renal survival. In order to prevent ESRD, diagnosis should be done in the early phases of renal involvement. Therefore, because of the clinical presentation very similar in MIDD and in the primary glomerulonephritis, the extensive use of all the diagnostic test available to detect monoclonal component is recommended in the evaluation of all the patients with nephropathy. Hematology treatment should be started immediately; in our experience it has been effective free of major related toxicities.

REFERENCES

1. Bridoux F, Delbes S, Sirac C. et al. Renal disorders associated with monoclonal gammopathies: diagnostic and therapeutic progress. Presse Med. 2012 Mar;41(3 Pt 1):276-89.
2. Korbet SM, Schwartz MM, Lewis EJ. Immuotactoid glomerulopathy (fibrillary glomerulonephritis). Clin J Am Soc Nephrol. 2006 Nov;1(6):1351-6.
3. Nasr SH, Valeri AM, Cornell LD et al. Renal monoclonal immunoglobulin deposition disease: a report of 64 patients from a single institution. Clin J Am Soc Nephrol. 2012 Feb;7(2):231-9.
4. De Sanctis L, Sestigiani B, Sgarlato V., et al. Il coinvolgimento renale nelle gammopatie monoclonali e nel mieloma. G Ital Nefrol 2010; 27 (S50): 19-33.
5. Merlini G, Pozzi C. Mechanisms of renal damage in plasma cell dyscrasias: an overview. Contrib Nephrol 2007; 153: 66-86.
6. Jourde-Chiche N, Dussol B, Daniel L. Kidney involvement in hematologic malignancies. Diagnostic approach. Rev Med Interne. 2010 Oct;31(10):685-96.

Resolution of AL hepatic amyloidosis

R. Abonour[1], M.D. Benson[2]

[1]Department of Medicine HEM/Oncology, Indiana University School of Medicine, Indianapolis, IN USA
[2]Department of Pathology and Laboratory Medicine, Indiana University School of Medicine, Indianapolis, IN USA

ABSTRACT

Background: Treatment of AL amyloidosis is targeted to control of the offending plasma cell dyscrasia so that progression of amyloid deposition is stopped. Whether tissue amyloid can then be reduced and organ function restored is a question posed for each individual patient.
Objective: We report five patients who presented with massive hepatomegally and AL amyloid proven by liver biopsy. Patients were monitored from four to 27 years to evaluate response to chemotherapy aimed at control of the plasma cell dyscrasia.
Methods: Ages of subjects at time of diagnosis ranged from 45 – 67 years. All were male. Three patients also had renal involvement with nephrotic syndrome, one with advanced renal insufficiency. Four were treated with melphalan and corticosteroid, two oral medications, two IV melphalan with stem cell rescue.
Results: Liver size in each patient returned to normal in 24 – 36 months and repeat liver histology for three patients demonstrated decrease in amyloid, one with complete resolution. Survival was four to 27 years without recurrence of amyloid.
Discussion: Massive hepatomegally from AL amyloid deposition is associated with a grave prognosis. Unfortunately progressive enlargement of the liver is ignored or unappreciated by many patients. This results in delayed diagnosis and, therefore, seriously impacts treatment options. Even so, favorable response may be obtained in the patients with a plasma cell clone that is responsive to chemotherapy. Resolution of hepatic amyloid may be related to the high level of metabolic activity of this vascular organ.
Conclusion: These cases demonstrate that hepatic amyloid, even with massive hepatomegally, can resolve and normal liver function restored if the plasma cell clone responds to therapy.

INTRODUCTION

Massive hepatomegaly is a relatively uncommon presentation for immunoglobulin light chain (AL) amyloidosis. While as high as 35 percent of AL patients have hepatomegaly at time of diagnosis only 12 – 15 percent will have enlarged liver as chief reason for seeking medical evaluation. In these patients the diagnosis is almost always made by liver biopsy since the correct diagnosis is not entertained prior to histologic documentation.

Prognosis for the patient with massive hepatic amyloid is usually guarded despite the fact that liver function remains relatively normal until late stages of the disease. The amyloid is progressive and response to therapy is unpredictable. Even so, some patients may have favorable response to therapy targeted to control or ablate the offending plasma cell clone which produces the amyloid fibril precursor protein.

CASE STUDIES

Clinical data for 5 patients who presented with massive hepatic amyloidosis and had favorable response to chemotherapy are listed in Table 1.

Table 1.

CASE	AGE @ Dx	TYPE LC	LIVER SIZE(MCL)	LIVER FUNCTIONS	OTHER SYSTEMS	Rx	AGE NOW	YEARS SINCE Dx
1	47	K	12 cm Large LL	SGOT 56 AP 159 Cardio-green 18%*	Carpal Tunnel Syndrome	Melphalan & Prednisone X 2 yrs. + Colc;hisine	74	27
2	67	λ	15 cm	SGOT 53 Alb 1.8 AP>300 Cardio-green 26%*	Nephrotic syndrome resolved @ 6 mos.	Melphalan & Prednisone X 2 yrs. (20 months) + Col	71	4** until death from Leukemia
3	50	K	17 cm	AST 50 AP 631 Alb 1.3	Nephrotic syndrome Dialysis	Alkaline Phosphatase, Melphalan & Prednisone 10 Courses Stem Cell Dialysis	59	9
4	46	λ	22 cm	SGOT 67 AP 1406	Nephrotic syndrome resolved Vertebral collapse	Stem Cell Rituximab	58	12
5	62	λ	16 cm	SGOT 20 AP343	Peripheral Neuropathy Heart CHF Nephrotic syndrome	Melphalan & Dexamethazone Thalidomide Velcade & Doxil	66	4

RESULTS AND DISCUSSION

Initial diagnosis of amyloidosis for each subject was made by liver biopsy. In none was the correct diagnosis contemplated prior to the biopsy. This lapse in differential diagnostic access may be a result of specialty care where the physician fails to consider other organ dysfunction. Four of the 5 subjects in Table 1 had large amounts of proteinuria. Only case 1 had isolated hepatic disease. Combination of hepatomegaly, nephrotic syndrome with or without heart failure should raise a suspicion of AL amyloidosis.

Each of the subject responded to chemotherapy and liver size returned to normal limits. Decrease in amyloid infiltration was documented in 3 patients by repeat percutaneous biopsy and one patient had complete absence of hepatic amyloid 4 years after initial diagnosis. This patient died with acute leukemia most likely related to treatment with alkylating agent. The nephrotic syndrome remitted within 12 months of treatment and liver size was normal by 24 months.

Case 1 with isolated hepatic amyloid is of special interest. He had elevated serum free κ-light chains at time of diagnosis and 27 years later, while having no evidence of amyloidosis, still has moderately elevated serum free κ-light chains.

All subjects in this series received melphalan and prednisone/dexamethosone in some format. Some also received other therapeutic agents as thought clinically indicates. None was a subject of prospective during trial.

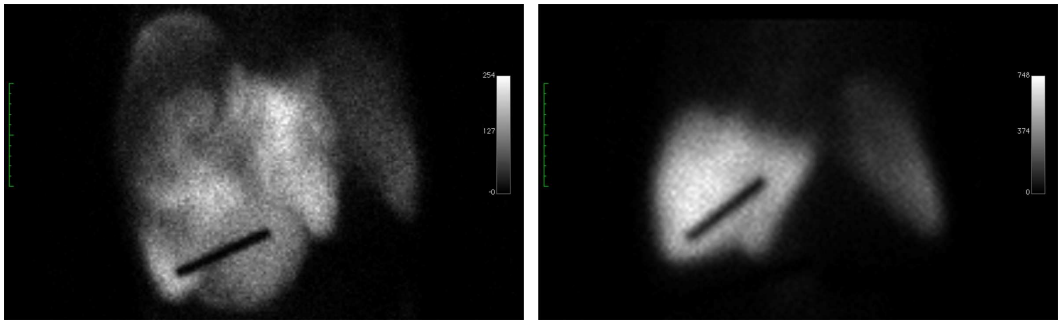

Figure 1. Case 4 – Liver scan at time of diagnosis (Left). Repeated after therapy (Right).

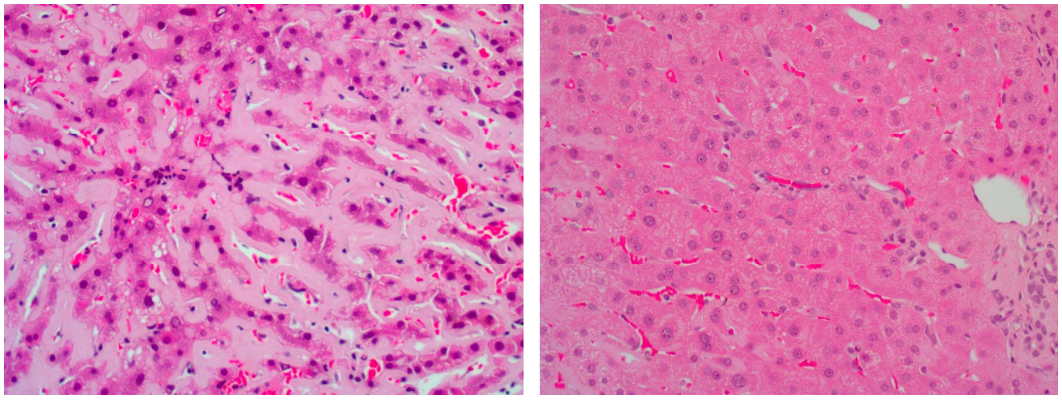

Figure 2. Case 3 – Liver biopsy at time of diagnosis (Left). 19 months later (Right).

CONCLUSIONS

1. Massive hepatic amyloidosis usually is associated with multisystem pathology.
2. While not predictable, treatment with chemotherapeutic agents may result in prolonged longevity.
3. Hepatic amyloid may completely resolve if therapeutic response is obtained.
4. Favorable response is probably related to unique drug sensitivity of offending plasma cell clone.

Case report: A 63-year-old man with AL amyloidosis presenting a predominant diffuse lymphadenopathy and a M-protein IgM κ

M. Di Girolamo (°) , M. Nowakowski (*)

(°) Dpt of Internal Medicine Fatebenefratelli Hospital – AFaR. Isola Tiberina Rome (Italy)
(*) Dpt of Internal Medicine "S. Giovanni di Dio" General Hospital. Melfi (Italy)

ABSTRACT

Systemic AL amyloidosis IgM manifesting with a generalized lymphadenopathy it is considered to have some clinical aspects similar to Waldenström macroglobulinemia (WM). However it is still a matter of debate whether these patients should receive or not the same chemotherapy regimens. We describe a long free survival of a patient with AL amyloidosis M-protein IgM unusually unresponsive to a prolonged chemotherapy and radiotherapy and discuss the possible cause.

INTRODUCTION

We performed a clinical review of some patients of our database with biopsy-proven AL amyloidosis, in order to evaluate the survival outcome [1-2], focusing upon the therapeutic strategy for the patients unresponsive to therapy [3-4].

Among these patients, we found a "*cold case*" of 15 years ago: a patient with IgM κ M-protein associated AL amyloidosis and a systemic lymphoadenopathy. The patient, nevertheless unusually unresponsive to a prolonged chemotherapy and radiotherapy, showed a favourable outcome, continuing to feel well during four years of follow up. For this reason we discussed the possible causes of his resistence to therapy.

METHODS

A 63-year-old man presented in 1990 an asymptomatic serum M-protein IgM κ. Four years later (1994) a palpable mass appeared in the laterocervical region. A CT scan showed very extensive lymphadenopathy (supraclavicular, axillary, mediastinal, thoracic, mesentheric, iliac, retroperitoneal, inguinal nodes) without predominance of any particular anatomical sites. There were no overt signs of organomegaly, macroglossia, neuropathy or nephropathy. Neither ECG nor echocardiography revelead any findings suggestive of amyloid heart disease. Bone marrow biopsy showed some aggregates of lymphoplasmacytoid cells and plasma cells (6%), without evidence of either leukemia, myeloma or WM. On a biopsy lymph node specimen (left laterocervical region), massive deposition of AL amyloid fibrils, positive for AL κ on immunohistochemistry,

subversiving lymph node structure (figure 1) was observed. Considering the M-protein present in serum and the finding of the small clonal cell expansion in the bone marrow, probably producing the precursor of immunoglobulin, the diagnosis was considered to be classificable as AL amyloidosis manifesting primarly as systemic lymphadenopathy.

The therapeutic approach, starting on 1994, consisted in a long-lasting chemotherapy for one year (cycles of Chlorambucil plus Prednisone, commonly employed in WM during past years) followed (1995-96) by a mantle field-radiotherapy (on the mediastinum and laterocervical, axillary lymph nodes) and on the inguinal lymph nodes. Clinical and instrumental controls were annually performed during the following four years from the diagnosis to evaluate the results of the therapy.

RESULTS

The patient showed a favourable outcome, continuing to feel well during four years of follow up, nevertheless unusually unresponsive to a prolonged chemotherapy and radiotherapy. The clinical and instrumental controls indicated no progression of disease, while CT imaging showed persistence of the systemic diffuse lymphadenopathy, unchanged nevertheless the radiotherapy. What would be the cause?

DISCUSSION

Amyloid fibrils deposition in AL amyloidosis, arising from immunoglobulin light chains usually occurs in visceral organs such as the heart and kidneys, while AL amyloidosis rarely shows lymphadenopathy as an initial and isolate manifestation [8-10] (in a frequency ranging from 17 to 37%).

The high rate of lymph-node involvement in small subgroup of patients with IgM-associated AL amyloidosis probably indicate that the light chains produced by the IgM clone of the plasma cells present a still undetermined biological peculiar tendency to deposit locally in the lymphatic system. These patients have characteristic clinical and laboratory features but it is no clear if that type of AL amyloidosis (IgM-associated) may be considered a distinct clinical entity, different from other AL type.

It has been proposed that, similarly to that observed in non-IgM patients with AL amyloidosis, these patients should be treated with the same chemotherapy regimens commonly used for other AL Amyloidosis or WM [6]. The retrospective studies of the hematologic response to chemotherapy regimens commonly applied in these patients indicate moreover a greatly improved survival [7].

In our patient, the CT control, during the following four years, irrespectively of the persistence of the M-protein, showed no obvious change in the size of lymph nodes, with clinical conditions persistently good and lab analyses in the normal range (table 1). There was not any therapeutic response on the extensive systemic lymph node involvement, after 12 cycles of chemotherapy and a intensive radiotherapy.

Our hypothesis is that this result could have been probably related to the diffuse and quick lymph nodes amyloid structural subversiving, instead of a refractory hematologic response.

CONCLUSIONS

Systemic amyloidosis can occur rarely as multiple masses with replacement of lymph nodes, causing lymphadenopathy, so all the retrospective studies on IgM associated AL amyloidosis are limited by the low number of patients [8-10].

This particular type of AL amyloidosis, presenting with M-protein IgM and systemic lymphadenopathy appear to have a better prognosis compared to WM. This feature could be partially explained with the extensive deposition of the fibrils in the lymph nodes, obviously not responding to traditional chemo/radiotherapy which could appear to be poorly efficacious or even sometimes useless.

We therefore suggest that between the prognostic factors of the AL amyloid patients with systemic lymphadenopathy should be carefully considered also the histological entity or grading of fibrillar amyloid lymph nodal deposition explaining the “lymph node unresponsiveness” to the therapy. Only an appropriate work-up in the follow up procedure should be undertaken to minimize the risk of a potential pitfall about the best therapeutic choice, and in the better interpretation of the data for the overall survival studies.

Table 1 Laboratory data

		1993 Jul	1994 Apr	1996 Mar	1996 Nov	1997 Nov	1998 Apr
Tot. proteins	*g/dl*	**7,7**	**7,7**	**7,4**	**6,8**	**6,5**	**6,4**
Albumin	*g/dl*	**4,08**	**3,69**	**3,72**	**3,64**	**3,64**	**3,59**
γ-globulin	*g/dl*	**2,69**	**2,59**	**1,79**	**1,53**	**1,44**	**1,37**
CM	*g/dl*		**2,05**		**1,5**	**1,4**	
IgG	*mg/dl*		**1148**	**864**	**850**	**932**	**870**
IgA	*mg/dl*		**139**	**135**	**105**	**115**	**120**
IgM	*mg/dl*		**2807**	**2236**	**1770**	**1743**	**1801**
VES	mm/h	**110**		**76**		**70**	
Creatinine	*< 1.3 mg/dl*	**0,9**	**0,9**	**0,9**	**0,9**	**0,90**	**1,0**
Glucose	*60-110 mg/dl*	**70**	**91**	**82**	**88**	**85**	**85**
Uric acid	*3.4 -7 mg/dl*	**5,7**	**5,2**	**4,3**			**5,6**
W.B.C	x mm^3	**6200**	**8100**	**10500**	**5000**	**6200**	**6100**
Hb	g/dl	**12,6**	**12,1**	**12,5**	**12,1**	**11,3**	**11,8**
Platelet	x mm^3	**209000**	**191000**	**227000**	**244000**	**135000**	**149000**
ALT	*10-50 U/l*	**14**	**14**	**17**	**13**		**25**
Alkaline Ph.	*56-270U/l*	**136**	**138**	**147**			**56**
γ GT	*10-66 U/l*	**6**	**9**	**7**			**15**
Lactate DH	*240-480 U/l*	**330**	**307**	**247**	**263**	**316**	**426**
Calcium	*8.8-10.2 mg/dl*		**8,8**	**8,8**	**9,0**		**8,0**

REFERENCES

1. Gertz MA, Kyle RA, Noel P. Primary systemic amyloidosis: a rare complication of immuno-globulin M monoclonal gammopathies and Waldenstrom's macroglobulinemia. J Clin Oncol 1993; 11:914-20.
2. Terrier B, Jaccard A, Harousseau JL, et al. The clinical spectrum of IgM-related amyloidosis: a French nationwide retrospective study of 72 patients. Medicine (Baltimore) 2008; 87:99-109.

3. Wechalekar AD, Lachmann HJ, Goodman HJ, Bradwell A, Hawkins PN, Gillmore JD. AL amyloidosis associated with IgM paraproteinemia: clinical profile and treatment outcome. Blood 2008; 112:4009-16
4. Merlini G and Palladini G. Amyloidosis: is a cure possible? Ann Oncol 2008; 19 Suppl 4:iv63-6.
5. Gertz MA, Comenzo R, Falk RH, et al. Definition of organ involvement and treatment response in immunoglobulin light chain amyloidosis (AL): a consensus opinion from the 10th International Symposium on Amyloid and Amyloidosis, Tours, France, 18-22 April 2004. Am J Hematol 2005; 79:319-28.
6. Dimopoulos MA, Gertz MA, Kastritis E, et al.. Update on treatment recommendations from the Fourth International Workshop on Waldenstrom's Macroglobulinemia. J Clin Oncol. 2009 120-126.
7. Merlini G, Baldini L, Broglia C, et al. Prognostic factors in symptomatic Waldenstrom's macroglobulinemia. Semin Oncol 2003; 30:211-5.
8. Matsuda M, Gono T et al. AL amyloidosis manifesting as systemic lymphoadenopathy Amyloid, June 2008; 15(2): 117-124
9. Ko HS, Davidson JW, Pruzanski. Amyloid lymphoadenopathy. Ann Intern. Med. 1976; 85: 763-764
10. Newland JR, Linke RP, Kleinsasser O. Lymph node enlargement due to amyloid . Virchow Arch. A. 1983; 399:233-236

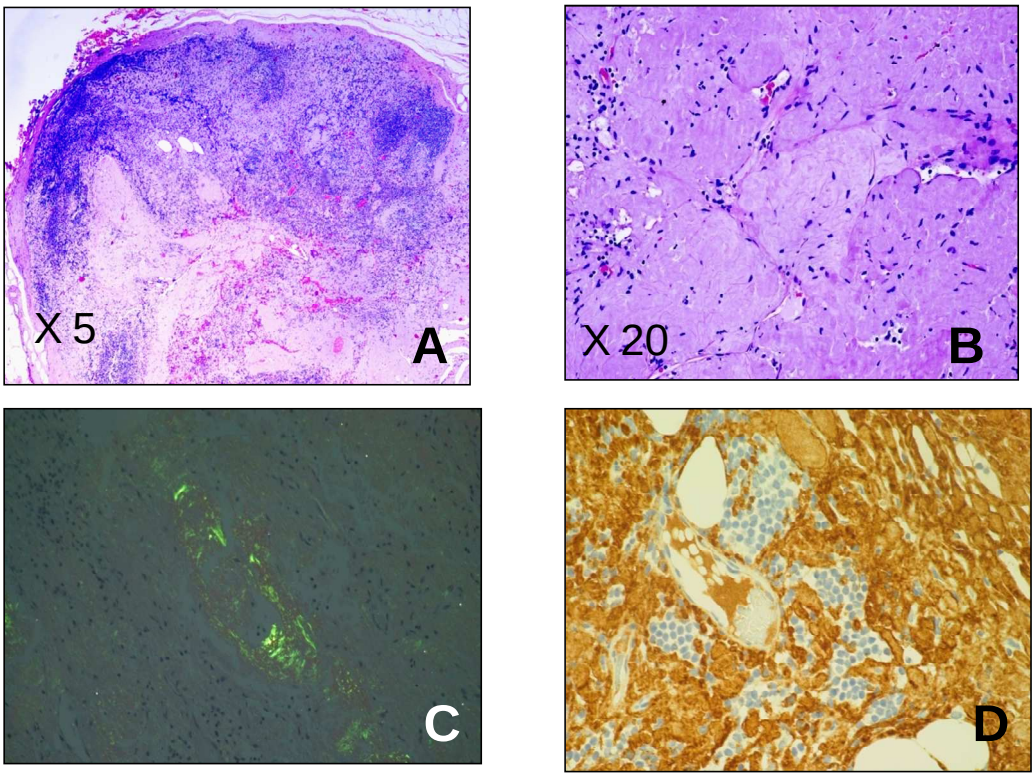

Histopathology of biopsied llymph node demonstrating massive deposition of amyloid: (A and B) HE staining; (C) Congo red staining with polarized light; (D) ALκpositivity on immunohistochemistry

Figure 1 Histopathology of biopsed left laterocervical lymph node

Successful treatment of small plasma cell clonal proliferation with improvement of target organ function - beyond amyloid

K. Barton, M.M. Picken

Loyola University Medical Center, Chicago, USA

Plasma cell dyscrasia may be associated with amyloidosis and other related disorders, including light chain deposition disease, light chain proximal tubulopathy and crystal storing histiocytosis. In a subset of patients, the tumor load may be very small such that the question may arise whether treatment of the underlying plasma cell proliferation should be considered. We report here on a patient who initially developed renal failure of unclear etiology. Light chain proximal tubulopathy (LCPT) was subsequently diagnosed in the renal transplant after a slow decline in allograft function[(1)].

A 58-year-old woman underwent living, related, kidney transplantation in 1997. In January 2002, worsening kidney function led to kidney biopsy, which identified the LCPT. Bone marrow aspirate and biopsy did not identify any B cell clonal process and plasma cells were less than 1%. Serum immunofixation identified a small IgG kappa monoclonal protein, and urine immunofixation showed kappa free light chains. Therapy was initiated with pulses of dexamethasone, and with relatively stable renal function.

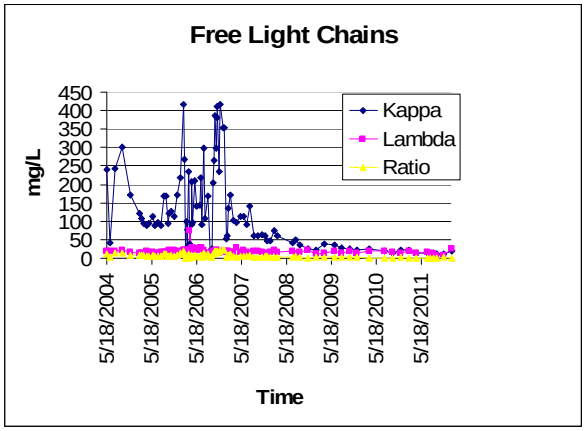

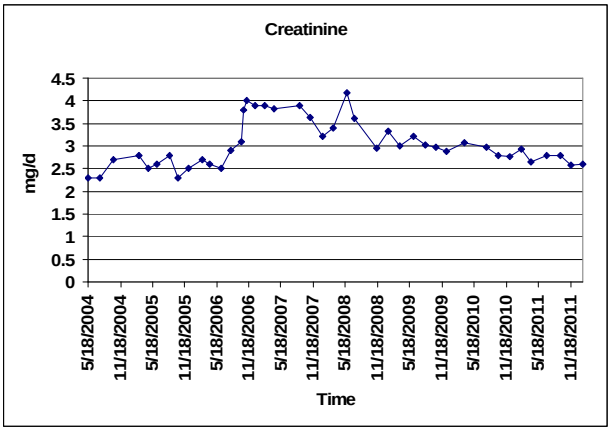

Serum free light chain assays were used for tracking her disease, beginning in 2004. In March 2005, she was switched to a bortezomib-based therapy because of increased free light chains. This was further adjusted to cyclophosphamide, bortezomib, and dexamethasone in April 2006. In late 2006, she developed fevers and sepsis of unclear etiology and therapy was halted temporarily with worsening of her renal function.

In December 2006, after resolution of her acute illness, lenalidomide therapy was instigated. Apart from some muscle cramping, she tolerated this therapy quite well. She showed a slow, steady improvement of her kappa free light chains and achieved complete hematologic remission with slow improvement of renal function.

CONCLUSION

Treatment of small clones is feasible and can lead to improvement of target organ function in at least some patients using immune modulatory drugs (IMIDs) such as lenalidomide[1,2].

REFERENCES

1. Kapur U, Barton K, Fresco R, Leehey DJ, Picken MM. Expanding the pathologic spectrum of immunoglobulin light chain proximal tubulopathy. Arch Pathol Lab Med; 131:1368-72, 2007
2. Merlini G, Stone MJ. Dangerous small B-cell clones. Blood; 108:2520-30, 2006.

Cardiac AL Amyloidosis – Winning the Battle and Losing the War

K.K. Mackie[1], K. Barton[2], M.M. Picken[3], E.E. Coglianese[4]

[1]Internal Medicine, [2]Hematology/Oncology, [3]Pathology, [4]Center for Heart and Vascular Medicine, Cardiology, Loyola University Medical Center, USA

A 58 year-old-woman, who was a lifetime nonsmoker with no prior cardiac history, presented with decompensated heart failure. Symptoms were present for several months.

On initial presentation, BUN was 28 with creatinine of 1. Troponin-I was 160pg/ml and BNP was1336pg/ml. Twenty-four-hour urine protein was 761mg/24h. Initial chest X-ray showed large right and smaller left pleural effusions. Initial echocardiogram demonstrated an 18mm interventricular septal wall thickness. Serum free lambda light chains were 350 mg/L and abdominal fat pad biopsy was positive for AL-lambda amyloid. Bone marrow biopsy demonstrated a lambda monoclonal plasma cell population with 5% plasma cells. The patient was treated with bortezomib and dexamethasone and quickly achieved a sustained reduction in her lambda light chains (Figure 1). However, the cardiac markers remained persistently elevated, suggesting that the damage from AL light chains was irreversible. Ultimately, the patient continued to have recurrent pleural effusions despite therapeutic thoracenteses and heart failure management, and ultimately, she died from cardiopulmonary arrest.

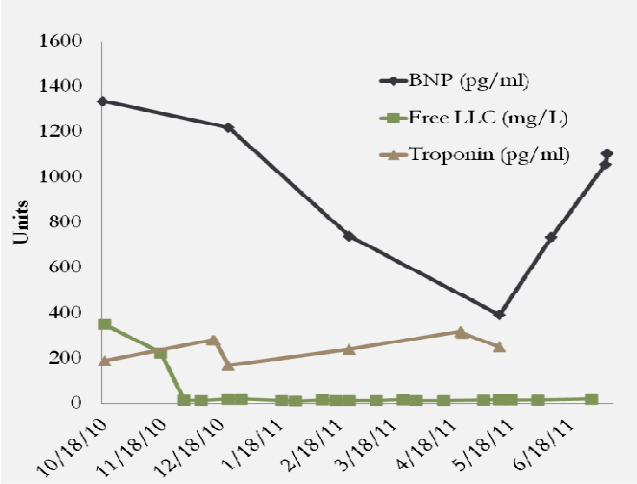

Figure 1

The poor prognosis of patients with advanced cardiac amyloid is well-established[1]. The reported median survival of patients with cardiac AL amyloidosis with heart failure is 5 months[2]. In this patient, progressive and irreversible organ dysfunction continued despite a complete hematological response of the abnormal light chains. Although criteria exist for initial cardiac transplantation evaluation, our patient was not considered to be a candidate for this procedure due to her unstable heart failure, and probable renal/possible pulmonary involvement by amyloidosis [3].

CONCLUSION

Late diagnosis of cardiac AL amyloidosis continues to be a major factor in poor survival, despite successful management of the underlying plasma cell dyscrasia.

REFERENCES

1. Varr BC, Liedke M, Arai S, Lafayette RA, Schrier SL, Witteles RM. Heart transplantation and cardiac amyloidosis: approach to screening and novel management strategies. J Heart Lung Transplant. 2012; 31:325-31.
2. Kapoor P, Thenappan T, Singh E, Kumar S, Greipp PR. Cardiac amyloidosis: a practical approach to diagnosis and management. Am J Med. 2011; 124:1006-15.
3. Lacy MQ, Dispenzieri A, Hayman SR et al. Autologous stem cell transplant after heart transplant for light chain (AL) amyloid cardiomyopathy. J Heart Lung Transplant. 2008; 27:823-9.

Systemic AL amyloidosis and synchronous Alzheimer's pathology identified at autopsy – incidental versus related?

K.K. Mackie[1], K. Barton[2], M.M. Picken[3], E.E. Coglianese[4], J.M. Lee[3]

[1]Internal Medicine, [2]Hematology/Oncology, [3]Pathology, [4]Center for Heart and Vascular Medicine, Cardiology, Loyola University Medical Center, USA

INTRODUCTION

This clinical case presents the unfortunate fate of a patient diagnosed with systemic AL amyloidosis who ultimately died from cardio-respiratory arrest. Interestingly, autopsy findings revealed a constellation of cerebral involvement, which included cortical neuritic amyloid plaque counts in a range consistent with a diagnosis of Alzheimer's disease.

CASE

A 58 year-old-woman, a lifetime nonsmoker with no prior cardiac history, presented with decompensated heart failure. Ultimately, her fat pad biopsy was positive for AL amyloidosis. Treatment was initiated with bortezomib and hematologic remission was obtained. However, despite hematologic response, her cardiac function deteriorated. Interestingly, over the course of disease progression, the patient's mental status changed with the onset of hallucinations and paranoia. She became withdrawn and depressed. The patient was seen by psychiatry and treated with antidepressants without improvement.

Ultimately, the patient died from cardio-respiratory failure. Post-mortem histological assessment determined the presence of AL-Amyloid deposition in the heart (the interventricular septum measured 2cm), kidneys, lungs, and adipose tissue that clearly persisted despite hematologic remission which was maintained for months.

Autopsy also reported cortical neuritic amyloid plaques counts that were in a range considered diagnostic of possible Alzheimer's disease(1). There was also amyloid in the vessels in the dura and choroid plexus. While neuritic plaques are associated with the deposition of βeta-amyloid protein, the involvement of the dura and choroid plexus most likely represented light chain deposition from the systemic amyloidosis, given that these areas do not contain a blood-brain barrier.

SUMMARY

Little is known about whether there is an increased incidence of Alzheimer's disease in AL amyloid patients. Whether the finding of cerebral parenchymal and systemic amyloidosis, in our relatively young patient, is

incidental or related, is an open question. It is feasible that an amyloidogenic-specific environment can exist within both the brain parenchyma and systemically, in particular in the heart.

REFERENCES

1. Mirra, S. et al. The Consortium to Establish a Registry for Alzheimer's Disease I (CERAD): Part II Standardization of the Neuropathologic Assessment of Alzheimer's Disease (1991) Neurology 41: 479-486.

SECTION VI

ATTR AMYLOIDOSIS


Ni Hao.
Wok & Fusion
"All you can eat"
Tuesday
你好中國城

STATE OF THE ART: Biology, clinic and prognosis in ATTR amyloidosis

Shu-ichi Ikeda

Department of Medicine (Neurology and Rheumatology), Shinshu University School of Medicine, Matsumoto 390-8621, Japan

ABSTRACT

Systemic amyloidosis is a heterogenous disease group, in which amyloidogenic precursor proteins accumulate as insoluble fine fibrils on several vital organs, ultimately leading to fatal multi-organ failure. Among them immunoglobulin light chain (AL)-derived amyloidosis is the most common and the next is transthyretin (ATTR)-related amyloidosis. I here review the recent advance in the extensive studies of ATTR amyloidosis.

INTRODUCTION

Transthyretin (TTR) is an amyloidogenic protein and produces two different forms of systemic amyloidosis: one is familial amyloidosis including familial amyloid polyneuropathy (FAP)[1] and the other is senile systemic amyloidosis (SSA)[2], which was previously called senile cardiac amyloidosis. In the former, an amyloid precursor protein is a variant type of TTR with one amino acid substitution, whereas in the latter it is wild-type TTR. TTR-related systemic amyloidosis is more prevalent disorder than previously recognized.

FAMILIAL ATTR AMYLOIDOSIS

This disorder can be classified into FAP and familial amyloid cardiopathy (FAC) and more than 100 variants of TTR have been identified as a causative amyloid precursor in this disease. FAP was once considered to be a disease peculiar to endemic areas, but FAP patients are now known to exist in many nations worldwide.

The clinical phenotypes of FAP have been shown to vary in different kindreds or individuals with diverse TTR gene mutations. Among many TTR variants the substitution of methionine for valine at position 30 (ATTR Val30Met) is the most common and even in FAP with ATTR Val30Met the clinical picture is considerably different between patients originated from endemic foci and those with non-endemic origins: in the former group the patients show an early onset, an autosomal dominant trait with a high penetration, equal sex distribution, polyneuropathy starting in the legs and prominent dysautonomia, while in the latter they show a late onset, male predominance and obscure family history. Additionally, apparent dissociated sensory loss and serious autonomic dysfunctions are not usually seen in the patients with a late onset, and in some patients upper limb symptoms preceded lower limb symptoms. In FAP with ATTR non-Val30Met clinical manifestations of polyneuropathy and autonomic dysfunction closely resembled to those of ATTR Val30Met FAP patients with

non-endemic origins. Among them serious cardiac amyloidosis is commonly seen and in some patients the disease starts as a carpal tunnel syndrome. A few rare forms of ATTR non-Val30Met selectively cause amyloid deposition on the leptomeninges and subarachnoid vessels in the central nervous system, where amyloid-induced thickened leptomeninges compressed the spinal cord and subarachnoidal and/or subcortical hemorrhages recurrently developed. This unique clinicopathologic finding is called as familial oculoleptomeningeal amyloidosis or familial meningocerebrovascular amyloidosis.

FAC is one form of hereditary ATTR amyloidosis showing a predominant clinical manifestation of cardiac amyloidosis and more than 30 variants of TTR are known to produce severe amyloid heart disease. Most patients with FAC had a later age of onset and usually lacked an apparent family history. Thus, they frequently seemed to be sporadic and the common initial mis-diagnosis for them was primary systemic AL amyloidosis.

SSA

SSA mainly affects the heart in the elderly and the prevalence of the disease was reported to be 22-25% based on examination of cardiac specimens obtained from autopsied individuals over 80 years old 3. Most patients with SSA were diagnosed on postmortem studies, but recent advance of diagnostic technology that include immunohistochemical demonstration of TTR-related amyloid deposits with no mutation of TTR gene enables us to make a correct clinical diagnosis of the patients with this disease 4. Thus, the number of SSA patients is now increasing.

SSA usually develops in individuals over 80 years of age, males being predominantly affected. However, recently several patients with SSA who were younger than 70 years at the time of antemortem diagnosis have been reported. The clinical manifestations consist of congestive heart failure, arrhythmia and/or conduction blocks and atrial fibrillation might be an initial sign of this cardiac disorder. Rarely SSA-related cardiac amyloidosis with impaired left ventricular wall motion and thickened endocardium causes systemic embolism, resulting in cerebral infarction 5. Another notable manifestation is carpal tunnel syndrome (CTS). Amyloid deposits are occasionally seen in biopsied tissue specimens obtained from carpal tunnel release and more than half of them are TTR immunoreactive. Among 33 patients with proven tenosynovial TTR amyloid deposition two of them were reported to develop systemic amyloidosis more than 9 years after the initial appearance of CTS. We also described two SSA cases whose initial manifestations were bilateral CTS. It is, therefore, very likely that in SSA CTS seems to precede cardiac manifestations several years.

IMPORTANCE OF WILD-TYPE TTR

Wild-type TTR is inherently an amyloidogenic protein and is well known to be an amyloid precursor protein in SAA. Additionally, the contribution of wild-type TTR to amyloid fibril formation in FAP been recently noted. Ongoing deposition of wild-type TTR-derived amyloid was first noted in the hearts of ATTR non-Val30Met FAP patients treated with liver transplantation, but it is now recognized that similar deposition of wild-type TTR-derived amyloid can also occur in other organs: postoperative changes in composition ratio between variant type and wild-type TTR were demonstrated in the renal amyloid of a FAP patient with ATTR Val30Met. An unexpectedly high ratio of wild-type TTR was found in the sciatic nerve amyloid (75% composition of its amyloid fibril protein was derived from wild-type TTR) obtained from an autopsied FAP patient with ATTR Thr60Ala who died 5 years after combined liver and heart transplantation. Moreover it has been shown that the amyloid fibrils

in abdominal fat tissues in non-transplanted FAP patients with ATTR Val30Met are composed of not only variant but also wild-type TTR and that the composition ratio of wild-type TTR in patients older than 50 years are significantly higher than those in patients younger than 50. This suggests that aging plays an important role in wild-type TTR-derived amyloid fibril formation in FAP patients.

DIAGNOSIS OF SYSTEMIC ATTR AMYLOIDOSIS

Cardiac amyloidosis, amyloid-related polyneuropathy and/or CTS are caused mainly by three different form of systemic amyloidosis including AL, hereditary TTR amyloidosis and SSA. It is, therefore, necessary to differentiate ATTR amylodiosis from AL amyloidosis. Histological and immunohistochemical analysis of tissue amyloid is an initial step for the diagnosis of this disease. After immunohistochemical demonstration of TTR-related amyloid deposits in biopsied tissues molecular analysis of TTR is required. A matrix-assisted laser desorption ionization/time-of-flight (MALDI/TOF) mass spectrometry system is easy and sensitive to detect variant forms of TTR in sera of patients and thus, immunoprecipitated serum TTR molecules of the patient is initially screened by this technique. Finally, direct DNA sequencing is necessary to demonstrate the mutations of TTR gene.

TREATMENT

As serum TTR is mainly produced in the liver, liver transplantation can abolish the hepatic source of variant TTR and this therapeutic strategy has been widely accepted for the treatment of FAP patients: long-term observation of the transplanted patients has clearly shown that early liver transplantation can improve FAP patients' survival and quality of life with histopathological regression of amyloid deposits in these patients. The prognosis of cardiac amyloidosis is generally poor. For patients with AL amyloidosis, the median survival is 4-6 months after the appearance of congestive heart failure, while that of patients with SSA is 5 years. Concerning organ dysfunction affected by amyloid deposition, soluble oligomers of amyloidogenic precursor proteins seem to produce the cytotoxic effects to the involved organs. Monoclonal immunoglobulin light chain is surmised to be more harmful to myocardium than amyloidogenic TTR molecule. Cardiac amyloidosis in SSA usually does not follow a rapidly progressive course and some patients with this disease have survived after heart transplantation. For the pathogenesis of TTR-related amyloidosis including variable hereditary forms it has been clearly shown that TTR tetramer dissociation, misfolding and misassembly are required for the process of amyloid fibril formation. Preferential stabilization of the native TTR tetramer over the dissociative transition state can be achieved by orally administered non-steroidal anti-inflammatory drugs (NSAIDs) and a clinical trial of this drug for the patients with ATTR-type familial amyloid polyneuropathy has been now ongoing.

REFERENCES

1. Ikeda S, Nakazato M, Ando Y, et al. Familial transthyretin-type amyloid polyneuropathy in Japan. Clinical and genetic heterogeneity. Neurology 2002;58:1001-1007.
2. Westermark P, Bergström J, Solomon A, et al. Transthyretin-derived senile systemic amyloidosis: clinicopathologic and structural considerations. Amyloid 2003;10 (Suppl. 1):48-54.

STATE OF THE ART: Essential therapies for FAP

Yukio Ando
Department of Neurology, Graduate School of Medical Sciences, Kumamoto University

ABSTRACT

It has been widely accepted that liver transplantation can halt the clinical manifestations of transthyretin (TTR) related familial amyloidotic polyneuropathy (FAP). However, the therapy has given rise to several problems. As the essential therapy for FAP, several different approaches have been investigated as an essential therapy for FAP: (1) reduction of variant TTR levels in plasma, (2) down-regulation of variant TTR gene mRNA, (3) inhibition of amyloid deposition, (4) stabilization of the tetrameric TTR structure and (5) replacement of the variant TTR gene with the normal TTR gene. We introduce those research strategies and trials and discuss the possibility of the optimal treatment for FAP.

INTRODUCTION

Because patients with FAP show various serious systemic symptoms, many trials have attempted to treat them. Although liver transplantation has become a well-established treatment for halting the progression of FAP-related clinical symptoms, no truly effective therapy has been designed, and several problems related to its use have arisen. We cannot use liver transplantation for these patients as long-term therapy. To overcome all these problems, we must develop a new noninvasive effective treatment.

The following methods can be considered potential FAP treatment strategies (Table 1): (1) reduction of variant TTR levels in plasma; (2) down-regulation of the variant TTR gene mRNA; (3) inhibition of amyloid deposition; (4) stabilization of the tetrameric TTR structure; and (5) replacement of the variant TTR gene with the normal TTR gene (which can be achieved by liver transplantation or by gene therapy) (Figure 1).

Here, we describe new therapeutic approaches for FAP that our group has recently investigated.

1. RETINAL LASER PHOTOCOAGULATION

The occurrence of ocular complications increases with time, even after liver transplantation, which leads to a halt in the progression of systemic neurologic complications. We investigated a new strategy to prevent ocular involvements. We used panretinal laser photocoagulation for 18 patinets, which damages the retinal pigment epithelium, the main location for synthesis of amyloidogenic transthyretin in ocular tissues, to treat 1 eye of each patient. After laser photocoagulation, we performed general ophthalmic examinations every 3 months for 3 years. Panretinal laser photocoagulation clearly prevented progression of amyloid deposition in the vitreous and on the retinal surface in both cases during 3 years of follow-up. No serious complications occurred.

Panretinal laser photocoagulation is a safe and well-known procedure that offers a new treatment option to mitigate ocular manifestations in FAP patients (1).

2. ANTIBODY THERAPY AGAINST MISFOLDED TTR

An anti-serum against β-strand H (a peptide TTR115-124, which constitutes the monomer-to-monomer interaction areas in the dimer, reacted only with ATTR in amyloid fibrils but not with normal plasma TTR (2). Those results suggested that there was an altered configuration of TTR within amyloid fibrils when compared with plasma TTR. The antiserum to TTR115-124, which so far has turned out to be amyloid specific, may serve as a valuable probe and may be useful in antibody therapies.

We produced a polyclonal antibody for TTR115-124 and injected it to transgenic rats which develop amyloid deposition in the large intestine at 12 -18 months after the birth. The antibody effectively prevented TTR deposition in the rats.

3. GENE SILENCING TOOLS

Ribozymes, antisense methods and small interfering RNAs (siRNAs) are effective gene silencing tools. Ribozymes are based on catalytic RNA originally found in the protozoan tetrahymena and can cleave a targeted RNA sequence or reverse the mRNA to generate correct sequences. The antisense oligonucleotides were recognized as the therapeutic tool in the 1970s and cause enzymatic degradation of mRNA by activating ribonuclease H1. RNA interference (RNAi) was first discovered in *Caenorhabditis elegans* as a phenomenon of sequence-specific post-transcriptional gene silencing. The inhibition of specific gene expression by RNAi has also been achieved in mammalian cells by passing the Dicer step and directly introducing synthesized small interfering RNAs (siRNAs). These technologies are expected to be a powerful tool for gene therapy. In fact, siRNA TTR supplied by Alnylam markedly reduced the TTR mRNA expression in ARPE-19 cells derived from retinal pigmental cells. Next, we injected rat and human TTR siRNA to the vitreous body of the transgenic rats which expressed mRNA TTR in the retina. Both type of siRNA suppressed rat and human variant TTR expression.

Propsting et al. reported specific cleavage of ATTR Val30Met mRNA in a cell culture system by using hammerhead ribozymes. They showed that chemically modified nuclease-stable Inosine(15.1)-Hammerhead ribozymes can target ATTR Val30Met mRNA with high specificity at the RNA level. Tanaka et al. reported that another ribozyme targeting a variant TTR (E61K) degraded the variant mRNA but not the wild-type mRNA. These ribozymes also reduced the amounts of TTR mRNA and protein in HepG2 cells and COS-1 cells transfected with TTR-E61K cDNA. Benson et al. demonstrated suppression of hepatic TTR mRNA levels and serum TTR levels by as much as 80% in mice transgenic for the human Ile84Ser TTR mutant gene by antisense oligonucleotides. Kurosawa et al. reported that an siRNA selectively silenced the mutant Val30Met TTR allele in cells expressing both wild type and Val30Met alleles. This project is now in on going phase study. Soon this therapy may become an essential therapy for FAP.

The strategy of using single-stranded oligonucleotides (SSOs) for gene therapy grew from studies that attempted to characterize and improve chimeraplasty. SSOs containing three phosphorothioate bonds at the 3' and 5' termini were more effective than the chimeraplasts in gene repair assays conducted with cell-free

extracts and a yeast system. SSOs are significantly less expensive than chimeraplasts and far simpler to synthesize and purify, so they may be an invaluable resource for treating a variety of genetic diseases.

To test the feasibility of gene therapy for FAP, via chimeraplasts and SSOs, that would halt production of variant TTR in the liver and retina, Nakamura et al. first applied chimeraplasts and SSOs to HepG2 cells secreting human wild-type TTR. They then demonstrated gene conversion by SSOs in rabbit eye expressing rabbit wild-type TTR and transgenic murine liver in which the intrinsic wild-type TTR gene was replaced by a TTR Val30Met gene. We are performing the experiments to produce hepatocytes with no variant TTR gene combining iPS cells from FAP patients and this gene conversion method.

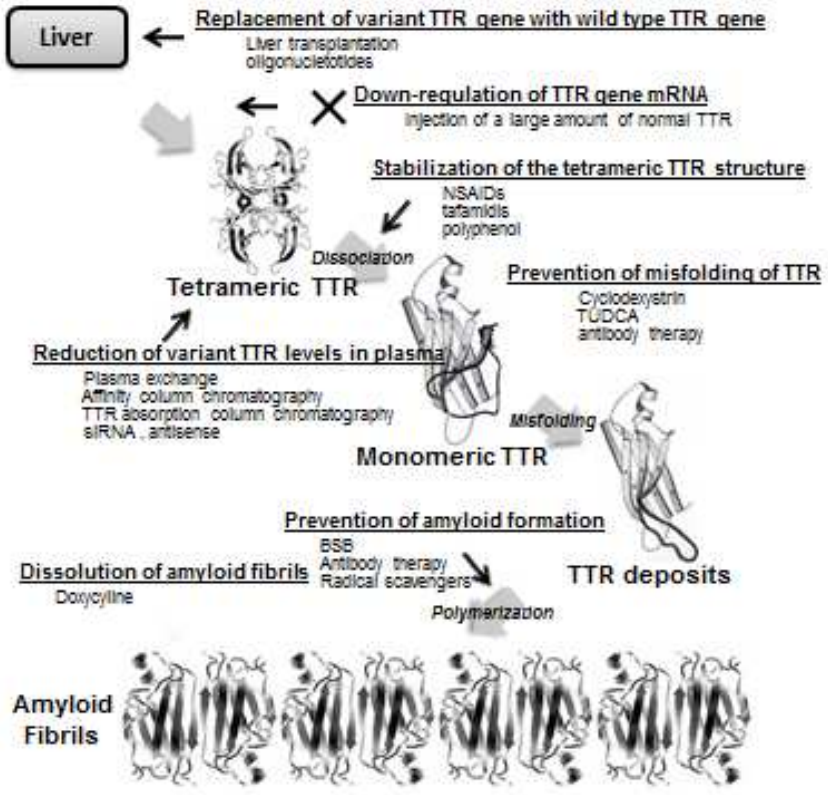

Figure 1. Amyloid formation mechanism in FAP and points of intervention for our treatments. Based on the pathogenesis of FAP, various therapeutic approaches can be considered as potential FAP treatment strategies

4. UNIQUE COMPOUND SUPPRESSING TTR MISFOLDING

TTR (transthyretin), a β-sheet-rich protein, is the precursor protein of familial amyloidotic polyneuropathy and senile systemic amyloidosis. Although it has been widely accepted that protein misfolding of the monomeric form of TTR is a rate-limiting step for amyloid formation, no effective therapy targeting this misfolding step is available. In the present study, we focused on CyDs (cyclodextrins), cyclic oligosaccharides composed of

glucose units, and reported the inhibitory effect of CyDs on TTR amyloid formation. Of various branched β-CyDs, GUG-β-CyD [6-O-α-(4-O-α-D-glucuronyl)-D-glucosyl-β-CyD] showed potent inhibition of TTR amyloid formation. Far-UV CD spectra analysis showed that GUG-β-CyD reduced the conformational change of TTR in the process of amyloid formation. In addition, tryptophan fluorescence and 1H-NMR spectroscopy analyses indicated that GUG-β-CyD stabilized the TTR conformation via interaction with the hydrophobic amino acids of TTR, especially tryptophan. Moreover, GUG-β-CyD exerted its inhibitory effect by reducing TTR deposition in transgenic rats possessing a human variant TTR gene in vivo. Collectively, these results indicate that GUG-β-CyD may inhibit TTR misfolding by stabilizing its conformation, which, in turn, suppresses TTR amyloid formation (3).

REFERENCES

1. Kawaji T, Ando Y, Hara R & Tanihara H. Novel Therapy for Transthyretin-related Ocular Amyloidosis A Pilot Study of Retinal Laser Photocoagulation. Ophthalmology. 2010;17, 552-555
2. Bergström J, Engström U, Yamashita T, Ando Y, Westermark P. Surface exposed epitopes and structural heterogeneity of in vivo formed transthyretin amyloid fibrils. Biochem Biopys Res Commun 2006; 348:532-539.
3. Jono H., Anno T., Motoyama K., Misumi Y., Tasaki T., Oshima T., Mori Y., Mizuguchi M., Ueda M., Shono M., Obayashi K., Arima H. & Ando Y.Cyclodextrin, a novel therapeutic tool for suppressing amyloidogenic transthyretin misfolding in transthyretin-related amyloidosis. Biochem J, 2011; 437:35-42.

PERSPECTIVE: Therapy of ATTR Amyloidosis

Steven R. Zeldenrust

Mayo Clinic, Rochester, MN, USA

INTRODUCTION

ATTR represents a relatively simple form of the systemic diseases known as amyloidoses. The simplicity is due to the fact that the disease is caused by single point mutations in a single gene, resulting in the ultimate deposition of TTR as amyloid fibrils. This is contrasted with AL amyloidosis, in which a vast variety of different light chain proteins are involved. Further, circulating TTR is produced predominantly by a single organ, the liver, as opposed to AL in which plasma cells scattered throughout the bone marrow are responsible for production of the pathogenic light chain. Studies have shown that outcomes in AL are impacted by multiple factors, including specific genetic events in the clonal plasma cells themselves, further complicating the treatment and prognosis in AL. No such factors have been reported for outcomes in ATTR, in which the only genetic event is the mutation within the TTR gene itself.

The pathway to organ damage in ATTR is also relatively simple, with TTR produced in the liver, circulating in the plasma and ultimately depositing as amyloid fibrils in various end-organs (Figure 1). These steps in the pathogenesis of ATTR have provided logical targets for therapeutic intervention.

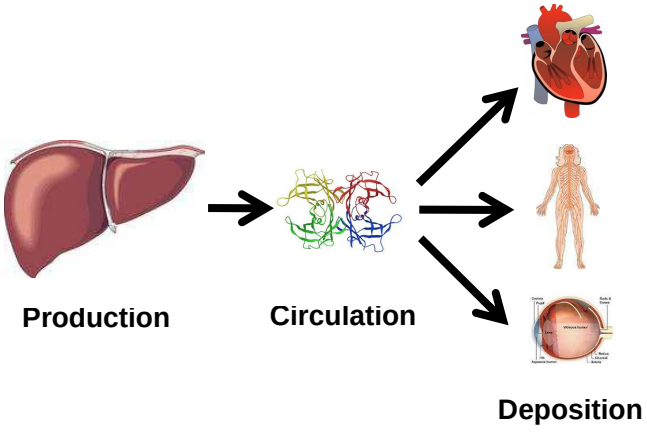

Figure 1. Pathway of disease pathogenesis in ATTR.

TTR PRODUCTION

The production of TTR by the liver is the first step in the pathway and the first to be exploited for therapeutic benefit. Since the liver is the predominant source of circulating TTR, it is logical that replacing the patient's liver that is producing the variant TTR with one from a healthy donor can effectively remove the source of the amyloid precursor protein. The first liver transplant for ATTR was performed in Sweden in 1990, in a patient with the V30M mutation common in that country. [1] Since the original report, over 1900 liver transplants have been performed worldwide according to the FAP World Transplant Registry. This approach would seem to be curative, since the source of the precursor protein is completely removed at the time of transplant. This principle is supported by long-term data that shows excellent outcomes for ATTR patients undergoing liver transplant, with 77% survival at 5 years post-transplant. [2] More recent data from Sweden and Japan have shown a clear survival advantage for V30M patients undergoing liver transplant. [3, 4]

Despite the initial optimism, it has become clear that not all ATTR patients benefit from liver transplantation and in some cases they may actually fare worse after transplant. [5, 6] This appears to be particularly relevant for patients with mutations other than V30M and those that have evidence of cardiac involvement at the time of transplant. The demonstration that amyloid deposits contain increased amounts of wild-type TTR following transplant suggests that the donor liver continues to contribute to progressive amyloid deposition in some cases.

Newer approaches to attack TTR production have begun to be tested in early clinical trials, using gene-silencing technology to block all TTR production by the liver. This approach has several advantages over liver transplant, including avoiding the significant morbidity and mortality related to the surgery itself. In addition, this approach blocks production of the wild-type TTR as well as the variant, which should avoid the formation of new amyloid deposits entirely. Importantly, patients with senile systemic amyloidosis, who develop amyloid deposits from the wild-type protein alone, may benefit from this approach as well. The results of clinical trials of gene silencing in ATTR are eagerly awaited.

CIRCULATION

The second step in the pathway to ATTR is the circulation of TTR in the plasma as it travels from the site of production to the ultimate site of deposition as amyloid fibrils. Compelling data have emerged suggesting that the point mutations in the TTR gene result in instability of the TTR tetramer, which is the native circulating form of TTR in the plasma. [7] This instability leads to increased dissociation of the tetramer to individual TTR monomers, which can undergo misfolding to amyloidogenic intermediates. This critical step in the pathogenesis of ATTR is a logical place to intervene. Several small molecules that bind to and stabilize the tetramer have been employed in clinical trials.

This approach has shown promise in a recent Phase III clinical trial in V30M patients with peripheral neuropathy. [8]A similar Phase III study of diflunisal is ongoing in patients with non-V30M mutations. These trials represent the first targeted therapeutic approach to any form of systemic amyloidosis. Additional studies to confirm the benefit of this approach in non-V30M patients and those with non-neurologic symptoms are needed.

DEPOSITION

The final step in the pathogenesis of ATTR is the ultimate deposition of amyloid fibrils in various end-organs. This portion of the pathway is the most recent to be exploited in clinical studies. Doxycycline has been shown to disrupt TTR amyloid fibrils in mouse models of ATTR and is currently being investigated in conjunction with tauroursodeoxycholic acid, which shows synergistic activity on TTR amyloid deposits. [9, 10]

A more generalized approach to attacking systemic amyloidosis has been the depletion of serum amyloid P (SAP) component from existing deposits. While depletion of circulating SAP did not appear to have a significant clinical effect, it appears that the subsequent delivery of an anti-SAP antibody may be helpful in clearing existing deposits. [11] This approach has the advantage of being applicable to all forms of amyloidosis, as SAP is a ubiquitous component of all amyloid deposits.

FUTURE THERAPIES

This is an exciting time for in the treatment of ATTR, with new therapies attacking different steps of the amyloid formation pathway being tested in clinical trials at multiple centers. One area which is currently not being adequately addressed is the link between amyloid fibril deposition and cell toxicity. Many groups are working to unravel the link between organ damage and amyloid deposition, but thus far the exact nature of the toxic process has remained elusive. Uncoupling the process of amyloid formation and organ damage has far-reaching potential for the treatment of patients with these devastating diseases.

With the growing number of therapies emerging in the treatment of ATTR, it seems likely that patients will benefit from some or all of these approaches. The current paradigm of treatment for ATTR with liver transplant as the only option is likely to change significantly in the years to come. While some patients may still benefit from liver transplant, a combination of approaches will likely be needed in most cases. By blocking multiple steps in the pathogenesis of ATTR, we are likely to see improved outcomes for all patients. Much like AIDS was once considered incurable, we may be able to achieve long-lasting benefit from employing multiple therapies over the course of the patient's life.

REFERENCES

1. Holmgren, G., et al., Biochemical effect of liver transplantation in two Swedish patients with familial amyloidotic polyneuropathy (FAP-met30). Clinical Genetics, 1991. 40(3): p. 242-6.
2. Herlenius, G., et al., Ten years of international experience with liver transplantation for familial amyloidotic polyneuropathy: results from the Familial Amyloidotic Polyneuropathy World Transplant Registry. Transplantation, 2004. 77(1): p. 64-71.
3. Okamoto, S., et al., Liver transplantation for familial amyloidotic polyneuropathy: impact on Swedish patients' survival. Liver Transplantation, 2009. 15(10): p. 1229-35.
4. Yamashita, T., et al., Long-term survival after liver transplantation in patients with familial amyloid polyneuropathy. Neurology, 2012. 78(9): p. 637-43.
5. Liepnieks, J.J., L.Q. Zhang, and M.D. Benson, Progression of transthyretin amyloid neuropathy after liver transplantation. Neurology, 2010. 75(4): p. 324-7.

6. Stangou, A.J., et al., Progressive cardiac amyloidosis following liver transplantation for familial amyloid polyneuropathy: implications for amyloid fibrillogenesis. Transplantation, 1998. 66(2): p. 229-33.
7. Hammarstrom, P., et al., Prevention of transthyretin amyloid disease by changing protein misfolding energetics. Science, 2003. 299(5607): p. 713-6.
8. Coelho, T., et al., Tafamidis for transthyretin familial amyloid polyneuropathy. Neurology, 2012.
9. Cardoso, I., et al., Synergy of combined doxycycline/TUDCA treatment in lowering Transthyretin deposition and associated biomarkers: studies in FAP mouse models. Journal of Translational Medicine, 2010. 8: p. 74.
10. Cardoso, I. and M.J. Saraiva, Doxycycline disrupts transthyretin amyloid: evidence from studies in a FAP transgenic mice model. FASEB Journal, 2006. 20(2): p. 234-9.
11. Bodin, K., et al., Antibodies to human serum amyloid P component eliminate visceral amyloid deposits. Nature, 2010. 468(7320): p. 93-7.

Baseline Demographics and Clinical Characteristics in THAOS—the Transthyretin Amyloidosis Outcomes Survey

O.B. Suhr on behalf of the THAOS Investigators

Umeå University Hospital, Umeå, Sweden.

Transthyretin (TTR) amyloidosis (ATTR) is a rare, systemic condition with two main forms: hereditary (associated with >100 identified genetic mutations) and wild-type (WT) (associated with advanced age). ATTR patients present with polyneuropathic, cardiac (cardiomyopathy or conduction disturbances), or mixed phenotypes, which can vary by genotype and geographic region. This analysis describes baseline demographic and disease characteristics of subjects in the Transthyretin Amyloidosis Outcomes Survey (THAOS), a global, multicenter, longitudinal, observational survey, as of September 1, 2011. Data are available for 975 subjects, including 688 symptomatic patients with WT (n=77) or variant (n=611) ATTR, and 274 asymptomatic carriers. Nineteen countries of origin and 43 *TTR* mutations are represented. ATTR phenotypes differed according to mutation. Quality of life for symptomatic patients with hereditary ATTR was comparable to or worse than that of age-matched patients with other serious diseases. THAOS demonstrates the value of an international registry to better understand presentations of ATTR.

INTRODUCTION

Transthyretin (TTR) amyloidosis (ATTR) is a rare, systemic condition with two main forms: hereditary and wild-type (WT) (1,2). ATTR is an autosomal dominant disease in which single site mutations in the *TTR* gene destabilize the native tetrameric structure of TTR, resulting in tetramer dissociation and extracellular deposition of insoluble protein fibrils primarily in nerves and heart. Patients with ATTR present with polyneuropathic, cardiac, or mixed phenotypes, which can vary by genotype and geographic region. Val30Met (p.Val50Met) is the most common *TTR* gene mutation associated with a predominantly polyneuropathic phenotype and is endemic in Portugal, Sweden, and Japan. Polyneuropathic ATTR most commonly presents in the third to sixth decade of life as a progressive sensory-motor neuropathy with autonomic manifestations. While penetrance is variable, the disease is fatal within 10–13 years of symptom onset.

Established in 2007, the Transthyretin Amyloidosis Outcomes Survey (THAOS) is a global, multicenter, longitudinal, observational survey that collects data on the natural history of ATTR and aims to document the efficacy and safety of treatment modalities.

METHODS

The present analysis describes baseline demographic and disease characteristics, as well as quality of life (QOL), of subjects in the THAOS registry as of September 1, 2011 (ClinicalTrials.gov: NCT00628745). Symptomatic individuals with confirmed WT or variant ATTR, and asymptomatic carriers of variant *TTR*, are eligible for enrollment. Data obtained during clinical evaluations are entered into the THAOS registry using a secure, interactive, Web-based system. Patient information collected includes cardiac and neurologic findings, renal function assessments, QOL assessments, hospitalizations, medications, and transplant history. Standardized methods as endorsed by national or international societies are recommended for all data collection assessments. There are currently 46 active sites in 19 countries represented in THAOS.

RESULTS

At the time of this analysis, data were available for 975 subjects, including 688 symptomatic patients with either WT (77 patients) or variant (611 patients) ATTR; there were 274 asymptomatic carriers of variant ATTR. Most patients enrolled in THAOS reside in Portugal (n=453), the United States (n=138), Japan (n=68), Italy (n=73), and Brazil (n=65). In total, 40 *TTR* mutations were detected across the THAOS population. Although patients with some *TTR* mutations presented with predominantly neuropathic (e.g., Val30Met) or predominantly cardiac (e.g., Val122Ile) symptoms, all *TTR* mutations were associated with multisystem involvement (Table 1). Val30Met was the most common *TTR* mutation reported in THAOS (n=649). The majority of symptomatic and asymptomatic Val30Met patients (67.6%, n=439) were from Portugal.

Table 1. Frequency of symptoms reported by genotype at time of enrollment in THAOS

TTR Genotype	Motor Neuropathy (%)	Sensory Neuropathy (%)	Gastro-Intestinal (%)	Autonomic Neuropathy (%)	Cardiac (%)	Other (%)
Val30Met (N=437)	35.9	90.8	73.7	56.8	33.6	43
Val122ILe (N=32)	15.6	56.3	21.9	25	96.9	50
Leu111Met (N=10)	0	10	10	10	70	50
Glu89Gln (N=13)	30.8	84.6	46.2	30.8	53.8	46.2
ILe68Leu (N=10)	40	70	20	30	80	50
Phe64Leu (N=12)	41.7	91.7	41.7	25	33.3	16.7
Ser77Tyr (N=13)	46.2	100	75.9	38.5	53.8	76.9
Thr60Ala (N=12)	33.3	83.3	41.7	50	83.3	58.3
Wild-Type (N=77)	14.3	32.5	11.7	23.4	94.8	31.2

For all symptomatic patients with *TTR* mutations, the median age of symptom onset was 39.0 years (range, 25.9–64.5 years); the median duration of ATTR-related symptoms was 3.99 years (range, 0.80–12.08 years). For the large Val30Met subgroup, the median age of onset and the duration of ATTR-related symptoms were 33.9 years (range, 25.2–59.8 years) and 3.96 years (range, 0.78–12.83 years), respectively. By contrast, the median age of symptom onset for non-Val30Met patients with *TTR* mutations was much older—54.5 years of age (range, 36.5–71.9 years) and the duration of symptoms was 4.19 years (range, 0.90–10.96 years). Symptom profiles in Val30Met patients varied according to whether age of onset was early (<50 years) or late (≥50 years of age) and according to country of birth.

Symptomatic patients with a *TTR* mutation reported significantly worse QOL (EQ-5D assessments) compared to the general US population (Table 2; $P \leq 0.0002$) (3). QOL tended to decline with age (data not shown here).

The QOL of WT symptomatic patients, all of whom were ≥50 years of age, did not differ from that of the general US population in those age ranges (data not shown). EQ-5D scores seen in symptomatic ATTR patients with *TTR* mutations were comparable to, or lower than, EQ-5D scores in patients with other serious diseases (Table 2) (3).

Table 2. Comparison of EQ-5D index scores reported in other diseases[a]

Disease	Age (years)	EQ-5D Index Score
THAOS symptomatic patients with *TTR* mutations in comparative age group (N=77)	50–64[b]	0.61
Diabetes (N=2,854)	60	0.758
Stroke (N=995)	67	0.694
Emphysema (N=597)	66	0.680
Breast cancer (N=236)	64	0.810
Rheumatoid arthritis (N=235)	59	0.661
General US population (N=8,375)	50–64[b]	0.84

[a]Non-THAOS data from Sullivan et al. (3)
[b]Age range of population studied, years.

CONCLUSION

The symptomatic ATTR patient population in THAOS presented with multisystem involvement regardless of the underlying *TTR* mutation. The most common *TTR* mutation observed in THAOS was Val30Met, and nearly two-thirds of these patients resided in Portugal. Val30Met patients tended to show phenotypic differences in ATTR-related symptoms according to age of onset and endemic region. Symptomatic patients with hereditary ATTR displayed a worse QOL than age-matched populations of healthy subjects. QOL was comparable to or worse than that of patients with other serious diseases. THAOS demonstrates the value of an international registry to better understand the diverse presentations of ATTR.

FUNDING

Data presented in this abstract are part of the THAOS registry, which is sponsored by Pfizer Inc.

REFERENCES

1. Plante-Bordeneuve V, Said G. Familial amyloid polyneuropathy. *Lancet Neurol*. 2011;10(12):1086-1097.
2. Rapezzi C, Quarta CC, Riva L, et al. Transthyretin-related amyloidoses and the heart: a clinical overview. *Nat Rev Cardiol.* 2010;7(7):398-408.
3. Sullivan PW, Lawrence WF, Ghushchyan V. A national catalog of preference-based scores for chronic conditions in the United States. *Med Care.* 2005;43(7):736-749.

Familial amyloid polyneuropathy in Galician population

Beatriz San Millán[1], Susana Teijeira[1], Irene Viéitez[1], Dolores Escriche[2], Jose M Fernández[3], Carmen Navarro[1]

Departments of Pathology [1], Neurology[2] and Neurophysiology[3], University Hospital of Vigo, Spain

ABSTRACT

Transthyretin-related familial amyloidotic polyneuropathy (TTR-FAP) is a systemic amyloidosis caused by mutations in the transthyretin gene. The first identified cause of FAP—the *TTR* Val30Met mutation—is still the most common of more than 100 amyloidogenic point mutations identified worldwide and it is transmitted as an autosomal dominant trait. The penetrance and age at onset of FAP among people carrying the same mutation vary between countries.

We evaluate the clinical, pathological and genetic features in patients of the Galician community with the progressive type of FAP. Probands suffered sensorial defects in the limbs. Electrophysiology, cardiac examinations, sural nerve biopsies and a post-mortem study were realized. Exon 2 of *TTR* gene was sequenced. Sural biopies showed variable loss of nerve fibers. Congo red and thioflavin T affinity confirmed endoneural and vascular amyloid deposits, positive for TTR. Ultrastructural examination demonstrated amyloid fibrils Postmortem studies revealed multi-organ involvement.

INTRODUCTION

Transthyretin-related familial amyloidotic polyneuropathy (FAP) is a fatal inherited autosomal dominant disease resulting from mutations in the transthyretin (*TTR*) gene.

This condition is characterized by systemic extracellular deposition of TTR amyloid fibrils, which originate from mutated transthyretin (mTTR). TTR amyloid preferentially accumulates in peripheral nerves, autonomic nervous system tissues, heart, kidneys, eyes, and gastrointestinal tract. Originally described by C. Andrade in Portugal, FAP was subsequently identified throughout the world. In Spain, several clusters of patients have been identified especially in Baleares, Huelva, Catalonia and Galicia.

Our objective was to evaluate the clinical, pathological and genetic features in patients of the gallician community with the progressive type of FAP.

METHODS

Probands were 15 adults from 34 to 70 years presenting with discomfort, numbness, painful disestesias and other sensorial defects in distal limbs. Exhaustive clinical, biochemical, electrophysiological and cardiac examinations were performed. Sural nerve biopsies were obtained and amyloid deposits were characterized by

their Congo red affinity, birefringence under polarized light and immunofluorescense analysis with thioflavin T. Immunohistochemical analyses included polyclonal antibodies against lambda and kappa light chains, amyloid A, substance P and transthyretin (TTR). Post-mortem studies were realized in one patient. Genealogic trees were elaborated and exon 2 of *TTR* gene was sequenced in probands and relatives who asked for presymptomatic molecular diagnosis.

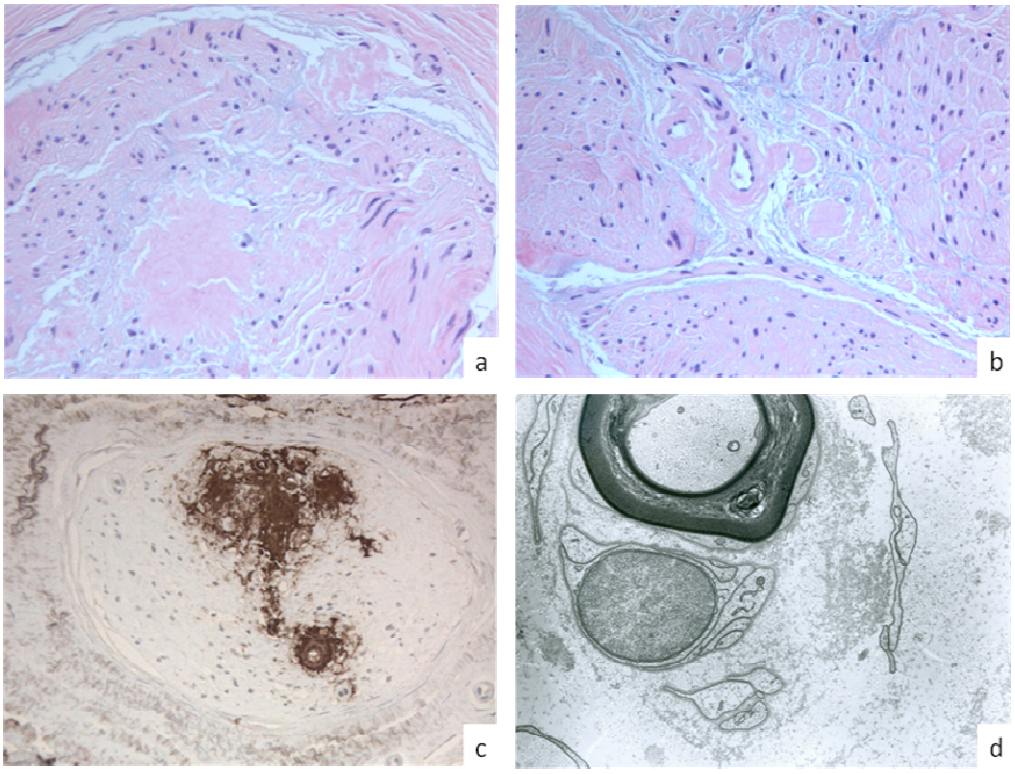

Figure 1. Endoneurial distribution of amyloid in sural nerve samples. a: Subperineurialand endoneural amyloid deposits were common. b: Note amyloid deposits surrounding endoneurial blood vessels and invading the vessel walls. c: Immunohistochemical studies detected TTR in the amyloid deposits. d: Electron micrograph showing amyloid fibrils surrounding myelinated and unmyelinated nerve fibers.

RESULTS

Significant variability of age at onset and clinical severity was observed. Pain, paresthesias and numbness of hands and feet with distal to proximal progression were the most common initial complaints. Patients in more advanced stages of the disease had walking difficulty or weakness. Autonomic manifestations included diarrhoea, constipation and orthostatic hypotension. Extra-neurological manifestations included weight loss and plantar ulcers in long-term cases. Most patients reported familial history of wheelchair-bound members. Sural nerve biopsies of all patients revealed eosinophilic amorphous deposits (Fig.1a-b), positive for Congo Red, thioflavin T, substance P and TTR (Fig.1c). Amyloid was characteristically found in the subperineurial space,

endoneurium, around blood vessels or within the vessel walls, causing occlusion of the lumen in severely affected patients. Nerve fibre density was markedly reduced and in advanced cases myelinated axons had almost disappeared. Endoneurial blood vessels were frequently surrounded and invaded by amyloid. Ultrastructural examination demonstrated straight non-ramified amyloid fibrils of 7-10 nm (Fig.1d). Systemic amyloid deposition was demonstrated by post-mortem examination in one case. Genetic analysis revealed an amino acid substitution of Val 30 for Met in exon 2 of *TTR* gene in probands and several relatives.

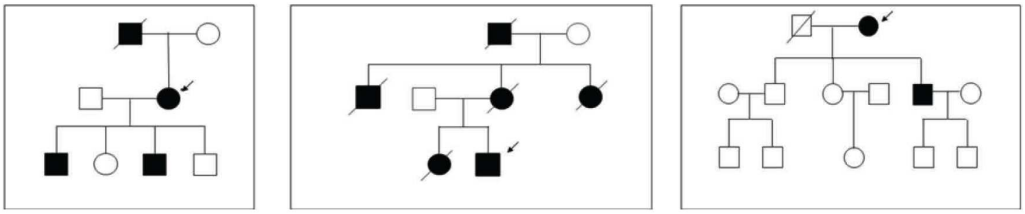

Figure 2. Genealogic trees demonstrated positive familial history and autossomal dominant transmission in most of the cases.

DISCUSSION

14 families were diagnosed, with variable age at onset and illness duration. Ninety per cent of patients referred familial history. Cardiac and autonomic involvement was detected in some patients. Our results are consistent with the Portuguese form of FAP first reported by C. Andrade in 1952.

In conclusion:

- *TTR-FAP has a high prevalence in the Galician community, probably due to its geographic vicinity to Portugal, as all of the patients harbour the Val30Met mutation.*
- *FAP must be considered in all patients with distal painful sensory-motor polyneuropathy of unclear cause.*
- *This rare dominantly inherited disorder can present as an isolated and nonfamilial form, particularly in late-onset cases.*
- *Sural nerve biopsy provides definite diagnosis in order to elaborate a treatment plan and assure a better prognosis and hope for extended life, improving organ function.*
- *Minute deposits can be difficult to identify as amyloid, so biopsy specimens must be carefully studied by a pathologist familiar with nerve pathology. Serial sections of the whole specimen are advisable if deposits are not found in preliminary sections.*
- *Molecular analysis should be offered to symptomatic and asymptomatic members of the families to get a conclusive diagnosis and to perform an adequate genetic counselling.*

ACKNOWLEDGEMENTS

We thank Soralla Barrera for her excellent technical assistance**.**

REFERENCES

1. Araki S, Ando Y. Transthyretin-related familial amyloidotic polyneuropathy-Progress in Kumamoto, Japan (1967-2010). Proc Jpn Acad Ser B Phys Biol Sci. 2010;86(7):694-706.
2. Misumi Y, Ueda M, Obayashi K, Jono H, Su Y, Yamashita T, Ohshima T, Ando Y, Uchino M. Relationship between amyloid deposition and intracellular structural changes in familial amyloidotic polyneuropathy. Hum Pathol. 2012 Jan;43(1):96-104.
3. Planté-Bordeneuve V, Ferreira A, Lalu T, Zaros C, Lacroix C, Adams D, Said G. Diagnostic pitfalls in sporadic transthyretin familial amyloid polyneuropathy (TTR-FAP). Neurology. 2007 Aug 14;69(7):693-8.
4. Said G, Planté-Bordeneuve V. Familial amyloid polyneuropathy: a clinico-pathologic study. J Neurol Sci. 2009 Sep 15;284(1-2):149-54.
5. Planté-Bordeneuve V, Said G.Familial amyloid polyneuropathy. Lancet Neurol. 2011 Dec;10(12):1086-97.
6. Zeldenrust SR. Genotype--phenotype correlation in FAP. Amyloid. 2012 Jun;19 Suppl 1:22-4.
7. Conceição I. Clinical features of TTR-FAP in Portugal. Amyloid. 2012 Jun;19 Suppl 1:71-2. Epub 2012 Apr 6.
8. Hellman U, Suhr O. Regional differences and similarities of FAP in Sweden. Amyloid. 2012 Jun;19 Suppl 1:53-4. Epub 2012 Apr 2.

Familial Dynamics, Attachment and Psychopathology in Familial Amyloidotic Polyneuropathy Patients

Lopes A [1,2], Rodrigues C[1], Sousa A[2], Cunha Z[2],Teixeira L[3], Coelho T[1]

1 Unidade Clínica de Paramiloidose, Centro Hospitalar do Porto, Portugal
2 Unidade de Psiquiatria de Ligação e Psicologia da Saúde, Centro Hospitalar do Porto, Portugal
3 Instituto de Ciências Biomédicas Abel Salazar, Porto, Portugal

Studies on familial dynamics, attachment and psychopathology in Familial Amyloidotic Polyneuropathy (FAP) are few. In 31 FAP patients and a control group (n=30) were applied: socio-demographic and familial description questionnaire, Adult Attachment Scale (AAS) and Brief Symptoms Inventory (BSI). Most of patients were females, married, had one child, were retired and 35,5% had lost one of parents at childhood/adolescence. Patients mean age was 42,4y (control group 36,8y). Statistically significant differences were found between groups for AAS dimensions (Closeness and Dependence, p<0,001). Female patients presented higher Anxiety (p<0,001). Also were found statistically significant differences between groups for all BSI dimensions (p<0,05) (except for Paranoid Ideation). Female patients had higher values for Depression, Anxiety and Obsessive-Compulsive dimensions (p<0,05). These imply that FAP patients are a special group with particular familial characteristics, with difficulties in attachment that may be responsible for psychopathology patterns. Females represent the more problematic group.

INTRODUCTION

Studies on familial dynamics and attachment in Familial Amyloidotic Polyneuropathy (FAP) patients are few. There isn't much information about psychopathology in these patients.

For a long time, patients with FAP lived with a disease that had no treatment, had to face a chronic and catastrophic evolution that most of them knew very well, since they had experienced it in other members of their families (parents, siblings and even other members of their communities). FAP has a great impact on mental and relational patients life (psychosocial and familial)[1,2].

The hereditary characteristics with variable adulthood age of onset and the variable symptomatic expression provokes uncertainty and anxiety; chronic and devastating evolution full of repulsive aspects of the body may decrease self esteem, evoke feelings of rejection, loneliness and depression. These patients live with a disease that imposes a strong psychological burden to them and their families[3]. Liver transplantation and most recently a new specific medication (tafamidis) have brought some hope for these patients but also a new source of anxiety (to be or not to be included, whether for transplantation or for medication)[4].

It is known that chronic diseases cause an important impact in families. In the area of other genetic late onset diseases a few studies have made relevant how these families may be more problematic (cohesion, emotions expression) and attachment issues have been also addressed[5,6].

Studies on families with FAP, concerning the psychosocial impact of disease on family structure are relevant to develop therapeutic strategies that may fit these population problems.

With this study we wanted to know if families with FAP do organize in a different way of families with no such problems, and if their members have particular attachment patterns and psychopathology?

METHODOLOGY

This is a preliminary, transversal and quantitative study. The sample was composed by two groups, one with patients consecutive attending consultation in Familial Amyloidotic Unit, Centro Hospitalar do Porto (*n*=31), and the other, control group (*n=30*), with subjects without known genetic or chronic disease. All of participants were more than 21 and less than 66 years old.

The following instruments were used: Socio Demographic Questionnaire, Familial Description Questionnaire, Adult Attachment Scale (AAS) and Brief Symptom Inventory (BSI).

AAS has 18 items for evaluation of 3 dimensions: *Closeness* (comfort in making relationships), *Dependence* (feelings of depending on others) and *Anxiety* (concerns about being abandoned or rejected by others)[7]. BSI has 53 items that evaluate 9 psychopathological dimensions (*Somatization*, *Obsessive/Compulsive*, *Interpersonal Sensivity*, *Depression*, *Anxiety*, *Hostility*, *Phobic Anxiety*, *Paranoid Ideation* and *Psychoticism*) and 3 global indexes (*Global Severity Index*, *Positive Symptom Distress Index* and *Positive Symptom Total*)[8]: In this study, besides the nine dimensions, we only consider the Global Severity Index which helps to measure the overall psychological distress level.

For statistical analysis was used the Student t test for independent samples. When was not verified the assumption of normality, was used the Mann-Whitney test. All analysis were performed using the SPSS version 17.0 and was considered the significance level p=0,05.

RESULTS

Most patients were waiting for liver transplantation (64,5%); 25,8% were in advanced stage and 9,7% have been transplanted; 64,5% were female and 67,7% were married (50% in the control group). Mean age of patients was 42,4y (*SD*=10,0) and 36,8y (*SD*=11,7) in control group. Most of patients had 1 child (44,8%) or none (24,1%); in control group, 56,7% had no children and 16,7% had one child. Most of patients had less than 9 years of school level and most of control group had more than 12 years of school level. Most of patients belonged to the working class and had no professional qualifications. 61,3% are retired and 89,5% of these, because of FAP. Only 3,6% are retired in the control group.

Results from Familial Description Questionnaire: the sick parent was in 58,6% the mother and all sick parents were deceased; parents age of beginning of sickness was 39,8 yrs (*SD*=10,8 yrs, *Min*=28 yrs, *Max*= 61 yrs) and the mean age of patients at that time was 13,3 yrs (*SD*=9,5 yrs, *Min*=1 yr, *Max*=30 yrs). At date of decease, the mean age of *parents* was 51,7 yrs (*SD*=11,4 yrs, *Min*=32 yrs, *Max*=77 yrs) and the mean age of *patients* was 23,7 yrs (*SD*=10,5 yrs, *Min*=5 yrs , *Max*=46 yrs).

Most of patients (80%) referred they had no separations or significant life changes after sick parents death.

Results from AAS: were found statistically significant differences between the two groups for dimensions Closeness and Dependence (p<0,001). Considering only the FAP group, were verified that women presented a higher score in Anxiety (p<0,001) and that there were no differences regarding the marital status (p>0,05 in all dimensions) or loss of progenitor in childhood/adolescence (p>0,05 in all dimensions).

Results from BSI: were found statistically significant differences between the two groups for all BSI dimensions (p<0,05) (except for Paranoid Ideation). FAP group had a higher median score for all BSI dimensions and, considering the results of this group regarding the gender, were verified that women had higher values and presented statistically significant differences for Obsessive-Compulsive (p=0,031), Depression (p=0,033), Phobic Anxiety (p=0,044) and Paranoid Ideation (p=0,041) dimensions.

DISCUSSION AND CONCLUSIONS

Patients had higher scores in almost all psychopathologic indexes than control group, which could define FAP patients as a vulnerable group with higher risks for emotional/psychiatric breakdowns. Depression and anxiety were the most common problems in these patients. Patients had also more difficulties with adult attachment. This means that FAP patients may be more vulnerable to problems of depending on others and closeness. This may have as consequence difficulties in adult relationships and intimacy.

When we considered the variable gender, we found that women with FAP are at higher risk for several psychopathological problems namely depression and anxiety.

In patients there were a very high percentage of sick or deceased parents during childhood and/or adolescence. Although we empirically know that those events may provoke significant life changes, in this sample such did not occur. Also no changes were found whether in psychopathology or attachment issues, related to these variables which according to literature of other domains, could be expected.

The study limitations namely the sample size and the fact that only few of studied patients had significant life changes after sick parent's sickness or death could explain that such implications were not relevant.

Emotional and psychopathological problems are common and relevant, so these patients should have available psychosocial support in multidisciplinary teams.

This is a preliminary study and although these results may be limited they represent certainly the need to obtain more rigorous knowledge about psychopathology, emotional problems and familial issues in FAP patients.

REFERENCES

1. Andrade C. A peculiar form of peripheral neuropathy: familial atypical generalized amyloidosis with special envolvement of the peripheral nerves. Brain 1952;75:408-427.
2. Coelho T, Sousa A, Lourenço E, Ramalheira J. A study of 159 Portuguese patients with familial amyloidotic polyneuropathy (FAP) whose parents were both unaffected. Journal of Medicine Genetics 1994;31:293-299.
3. Lopes A, Fleming M. Aspectos Psicológicos da Polineuropatia Amiloidótica Familiar: a trama subterrânea intergeracional. Brotéria Genética 1998;XIX(XCIV):183-192.
4. Jonsene E, Athlin E, Suhr O. Familial amyloidotic patient's experience of the disease and of liver

transplantation. Journal of Advanced Nursing 1998;27:52-58.

5. Rolim L, Zagalo-Cardoso J, Paul C, Sequeiros J, Fleming M. The Perceived Advantages and Disadvantages of Presymptomatic Testing for Machado-Joseph Disease: Development of a New Self-Response Inventory. Journal of Genetic Counseling 2006 Oct:15(5):375-91.
6. Van der Meer L, Timman R, Trijsburg W, Duisterhof M, Erdman R, Van Elderen T, Tibben A. Attachment in families with Huntington's disease. A paradigm in clinical genetics. Patient Education and Counseling. 2006 Oct;63(1-2):246-54.
7. Canavarro MC. Inventário de sintomas psicopatológicos – BSI. In Simões MR, Gonçalves M, Almeida LS (Eds.), Testes e Provas Psicológicas em Portugal (II vol.). Braga: APPORT/SHO.1999.
8. Collins NL, Read SJ. Adult attachment: working models, and relationship quality in dating couples. Journal of Personality and Social Psychology 1990;58(4):644-663.

The Prevalence of Holter Abnormalities in ATTR Cardiac Amyloidosis

A. Reshad Garan[1], Sheela Kolluri[2], Ilise Lombardo[2], and Mathew S. Maurer[1]

[1]Columbia University Medical Center, New York, NY, USA, [2]Pfizer, Inc., New York, NY, USA

ABSTRACT

Little is known about the prevalence of cardiac arrhythmias in patients with ATTR cardiac amyloidosis. Furthermore, there is little known about the prognostic importance of ventricular arrhythmias in this population. We sought to characterize cardiac arrhythmias in ATTR cardiac amyloidosis patients. We analyzed 24 hour Holter data from 34 patients with ATTR cardiac amyloidosis in order to determine the prevalence of arrhythmias in this population. Sixteen patients (45.7%) were taking a beta-blocker, eight (22.9%) were taking amiodarone, and two (5.7%) were taking another anti-arrhythmic medication. Non-sustained ventricular tachycardia (NSVT) was present in 20 patients (58.8%). No patients had sustained ventricular tachycardia. There was no difference in overall survival between those with and without NSVT on the 24 hour Holter monitor. In this sample, malignant ventricular arrhythmias were present in the majority of patients with ATTR cardiac amyloidosis, though the presence of NSVT on Holter monitor did not confer a worse survival.

INTRODUCTION

Survival in the amyloidoses is dependent upon the extent of cardiac involvement. Moreover, cardiac complications are major predictors of morbidity and mortality in patients with ATTR amyloidosis following orthotopic liver transplant (OLT).[1] Most studies identifying prognostic markers in cardiac amyloid have either focused solely on patients with AL amyloid or have included only a minority of patients with ATTR; much less is known about predictors of survival in the latter population.

Non-sustained ventricular tachycardia (NSVT) is prognostically important in several types of cardiomyopathies. In AL amyloid, the presence of ventricular arrhythmias on 24 hour ambulatory Holter monitoring was an independent predictor of survival[2] and may be a predictor of sudden death.[3] Relatively little is known about ventricular tachyarrhythmias in the ATTR population. The aim of the current study is to characterize the prevalence and significance of ventricular arrhythmias during 24 hour ambulatory Holter monitoring in patients with ATTR cardiac amyloidosis.

METHODS

The data analyzed were collected as part of NCT00694161, an open label, multicenter, single-treatment study examining the efficacy and safety of Tafamadis in patients with ATTR amyloid cardiomyopathy. Subjects were

eligible if they were age forty or older and had ATTR amyloid cardiomyopathy, either due to V122I mutation or wtATTR. After obtaining informed consent according to the institutional review board of participating centers, baseline data were obtained from 34 patients. All subjects underwent 24 hour ambulatory Holter monitoring. The primary end-point for the present analysis was all cause mortality. Baseline demographic, clinical, and echocardiographic data were compared for those with and those without non-sustained ventricular tachycardia using the Fisher exact test for categorical variables and the Wilcoxon rank-sum test for continuous variables. Time-to-event analysis was conducted by Kaplan-Meier estimate curves for the presence or absence of NSVT on 24-hour Holter monitor. A p-value ≤ 0.05 was considered significant.

RESULTS

Thirty-four patients were enrolled. Table 1 details the demographic information of patients divided into those with and without NSVT. There were no significant differences between the population of patients with NSVT and that without NSVT. NSVT (<30 beats) was observed in 58.8% of the study population.

Table 1. Patient Demographics

	All (N=34)	With NSVT (N=20)	Without NSVT(N=13)*
Gender (% Female)	8.8	15.0	0
Age (years)	76±4.6	75±4.4	76±5.1
LVEF (%)	46±14	46±16	46.5±11
Wild Type (%)	88.2	85.0	92.3
NYHA class (%)			
I	11.8	20.0	0
II	82.4	75.0	92.3
III	5.9	5.0	7.7
IV	0	0	0
Anti-arrhythmics (%):			
Beta-blocker	44.1	40.0	46.1
Amiodarone	35.3	25.0	46.1
Other	8.8	10.0	7.7
IV Septal Thickness (mm)	20.8±3.6	21.2±3.8	20.4±3.5
NT pro-BNP (pg/ml)	4950±4159	3758±2493	6914±5691
Troponin I (ng/ml)	0.14±0.08	0.14±0.07	0.14±0.10
Troponin T (ng/ml	0.05±0.04	0.05±0.03	0.05±0.04
Defibrillator (%)	20.6	10.0	30.8
Permanent Pacemaker (%)	38.2	30.0	46.1

*All p-values comparing values for patients with NSVT and without NSVT > 0.05

Six patients met the primary end-point of death from any cause. The presence of NSVT did not correlate with mortality (Figure 1).

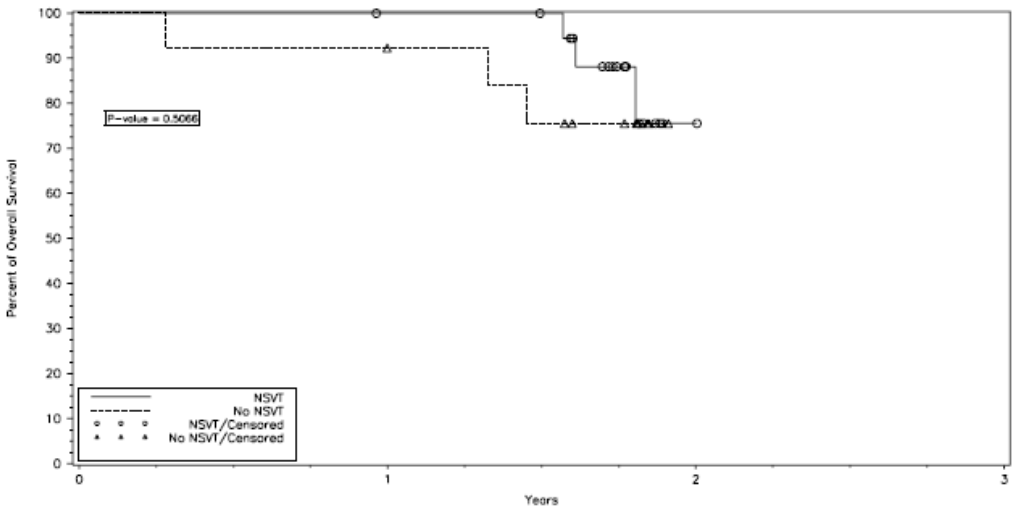

Figure 1. Kaplan-Meier survival estimates stratified by presence or absence of NSVT on baseline Holter

DISCUSSION

Ventricular arrhythmias are common in this patient population with more than 50% of patients exhibiting NSVT on Holter monitor. The prognostic value of NSVT has been examined in numerous populations of cardiomyopathy patients, including those with ischemic and hypertrophic cardiomyopathies. However, unlike in these populations of patients, NSVT did not confer a worse prognosis in our cohort of patients with ATTR cardiac amyloidosis.

ACKNOWLEDGEMENTS

This study was an analysis of the baseline Holters performed in the Fx1B-201 Study (NCT00694161) which was sponsored by FoldRx Pharmaceuticals, Inc, that is a wholly owned subsidary of Pfizer, Inc.

REFERENCES

1. Okamoto S, Hörnsten R, Obayashi K, Wijayatunga P, Suhr OB. Continuous development of arrhythmia is observed in Swedish transplant patients with familial amyloidotic polyneuropathy (amyloidogenic transthyretin Val30Met variant). Liver Transpl. 2011;17:122-8.
2. Palladini G, Malamani G, Cò F, et al. Holter monitoring in AL amyloidosis: prognostic implications. Pacing Clin Electrophysiol. 2001;24:1228-33.
3. Falk RH, Rubinow A, Cohen AS. Cardiac arrhythmias in systemic amyloidosis: correlation with echocardiographic abnormalities. J Am Coll Cardiol. 1984;3:107-13.

Relationship between age at symptom onset and left ventricular wall thickness in ATTR amyloid—THAOS survey

C. Rapezzi,[1] M.S. Maurer,[2] on behalf of the THAOS Investigators

1. University of Bologna, Bologna, Italy; 2. Columbia University College of Physicians and Surgeons, New York, NY.

Transthyretin amyloidosis (ATTR) is a rare hereditary disorder presenting primarily as polyneuropathy and cardiomyopathy. A relationship between age at symptom onset and development of cardiomyopathy has been suggested. In symptomatic ATTR patients enrolled in THAOS (Transthyretin Amyloid Outcomes Survey), the association of echocardiographic measures of left ventricular (LV) wall thickness with age of symptom onset, gender, mutation, blood pressure, and liver transplant history was evaluated. In ATTR, cardiac manifestations are more pronounced in patients with late symptom onset. Late symptom onset (≥50 years) was also associated with greater LV wall thickness than early onset (<50 years, P<0.01) in both V30M and non-V30M patients. Age at echocardiographic measurement is independent of gender as a predictor of cardiac involvement in ATTR (as determined by LV wall thickness) across *TTR* mutations. Thus, more severe cardiac manifestations in ATTR are more pronounced in patients with late symptom onset regardless of the specific mutation(s) studied.

BACKGROUND AND OBJECTIVES

Transthyretin (TTR) amyloidosis (ATTR) is an autosomal dominant or acquired disorder in which the native tetrameric structure of TTR is destabilized, resulting in extracellular deposition of insoluble protein fibrils primarily in nerves and the heart (1). ATTR has been associated with wild-type (WT) *TTR* and more than 100 identified *TTR* mutations that promote the misfolding and aggregation of TTR into amyloid. ATTR is phenotypically heterogeneous; presenting symptoms include polyneuropathy and/or cardiomyopathy (2,3). Cardiac symptoms are more pronounced in some genotypes (e.g., Val122Ile, Leu111Met, Thr60Ala, Ile68Leu, and WT *TTR*) than in others (e.g., Val30Met). A relationship between age at symptom onset, gender, and development of cardiac manifestations (e.g., interventricular septum thickness) has been suggested (4). This analysis utilizes data from symptomatic patients enrolled in the Transthyretin Amyloidosis Outcomes Survey (THAOS) to evaluate variables associated with cardiac involvement in ATTR.

METHODS

THAOS is a global, multicenter, longitudinal, observational survey that collects data on the natural history of ATTR. The association of left ventricular (LV) wall thickness with gender, age at symptom onset, and age at

echocardiographic testing was assessed in the THAOS population. The Wilcoxon rank-sum test was used to compare mean differences in LV wall thickness between 2 genotype subgroups. Multivariate regression analysis was conducted using LV wall thickness divided by height as the dependent variable and using gender and age at echocardiographic testing as independent variables.

RESULTS

Patients from the THAOS population included in this study represented 28 *TTR* variants (Table 1).

Table 1. Baseline Characteristics: Symptomatic THAOS Patients with LV Wall Thickness Measures

Characteristic	Symptomatic THAOS Population (N=227)
Age at symptom onset, years	
Mean ± SD	53 ± 18
Median	55
Range	18–87
Age at echocardiography, years	
Mean ± SD	58 ± 17
Median	61
Range	26–89
Gender, n (%)	
Male	169 (74.4)
Female	58 (25.6)
Ethnicity, n (%)	
Caucasian	165 (72.7)
Asian	27 (11.9)
African descent	22 (9.7)
Latino	7 (3.1)
Other	4 (1.8)
Missing	2 (0.9)
TTR genotype, n (%)	
Ala97Ser	2 (0.9)
Glu89Gln	7 (3.1)
His88Arg	2 (0.9)
Ile107Val	4 (1.8)
Ile68Leu	4 (1.8)
Leu111Met	5 (2.2)
Phe64Leu	3 (1.3)
Ser50Arg	3 (1.3)
Ser77Tyr	4 (1.8)
Thr49Ala	2 (0.9)
Thr59Lys	2 (0.9)
Thr60Ala	5 (2.2)
Val122Ile	21 (9.3)
Val20Ile	3 (1.3)
Val30Met	86 (37.9)
Wild-type	51 (22.5)
Other	23 (10.1)

LV wall thickness was significantly greater in men (P<0.0001), in patients with later symptom onset (≥50 years, P<0.0001) and in those ≥50 years of age at the time of measurement (P<0.0001) across all mutation groups. LV wall thickness was significantly greater in patients with cardiac *TTR* mutations (Val122Ile, Leu111Met, Thr60Ala, and Ile68Leu) and in WT patients, compared with those with the V30M mutation (P<0.0001 for both measures). There was no difference between the WT and cardiac mutation groups. Age at symptom onset coincided with

age at echocardiographic testing for the 3 subgroups (Figure 1A). LV wall thickness increased with age at measurement across subgroups (Figure 1B).

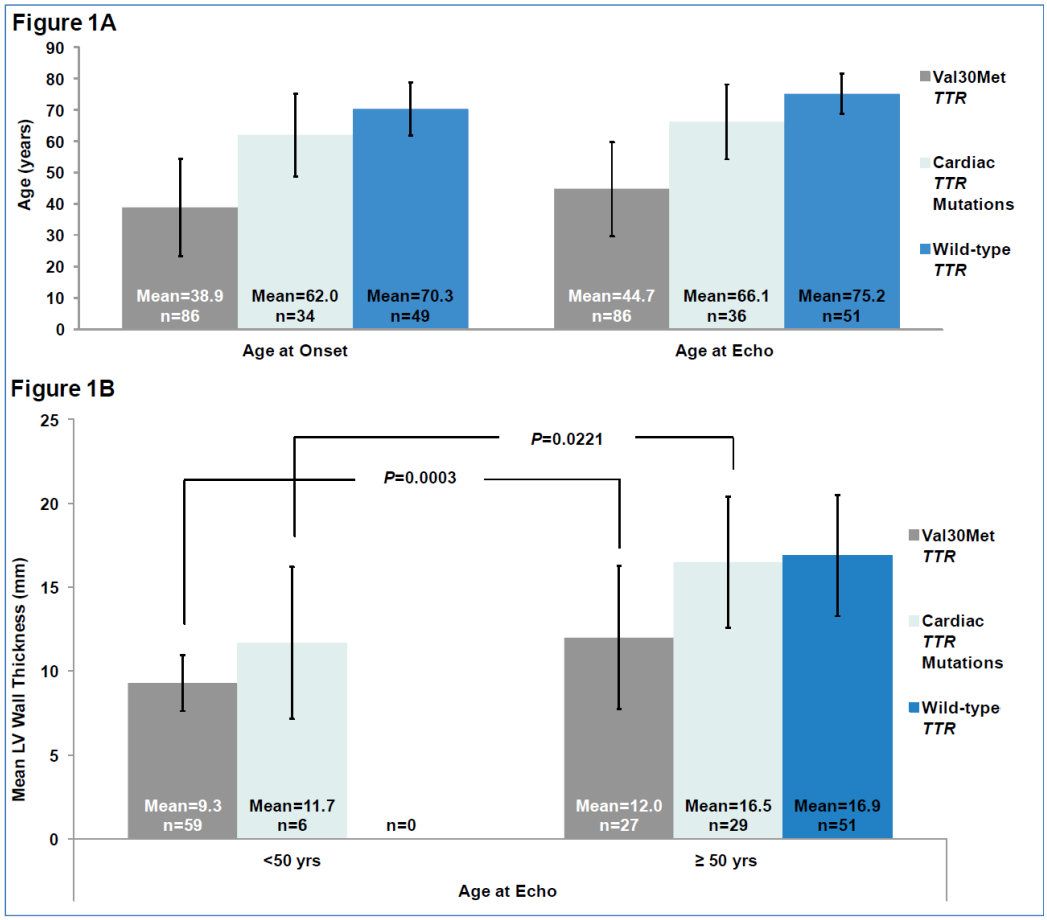

Figure 1. Age and Genotype. (A) Age at Symptom Onset and Age at Echocardiographic Testing by Genotype. (B) LV Wall Thickness by Age at Echocardiographic Testing and Genotype.

While both gender and age at echocardiographic testing were independent predictors of LV wall thickness in symptomatic patients, only age at echocardiographic testing was a significant predictor of LV wall thickness in patients with cardiac *TTR* mutations and patients with V30M mutations.

CONCLUSION

In ATTR, cardiac manifestations were more pronounced in patients with late symptom onset and in older patients. Furthermore, age (at echocardiographic testing) was an independent determinant of severity of cardiac involvement as determined by LV wall thickness.

FUNDING

Data presented in this abstract are part of the THAOS registry, which is sponsored by Pfizer Inc.

REFERENCES

1. Rapezzi C, Quarta CC, Riva L, et al. Transthyretin-related amyloidoses and the heart: a clinical overview. *Nat Rev Cardiol*. 2010;7(7):398-408.
2. Benson MD, Kincaid JC. The molecular biology and clinical features of amyloid neuropathy. *Muscle Nerve*. 2007;36(4):411-423.
3. Planté-Bordeneuve V, Said G. Familial amyloid polyneuropathy. *Lancet Neurol*. 2011;10(12):1086-1097.
4. Hornsten R, Pennlert J, Wiklund U, et al. Heart complications in familial transthyretin amyloidosis: impact of age and gender. *Amyloid*. 2010;17(2):63-68

Heart failure secondary to severe cardiomyopathy: clinical presentation of familial amyloid polyneuropathy with Val30Met mutation

C. Monteiro[1], T. Sequeira[2], M. Santos[3], A. Marinho[2], I. Sá[3], H. Reis[3], T. Coelho[4,5]

1- Neurology department, 2-Internal medicine department, 3-Cardiology department,4-FAP clinic, 5-Neurophysiology department, Hospital de Santo António, Porto, Portugal.

ABSTRACT

Severe restrictive cardiomyopathy is not commonly observed in Portuguese patients with familial amyloid polyneuropathy caused by Val30Met mutation (FAP ATTRV30M). We report a case of a 47-years-old man who presented with congestive heart failure along with minimal neuropathic symptoms as the first clinical manifestation of FAP ATTRV30M.

INTRODUCTION

Familial amyloid polyneuropathies are a group of multisystemic hereditary diseases most commonly caused by mutations in transthyretin. The Val30Met mutation (FAP ATTRV30M) is particularly common in Portugal and it is clinically characterized by a length-dependent polyneuropathy with autonomic dysfunction. Heart involvement is frequent in Portuguese patients; conduction disturbances represent the most common cardiac manifestations in FAP ATTRV30M patients (1). Among the cardiac manifestations, cardiomyopathy is uncommon in Portuguese patients. We report a patient with TTR Val30Met mutation in whom the clinical presentation was a severe restrictive cardiomyopathy.

METHODS

Case report and literature review.

RESULTS

A 47-years-old man, with diabetes and no known family history of cardiac or neurological disease, presented with one year of fatigue, exertional dyspnea, periorbital and lower limbs edema; on admission he had a heart failure class III on NYHA classification. He also reported erectile dysfunction, minor feet paresthesias, and more recently, reduced left visual acuity. Neurological signs including orthostatic hypotension were absent; there was no macroglossia. Echocardiography and cardiac magnetic ressonance imaging revealed an infiltrative cardiomyopathy suggestive of amyloidosis. Endomyocardial biopsy was therefore performed, showing no

staining with Congo red; salivary gland biopsy was also negative. Electromyography revealed bilateral carpal tunnel syndrome. Serum and urine immunofixation electrophoresis were negative; other causes of restrictive cardiomyopathy like sarcoidosis and hemochromatosis were excluded. DNA analysis of the TTR gene was performed and a Val30Met mutation was detected. After the genetic diagnosis, left eye vitrectomy was performed, with detection of amyloid in the vitreous.

DISCUSSION

The patient presented with a severe restrictive cardiomyopathy, associated with minor sensory and autonomic symptoms, raising the suspicion of AL amyloidosis, which was not confirmed either by biopsy or immunoelectrophoresis. Although it was not possible to detect amyloid on the examined tissues, TTR amyloidosis was suspected and unpredictably a Val30Met mutation was found (2). Heart failure due to restrictive cardiomyopathy is an atypical clinical presentation of FAP ATTRV30M. Our case report also highlights the need to consider FAP in the differential diagnosis of cardiac amyloidosis.

REFERENCES

1. Planté-Bordeneuve V, Said G. Familial amyloid polyneuropathy. Lancet Neurol 2011;10:1086–97
2. Hörnsten R, Pennlert J, Wiklund U, Lindqvist P, Jensen SM, Suhr OB. Heart complications in familial transthyretin amyloidosis: impact of age and gender. Amyloid. 2010;17:63-8

Urinary biomarkers for kidney disease in ATTR amyloidosis

A. Rocha[1], F. Bravo[2], I. Beirão[1,3,4], J.C. Oliveira[2], L. Lobato[1,3,4]

[1]Department of Nephrology, [2]Department of Clinical Chemistry and [3]Unidade Clínica de Paramiloidose, Hospital de Santo António, Centro Hospitalar do Porto, Porto, Portugal; [4]UMIB, Instituto de Ciências Biomédicas Abel Salazar - ICBAS, University of Porto, Porto, Portugal
Corresponding author: Luísa Lobato lmlobato@icbas.up.pt

ABSTRACT

The detection and prognosis of nephropathy in ATTR V30M depends on albuminuria and renal function. Urinary levels of alpha-1 microglobulin (A1M) and beta-2 microglobulin (B2M) reflect tubular dysfunction, urinary alpha-2 macroglobulin (A2M) implies glomerular damage. Measurements in 30 patients and 11 asymptomatic carriers: urinary A1M, B2M, A2M, albumin and creatinine; serum creatinine and cystatin C. Patients: 49.4±12.6 years; pathological urinary A1M was detected in 17, A2M in 5; 5 had albuminuria (mg/g creatinine) 30-300 and in 20 >300. Asymptomatic: 41.4±15 years; urinary A1M in 1, no A2M, albuminuria >30 in 1. The excretion rates of A1M and B2M were positively correlated with albuminuria (P<0.001), serum creatinine (P<0.05) and cystatin C (P<0.001). Urinary A2M was almost exclusively found in the presence of albuminuria, although their levels do not correlate. Urinary biomarkers emerge as a potential approach to detect renal disease. Unexpectedly, urinary A2M was not a marker of severity of albuminuria.

INTRODUCTION

The amyloidoses associated with transthyretin (ATTR) are autosomal-dominant diseases due to at least 100 different transthyretin (TTR) mutations, being the single amino-acid substitution of methionine for valine at position 30 the most common. Although this disorder was initially thought to follow a benign course concerning the kidney, it was recognized that progression to end-stage renal disease (ESRD) occurs in up to 10 percent of patients in the pre-transplant era. The detection and prognosis of ATTR nephropathy depend on the presence of albuminuria and/or an elevated serum creatinine concentration. Both are correlated with heavy amyloid deposition in the glomeruli, arterioles, and medium vessels, but not with deposition in medullary tissues (1). Ideally, we should have early markers of nephropathy in initial stages of ATTR, even before neurological manifestations.

In past decades, several urinary proteins have been identified as early prognostic markers in different kidney diseases (2). Here, we report the value of urinary alpha 1-microglobulin (A1M), beta-2 microglobulin (B2M) and

alpha-2 macroglobulin (A2M) as predictors of outcome of nephropathy in a cohort of 41 subjects with TTR V30M mutation.

PATIENTS AND METHODS

Thirty patients and 11 asymptomatic gene carriers were randomly selected. Information about patient demographics and clinical characteristics was collected.

On the day of the urine sample collection, the following key laboratory measures were assayed: urinary creatinine, albumin, B2M, A1M and A2M and serum creatinine. The glomerular filtration rate (GFR) was estimated by serum cystatin C. The amount of albuminuria was estimated by the albumin to creatinine ratio (mg/g). Albuminuria <30 mg/g was considered normal. Urinary values of A1M >12 mg/L, A2M > 9.4 mg/L and B2M > 300 ng/mL were considered abnormal.

Correlations were assessed by Spearman correlation coefficient test. $P<0.05$ was selected as the level of significance. Values are expressed as mean ± standard deviation.

RESULTS

The patients, 18 females and 12 males, had 49.4±12.6 years of age and an evolution of neuropathy of 5.0 ± 4.4 years. Asymptomatic gene carriers, 9 females and 2 males, had 41.4 ± 15 years of age.

The laboratory data are summarized in Table 1. Eleven patients showed overt renal failure, with 5 of them progressing to dialysis.

Table 1. Study population laboratory parameters

	Patients (*n* = 30)	Asymptomatic gene carriers (*n* = 11)
uAlb (mg/g)	1663.9 ± 2019.9	11.5 ± 14.1
sCr (mg/dl)	1.71 ± 2.17	0.72 ± 0.14
sCys (mg/dl)	1.54 ± 1.15	0.66 ± 0.12
GFR (ml/min)	76.9 ± 52.6	137.4 ± 32.5

uAlb: albuminuria; sCr: serum creatinine; sCys: serum cystatine

Pathological urinary A1M, B2M and A2M levels were detected in patients, not in asymptomatic gene carriers (Table 2). The A1M biomarker was present more often in patients and it was the single detected in the absence of neuropathy. None of the patients showed glycosuria.

Table 2. Pathological excretion of urinary biomarkers in the subjects

	A1M		A2M		B2M	
	n (%)	level	n (%)	level	n (%)	level
Patients	17 (56.7)	45.2 ± 41.3	5 (16.7)	28.6 ± 34.3	6 (20)	22592.8 ± 27047.6
Asymptomatic	1 (9.1)	12.1	0	absent	absent	absent

A1M: alpha 1-microglobulin, B2M: beta-2 microglobulin; A2M: alpha-2 macroglobulin

Six patients had albuminuria <30 mg/g, 4 between 30 and 300 mg/g and 20 >300 mg/g. Among normoalbuminuric we found 1 patient with urinary pathological levels of A2M and A1M and another with abnormal B2M.

The excretion rates of A1M and B2M were positively correlated with albuminuria (P<0.001), serum creatinine (P<0.05), cystatin C (P<0.001) and GFR (P<0.001) Excretion of A2M was almost exclusively found in the presence of albuminuria >30 mg/g, although their levels do not correlate with the severity of albuminuria. Among 14 patients who evolved to ESRD, 5 presented simultaneous detection of A1M and A2M.

DISCUSSION

Definite diagnosis of ATTR nephropathy is based on renal biopsy findings. In our experience, however, the diagnosis can be reliably made in patients with microalbuminuria in the unequivocal presence of neuropathy. Conversely, we face two constraints; microalbuminuria is not a marker of tubulointerstitial damage and in 10 percent of patients who progress to ESRD this marker was absent.

Thus, improved methods for detect onset of kidney amyloid deposits, even before clinical disease, are needed to allow earlier treatment. We used a urine analysis approach to identify non-invasive and cost-effective markers.

One third of our patients presented a clear glomerular proteinuria, although significant tubular component was also seen. Urinary excretion of low-molecular proteins A1M and B2M, which are reliable indicators of tubular impairment, was present in 60 percent of patients. To explain the occurrence of low molecular weight proteinuria despite the absence of typical tubular syndrome we must regard that megalin, a multiligand receptor expressed on the renal proximal tubules, functions as a specialized chaperone protein for internalization and degradation of a number of proteins, including A1M and B2M (3). We speculate that the mechanism for low molecular weight proteinuria is not tubular damage but actually a saturation of the megalin-mediated endocytosis. So, the protein overload present in the lumen of the proximal tubule results in a combined low and high molecular weight proteinuria. We suppose that urinary excretion of tubular proteins is related with severity of kidney injury and it is not a precocious marker.

The progressive dysfunction of the glomerular barrier leads to nonselective waste of high molecular weight proteins. It would be expected that excretion of A2M was related with the severity of albuminuria. Unexpectedly, this correlation was not found. However, the combined excretion of low and high molecular weight proteins was exclusively found in patients who progressed to ESRD.

It is likely that a combination of biomarkers will be required for assessing disease detection and future response to a treatment. A1M, B2M and A2M were good markers to estimate injury severity and define prognostic information. We recommend the use of urinary low and high molecular weight proteins for definition and monitoring the progression of renal lesion in ATTR V30M.

REFERENCES

1. Lobato L, Beirão I, Guimarães SM, Droz D, Guimarães S, Grünfeld JP, Noël LH. Familial amyloid polyneuropathy type I (Portuguese): distribution and characterization of renal amyloid deposits. Am J Kidney Dis. 1998; 31:940-946.
2. Petrica L, Petrica M, Vlad A, Jianu DC, Gluhovschi, Ianculescu C et al. Proximal tubule dysfunction is dissociated from endothelial dysfunction in normoalbuminuric patients with type 2 diabetes mellitus: a cross-sectional study . Nephron Clin Pract. 2011;118(2):c155-64.

3. Vinge L, Lees GE, Nielsen R, Kashtan CE, Bahr A, Christensen EI. The effect of progressive glomerular disease on megalin-mediated endocytosis in the kidney. Nephrol Dial Transplant. 2010 Aug;25(8):2458-67.

Analysis of TTR-related amyloidosis in the field of orthopedics

A. Yanagisawa[1,3], T. Sueyoshi[3], M. Ueda[1,2], M. Tasaki[1,2], T. Oshima[2], H. Jono[1], K. Obayashi[1,2], Y. Misumi[2], T. Yamashita[2], K. Yawatari[4], H. Irie[3], A. Sei[3], J. Ide[3], H. Mizuta[3], & Y. Ando[2]

[1] Department of Diagnostic Medicine, [2] Department of Neurology, and [3] Department of Orthopaedic Surgery, Faculty of Life Sciences, Kumamoto University, Kumamoto, Japan, and [4]Kumamoto Orthopedic Hospital, Kumamoto, Japan

ABSTRACT

Transthyretin (TTR) amyloid deposition is often detected in ligaments and tendons in the field of orthopedics, especially in elderly people. However, detailed incidence and clinical significance of TTR amyloid deposition in ligaments and tendons remains largely unknown. In this study, we analyzed TTR-related amyloidosis in the field of orthopedics. We studied 126 specimens from patients with carpal tunnel syndrome, rotator cuff tears, and lumbar spinal canal stenosis. We identified 61 amyloid-positive samples, 46 of which contained TTR-derived amyloid. Although correlation between the serum TTR levels and amount of amyloid deposition was not observed, age-dependent increase of the affinity between wild type TTR-related amyloid and ligamentum flavum was observed in patients with lumbar spinal canal stenosis. These results suggest that relationship between this phenomenon and senile systemic amyloidosis may be present.

INTRODUCTION

Transthyretin (TTR) has a β-sheet-rich structure and is highly amyloidogenic protein [1, 2] that causes two types of amyloid diseases: familial amyloid polyneuropathy (FAP), caused by mutant TTR [3, 4], and senile systemic amyloidosis (SSA), caused by wild-type (WT) TTR [3, 4]. Recently, it has been well documented that TTR-related amyloid shows high affinity for ligaments and tendons, especially in elderly people [5]. However, detailed incidence of amyloid deposition or relationship between amyloid deposition in these tissues and serum levels of TTR in amyloid deposited subjects has not been well understood.

In this report, we examined whether TTR-related amyloid deposition detected in ligaments and tendons lead to SSA.

MATERIALS AND METHODS - PATIENTS

We studied 126 specimens obtained from patients (66 men and 60 women) with carpal tunnel syndrome: CTS (54 specimens), rotator cuff tears: RCT (21 specimens), or lumbar spinal canal stenosis: LSCS (51 specimens).

These patients were diagnosed at the Department of Orthopaedic Surgery in Kumamoto University Hospital and its associated hospitals based on clinical findings and radiological examinations from 2008 to 2011. At the time of surgery, the patients were between 46 and 83 years old (mean: 71 years old).

CONGO RED STAINING

Tissue samples were fixed with 10% formalin, embedded in paraffin, serially sectioned at a thickness of 4 μm, and placed on microscope slides. After sections were stained with hematoxylin-eosin and alkaline Congo red, amyloid deposition were examined under polarized light for the presence of green birefringence.

IMMUNOHISTOCHEMICAL STAINING

To identify precursor proteins of amyloid, we performed immunohistochemical staining using antibodies that react with TTR. For immunohistochemistry with rabbit polyclonal anti-human TTR IgG (DAKO, Glostrup, Denmark), the same tissues as those examined by means of Congo red staining were deparaffinized, dehydrated in a modified alcohol series, and incubated in blocking buffer (1% BSA and 4% horse serum in PBS) for 30 minutes at 37℃ in a moist chamber. Overnigh t incubation with the appropriately diluted primary antibody in blocking buffer was then performed at 4℃. Rabbit polyclonal anti-human TTR IgG served as the primary antibody. Reactivity was visualized via the DAB Liquid System (DAKO), as described by the manufacturer. For parallel control sections, blocking buffer replaced the primary antibody.

MEASUREMENT OF SERUM TTR CONCENTRATIONS

For measuring TTR concentrations, 7 serum samples of TTR deposition cases (73.7 ± 2.8 years old) and 8 serum samples of non-TTR deposition cases (68.3 ± 5.4 years old) were employed. Serum TTR concentrations were measured by nephelometry.

MASS SPECTROMETRY OF TTR IN SERUM

To confirm the patients who did not have variant TTR in serum, we performed Mass spectrometry using surface-enhanced laser desorption/ ionization time-of-flight mass spectrometry (SELDI-TOF MS) [6].

ETHICS

The study protocol was approved by the institutional review board of Kumamoto University, and a signed consent form was obtained from all patients or their family member. All family members of patients gave informed consent for performance of biopsies.

RESULTS

Congo red staining revealed 61 (48.4%) amyloid-positive specimens obtained from 126 patients with carpal tunnel syndrome, rotator cuff tears, or lumbar spinal canal stenosis. Anti-TTR antibody reacted with 46 (75.4%) specimens with amyloid deposition: 18 samples of tenosynovium, 5 samples of rotator cuff tendon, and 23 samples of ligamentum flavum. The occurrence of TTR amyloid deposition was increased with age (<40's: 0%, 50's: 12.1, 60': 33.3, 70's: 59.5, >80's: 83.3). In 15 samples, none antibodies reacted with lesions in which

Congo red staining was positive. The mean age in TTR depositon cases was higher compared to that of non-TTR cases in tenosynovium and ligamentum flavum (71.1 ± 9.3 vs.58.8 ± 9.6 years old, p<0.001, 72.4 ± 6.5 vs.66.7 ± 6.6 years old, p<0.01, respectively), but not significantly in rotator cuff tendons (65.4 ± 6.2 vs.63.9 ± 7.4 years old, p=0.69).

In LSCS cases, a significant and moderate positive correlation between amount of TTR amyloid deposition in ligamentum flavum and age was observed. The mean serum TTR levels of TTR deposition cases did not significantly change compared with those of non-TTR cases (22.9 ± 5.9 vs.23.9 ± 5.6 mg/ dl, p=0.74). SELDI/ TOF MS revealed that all patients of TTR cases did not have any mutated TTR.

DISCUSSION

In this study we demonstrated that not only the occurrence but also the amount of WT TTR amyloid deposition was increased with age. The occurrence of SSA in elderly Japanese cases (>80 years old) was found to be about 12% based on examination of autopsy-derived cardiac specimens [7]. Because the occurrence of TTR amyloidosis in ligaments and tendons (>80 years old) was above 80%, this was much higher than that of SSA. These findings suggest that most of TTR amyloidosis in ligaments and tendons may be a localized form. On the other hand, the mean age of TTR amyloidosis TTR amyloidosis in ligaments and tendons was much younger than that of SSA (71 vs. 83 years old). And 13% of the SSA patients showed symptoms of CTS [8], in addition, several case reports indicated that some patients with CTS developed SSA [8, 9, 10]. These findings suggest that some of TTR amyloidosis in ligaments and tendons may develop SSA.

We should carefully follow the clinical course of the patients with WT TTR amyloid deposition in ligaments and tendons in the field of orthopedics, because a part of those patients could develop SSA.

ACKNOWLEDGEMENT

We thank Ms. H. Katsura for her technical support with the histopathological analyses.

REFERENCES

1. Misumi Y, Ando Y, Ueda M, Obayashi K, Jono H, Su Y, Yamashita T, Uchino M. Chain reaction of amyloid fibril formation with induction of basement membrane in familial amyloidotic polyneuropathy. *J Pathol* 2009; 219:481-490.
2. Hamilton JA, Benson MD. Transthyretin: a review from a structural perspective. *Cell Mol Life Sci* 2001; 58:1491-1521.
3. Ando Y, Nakamura M, Araki S. Transthyretin-related familial amyloidotic polyneuropathy. *Arch Neurol* 2005; 62: 1057-1062.
4. Ando Y, Ueda M. Novel methods for detecting amyloidogenic proteins in transthyretin related amyloidosis. *Front Biosci* 2008; 13:5548-5558.
5. Sueyoshi T, Ueda M, Jono H, Irie H, Sei A, Ide J,Ando Y, Mizuta H. Wild type transthyretin-derived amyloidosis in ligaments and tendons of various organ sites. *Human Pathol* 2011; 42: 1259-1264.

6. Ueda M, Misumi Y, Mizuguchi M, Nakamura M, Yamashita T, Sekijima Y, Ota K, Shinriki S, Jono H, Ikeda SI, Suhr OB, Ando Y. SELDI-TOF MS evaluation of variant transthyretins for diagnosis and pathogenesis of familial amyloidotic polyneuropathy. *Clin Chem* 2009; 55: 1223-1227.
7. Ueda M, Horibata Y, Shono M, Misumi Y, Oshima T, Su Y, Tasaki M, Shinriki S, Kawahara S, Jono H, Obayashi K, Ogawa H, Ando Y. Clinicopathological features of senile systemic amyloidosis: an ante- and post-mortem study. *Mod Pathol* 2011; 24: 1533-1544.
8. Rapezzi C, Merlini G, Quarta CC, Riva L, Longhi S, Leone O, Salvi F, Ciliberti P, Pastorelli F, Biagini E, Coccolo F, Cooke RM, Bacchi-Reggiani L, Sangiorgi D, Ferlini A, Cavo M, Zamagni E, Fonte ML, Palladini G, Salinaro F, Musca F, Obici L, Branzi A, Perlini S. Systemic cardiac amyloidoses: disease profiles and clinical courses of the 3 main types. *Circulation* 2009; 120:1203-1212.
9. Takei Y, Hattori T, Gono T, Tokuda T, Saitoh S, Hoshi Y, Ikeda S. Senile systemic amyloidosis presenting as bilateral carpal tunnel syndrome. *Amyloid* 2002; 9:252-255.
10. Kodaira M, Sekijima Y, Tojo K, Tsuchiya A, Yazaki M, Ikeda S, Sekijima Y, Hoshii Y, Tachibana S. Non-senile wild-type transthyretin systemic amyloidosis presenting as bilateral carpal tunnel syndrome. *J Peripher Nerv Syst* 2008; 13:148-150.

Amyloid arthropathy in a patient with ATTR-Val122Ile amyloidosis

Pauline Klooster, Johan Bijzet and Bouke P. Hazenberg

Department of Rheumatology & Clinical Immunology, University of Groningen, University Medical Center Groningen, The Netherlands

INTRODUCTION

ATTR amyloidosis is usually characterized by neuropathy and cardiomyopathy. Arthropathy is not a typical feature although carpal tunnel syndrome may be seen sometimes. We describe a patient with cardiomyopathy caused by ATTR-Val122Ile amyloidosis who had aso prominent arthropathy of the shoulders and knees.

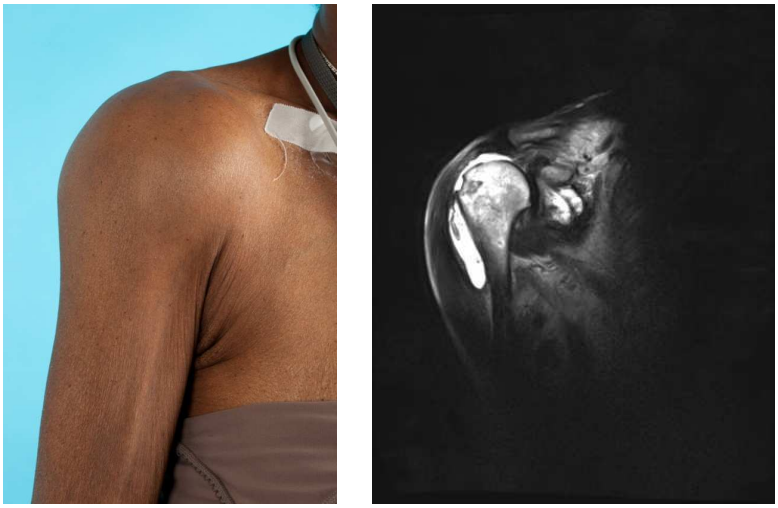

Figure 1. Left picture: Right shoulder with the typical 'shoulder pad sign'. Right picture: MRI scan of the shoulder showing swelling of the bursa subacromialis and glenohumeral joint.

CASE

A 66-year-old Afro-Caribbean woman was referred to our tertiary centre because of possible amyloid cardiomyopathy suspected by cardiac ultrasound because of right-sided cardiac failure and thickened ventricular walls. She had a history of hay fever, hypothyroidism, and recent surgery for a left-sided carpal tunnel syndrome. About one year she complained about shortness of breath and edema of both ankles that

responded well to diuretics. She had lost about 15 kg weight and complained about anorexia and palpitations. Her right knee was thickened for about eight years, but did not hurt at all. Her right shoulder was also swollen for about one year and also painless. She had numbness, tingling and pain in both hands (especially left side) that had improved considerably after CTS surgery. Some family members suffered from thyroid disease and one sister was known with unspecified heart disease.

Physical examination disclosed prominent arthropathy of both shoulders (typical “shoulder pads”, see Figure 1), swelling of both knees, and a peritendinous swelling of the dorsal part of both hands. No tongue enlargement, organomegaly, or bruising was present. There were no signs of peripheral or autonomic neuropathy.

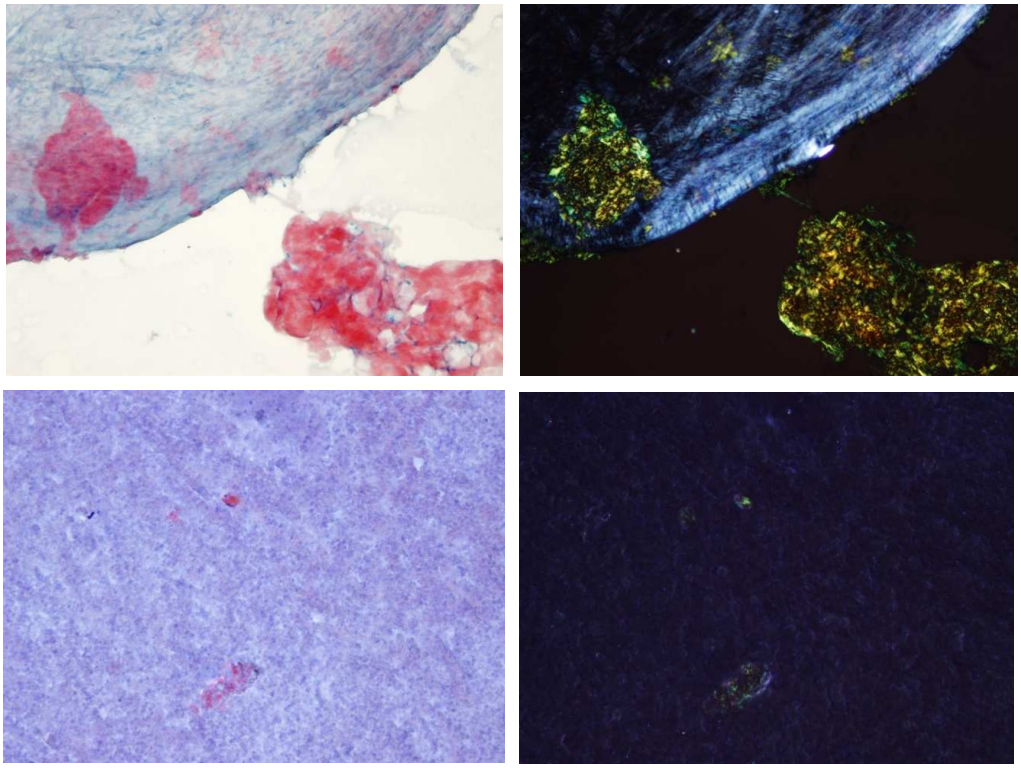

Figure 2. Congo red-stained subcutaneous fat tissue specimen (upper two pictures) and shoulder joint fluid sediment (lower two pictures). The left two pictures show the red-stained amyloid deposits in bright light, whereas the right two pictures show the characteristic apple green birefringence in polarized light.

Laboratory investigation showed a marginally elevated free kappa immunoglobulin-light chain (27.7 mg/L, N < 20 mg/L) while no other signs of a plasma cell dyscrasia were found in blood and urine. Serum CRP and uric acid were normal and anti-CCP, ANA and rheumatoid factor were absent. Serum levels of NT-proBNP and troponines were clearly elevated. Bone marrow biopsy did not show amyloid and less than 5% plasma cells were seen without any clonal restriction. Aspiration of abdominal subcutaneous fat tissue aspirate and synovial

fluid of both shoulders and right knee revealed Congo red-positive material with apple green birefringence in polarized light that was characteristic of amyloid (Figure 2). A few leukocytes and no crystals were found in the joint fluid.

Echocardiography showed a thickened left ventricular posterior wall (16 mm), intraventricular septum (19 mm), and right ventricular wall (6 mm) as well as diastolic dysfunction and decreased left ventricular ejection fraction (30%). Supraventricular and ventricular tachyarrhythmias were observed during 24h Holter registration.

Plain radiographs of shoulders and knees only showed soft tissue swelling without erosions. MRI scan of the right shoulder showed swelling of the subacromial burse and glenohumeral joint with deposits of amorph material that was visualized after injection of gadolinium (Figure 1). Serum amyloid P component (SAP) scintigraphy showed increased uptake only in shoulders, wrists, and knees (Figure 3). Bisphosphonate bone scintigraphy showed uptake in shoulders, wrists, and knees and in the heart and diffusely in soft tissue instead of bones (Figure 3).

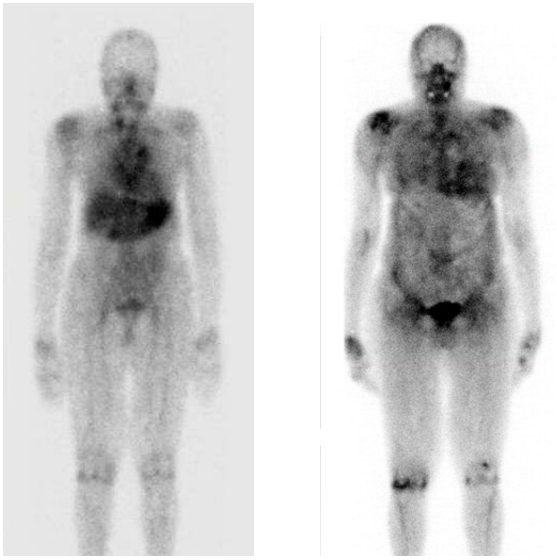

Figure 3. Left picture: Serum amyloid P component (SAP) scintigraphy shows specific uptake of shoulders, wrists and knees. Also visible is some non-specific uptake in the blood pool (heart and liver) and stomach. Right picture: Bisphosphonate bone scintigraphy shows uptake in shoulders, wrists, and knees and in heart and diffusely in soft tissue instead of bones.

DISCUSSION

Because of the clinical picture of amyloid cardiomyopathy and amyloid arthropathy our thoughts initially went to the possibility of AL amyloidosis. However, we did not find an increased free light chain production in serum and urine, nor did we find a clonal plasma cell dyscrasia in the bone marrow. Because of cardiomyopathy we looked for a TTR gene mutation and learned that our patient was homozygous for the TTR-Val122Ile mutation. The semi-quantitative amount of amyloid in the fat aspirate was 4+, whereas precursor quantification in this fat aspirate showed a TTR concentration of 936 ng/mg fat tissue (N < 4.4 ng/mg fat tissue) with normal

concentrations of amyloid A and kappa and lambda light chains. Amyloid was present in the synovial fluid whereas no other cause of the arthropathy was found. We therefore concluded that this patient suffered from ATTR-Val122Ile amyloidosis characterized by cardiomyopathy and arthropathy.

The 'shoulder pad sign' is virtually pathognomonic for AL amyloidosis [1]. Soft tissues (muscles, synovial and peri-articular tissue) are infiltrated by amyloid. Shoulders, wrists and knees are most frequently affected. Analysis of the synovial fluid is a hardly invasive and most straightforward approach, but skill and experience are necessary for a reliable result [2]. Therefore, a synovial biopsy is the best approach in daily practice. Our patient, however, did not suffer from AL amyloidosis but from ATTR amyloidosis. Amyloid arthropathy has been described in only a few cases with ATTR amyloidosis [3, 4]. Contrary to our patient neuropathy is a prominent sign in these cases giving rise to a Charcot-like arthropathy.

The abdominal subcutaneous fat aspiration is a simple and extremely useful way to detect systemic amyloidosis [5]. The TTR Val122Ile mutation is present in about 3% of the Afro-American population younger than 60 years. This percentage increases to 10% in the Afro-American population with cardiac failure older than 60 years [6]. The presentation with clinical cardiomyopathy is most frequent in the sixth decade. The mortality of patients with the TTR Val122Ile mutation is slightly higher than in the general population [7].

CONCLUSIONS

Typical amyloid arthropathy of shoulders as disease manifestation of ATTR amyloidosis to our knowledge has not been described before and can thus be added to the clinical manifestations of this disease. This case shows the benefits of performing two minimally invasive procedures, i.e. a subcutaneous abdominal fat tissue aspiration and joint fluid aspiration, for both detection and typing of amyloid.

REFERENCES

1. Guerreiro de Moura CG, Pinto de Souza S. Images in clinical medicine: Shoulder pad sign. N Engl J Med 2004; 351:e23.
2. Lakhanpal S, Li CY, Gertz MA, Kyle RA, Hunder GG. Synovial fluid analysis for diagnosis of amyloïd arthropathy. Arthritis Rheum 1987; 30:419-23.
3. Shirashi M, Ando Y, Mizuta H, Nakamura E, Takagi K, Ando M. Charcot knee arthropathy with articular amyloid deposition in familial amyloidotic polyneuropathy. Scand J Rheumatol 1997; 26:61-64.
4. Pruzanski W, Baron M, Shupak R. Neuroarthropathy (Charcot joints) in familial amyloid polyneuropathy. J Rheumatol 1981; 8:477-81.
5. van Gameren II, Hazenberg BP, Bijzet J, van Rijswijk MH. Diagnostic accuracy of subcutaneous abdominal fat tissue aspiration for detecting systemic amyloidosis and its utility in clinical practice. Arthritis Rheum 2006; 54:2015-21.
6. Buxbaum J, Jacobson DR, Tagoe C, et al. Transthyretin V122I in African Americans with congestive heart failure. J Am Coll Cardiol 2006; 47:1724-5.
7. Buxbaum J, Alexander A, Koziol J, Tagoe C, Fox E, Kitzman D. Significance of the amyloidogenic transthyretin Val 122 Ile allele in African Americans in the Arteriosclerosis Risk in Communities (ARIC) and Cardiovascular Health (CHS) Studies. Am Heart J 2010; 159:864-70.

Clinical and laboratory features of leptomeningeal type of TTR amyloidosis

M. Ueda, M. D. Benson, J. Hardwick, W. Ishii, L. Du, B. Kluve-Beckerman, and J.J. Liepnieks

Department of Pathology and Laboratory Medicine, Indiana University School of Medicine, Indianapolis, IN, USA.

ABSTRACT

In the present study, we investigated clinical and laboratory features in leptomeningeal (LM) type of TTR amyloidosis patients (Gly30, Arg53, Ser64, His69, and Cys114). In most of those patients, the initial symptom was transient stroke-like symptom or seizure. In the same patients, vitreous opacities were the first manifestation. Brain MRI showed diffuse abnormal leptomeningeal enhancement without focal parenchymal mass lesion. In most of the patients, symptoms and laboratory findings in other organs than central nervous system and eyes were not observed or very mild, and amyloid deposition was not observed in the skin and rectal biopsy specimens. In an autopsy case with TTR Gly30, severe leptomeningeal amyloid deposits were observed. However, no amyloid deposition was observed in other tissue sites. To make an accurate and timely diagnosis of the disease, we should be aware that tissue biopsies (skin, gastrointestinal, fat, cardiac) may be of limited value for detecting amyloid deposits.

INTRODUCTION

To date, over 112 transthyretin (TTR) mutations have been identified as the cause of hereditary systemic amyloidosis.[1,2] It has been reported that TTR amyloidosis can be classified into several clinical phenotypes, such as peripheral neuropathy (PN) type, cardiomyopathy type, and leptomeningeal (LM) type, which correlate with types of TTR mutations.[1,2] Thirteen TTR mutations (Pro12, Gly18, Thr25, Gly30, Pro36, Pro49, Glu53, Ala53, Arg53, Arg55, Ser64, His69, and Cys114) reportedly cause LM type amyloidosis.[1-6] Some familial amyloidotic polyneuropathy (FAP) patients having TTR Met30 mutation, which was the first to be identified and is the best known mutation found throughout the world,[7] also develop LM amyloidosis in addition to the other systemic symptoms such as PN.[8]

METHODS

In the present study, we investigated clinical and laboratory features, such as cerebrospinal fluid tests, MRI, biopsies, and systemic symptoms based on blood tests, nerve conduction velocity test, and echocardiography in LM type of TTR amyloidosis patients (seven of Gly30, one of Arg53, one of Ser64, three of His69, and one of Cys114) (Table 1). We also analyzed an autopsy case with TTR Gly30.

Table 1. Clinical findings of LM amyloidosis patients.

No.	TTR mutation	Age of onset	Sex	CNS symptoms	Eye symptoms	Brain MRI	Other symptoms	Biopsies
1	Gly30	41	F	S, HA, TA, TL, BH	VO	LE	None	R (-), S (-)
2	Gly30	38	M	TL, D, HA, S	VO	NE	None	NE
3	Gly30	50	M	TL, TDC, TA	VO	NE	GI	NE
4	Gly30	45	F	S, TA	VO, G	NE	None	S (+)
5	Gly30	37	F	TL, S, HI	VO	LE	None	NE
6	Gly30	34	F	TL, TA, HA, TDC	VO	Normal	GI	S (-)
7	Gly30	28	F	HA, D	None	NE	None	S (-), R (-)
8	Arg53	48	F	TL, S, HC,CI	NA	NA	None	B (+)
9	Ser64	28	M	HA, HI	VO	NE	N, U	NE
10	His69	48	M	S, TA, TL, CI	VO	LE	None	S (+), H (+)
11	His69	50	F	S, TL, CI	VO	Normal	None	NE
12	His69	37	F	None	None	Normal	N (?)	S (-)
13	Cys114	30	M	D, CI, BH	VO	LE	N, GI, U	R (+)

Sex: F, female; M, male. CNS symptoms: BH, brain hemorrhage; CI, cognitive impairment; D, dizziness; HA, headache; HC, hydrocrphalus; HI, hearing impairment; S, seizure; TA, transient aphasia; TDC, transient disturbance of consciousness; TL, TIA-like symptoms. Eye symptoms: G, glaucoma; VO, vitreous opacity. Brain MRI: LE, leptomeningeal enhancement. Other symptoms: GI, gastrointestinal symptoms; N, neuropathy; U, urinary disturbance. Biopsy: B, brain biopsy; H, heart biopsy; R, rectal biopsy; S, skin biopsy. NE, not examined; NA, not available.

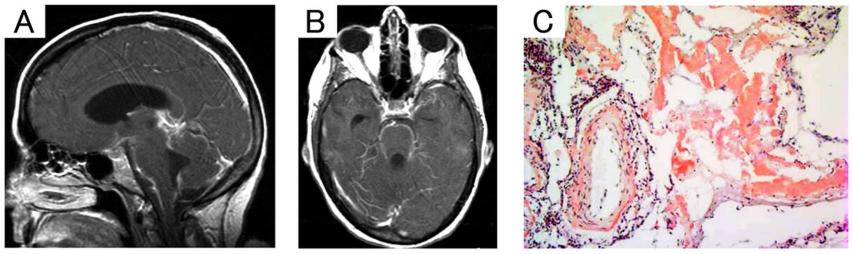

Figure 1. MRI and histopathological findings of a patient with TTR Gly30 (Case No. 1).
(A, B) T1-weighted MRI shows gadolimium enhancement of leptomeninges. Sagittal view (A), and horizontal view (B). (C) Brain specimen stained with Congo-red.

RESULTS

In most of those patients, the initial symptom was transient stroke-like symptom or seizure. They also had dizziness, headache, cerebral hemorrhage, transient disturbance of consciousness, amnesia, and blurred vision. In the same patients, vitreous opacities were the first manifestation. Several patients had hydrocephalus

and underwent a shunt operation, which could delay progression of symptoms such as seizure. Brain MRI showed diffuse abnormal leptomeningeal enhancement without focal parenchymal mass lesion (Figure 1A and B). Protein concentrations in cerebrospinal fluid of those patients were over 100 mg/dl. Serum TTR concentrations in LM amyloidosis patients were about half of those in healthy volunteers. In most of those patients, except for a patient with TTR Cys114, symptoms and laboratory findings in other organs than central nervous system and eyes were not observed or very mild, and amyloid deposition was not observed in the skin and rectal biopsy specimens. In an autopsy case with TTR Gly30, severe leptomeningeal amyloid deposits were observed (Figure 1C). However, no amyloid deposition was observed in other tissue sites.

DISCUSSION

The patients having those five kinds of TTR mutations showed CNS symptoms with severe amyloid deposits. These findings are congruent with the previous studies.[4-6] It is generally believed that LM TTR amyloid deposits are derived from TTR produced by the choroid plexus of the brain. The reason why those TTR mutations cause LM amyloidosis remains unclear.

FAP is usually diagnosed on the basis of biopsies of several tissue sites, such as subcutaneous adipose tissue of the abdominal wall, and gastrointestinal (GI) tract. However, most of the patients of LM type amyloidosis did not show amyloid deposits in those tissue sites. To make an accurate and timely diagnosis of the disease, we should be aware that tissue biopsies (skin, fat, and GI) may be of limited value for detecting amyloid deposits.

REFERENCES

1. Zeldenrust S, Benson MD. Familial and senile amyloidosis caused by transthyretin. In Protein Misfolding Diseases: Current and Emerging Principles and Therapies. Edited by Alvarado M, Kelly JW, Dobson CM. Hoboken, NJ: John Wiley & Sons; 2010:795–815.
2. Mutations in Hereditary Amyloidosis. Available from: http://amyloidosismutations.com/attr.html
3. Petersen RB, Goren H, Cohen M, Richardson SL, Tresser N, Lynn A, et al. Transthyretin amyloidosis: a new mutation associated with dementia. Ann Neurol. 1997;41:307–313.
4. Dowell JD, Fleck JD, Vakili ST, Benson MD. Familial oculoleptomeningeal amyloidosis associated with primary angiitis of the CNS. Neurology. 2007;68:77–78.
5. Uemichi T, Uitti RJ, Koeppen AH, Donat JR, Benson MD. Oculoleptomeningeal amyloidosis associated with a new transthyretin variant Ser64. Arch Neurol. 1999;56:1152-1155.
6. Blevins G, Macaulay R, Harder S, Fladeland D, Yamashita T, Yazaki M, et al. Oculoleptomeningeal amyloidosis in a large kindred with a new transthyretin variant Tyr69His. Neurology. 2003;60:1625–1630.
7. Ando Y, Nakamura M, Araki S. Transthyretin-related familial amyloidotic polyneuropathy. Arch Neurol 2005;62:1057–1062.
8. Herrick MK, DeBruyne K, Horoupian DS, Skare J, Vanefsky MA, Ong T. Massive leptomeningeal amyloidosis associated with a Val30Met transthyretin gene. Neurology 1996;47:988–992.
9. Sekijima Y, Wiseman RL, Matteson J, Hammarström P, Miller SR, Sawkar AR, et al. The biological and chemical basis for tissue-selective amyloid disease. Cell. 2005;121:73–85.

Detection of Microbleeds in Hereditary Cerebral Amyloid Angiopathy Associated with Amyloidogenic Transthyretin Tyr114Cys Using Susceptibility-weighted Imaging

T Yamashita[1], T Hirano[1], T Hirai[2], T Oshima[1], K Okumura[1], M Tateishi[1], M Yohei[1], S Yamashita[1], Y Maeda[1], S Shinriki[3], M Ueda[3], K Obayashi[3], Y Ando [1]

[1]Department of Neurology, [2]Department of Medical Diagnostic Radiology, [3]Department of Diagnostic Medicine, Faculty of Life Sciences, Kumamoto University

Patients with hereditary cerebral amyloid angiopathy (CAA) associated with amyloidogenic transthyretin (ATTR) Tyr114Cys present with rapidly progressive dementia and fatal lobar hemorrhage. However, cerebral microbleeds (CMBs) have not been well elucidated in the patients. This study investigated whether the patients developed CMBs using susceptibility-weighted imaging (SWI). Patient 1 underwent liver transplantation at the age of 39, and developed slowly progressive cognitive impairment subsequently. Patient 2 underwent liver transplantation at the age of 34, and developed slowly progressive cognitive impairment at the age of 39. SWI demonstrated CMBs in the cerebellum, bilateral subcortical white matter, and the thalamus. In this study, we demonstrated that CAA ATTR Tyr114Cys patients developed CMBs. Liver transplantation for this disease prevented fatal lobar hemorrhage caused by CAA removing ATTR in the circulating blood. However, transplanted patients could show cognitive impairment and CMBs because of ATTR in the cerebrospinal fluid produced by the choroid plexus.

INTRODUCTION

Amyloidogenic transthyretin (ATTR)-related amyloidosis is the most common type of hereditary systemic amyloidosis in the world.[1] According to the Familial Amyloidotic Polyneuropathy World Transplant Registry, more than 1900 liver transplantations have been performed for this fatal disorder in attempts to remove ATTR, which had been synthesized by the original liver, from the plasma.[2,3]

Patients with ATTR Tyr114Cys develop amyloid deposits in cerebral blood vessels and fatal lobular intracranial hemorrhage presenting CAA in addition to rapidly progressive dementia, fluctuating consciousness, convulsion, visual hallucination, transient focal neurological symptoms and signs (TFNSS), cardiopathy, vitreous opacity, mild amyloid polyneuropathy.[4,5,6,7] Liver transplantation decreases the mortality, occurrence of cerebral hemorrhage, and the volume of cerebral hemorrhage.[8]

Cerebral microbleeds (CMBs) are a potential risk factor for intracranial hemorrhage with recent increased attention on amyloid beta-related CAA.[9] However, CMBs have not been well elucidated in CAA with ATTR

Tyr114Cys. Susceptibility-weighted imaging (SWI) is a newer technique that is more sensitive than conventional T2* gradient echo imaging in detecting CMBs.

This study investigated whether CAA with ATTR Tyr114Cys patients developed CMBs using SWI.

PATIENTS AND METHODS

A 49-year-old man (patient 1) and a 47-year-old woman (patient 2) with ATTR Tyr114Cys mutation were examined neuroradiologicaly using SWI at 3.0 tesla.

Patient 1 developed vitreous opacity at the age of 30, underwent liver transplantation at the age of 39, and showed slowly progressive cognitive impairment subsequently. On admission, neurological examination revealed visual hallucination (Charles Bonnet Syndrome), loss of visual acuity, loss of light reflexes, distal dominant muscle weakness and atrophy, and absent Achilles tendon reflexes. The patient complained of thermohypoesthesia under knees, hypalgesia under knees. The patient exhibited dysuria, and could not stand up and walk.

Patient 2 developed vitreous opacity at the age of 31, underwent liver transplantation at the age of 34, and showed slowly progressive cognitive impairment at the age of 39. On admission, neurological examination revealed visual hallucination (Charles Bonnet Syndrome), loss of visual acuity, loss of light reflexes, diffuse muscle weakness and atrophy, and absent all tendon reflexes. The patient complained of thermoanesthesia under ankles, hypalgesia under ankles, hypesthesia under ankles, decreased vibration sense, and decreased position sense. The patient exhibited dysuria and could walk.

We studied SWI of the brain in the 2 CAA ATTR Tyr114Cys patients.

The Institutional Review Board of Faculty of Life Sciences, Kumamoto University approved the performance of this study (No. 1172).

RESULTS

Axial 2-mm-thick SWI at the level of the cerebellum revealed hypointense signals in the right hemisphere of patient 1. SWI at the level of the basal ganglia demonstrated bilateral hypointense foci in subcortical white matter and thalamus.

DISCUSSION

In this study, we demonstrated that CAA ATTR Tyr114Cys patients developed CMBs. To our knowledge, the present results provide the first evidence of CMBs in patients with ATTR-related CAA. SWI was effective to detect CMBs in CAA ATTR Tyr114Cys. Amyloid beta-related CAA is typically associated with CMBs in the lobular brain lesions, whereas hypertensive vasculopathy is associated with CMBs in the basal ganglia, thalamus, brainstem, and cerebellum.[9] In contrast, CMBs of CAA ATTR Tyr114Cys patients were detected in the cerebellum, subcortical white matter, and thalamus. CMBs may affect CNS manifestation in CAA CAA ATTR Tyr114Cys.

Liver transplantation for this disease prevented fatal lobar hemorrhage caused by CAA removing ATTR in the circulating blood. [8.10] However, transplanted patients could show slowly progressive cognitive impairment and CMBs, because of pre-existing deposits of amyloid or continuing amyloid fibril formation from circulating wild-type TTR produced by the transplanted liver or form ATTR in the cerebrospinal fluid produced by the choroid

plexus. In addition to liver transplantation, disease modifying therapy such as tetramer stabilizers are needed for CAA ATTR Tyr114Cys.

REFERENCES

1. Ando Y, Nakamura M, Araki S. Transthyretin-related familial amyloidotic polyneuropathy. Arch Neurol. 2005;62:1057-1062.
2. Wilczek HE, Larsson M, Ericzon BG; FAPWTR. Long-term data from the Familial Amyloidotic Polyneuropathy World Transplant Registry (FAPWTR). Amyloid. 2011;18:188-190.
3. Yamashita T, Ando Y, Okamoto S, Misumi Y, Hirahara T, Ueda M, Obayashi K, Nakamura M, Jono H, Shono M, Asonuma K, Inomata Y, Uchino M. Long-term survival after liver transplantation in patients with familial amyloid polyneuropathy. Neurology. 2012;78:637-643.
4. Ueno S, Fujimura H, Yorifuji S, Nakamura Y, Takahashi M, Tarui S, Yanagihara T. Familial amyloid polyneuropathy associated with the transthyretin Cys114 gene in a Japanese kindred. Brain. 1992;115:1275-1289.
5. Nakamura M, Yamashita T, Ueda M, Obayashi K, Sato T, Ikeda T, Washimi Y, Hirai T, Kuwahara Y, Yamamoto MT, Uchino M, Ando Y. Neuroradiologic and clinicopathologic features of oculoleptomeningeal type amyloidosis. Neurology. 2005;65:1051-1056.
6. Kawaji T, Ando Y, Nakamura M, Yamashita T, Wakita M, Ando E, Hirata A, Tanihara H. Ocular amyloid angiopathy associated with familial amyloidotic polyneuropathy caused by amyloidogenic transthyretin Y114C. Ophthalmology. 2005;112:2212.
7. Yamashita T, Ando Y, Katsuragi S, Nakamura M, Obayashi K, Haraoka K, Ueda M, Xuguo S, Okamoto S, Uchino M. Muscular amyloid angiopathy with amyloidgenic transthyretin Ser50Ile and Tyr114Cys. Muscle Nerve. 2005;31:41-45.
8. Yamashita T, Ando Y, Ueda M, Nakamura M, Okamoto S, Zeledon ME, Hirahara T, Hirai T, Ueda A, Misumi Y, Obayashi K, Inomata H, Uchino M. Effect of liver transplantation on transthyretin Tyr114Cys-related cerebral amyloid angiopathy. Neurology. 2008;70:123-128.
9. Mesker DJ, Poels MM, Ikram MA, Vernooij MW, Hofman A, Vrooman HA, van der Lugt A, Breteler MM. Lobar distribution of cerebral microbleeds: the Rotterdam Scan Study. Arch Neurol. 2011;68:656-659.
10. Sakashita N, Ando Y, Jinnouchi K, Yoshimatsu M, Terazaki H, Obayashi K, Takeya M. Familial amyloidotic polyneuropathy (ATTR Val30Met) with widespread cerebral amyloid angiopathy and lethal cerebral hemorrhage. Pathol Int. 2001;51:476-480.

Neurological manifestations of senile systemic amyloidosis

Shu-ichi Ikeda[1], Yoshiki Sekijima[1], Kana Tojo[1], Michitaka Nakagawa[1], Jun Koyama[2]

1) Department of Medicine (Neurology and Rheumatology), 2) Division of Cardiovascular Medicine, Shinshu University School of Medicine, Matsumoto 390-8621.

ABSTRACT

Senile systemic amyloidosis (SSA) usually develops as intractable heart failure with arrhythmia in elderly individuals and neurological manifestations have not been noted yet. We here report that carpal tunnel syndrome and cerebral infarction might precede the cardiac manifestations in this disease.

INTRODUCTION

Senile systemic amyloidosis (SSA), which was previously called senile cardiac amyloidosis, is known to be a disorder selectively affecting the heart in the elderly individuals[1] and is caused by the deposition of wild-type transthyretin (TTR)-derived amyloid fibrils[2]. Most patients with this disease were diagnosed on postmortem studies. However, current advance of diagnostic technology that includes immunohistochemical demonstration of TTR-related amyloid deposits with no mutation of TTR gene enables us to make a correct clinical diagnosis of the patients with SSA[3]. Although main clinical picture of SSA is intractable heart failure with arrhythmia, our previous reports have suggested that carpal tunnel syndrome (CTS) might precede the cardiac manifestations in this disease[4,5]. In this study we tried to clarify the natural course of SSA with a special attention to the neurological manifestations, showing that CTS and cerebral embolism are frequent initial symptoms of this disease.

MATERIALS AND METHODS

During past 5 years 20 patients who were supposed to be suffering from SSA were referred to us: they had a history of congestive heart failure. Chest X-ray showed an enlarged cardiac shadow (cardiothoracic ratio□50%) and electrocardiographic findings consisted of low voltage in the standard limb leads and QS pattern in the right precordial leads with or without conduction blocks[6]. Echocardiography showed marked symmetrical thickening of ventricular walls and ventricular septum with hyperrefractile myocardial echoes (the so called granular sparkling appearance). Myocardial technetium-99m pyrophosphate (Tc-99m-PYP) scintigraphy revealed a positive shadow and high serum level of BNP (brain natriuretic peptide) was referred.

MOLECULAR ANALYSIS OF TTR

Serum samples obtained from the patients were immunoprecipitated and TTR molecules were analyzed by matrix-assisted laser desorption ionization/time-of-flight (MALDI/TOF) mass spectrometry, showing that wild type of TTR had two major ion peaks (wild type TTR and that with a cystein residue). In the sera of FAP patients with ATTR Val30Met two additional peaks that indicate the presence of a variant form of TTR are seen. To confirm these findings, direct DNA sequencing of all 4 exons of the TTR gene was also carried out.

HISTOPATHOLOGICAL STUDY

Surgical biopsy of abdominal skin was carried out for all patients: this biopsy sample was about 1.5cm wide and the same size depth including a deep subcutaneous fat tissue layer. Endomyocardial biopsy from right ventricle and/or gastroduodenal mucosal biopsy under endoscopic control were also performed for some of the patients with SSA. Formalin-fixed and paraffin-embedded sections were stained with H&E and phenol Congo red10, and amyloid deposits were identified as characteristic apple green birefringence under a polarized microscopy. Immunostaining was carried out using a Ventana XT automated immunohistochemistry system (Ventana Medical Systems, AZ) and the primary antibodies used were anti-Aλ, Aκ, AA, TTR11. For TTR immunostaining all sections were pre-treated with 98% formic acid for 5 minutes.

RESULTS

The patients consisted of 14 males and 6 female and their ages ranged from 60 to 97 years. Among them 13 showed carpal tunnel syndrome and 4 suffered from cerebral infarctions. The vast majority of them neurological manifestations preceded congestive heart failure (Table 1).

Table 1. Summarized clinical pictures of SSA patients examined

Case	Sex	Age at onset	Age at diagnosis	Initial symptom	Other symptoms	Age at death	Tissue amyloid deposition
1	M	60	67	CTS	CVD		myocardium, skin
2	M	60	76	CTS		81	gastric mucosa
3	M	65	75	CTS		80	gastric mucosa
4	M	65	72	CTS	CKD		myocardium, skin
5	M	67	70	CTS	CKD		myocardium
6	M	67	69	CHF			myocardium
7	M	67	68	Af			myocardium
8	M	68	78	CTS			carpal ligament
9	M	69	71	CTS			myocardium
10	M	70	70	CHF			myocardium
11	F	70	74	CTS			gastric mucosa
12	M	71	73	CHF	CTS		myocardium
13	M	71	73	Renal infarction			myocardium
14	M	73	73	CHF			myocardium
15	M	73	83	CHF	CVD		myocardium
16	F	75	85	CHF		88	skin
17	F	77	84	CTS	TIA		skin, gastric mucosa
18	F	78	78	CHF	CKD	81	myocardium
19	F	80	83	CTS			skin
20	F	97	97	CVD		97	skin

Abbreviations TIA: transient cerebral ischemic attack
CTS: carpal tunnel syndrome, CVD: cerebral infarction, CKD: chronic renal disease

DISCUSSION

Wild-type TTR is inherently an amyloidogenic protein and is well known to be an amyloid precursor protein in SAA. The clinical manifestations of this disease consist of congestive heart failure, arrhythmia and/or conduction blocks and atrial fibrillation might be an initial sign of this cardiac disorder. Rarely SSA-related cardiac amyloidosis with impaired left ventricular wall motion and thickened endocardium causes systemic embolism, resulting in cerebral infarction[6,7]. Another notable manifestation is carpal tunnel syndrome (CTS)[8]. Amyloid deposits are occasionally seen in biopsied tissue specimens obtained from carpal tunnel release and more than half of them are TTR immunoreactive. Among 33 patients with proven tenosynovial TTR amyloid deposition two of them were reported to develop systemic amyloidosis more than 9 years after the initial appearance of CTS. We also described two SSA cases whose initial manifestations were bilateral CTS. It is, therefore, very likely that in SSA CTS seems to precede cardiac manifestations several years. A possible natural course of SSA can be supposed as follows: CTS appears between 50 to 60 years old and next atrial fibrillation adds, occasionally leading to the complication of cerebral embolism. Finally congestive heart failure develops. TTR-related amyloidosis seems to be treatable: TTR tetramer dissociation, misfolding and misassembly are required for the process of amyloid fibril formation. Preferential stabilization of the native TTR tetramer over the dissociative transition state can be achieved by orally administered non-steroidal anti-inflammatory drugs (NSAIDs)[9,10].

REFERENCES

1. Westermark P, Bergström J, Solomon A, et al. Transthyretin-derived senile systemic amyloidosis: clinicopathologic and structural considerations. Amyloid 2003;10 (Suppl. 1):48-54.
2. Westermark P, Sletten K, Johansson B, et al. Fibril in senile systemic amyloidosis is derived from normal transthyretin. Proc Natl Acad Sci USA 1990;87:2843-2845.
3. Ikeda S, Sekijima Y, Tojo K, Koyama J. Diagnostic value of abdominal wall fat pad biopsy in senile systemic amyloidosis. Amyloid 2011;18:211-215.
4. Takei Y, Hattori T, Gono T, et al. Senile systemic amyloidosis presenting as bilateral carpal tunnel syndrome. Amyloid 2002;9:252-255.
5. Takei Y, Hattori T, Tokuda T, et al. Senile systemic amyloidosis presenting as bilateral carpal and left cubital tunnel syndrome. Intern Med 2003;42:1050-1051.
6. Yamano M, Azuma A, Yazaki M, et al. Early cardiac involvement in senile cardiac amyloidosis: a case report. Amyloid 2008;15:54-59.
7. Nakagawa M, Tojo K, Sekijima Y, et al. Arterial thromboembolism in senile systemic amyloidosis: report of two cases. Amyloid 2012;19:118-121.
8. Sekijima Y, Uchiyama S, Tojo K, et al. High prevalence of wild-type transthyretin depositioin in patients with idiopathic carpal tunnel syndrome: a common cause of carpal tunnel syndrome in the elderly. Hum Pathol 2011;42:1785-1791.
9. Sekijima Y, Wiseman RL, Matteson J, et al. The biological and chemical basis for tissue-selective amyloid disease. Cell 2005;121:73-85.
10. Tojo K, Skijima Y, Kelly JW, et al. Diflunisal stabilizes familial amyloid polyneuropathy-associated transthyretin variant tetramer in serum against dissociation required for amyloidogenesis. Neurosci Res 2006;56:441-449.

New transthyretin variant Glu54Gln associated with familial amyloidosis

D. Coriu[1,2], C. Ailenei[1], R. Talmaci[1], S. Badelita[1,2], C. Dobrea[1,2], C.L. Murphy[3], D.Kestler[3], & A. Solomon[3]

[1] University of Medicine "Carol Davila", Bucharest, Romania

[2] Department of Hematology, Fundeni Clinical Institute, Bucharest, Romania

[3] University of Tennessee Graduate School of Medicine, Knoxville, TN, USA

INTRODUCTION

Transthyretin (TTR) amyloidosis is the most prevalent type of hereditary systemic amyloidosis that results from a series of dominant mutation in the TTR gene.

To date over 100 such alterations have been described and now we wish to report yet another variation detected in two unrelated Romanian individuals with TTR amyloidosis.

PATIENTS AND METHODS

Case 1

The first patient (Gre) is a 54-year-old man with a progressive peripheral sensory motor polyneuropathy, autonomic dysfunction, and a restrictive cardiomyopathy. At 45, he had the onset of orthostatic hypotension, paresthesias of the lower extremities, dysphagia, and chronic diarrhea. Subsequently, there was rapidly progressive cardiac dysfunction, heart failure and pulmonary hypertension. Notably, his father was diagnosed with idiopathic cardiomyopathy at age 50 and died a few years latter.

Case 2

The second patient (Del) is a 46-year-old woman who presented with restrictive cardiomyopathy and a bilateral carpal tunnel syndrome. At age 40 she developed symptoms of heart disease and also had a carpal tunnel syndrome treated surgically. Her father died at age 50 after a long standing history of cardiomyopathy and severe sensori-motor neuropathy.

Samples of subcutaneous fat aspirate and rectal biopsy were stained with Congo-red and examined in polarized light. In both cases, all the investigations performed excluded light chain amyloidosis. Genomic DNA was extracted from peripheral blood. PCR amplification of TTR exons 2, 3, and 4 was ran using the following primers (1) :

TTREX2-F: 5'- CCAGGGCACCGGTGAATCC-3';

TTREX2-R: 5'- CCAAGTGAGGGGCAAACGGG-3'

TTREX3-F: 5'-TGTGTGTTAGTTGGTGGGGGTGT-3';
TTREX3-R: 5'- TGGGGAGATGCCAAGTGCCT-3';
TTREX4-F: 5'- GGTCAGTCATGTGTGTCATCTG-3';
TTREX4-R: 5'- TTAGTAAAAATGGAATACTCTTGG-3'

Direct genomic sequencing of the amplified products was performed using the ABI 3100 Avant sequencer (Applied Biosystems). TTR was isolated from serum by immunoprecipitation for ESI-MS (2).

RESULTS

In both cases, biopsies of abdominal subcutaneous fat and rectum showed birefringent deposits after Congo red staining.

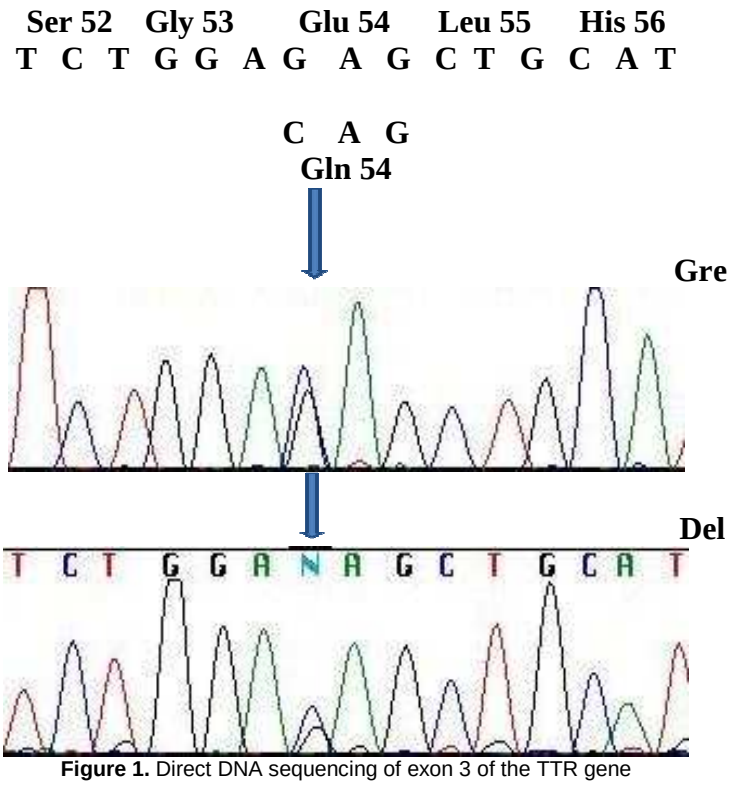

Figure 1. Direct DNA sequencing of exon 3 of the TTR gene

Direct DNA sequencing of exon 3 of the TTR gene (for Gre and Del) demonstrates heterozygosity at the first base position in codon 54 where both G and C are observed. Glutamic Acid (GAG) and Glutamine (CAG) are both predicted to be expressed by these patients (fig 1).

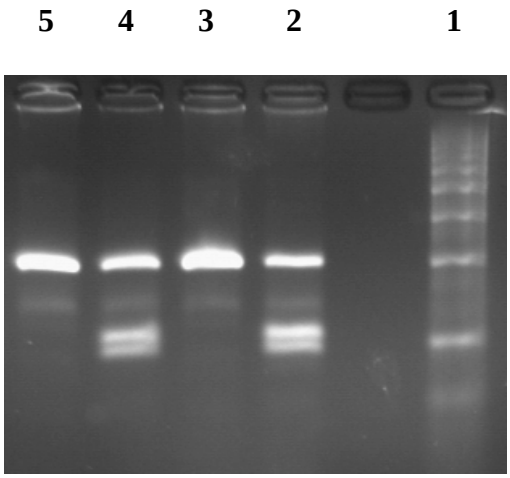

Figure 2. PCR-RFLP analysis of exon 3.

Enzymatic digestion with PVU II on unrelated normal control samples (lanes 3, 5) was compared to the patient Gre (lane 2) and patient Del (lane 4). Fragments at positions corresponding to 109 bp and 96 bp in length were noted in addition to the intact PCR product at 205 bp in the control samples. This indicated the creation of a restriction enzymes site in the patients confirming the presence of a heterozygous G to C purine transition mutation in exon 3. Lane 1 contains a standard marker of sequentially increasing 100 base pair bands (fig 2).

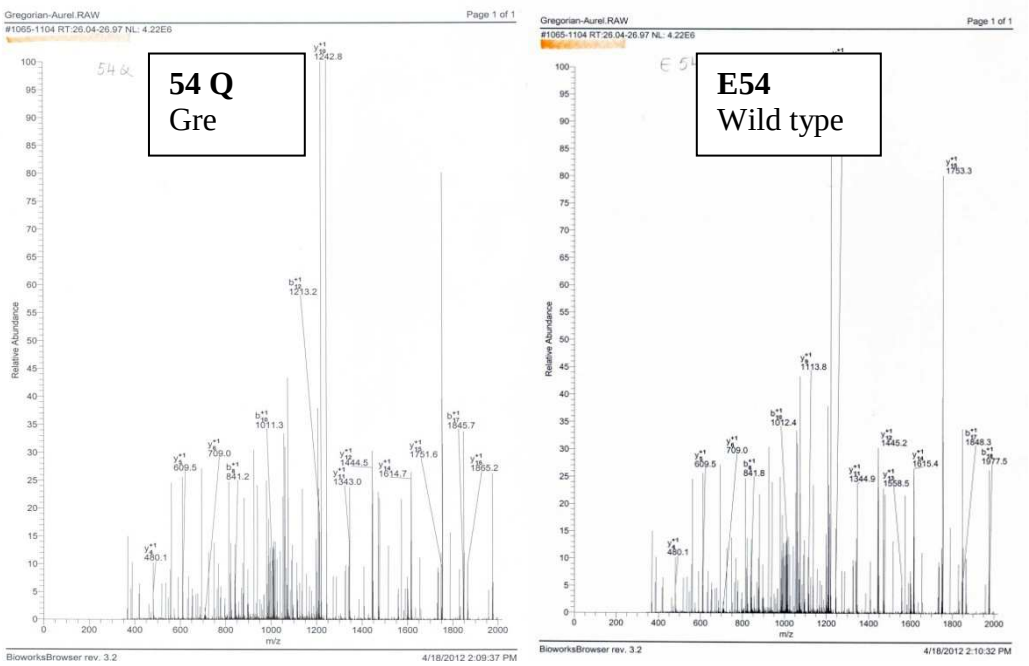

Figure 3. MS studies.

Molecular analysis of TTR imunoprecipitants from serum samples obtained from the patient Gre and control. The critical peptide masses are shifted by one unit (fig 3). However, currently available MS methods are not sufficient to resolve this E54Q misense mutation definitively. Future MS resolution of such E to Q substitution will rely on use of newer methodologies such as energy-resolved MS.

CONCLUSION

To the best of our knowledge these are the first reported cases of E54Q –associated TTR amyloidosis.

ACKNOWLEDGMENTS

The study was funded by the National Research Project CEEX 41-074/2006 and the Aslan Foundation.

REFERENCES

1. Teruhisa Tsuzuki, Shuji MitaS, Shuichiro Maeda, Shukuro ArakiS, and Kazunori Shimada. Structure of the Human Prealbumin Gene. The Journal of Biological Chemistry 1985; 260 (22), 12224-12227
2. Ranlov I, Ando Y, Ohlsson PI, Holmgren, and Suhr OB. Rapid screening for amyloid-related variant forms of transthyretin is possible by electrospray ionization mass spectrometry. European J Clin Invest 1997 ; 27, 956-959.

Detection of autoantibodies against ATTR in patients with FAP ATTR V30M

K. Obayashi [1], M. Tasaki [2], T. Ohshima [3], O.B. Suhr [4], I. Anan [4], Y. Misumi [3], M. Ueda [2], T. Yamashita [3], H. Jono [2] and Y. Ando [2, 3]

[1] Diagnostic Unit for Amyloidosis, Department of Laboratory Medicine, [2] Department of Diagnostic Medicine and [3] Department of Neurology, Graduate School of Medical Sciences, Kumamoto University, Kumamoto, Japan; [4] Department of Medicine, Umeå University Hospital, Umeå, Sweden

ABSTRACT

We examined whether a relationship exists between the incidence of autoantibodies against ATTR and the phenotype of FAP ATTR V30M. Three of 25 Japanese and 5 of 6 Swedish patients have high levels of autoantibodies against ATTR, and these 8 patients were all late onset cases. In addition, ratio of ATTR V30M to wild-type TTR in serum of the high autoantibody group was lower than those of low autoantibody group. Moreover, our ELISA data suggested that there were some epitopes at positions 24-35 or 105-115 of ATTR V30M in these patients, and significant positive correlation between the levels of the autoantibody which the epitope was at position 24-35 and the age of onset was observed in these patients. Age-dependent increase in the incidence of autoantibodies was observed in patients with FAP ATTR V30M. This phenomenon may influence the clinicopathological differences between both early and late onset cases of the disease.

INTRODUCTION

It has been well documented that conformational changes via instability of tetrameric form TTR occurs during the process of amyloid formation in FAP [1)]. Some criptic epitopes expose on amyloidogenic TTR (ATTR) molecule surface during the process in sera of FAP patients [2 - 8)]. There is a possibility that *de novo* antibodies responded to criptic epitopes of ATTR may be synthesized in serum of FAP patients. In this study, we examined whether a relationship exists between the incidence of autoantibodies against ATTR and the phenotype of FAP ATTR V30M.

METHODS

Serum samples were collected from 25 Japanese (13 females and 12 males; 28-32 years old) and 8 Swedish (5 females and 3 males; 67-81 years old) FAP ATTR V30M patients, 4 Japanese gene carriers of ATTR V30M (3 females and 1 male; 21-27 years old), and 24 Japanese healthy controls which had no genetic mutations of TTR (12 females and 12 males; 26-36 years old). To detect the presence or levels of autoantibodies against ATTR in these serum samples, enzyme-linked immunosorbent assay (ELISA) using recombinant ATTR V30M

protein was immobilized on a polystyrene microtiter plates. Ratio of wild-type TTR to ATTR V30M in these serum samples was also determined by means of SELDI-TOF MS [4]. In addition, to detect the conformational epitopes binding to the autoantibodies, we tried ELISA immobilized some recombinant ATTR V30M fragment peptides on polystyrene microtiter plates. Moreover, correlation between the data of the ELISA and age of the subjects or duration of FAP was investigated.

RESULTS

Three of 25 Japanese and 5 of 6 Swedish FAP ATTR V30M patients have high levels of autoantibodies against ATTR, and these 8 patients were all late onset cases. In addition, ratio of ATTR V30M to wild-type TTR in serum of the high autoantibody group was lower than those of low autoantibody group (Figure 1).

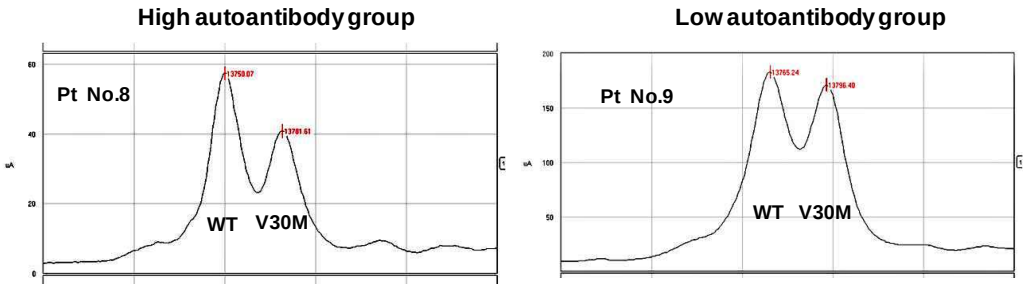

Figure 1. A sample of the ratio of wild-type TTR to ATTR V30M in serum.

Moreover, our ELISA data suggested that there were some epitopes at positions 24-35 or 105-115 of ATTR V30M in these patients, and significant positive correlation between the levels of the autoantibody which the epitope was at position 24-35 and the age of onset was observed in these patients ($r=0.833$, $p<0.05$, Figure 2).

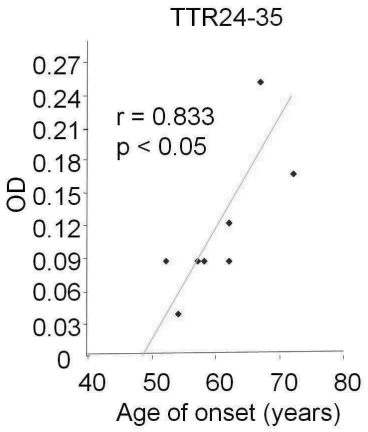

Figure 2. Correlation with the data of ELISA in all FAP ATTR V30M patients and age of onset.

DISCUSSION

Age-dependent increase in the incidence of autoantibodies was observed in patients with FAP ATTR V30M. This phenomenon may influence the clinicopathological differences between both early (<50 years old) and late (more than 50 years old) onset cases of the disease.

ACKNOWLEDGEMENT

This study was supported by grants from the Regeneration Project of Regional Base Health Care of Kumamoto prefecture.

REFERENCES

1. Quintas A, Vaz DC, Cardoso I, Saraiva MJ, Brito RM. Tetramer dissociation and monomer partial unfolding precedes protofibril formation in amyloidogenic transthyretin variants. J Biol Chem 276: 27207-27213, 2001.
2. Palha JA, Moreira P, Olofsson A, Lundgren E, Saraiva MJ. Antibody recognition of amyloidogenic transthyretin variants in serum of patients with familial amyloidotic polyneuropathy. J Mol Med (Berl) 78: 703-707, 2001.
3. Ando Y, Terazaki H, Haraoka K, Tajiri T, Nakamura M, Obayashi K, Misumi S, Shoji S, Hata K, Nakagawa K, Ishizaki T, Uemoto S, Inomata Y, Tanaka K, Okabe H. Presence of autoantibody against ATTR Val30Met after sequential liver transplantation. Transplantation 73: 751-755, 2002.
4. Suhr OB, Lundgren E. Presence of autoantibody against ATTR Val30 Met after sequential liver transplantation. Transplantation 73: 674-675, 2002.
5. O'Nuallain B, Wetzel R. Conformational Abs recognizing a generic amyloid fibril epitope. Proc Natl Acad Sci USA 99: 1485-1490, 2002.
6. Bergström J, Engström U, Yamashita T, Ando Y, Westermark P. Surface exposed epitopes and structural heterogeneity of in vivo formed transthyretin amyloid fibrils. Biochem Biophys Res Commun 348: 532-539, 2006.
7. Terazaki H, Ando Y, Fernandes R, Yamamura K, Maeda S, Saraiva MJ. Immunization in familial amyloidotic polyneuropathy: counteracting deposition by immunization with a Y78F TTR mutant. Lab Invest 86: 23-31, 2006.
8. Su Y, Jono H, Torikai M, Hosoi A, Soejima K, Guo J, Tasaki M, Misumi Y, Ueda M, Shinriki S, Shono M, Obayashi K, Nakashima T, Sugawara K, Ando Y. Antibody therapy for familial amyloidotic polyneuropathy. Amyloid 19 (Suppl 1): 45-46, 2012.
9. Kawahara S, Ueda M, Miyazaki A, Yuki U, Shono M, Horibata Y, Jono H, Obayashi K, Ikeda K, Tanase S, Ando Y. Age-dependent increase in thiol conjugated forms of transthyretin (TTR) in the elderly: quantitative analyses by the surface-enhanced laser desorption/ionization time-of-flight mass spectrometry (SELDI-TOF MS) protein chip system. Amyloid 18 (Suppl 1): 9-11, 2011.

Baseline Profile of Patients Undergoing Tafamidis Treatment in THAOS – the Transthyretin Amyloidosis Outcomes Survey

T. Coelho[1], M.S. Maurer[2], M. Waddington Cruz[3], on behalf of the THAOS Investigators

[1]Hospital Santo António, Porto, Portugal; [2]Columbia University Medical Center, New York-Presbyterian Hospital, New York, USA; [3]Hospital Universitário Clementino Fraga Filho, Rio de Janeiro, Brazil.

THAOS is a worldwide registry of patients with transthyretin (TTR) amyloidosis. Of 975 subjects enrolled, we analyzed 84 patients who were receiving tafamidis, including those with polyneuropathy (TTR-FAP) or cardiomyopathy (TTR-CM). At the time of enrollment, symptom duration was 6.0±5.4 years (mean±SD) and length of treatment was 2.4±0.8 years. 67 patients had TTR-FAP-associated mutations (V30M, I107V, F64L, S77F, and S77Y) with a mean age of 43.4±14.1 years, symptom onset at 37.4±14.6 years; symptoms included sensory neuropathy (98.5%), gastrointestinal disturbances (80.0%), and autonomic neuropathy (56.9%). Neurological assessments revealed deterioration consistent with length-dependent axonal degeneration. Seventeen patients with TTR-CM-associated phenotypes (wild-type, V122I, L58H, and T60A) were older (74.6±6.8 years) and reported later symptom onset (68.7±9.5 years), including cardiac problems (88.2%) and sensory neuropathy (64.7%). These patients had abnormal electrocardiograms. Follow-up data for all patients are currently being recorded, with the goal of demonstrating disease progression and disease-modifying effects of any treatment.

BACKGROUND AND OBJECTIVES

Liver transplantation is the current standard of care for transthyretin (TTR) amyloidosis (1), and while it demonstrates clear benefits, there are many patients who do not undergo this procedure for various reasons and may benefit from one of a number of promising new pharmacotherapies being developed (2). One such therapy, tafamidis, is a novel, specific stabilizer of TTR (3) that has demonstrated a clinical benefit for patients with V30M TTR amyloidosis in a phase 2/3 trial (4). Tafamidis recently gained approval for use in the European Union, and is the first pharmacologic agent specifically approved for the treatment of early stage TTR amyloidosis (5).

The Transthyretin Amyloidosis Outcomes Survey (THAOS) is a global, multicenter, longitudinal, observational survey established in 2007 that collects data on the natural history and treatment of TTR amyloidosis. As of September 2011, the registry included 975 patients in 46 sites and 19 countries. A number of these patients are being actively treated with pharmacotherapy in clinical trials. Here we describe the patient population in THAOS who have received treatment with tafamidis.

METHODS

Baseline data as of September 1, 2011, were analyzed for 84 patients receiving tafamidis treatment, separated by genotype according to its associated predominant phenotype – polyneuropathy (TTR-FAP) or cardiomyopathy (TTR-CM).

RESULTS

Overall characteristics of tafamidis-treated patients are summarized in Table 1. They were similar in age, gender distribution, and age at disease onset to the untreated population in THAOS (data not shown). A slightly higher percentage of tafamidis-treated patients with *TTR* mutation reported a family history of TTR amyloidosis, compared to the untreated population (93.0% vs 83.9%).

Table 1. Baseline characteristics of the tafamidis-treated population in THAOS

	TTR-FAP Genotype	TTR-CM Genotype
Total (men)	67 (31)	17 (14)
Mean age, years (SD)	43.4 (14.1)	74.6 (6.8)
Mean age at disease onset, years (SD)	37.4 (14.6)	68.7 (9.5)
Mean length of tafamidis treatment, years (SD)	2.4 (0.9)	2.6 (0.4)
TTR genotype (%)	V30M (91.0) S77Y (3.0) S77F (1.5) F64L (1.5) I107V (1.5) G6S/V30M (1.5)	Wild-type (76.5) L58H (11.8) T60A (5.9) V122I (5.9)
Country of residence (%)	Portugal (59.7) France (28.4) Brazil (10.5) United States (1.5)	United States (100.0)
Patients with family history of ATTR, n (%)[a] Father with ATTR, % Mother with ATTR, % Other with ATTR, % Unknown with ATTR, %	63 (94.0) 39.7 57.1 1.6 1.6	3 (75.0) 33.3 33.3 33.3

ATTR = transthyretin amyloidosis. [a]Patients with *TTR* mutation only.

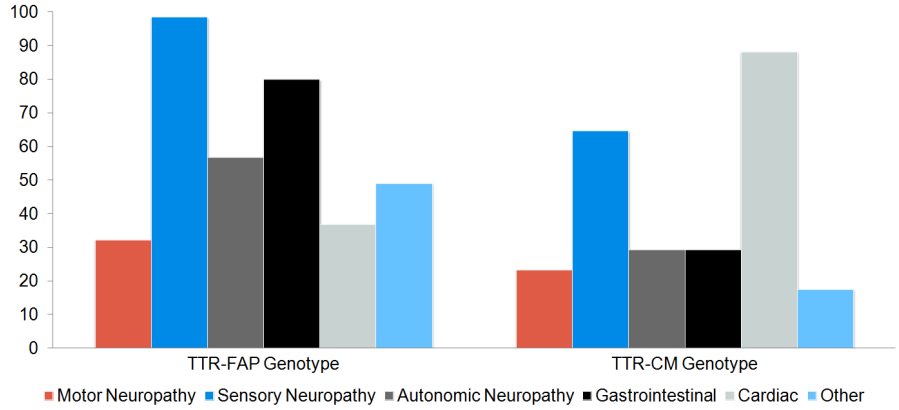

Figure 1. Baseline symptoms reported by tafamidis-treated patients in THAOS.

Patient-reported symptoms related to TTR amyloidosis at the time of enrollment, recorded as part of a patient's medical history, are shown in Figure 1. These patterns were similar for treated and untreated (data not shown) patients.

Detailed medical assessments recorded for each patient indicated that most TTR-FAP patients showed evidence of neuropathic pain or paresthesia, and up to a third demonstrated gastrointestinal complications (e.g. constipation). Among TTR-CM patients, most had signs of stage II heart failure and some reported neuropathic complications, but few had gastrointestinal disturbances.

Decreased or absent pinprick and light touch sensation and cold temperature insensitivity in the toe were common neurologic findings in TTR-FAP patients (n=65). The observed distal-to-proximal pattern of sensation loss is consistent with length-dependent axonal degeneration.

100% of TTR-CM patients (n=12) exhibited abnormal electrocardiograms, including abnormalities in rhythm, pacemaker function, conduction, and Q waves.

CONCLUSIONS

At the time of THAOS enrollment, many tafamidis-treated patients with TTR-FAP genotypes exhibited sensory neuropathy and gastrointestinal symptoms, and demonstrated length-dependent axonal degeneration. Abnormal electrocardiograms and cardiac and sensory neuropathy symptoms were characteristic of patients with TTR-CM genotypes. As more patients commence treatment with tafamidis, physicians will be encouraged to enroll these patients in THAOS and to record their progress. It is hoped that these additional data can help inform future analyses, patient care, and directions for the registry.

FUNDING

Data presented in this abstract are part of the THAOS registry, which is sponsored by Pfizer Inc.

REFERENCES

1. Holmgren G, Ericzon BG, Groth CG, Steen L, Suhr O, Andersen O, et al. Clinical improvement and amyloid regression after liver transplantation in hereditary transthyretin amyloidosis. *Lancet*. 1993;341:1113-1116.
2. Planté-Bordeneuve V, Said G. Familial amyloid polyneuropathy. *Lancet Neurol*. 2011;10:1086-1097.
3. Bulawa CE, Connelly S, Devit M, Wang L, Weigel C, Fleming JA, et al. Tafamidis, a potent and selective transthyretin kinetic stabilizer that inhibits the amyloid cascade. *Proc Natl Acad Sci USA*. 2012;109:9629-9634.
4. Coelho T, Maia LF, Martins da Silva A, Cruz MW, Planté-Bordeneuve V, Lozeron P, et al. Tafamidis for transthyretin familial amyloid polyneuropathy: a randomized, controlled trial. *Neurology*. 2012;79(8)785-792.
5. Said G, Grippon S, Kirkpatrick P. Tafamidis. *Nat Rev Drug Discov*. 2012;11:185-186.

Using Nutritional Status Measured by BMI and mBMI for Monitoring Clinical Progress in Patients with Transthyretin Familial Polyneuropathy: Data from Two Tafamidis Studies

O.B. Suhr[1], I.M. Conceição[2], O. Karayal[3], F.S. Mandel[3], B.-G. Ericzon[4]

[1]Umeå University Hospital, Umeå, Sweden; [2]Hospital de Santa Maria, Lisbon, Portugal; [3]Pfizer Inc, New York, New York, USA; [4]Karolinska Institutet, Stockholm, Sweden.

Transthyretin familial polyneuropathy (TTR-FAP) is often characterized by degenerative gastrointestinal symptoms such as involuntary weight loss, malnutrition, and cachexia. Deterioration in nutritional status may be reflected by reduction in body mass index (BMI) or modified body mass index (mBMI; BMI × serum albumin). BMI and mBMI were recorded during a double-blind 18-month clinical trial of tafamidis in TTR-FAP patients (Study Fx-005, N=125) and an open-label 12-month extension study (Fx-006, N=71). In Fx-005, mBMI decreased after 18 months in placebo patients (P<0.05 vs baseline), and increased in tafamidis patients (P<0.01 vs baseline; P<0.0001 vs placebo). Changes in BMI demonstrated similar but statistically non-significant trends. Decline in nutritional status in Fx-005 placebo patients was reversed following initiation of open-label tafamidis, with significant increases from Fx-006 baseline in mBMI (P<0.0001) and BMI (P<0.01). Thus, tafamidis therapy resulted in improvement in nutritional status, suggesting its potential for improving clinical outcomes in patients with TTR-FAP.

BACKGROUND AND OBJECTIVES

In addition to polyneuropathic and cardiomyopathic symptoms, transthyretin familial polyneuropathy (TTR-FAP) is characterized by degenerating gastrointestinal symptoms such as involuntary weight loss, malnutrition, and cachexia, reflected in reduced body mass index (BMI: kg/m^2). BMI is influenced by edema due to low serum albumin, and high BMI is observed despite malnutrition. Therefore, the product of serum albumin and BMI, modified body mass index (mBMI; BMI × serum albumin), is an effective tool for monitoring TTR-FAP progression, and has been shown to predict survival in these patients (1).

Tafamidis meglumine is a small molecule that stabilizes tetrameric TTR and prevents its dissociation into amyloidogenic monomers. In an 18-month controlled trial, tafamidis slowed the progression of peripheral neurologic impairment in TTR-FAP patients with Val30Met variant TTR (2). The objective of the present analysis was to evaluate nutritional status in patients with TTR-FAP in the tafamidis clinical trials.

METHODS

Data were analyzed from two clinical trials: Study Fx-005, a double-blind, randomized trial in Val30Met patients who received tafamidis 20 mg or placebo once daily for 18 months; and Study Fx-006, an open-label 12-month extension of Fx-005. Patients who completed the month 18 visit of Fx-005 were eligible to enroll in Fx-006. In the extension study, there were two treatment sequence groups: *Placebo-tafamidis*, patients randomized to 18 months of placebo in Fx-005 who were switched to tafamidis, and *tafamidis-tafamidis*, patients randomized to 18 months of tafamidis in Fx-005 who continued to receive tafamidis.

Nutritional status was evaluated by recording baseline height (m), and body weight (kg) and serum albumin (g/L) at baseline and 6-month intervals. BMI was calculated as body weight (kg)/(baseline height [m])^2 and mBMI as BMI (kg/m^2) × serum albumin (g/L). Analyses were performed in the intent-to-treat (ITT) population, defined as all patients who received ≥ 1 dose of tafamidis. For the Fx-005/Fx-006 analyses, only those Fx-005 patients who enrolled in Fx-006 were included in the ITT population.

RESULTS

A total of 128 patients were enrolled in study Fx-005 and randomized to tafamidis (n = 65) or placebo (n = 63). Of the 91 eligible patients completing study Fx-005, 85 enrolled and received ≥ 1 dose of tafamidis in Fx-006. Treatment groups were similar with respect to baseline characteristics.

Over the Fx-005 18-month treatment period, patients treated with placebo experienced a reduction in mBMI at each on-treatment study visit, while those treated with tafamidis experienced an increase in mBMI at each on-treatment study visit. By the end of Fx-005, mBMI change from baseline in the tafamidis group was significantly different from that in the placebo group ($P < 0.0001$). A statistically significant difference between the two treatment groups was also found in their serum albumin change ($P = 0.0226$) but not BMI change (P = NS).

Worsening of nutritional status in patients receiving placebo during the double-blind study Fx-005 was reversed following the initiation of tafamidis in the open-label extension study Fx-006 (Figure 1). Mean mBMI, BMI, and serum albumin were significantly improved from Fx-006 baseline (month 18) at the end of Fx-006 (month 30).

CONCLUSIONS

Nutritional status, as measured by mBMI, was maintained or increased with tafamidis treatment, in contrast to the decline observed with placebo. A reversal of the decline in nutritional status was seen in the placebo group following the switch to tafamidis. Improvement was noted for s-albumin and also for BMI suggesting that both increased body weight and s-albumin contributed to the improved nutritional status.

The improvement in mBMI in this combined 30-month-long trial is consistent with improvements in neurologic function and quality of life (2,3). This, together with previous reports (1,4) suggests that the mBMI may be a useful tool for monitoring clinical status and response to treatment in individuals with TTR-FAP.

This study was sponsored by FoldRx Pharmaceuticals, which was acquired by Pfizer Inc in October 2010.

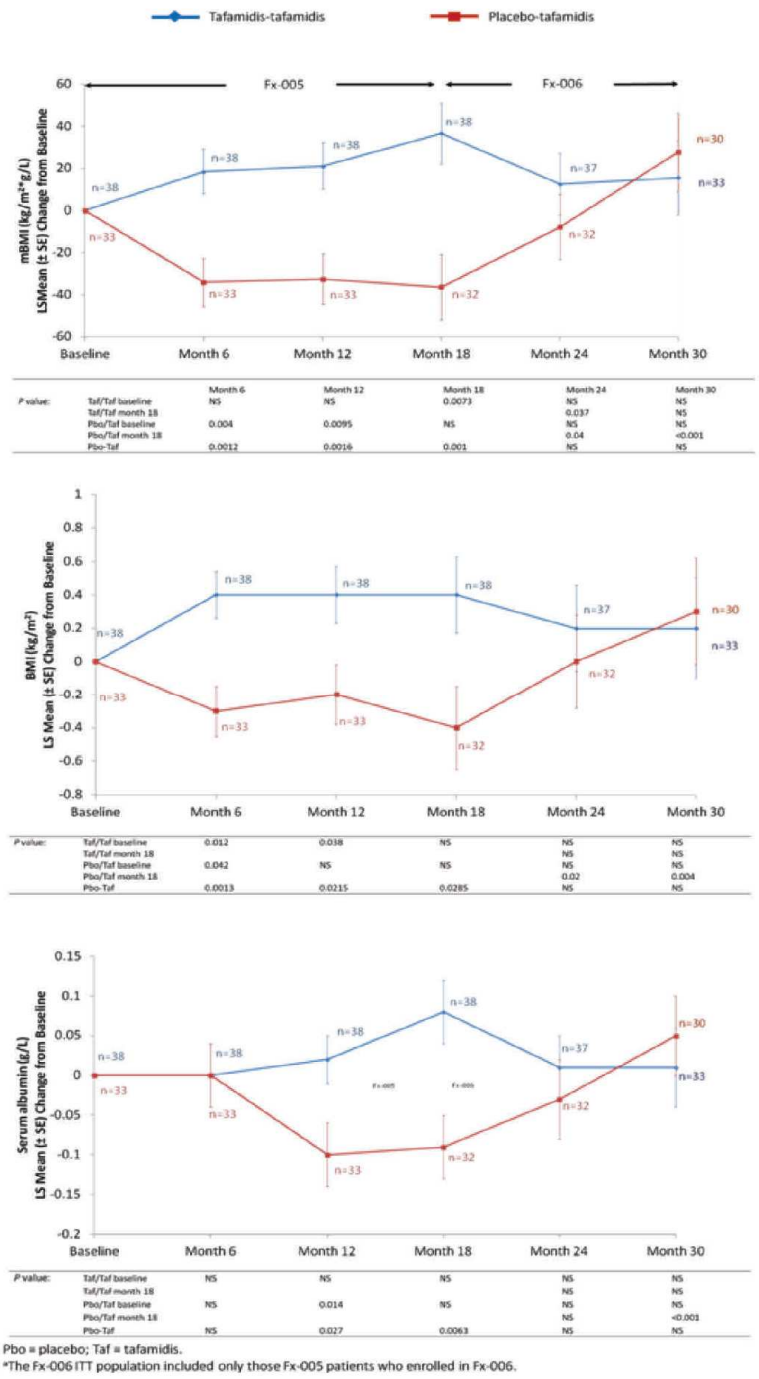

Figure 1. mBMI, BMI, and serum albumin change from baseline to on-treatment time points (Fx-006 intent-to-treat, observed cases population) in Fx-005 and Fx-006.

REFERENCES

1. Suhr O, Danielsson A, Holmgren G, Steen L. Malnutrition and gastrointestinal dysfunction as prognostic factors for survival in familial amyloidotic polyneuropathy. J Intern Med. 1994;235:479-485.
2. Coelho T, Maia LF, Martins da Silva A, Cruz MW, Planté-Bordeneuve V, Lozeron P, et al. Tafamidis for transthyretin familial amyloid polyneuropathy: a randomized, controlled trial. Neurology. 2012;79(8)785-792.
3. Coelho T. New pharmacological treatment. J Neurol. 2011;258:S4.
4. Suhr OB, Friman S, Ericzon BG. Early liver transplantation improves familial amyloidotic polyneuropathy patients' survival. Amyloid. 2005;12:233-238.

Cardiac Safety and Tolerability, and Effects on Cardiac Function, of Tafamidis in Patients With Non-V30M TTR-FAP

Thibaud Damy,[1] Daniel Judge,[2] Ahmet Dogan,[3] Karine Berthet,[4] Violaine Planté-Bordeneuve[1]

1. CHU Henri Mondor, Créteil, France; 2. Johns Hopkins University Center for Inherited Heart Disease, Baltimore, MD, USA; 3. Mayo Clinic, Rochester, MN, USA; 4. Pfizer Inc, Paris, France.

Transthyretin familial amyloid polyneuropathy (TTR-FAP) is characterized by extracellular TTR amyloid deposition in the nerves and heart. Progressive cardiomyopathy due to amyloidosis is described in TTR-FAP patients despite treatment with liver transplant to remove the source of mutant TTR. Tafamidis prevents TTR monomer dissociation into amyloid fibrils. Twenty-one patients with TTR-FAP due to non-V30M *TTR* mutations received tafamidis in a phase 2, open-label safety trial . Mean (SD) age, LVEF, troponin I, and NT-pro-BNP at baseline were 63.1 (9.86) years, 60.3 (9.96) %, 0.023 (0.04) ng/mL, and 1,248.9 (1,529.4) pg/mL, respectively. Cardiac outcomes did not significantly change for 18 patients completing the study. Of 9 patients with a history of cardiac events, 6 experienced peripheral edema or dyspnea related to heart failure; 3 were hospitalized for other cardiovascular events. The percentage of patients with normal heart rate variability increased from 21% (4/19) at baseline to 42% (8/19) at month 12.

INTRODUCTON

Transthyretin familial amyloid polyneuropathy (TTR-FAP) is an autosomal dominant disease in which single site mutations in the transthyretin (*TTR*) gene destabilize the native tetrameric structure of TTR, resulting in tetramer dissociation and extracellular deposition of insoluble protein fibrils primarily in nerves and heart (1,2). Orthotopic liver transplant (OLT) has until recently been the only effective treatment option (3). Cardiomyopathy due to continuing amyloidosis typically progresses after OLT, particularly in patients with non-V30M mutations (3). Tafamidis meglumine is a small molecule that stabilizes the native tetrameric form of TTR and prevents its dissociation into amyloidogenic monomers. A previous 18-month controlled trial demonstrated that tafamidis slowed progression of peripheral neurologic impairment in patients with V30M TTR-FAP (4). Here we report on exploratory cardiac outcomes in a 12-month study of tafamidis in patients with TTR-FAP due to non-V30M *TTR* mutations, a group in which significant cardiac involvement is likely.

METHODS

This was a 12-month, phase 2, open-label study of tafamidis 20 mg QD in adults with biopsy-confirmed TTR amyloidosis due to non-V30M mutation. The primary endpoint was TTR stabilization rate at week 6. The effects

of treatment on selected cardiac parameters were evaluated at baseline, month 6, and month 12. Analyses were performed in the intent-to-treat (ITT) population, defined as all patients who received at least 1 dose of tafamidis. All analyses were based on observed data without imputation of missing values.

RESULTS

Of the 21 patients enrolled in the study, 61.9% were male and the mean age (standard deviation [SD]) was 63.1 (9.86) years. Mean disease duration was 64.7 (60.77) months with an age of onset of 59.3 (9.15) years. Eight *TTR* variants were represented in the study population: p.Ser77Tyr (n=2), p.Gly47Ala (n=3), p.Phe64Leu (n=4), p.Asp38Ala (n=1), p.Thr60Ala (n=4), p.Leu58His (n=4), p.Ser77Phe (n=1), and p.Ile107Val (n=2). Eighteen patients (85.7%) completed the study.

All patients had at least 1 echocardiographic abnormality at baseline, the most common of which were left ventricular (LV) posterior wall thickness and LV septal thickness ≥ 13 mm in 17 (89.5%) patients and valve thickening in 16 (84.2%) patients. Echocardiographic values showed no clinically meaningful changes from baseline to month 12 (Table 1).

Table 1. Echocardiographic Assessment: ITT Population

Measurement	Baseline	6 month	12 month
LVEF, %			
N	21	18	18
Mean ± SD	60.3 ± 9.96	57.9 ± 10.94	60.2 ± 6.44
Median	61.0	57.5	59.0
Range	34 - 77	37 - 79	50 - 70
LV posterior wall thickness, mm			
N	19	16	14
Mean ± SD	14.6 ± 2.6	14.9 ± 3.2	15.1 ± 2.7
Median	14.0	15.0	15.0
Range	9.0 - 20.0	9.0 - 20.0	11.0 - 20.0
Interventricular septal thickness, mm			
N	19	16	14
Mean ± SD	15.24 ± 2.77	16.06 ± 3.30	16.21 ± 3.24
Median	15.0	17.0	15.5
Range	8.5 - 20.0	9.0 - 20.0	10.0 - 21.0
Fractional shortening, %			
N	18	15	14
Mean ± SD	31.2 ± 5.7	30.9 ± 5.9	30.6 ± 7.1
Median	32.0	31.0	30.0
Range	17 - 42	20 - 40	20 - 43
E/A ratio			
N	18	14	17
Mean ± SD	1.46 ± 0.67	1.44 ± 0.75	1.35 ± 0.69
Median	1.30	1.15	1.20
Range	0.60 - 3.10	0.70 - 3.10	0.50 - 3.10
IVRT, ms			
N	10	6	12
Mean ± SD	84.1 ± 17.5	94.2 ± 12.45	88.5 ± 17.7
Median	81.0	97.5	94.0
Range	56 - 108	77 - 106	52 - 106

Troponin I elevation has been observed in TTR-FAP patients (5). Mean troponin I levels in the study population were normal at baseline compared with established ranges and remained stable throughout the study (Table 2). Mean baseline NT-proBNP values were elevated but also remained stable over the course of the study with no

clinically relevant changes observed. NT-proBNP values >1,000 pg/mL, indicative of heart failure, were measured in 10 patients; 9 had previously experienced cardiac events. Patients at low risk of heart failure (NT-proBNP values <300 pg/mL) showed no increase in NT-proBNP levels; no serious cardiovascular events occurred.

Table 2. Biomarker Measurement in ITT Population

Measurement	Baseline	6 Months	12 Months
Troponin I, ng/mL			
N	20	18	18
Mean ± SD	0.023 ± 0.04	0.03 ± 0.04	0.02 ± 0.04
Median	0.00	0.00	0.00
Range	0.00–0.13	0.00–0.13	0.00–0.13
NT-proBNP, pg/mL			
N	19	18	16
Mean ± SD	1,248.9 ± 1,529.4	1,132.2 ± 1,264.5	1,253.9 ± 1,937.3
Median	799.0	829.5	752.4
Range	43.0–6,216.0	50.0–4,087.0	41.0–7,902.0

Changes from baseline in 24-hour average heart rate were minimal, with the pattern of electrographic abnormalities similar at baseline and during treatment. The percentage of patients with normal HRV increased was 21% (4/19) at baseline, 29% (4/14) at 6 months, and 42% (8/19) at 12 months. Echocardiographic and electrocardiographic abnormalities observed after treatment initiation were consistent with underlying cardiac morbidity. Tafamidis was not associated with abnormalities in blood urea nitrogen or measures of thyroid function. Seventeen patients (81%) experienced ≥1 adverse event (AE), most commonly falls (5 patients, 24%), diarrhea (5 patients, 24%), extremity pain (4 patients, 19%), and dizziness, dyspnea, vomiting, and constipation (3 patients each, 14%). Four serious AEs were considered possibly related to treatment (ankle fracture, malaise, urinary retention, and transient ischemic attack). No patients died during the study.

CONCLUSION

In conclusion, tafamidis was safe and well tolerated over 12 months in patients with non-V30M TTR-FAP. Most echocardiographic parameters were stable over 12 months of tafamidis treatment, and there were no clinically significant changes over time. There were no clinically relevant changes in troponin I or NT-proBNP levels. Although baseline Holter monitoring results indicated impaired cardiac autonomic function in most patients, electrographic analysis of heart rate and HRV demonstrated no adverse effects of tafamidis treatment. By month 12, measures of HRV appeared to improve.

FUNDING

This study was sponsored by FoldRx Pharmaceuticals, which was acquired by Pfizer Inc in October 2010.

REFERENCES

1. Planté-Bordeneuve V, Said G. *Lancet Neurol*. 2011;10(12):1086-1097.
2. Rapezzi C, Quarta CC, Riva L, et al. *Nat Rev Cardiol*. 2010;7(7):398-408.

3. Stangou AJ, Hawkins PN, Heaton ND, et al. *Transplantation*. 1998;66(2):229-233.
4. Coelho T, Maia L, Martins da Silva A, et al. *Neurology*. 2012;79(8)785-792.
5. Suhr OB, Anan I, Backman C, et al. *J Intern Med*. 2008;263(3):294-301.

Transthyretin Stabilization, Efficacy and Safety of Tafamidis for the Treatment of Transthyretin Amyloidosis

G. Merlini[1], T. Coelho[2], R.H. Falk[3], D.P. Judge[4], I. Lombardo[5]

[1]Foundation IRCCS Policlinico San Matteo, University of Pavia, Pavia, Italy; [2]Hospital Santo António, Porto, Portugal; [3]Brigham and Women's Hospital Cardiac Amyloidosis Program, Boston, USA; [4]Johns Hopkins University School of Medicine, Baltimore, USA; [5]Pfizer Inc, New York, USA

Transthyretin (TTR) stabilization, efficacy and safety of tafamidis, a kinetic stabilizer, were evaluated in a phase 2/3 double-blind, randomized trial (Fx-005, n=125) and open-label extension (Fx-006, n=71) in V30M TTR amyloidosis polyneuropathy patients, and phase 2 open-label studies in non-V30M polyneuropathy patients (Fx1A-201, n=21) and wild-type or V122I patients with cardiomyopathy (Fx1B-201, n=35). At final timepoints, TTR was stabilized in most patients (Fx-005: tafamidis 97.9%, placebo 0%, P<0.0001; Fx-006: tafamidis-tafamidis 94.1%, placebo-tafamidis 93.3%; Fx1A-201: 100%; Fx1B-201: 87.5%). In Fx-005, tafamidis resulted in less deterioration in Neuropathy Impairment Score-Lower Limbs (P=0.0271), Norfolk Quality of Life-Diabetic Neuropathy total score (P=0.1157) and modified body mass index (P<0.0001). These effects were sustained in Fx-006. Similar benefits were observed in Fx1A-201. In Fx1B-201, change from baseline in cardiac biomarkers and functional assessments was minimal suggesting no substantial deterioration in cardiac status. Thus, treatment with tafamidis was associated with stabilized TTR and slowed disease progression.

BACKGROUND AND OBJECTIVES

TTR amyloidosis, characterized by progressive neuropathy (TTR-FAP) and cardiomyopathy (TTR-CM), is both a genetic and a sporadic disease resulting from variant (or wild-type) TTR tetramer dissociation into monomers that ultimately form amyloid deposits (1). Tafamidis is a small molecule that kinetically stabilizes the native tetrameric form of TTR (2), a process that is predicted to slow amyloidogenesis and disease progression in TTR amyloidosis patients. Tafamidis was approved in Europe in November 2011 for the treatment of early-stage TTR-FAP (3). Here we describe the plasma TTR stabilization by tafamidis and the efficacy and safety of oral 20 mg daily tafamidis treatment in four clinical trials.

METHODS

Studies are described in Table 1. Key efficacy variables in the TTR-FAP studies included the Neuropathy Impairment Score-Lower Limbs (NIS-LL) and Σ5 NCS nds composite score measuring large nerve fiber; the total score of the Norfolk Quality of Life-Diabetic Neuropathy questionnaire (TQOL) and modified body mass

index (mBMI, equivalent to BMI × serum albumin), which is a measure of wasting and autonomic gastrointestinal function. N-terminal pro brain-type natriuretic peptide (NT-proBNP), troponin I and T levels, and 6-minute walk test (6MWT) were recorded in Fx1B-201.

Table 1. Summary of Clinical Trials Evaluating Tafamidis

Study	Description	ITT population	Genotypes
Fx-005 (TTR-FAP)	18-month, randomized, controlled, double-blind	Tafamidis n=64, Placebo n=61	Val30Met
Fx-006 (TTR-FAP)	12-month open-label extension of Fx-005	Tafamidis-tafamidis n=38, Placebo-tafamidis n=33	Val30Met
Fx1A-201 (TTR-FAP)	12-month, open-label	Tafamidis n=21	Non-Val30Met
Fx1B-201 (TTR-CM)	12-month, open-label	Tafamidis n=35	Wild-type (n=31), Val122Ile (n=4)

ITT=intent to treat, defined as all randomized patients with ≥1 post-baseline assessment (Fx-005, Fx-006) or all patients who received ≥1 dose of study medication (Fx1A-201, Fx1B-201).

Samples were subjected to urea-denaturing conditions followed by crosslinking in an immunoturbidity assay, in which only intact folded TTR tetramers are recognized. Under these conditions, TTR irreversibly dissociates into unfolded monomers, but tafamidis-bound tetramers are stabilized. Percent TTR stabilization was calculated as the relative difference in “fraction of initial” (FOI, amount of tetramer remaining after denaturation divided by amount of tetramer before denaturation) between dosed and baseline samples. Stabilization was deemed if values were above the 95% confidence interval of values for healthy volunteers in a previous phase 1 study (32% stabilization).

RESULTS

TTR stabilization was observed across all TTR genotypes evaluated, including wild-type. In nearly all (95%-100%) tafamidis-treated patients, TTR was stabilized at the first assessed time point (week 6 or week 8), compared with only 7% of placebo-treated Val30Met patients. Results in tafamidis-treated patients were sustained to the end of the treatment period; none of the placebo-treated patients had stabilized TTR at month 18 of study Fx-005.

During the Fx-005 study, Val30Met patients receiving tafamidis experienced less deterioration in NIS-LL, TQOL, and mBMI than those receiving placebo. In the ITT population, 45.3% of tafamidis-treated patients had no disease progression (NIS-LL change from baseline <2 points) at month 18 compared with 29.5% of placebo patients (P=0.0682); least squares mean ± standard error changes from baseline to month 18 in TQOL scores were 2.0 ± 2.3 and 7.2 ± 2.4 for the tafamidis and placebo groups, respectively (P=0.1157). Compared with placebo, tafamidis patients experienced a significant reduction in change from baseline at month 18 in NIS-LL (P=0.0271) and mBMI (P<0.0001) and numerically smaller decline in TQOL (P=0.2090).

Fx-006 outcomes reflected a sustained slowed progression of disease in the tafamidis-tafamidis group and a reduction in disease progression in placebo-tafamidis patients who started tafamidis treatment 18 months later. Slower disease progression was also observed in non-Val30Met TTR-FAP patients in the Fx1A-201 study (Figure 1).

In the Fx1B-201 study, cardiac health was evaluated in TTR-CM patients by comparing cardiac biomarkers and functional assessments at baseline and at 12 months. Change from baseline in NT-proBNP and 6MWT was

minimal compared with non-randomized, historical controls, and troponin I and T levels were stable, suggesting no substantial deterioration of cardiac status.

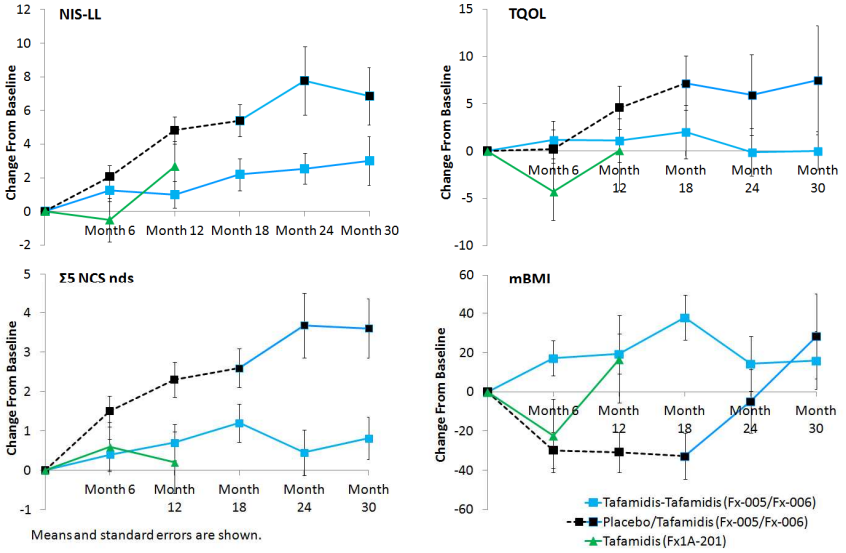

Figure 1. Changes from baseline to on-treatment visits (Fx-005, Fx-006, Fx1A-201; ITT, observed cases).

There were 5 deaths in the Fx-005 study (2 receiving tafamidis, 3 receiving placebo), all after liver transplant. No deaths were reported in Fx-006 or Fx1A-201. Two TTR-CM patients died during the Fx1B-201 study (causes of death were hemorrhagic stroke and primary amyloidosis) and 2 deaths occurred >30 days after study completion (intracranial hemorrhage due to glioblastoma multiforme and unknown). The most common adverse events were diarrhea (n=28, 22.0%) and urinary tract infection (n=26, 20.5%) among TTR-FAP patients, and dyspnea (n=11, 31.4%), congestive heart failure (n=9, 25.7%), fatigue (n=8, 22.9%), dizziness (n=7, 20.0%), and diarrhea (n=7, 20.0%) among TTR-CM. Differences between study groups are likely due to the underlying differences in patient characteristics such as age and comorbid conditions.

CONCLUSIONS

Tafamidis stabilized TTR in most patients with wild-type or mutant TTR, and tafamidis-treated patients experienced less neurologic deterioration and maintained quality of life and nutritional status.

FUNDING

This study was sponsored by FoldRx Pharmaceuticals, which was acquired by Pfizer Inc in October 2010.

REFERENCES

1. Kelly JW. Alternative conformations of amyloidogenic proteins govern their behavior. Curr Opin Struct Biol. 1996;6:11-17.

2. Bulawa CE, Connelly S, Devit M, Wang L, Weigel C, Fleming JA, et al. Tafamidis, a potent and selective transthyretin kinetic stabilizer that inhibits the amyloid cascade. Proc Natl Acad Sci USA. 2012;109:9629-9634.
3. Said G, Grippon S, Kirkpatrick P. Tafamidis. Nat Rev Drug Discov. 2012;11:185-186.

Treatment of Advanced Heart Failure in Cardiac Amyloidosis with Left Ventricular Assist Device Therapy

Paul L. Swiecicki[1], Brooks Edwards[2], Sudhir Kushwaha[2], Angela Dispenzieri[1], Soon J. Park[3], Morie A. Gertz[1]

[1]Division of Hematology, Mayo Clinic, Rochester, MN, United States;[2]Division of Cardiovascular Diseases, Mayo Clinic, Rochester, MN, United States; [3]Division of Cardiovascular Surgery, Mayo Clinic, Rochester, MN, United States.

ABSTRACT

Left ventricular assist devices (LVAD) are frequently used in heart failure secondary to dilated cardiomyopathy but no study has investigated their use in cardiac amyloidosis. We analyzed the outpatient outcomes in seven patients with cardiac amyloidosis treated with LVAD implantation between December 2008 and October 2011.

All patients were NYHA Class IV and had a significantly decreased cardiac index. All patients tolerated LVAD placement well, the most common post-operative complication being bleeding. Post-operatively, 1 patient developed transient right heart failure. Mean hospitalization was 24 days and none of the patients were re-hospitalized within 30 days. Only 1 patient died since the procedure and all patients reported significantly improved NYHA Class.

In patients with advanced heart failure secondary to cardiac amyloidosis, LVAD implantation may be an acceptable therapeutic option. Firm conclusions cannot be drawn but these observations suggest consideration of LVAD implantation in patients with end stage cardiac amyloidosis.

INTRODUCTION

Amyloidosis is a multisystem disease, the most serious manifestation being that of cardiac amyloidosis. No effective treatment options exist outside of transplantation which most patients are not eligible for due to the systemic nature of the disease and concern for reoccurrence. In the last decade there has been considerable research in the treatment of end-stage heart failure. Namely, left ventricular assist devices (LVADs) were developed. Originally used to bridge patients to transplant, they are now also used in non-transplant candidates as 'destination therapy'. LVAD use has been found to have low risk of adverse events and improve quality of life (1). Patients with cardiac amyloidosis are rarely transplant candidates due to the nature of the disease (2). No study has fully addressed LVAD placement in patient with cardiac amyloidosis. In this study, we sound to examine the characteristics, surgical complications, and post-hospital outcomes in 7 patients who received LVADs for end stage cardiac amyloidosis.

METHODS

During the period December 1, 2008 and October 31, 2011 7 patients received continuous axial flow LVAD (Heart Mate II, Thoratec, Pleasanton, CA) for treatment of cardiac amyloidosis. The diagnosis of cardiac amyloidosis had been established by tissue biopsy and mass spectrometry in each patient. The records of each patient were then analyzed. The study protocol was reviewed and approved by the institutional review board at Mayo Clinic, Rochester, MN

RESULTS

Five patients had the diagnosis of SSA, one had TTR familial amyloidosis, and one patient had AL amyloidosis. The patient (#5) with TTR familial amyloidosis was found to have a mutation resulting in the amino acid substitution p.Asp18Asn. All patients were classified as NYHA functional class IV at time of presentation. Four of the seven patients were given a score less than 3 as defined by the Interagency Registry for Mechanically Assisted Circulatory Support scale. Baseline echocardiography demonstrated increased septal and posterior thickness in the majority of the patients. Baseline cardiac catheterization data was available for 6 of the patients, all of which demonstrated mean pulmonary artery pressure, mean wedge pressure, and pulmonary vascular resistance to be significantly elevated. The one patient with a history of AL amyloidosis had underwent 8 months of chemotherapy with Melphalan, Prednisone, and Lenalidomide and was in complete hematologic remission prior to LVAD implantation.

The procedure was well tolerated by all patients. Postoperatively, no patients required prolonged intubation, developed acute renal failure, acute cerebral events, or had thromboembolic events. One patient post-operatively developed significant right sided heart failure necessitating dopamine support. His right heart failure resolved and inotropic support was able to be weaned prior to discharge. The median ICU stay for the patients was 8.6 days (5, 15) and average length of hospitalization was 29.4 days (14, 62). All patients were discharged home after intensive inpatient cardiac rehabilitation. No patients were readmitted within 30 days of discharge.

Table 1. Baseline Demographics

Patient:	**#1**	**#2**	**#3**	**#4**	**#5**	**#6**	**#7**
Age	73	58	68	75	46	55	70
Sex	M	M	M	M	M	M	M
Amyloid Type	ATTR SSA	ATTR SSA	ATTR SSA	ATTR SSA	TTR Familial	AL	ATTR SSA
NYHA Class	IV	IV	IV	IV	IV	IV	IV
Cardiac Index ($L/min/m^2$)	1.83	1.79	2.02	1.66	2.33	2.1	2.36

No patients have been lost to follow-up with an average time since procedure of 12.1 months (2, 30). Since LVAD placement, one patient had died (support day 59) and another had proceeded to receive a dual heart/liver transplant (support day 167). Compared to symptoms prior to the LVAD implantations, all discharged patients have had significant improvement in symptoms and NYHA functional class. The most common adverse event has been gastrointestinal bleeding necessitating hospitalization. Follow up echocardiography demonstrated improvement in left heart filling pressures but development of worsening right ventricular dysfunction in many of the patients.

Table 2. Post-Operative Outcomes

Patient:	**#1**	**#2**	**#3**	**#4**	**#5**	**#6**	**#7**
Most recent follow up, months*	2	10	15	30	16	10	2
Deceased	Yes	No	No	No	No	No	No
Length of hospitalization, days	44	22	14	24	26	14	62
Current NYHA Class	III	III	III	III	II	III	III
GI Bleeds	No	Yes	Yes	No	No	Yes	No
Degree of RV Dysfunction	Moderate	Severe	Normal	Mild	Severe	Moderate	Mild

* follow up time post LVAD implantation date

DISCUSSION

This is the first study to describe post-hospital outcomes after use of left ventricular assist devices (LVADs) in the treatment of patients with cardiac amyloidosis. Particularly important is that all patients have had improved heart failure symptoms and only one death has occurred during follow-up. In addition, with LVAD support one patient was able to be bridged to possibly curative dual heart and liver transplant. Most patients receiving LVADs were still noted to develop worsening or severe right ventricular dysfunction. However, only one patient developed temporary right ventricular failure as defined as the need for inotropic or biventricular assist device support.

There is currently a lack of efficacious treatments for non-AL amyloid cardiomyopathy outside of cardiac transplantation. If the cardiac damage is too severe, chemotherapy may be inadequate to alter the natural history of AL amyloidosis. The exception is that of familial amyloidosis where multi-organ transplants may be curative. Medical management is often not effective. There has only been one past study looking at the role of LVAD implantation in restrictive cardiomyopathy which demonstrated no difference in mortality between patients receiving LVADs for restrictive or hypertrophic cardiomyopathy vs. those receiving LVADs for idiopathic or ischemic cardiomyopathy (3). Of note, the aforementioned study on restrictive and hypertrophic cardiomyopathy included 3 of the patients which were identified in this study.

In summary, this study showed that 7 patients with cardiac amyloidosis who underwent LVAD implantation for end stage heart failure experienced improved heart failure symptoms with low post-hospital morbidity and mortality. As there are few treatment options available to these patients, LVAD implantation may be an acceptable therapeutic option.

REFERENCES

1. Moskowitz AJ, Weinberg AD, Oz MC, Williams DL. Quality of life with an implanted left ventricular assist device. The Annals of thoracic surgery. 1997; 64:1764-1769.
2. Kpodonu J, Massad MG, Caines A, Geha AS. Outcome of heart transplantation in patients with amyloid cardiomyopathy. The Journal of heart and lung transplantation: the official publication of the International Society for Heart Transplantation. 2005;24:1763-1765.nll.

3. Topilsky Y, Pereira NL, Shah DK, et al. Left ventricular assist device therapy in patients with restrictive and hypertrophic cardiomyopathy. Circulation. Heart failure. 2011;4:266-275.

SECTION VII

OTHER TYPES OF AMYLOIDOSIS


Wednesday

STATE OF THE ART: AA Amyloidosis

Ilan Ben-Zvi[1], Lesya Kukuy[2], Avi Livneh[3]

[1,2,3]The Heller Institute of Medical Research, Sheba Medical Center and [1,3]Sackler School of Medicine, Tel Aviv University, Tel Aviv Israel

BACKGROUND

AA amyloidosis (AA-A) went through many changes over the last 20 years.

AIM

To describe clinical aspects of AA amyloidosis, focusing on recent developments.

METHODS

Pubmed search of articles appeared over the last 20 years, focusing on those heralding an important change.

FINDINGS

Definition and pathogeneses

AA amyloidosis occurs as a result of tissue deposition of the N-terminal fragment of serum amyloid A (SAA) in association with continuously elevated SAA. Recent studies have shown that elevated SAA levels not only cause the disease, but also determine the prognosis, that is, disease progression, renal deterioration, and the inevitable fatal outcome (1). SAA is an acute phase protein, produced mainly by the liver, with 3 main isoforms (SAA-1,-2,-4). Its normal serum level is 0.5-5 mg/L. Its acute rise during inflammation is regulated by inflammatory cytokines such as IL-1β, IL-6, and TNF α. Its N-terminal fragment of ± 76 a.a. (8KD) is the source of AA.

The diseases causing increased generation of SAA, and thereby underlying amyloidosis, are stratified to chronic inflammatory, chronic infectious, neoplastic and other diseases. The classical and most common of these, as well as "newer" conditions, noted over the last decade are presented in Table 1. A major epidemiological change, namely a shift in the distribution of the underlying diseases from mainly infectious to mainly inflammatory, accompanied by a sharp rise in the rate of primary AA amyloidosis (or amyloidosis of unknown cause), over the last 50 years has been also observed. These modifications actually reflect the

favorable change in the standard of living and the better medical care available for both, first the infectious and then the inflammatory diseases underlying amyloidosis (Table 2).

Table 1. AA-A: Classical/common and non-classical underlying diseases

Infectious diseases - classical/common	**Infectious diseases - non-classical and new**
Tuberculosis, Bronchiectasis, Osteomyelitis, Injection-drug abuse,	Hepatitis B, Ch filariasis, Whipple's, HIV, Skin infection associated with paraplegia/ IVDA, Visceral leishmaniasis
Inflammatory diseases	**Inflammatory diseases**
Rheumatoid arthritis, Juvenile idiopathic arthritis, Psoriatic arthritis, FMF, Crohn's disease, Behcet's,	Gout, Autoinflammatory diseases, Scleroderma, Wegeners, SLE, PMR, Sjogren, Inclusion body myositis,
Neoplasms	**Neoplasms**
Hypernephroma, Carcinoma of lung or GIT, Hodgkin's lymphoma, Castelman's,	Schnitzler's disease, Non-Hodgkin's lymphoma, Hepatic adenoma
Others	**Others**
Sarcoidosis, Cystic fibrosis, Unknown	Common variable immunodeficiency, Cyclic neutropenia, Multiple sclerosis, Morbid obesity, Histiocytosis X, Unknown

Not all patients with chronically elevated SAA will develop amyloidosis. In familial Mediterranean fever (FMF) AA-A may involve more than 50% of untreated individuals, while in rheumatoid arthritis (RA) its rate spans between 5-25%. What determines the difference in the rate of amyloidosis between diseases and between individuals with the same disease is not completely understood. However, genetic and other risk factors which increase probability for the development of AA-A have been identified. Table 3 shows risk factors found in amyloidosis of FMF. As might be seen, most risk factors are associated with SAA, its amount, duration of exposure to it, its susceptibility to abnormal proteolysis, its solubility, folding capacity and propensity to sediment and form amyloid fibrils. Comparable findings were also observed in RA, one of which, old age of RA onset has been described only recently by Okuda et al (5).

Table 2. New trends in underlying categories causing AA amyloidosis disease (1-4)

Cause of amyloidosis	**Mayo Clinic (1931- 1946) (%)**	**Paris (1990-2005) (%)**	**London (1990-2005) (%)**	**Boston (2000-2010) (%)**
Infections	63	40	15	9
Inflammation	13	48.5	76	56
Neoplasms	23	10	3	5
Primary AA	0	1.5	6	30

Course

AA-A is primarily a sort of nephropathy. The subclinical stage, may last for a mean of 20 years. In almost all cases, the disease first appears as nephropathy, with proteinuria, evolving gradually to nephrotic syndrome, followed by gradual development of chronic renal failure, up to end stage kidney disease. This course leads to kidney replacement therapy within a mean of 20 years, with ±equal length in each stage. However, AA-A is a systemic disease, and when manifested clinically, with proteinuria of various degrees, amyloid deposits are already present in several organs, from which biopsy is available. Chances to obtain a positive biopsy from a clinically non-symptomatic organ are presented here (Table 4). They increase with time as the disease progresses.

Table 3. Risk factors to develop amyloidosis in FMF

Risk factors to develop amyloidosis	Odds ratio	Possible pathogenesis (with SAA related orientation)
Homozygousity to M694V mutation	**5**	More intense inflammation
Homozygousity to SAA1.1 allele (Caucasians)	3	Better susceptibility to abnormal proteolysis
Country of residence (Europe/ Israel/ Armenia/ Turky/ Arab countries)	1/ 1.5/ 2.8/ 3.1/ 3.2	Worse availability of medical care
Arthritis as part of the FMF picture	2.5	Marker of a more severe disease
Male sex	2	???
SAA levels	2	More Substrate
Carriage of Arg753Gln change in the TLR -2 gene (Recognition of bacteria)	2	???
Family history of AA-A		Predisposition to inflammation
Disease duration		Longer exposure to inflammation
Absence of treatment		More inflammation

Several exceptions to this course may occur. One with a favorable effect is caused by vigorous treatment against the underlying disease. This may extend dramatically the duration of each stage of the amyloid kidney disease, cause resolution of proteinuria and reversal of nephrotic syndrome (6). The second one, also with favorable effect, is determined by histological factors. In general, vascular deposition, low amyloid amount and absence of inflammation may slow down progression to renal impairment. The third deviation from the regular course is caused by a condition termed by us **amyloid storm**. This phenomenon may shorten dramatically the course of amyloid nephropathy. It occurs mostly in association with infection, usually pneumonia or gastroenteritis, and manifests mainly with rapidly progressive renal failure, diarrhea and malabsorption, sudden increase in the amount of urine protein to a mean of 10-20 grams a day and life threatening hypoalbuminemia (6). The reason for this development is unclear. It was thought to represent an amyloid enhancing factor (AEF) effect, but based on 2 kidney biopsies, with moderate amount of amyloid deposits, this speculation remains questionable.

Table 4. Biopsy from clinically un-affected organs in renal AA amyloidosis

Site of biopsy	Percent success
Rectum	80
Duodenum/ antrum/ esophagus	100/ 80/ 45
Gingiva	30
Abdominal subcutaneous fat	8 per histology

Other organs usually manifest many years after the onset of nephropathy. Prolongation of life by kidney replacement therapy, allows more of these become symptomatic. Uncommonly they manifest at an earlier stage, simultaneously, or before clinical expression of kidney disease. Nevertheless, the rule that the kidney presents first, remain strong enough to become very cautious with attributing a clinical manifestation to AA amyloidosis before kidney disease has evolved to its full entirety. Thus, over the course of the disease, the clinical picture may be complicated and include more manifestations than just those arising from nephropathy (Table 5).

Table 5. Common and uncommon manifestations of FMF - AA-A

Organ involvedvolved	Manifestations
Kidney	Proteinuria, nephrotic syndrome, chronic RF, Ac on Ch RF, electrolyte and acid base disorders, glycosuria, Nephro DI
GI tract	Diarrhea, malabsorption, bleeding, obstruction
Spleen	Splenomegaly, hyposplenism, spleen fracture
Liver	Hepatomegaly, elevated enzymes
Heart	Diastolic and systolic dysfunction, Rhythm and conduction disturbances, early ECG abnormalities
Peripheral NS	Neuropathy
Autonomic NS	Autonomic dysfunction
Genitourinary tract	Bleeding, testicular dysfunction
Lungs	Parenchimal nodular infiltrates
Adrenal	Addison's dis
Thyroid	Goiter, hypothyroidism
Coagulopathy	RVT, Hypercoagulation
Skin, Joints, Lymph Ns	Usually asymptomatic

Diagnosis

Diagnosis must base on biopsy, best from the affected organ. Relying on clinical circumstances may mislead. For instance, in 7 of 27 FMF patients, presented with proteinuria above 0.5 g/24 hours, biopsy revealed kidney disease other than amyloidosis, which was the presumed, pre biopsy diagnosis (Kukuy L et al, p 406 in this book). Demonstration of anti AA antibody reactivity of the Congo red positive deposits is still the mainstay of the diagnosis of AA-A. Alternatively, instead of tissue immunoreactivity, the amyloid can be extracted and analyzed, using sequence or mass spectrometry techniques (Kaplan B et al, p190 in this book). Yet, biopsy-dependent diagnosis is limited by being invasive, site restricted and therefore clinically inadequate. To date no scintigraphy procedure for AA-A diagnosis is currently widely available. More significant efforts must be invested in this direction.

Treatment

While the incidence of reactive amyloidosis is continuously dropping, due to effective treatments to most underlying inflammatory and infectious diseases, treatment of AA amyloidosis for those who present with an established disease is still generally unsatisfactory and disappointing and basically still directed at suppression of the underlying disease. The introduction of biologics for the treatment of the underlying diseases, caused major change with respect to resorption of the amyloid deposit and regression of its manifestations. This impression is based on individual cases or small series (7-9). Controlled trials are still awaited (Table 6). Future treatments are currently in a process of research; they are targeted at fibril components, including SAA itself (by directly inhibiting its production), or at SAA associated molecules, SAP and GAGs and thereby inhibiting fibril formation (10-12).

A yet unexplained phenomenon is the clinical histological discordance. Namely, rapid resolution of proteinuria, without much regression of amyloid deposits. Because this observation is universal for amyloidosis, and may occur in AL- amyloidosis after chemotherapy, as well as in AA- A after different drug schedules, it may suggest that the sole termination of active fibrillogenesis is the major factor that accounts for the regression of proteinuria.

Prognosis

Prognosis remains poor. In recent studies, five year survival is around 50% and per Lachmann et al (**1**) is adversely associated with old age, end stage renal failure at presentation, reduced serum albumin level, and persistent higher levels of SAA concentration. In another study by Bergesio et al, we see a new player for prognosis in AA-A, cardiac involvement, which negatively determines the survival outcome by a factor of 3.

Table 6. New treatments and therapeutic approaches

Treatment	Author (7-9)	Examples
Anti – IL-1 (Anakinra)	Stankovic K	Anakinra given to 9 FMF- amyloidosis pts, dramatically improved diarrhea, proteinuria, inflammatory markers and FMF attacks.
Anti IL- 6 – (Tocilizumab)	Hattori Y	TCZ administerred to 5 RA-amyloidosis pts, dramatically improved diarrehea, ileus, proteinuria and resolution of amyloid deposites.
Anti TNF agents (Infliximab, etanercept, adalimumab)	Kuroda T	Anti TNF agents caused striking effect on GI tract in 14 RA- AA patients, with a decrease in amyloid deposits ($p = 0.003$). Cr-Cl improved in only 4 and protein excretion decreased in only 3.

CONCLUSIONS

In this generation we witness a shift in underlying diseases, with fewer cases related to infections and inflammation and more to unknown causes. Further improvement with additional decline in inflammatory causes is almost here. The diagnosis, treatment and prognosis, still remain stationary, but hopes for improvement in the near future start to be more realistic

REFERENCES

1. Lachmann HJ, Goodman HJ, Gilbertson JA, et al. Natural history and outcome in systemic AA amyloidosis. N Engl J Med. 2007;356:2361-71.
2. Dahlin DC. Secondary amyloidosis. Ann Intern Med. 1949;31:105-19.
3. Verine J, Mourad N, Desseaux K, et al. Clinical and histological characteristics of renal AA amyloidosis: a retrospective study of 68 cases with a special interest to amyloid-associated inflammatory response. Hum Pathol. 2007;38:1798-809.
4. Girnius S, Dember L, Doros G, Skinner M. The changing face of AA amyloidosis: a single center experience. Amyloid. 2011;18 Suppl 1:221-3.
5. Okuda Y, Yamada T, Matsuura M, Takasugi K, Goto M. Ageing: a risk factor for amyloid A amyloidosis in rheumatoid arthritis. Amyloid. 2012;19:58.
6. Livneh A, Zemer D, Langevitz P, Laor A, Sohar E, Pras M. Colchicine treatment of AA amyloidosis of familial Mediterranean fever. An analysis of factors affecting outcome. Arthritis Rheum. 1994;37:1804-11.
7. Stankovic Stojanovic K, Delmas Y, Torres PU, et al. Dramatic beneficial effect of interleukin-1 inhibitor treatment in patients with familial Mediterranean fever complicated with amyloidosis and renal failure. Nephrol Dial Transplant. 2012;27:1898-901.
8. Hattori Y, Ubara Y, Sumida K, et al. Tocilizumab improves cardiac disease in a hemodialysis patient with AA amyloidosis secondary to rheumatoid arthritis. Amyloid. 2012;19:37-40.

9. Kuroda T, Wada Y, Kobayashi D, et al. Effective anti-TNF-alpha therapy can induce rapid resolution and sustained decrease of gastroduodenal mucosal amyloid deposits in reactive amyloidosis associated with rheumatoid arthritis. J Rheumatol. 2009 ;36:2409-15.
10. Kluve-Beckerman B, Hardwick, Du L, Benson MD. AA amyloidosis: potential therapy with antisense oligonucleotides. Amyloid. 2011;18 Suppl 1:195-7.
11. Bodin K, Ellmerich S, Kahan MC, et al. Antibodies to human serum amyloid P component eliminate visceral amyloid deposits. Nature. 2010 Nov 4;468:93-7.
12. Dember LM, Hawkins PN, Hazenberg BP, et al. Eprodisate for the treatment of renal disease in AA amyloidosis. N Engl J Med. 2007;356:2349-60.

PERSPECTIVES: AA and other types of amyloidosis

Martha Skinner

Amyloidosis Treatment and Research Center, Boston University School of Medicine, Boston MA, USA

In this session, some of the more rare types of systemic amyloidosis were discussed. The session also included a comprehensive report on a series of patients with AA amyloidosis. The more rare, inherited and non-inherited, types of amyloidosis that were discussed included: ALoc, amyloidosis localized to the airway; ApoAI, amyloidosis caused by a mutant form of apolipoprotein AI; AFib, amyloidosis caused by a mutant form of fibrinogen Aα; ALys, amyloidosis caused by a mutant form of lysozyme, and ALect2, amyloidosis caused by deposits of the protein lectin.

Table 1 gives a brief review of the discovery of each form discussed in this session and the International Symposium at which it was first presented.

Table 1. Discovery and Presentation of Amyloid Types in this Session

Protein	Discovery	Symposium presentation
ALoc (larynx)	1938 New and Erich (1) 9 cases of amyloid among 722 benign laryngeal tumors	1993 VIIth, Kingston (2) Kongsrud, et al (horse Ig LC); Berg, et al (human kI) Liepnieks, et al (human lIII)
AA amyloidosis	1971 Benditt, et al (4)	1967 Ist, Groningen (3) Bywaters, et al
Apo AI	1988 Nichols and Benson (5)	2006 XIth, Woods Hole (8) Obici, et al Leu75Pro
Fibrinogen Aα	1993 Benson, et al (6)	1993 VIIth, Kingston Uemichi and Benson
Lysozyme	1993 Pepys, et al (7)	1993 VIIth, Kingston Pepys, et al
Lect2	2008 Benson, et al (9)	2010 XIIth, Rome (10) Dogan, et al; Murphy, et al

Dr. Aldert Hazenberg, son of our host Dr. Bouke Hazenberg, reported on localized amyloidosis of the larynx. Localized amyloidosis of the larynx is well recognized, and as far back as in 1938 a report on benign tumors of the larynx noted 9 cases among 722 benign tumors of the larynx (1). Years later, in 1993 it was reported at the VIIth International Symposium in Kingston, Canada, where it was reported that amyloid deposits in these tumors were of light chain protein type. At that Symposium 3 presentations reported localized airway amyloid deposits in humans and animals (2). Dr. Hazenberg's reported that surgery was effective for 15 patients, with revision surgery needed for some years later.

In 1967 when the First Symposium on Amyloidosis was held in Groningen, the Netherlands about 40 researchers gathered to report on the results of studies on amyloid proteins and to discuss the clinical findings of the diseases known to be amyloidosis. The clinical syndrome of systemic amyloidosis associated with chronic inflammation was one of the few clinical reports at that first Symposium in 1967 (3). Professor Eric Bywaters from Taplow, UK reported 16 cases of amyloidosis diagnosed by kidney or liver biopsies in a series of 389 patients with juvenile rheumatoid arthritis. This early clinical report was important as it indicated there were types of amyloidosis associated with chronic inflammation that differed from other types that occurred without inflammation or that were familial in nature. A few years later in 1971, Dr. Earl Benditt identified the amyloidosis associated with chronic inflammation as protein AA, a fragment of the serum amyloid A (SAA) protein (4).

After training both of Dr. Helen Lachmann's parents, Professor Bywaters would have been proud of Dr. Lachmann's report at this Symposium on 493 cases of AA amyloidosis. Using the incredibly comprehensive patient database at the National Amyloidosis Centre in London, Dr. Lachmann reviewed 20 years of collected data on patients with AA amyloidosis. Dr. Lachmann found there were an increasing number of patients with uncharacterized inflammatory disorders, in addition to cases associated with the well known chronic inflammatory diseases. She also noted that the rate of diagnosis of AA amyloidosis has recently become stable after increasing for many years, and that there has been a significant increase in the age at death for patients with AA amyloidosis. This report suggests important advances in AA amyloidosis. First, technology has allowed us to identify the type of amyloidosis as AA in patients even when they do not have a recognized underlying inflammatory disorder. Secondly, Dr. Lachmann's report suggests that improved treatment of underlying inflammatory disorders has decreased the number of cases being diagnosed, and lastly, patients with AA amyloidosis are benefiting from improvements in treatment and living longer.

Dr. Arie Stangou reported on organ transplants, kidney or liver or both, for 3 types of rare familial amyloidoses. These very rare types, AApoAI (apolipoprotein AI), AFib (fibrinogen Aα), and ALys (lysozyme) have been identified in recent years (5, 6, 7). Benson reported the AFib amyloidosis type and Pepys reported the ALys amyloidosis type at the VIIth International Symposium in Kingston (2). The AApoAI type was reported by Benson and by Obici at the XIth International Symposium in Woods Hole (8). Dr. Stangou's report shows how far we have come in now being able to suggest treatment which, even though it is a supportive treatment, is a breakthrough for these rare types of amyloidosis.

The report on ALect2 (leukocyte chemotactic factor) by Dr. Oren Fix indicated the clinical involvement of patients with this disorder are even more extensive than we realized. Initially reported by Benson, et al in 2008, Lect2 is one of the most recent proteins to be recognized as a cause of amyloidosis involving the kidney (9). Two reports of ALect2 were given at the XIIth International Symposium in Rome and indicated the more widespread nature of the disease and predominance of patients with Hispanic ancestry among those affected (10). Dr. Fix reported a case of ALect2 with primary liver involvement and acute liver failure that underwent liver and renal transplantation.

Now 45 years after that first Symposium, we can address clinical findings and treatment of amyloid diseases as well as research on amyloid proteins. We have classified amyloidosis as localized and systemic, more common and more rare, inherited and acquired, and we are making good progress towards effective treatments.

REFERENCES

1. New GB and Erich JB: Benign tumors of the larynx. Arch Otolaryngology, 28: 841-910, 1938.
2. Amyloid and Amyloidosis, Ed by R Kisilevsky, MD Benson, B Frangione, J Gauldie, TJ Muckle, and ID Young Parthenon Publishing Co., New York, 1994.
3. Amyloidosis, Ed. by E Mandema, L Ruinen, JH Scholten, AS Cohen, Exerpta Medica, Amsterdam, 1968.
4. Benditt EP, Eriksen N, Hermodson MA, and Ericsson LH: FEBS Letters, 19: 169, 1971.
5. Nichols WC, Dwulet FE, Liepnieks J, Benson MD: Variant apolipoprotein AI as a major constituent of human hereditary amyloid. Biochem Biophys Res Comm, 156: 762-68,1988.
6. Benson MD, Liepnieks J, Uemichi T, Wheeler G, Correa R: Hereditary renal amyloidosis associated with a mutant fibrinogen α-chain. Nature Genetics, 3: 252-55,1993.
7. Pepys MB, Hawkins PN, Booth DR, Vigushin DM, Tennent GA, Soutar AK, et al: Human lysozyme gene mutations cause hereditary systemic amyloidosis. Nature, 362: 553-57, 1993.
8. Amyloidosis, Ed. by M Skinner, J Berk, L Connors, and D Seldin, CRC Press, 2007.
9. Benson MD, James S, Scott K, Liepnieks JJ, Kluve-Beckerman B: Leukocyte chemotactic factor 2: a novel renal protein, Kidney International 74: 218-22, 2008.
10. Amyloid: J Protein Folding Disorders, Suppl 1, Ed by G Merlini, L Obici, G Palladini, Vol 18, 2011.

Basic and clinical significance of Interleukin 6 (IL-6) in AA amyloidosis

Kazuyuki Yoshizaki [1) 2)]

1) Dept. of Immuno-Medicai Science, Division of Applied Chemistry, Graduate School of Engineering, Osaka University
2) Tokushukai Medical Coporation

ABSTRACT

The mechanism of Serum amyloid A (SAA), a precursor molecule of AA protein, production was examined in detail by utilizing hepatoma-derived cell lines. Interleukin 6 (IL-6) activated STAT3, a transcripitional factor, which is essential for induction of SAAmRNA. Further, IL-6 combined with TNF-α or IL-1 as complementary activators, augmented SAAmRNA induction. Since IL-6 was a pivotal cytokine for induction of SAA, IL-6 blockade completely inhibited the production of SAA. It is known that serum levels of SAA decrease and become normalized after IL-6 blocking therapy, while SAA levels decreased but hardly reach the normal range as a result of TNF-α blocking therapy.

Therefore, an anti-IL-6R antibody, tocilizumab or Actemura, seems to be an ideal therapeutic reagent for prevention and improvement of AA amyloidosis. Accordingly, we are now carrying out a clinical study of treatment with tocilizumab for patients with AA amyloidosis.

INTRODUCTION

AA amyloidosis is initiated and progresses in a chronic inflammatory environment in which acute phase proteins such as C-reactive protein (CRP), serum amyloid A (SAA), and fibrinogen levels remain elevated in serum for a long time. While it is known that SAA, a precursor molecule of AA amyloid protein, is produced by the stimulation of pro-inflammatory cytokines, the details of the mechanism of SAA production in association with cytokines need to be clarified. To this end, we examined this mechanism stimulating IL-6, IL-1 and TNF-α in hepatoma-derived cell lines, and analyzed the induction and augmentation of SAA at the levels of signal transduction pathways.

METHODS AND RESULTS

1. Induction of SAAmRNA by IL-6 and its augmentation by IL-6 combined with IL-1 or TNF-α.

Human hepatoma-derived cell lines were stimulated with IL-6, IL-1 and/or TNF-α. For the detection of SAAmRNA, SAA real-time quantitative RT-PCR using SAA-specific primers was performed. SAAmRNA was

significantly induced by stimulation only by IL-6, but not by IL-1 or TNF-α. However, the combination of IL-6 and IL-1, or IL-6 and TNF-α, synergistically induced SAAmRNA, but surprisingly, the combination of IL-1 and TNF-α did not. This results indicates that, of the three cytokines, IL-6 is pivotal and that TNF-α or IL-1 function as supplementary activators for augmentation of SAAmRNA induction.[1)]

2. STAT3 is essential for synergistic induction of SAA gene with IL-6 and IL-1.

After IL-6 binds to its receptor (IL-6R), the IL-6 signal activates transcriptional factor STAT3 via activation of gp130, another component of the IL-6 receptor system and the signal transducer. However, no consensus STAT3 response element (RE) is located in the promoter region of SAA. To determine whether STAT3 response promotes SAAmRNA expression, we therefore generated over-expression of wild type (WT) STAT3 and created dominant negative (dn) STAT3 pGL3 promoter-luciferase constructs. We found that the co-expression of dn STAT3 completely inhibited transcriptional activity of pGL3-SAA even after stimulation with IL-6+IL-1. Co-expression with wt STAT3, on the other hand, resulted in augmention. For identification of the STAT3 binding site, 5'deletion mutants of the promoter were used and the results suggested that STAT3 may interact with the entire domain, from c/EBPβ RE to NF-kB RE.[2)]

3. Presence of STAT3 on the SAA gene promoter 3' downstream of NF-kB RE after stimulation by IL-6+IL-1

To detect the presence of STAT3 on the promoter, an electro-mobility shift assay (EMSA) using a long oligo-nucleotide from -196 to -73 in the SAA1 promoter was performed and a nucleoprotein complex enhanced by IL-6 and IL-1 stimulation was detected. To identify the components of this complex, super-shift assay was performed using specific antibodies against transcriptional factors. We could confirm that this complex was composed at least of NF-kB p65 and phospho-STAT3 ser727 with a cofactor, p300, downstream of NF-kB RE.[2)] We are now trying to identify the non-consensus novel STAT3 binding site by using the Z score assay with nucleotide-protein binding energy.[3)]

On the basis of our findings, we propose a model for the induction and augmentation of the SAA gene comprising the transcriptional complex composed of NF-kB p65, phospho-STAT3 ser727 and co-factors of p300 in the SAA promoter region downstream of NF-kB RE.

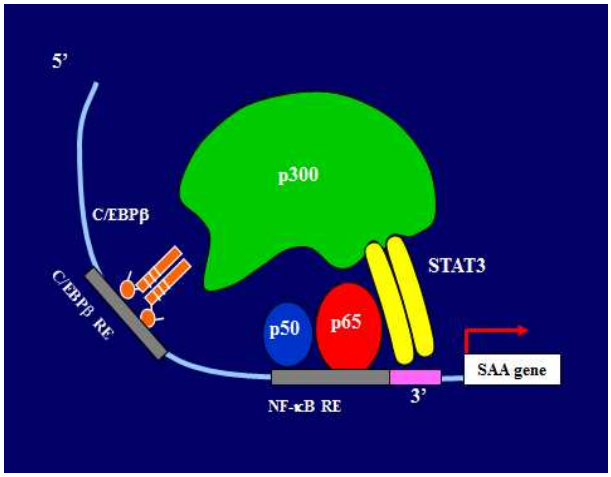

Figure 1. Cytokine-driven Transcriptional Activity of human SAA gene (Working Model). Transcriptional activity of STAT3 is augmented by interaction with NF-kB p65 and binding at 3'-site of NF-kB RE.

4. IL-6 blockade by an anti-IL-6 receptor antibody completely inhibited the production of SAA in vitro and normalized serum SAA levels in RA patients.

Augmentation of SAAmRNA expression in hepatocytes through stimulation by the trio of IL-6, IL-1 and TNF-α was completely inhibited by blocking with the anti-IL-6 receptor antibody tocilizumab. On the other hand, blocking with the IL-1 receptor antagonist produced only partial inhibition and with the TNF-α antibody none at all.In the case of tocilizumab therapy to for RA, serum CRP and SAA levels were not only reduced but actually normalized. [4] TNF-α blockade, on the other hand, induced a reduction in serum levels of CRP and SAA, but almost no normalization. These findings indicate that IL-6 blockade may be more effective than TNF-α blockade for the suppression of SAA production both in vitro and in vivo.

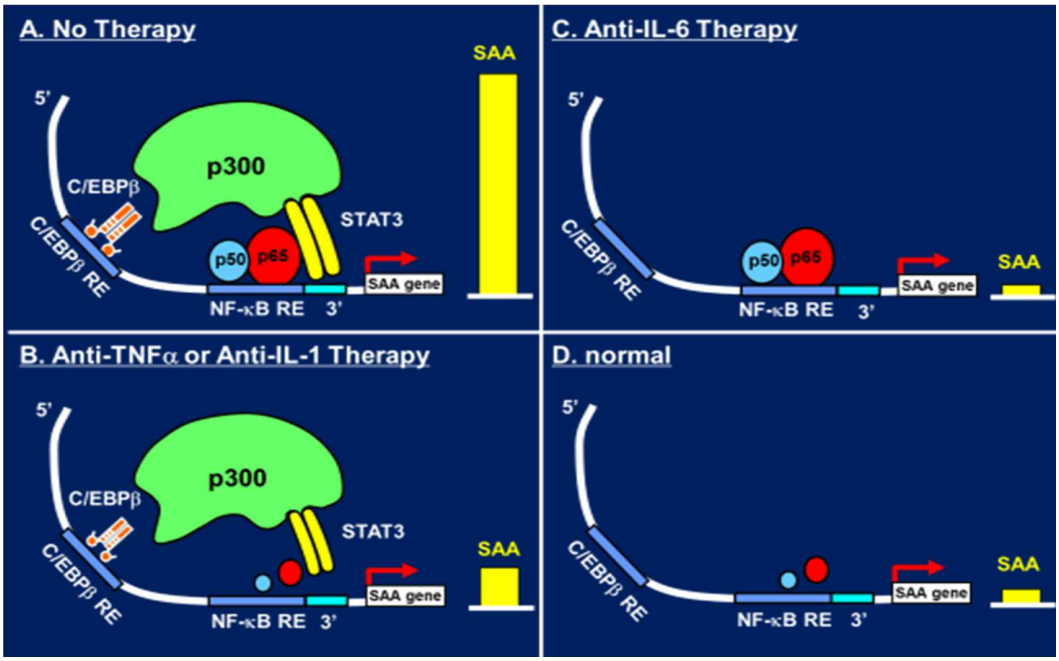

Figure 2. Effect of cytokine blocking therapy on serum SAA levels and its transcription mechanism in RA patients

5. Reduction of AA amyloid deposition and improvement in renal function resulting from treatment with tocilizumab for a JIA and an RA patient with AA amyloidosis: two case reports.

A JIA patient and an RA patient with AA amyloidosis were treated with tocilizumab for a year and a half, as reported by Okuda et al. and Nishida et al., respectively. AA amyloid fibril deposits on the duodenal or colon wall were reduced. No proteinuria was detected and renal functions such as creatine level and creatinine clearance improved after the tocilizumab therapy. [5, 6]

DISCUSSION

Once a patient has been diagnosed with AA amyloidosis accompanied by chronic inflammatory conditions, the disease gradually progresses and leads to a fatal outcome, mainly caused by renal failure associated with accumulating deposits consisting of AA fibrils on renal interstitial tissue. It has proven to be very difficult to block

this increase of AA protein deposits, even by treatment with continuous high doses of steroids and immune suppressants. Most clinicians are therefore eager to obtain an effective therapy against AA amyloidosis. In this context, it is highly relevant that serum amyloid A (SAA), a precursor molecule of AA protein, is produced and enhanced in serum in inflammatory diseases such as rheumatoid arthritis (RA). Gillmore, and Hawkins et al. reported that normalization of SAA levels in serum is essential for the prevention and reduction of disease activity. However, with previous and current therapies it is still too problematic to attain a normal range of serum SAA levels, and there has been little evidence concerning the SAA producing mechanism. To determine the exact mechanism of SAA induction, we analyzed the transcriptional mechanism of SAA production by using cytokine-stimulated hepatocytes. As a result of this analysis, we can propose a model for the transcriptional mechanism of induction and augmentation of SAA expression both in vitro and in vivo. Our findings demonstrate that activation of serine phosphorylated STAT3 by IL-6 stimulation, and binding of STAT3 to the novel non-consensus response element in the SAA promoter region are both essential for the induction of SAA and augmentation of SAA expression. This induction and augmentation are the result of STAT3 activation via stimulation of IL-6 by NF-kB activation, which in turn is the result of TNF-α or IL-1 stimulation. This proposed mechanism implies that IL-6 inhibition may be most effective therapeutic strategy for the blocking of AA fibril deposition on tissue. In fact, we previously reported achieving reduction of AA deposition and improvement of renal function in a patient with AA amyloidosis who was treated with tocilizumab, an anti-IL-6R antibody. Tocilizumab may therefore prove to be an efficacious reagent for the treatment of AA amyloidosis. It is therefore hoped that AA amyloidosis, an as yet incurable disease, can be conquered in the near future.

ACKNOWLEGEMENTS

The author thanks Dr. K.Hagihara, T.Nishikawa, S.Nakazawa, T.Isobe for proceeding the experiments, and Ms. M.Tanigawa for secretarial assistance.

REFERENCES

1. Biochem. Biophys. Res. Commun. 314:363-369, 2004.
2. Genes to Cells 10:1051-1063, 2005.
3. Prediction and experimental validation of putative non-consensus binding sites for transcription factor STAT3 in Serum amyloid A gene promoter. In preparation.
4. Arthritis Rheum, 50:1761-1769, 2004.
5. J. Neurosci. Res, 76:265-276, 2004.
6. Ann Rheum Dis. Res, 68(7):1235-1236, 2009.

HLA Typing in Amyloidosis of Familial Mediterranean Fever

Y. Shinar[1], M. Rubinstein[2], E. Ben-Chetrit[3], Y. Berkun[3], I. Ben Zvi[1,2], M. Lidar[1,2], R. Loewenthal [4], A. Livneh [1,2]

[1]Heller Institute of Medical Research, Sheba Medical center, [2]Medicine F, Sheba Medical Center, [3]Pediatric Department, Hadassah Hebrew University Medical Center, [4]Tissue Typing Unit, Sheba Medical Center, Israel.

ABSTRACT

AA amyloidosis is a threat to FMF patients, even in the era of colchicine. Beside FMF, AA amyloidosis also develops in diseases associated with certain HLA types. We therefore studied HLA-A, HLA-B, and HLA-DR variants distributions in FMF patients with amyloidosis, including 11 of Israeli Arab and 19 of North African Jewish (NAJ) origin. The HLA-B38 antigen frequency was higher in unrelated Arab patients than in historical unaffected Arab subjects (OR=7.7, 95%CI 2.3-25, p=0.02). In NAJ patients the HLA-B13 antigen frequency was higher when compared to an origin matched reference group (OR 3.1, 95% CI 1.1-9.1, p=0.04). No differences were evident in the frequencies of HLA-A or HLA-DR variants. Because HLA-B38 often appears in haplotype with the FMF modifier, MICA-A9 allele, its significance in amyloidosis of FMF may warrant further study.

INTRODUCTION

FMF is a prototype of the hereditary recurrent fevers (HRF), a group of diseases whose recurrent, self-limited inflammatory bouts are caused by a proinflammatory genetic defect in innate inflammatory pathways. HRF patients are prone to develop secondary amyloidosis causing renal failure, due to recurrent surges of serum amyloid A, (SAA), the precursor protein of amyloid A, during disease attacks. The risk of amyloidosis is highest for FMF patients that are non-compliant or non-responsive to colchicine. Other risk factors include the highly pathogenic p.M694V homozygous Mediterranean fever gene (*MEFV)* genotype, the alpha/alpha variant of SAA and the male gender. In addition, environmental, or country based risk factors, have been demonstrated by epidemiological studies [1]. All these factors however fall short of predicting actual cases of amyloidosis outbreak.

AA amyloidosis also develops in chronic inflammatory conditions known to associate with specific HLA types. Examples are: Rheumatoid arthritis associated with DR4 and DR1, ankylosing spondelytis associated with HLA-B27, Crohn's disease associated with HLA-B7, and ulcerative colitis with HLA-DR1. Notably, a study from Japan depicted increased amyloidosis rate in RA patients with a double dose of HLA-DR4 [2]. In the HLA-associated diseases a severe innate type inflammation is a well-documented component.

Early studies in FMF patients found no significant deviation in the frequency of the HLA-A and B antigens in FMF patients from origin matched healthy controls, and ruled out segregation of disease with the HLA complex

in families. Later studies found a relationship between HLA-DR4 and the *MEFV* gene, and a significant relationship between HLA-DR and HLA-DQ types and specific *MEFV* gene mutations. Studies on association between amyloidosis and HLA types in FMF patients are also equivocal. Fradkin *et al* found no association while Karahan *et al* depicted association with the HLA-B58 antigen with amyloidosis in end stage renal diseases [3,4]. In this study we examined whether certain HLA types are associated with the development of amyloidosis in FMF, in two Israeli ethnic groups.

METHODS

The study included all 30 amyloidotic FMF patients of two origins, namely 11 Israeli Arabs and 19 North-African Jews that were HLA-typed before kidney transplantation, between the years 1997-2007**.** Typings were retrieved from the national tissue typing center registry, at Sheba Medical Center, Tel-Hashomer. Three Arab patients were sibs of one family, and 2 of a second family. The class 1 antigens were defined serologically; HLA-C data, available for only 20/30 patients, was not analyzed. Class 2 HLA-DRB1 gene variants were defined by low resolution DNA oligotyping. HLA variants frequencies in unrelated patients (including only one patient of each Arab Israeli family) were compared to those in same or similar origin populations. For North African Jews, whose HLA allele frequencies vary across countries of origin, revealing the degree of ancestral admixture with European Jews, a virtual reference group was established, matched to the country-cluster origin of the patients (Moroccan/ Algerian Jews or Libyan/ Tunisian Jews) [5]. Allele frequency data was derived from the HLA allele database (http://www.allelefrequencies.net/hla). The allele frequency (AF) is n/2N, where n is the count of chromosomes with a specific *MEFV* allele, and 2N is the total number *of MEF*V chromosomes.

MEFV pathogenic variants and demographic data were extracted from medical files and a questionnaire. Patients lacking *MEFV* genotyping were genotyped for 2 most common pathogenic variants: p.M694V, p.V726A and the p.E148Q, a clinically debated variant, whose presence on the same allele with p.V726A was reported to associate with amyloidosis [6].

RESULTS

Class I antigens. Eight HLA-A and 12 HLA-B variants were identified in the 11 Israeli Arab amyloidotic FMF patients. The HLA-B38 allele was overrepresented in the patients group; It was present in 5/8 unrelated amyloidotic FMF patients (AF=0.31), but only in 13/117 unaffected Israeli Arab subjects (AF=0.05, OR=7.7, 95% CI 2.3-25, p=0.02). A serological related antigen, HLA-B39 (a B16 split) was present in 3 members of one family, and in 2/117 unaffected subjects (AF=0.01). When considering explicitly unrelated patients (n=8), HLA-B38 and HLA-B39 antigens in combination presented an OR of 8.8 to develop FMF with amyloidosis in this ethnic group (95% CI 2.8-27, p=0.001).

The NAJ patients (n=19) were from several countries: Morocco (n=7), Libya (n=3) Tunisia (n=3), Morocco/Tunisia (n=2), Algeria (n=1), Morocco/Algeria (n=1) and unspecified (n=2). Twelve HLA-A and 16 HLA-B variants were identified in this NAJ patients group. The HLA-B13 allele frequency was higher in the NAJ patients than in the reference group with matched country cluster of origin (see methods, AF=0.11 vs.0.048, respectively, OR 3.1, 95% CI 1.1-9.1, p=0.04). The HLA-B38 antigen frequency did not differ between the NAJ patients and the reference group (AF=0.08 and 0.065, respectively).

Class II antigens. Six HLA-DR types were identified in the Arab patients group. HLA-DR11 was present in all members of the two families of Arab origin, at least once. When only unrelated alleles were considered, the HLA-DR11 rate was not significantly increased in patients (AF=0.25) over the population sample (AF=0.21).

Eight DR types were found in the NAJ patients. None had an increased frequency in the patients over the historical reference group. In particular, the HLA-DR4 was not associated with amyloidosis in the patients group (AF=0.13 in patients, vs. 0.15 in controls) and HLA- DR1 was not present in the amyloidotic patients at all (AF= 0.054 in controls, p=non-significant).

***MEFV* gene mutations.** All NAJ patients, including 5 patients with the HLA-B13 allele, were homozygous for the p. M694V mutation. The Arab patients had various genotypes: p.[E148;V726];[E148;V726]; (3 sibs), p.[M694I];[M694I]; (one sib in other family), p. [M694V;M694V] (n=3), p.[726];[726] (n=1), not known (n=3). No association was found between a certain *MEFV* mutation or genotype and the HLA-B38 alleles.

DISCUSSION

Our study depicted an increased frequency of two HLA-B alleles in a group of FMF patients with amyloidosis, compared to the origin matched population, each in a different ethnic group. HLA-B38 was overrepresented about 6 fold in the Arab patients. HLA-B13 was about twice more frequent in the NAJ patients, but was not encountered in the Arab patients group. Of note, the HLA-B38 antigen is a pan-ethnic risk factor for psoriatic arthritis (PsA) [7]. Early staged PsA is now viewed upon as an aggravated auto-inflammatory response to micro-trauma, and a trigger to chronic, HLA-associated autoimmune response targeting innate inflammation factors at the local tissue ([8]. Interestingly, the B38 allele is tightly linked by haplotype to the proximate MHC class I chain-related A (MICA) A9 allele [9]. The MICA gene is a modifier of FMF [10]. Since enhancement of amyloidosis by MICA variants has been excluded, the contribution of HLA-B38 itself to amyloidosis, and perhaps in concurrence to PsA, may warrant further study.

Previously reported HLA associations with amyloidosis were not corroborated by our study [2,4]. However our study group was small, and insensitive to weak associations typically characterizing HLA-susceptibility. This also implicates that the present positive results of the study need to be confirmed in a larger study.

REFERENCES

1. van der Hilst JC, Simon A, Drenth JP. Hereditary periodic fever and reactive amyloidosis. Clin Exp Med. 2005;5:87-98.
2. Migita K, Nakamura T, Maeda Y, Miyashita T, Origuchi T, Yatsuhashi H, Nakamura M, Ishibashi H, Eguchi K. HLA-DRB1*04 alleles in Japanese rheumatoid arthritis patients with AA amyloidosis. J Rheumatol. 2006;33:2120-3.
3. Fradkin M, Pras M, Zemer D, Gazit E. Familial Mediterranean fever: no association of HLA with amyloidosis or colchicine treatment response. Isr. J. Medical Sci. 1985;21:757.
4. Karahan GE, Seyhun Y, Oguz FS, Kekik C, Onal AE, Yazici H, Turkmen A, Aydin AE, Sever MS, Eldegez U, Carin MN. Impact of HLA on the underlying primary diseases in Turkish patients with end-stage renal disease. Ren Fail. 2009;31:44-9.

5. Campbell CL, Palamara PF, Dubrovsky M, Botigué LR, Fellous M, Atzmon G, Oddoux C, Pearlman A, Hao L, Henn BM, Burns E, Bustamante CD, Comas D, Friedman E, Pe'er I, Ostrer H. North African Jewish and non-Jewish populations form distinctive, orthogonal clusters. Proc Natl Acad Sci U S A. 2012 Aug 6 (Epub ahead of print).
6. Gershoni-Baruch R, Brik R, Shinawi M, Livneh A. The differential contribution of MEFV mutant alleles to the clinical profile of familial Mediterranean fever. Eur J Hum Genet. 2002;10:145-9.
7. Espinoza LR, Vasey FB, Oh JH, Wilkinson R, Osterland CK. Association between HLA-BW38 and peripheral psoriatic arthritis. Arthritis Rheum. 1978;21:72–75.
8. McGonagle D. Enthesitis: an autoinflammatory lesion linking nail and joint involvement in psoriatic disease. Eur Acad Dermatol Venereol. 2009 Sep;23 Suppl 1:9-13.
9. Pollock R, Chandran V, Barrett J, Eder L, Pellett F, Yao C, Lino M, Shanmugarajah S, Farewell VT, Gladman DD. Differential major histocompatibility complex class I chain-related A allele associations with skin and joint manifestations of psoriatic disease. Tissue Antigens. 2011; 77:554-61.
10. Turkcapar N, Tuncali T, Kutlay S, Burhan BY, Kinikli G, Erturk S, Duman M. The contribution of genotypes at the MICA gene triplet repeat polymorphisms and MEFV mutations to amyloidosis and course of the disease in the patients with familial Mediterranean fever. Rheumatol Int. 2007;27:545-51.

An exploratory case-control study of progression of AA amyloidosis in rheumatic diseases

John Hunter; Snehashish Banik; Meng May Chee
Rheumatology Department, Gartnavel General Hospital, Glasgow, G12 0YN, Scotland.

ABSTRACT

Background: Renal impairment is not uncommon in rheumatic diseases, but it is infrequently due to amyloidosis.
Objective: To demonstrate differences in progression of renal disease in patients with AA amyloid.
Methods: Patients with AA amyloidosis were identified from a West of Scotland registry. During the period patients were recruited to the registry, a control group of patients were identified because of referral for biopsy where amyloid was sought. Follow up data on the rate of deterioration of serum creatinine and time from recruitment to dialysis were obtained by case record review.
Results: 11 patients with AA amyloid (9 with rheumatoid arthritis, 1 ankylosing spondylitis & 1undifferentiated polyarthritis) were identified, all diagnosed between 2000 & 2010. 16 control subjects had rheumatoid arthritis (12), undifferentiated polyarthritis (2), psoriatic arthritis (1), & ankylosing spondylitis (1). Biopsies failed to show amyloid in rectal, renal, abdominal fat & carpal tunnel tissue in control subjects and 1 biopsy was declined because of anticoagulants. Median baseline serum creatinine was 134 micromol/l in control subjects & 125 in patients with AA amyloid. During follow up in controls (median 42 months), 5(31%) doubled serum creatinine but no patients were started on dialysis. During follow up of AA amyloid (median 27months) 5(45%) required dialysis & a total of 8(72%) doubled serum creatinine. 6 amyloid patients received biologic suppressive therapies (anti-TNF, rituximab & anakinra). Baseline serum creatinine failed to distinguish those with a better renal prognosis but no measurable urinary protein was present in 2 of 3 who neither doubled serum creatinine nor received dialysis therapy during between 54 & 108 months' follow up. Likewise 2 of these 3 received biologic therapies.
Conclusion: In this small study AA amyloid complicating inflammatory rheumatic diseases required renal replacement therapy more frequently than control patients with similar presentations.

INTRODUCTION

Previous observations have suggested that impaired renal function is not uncommon in inflammatory rheumatic diseases. In most cases renal impairment is not related to amyloidosis. However in cases of AA amyloidosis renal progression is the rule such that the majority of patients will require renal replacement therapy (dialysis or renal transplant) some 5-10 years following the initial demonstration of amyloid. This gives the opportunity to perform a case-control study. The aim of this study is therefore to see whether there are differences between

patients with renal impairment where AA amyloid has been demonstrated and patients with rheumatic diseases who have impaired renal function in whom amyloid has not been demonstrated. The larger such a study is the more likely it is to provide insight. This exploratory study has been performed to see how readily available data can be accessed.

METHODS

Patients: Between 2000 and 2010, 11 patients with AA amyloid were identified using the West of Scotland registry. A further 9 patients were recorded on the registry as being diagnosed between 2000 and 2010 but in these cases the case records were unavailable, either because they attended distant hospitals or because case records were missing. 16 control patients were identified among those who had been referred because their clinical presentation was thought to be consistent with a diagnosis of AA amyloidosis. Renal disease dominated amongst the reasons for referral but amyloid was not shown in rectal, renal, abdominal fat and carpal tunnel tissue when biopsies were examined in these control cases. Case record review allowed an estimation of deterioration of renal function over time from initial presentation. Factors that might have influenced renal deterioration such as baseline serum creatinine, baseline urine protein loss and treatments used were examined to see if they influenced outcome.

RESULTS

AA amyloid patients: 9 had rheumatoid arthritis, 1 had ankylosing spondylitis and 1 patient presented to the hospital with renal and gastro-intestinal features of amyloid, an inflammatory polyarthritis and later developed gout. The median age at demonstration of AA amyloid was 67 (range 35-76) and the median duration of the pre-existing arthritis was 29 (range 5-32) years. Other factors that may have contributed to the development of amyloidosis included bronchiectasis in 3 patients, septic arthritis in 2, renal tumours in 2, childhood tuberculosis in 2, and osteomyelitis, recurrent urinary infections and co-existent gout alongside rheumatoid arthritis each in 1 case. The presentation of AA amyloid involved an elevated serum creatinine in 4 cases, proteinuria in 6 cases (in 3 manifesting as nephrotic syndrome) and the diagnosis was an incidental finding at renal biopsy for a renal mass in 2 cases and for investigation of proteinuria accompanying type 2 diabetes in 1 patient.

Control patients: 16 patients were identified who had been referred because of clinical suspicion of AA amyloid. In biopsies of kidney, rectum and in abdominal fat aspirate amyloid was not demonstrated. In 1 patient congophilic material was demonstrated in tissue examined after carpal tunnel decompression but further examination failed to demonstrate evidence of amyloidosis of any type. The background rheumatological diagnosis was rheumatoid arthritis in 12 patients, undifferentiated inflammatory polyarthritis in 2, psoriatic arthritis in 1 and ankylosing spondylitis in 1 patient. Renal diagnoses included IgA nephropathy, renovascular disease and chronic pylonephritis. Other diagnoses accompanying the rheumatic disorder that might have contributed to a propensity to AA amyloid among the control patients were gout in 2 patients and Crohn's disease, bronchiectasis, leucopenia, endocarditis, septic arthritis, recurrent urinary infections and a renal tumour each in 1 patient. The presentations that led to consideration of amyloid included raised serum creatinine in 11 patients and proteinuria in 9 which was in the nephrotic range in 2 patients. The median age for initial data collection concerning progression of renal impairment was 65.5 years (range 42-80).

Renal outcomes: Baseline serum creatinine in the amyloid group was median 125 micromol/l. (range 57-310). The median baseline serum creatinine in the control group was similar at 134 micromol/l (range 65-320). The median period of follow up was 27 months (range 1-108) in the amyloid group and 42 months (range 1-245) in the control group.

During the follow up periods 5 (45%) amyloid patients and no control patients required dialysis or other renal replacement therapy. Similarly the level of serum creatinine doubled from baseline in 8 (72%) amyloid patients and 5 (31%) control patients. 1 of the amyloid patients had a renal transplant following dialysis. His treatment before the transplant was with Etanercept but he developed leucopenia and he has been continuously treated since with Anakinra. 3 other patients remain well on anti-TNF therapy. 1 died in end stage renal failure with an accompanying vascular dementia. 2 patients received Rituximab, 1 of whom died from sepsis after several cycles of Rituximab therapy associated with improvement in his rheumatoid arthritis. Rituximab failed to give symptomatic improvement of rheumatoid disease and was followed by rapid renal progression in the other patient who received it. Other treatments used that may have suppressed inflammation included Leflunomide, Methotrexate, Minocycline and Captopril.

In 2 of the 3 patients who neither doubled the serum creatinine nor required dialysis during a median follow up period of 66 months, the finding of AA amyloid on biopsy was unexpected. 2 of these 3 patients received anti-TNF therapy (a similar proportion to the group as a whole), but the median baseline creatinine (180 micromol/l) was higher than the median baseline serum creatinine in the remainder of the AA amyloid group. Similarly 2 of the 3 patients who did well had less than 0.25 g/l proteinuria at presentation whereas the remaining AA amyloid patients had a median baseline urine protein concentration of 2 g/l (range 0.4-9.3).

DISCUSSION

This small study of AA amyloid complicating inflammatory rheumatic diseases shows that renal replacement therapy was required more frequently in amyloid patients compared to those patients with rheumatic diseases who present with similar problems. Renal deterioration as assessed by the doubling of serum creatinine was also more frequent among patients who had AA amyloid. There was no obvious therapeutic benefit from using biologic suppressive therapies in this series when those patients with AA amyloid, who received biologic therapies were compared with those who did not. However, those who did not receive them did so either because the demonstration of AA amyloid was a surprise (a patient presenting with diarrhoea with a previous history of colitis and no detectable proteinuria or elevation of serum creatinine and in patient with diabetes and proteinuria) or because biologics were contra-indicated because of intercurrent sepsis or recent history of malignancy.

There were 3 patients with AA amyloid who neither doubled their serum creatinine during the follow up period nor required renal replacement therapy. These patients did not have unusually low levels of serum creatinine but proteinuria at presentation was at low levels. This is consistent with previous observations among AA amyloid patients in the West of Scotland and proteinuria has previously been thought to be a significant prognostic factor in chronic kidney disease.

Retrospective surveys such as this are prone to bias. Because of the established interest in AA amyloidosis in the West of Scotland patients are registered prospectively by one doctor (JH) and it is unlikely that patients with AA amyloidosis secondary to rheumatic disorders attend elsewhere. Patient selection in the control group is influenced by referral practice and more of these patients came from hospitals in which the authors practice

than from hospitals further afield in the West of Scotland. Nevertheless, the results are consistent with a previous audit of patients attending rheumatology clinics in Gartnavel General Hospital in that progressive renal disease is uncommon in patients where a degree of chronic kidney disease has already been established.

This study has demonstrated that it is possible to abstract information from case record review to explore for possible prognostic factors in patients with AA amyloidosis and clearly it is hoped that additional information might be derived from a larger study over a more prolonged period. Whilst ideally this might be a prospective study, recruitment would be likely to be slow and learning from those patients we have already served may give worthwhile information.

Renal Biopsy in Familial Mediterranean Fever With Proteinuria – Is It Justified?

O.(L.) Kukuy[1], I. Ben-Zvi[2], A. Ben-David[1], J. Kopolovic[4], A. Volkov[3], Y.Shinar[2], E. Holtzman[1], D.Dinour[1], A. Livneh[2]

Institute of Nephrology and Hypertension, Sheba Medical Center, Tel Hashomer, Israel (1); Heller Institute of Medical Research, Sheba Medical Center, Tel Hashomer, Israel (2); Department of Pathology , Sheba Medical Center, Tel Hashomer, Israel (3) Department of Pathology, Hadassah-Hebrew University Medical Center, Jerusalem, Israel (4)

ABSTRACT

FMF patients may develop various kidney diseases, manifested with proteinuria. AA amyloid nephropathy is the most common one, therefore kidney biopsy is usually avoided. Thus, the rate and the course of other kidney diseases reported in FMF are generally unknown. In 27 FMF patients, who developed proteinuria above 0.5 g/24 hrs and underwent kidney biopsy, nephropathy other than AA amyloidosis was studied for its rate, and clinical, genetic and laboratory features. Data was abstracted from patient files, looking specifically for parameters, useful for prediction of pathological diagnosis prior to biopsy. Only 60% of these patients had biopsy proven AA amyloidosis. Patients with amyloidosis differed from patients with non-amyloid nephropathy on several parameters, including severity of FMF, degree of proteinuria and rate of hypertension. Poor prognosis with higher rate of ESRD and mortality also characterized the amyloidosis group. Kidney biopsy in FMF patients, who develop proteinuria, is highly warranted.

BACKGROUND

Familial Mediterranean fever (FMF) is a genetically transmitted autoinflammatory disease, which may be complicated with reactive amyloidosis (AA) (1). The kidney is the major affected organ, and its involvement with amyloidosis is manifested initially with proteinuria. It is common practice to view proteinuria in FMF as resulting from amyloidosis and avoid kidney biopsy. However, nephropathy other than amyloidosis has been described in FMF, but its rate and other features are unknown (2).

OBJECTIVE

To appreciate the fraction of FMF patients with proteinuria unrelated to amyloidosis, and characterize the course and underlying pathology of non-amyloidotic proteinuria.

METHODS

We have collected data retrospectively, on FMF patients, undergoing kidney biopsy for proteinuria above 0.5 gram/24 hours, over the last 10 years (since 2001). Clinical, laboratory and genetic data were abstracted from patient files, and patients were interviewed to complete the missing information. All kidney biopsies were viewed by an experienced pathologist, using accepted methods as light, immunofluorescence and electron microscopy and stained with Congo red and AA antibodies to detect amyloid.

RESULTS

Of 27 FMF patients with proteinuria above 0.5 g/24 hrs, referred to kidney biopsy, only 16 were diagnosed with AA amyloidosis (59.3%), 11 were diagnosed with other nephropathies (focal glomerulonephritis-5, focal segmental glomerular sclerosis-2, IgA nephropathy -1, minimal change disease-1, focal glomerulonephritis with signs of thrombotic microangiopathy-1). In 10 of 27 patients the pre-biopsy diagnosis was changed following kidney biopsy (7 from suspected amyloidosis to other nephropathies and 3 from suspected other nephropathies to amyloidosis). Table 1 shows demographic, clinical, genetic and kidney disease parameters in the two patient groups. Table 2 compares the course and prognosis of the two patient groups.

Table 1. Predictors of amyloidosis in FMF patients undergoing biopsy for proteinuria

Predictors parameters	**Amyloidosis group**	**Other kidney diseases**	**P value**
Number of patients	16	11 (41%)	
Age	43.9±14.9	43.3±13.4	0.884
Male Sex	8	9	
North African origin	14	7	
Mutation	694/694- 80% Other - 20%	694/694 - 54% Other – 46%	0.27
Severe FMF	10/16	3/11	<0.05
Degree of proteinuria at biopsy (g/24h)	6.46±4.3	2.4±1.7	0.0136
Urine sediment (%)	81	72	0.958

Table 2. Course and prognosis of the disease

Parameters	**Amyloidosis group**	**Other kidney diseases**	**P value**
ESRD/transplant	75%	27.2%	0.02
Time interval from onset of proteinuria to ESRD (years)	19.14	NA	
Years from onset of FMF until ESRD	44.7±14.4	25.7±3.05	0.111
HTN (onset unknown)	10/16	2/11	0.05
Death	37.5%	9%	0.227
Causes of death	Progressive amyloidosis-4 Septic foot-1 Creutzfeldt-Jacob disease-1 Unknown-1	Uncontrolled bleeding and pneumonia - 1	

DISCUSSION AND CONCLUSION

Almost 50% of patients with FMF and proteinuria were diagnosed with nephropathy other than amyloidosis on kidney biopsy, which includes conditions with more favorable outcome. It is highly suggested to obtain biopsy from patients with FMF and proteinuria more than 0.5 gr/24 hours.

REFERENCES

1. Livneh A, et al. Colchicine treatment of AA amyloidosis of familial Mediterranean fever. An analysis of factors affecting outcome. Arthritis Rheum. 1994 Dec;37(12):1804-11.
2. Said R, et al. Spectrum of renal involvement in familial Mediterranean fever. Kidney Int. 1992 Feb;41(2):414-9.

Lessons from amyloidosis of FMF in a subset of kidney-transplanted patients

Ilan Ben-Zvi, Shaye Kivity, Iveta Danilesko, Gilad Yahalom, Olesya Kukuy, Ruth Rahamimov, Avi Livneh

Department of Internal Medicine F, Rheumatology Unit, Sheba Medical Center, Ramat-Gan, Israel

ABSTRACT

Amyloidosis of FMF may lead to end-stage renal failure, culminating in some patients in kidney transplantation. We aimed to assess demographic, clinical and genetic risk factors for the development of FMF-amyloidosis in a subset of kidney transplanted patients, and to evaluate the impact of transplantation on the course of FMF. Demographic, clinical and genetic data of 16 kidney-transplanted FMF-amyloidosis patients was compared to18 FMF patients without amyloidosis. Compliance with colchicine treatment in FMF-amyloidosis patients was much lower than in FMF without amyloidosis. Post kidney-transplantation, the frequency of typical FMF serosal attacks was significantly lower than before transplantation. FMF-amyloidosis patients carried only M694V mutations in the FMF gene, while FMF without amyloidosis featured other mutations as well. In conclusion, kidney transplantation in patients with AA amyloidosis of FMF seems to prevent FMF attacks. Compliance with treatment and genetic makeup but not severity of FMF constitute the major risk factors for the development of amyloidosis in FMF.

INTRODUCTION

Familial Mediterranean fever (FMF) is a genetic auto-inflammatory disease, caused by mutations in the MEditerranean FeVer gene (*MEFV*) and characterized by recurrent episodes of fever accompanied by polyserositis. The most devastating complication of FMF is renal amyloidosis, occurring in up to 50-60% of untreated patients (1). Several risk factors for the development of amyloidosis among FMF patients have been described previously, including a family history of FMF- amyloidosis, consanguinity of patients' parents, homozygosity for the M694V mutation, ethnicity (higher in North African Jewish ancestry and Turks, and less common in Arabs), male gender, high SAA levels, the α/α isoform of SAA and country of residence (2,3). The insertion of colchicine to the treatment regimen of FMF, first reported by Zemer et al (4), significantly diminished the incidence of amyloidosis in FMF patients. Higher rates of FMF-related amyloidosis are noted in patients with low compliance to colchicine therapy and in patients who initiated colchicine at an older age (5,6). Continuous colchicine treatment was shown to prevent amyloid re-accumulation in the grafted kidney of FMF patients with amyloidosis (6).

Here we aimed to evaluate several factors, which underlined the evolvement of amyloidosis in a subset of FMF patients, who underwent kidney transplantation, and determines the effect of transplantation on the course of FMF.

METHODS

Patients groups: We retrospectively compared the demographic, clinical and genetic data of FMF patients with and without amyloidosis. All 16 amyloidosis patients have undergone kidney transplantation. The diagnosis of kidney amyloidosis was determined by kidney biopsy, or by typical clinical presentation of renal amyloidosis with amyloid-positive extrarenal biopsy. The control group consisted of 18 consecutive FMF patients, without amyloidosis (as attested by normal urine analysis), or other kidney-related diseases. In both groups, the Tel-Hashomer criteria were used for the diagnosis of FMF (7). All patients were interviewed, examined and completed a questionnaire detailing clinical, demographic and genetic characteristics. The FMF severity was assessed using the FMF severity scale of Mor et al (8).

The 3 most common *MEFV* mutations, M694V, V726A, and E148Q, identifying 70% of the FMF alleles in the Israeli-Jewish FMF patients population, were determined, using polymerase chain reaction amplified segments of exon 10 and exon 2 of *MEFV* and enzyme restriction analysis, as previously described (9).

RESULTS

Demographic parameters

The study and control groups were comparable with respect to sex, age at recruitment and age at diagnosis but differed in ethnic origin, where most amyloidosis patients were North African (87% vs. 44%, P=0.01). Male preponderance and older age characterized the kidney-transplanted FMF-amyloidosis group. The other distinct patient ethnicities in the study group, varied insignificantly from those of the control group.

Clinical parameters

The clinical parameters of the FMF-amyloidosis group and the FMF-control group at the pre-transplantation period appeared to be comparable. This included rate of attacks in each site, rate of attacks accompanied by fever, duration of attacks, pain score during attacks, colchicine dose, age of onset, diagnosis delay, and disease severity score.

Colchicine treatment

Both patient groups were prescribed a mean of 1.5 mg colchicine a day by their treating physicians. However, while patients of the control group reported a 94% compliance rate, the kidney-transplanted FMF-amyloidosis patients admitted only a 50 % compliance rate at the pre-transplantation period (p=0.05).

Genetics

MEFV mutations are shown in Table 1. Fourteen of the 16 kidney-transplanted FMF-amyloidosis underwent genetic analysis, which resulted in the detection of the *MEVF*- M694V mutation in all (12 homozygous, and 2 heterozygous). By contrast, among all 18 FMF patients without amyloidosis, only 12 (66%) had any M694V mutation. The rest had other mutations or no mutations at all (n=6). The difference between the patient and control groups in carriage of at least one M694V mutation was significant (p=0.02). There was no difference on the rate of homozygosity to the M649V mutation, the main known genetic risk factor for amyloidosis.

Table 1. MEFV mutations in FMF patients with and without amyloidosis

MEFV genotypes	FMF with amyloidosis (n=14)*	FMF without amyloidosis (n=18)
M694V/M694V	12	9
M694V/0	2	1
E148Q/M694V	0	2
Other genotypes	0	7
Not performed	2	0
No mutations	0	1

* 14 of 16 patients analyzed

Post-transplantation course of FMF

Study patients were 6.75±6.75 years in average after kidney transplantation. Eighty-one percent of them underwent dialysis treatments during 2.37±1.7 years, before transplantation. All reported 100% compliance with colchicine and with the prescribed immunosuppressive therapy, which included mycophenolate mofetil (MMF) along with tacrolimus or cyclosporine or azathioprine, with or without prednisone. While FMF patients without amyloidosis recalled their most recent FMF attack to occur 143 days (average) before the day they completed the questionnaire, in FMF-amyloidosis patients it occurred 2214 days before the questionnaire time ($p = 0.01$).

CONCLUSIONS

Kidney transplantation in patients with AA amyloidosis of FMF seems to prevent FMF attacks. A protective role of immunosuppressive therapy in this regard cannot be excluded. Compliance with treatment and genetic makeup but not severity of FMF constitute the major risk factors for the development of amyloidosis in FMF.

REFERENCES

1. Pras M, Bronshpigel N, Zemer D, Gafni J. Variable incidence of amyloidosis in familial Mediterranean fever among different ethnic groups. Johns Hopkins Med J. 1982 Jan;150(1):22-6.
2. Livneh A. [Amyloidosis of familial Mediterranean fever (FMF)--insights to FMF phenotype II]. Harefuah. 2006 Oct;145(10):743-5, 82.
3. Gershoni-Baruch R, Brik R, Zacks N, Shinawi M, Lidar M, Livneh A. The contribution of genotypes at the MEFV and SAA1 loci to amyloidosis and disease severity in patients with familial Mediterranean fever. Arthritis Rheum. 2003 Apr;48(4):1149-55.
4. Zemer D, Revach M, Pras M, et al. A controlled trial of colchicine in preventing attacks of familial mediterranean fever. N Engl J Med. 1974 Oct 31;291(18):932-4.
5. Sevoyan MK, Sarkisian TF, Beglaryan AA, Shahsuvaryan GR, Armenian HK. Prevention of amyloidosis in familial Mediterranean fever with colchicine: a case-control study in Armenia. Med Princ Pract. 2009;18(6):441-6.

6. Livneh A, Zemer D, Siegal B, Laor A, Sohar E, Pras M. Colchicine prevents kidney transplant amyloidosis in familial Mediterranean fever. Nephron. 1992;60(4):418-22.
7. Livneh A, Langevitz P, Zemer D, et al. Criteria for the diagnosis of familial Mediterranean fever. Arthritis Rheum. 1997 Oct;40(10):1879-85.
8. Mor A, Shinar Y, Zaks N, et al. Evaluation of disease severity in familial Mediterranean fever. Semin Arthritis Rheum. 2005 Aug;35(1):57-64.
9. Kogan A, Shinar Y, Lidar M, et al. Common MEFV mutations among Jewish ethnic groups in Israel: high frequency of carrier and phenotype III states and absence of a perceptible biological advantage for the carrier state. Am J Med Genet. 2001 Aug 15;102(3):272-6.

Renal amyloidosis associated with a novel fibrinogen A alpha chain (AFib) mutation

Yvonne A. Efebera[1], Dorota Rowczenio[2], Anjali Satoskar[3], Don M. Benson[1], Tibor Nadasdy[3], Philip N. Hawkins[2]

[1] Division of Hematology, The Ohio State University Comprehensive Cancer Center, Columbus, OH; [2] Division of Medicine, UCL Medical School, Royal Free Hospital, London, NW3 2PF; [3] Department of Pathology, The Ohio State University, Columbus, OH

INTRODUCTION

We present an elderly patient with renal amyloidosis associated with a novel fibrinogen A alpha chain (AFib) mutation, who presented with slowly progressive renal insufficiency and proteinuria.

PATIENT

An 80 year old man who was known to have mild renal insufficiency since 1998, and low-level proteinuria since 2005, presented in October 2011 to the nephrology service with worsening creatinine over a six month period. His creatinine was 5.95 mg/dl (normal <1.3) and his urine protein was 6,379 mg/day (normal 40-225). He had no shortness of breath, dizziness, bruising, diarrhea or constipation. His past medical history was well controlled hypertension, hyperlipidemia and abdominal aortic aneurysm repair in 2004. He remained very active, and had no family history of renal disease. His parents were Russian and had died at age 72 and 75 years. His physical exam was unremarkable except for trace edema of the lower extremities.

INVESTIGATIONS AND RESULTS

Renal biopsy showed glomerular amyloid deposits (Figure 1) that stained strongly with antibodies to fibrinogen. He did not have a monoclonal protein by laboratory work and his bone marrow biopsy was unremarkable. There was no cardiac, liver, gastrointestinal, neurologic or other organ involvement.

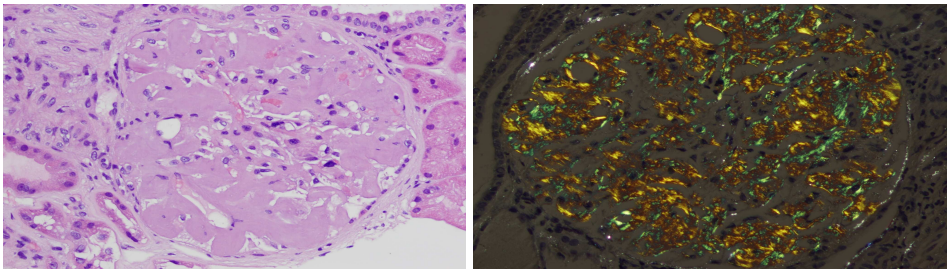

Figure 1. Smudgy acellular amyloid deposits in expanded mesangium 400x with apple green birefringence

Liquid chromatography tandem mass spectrometry (LC MS/MS) showed the amyloid deposits were primarily composed of fibrinogen alpha peptides consistent with AFib-type amyloid deposition. Direct DNA sequencing of the FGA gene revealed a novel fibrinogen mutation resulting from a single base substitution (c.1633G>A) altering the codon at position 526 from glutamic acid to lysine (E526K).

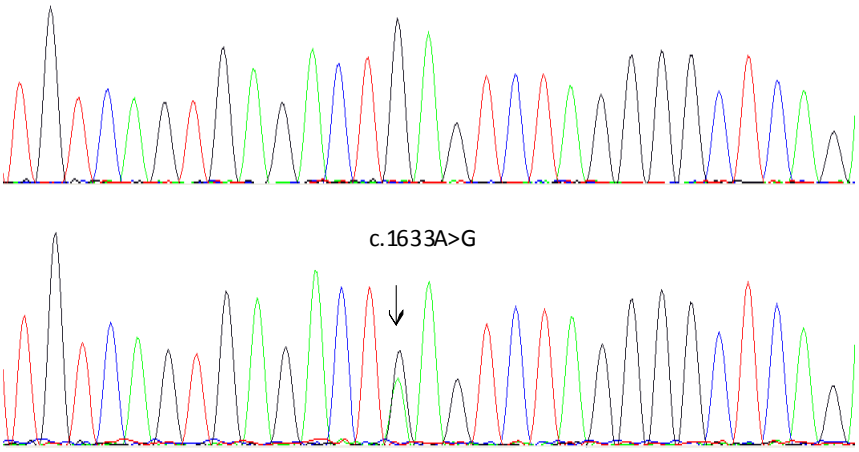

Figure 2. Novel mutation in the FGA gene; the top panel shows the wild-type sequence and the lower G to A single base substitution (c.1633 G>A) encoding the p.E526K variant, indicated by an arrow.

CONCLUSION

This is the first report of this novel fibrinogen mutation. The clinical presentation was indistinguishable from that of the most common AFib mutation (E526V- glutamic acid to valine), i.e. with a late onset of hypertension and proteinuric renal insufficiency without other amyloidotic organ involvement. The histological picture of major glomerular amyloid deposition was also similar. A major difference is that this patient had Russian ancestry while the majority of E526V mutation appear to be of British decent. Since his diagnosis, he continues to work full time and has not yet required dialysis.

REFERENCES

1. Talmud P, Tybjaerg-Hansen A, Bhatnagar D, Mbewu A, Miller JP, Durrington P, et al. Rapid screening for specific mutations in patients with a clinical diagnosis of familial hypercholesterolaemia. Atherosclerosis. 1991 Aug;89(2-3):137-41.
2. Gillmore JD, Lachmann HJ, Rowczenio D, Gilbertson JA, Zeng CH, Liu ZH, et al. Diagnosis, pathogenesis, treatment, and prognosis of hereditary fibrinogen A alpha-chain amyloidosis. J Am Soc Nephrol. 2009 Feb;20(2):444-51.
3. Stangou AJ, Banner NR, Hendry BM, Rela M, Portmann B, Wendon J, et al. Hereditary fibrinogen A alpha-chain amyloidosis: phenotypic characterization of a systemic disease and the role of liver transplantation. Blood. Apr 15;115(15):2998-3007.

The role of liver transplantation in the hereditary amyloidoses; the U.K experience

A.J. Stangou[1], B. Gunson[1], P. Ashcroft[1], D.Mirza[1], M. Rela[2], J O'Grady[2], N.D.Heaton[2], P.Muiesan[1]

[1]Birmingham NIHR Biomedical Research Unit in Liver Disease, Liver Unit, Queen Elizabeth Hospital, Birmingham, UK. [2]Liver Unit, King's College Hospital, London, UK

ABSTRACT

We evaluated the role of liver transplantation (LT) in the hereditary amyloidoses and present the UK experience of LT for fibrinogen A-α chain (AFib), apolipoprotein apoAI (AApoAI) and lysozyme (ALys) amyloidosis. Ten patients with E526V AFib amyloidosis and renal failure received combined liver and kidney transplant (LKT). The combined transplant procedure was curative but associated with significant perioperative risk. Three patients received LKT for AApoAI amyloidosis with renal and liver failure. All maintain normal dual graft function and have exhibited systemic amyloid regression. Two siblings with hepatic amyloidosis in association with ALys (Asp67His) received emergency LT for spontaneous liver rupture. The first patient survived 12 years, while the second remains well with normal graft function at 7 years. Liver transplantation may be curative in AFib, has a role of life-saving treatment in hepatic failure due to ALys, and is reserved for the indication of end-stage amyloid liver disease in AApoAI

INTRODUCTION

The clinical syndromes of autosomal dominant hereditary renal amyloidoses encompass a group of systemic amyloidoses due to mutations in the lysozyme (ALys), apolipoprotein AI (AApoAI), ApoAII and fibrinogen α-chain genes, which all share in common the manifestation of amyloid nephropathy in middle age with variable systemic involvement (1,2). Liver is the exclusive site of fibrinogen synthesis and thus the exclusive source of amyloid production in AFib. Approximately 50% of the variant ApoAI is produced by the liver, and in ALys the aberrant protein production is extrahepatic. Here we evaluate the role of liver transplantation in AFib and AApoAI patients with renal failure (AFib) or liver and renal amyloid related end stage disease (AApoAI) and in 2 cases of ALys with extensive hepatic amyloidosis causing spontaneous liver rupture.

PATIENTS AND METHODS

Between 1993-2011, fifteen patients with hereditary amyloid forms received liver transplantation between Queen Elizabeth Hospital and King's College Hospital, and are followed up at the Amyloid Clinic at Queen Elizabeth Hospital, Birmingham.

Fibrinogen α-chain amyloidosis: Nineteen patients with the E526V and one with R554L AFib variant with end-stage renal failure were assessed for combined liver and kidney transplantation. Amyloid scintigraphy revealed renal and splenic amyloid in all E526V cases. Ten patients had cardiac autonomic parasympathetic dysfunction and coronary atherosclerosis was documented in 66.6% of cases, including 70% LAD or RCA stenosis in 4 pre-dialysis patients. None of the patients were diabetic. Vascular dopplers showed carotid or systemic vascular disease in 50% of cases. The excised carotid atheroma in a patient with E526V AFib contained amyloid fibrils composed purely by variant fibrinogen. Extrarenal amyloid deposits involved the heart, spleen, vessel walls, however none of the cases fulfilled criteria for cardiac amyloidosis. Ten patients (median age 58 years) with E526V AFib amyloidosis and end stage renal failure received combined liver and kidney transplant.

Apolipoprotein ApoAI amyloidosis (AApoAI): Three patients aged 50, 52 and 56 years received combined LKT for AApoAI amyloidosis with renal and liver failure. All patients had documented hepatic and renal amyloidosis and were on renal replacement therapy. Cardiac parasympathetic dysfunction was documented in all patients, requiring prophylactic pacemaker insertion before transplant.

Lysozyme amyloidosis: Two siblings with ALys (Asp67His) associated hepatic amyloidosis which caused spontaneous liver rupture or massive hepatic haematoma received emergency LT as a life-saving procedure at 15 and 24 years of age respectively.

RESULTS

Fibrinogen α-chain amyloidosis: At median follow-up of 76 months (range 9-172), 7 patients are alive (cumulative survival 70%). Three fatal outcomes occurred in the peri-operative period due to vascular events or biliary complications, and involved patients who were older or on long- term renal replacement therapy. At median follow up of 76 (11-72) months all but one survivors maintain normal dual graft function with no amyloid progression. Two patients transplanted pre-emptively before RRT retain stable native kidney function at 8 and 7 years post-LKT. One patient lost the kidney graft due to chronic allograft nephropathy and has received a second kidney graft in a successful live related kidney transplant.

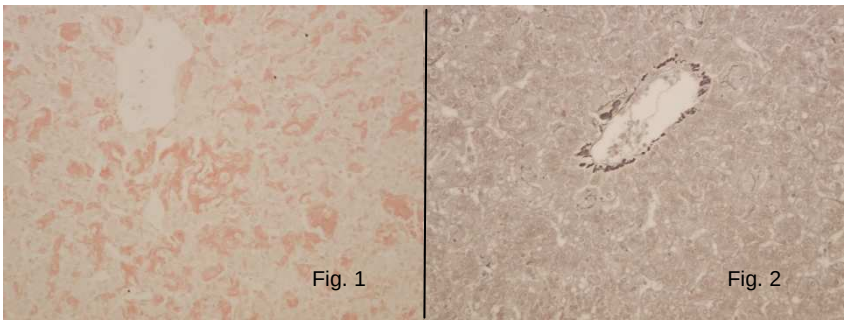

Figure 1. Histology of the explanted ALys liver exhibits extensive sinusoidal amyloid deposition

Figure 2. Marked depletion of sinusoidal reticulin in same sample, consistent with ‘fragile liver’.

Apolipoprotein ApoAI amyloidosis: Liver transplantation was uncomplicated and all AApoAI patients maintain normal dual graft function with no amyloid progression at 36, 109 and 152 months post-LKT. A further ApoAI

amyloidosis patient wit end stage hepatic amyloidosis and chronic kidney disease due to renal amyloidosis died on the waiting list for combined LKT due to complications of liver failure.

Lysozyme amyloidosis: The first patient who received life-saving emergency liver transplantation for hepatic rupture due to extensive hepatic amyloidosis survived 12 years post-LT. He died with massive GI haemorrhage related to mucosal amyloidosis. The second patient is alive and well at 7 years.

DISCUSSION

Fibrinogen α-chain amyloidosis is the commonest form of hereditary amyloid nephropathy in the United Kingdom, Ireland and the US. The disease is autosomal dominant with variable penetrance and commonly presents in middle age. The renal aspect of the disease is characterised by rapid progression to end stage renal failure within 1-5 years from presentation with proteinuria and hypertension. Fibrinogen is exclusively produced by the liver, and outcomes of isolated renal transplantation are poor due to amyloid recurrence (10-year renal graft survival <10%). Our observations in this series suggest that the disease phenotype may be more diverse and systemic than previously described, and in particular AFib may be another amyloid disease associated with amyloid atheromatosis. Combined liver and kidney transplantation is curative because it eliminates the exclusive source of amyloid production through liver replacement and restores kidney function through the kidney graft. It is however associated with high perioerative mortality risk, which in our series was 30%. We support evaluation of isolated liver transplantation in prospective Ethically approved studies as a novel indication for AFib patients with evidence of disease evolution, progressive renal involvement and early nephrotic syndrome with preserved GFR (60-70 mls/min). The same approach may apply to AFib kidney transplant recipients who exhibit early kidney graft recurrence if they are otherwise eligible in terms of cardiovascular assessment.

Approximately 50% of ApoAI is produced by the liver; the disease course is one of slow progression, and in contrast to AFib, long-term outcomes of isolated kidney or combined heart/ kidney transplantation without liver replacement are satisfactory. The indication for the addition of liver transplantation to kidney graft is reserved for the indication of amyloid liver failure.

The indication for liver transplantation in lysozyme amyloidosis (ALys) is not with curative intent as production of variant lysozyme is extrahepatic. Liver transplantation has the role of life-saving emergency procedure to replace the acutely failing amyloid laden liver through spontaneous rupture or liver haemorrhage. Survival of 12 years in our first recipient after a life-saving ‘palliative’ procedure is remarkable. The patient succumbed to extrahepatic amyloid complications whilst maintaining satisfactory liver function. Both ALys recipients in our series required emergency liver transplantation at very young age and post-LT patient and graft survival were satisfactory and justify consideration or urgent liver transplant for this indication.

CONCLUSIONS

Combined liver and kidney transplant for end-stage renal failure in AFib is curative, but incurs significant risks. Preemptive isolated LT at early stages of amyloid nephropathy merits prospective evaluation. The addition of liver transplant to kidney graft may be curative in AApoAI amyloidosis, however, the indication of liver transplant in AApoAI is reserved for liver failure. Life saving, albeit not curative, liver transplant is justified in patients with ALys amyloid related liver failure, and posttransplant life expectancy is acceptable.

ACKNOWLEDGEMENTS

We thank Professor Philip N Hawkins and Staff at the National Amyloidosis Centre, Royal Free Hospital, our colleagues and Staff at the Liver Unit, Queen Elizabeth Hospital, and Liver Unit and Nephrology Department King's College Hospital, and all the Physicians and teams involved in the care of these patients in the UK.

REFERENCES

1. Pepys MB, Hawkins PN, Booth DR, et al. Human lysozyme gene mutations cause hereditary systemic amyloidosis. *Nature*. 1993;362(6420):553-557.
2. Benson MD, Liepnieks J, Uemichi T, Wheeler G, Correa R. Hereditary renal amyloidosis associated with a mutant fibrinogen alpha-chain. *Nat Genet*. 1993;3(3):252-255.

LECT2 Amyloidosis Involving the Liver in Three Patients: A Case Series

A. Darnell[1], M. Fischer[2], R. Vuppalanchi[2], M. Benson[1], and O. Cummings[1]

Indiana University School of Medicine, Department of Pathology[1] & Department of Medicine[2]

ABSTRACT

LECT2 (leukocyte cell-derived chemotaxin 2) is a new member of the group of proteins known to cause amyloidosis. Previously, LECT2 amyloidosis has been exclusively described in the kidney. It is also notable for its increased occurrence in Hispanic patients. Here we present three cases of LECT2 amyloidosis involving the liver. The first patient was a 56 year old Hispanic female with a presumed diagnosis of autoimmune hepatitis who presented for liver biopsy. The second patient was a 66 year old Hispanic man with presumed cirrhosis. The demographics of the third patient are unknown. The liver histology revealed similar findings in all three patients: globular deposits of amyloid in the portal tracts. Immunohistochemical stains for AL (immunoglobulin light chain or primary amyloidosis) and AA (Amyloid A protein) were negative. However, recent recognition of LECT2 as a significant form of renal amyloidosis prompted an immunohistochemical stain for LECT2, which was strongly positive.

INTRODUCTION

LECT2 (leukocyte cell-derived chemotaxin 2) is a new member of the group of proteins known to cause amyloidosis (1). LECT2 is synthesized by the liver and it is a downstream target of β-catenin (2,3). Several biochemical functions have been attributed to LECT2: neutrophilic chemotaxis, NK T cell homeostasis, tissue remodeling and repair (1). Previously, LECT2 amyloidosis has been exclusively described in the kidney; predominately in patients with proteinuria. It is also notable for its increased occurrence in patients of Hispanic origin (4). Here we present three cases of LECT2 amyloidosis involving the liver.

METHODS

The first patient was a 56 year old Hispanic female with a presumed diagnosis of autoimmune hepatitis who presented for liver biopsy. Relevant laboratory values included an ANA titer of 1:640, IgG 1960 mg/dl, AST 221 IU/L ALT 210 IU/L, negative hepatitis B and C serologies, and serum protein 8.3 g/dl. The serum protein electrophoresis showed polyclonal gammopathy. There was no clinical evidence of kidney disease such as elevated serum creatinine or proteinuria hence urine protein electrophoresis and kidney biopsy was not performed in this patient. This does not rule out renal involvement as there has been a previous report of renal

LECT2 amyloidosis without proteinuria (5). She was treated with oral budesonide and mycophenolate mofetil (due to intolerance of azathioprine) and her liver chemistries normalized.

The second patient was a 66 year old Hispanic man with presumed cirrhosis. The demographics of the third patient are unknown.

RESULTS

The liver histology revealed similar findings in all three patients: globular deposits of amyloid in the portal tracts (Figure 1). Immunohistochemical stains for AL (immunoglobulin light chain or primary amyloidosis) and AA (Amyloid A protein or secondary amyloidosis) were negative. However, recent recognition of LECT2 as a significant form of renal amyloidosis when AL and AA are negative, particularly in Hispanic patients, prompted an immunohistochemical stain for LECT2, which was strongly positive (Figure 2).

In all three patients, DNA sequencing of peripheral blood revealed homozygosity for the G allele at nucleotide 172, which forms the codon GTC (Valine) at position 40/58. A finding previously described and found to be characteristic of individuals with LECT2 amyloidosis (4).

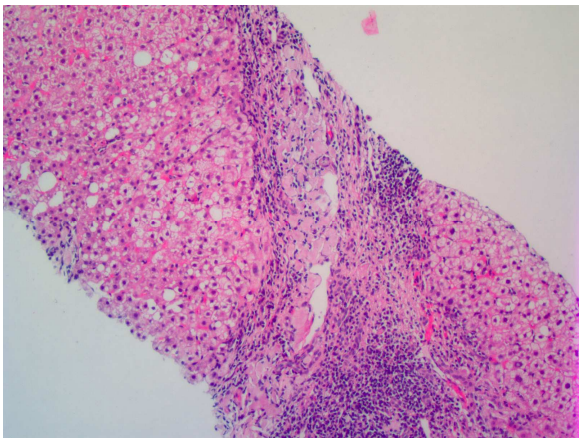

Figure 1. H&E 10x magnification

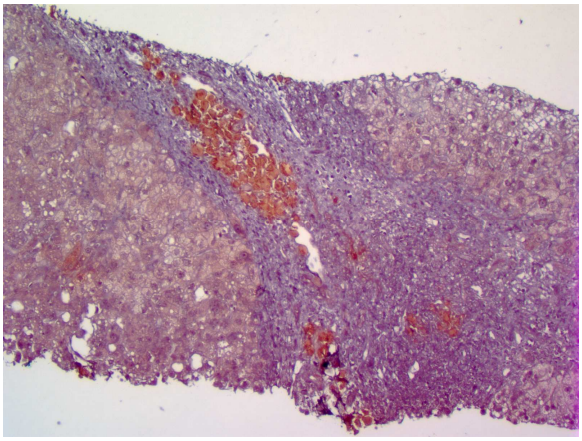

Figure 2. LECT2 immunostain 10x magnification

DISCUSSION

LECT2 amyloid was originally described in a patient with nephrotic syndrome and slowly progressive renal failure (6,7). Clinical evaluation and renal biopsy could not elucidate the type of amyloid until incidentally the patient developed renal cell carcinoma which led to nephrectomy. It was then that biochemical analysis was performed and LECT2 amyloid was discovered.

The pathogenesis of LECT2 amyloidosis in the liver is unclear. Recent evidence suggests that β-catenin, an important regulator of LECT2 production plays an important role in various aspects of liver biology including liver development (both embryonic and postnatal), liver regeneration following partial hepatectomy, HGF-induced hepatomegaly, liver zonation, and pathogenesis of liver cancer (8).

It is conceivable that the LECT2 synthesized by hepatocytes that are damaged or destroyed by autoimmune hepatitis can accumulate to a level locally that leads to fibril formation and deposition. This hypothesis would oppose to what has been shown in mouse models; in Concanavalin A-induced hepatitis, an experimental model for human autoimmune hepatitis, the expression of LECT2 is rather transiently decreased (9,10). Another explanation is that the ongoing inflammation in the presence of autoimmune hepatitis may interfere with local catabolic pathways, leading to a relative local LECT2 excess with eventual fibril formation and deposition. It has been shown that LECT2 expression throughout the body varies between organs, cell types and in different diseases. For instance, endothelial cells, smooth muscle cells, cerebral nerve cells and squamous cells of the upper epidermis are among the group of cells with the most consistent LECT2 expression. However, these cells lose LECT2 expression when involved by severe inflammation or neoplastic process: vascular endothelial cells become LECT2 negative in vasculitis, and squamous cells become LECT2 negative in squamous cell carcinoma of the esophagus. Conversely, cells that generally lack LECT2 expression show positive expression in certain disease states: osteoblasts after a bone fracture and thyroid epithelial cells in follicular carcinoma (1).

According to a recent publication LECT2 amyloidosis was the 3rd most common type of amyloid identified in kidney biopsy specimens, ahead of ATTR (transthyretin)(4). In our case2, LECT2 was found in the liver. We recommend that LECT2 amyloidosis is included in the differential of amyloidosis irrespective of the type of organ involved after the more common AL or AA subtypes are ruled out.

REFERENCES

1. Nagai, H., et al., Systemic expression of a newly recognized protein, LECT2, in the human body. Pathol Int, 1998. 48(11): p. 882-6.
2. Ovejero, C., et al., Identification of the leukocyte cell-derived chemotaxin 2 as a direct target gene of beta-catenin in the liver. Hepatology, 2004. 40(1): p. 167-76.
3. Yamagoe, S., et al., Expression of a neutrophil chemotactic protein LECT2 in human hepatocytes revealed by immunochemical studies using polyclonal and monoclonal antibodies to a recombinant LECT2. Biochem Biophys Res Commun, 1997. 237(1): p. 116-20.
4. Murphy, C.L., et al., Leukocyte chemotactic factor 2 (LECT2)-associated renal amyloidosis: a case series. Am J Kidney Dis, 2010. 56(6): p. 1100-7.
5. Holanda, D.G., et al., Atypical presentation of atypical amyloid. Nephrol Dial Transplant, 2011. 26(1): p. 373-6.

6. Benson, M.D., LECT2 amyloidosis. Kidney Int, 2010. 77(9): p. 757-9.
7. Benson, M.D., et al., Leukocyte chemotactic factor 2: A novel renal amyloid protein. Kidney Int, 2008. 74(2): p. 218-22.
8. Thompson, C., et al., Signaling by the cysteinyl-leukotriene receptor 2. Involvement in chemokine gene transcription. J Biol Chem, 2008. 283(4): p. 1974-84.
9. Tiegs, G., J. Hentschel, and A. Wendel, A T cell-dependent experimental liver injury in mice inducible by concanavalin A. J Clin Invest, 1992. 90(1): p. 196-203.
10. Saito, T., et al., Increase in hepatic NKT cells in leukocyte cell-derived chemotaxin 2-deficient mice contributes to severe concanavalin A-induced hepatitis. J Immunol, 2004. 173(1): p. 579-85.

Long term effectiveness of surgery in localized laryngeal amyloidosis

Aldert J. Hazenberg[1], Frederik G. Dikkers[2], and Bouke P. Hazenberg[1]

Department of Otorhinolaryngology, Refaja Hospital, Stadskanaal (1) and Departments of Otorhinolaryngology (2) and Rheumatology & Clinical Immunology (3), University Medical Center Groningen, University of Groningen, Groningen, The Netherlands.

OBJECTIVE

To assess long term effectiveness of surgical treatment in localized laryngeal amyloidosis.

METHODS

This retrospective study comprised all consecutive patients with localized laryngeal amyloidosis who visited our tertiary referral center between 1994 and 2012 and who were treated with surgery. Systemic amyloidosis was made unlikely by thorough clinical evaluation [1]. Recurrence rate, number of revision surgery procedures, progression to systemic amyloidosis and changes in voice were monitored yearly.

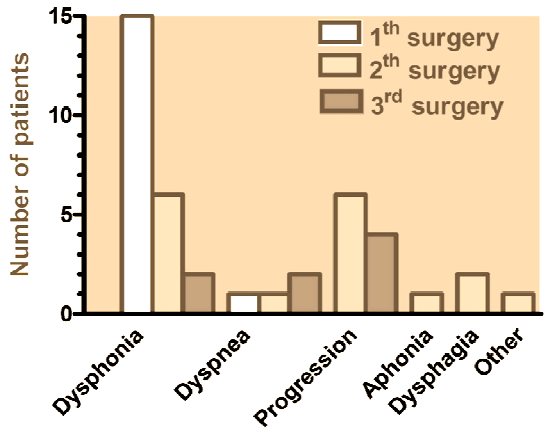

Figure 1. Indications for surgery.

RESULTS

Fifteen patients (4 women) were included. Median age was 49 years (21-77 years) and median follow-up was 5.9 years (1.5-14.5 years). Amyloid was found subglottic (3), glottic (4), in false vocal folds (8) and in other

supraglottic areas (5), in more than one larynx region (10) and bilaterally (7). Combinations of localizations occurred in contiguous regions. One patient had a small plasma cell clone in the bone marrow without systemic amyloidosis. Blunt dissection was used at the glottis and CO2-laser- excision, sometimes assisted by microdebrider, at other laryngeal areas.

Ten patients needed one revision, four of them needed a second revision and one patient needed a third revision. Revision was indicated because of progression with dysphonia (8), dyspnea (3), exclusion of malignancy (1), dysphagia (1) and aphonia (1). Time until first revision surgery was median 2.4 years (2 months – 11.5 years). One patient had been treated with radiotherapy elsewhere nine years before she was seen with progression of amyloid necessitating revision surgery. No patient developed systemic amyloidosis during follow-up.

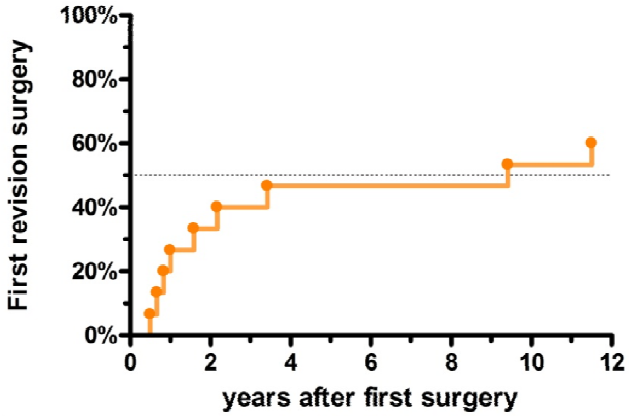

Figure 2. Most frequent recurrences in the first four years.

DISCUSSION

Although local progression urges revision surgery in the first four years postoperatively, progression seems to slow down after four years. Late progression, however, remains possible as shown in two patients, nine and eleven years after radiotherapy and surgery, respectively. Localized laryngeal amyloidosis does not progress to systemic amyloidosis.

REFERENCES

1. Bartels H, et al. Ann Otol Rhinol Laryngol 2004;113:741-8.

Subcutaneous amyloid deposition at insulin injection sites in two patients with type II diabetes mellitus

P. de Graeff[1], P.M. Kluin[2], and B.P. Hazenberg[3]

Departments of (1) Internal Medicine, (2) Pathology and (3) Rheumatology & Clinical Immunology, University Medical Center Groningen, University of Groningen, the Netherlands

CASES

Two patients with insulin dependent diabetes mellitus, one male aged 61 years old (patient 1) and one female aged 53 years old (patient 2), developed a localized subcutaneous abdominal mass at their respective insulin injection sites (Figure 1). Both patients had been treated with recombinant human insulin or insulin analogues for more than 10 years. Biopsies were taken under the suspicion of malignant disease.

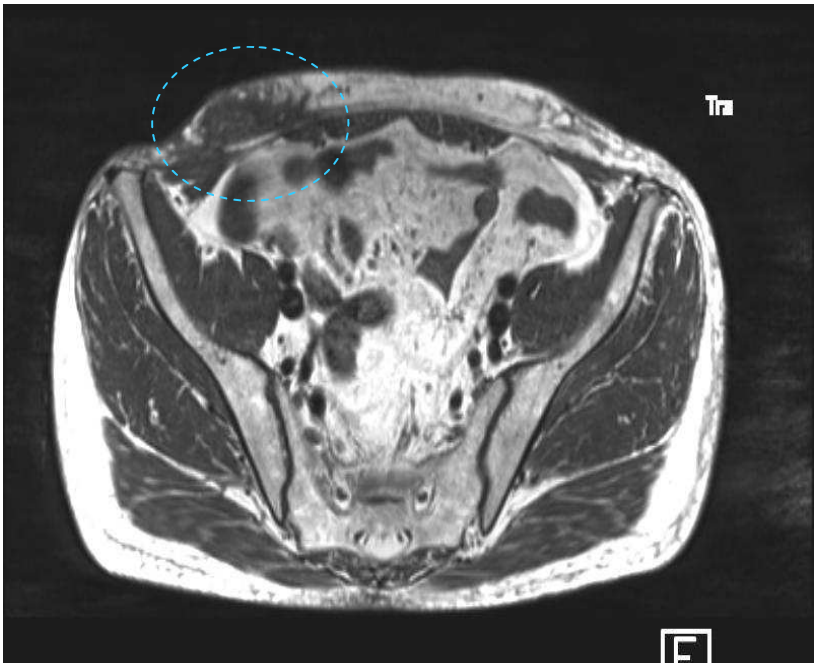

Figure 1. Abdominal CT scan of patient 1 showing a mass in the right lower quadrant

RESULTS

However, histopathological examination of tumor biopsies demonstrated adipose tissue with deposits of amorphous eosinophilic material. After Congo red staining, samples showed apple-green birefringence in polarized light typical of amyloid. Antibodies against serum amyloid P (SAP) and serum amyloid A (SAA) stained negative. Additional evaluation including serum protein electrophoresis, serum immunoglobulin free light chain levels, bone marrow aspiration and (123)I-SAP scintigraphy revealed no signs of systemic AL amyloidosis. Finally, additional immunohistochemical staining (Figure 2) revealed strong insulin positivity leading to the diagnosis of localized amyloidosis composed of iatrogenic amyloid insuline (AIns) type amyloid. In both patients, blood glucose levels markedly improved after they changed their injection site suggesting that that in these cases, insulin resistance may be partly explained by accumulation of insulin in the amyloid mass, resulting in decreased bioavailability.

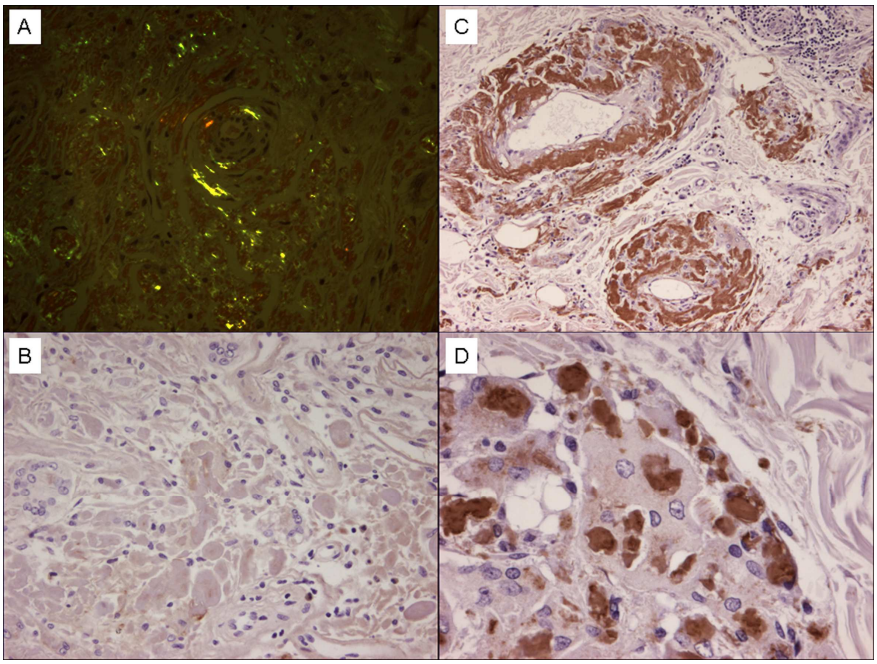

Figure 2. Patient 2 (A) Congo red-stained tissue showing the characteristic apple green birefringence in polarized light; (B) negative serum amyloid P (SAP) staining; (C, D) additional immunohistochemical staining showing strong strong insulin positivity and the presence of giant cells

So far, twelve cases of localized insulin-derived amyloidosis have been described in literature [1, 2]. Given the high prevalence of insulin-dependent diabetes mellitus, its occurrence is likely to be underestimated. This diagnosis should be considered in every patient using either porcine or recombinant human insulin presenting with a subcutaneous tumor at their injection site, especially in case of insulin-refractory disease. AIns amyloid is

the exception of the rule that amyloid in subcutaneous abdominal fat tissue proves the presence of systemic amyloidosis.

CONCLUSIONS

AIns type amyloid should be considered in every patient using insulin presenting with a subcutaneous tumor at their injection site, especially in case of insulin-refractory disease. AIns amyloid is the exception of the rule that amyloid in subcutaneous abdominal fat tissue proves the presence of systemic amyloidosis.

REFERENCES

1. Shikama Y, Kitazawa J, Yagihashi N, Uehara O, Murata Y, Yajima N, Wada R, Yagihashi S. Localized amyloidosis at the site of repeated insulin injection in a diabetic patient. Intern Med. 2010;49(5):397-401.
2. Störkel S, Schneider HM, Müntefering H, Kashiwagi S. Iatrogenic, insulin-dependent, local amyloidosis. Lab Invest. 1983 Jan;48(1):108-11.

SECTION VIII

DESIGN OF TARGETED MOLECULES AND INNOVATIVE DRUGS


Groninger
Museum

STATE OF THE ART AND PERSPECTIVES FOR THE FUTURE: Design Of Targeted Molecules And Innovative Drugs

D.C. Seldin[1] and M.D. Benson[2]

[1]Amyloid Treatment and Research Program, Department of Medicine, Boston University School of Medicine and Boston Medical Center, Boston, Massachusetts, USA
[2]Indiana University School of Medicine, Department of Pathology and Laboratory Medicine; and,
Richard L. Roudebush Veterans Affairs Medical Center, Indianapolis, Indiana USA

HISTORICAL PERSPECTIVE

The Proceedings of the First International Symposium on Amyloidosis held at the University of Groningen, The Netherlands, September 24-28, 1967, document only one article which addressed treatment of patients with systemic amyloidosis. Professor H.P. Missmahl presented results of studies conducted over a 30 year period on patients with amyloidosis, describing diagnostic methodologies and treatments. Professor Missmahl described “pericollagen” and “perireticulin” deposition of amyloid, andd favorable results using methotrexate and chloroquine in both types. At this time, the distinction between AL and AA had not yet been made. Fortunately, the last 45 years have shown tremendous advances in the basic science study of amyloidosis, chemical characterization of the different types of amyloid, and development of specific therapies.

The first effective therapy for one form of systemic amyloidosis was based upon the recognition that AL amyloidosis is a direct result of a bone marrow plasma cell dyscrasia. This led to the use of anti-plasma cell chemotherapy to suppress or eliminate the monoclonal plasma cells synthesizing the amyloid pre-fibrillar light chain protein. Improvements were seen with the use of oral melphalan, an alkylating agent, coupled with prednisone. However, many patients had little hematologic response and hence clinical improvement was uncommon, and survival benefits were modest. In the last 20 years, high-dose intravenous melphalan with autologous stem cell rescue has become the most successful form of treatment in patients who are not at high-risk because of advanced vital organ involvement. More recently, proteasome inhibitors such as bortezomib, and the immunomodulatory drugs thalidomide and lenalidomide, have been added to the therapeutic armamentarium. While less myeloablative and toxic than high-dose melphalan, even these agents have side effects in patients with amyloid organ disease.

The second disease for which the source of the pre-fibrillar protein could be eliminated was ATTR. For patients producing a mutant amyloid-prone form of TTR primarily in the liver, orthotopic liver transplantation can eliminate the source of the pre-fibrillar protein precursor. Of course, this comes at great cost in terms of major

surgery and subsequent need for life-long immunosuppression. Furthermore, not all patients benefit, as for some, ongoing production of the wildtype TTR protein appears to be capable of augmenting fibril deposition, and also, non-hepatic sources of production of TTR such as the choroid plexus are not corrected with this approach.

For AA (secondary) amyloidosis caused by chronic infection or inflammatory disorders, the mainstay of therapy has been to reduce SAA production using antibiotics or anti-inflammatory drugs. This has been very effective for many patients, and the incidence of AA seems to be declining, with an increasing proportion of patients with AA found to have unusual hereditary periodic fever syndromes or other cytokine-producing diseases. As for the therapies for AL and ATTR, this approach goes after the source of the precursor protein, but does not address the function and activity of the amyloid-forming protein itself.

THE LONG ROAD TO THE FIRST TARGETED THERAPEUTICS

The first successful agent to interfere with the process of fibril formation at the level of the pathologic protein and its chaperones and accessory molecules was eprodisate (Fibrillex, or Kiacta). The results of a phase III randomized double-blind trial carried out from 2001-2003, and reported in the New England Journal of Medicine in 2007, demonstrated that eprodisate slowed progression of renal failure in patients with AA amyloidosis. The science behind eprodisate had its origin in the mid-1980s, when Kisilevsky working with colleagues Snow, Ancsin, and other collaborators across the globe made the observation that glycosaminoglycans (GAGs) are co-deposited with all forms of amyloid. They hypothesized that the GAGs promote amyloid formation, found evidence *in vivo* and *in vitro* to support this notion, and then tested polyanionic GAG-mimetics as agents to retard amyloid formation. This work led to the development of eprodisate, which is now undergoing a second confirmatory phase III trial, required by the FDA. If that trial is positive, eprodisate will be approved, ~30 years after the initial observations that led to its development.

The second success has been with agents that stabilize TTR in its native tetrameric state. This approach came out of the insight of Kelly and collaborators at the Scripps Research Institute. In the late 1990s, Prof. Kelly demonstrated that dissociation of the TTR tetramer was the rate-limiting step in formation of oligomers and then fibrils on the pathway to amyloid formation. They found that small molecules that dock in the thyroxine binding site of the TTR tetramer inhibit its dissociation, and identified diflunisal and tafamidis (Vyndaqel) as compounds with such activity. Diflunisal is being investigated in a randomized phase III double-blind study supported by the FDA and NIH that has completed accrual, and will be analyzed in late 2012. Tafamidis became the lead compound of the company FoldRx, subsequently purchased by Pfizer. With their support, the tafamidis trial accrued quickly, and positive results were reported at this meeting, having led to approval by the European Medicines Agency in November 2011. Approval in the U.S. is pending, with the FDA potentially requiring more information or a confirmatory second trial. Regardless, the time-line from laboratory observation to translation into a successful drug in this case took place over about a 15 year period, half that of eprodisate.

Important lessons can be learned from the development of these two agents. Firstly, innovative therapies depend upon insightful laboratory insights made by creative scientists. Secondly, translating these insights into effective drugs is a long and expensive process. However, as the field progresses and we gain better understanding of drug developmental pathways, the pace of drug development will undoubtedly accelerate.

MANY PROMISING ROUTES TOWARDS NEW THERAPIES

The talks presented in Session 12: “Design of Targeted Molecules and Innovative Drugs” show many potential paths for development of new therapeutics. Successful drug development depends upon accurate identification of the fibril precursor; a sophisticated understanding of the process of fibril formation including misfolding, aggregation, oligomer and fibril formation, and of the role of accessory molecules and chaperones; *in vitro* and *in vivo* assays for drug screening; animal models for *in vivo* testing; and clinical trials with meaningful endpoints in terms of organ function and quality of life as well as survival. These steps are now in place for many of the systemic amyloid diseases, and the exciting oral presentations in this session highlighted a variety of innovative translational research approaches.

A series of presentations described the use of small interfering RNAs (siRNA) and antisense oligonucleotides (ASO) to disrupt plasma cells and amyloid precursor synthesis at the RNA level. In the first oral presentation, OP66, Zhou and colleagues described induction of apoptosis in human plasma cell lines treated with lambda light chain siRNA. In OP73, Ackermann and colleagues from Isis Pharmaceuticals, and their academic collaborators, described the preclinical studies and design of a phase I trial to measure pharmacokinetics and pharmacodynamics of an ASO against TTR. In OP74, Coelho reported on behalf of her colleagues and co-investigators at Alnylam Pharmaceuticals on the phase I results of a first generation ALN-TTR01 siRNA incorporated into a lipid nanoparticle. In OP75, Tasaki and colleagues described the use of an siRNA against TTR conjugated with cholesterol to treat the ocular manifestations of TTR disease, in cells and in rats by intravitreal injection.

Other presentations described interesting and innovative small molecule therapeutics. In OP67, Snow and colleagues at ProteoTech reported on the ability of the small molecule Systebryl to reduce AA amyloid formation and promote resorption in animal models. This promising agent is entering phase I clinical trials. In OP68, Garceau, representing Bellus Health, Celtic Therapeutics, and their academic collaborators, described the design of the confirmatory phase IIII trial of eprodisate for treatment of AA amyloidosis that has recently begun. In OP69, Berk, on behalf of the diflunisal consortium of investigators, updated information on demographics, baseline studies, and the limited number of adverse events in that phase III study so far. In OP70, Ferreira *et al.* reported that curcumin increases stability of TTR in the plasma of mice, and reduces tissue deposits and biomarkers of ER stress and protein oxidation. In OP71, Obici *et al.* describes preliminary results of a phase II study combining doxycycline and tauroursodeoxycholic acid for treatment of patients with ATTR and SSA; so far the combination has been well-tolerated, and only 1 of 22 patients had come off study because of neurological progression at 6 months.

Monoclonal antibodies have proven roles in cancer therapeutics. In OP72, Su and colleagues described the specificity of a TTR fibril monoclonal antibody that could potentially be used to promote fibril opsonization and resorption.

THE FUTURE

After many years of critical basic science studies including biochemical characterization of amyloid proteins, biophysical analysis of oligomers and fibrils, and development of tissue culture and animal model systems, the era of targeted amyloid therapeutics is now upon us. There is much to be optimistic about, and certainly by the time of the next symposium we expect many further advances in this area.

SELECTED REFERENCES

1. Merlini G, Seldin DC, Gertz MA. 2011. Amyloidosis: pathogenesis and new therapeutic options. Journal of Clinical Oncology 29(14):1924-33.
2. Skinner M, Lewis WD, Jones LA, Kasirsky J, Kane K, Ju ST, et al. 1994. Liver transplantation as a treatment for familial amyloidotic polyneuropathy. Ann Intern Med.120(2):133-4.
3. Snow AD, Kisilevsky R. 1985. Temporal relationship between glycosaminoglycan accumulation and amyloid deposition during experimental amyloidosis. A histochemical study. Lab Invest.53(1):37-44.
4. Dember LM, Hawkins PN, Hazenberg BP, Gorevic PD, Merlini G, Butrimiene I, et al. 2007. Eprodisate for the treatment of renal disease in AA amyloidosis. N Engl J Med 356(23):2349-60.
5. Kelly JW, Colon W, Lai Z, Lashuel HA, McCulloch J, McCutchen SL, et al. 1997. Transthyretin quaternary and tertiary structural changes facilitate misassembly into amyloid. Adv Protein Chem.50:161-81.
6. Berk JL, Dyck PJ, Obici L, Zeldenrust SR, Sekijima Y, Yamashita T, et al. 2011. The diflunisal trial: update on study drug tolerance and disease progression. Amyloid : the international journal of experimental and clinical investigation : the official journal of the International Society of Amyloidosis.18 Suppl 1:191-2.
7. Coelho T, Maia LF, Martins da Silva A, Waddington Cruz M, Plante-Bordeneuve V, Lozeron P, et al. 2012. Tafamidis for transthyretin familial amyloid polyneuropathy: A randomized, controlled trial. Neurology.

A clinical Phase 3 confirmatory trial of eprodisate in the treatment of AA amyloidosis patients

D. Garceau[1] , H. Lachmann[2], T. Sablinski[3], L.M. Dember[4]

[1] Bellus Health, Laval, Canada; [2] Royal Free and University College Medical School, London, United Kingdom; [3] Celtic Therapeutic, New York, USA [4] University of Pennsylvania, Philadelphia, US

AA amyloidosis occurs in chronic inflammatory conditions as a result of abnormal deposition of amyloid A protein in tissues, predominantly the kidneys, leading to progressive organ dysfunction. Eprodisate (NC-503, Kiacta™) inhibits the interaction between glycosaminoglycans and amyloid protein thereby preventing amyloid fibril formation and deposition. In a first clinical Phase 2/3 study conducted in 183 AA patients, eprodisate administered for 2 years reduced the risk of renal function deterioration and death as compared to placebo (Cox proportional hazards regression analysis: HR=0.58; 95% CI (0.37, 0.93); p=0.025). Eprodisate appeared to be safe and well tolerated in AA patients. To confirm the safety and efficacy of eprodisate, a second multicenter, randomized, placebo-controlled clinical Phase 3 trial has recently been initiated. Comparison of study design, statistical approached and patient profile are made between the two eprodisate clinical studies and the rationale for differences is discussed.

INTRODUCTION

AA amyloidosis is associated with chronic inflammatory diseases and it develops when proteolytic fragments of serum amyloid A (SAA), an acute phase reactant protein, are deposited in tissues as amyloid fibrils. The kidney is the organ most frequently affected in AA amyloidosis and kidney involvement is characterised by nephrotic syndrome and progressive loss of renal function.

There is currently no specific treatment for AA amyloidosis. Treatments that suppress the underlying inflammatory condition may slow the progression of AA amyloidosis by decreasing the production of the SAA precursor protein. However, these treatments are not sufficiently effective for many patients and have substantial toxicity. Eprodisate is a low molecular weight, negatively charged and sulfonated molecule that was specifically designed to interfere with interactions between AA protein and glycosaminoglycans. The compound was found to inhibit amyloid fibrils deposition in a mouse model of AA amyloidosis (1,2). The efficacy and safety of eprodisate was first investigated in a Phase 2/3 clinical trial involving 183 patients with AA amyloidosis. In this first Phase 2/3 trial, eprodisate reduced by 42% (p=0.025) the risk of the composite outcome of renal function deterioration or death as compared to placebo (3). The compound appeared to be safe and well

tolerated in AA patients. To further evaluate the safety and efficacy of eprodisate for the treatment of AA amyloidosis, a second multicenter, randomized, double-blind and placebo-controlled phase 3 trial has been recently been initiated.

METHOD

230 patients with AA amyloidosis will be enrolled in approximately 78 study sites in 28 countries. The diagnosis of AA amyloidosis has to be confirmed by a tissue biopsy (Congo red staining and immunohistochemistry or immunoelectron microscopy). Presence of renal involvement defined by proteinuria ≥ 1 g/day is required. The key exclusion criteria include kidney diseases other than AA amyloidosis and creatinine clearance ≤ 25 ml/min/1.73m^2. The primary efficacy outcome is time to earliest of the following events: persistent ≥ 40% decrease CrCl; persistent ≥ 80% increase SCr; or progression to ESRD/dialysis.

This is a randomized, doubled-blind and placebo-controlled event-driven study. The study will end when 120 primary events have occurred. The primary efficacy endpoint will be analysed with a Log rank test. Participants will be evaluated every 3 months throughout the duration of the study.

RESULTS

The confirmatory clinical Phase 3 study is still ongoing. As of May 10, 2012, a total of 192 were screened: 90 patients of them were randomized and 32 were in-screening phase. A total of 62 patients were screen failed; the main reason being creatinine clearance less than 25 ml/min/1.73m^2 (n=25), proteinuria less than 1g/day (n=19) and negative biopsy results (n=12). The greater proportions of patients have been recruited from Eastern Europe (42%) and Middle East/Asia (28%), followed by Western Europe (18%) and America (12%). Fifty five percent of patients enrolled in the study to date are male, the mean age of study patients is 52 years and the baseline median levels of serum creatinine, creatinine clearance and proteinuria are 1.1 mg/dl, 64 ml/min/1.73 m^2 and 4.3 g/day, respectively. Comparisons of patient population between first phase 2/3 (P 2/3) study and ongoing phase 3 (P 3) study shows comparable population with respect to underlying inflammatory disease (Figure 1).

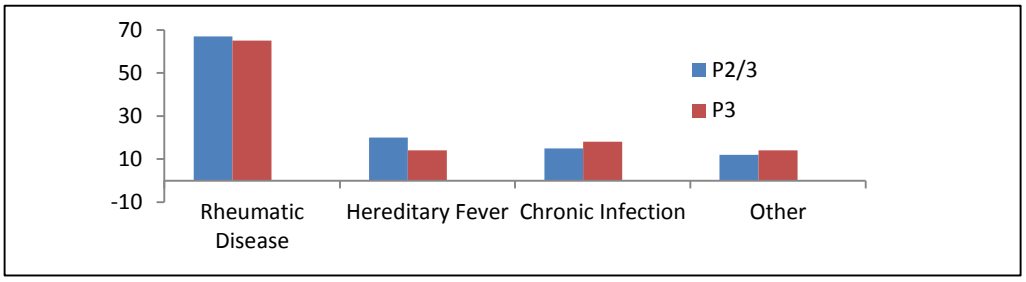

Figure 1. Underlying Inflammatory Diseases of Study Population (%)

DISCUSSION

Following the completion of a first successful Phase 2/3 study showing the protective effect of eprodisate on renal function in AA patients, a confirmatory Phase 3 trial has recently been initiated. The design of the confirmatory Phase 3 trial was informed by the data obtained from the first Phase 2/3 trial. The key differences in the primary endpoint, the study design and the inclusion criteria are shown in Table 1.

Table 1. Key Differences between first Phase 2/3 and Confirmatory Phase 3 Trial Designs

First Phase 2/3 study	**Confirmatory Phase 3 study**
Primary endpoint: ≥ 50% decrease in CrCl, ≥ 100% increase in SCr; progression to ESRD or death	*Primary endpoint:* persistent* ≥ 40% decrease in CrCl, persistent ≥ 80% increase in SCr, or progression to ESRD
2-year fixed study duration	Event-driven trial (study will end when 120 events have occurred)
Inclusion criteria: Proteinuria ≥ 1g/day or CrCl ≤ 60 ml/min/1.73m^2 CrCl ≥ 20 ml/min/1.73m^2	*Inclusion criteria:* Proteinuria ≥ 1 g/day CrCl ≥ 25 ml/min/1.73m^2

**persistence is demonstrated by the presence of the event in a confirmatory visit scheduled 4-6 weeks after event was first reported*

Death has been removed from the primary composite endpoint because data from the phase 2/3 study indicated that deaths were usually related to complications of the underlying inflammatory disease and the cause of death was not always well defined. Since eprodisate does not affect the underlying inflammatory disease, inclusion of death in the primary composite endpoint adds noise thereby reducing the ability to detect effects of the drug. Death will remain an important outcome as a secondary efficacy endpoint and safety analyses. The thresholds for decrease in creatinine clearance and increase in serum creatinine level have been slightly lowered in order to increase the total number of events while still retaining events that are clinically meaningful. The criterion of persistence of the alteration of kidney function has been added to improve the robustness of the primary outcome.

The data from the phase 2/3 study were also used to calculate the sample size (i.e. number of events) of the confirmatory Phase 3 trial. A total of 120 events, in both treatment group combined, is expected to provide a statistical power of approximately 90%, assuming a treatment effect comparable to that seen in the Phase 2/3 study and a significance level of 0.05.

In the Phase 3 trial, proteinuria of ≥ 1g/day is required for all participants. This change was made based on the analysis of the phase 2/3 study revealing that patients with high proteinuria levels exhibited faster renal function decline and thus were more likely to have renal outcome event during a relatively short follow-up period. Finally, the lower limit of CrCl as entry criterion was increased from 20 to 25 ml/min/1.73m^2 to avoid enrolment of participants with disease likely to require renal replacement therapy before eprodisate could exert an effect.

In conclusion, results from the first Phase 2/3 study showing the statistically significant and clinically meaningful renal protective effect of eprodisate in AA patients are quite encouraging. The improvement in the study design of the second Phase 3 trial should help confirming the efficacy of eprodisate in the treatment of AA amyloidosis.

REFERENCES

1. Kisilevski R, Lemieux LJ, Fraser PE, et al. Arresting amyloidosis in vivo using small molecule anionic sulphonates or sulphates: implications for Alzheimer's Disease. Nat Med 1995; 1: 143-8.
2. Gervais F, Morissette C, Kong X. Proteoglycans and amyloidogenic proteins in peripheral amyloidosis. Curr Med Chem Immun, Endocr Metab Agents. 2003; 3: 361-70.
3. Dember LM, Hawkins PN, Hazenberg BPC, et al. Eprodisate for the treatment of renal disease in AA amyloidosis. N Engl J Med 2007; 356 (23); 2349-60.

Phase I study of MLN9708, a novel, investigational oral proteasome inhibitor, in patients with relapsed or refractory (rel/ref) light-chain amyloidosis (AL)

V. Sanchorawala (1), J.A. Zonder (2), R.L. Comenzo (3), S.O. Schönland (4), A. Dispenzieri (5), D. Berg (6), G. Liu (6), N. Gupta (6), A-M. Hui (6), G. Merlini (7).

(1) Amyloid Treatment and Research Program, Boston University School of Medicine, Boston, MA, USA; (2) Barbara Ann Karmanos Cancer Institute, Detroit, MI, USA; (3) Tufts Medical Center, Boston, MA, USA; (4) Amyloidosis Center, Department of Internal Medicine, University of Heidelberg, Heidelberg, Germany; (5) Division of Hematology, Mayo Clinic, Rochester, MN, USA; (6) Millennium Pharmaceuticals Inc., Cambridge, MA, USA; (7) Amyloidosis Research and Treatment Center, Fondazione IRCCS Policlinico San Matteo, University of Pavia, Italy.

Safety, maximum tolerated dose (MTD), and recommended phase 2 dose (RP2D) of oral MLN9708 was assessed in patients with rel/ref AL. Increasing doses of oral MLN9708 (standard 3+3 design) were administered on days 1, 8, and 15 of 28-day cycles (up to12 cycles). Of 14 patients enrolled at MLN9708 4.0 mg and 5.5 mg, 13 were evaluable. Patients received median 3 cycles (range, 1–10). The MTD was 4.0 mg (3 patients had dose-limiting toxicities (DLT). Twelve patients had any adverse event (AE) (11 drug-related); most common included: nausea, fatigue, and thrombocytopenia. No AE-related on-study deaths were reported. Eight patients were ongoing; 5 discontinued due to disease progression. Preliminary hematologic responses included 3 very good partial response (VGPR).

INTRODUCTION

The proteasome inhibitor bortezomib provides durable hematologic responses in relapsed AL patients (1,2). MLN9708 is an investigational, oral, potent, reversible, and specific 20S proteasome inhibitor (3) that in preclinical studies has demonstrated faster dissociation rates and greater tissue penetration compared with bortezomib (4). MLN9708 has also demonstrated antitumor activity in solid tumor and hematologic malignancy xenograft models (3,5,6). This phase 1 study (NCT01318902) assessed weekly doses of oral MLN9708 in patients with rel/ref AL.

The primary objective of the study was to determine: the safety, tolerability, and MTD of oral weekly MLN9708 in patients with rel/ref AL; and the RP2D. The secondary objective of the study was to: characterize the plasma pharmacokinetics (PK) and whole blood pharmacodynamic effects of MLN9708; and to assess the overall hematologic response rate, time to and duration of hematologic and organ response, and progression-free and overall survival.

METHODS

Patients aged ≥18 years with cardiac biomarker risk stage I/II rel/ref AL and measurable major organ (heart/kidney) involvement received increasing doses of oral MLN9708 (standard 3+3 dose-escalation), up to the MTD determined in multiple myeloma (7), on days 1, 8, and 15 of 28-day cycles for up to 12 cycles. Patients with no hematologic response (<PR) after 3 cycles could add dexamethasone. MTD was defined as the highest dose resulting in DLTs during cycle 1 in ≤1/6 patients.

Adverse events were graded using NCI-CTCAE version 4.03 (8). Blood samples were collected for PK analysis during cycle 1: Day 15 pre-dose, and post-dose at 30 minutes, 1 hour, 2 hours, 4 hours, 6 hours, 24 hours (day 16), and 168 hours (day 22). For the hematologic response and amyloid-related organ assessments, response-evaluable patients had received 1 cycle of MLN9708, measurable disease at baseline, and at least 1 post-baseline hematologic response assessment.

RESULTS

At data cut-off (March 27, 2012) 14 patients (5 male, 8 female) had been enrolled to 2 dose cohorts: 4.0 mg cohort (n=9); 5.5 mg cohort (n=5). Of these 14 patients, 13 had received at least one MLN9708 dose and were included in the safety analysis. These patients had a median age of 66 years (range, 54–77) with a median of 3 prior therapies (range, 1–7); 5 patients received prior bortezomib therapy; 8 received a prior IMiD (lenalidomide (n=6) or thalidomide (n=2). Major organ involvement at study entry included kidney (n=8) and cardiac (n=8).

Patients received a median of 3 cycles (range 1–10); 7 patients (54%) received ≥3 cycles and 5 patients (38%) received ≥5 cycles. One patient in the 4.0 mg cohort experienced a DLT (grade 3 thrombocytopenia) and 2 patients in the 5.5 mg dose cohort experienced DLTs (grade 3 diarrhea; grade 2 acute renal failure and dyspnea, and grade 4 cardiac arrest). The MTD was determined to be 4.0 mg. A summary of AEs is shown in Table 1. No AEs resulted in study drug discontinuation and there were no on-study deaths. The most common drug-related AEs included nausea, thrombocytopenia, abdominal pain, and fatigue (Table 2).

Table 1. MLN9708 safety profile

	MLN9708 dose		
Patients, n	**4.0 mg (n=8)**	**5.5 mg (n=5)**	**Total (N=13) n (%)**
Any AE	7	5	12 (92)
Drug-related AE	6	5	11 (85)
Grade ≥3 AE	5	4	9 (69)
Drug-related grade≥3 AE	3	4	7 (54)
Serious AE	3	5	8 (62)
Drug-related serious AE	1	3	4 (31)
AE resulting in study drug discontinuation	0	0	0
On-study deaths	0	0	0

Of 7 response-evaluable patients (6 in the 4.0 mg and 1 in the 5.5 mg cohort) 4 (57%) achieved a hematologic response. Three patients achieved VGPR and 1 achieved partial response (all in the 4.0 mg dose cohort); 3 patients showed no change. To date, duration of hematologic response of up to 8.5 months has been reported. Eight patients remain on treatment, including the 3 patients that achieved VGPR. Five patients have discontinued treatment due to disease progression (n=4) and an unsatisfactory therapeutic response (n=1). Preliminary PK data showed that: MLN9708 was rapidly absorbed, with a median T_{max} of 1 hour (range, 0.5–6

hours); day 15 plasma C_{max} was 52.2 ± 32.4 ng/mL (mean ± SD) and AUC_{0-168} was 1190 ± 740 ng*hr/mL (n=4 at 4.0 mg dose cohort); and AUC from this study was similar to that seen in other MLN9708 studies.

Table 2. Most common all-cause and all-cause grade ≥3 AEs

	MLN9708 dose (n)		
Most common (>20%) all-cause AE, n	**4.0 mg (n=8)**	**5.5 mg (n=5)**	**Total (N=13) n (%)**
Nausea	4	3	7 (54)
Fatigue	3	2	5 (38)
Diarrhea	3	1	4 (31)
Dyspnea	1	3	4 (31)
Thrombocytopenia	3	1	4 (31)
Abdominal Pain	1	2	3 (23)
Decreased appetite	2	1	3 (23)
Edema peripheral	3	0	3 (23)
All-cause grade ≥3 AEs (≥2 patients)			
Dyspnea	1	2	3 (23)
Abdominal pain	1	1	2 (15)
Thrombocytopenia	1	1	2 (15)

DISCUSSION

These preliminary data suggest weekly oral administration of MLN9708 is feasible in patients with rel/ref AL. The MTD of MLN9708 in rel/ref AL was determined as 4.0 mg weekly. Enrollment continues into the MTD/RP2D 2 expansion cohorts: proteasome-inhibitor naïve patients and proteasome inhibitor exposed patients. MLN9708 PK in rel/ref AL appears to be similar to MLN9708 PK in other disease populations. Assessment is ongoing, with preliminary evidence of hematologic responses noted.

ACKNOWLEDGEMENTS

The authors would like to acknowledge all patients involved in this study, their families, and the participating physicians, research nurses, study coordinators, and other research staff. The authors would also like to acknowledge the writing assistance of Helen Wilkinson of FireKite during the development of this poster, which was funded by Millennium Pharmaceuticals Inc.

REFERENCES

1. Kastritis E, et al. J Clin Oncol 2010;28:1031–7.
2. Reece DE, et al. Blood 2011;118:865–73.
3. Kupperman E, et al. Cancer Res 2010;70:1970–80.
4. Fisher RI, et al. J Clin Oncol 2006;24:4867–74.
5. Lee EC, et al. Clin Cancer Res 2011;17:7313–23.
6. Chauhan D, Tian Z, Zhou B, Kuhn D, Orlowski R, Raje N, et al. Clin Cancer Res 2011;17:5311–21.
7. Kumar S, et al. ASCO Annual Meeting Abstracts; 2012. June 1–5; Chicago, IL.
8. U.S. Department of Health and Human Services, National Institutes of Health National Cancer Institute. Common Terminology Criteria for Adverse Events (CTCAE). Version 4.03. 14 June 2010.

Curcumin as a novel natural compound acting as TTR amyloidosis inhibitor in vivo

N. Ferreira [1], M.J. Saraiva [1,2], M.R. Almeida [1,2]

[1] Grupo de Neurobiologia Molecular, IBMC – Instituto de Biologia Molecular e Celular, Rua do Campo Alegre, 823, 4150-180 Porto, Portugal.
[2] Departamento de Biologia Molecular, ICBAS – Instituto de Ciências Biomédicas Abel Salazar, Universidade do Porto, Rua de Jorge Viterbo Ferreira n.º 228, 4050-313 Porto, Portugal.

Many small aromatic compounds acting as inhibitors of amyloid fibril formation have been proposed for the prevention and treatment of transthyretin (TTR) amyloidosis. Herein, we studied the effect of curcumin, one of those compounds, on TTR amyloidogenesis *in vivo*, using a well characterized mouse model for Familial Amyloidotic Polyneuropathy (FAP). Mice were given dietary curcumin or control diet for a six weeks period.

Analysis of plasma proteins after treatment revealed that curcumin selectively competed with thyroxine for the binding to TTR in treated mice increasing plasma TTR stability. Semi-quantitative immunohistochemistry demonstrates that curcumin treated mice present decreased oxidative and apoptotic biomarkers associated with TTR deposition. Most important, curcumin supplementation significantly reduced TTR toxic aggregates throughout the gastrointestinal tract. In conclusion, the present study adds to the number of natural potent TTR amyloid inhibitors and points towards the potential use of curcumin as a lead molecule for the design of new TTR amyloid inhibitors.

INTRODUCTION

Familial Amyloidotic Polyneuropathy (FAP) is a fatal hereditary amyloidosis characterized by systemic extracellular deposition of mutant transthyretin (TTR) amyloid fibrils throughout the connective tissue, affecting predominantly the peripheral (PNS), autonomic and motor nervous system. Although the molecular mechanism underlying TTR amyloidosis is still not completely understood, it is generally accepted that TTR point mutations induce tetramer dissociation into non-native partially unfolded TTR monomers that aggregate into toxic oligomers, form protofibrils and elongate into mature fibrils [1]. Curcumin (diferulomethane), a yellow pigment in turmeric, presents structural similarities with thyroxine (T_4), a physiologic TTR ligand, and has been suggested for the treatment of different neurodegenerative disorders such as Alzheimer's [2]. In the present study, we aim to assess the effect of curcumin on TTR amyloidogenesis *in vivo*, using a well characterized mouse model for FAP.

MATERIALS AND METHODS

Knockout mice for endogenous TTR but expressing human TTR V30M [3] were fed a diet consisting of standard mouse chow with 2% curcumin (w/w) ad libitum over 6 weeks. After this period, mice were sacrificed after anesthesia with ketamine/ medetomidine. Blood samples were collected and competition of curcumin with T_4 for the binding to plasma TTR was assayed by gel electrophoresis as previously described [4]. Plasma TTR resistance to dissociation was assessed by IEF under semi-denaturing conditions according to Ferreira and colleagues [4]. All mice's gastrointestinal tract was excised and frozen at −70 ℃ or fixed in 4% neut ral buffered formalin and embedded in paraffin for light microscopy techniques. Tissues were analyzed by Western blot and semi-quantitative immunohistochemistry (IHC) to detect TTR deposition in tissues and also associated biomarkers, specifically ER-stress marker Bip, Fas death receptor and 3-Nitrotyrosine. The conditions used were as previously described [5].

RESULTS

Curcumin selectively binds to TTR and increases its resistance to dissociation

PAGE analysis of plasma, from treated and control mice, incubated with radiolabelled T_4 (^{125}I-T_4), showed that curcumin strongly competed with T_4 for the binding to plasma TTR, indicating that curcumin selectively interacts with TTR over all thyroxine-binding proteins in plasma. By IEF analysis of plasma samples from treated hTTR V30M and control mice we found that curcumin binding to plasma TTR increases tetramer resistance to dissociation into non-native monomeric species, indicating that curcumin increases TTR conformational stability.

Curcumin decreases TTR load and associated markers in tissues

After curcumin treatment different mice tissues from the gastrointestinal (GI) tract were analysed by immunohistochemistry (IHC) and Western blot analysis. We found that curcumin treated hTTR V30M mice presented a potent reduction of the TTR extracellular load in tissues and a consistent significant reduction of the associated tissue biomarkers. In stomach, the target organ of TTR deposition in this particular mice model, we found a decrease of about 60 % of deposited TTR (Figure 1).

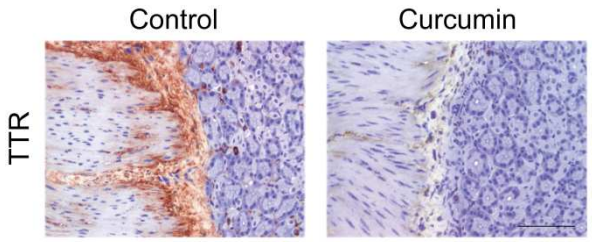

Figure 1. Curcumin treatment decreases TTR deposition in stomach of hTTR V30M mice. Scale bar 100 µm.

DISCUSSION AND CONCLUSION

Recently, we have reported that curcumin strongly suppresses TTR amyloid fibril formation *in vitro* by stabilization of TTR tetramer or by generating small intermediates that are innocuous to cultured neuronal cells [6]. These findings encouraged us to investigate the effect of subchronic supplementation of curcumin *in vivo*,

using well established FAP mice models at different stages of TTR deposition. We observed that curcumin selectively binds to plasma TTR and increases TTR conformational stability. Most important, dietary curcumin lowers TTR toxic aggregate deposition and associated tissue markers in the GI tract of treated FAP mice, namely endoplasmic reticulum (ER)-stress and protein oxidation markers. Although our results indicate that curcumin directly modulates TTR amyloidogenicity we do not disregard that its ability to interfere with multiple signaling pathways involved in inflammation and oxidative stress [7] might synergistically potentiate its anti-amyloidogenic effect *in vivo*. In conclusion, the present study highlights the potential use of curcumin as a lead molecule for the design of new potent TTR amyloid inhibitors.

REFERENCES

1. Quintas A, Saraiva MJ, Brito RM. The amyloidogenic potential of transthyretin variants correlates with their tendency to aggregate in solution. FEBS Lett. 1997; 418(3):297-300.
2. Hamaguchi T, Ono K, Yamada M. Curcumin and Alzheimer's disease. CNS Neurosci Ther. 2010; 16(5): 285-97.
3. Kohno K, Palha JA, Miyakawa K, Saraiva MJ, Ito S, et al. Analysis of amyloid deposition in a transgenic mouse model of homozygous familial amyloidotic polyneuropathy. Am J Pathol 1997; 150: 1497-1508.
4. Ferreira N, Cardoso I, Domingues MR, Vitorino R, Bastos M, Bai G, Saraiva MJ, Almeida MR. Binding of epigallocatechin-3-gallate to transthyretin modulates its amyloidogenicity. FEBS Lett 2009; 583(22): 3569-76.
5. Ferreira N, Saraiva MJ, Almeida MR. Epigallocatechin-3-gallate as a potential therapeutic drug for TTR-related amyloidosis: "in vivo" evidence from FAP mice models. PLoS One. 2012; 7(1):e29933.
6. Ferreira N, Saraiva MJ, Almeida MR. Natural polyphenols inhibit different steps of the process of transthyretin (TTR) amyloid fibril formation. FEBS Lett 2011; 585(15): 2424-30.
7. Goel A, Kunnumakkara AB, Aggarwal BB. Curcumin as "Curecumin": from kitchen to clinic. Biochem Pharmacol. 2008; 75(4):787-809.

Antibody therapy against amyloid forms of transthyretin for familial amyloidotic polyneuropathy

Y. Su[1, 3], H. Jono[1], M. Torikai[2], A. Hosoi[2], K. Soejima[2], J. Guo[1, 3], M. Tasaki[1, 3], Y. Misumi[3], M. Ueda[1], S. Shinriki[1], M. Shono[1], K. Obayashi[1], T. Nakashima[2], K. Sugawara[2], and Y. Ando[1, 3]

[1]Department of Diagnostic Medicine, and [3]Department of Neurology, Graduate School of Medical Sciences, Kumamoto University, Kumamoto, Japan, [2]Research Department 1, Kikuchi Research Center, The Chemo-Sero-Therapeutic Research Institute, Kumamoto, Japan.

Transthyretin (TTR)-related familial amyloidotic polyneuropathy (FAP) induced by amyloidogenic transthyretin (ATTR) is characterized by systemic accumulation of amyloid fibrils. It is believed that altered conformations exposing cryptic regions are intermediary and critical steps in TTR amyloid formation. However, no effective therapy targeting this step is available. In this study, to establish the antibody therapy for FAP, we generated a monoclonal TTR antibody (MAb ATTR), which specifically reacts with surface epitopes of TTR, and evaluated its binding affinity and specificity for TTR amyloid fibrils. MAb ATTR showed specific binding affinity for TTR amyloid fibrils extracted from kidney of V30M patient and induced by acid condition, but not for native forms, indicating that MAb ATTR showed binding affinity and specificity for TTR amyloid fibrils *in vitro* and *ex vivo*. MAb ATTR may have a potential to suppress TTR amyloid formation and become a candidate for the antibody therapy for FAP.

INTRODUCTION

Familial amyloidotic polyneuropathy (FAP), which is induced by amyloidogenic TTR (ATTR), is characterized by systemic accumulation of amyloid fibrils [1, 2]. Although liver transplantation has become a well-established therapy, this therapy has several problems, and no other essential therapies have been practically established [3]. It has been proposed that tetrameric TTR is not itself amyloidogenic, but dissociation of the tetramer into a non-native monomer with low conformational stability can lead to amyloid fibril formation [4]. Previous works have also shown that altered conformations exposing cryptic regions are intermediary and critical steps in the mechanism of TTR amyloid formation [5, 6]. However, no effective therapy targeting this step is available as of this moment. Our previous study showed that the polyclonal TTR antibody, which specifically reacts with surface epitopes only exposed in amyloid forms of TTR, significantly inhibited TTR deposition in transgenic rats possessing human ATTR V30M gene. It suggests that immune therapies targeting these special surface epitopes may be considered as a potential therapeutic strategy for FAP.

In this study, to establish the antibody therapy for FAP, we developed a monoclonal TTR antibody (MAb ATTR), which specifically reacts with the special surface epitopes of TTR. The binding affinity and specificity of MAb ATTR for TTR amyloid fibrils were examined.

MATERIALS AND METHODS

The study followed the guidelines of the ethical committee at Kumamoto University. MAb ATTR was generated by The Chemo-Sero-Therapeutic Research Institute (KAKETSUKEN). Autopsied frozen heart and kidney specimens from FAP ATTR V30M patients were analyzed by Congo red and immunohistochemical staining. TTR amyloid fibrils were extracted from those autopsied frozen kidney tissues from FAP V30M patients. Serum samples were obtained from healthy volunteers and FAP V30M patients. For TTR amyloid fibril formation, TTR were diluted in 50 mM glycine-HCl and 100 mM NaCl at pH 3 and incubated at 37 ℃. To evaluate the binding affinity and specificity of MAb ATTR for serum TTR and TTR amyloid, immunoblotting and ELISA was performed.

RESULTS AND DISCUSSION

We first examined the reactivity and specificity of MAb ATTR for TTR amyloid deposition in the tissue specimens which showed a high incidence of amyloid deposition of FAP ATTR V30M patients. By immunohistochemical staining, the immunoreactivities of MAb ATTR were observed in the heart and kidney specimens from FAP ATTR V30M patients, coincident with those of anti TTR polyclonal antibody. Moreover, MAb ATTR indeed showed the high consistency with Congo red positive areas in those tissue specimens, suggesting that MAb ATTR was able to bind for TTR amyloid fibrils in tissue specimens from FAP ATTR V30M patients specifically.

We next performed immunoblotting and ELISA assay using MAb ATTR to determine the binding affinity and specificity for TTR amyloid fibrils. By immunoblotting, the specific binding affinity of MAb ATTR for both TTR amyloid fibrils extracted from kidney of FAP ATTR V30M patient and induced by acid condition *in vitro* were confirmed, while not for native form of TTR. Moreover, by ELISA assay, MAb ATTR also showed the specific binding affinity for both TTR amyloid fibrils extracted from kidney of V30M patient and induced by acid condition in a concentration dependent manner, but not for native forms of TTRs. Collectively, these data clearly indicates that MAb ATTR shows binding affinity and specificity for TTR amyloid fibrils *in vitro* and *ex vivo*.

In conclusion, MAb ATTR may have a potential to suppress TTR amyloid formation and become a candidate for the antibody therapy for FAP, in addition to liver transplantation and other developing therapies. Further investigation to determine the inhibitory effect of MAb ATTR on TTR amyloid formation and deposition will be required for establishing a novel therapy for FAP.

REFERENCES

1. Ando Y, Nakamura M, Araki S. Transthyretin-related familial amyloidotic polyneuropathy. Arch Neurol. 2005;62:1057–1062
2. Benson MD, Uemichi T. Transthyretin amyloidosis. Amyloid. 1996;3:44–56
3. Ando Y. Liver transplantation and new therapeutic approaches for familial amyloidotic polyneuropathy

(FAP). Med Mol Morphol 2005;38:142-54.

4. Quintas A, Saraiva MJ, Brito RM. The tetrameric protein transthyretin dissociates to a non-native monomer in solution. A novel model for amyloidogenesis. J. Biol. Chem. 1999;274:32943-32949
5. Goldsteins G, Persson H, Andersson K, et al. Exposure of cryptic epitopes on transthyretin only in amyloid and in amyloidogenic mutants. Proc Natl Acad Sci USA. 1999;96:3108–3113
6. Bergström J, Engström U, Yamashita T, Ando Y, Westermark P. Surface exposed epitopes and structural heterogeneity of in vivo formed transthyretin amyloid fibrils. Biochem Biophys Res Commun. 2006;348:532-539.

Green Tea Halts Progression of Cardiac Transthyretin Amyloidosis – A Pilot Study

A.V. Kristen[1], S. Buss[1], D. Mereles[1], H. Steen[1], R. Schreiner[2], P.A. Schnabel[3], R.P. Linke[4], C. Röcken[5], E.E. Wanker[6], T. J. Dengler[1], K. Altland[7], H.A. Katus[1]

[1]*Department of Cardiology, Angiology, and Respiratory Medicine, INF 410, D-69120 Heidelberg, Germany*
[2]*Laboratory of Dr. Limbach and Associates, Im Breitspiel 15, D-69126 Heidelberg, Germany*
[3]*Institute of Pathology; Heidelberg University, INF 220/221, D-69120 Heidelberg, Germany*
[4]*Reference Center of Amyloid Diseases, amYmed, Am Klopferspitz 19, D-82152 Martinsried, Germany*
[5]*Institute of Pathology, Christian-Albrechts-University, Arnold-Heller-Straße 3/14, D-24105 Kiel, Germany*
[6]*Max Delbrück Center for Molecular Medicine, AG Neuroproteomics, D-13092 Berlin, Germany*
[7]*Institute of Human Genetics, Giessen University, Schlangenzahl 14, D-35392 Giessen,* Germany

ABSTRACT

Epigallocatechin-3-gallate, the most abundant catechin in green tea (GT), inhibits fibril formation from transthyretin (TTR) in vitro. It might halt progression of TTR-related amyloidosis. In total 19 patients with cardiac TTR amyloidosis were evaluated by echocardiography and cardiac MRI (n=9) while consuming GT for 12 months. Patients were not followed-up for reasons of death (n=2), discontinuation of GT consumption (n=2), and heart transplantation (n=1). After consumption of GT for 12 months no increase of LV wall thickness and LV myocardial mass was observed by echocardiography. In the subgroup of patients evaluated by cardiac MRI a decrease of LV myocardial mass was detected in all patients resulting in a mean decrease of -12.5%. This was accompanied by an increase of mitral annular systolic velocity (9%). No serious adverse side-effects were reported. GT appears to represent a promising therapeutic tool to halt the progression of cardiac amyloid load in patients with cardiac TTR amyloidosis.

INTRODUCTION

Cardiac ATTR amyloidosis is associated with distinct mutations in the TTR gene also known as familial amyloid cardiomyopathy (FAC) and represents the major complication of in patients of advanced age with familial amyloid polyneuropathy (FAP). Wild-type TTR (SSA) has been found in 25 % of post-mortem cardiac biopsies from patients older than 85 years [3]. Pre-mortem diagnosis is rare, but prevalence appears to be underestimated. By routine scintigraphic skeletal imaging SSA has been detected in 2 males among 374 consecutive admissions older than 60 years, indicating a prevalence of about 0.5 % [4].

Treatment concepts for patients with advanced cardiac involvement in TTR amyloidosis are still limited. Patients with advanced cardiac amyloidosis are deemed ineligible for liver transplantation due to high treatment-

related mortality. Furthermore, progression of cardiac amyloid deposition has been observed rather frequently after liver transplantation [7]. Heart transplantation is limited to patients at age < 65 years.

Recent in vitro experiments have shown that epigallocatechin-3-gallate (EGCG), the most abundant catechin in green tea (GT), efficiently inhibits fibril formation from TTR [15] and converts existing fibrils into non-fibril conformers [16]. In a FAP transgenic mouse model a reduction of amyloid deposition was observed after treatment with 100 mg EGCG per kg body weight per day over a period of six weeks [17].

METHODS

In total, 19 patients (15 male, 4 female, 66±3 years) with hereditary (n=10) or wild-type (n=9) cardiac ATTR amyloidosis and compensated heart failure were observed over a period of 12 months while consuming GT and/or GT extract. All patients had biopsy-proven ATTR. In addition to cardiac involvement there was clinical evidence for involvement of gut (n=4), and/or peripheral nerves (n=8). NYHA heart failure class was 2.0±0.2.

Patients were evaluated by routine protocols of echocardiography and cardiac MRI (cMRI). Follow-up control was performed 12 months after study inclusion. All echo and cMRI were evaluated independently by 3 expert investigators blinded by time point.

All patients were asked for a daily intake of approximately 500-700 mg EGCG either by drinking 2 liters of GT per day (10 g/L Green Darjeeling, FTGFOP1, Teekampagne Projektwerkstatt GmbH, Berlin, Germany; brewed 3-5 min at 100℃, and containing about 340 mg EGCG/ L [32]) or by the intake of caffeine-free GTE capsules (praevent-loges®, Dr. Loges+Co GmbH, Winsen/Luhe, Germany, 75 mg EGCG/capsule).

RESULTS

During the study period 5 patients were lost either due to death (n=2), or discontinuation of GT (n=2), or heart transplantation (n=1). Due to prior placement of cardiac pacemaker (n=2), internal defibrillator (n=1), orthopaedic prosthesis (n=1), or claustrophobia (n=1) cMRI images were obtained only from 9 of the 14 study patients. Modified BMI was 1080 ± 46. TTR types were Val30Met (n=8), Gly47Glu (n=1), Gly47Ala (n=1), Ile107Val (n=1), SSA (n=6). The main clinical demographics of the 14 patients with 12 months follow-up are shown in Table 1. Mean oral EGCG intake was calculated as 547±49 mg per day. No serious adverse effects were reported. During the observation period mean total cholesterol and LDL cholesterol decreased from 191.9 ± 8.9 mg/dL to 172.7 ± 9.4 mg/dL ($p<0.01$) and from 105.8 ± 7.6 mg/dL to 89.5 ± 8.0 mg/dL ($p<0.01$), respectively. Mean HDL cholesterol remained unchanged (58.9 ± 3.9 mg/dL to 55.4 ± 4.6 mg/dL).

During 12 months of GT/GTE intake a significant decrease by 6.5% of the thickness of IVS was observed. Thickness of IVS decreased in 12/14 patients, remained unchanged in 1 patient and increased 2 mm in 1 patient. Mean LV myocardial mass remained stable during the observational period of GT/GTE intake. A significant improvement of the mean systolic velocity of the lateral mitral annulus was observed (improved in 10/14 patients; diminished in 4/14 patients). Inter-observer variability of echocardiography was 7.6%. By cMRI we observed a significant average decline of LV myocardial mass by 12.5%. LV ejection fraction remained unchanged (57±5% vs. 57±4%; n. s.). Intra-observer variability of MRI was 4.2%.

DISCUSSION

This is the first single center observation of myocardial parameters during daily consumption of EGCG as GT(E) in patients with cardiac ATTR amyloidosis. No progression of cardiac wall thickness and mass as indicators of ATTR amyloid deposition was observed during the one year observation period.

Laboratory experiments have shown that EGCG binds to recombinant wild type as well as variant TTR tetramers at three sites different from the thyroxine binding site (1). Using a transgenic mice model an inhibitory effect of EGCG on amyloid deposition as well as a degrading effect on preformed amyloid fibrils was demonstrated (2). The described data, however, were achieved using a 10 to 100 fold excess of EGCG over TTR, far above the observed plasma concentration (0.5 µM) and applied doses (1 mmol) of EGCG in this trial. The binding sites of EGCG have been described to be different from tafamidis. Thus a combined treatment with GT/GTE and tafamidis may complement each other and increase the observed beneficial effects against the major problems of ATTR amyloidosis patients.

Cardiac MRI has been used as an endpoint in several interventional studies, either for reduction of left ventricular mass, e. g. arterial hypertension (5), and M. Fabry (6). In the present cohort the reduction of LV myocardial mass by cMRI was more pronounced than the blinded inter-observer variability, but appears to be slow. However, improved mitral annulus velocity was observed as the most accurate diastolic measure to detect early LV dysfunction in patients with AL amyloidosis (7).

Progression of left ventricular wall mass within a time span of one year was observed in a different group of untreated patients with mutant ATTR and cardiac involvement (3). It is well known that left ventricular mass varies within the mutation involved, with age at onset of the disease. Survival of patients with cardiac TTR amyloidosis appears to be much better than survival of patients with light-chain amyloidosis (4). There is, however, a wide variation of 5-year survival rates for patients with different TTR mutations (30 to 55%) and among patients with wild-type TTR amyloidosis (40 to 75%). The patients in Benson's study group (3) were about 12 years younger than the patients of our cohort and included individuals with mutations different from those of our patients. Therefore, the results of Benson's and our present study may not be comparable in a clean scientific approach. The lack of an appropriate control group will affect a final conclusion from the present observation.

GT has been proven beneficial by consumption for several thousands of years by many millions of individuals and is part of the daily routine in the Far East without any reported side-effects. Therefore, its use may be of interest for FAC patients and those at age beyond 65 years with no access to heart transplantation. Randomized, placebo-controlled investigations with longer study periods and larger samples of patients should confirm the results of this observation, determine the optimal dosage of GT/GTE for treatment, and identify undesirable side effects.

REFERENCES

1. Ferreira N, Cardoso I, Domingues MR, et al. Binding of epigallocatechin-3-gallate to transthyretin modulates its amyloidogenicity (2009) FEBS Lett 19;583:3569-3576.
2. Ferreira N, Saraiva MJ, Almeida MR. Epigallocatechin-3-gallate as a potential therapeutic drug for TTR-related amyloidosis: "in vivo" evidence from FAP mice models (2012) PLoS ONE 7:e29933.
3. Benson MD, Teague SD, Kovacs R, et al. Rate of progression of transthyretin amyloidosis (2011) Am J Cardiol 108:285-289.

4. Rapezzi C, Merlini G, Quarta CC, et al.. Systemic cardiac amyloidoses: disease profiles and clinical courses of the 3 main types (2009) Circulation 120:1203-1212.
5. Reichek N, Devereux RB, Rocha RA, et al.. Magnetic resonance imaging left ventricular mass reduction with fixed-dose angiotensin-converting enzyme inhibitor-based regimens in patients with high-risk hypertension (2009) Hypertension 54:731-737.
6. Hughes DA, Elliott PM, Shah J, et al. Effects of enzyme replacement therapy on the cardiomyopathy of Anderson-Fabry disease: a randomised, double-blind, placebo-controlled clinical trial of agalsidase alfa (2008) Heart 94:153-158.
7. Al Zahrani GB, Bellavia D, Pellikka PA, et al. Doppler myocardial imaging compared to standard two-dimensional and Doppler echocardiography for assessment of diastolic function in patients with systemic amyloidosis (2009) J Am Soc Echocardiogr 22:290-298.

SOM0226: A reprofiled drug intended for the prevention and treatment of familial transthyretin amyloidosis

M. Centellas[1], A. Planas[2], N. Reig[1], N. Gavaldà[1] and R. Insa[1]

[1] SOM Biotech, Barcelona Science Park, University of Barcelona, Barcelona, Spain. [2] Laboratory of Biochemistry, Institut Químic de Sarrià, University Ramon Llull, Barcelona, Spain

ABSTRACT

SOM0226 is a reprofiled drug intended for the treatment and prevention of familial transthyretin amyloidosis (ATTR). The drug has been identified by virtual screening and tested *in vitro* by a kinetic turbidity assay. SOM0226 shows a greater effect as a fibril formation inhibitor than the reference compound tafamidis, recently approved by EMA. SOM0226 is a drug approved for a non-amyloidogenic indication with an available pharmacology and safety profile in humans. As a repositioned drug, SOM0226 can bypass much of the early cost and time needed to bring a drug to market and is currently ready to initiate a clinical phase II proof of concept study in ATTR patients.

INTRODUCTION

Familial Transthyretin Amyloidosis (ATTR) is a rare disease caused by mutations in the TTR gene. It is characterized by a misfolding of the TTR protein that leads to its aggregation and deposition as amyloid fibrils in nerves and heart leading to a slowly progressive neuropathy, cardiomyopathy and nephropathy. ATTR can result in severe wasting, immobility and death within 5-15 years after symptoms first develop.

Currently, the only effective therapy for ATTR is the liver transplantation, which removes the main production site of the amyloidogenic protein. Also, tafamidis - a benzoxazole derivative - has recently obtained a conditional approval for the treatment of ATTR in the EU.

SOM0226 is a reprofiled compound identified by SOM Biotech by virtual screening, which presents a more cost-effective therapeutic alternative to the liver transplantation and a better efficacy and well-known safety profile than the benzoxazole derivative.

The compound has been evaluated *in vitro* and *ex vivo* for this indication. Also it has been thoroughly tested *in vivo* and clinically for the current marketed indication, allowing a faster and less risky development process in the new orphan indication. SOM0226 is currently ready to initiate clinical Phase II Proof of Concept studies in ATTR patients.

METHODS.

In silico ligand-based and receptor-based virtual screening: Tafamidis physicochemical and target binding properties were compared with a chemical database comprising molecules that are or have been used in humans. Thirty compounds were selected to be tested *in vitro*.

SOM0226 has been tested using a kinetic turbidity assay specifically developed to identify potential TTR inhibitors (1). A rapid evaluation of potential amyloid fibril inhibitors (1.5 h) was carried out using the highly amyloidogenic Y78F mutant of human transthyretin. Recombinant mutant protein was treated with different concentrations of inhibitor (from 0 to 40 µM) and fibril formation was induced by lowering the pH. Aggregate formation was detected by monitoring absorbance. Tafamidis was used as a reference compound. The parameters studied were the inhibitor concentration at which the initial rate of fibril formation is one-half than without inhibitor (IC50), and RA (%), the percent reduction of fibril formation rate at high inhibitor concentration relative to the rate without inhibitor.

RESULTS

A potent fibril formation inhibitor according to this assay is defined as having values of IC50 below 20µM and RA (Amyloidosis Reduction) over 80%.

Table 1. Results of turbidimetric kinetic assay.

Compound	IC50 (µM)	RA (%)	n	Fibril formation inhibitor
SOM0226	4.8	90	4	Potent inhibitor
Reference compound				
Tafamidis	16.9	99	6	Potent inhibitor
Bibliographic data (1)				
Diflunisal	16.3	87	4	Potent inhibitor
Flurbiprofen	>50	44	4	Poor inhibitor

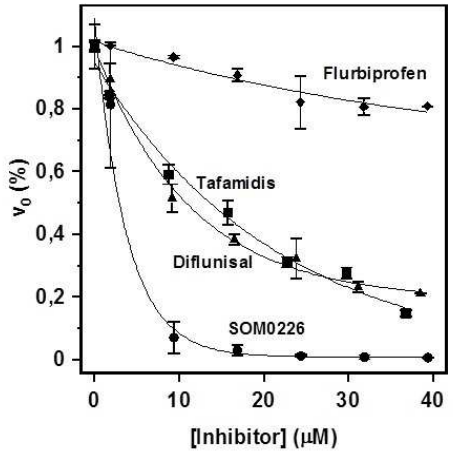

Figure 1. Relative initial rates of fibril formation (V_0%) against inhibitor concentration.

DISCUSSION

SOM0226, a drug already approved for a non amyloidogenic indication for chronic use, has been identified by SOM's *in silico* platform as a potent TTR amyloid fibril inhibitor *in vitro*. Specifically, SOM0226 is four times more active than Tafamidis (*Vyndaqel*®) in a kinetic turbidity assay and thus presents a promising alternative to current treatments for the orphan disease ATTR.

The potential of SOM0226 as a treatment for ATTR has been recently confirmed by a variety of cellular and *ex vivo* assays designed to study the efficacy of SOM0226 at the different steps of the TTR amyloid fibril formation process. The efficacy of SOM0226 is superior to tafamidis in all the experiments performed, confirming its potential for the treatment of ATTR. A clinical proof of concept study is planned to start in 2013 to evaluate the efficacy of SOM0226 in patients suffering from ATTR.

ACKNOWLEDGEMENTS

SOM Biotech is a drug reprofiling company located at the Bioincubator Santander of the Barcelona Science Park. SOM Biotech would like to thank the following institutions for funding support: "Generalitat de Catalunya (ACC10 and AGAUR)", "Ministerio de Sanidad y Consumo" and "Ministerio de Ciencia e Innovación".

REFERENCES

1. Dolado I et al.; J. Comb. Chem.; 2005;7;246-252.

RNAi therapy using cholesterol-conjugated siRNA for TTR-related ocular amyloidosis

M. Tasaki[1,4], H. Jono[1], A. Sugasaki[1], M. Ueda[1], R. Hara[2], K. Obayashi[1], T. Kawaji[2], H. Tanihara[2], D. Sah[3], Y. Fan[3], T. Yamashita[4], Y. Ando[1,4]

[1]Department of Diagnostic Medicine, Graduate School of Medical Sciences, Kumamoto University, Kumamoto, Japan. [2]Department of Ophthalmology and Visual Science, Graduate School of Medical Sciences, Kumamoto University, Kumamoto, Japan. [3]Alnylam Pharmaceuticals, Inc. [4]Department of Neurology, Graduate School of Life Sciences, Kumamoto University, Kumamoto, Japan.

ABSTRACT

Transthyretin (TTR)-related familial amyloidotic polyneuropathy (FAP) is characterized by systemic accumulation of amyloid fibrils caused by a point mutation in the TTR gene. In FAP patients, ocular manifestations are commonly found and cause loss of visual acuity. It has been reported that amyloidogenic TTR (ATTR) synthesized by retinal pigment epithelium (RPE) plays an important role in the progression of ocular manifestations. In this study, we generated a cholesterol-conjugated TTR (Cho-TTR) small interfering RNA (siRNA) against TTR to effectively suppress TTR expression and evaluated its effect both *in vitro* and *in vivo*. Cho-TTR siRNA markedly reduced TTR mRNA expression in human RPE cell line (ARPE-19). In *in vivo* examinations, Cho-TTR siRNA efficiently and sustainably reduced the expression of TTR in the RPE and aqueous humor at both mRNA and protein levels. Taken together, these data suggest that Cho-TTR siRNA treatment may represent a novel therapeutic strategy for TTR-related ocular amyloidosis.

INTRODUCTION

Familial amyloidotic polyneuropathy (FAP) is systemic amyloidosis characterized by amyloid deposition caused by amyloidogenic transthyretin (ATTR). Because ATTR is mainly produced by liver, liver transplantation that eliminates ATTR production, is currently the only promising therapy to prevent progression of clinical symptoms in FAP patients (1). However, ocular manifestations such as abnormal conjunctival vessels, pupillary abnormalities, vitreous opacity, and glaucoma progressively worsen even after liver transplantation (2), because the retinal pigment epithelium (RPE) cells independently produce ATTR (3). Therefore, new therapeutic strategies to prevent the progression of ocular manifestations are urgently needed. Our previous studies showed that retinal laser photocoagulation, which reduced the RPE cells, prevented the progression of amyloid deposition in the vitreous, indicating that effective suppression of ATTR expression in the RPE cells may became a novel therapy for ocular amyloidosis (4).

RNA interference (RNAi) is a sequence-specific gene-silencing mechanism triggered by double-stranded RNA and offers a powerful tool for gene function study and RNAi therapy. Our previous data showed that an siRNA directed against TTR significantly reduced TTR expression both *in vitro* and *in vivo*. However, the effect of siRNA persisted for only a short time.

In this study, since it has been reported that cholesterol-conjugated siRNA effectively knocked down target gene expression in the RPE cells (5), we generated a cholesterol-conjugated TTR siRNA (Cho-TTR siRNA) designed for improving knockdown effect and evaluated its effect both *in vitro* and *in vivo*.

METHODS

Chemically modified Cho-TTR and control siRNAs were kindly provided by Alnylam Pharmaceuticals, Inc. (Cambridge, MA, USA). The effect of siRNA on TTR expression was evaluated by real-time quantitative PCR (qRT-PCR) and ELISA. ARPE-19 cells were transfected with siRNA using Lipofectamine 2000 (Invitrogen) *in vitro*. For *in vivo* examinations, we used DA (normal) rats. siRNAs were administered by direct intravitreal injection. After 14 and 21 days, the RPE and aqueous humor were isolated to evaluate the effect of siRNA on TTR expression. To assess inflammatory response, inflammatory cytokine (IL-6, IL-1β, TNF-α) expression was measured by qRT-PCR. In addition, isolated ocular specimens were fixed in formalin, embedded in paraffin, and stained with hematoxylin and eosin to evaluate morphologically any potential effect of intravitreal siRNA administration on the retina.

RESULTS

We first evaluated the effect of Cho-human TTR siRNA on TTR expression in ARPE-19 cells. Cho-human TTR siRNA significantly reduced TTR expression in a dose-dependent manner. To evaluate the effect of the siRNA *in vivo*, we injected siRNA into the eyes of DA rats. Cho-rat TTR siRNA potently knocked down endogenous rat TTR mRNA expression in the RPE 14 days after intravitreal injection compared with previous data. Moreover, even at 21 days after Cho-TTR siRNA injection, TTR mRNA and protein levels remained potently suppressed in the RPE and aqueous humor. In addition, no significant inflammatory responses and no histological change were observed on the retina.

DISCUSSION

In this study, we provide direct evidence that Cho-TTR siRNAs efficiently and sustainably reduced the expression of TTR in the RPE at both mRNA and protein levels, and was well-tolerated *in vivo* when administered intravitreally. Since it is well-documented that cholesterol-conjugated siRNA potently reduced target gene expression in the liver (6) and RPE (5), these results suggest that TTR siRNA were efficiently induced into RPE cells by cholesterol-modification, which in turn, effectively suppressed TTR expression compared to TTR siRNA directed against TTR. Our previous studies have shown that ocular manifestations were prevented by reducing about 30% of whole RPE cells by retinal laser photocoagulation in FAP patients (4). Because our results clearly showed that Cho-siRNA could suppress TTR levels about 40-50% *in vivo*, Cho-siRNA treatment by intravitreal injection may represent a promising therapeutic strategy for TTR-related ocular amyloidosis. Further investigation to determine how to efficiently deliver the siRNA to the RPE cells or evaluate

the effect of intraviteal siRNA administration on the retina will be required for establishing a novel therapy for ocular amyloidosis.

REFERENCES

1. Ando Y, Tanaka Y, Ando E, Yamashita T, Nishida Y, Tashima K, Suga M, Uchino M, Ando M. Effect of liver transplantation on autonomic dysfunction in familial amyloidotic polyneuropathy type I. Lancet. 1995;345:195-6.
2. Hara R, Kawaji T, Ando E, Ohya Y, Ando Y, Tanihara H. Impact of liver transplantation on transthyretin-related ocular amyloidosis in Japanese patients. Arch Ophthalmol. 2010 Feb;128:206-10.
3. Cavallaro T, Martone RL, Dwork AJ, Schon EA, Herbert J. The retinal pigment epithelium is the unique site of transthyretin synthesis in the rat eye. Invest Ophthalmol Vis Sci. 1990;31:497-501.
4. Kawaji T, Ando Y, Hara R, Tanihara H. Novel therapy for transthyretin-related ocular amyloidosis: a pilot study of retinal laser photocoagulation. Ophthalmology. 2010;117:552-5.
5. Kleinman ME, Yamada K, Takeda A, Chandrasekaran V, Nozaki M, Baffi JZ, Albuquerque RJ, Yamasaki S, Itaya M, Pan Y, Appukuttan B, Gibbs D, Yang Z, Karikó K, Ambati BK, Wilgus TA, DiPietro LA, Sakurai E, Zhang K, Smith JR, Taylor EW, Ambati J. Sequence- and target-independent angiogenesis suppression by siRNA via TLR3. Nature. 2008;452:591-7.
6. Soutschek J, Akinc A, Bramlage B, Charisse K, Constien R, Donoghue M, Elbashir S, Geick A, Hadwiger P, Harborth J, John M, Kesavan V, Lavine G, Pandey RK, Racie T, Rajeev KG, Röhl I, Toudjarska I, Wang G, Wuschko S, Bumcrot D, Koteliansky V, Limmer S, Manoharan M, Vornlocher HP. Therapeutic silencing of an endogenous gene by systemic administration of modified siRNAs. Nature. 2004;432:173-8.

SECTION IX

LOOKING FOR CONSENSUS IN DIAGNOSIS AND THERAPY


Der AA Church

Early detection of amyloid and its reporting: where are we and where are we heading?

Maria M. Picken, Bouke P. Hazenberg, Per Westermark

Department of Pathology, Loyola University Medical Center, Chicago, USA
Department of Rheumatology & Clinical Immunology, University Medical Center Groningen, Groningen, The Netherlands
Rudbeck Laboratory, Department of Immunology, Genetics and Pathology, Uppsala University, Uppsala, Sweden

Amyloidosis is a rare disease and its diagnosis presents a continuing challenge. Despite many advances in our knowledge concerning various types of amyloid and the steady development of treatments, amyloid diagnosis continues to be tissue-based: it relies overwhelmingly on the Congo red stain, which has been in use since 1922. It is increasingly evident that the early detection of amyloid is essential for the success of various treatments; moreover, there is also evidence that tissue damage has already occurred in the pre-amyloidotic phase. Hence, now, more than ever before, early diagnosis is imperative.

This report, which is based on a consensus session held during the XIIIth International Symposium on Amyloidosis, addresses several possibilities for improvement in the early diagnosis of amyloid, including the following: (i) possible improvements in the Congo red stain itself leading to increased sensitivity; (ii) the use of other stains as alternatives (or in addition) to Congo red; and (iii) the wider application of fat biopsies, not only to the initial, generic diagnosis but also to subsequent patient management. Recommendations for the diagnosis & reporting of amyloid, incorporating the response of the audience to 10 questions asked during the meeting session, are also included. Future developments, including alternatives to tissue diagnosis and the Congo red stain, are briefly mentioned here as they are discussed elsewhere in this book.

For the diagnosis of amyloid, a Congo red stain viewed under polarized light is still considered to be the gold standard (1). While advanced amyloid can be suspected on a routine (H&E) stain as an accumulation of amorphous eosinophilic material, early deposits may be inconspicuous and a high index of suspicion is needed to examine sections with Congo red stain. The stain, and its interpretation under polarized light, are not entirely straightforward and are not general-pathologist-friendly. Demonstration of the diagnostic “green birefringence” requires good optics, strong light source, an appropriate environment for reading and an experienced pathologist. Thus, an easier method, which would allow not only earlier detection but possibly also the screening of large numbers of cases, would be highly desirable.

IMPROVED CONGO RED STAIN

The improved Congo red stain, based on the 1962 modification by Puchtler, was recently proposed by Per Westermark as an alternative (1). For this, a saturated solution of Congo red and NaCl in 80% ethanol is prepared, filtered and diluted 1:10 with saturated NaCl in 80% ethanol. One ml of 1% NaOH is added to 100 ml of the stain solution and sections are stained for 60 min (or more, even overnight), before being dehydrated and mounted. A microscope with a strong light source and good polarizers, as well as an experienced examiner, are required. The main advantage of this improved method is the absence of background stain.

CONGO RED AS A FLUOROCHROME

The Congo red stain itself can act as a fluorochrome and this feature has been successfully used for the detection of amyloid since the middle of the last century. Interestingly, a Congo red stain viewed under fluorescent light is more sensitive than one viewed under polarized light. In part, this is due to the fact that, in fluorescent light, the *entire* area with amyloid is visualized. This is in contrast to Congo red stained sections examined under polarized light, where only a portion of the amyloid is highlighted, while other parts are obscured by the *soi-disant* "polarization shadow". Only by rotating the microscope stage can these obscured parts be demonstrated, while, in turn, those parts which were previously seen will now become obscured. The "polarization shadow" phenomenon decreases the sensitivity of detection of Congo red/polarization and may make the detection of small deposits particularly challenging. On the other hand, this phenomenon can even help in amyloid detection by rotating the polarizer back and forth. If this is done, small amyloid spots appear as "twinkling stars". But this practice requires experience. Thus, while examination of Congo red stained slides under polarized light may barely detect small deposits of amyloid, the latter are much more easily visible in the same sections examined under fluorescence light. This technique has been used since the 1940-50s and Linke has written extensively about the advantages of this method (2). Various filters can be used (FITC, TRITC, TEXAS RED) depending on the personal preference of the investigator. However, Congo red fluorescence is not entirely specific; hence, the verification of results by Congo red polarization is highly recommended (3). Other stains are less sensitive and less specific. For example, SAB (sulphated alcian blue) stains GAGs (glycosaminoglycans) rather than the actual amyloid fibrils.

THIOFLAVIN STAINS

Thioflavin T has been in use as a potent fluorescent marker of amyloid for histology since 1959 (recently reviewed in 4). It selectively localizes to amyloid deposits, thereupon exhibiting a dramatic increase in fluorescent brightness. The sensitivity of the Thioflavin stain is superior to that of the Congo red stain, in part due to elimination of the "polarization shadow" phenomenon. The binding of the dye is linked to the presence of cross-β structure in the fibrils and the mechanism of action is explained by the "channel" model, where Thioflavin binds to β-sheets along surface side-chain grooves that run parallel to the long axis of the β-sheet. In Thioflavin stains (T or S) a distinct bright yellow-green fluorescence highlights the *entire* amyloid-containing area, without the equivalent of a "polarization shadow". The stain is viewed using a standard fluorescence microscope with either an FITC or DAPI filter. The stain can be applied either to paraffin or frozen sections. While the stain fades over time, the slides can be re-stained. The Thioflavin stain is easy to perform, the outcome is predictable and the interpretation is straightforward. Thioflavin stains are, however, not entirely

specific for amyloid and, besides amyloid, also stain fibrin, keratin and other structures. Thus, a confirmation of the findings by the Congo red stain itself may be needed. These drawbacks notwithstanding, the addition of a Thioflavin stain to the staining protocol may be helpful in the clinical diagnosis of amyloid. Thioflavin stain is a particularly useful option for renal- and dermato-pathologists who are familiar with fluorescence microscopy. Thioflavin derivatives have also been tested as alternative amyloid stains in the medical imaging of amyloid in living patients and have been used extensively in research (4).

Among the audience, 63.8% of respondents used the Congo red stain with polarization (exclusively or predominantly), while 16.1% used Congo red stain-polarization in combination with Congo red-fluorescence. Only 6% used Thioflavin. 11.6% of respondents used all of these methods. Only 2.5% of respondents used other methods. While 48.1% of respondents used a commercial stainer and a commercial Congo red staining solution, 36.1% used their own Congo red stain. The remaining respondents used either their own other stain (4.4%), electron microscopy (9.8%) or sent out slides for staining elsewhere (1.6%).

FAT TISSUE FOR SCREENING, DIAGNOSIS AND BEYOND

Abdominal subcutaneous fat tissue is easily aspirated at the bedside using readily available materials (see: www.amyloid.nl). When a 16 gauge needle is used, adequate quantities (about 100-200 mg) of tissue can easily be obtained. A positive Congo red stain with apple-green birefringence in polarized light is still the gold standard for detection of amyloid. Specificity is high and reaches almost 100% in experienced hands. However, if only minute amyloid deposits are present, supportive evidence should be obtained before the patient receives any treatment with potentially high toxicity. Also, AIns (insulin) amyloidosis should be excluded in patients with diabetes mellitus. AIns is an iatrogenic amyloid in which insulin-derived amyloid is deposited in abdominal fat tissue after repeated insulin injections at that particular site. Sensitivity is variable (54-93%) and depends on the adequacy of the tissue specimens, the quality of staining, the number of glass slides, the number of observers, and the time taken for careful observation. Pooled data have shown the sensitivity and specificity to be 79% and 97%, respectively, with a positive predictive value of 94% and a negative predictive value of 87% (5).

While the typing of amyloid is now considered mandatory, the immunohistochemical staining of subcutaneous fat tissue is fairly difficult due to non-specific reactions. Nonetheless, immunofluorescence on frozen sections and immuno-electron microscopy have been applied successfully to this problem. Several immunochemical methods, such as enzyme-linked immunosorbent assay (ELISA) and Western blot analysis, have been developed for typing amyloid in fat tissue with useful results. In Groningen, immunochemical methods are used to quantify the concentration in fat tissue of the four major amyloid proteins, i.e. amyloid A protein (> 11.6 ng/mg tissue), TTR (> 4.36 ng/mg fat tissue), light chain kappa (> 24.4 ng/mg fat tissue), and light chain lambda (> 10.6 ng/mg fat tissue) (5). The application of proteomics-based techniques to fat tissue has proven its utility and has also shown promise in the detection of changes in amino acid sequence and composition, specific mutations and variants, and the assessment of relative amounts of mutated versus wild-type proteins. The detection and diagnosis of amyloid type, with confidence (and with the exclusion of other types), occurs with a high sensitivity (87%) and specificity (98%). The role of wild-type protein, variants and mutants of amyloidogenic proteins, the role of enzymatic cleavage and other modifications of precursor proteins, and the role of amyloid constituents such as SAP, laminin, entactin, collagen IV, and GAGs in the formation, deposition, and removal of amyloid may also be studied in fat tissue using proteomics methods.

Monitoring the quantity of amyloid deposition in tissue may help us to learn more about the balance between accumulation and break-down of the total amyloid load of the body. Subcutaneous abdominal fat tissue is suitable for this purpose because it is easily available by aspiration, amyloid can almost always be found if present, and aspiration can be repeated at intervals during the course of the disease. A semi-quantitative scoring system has been developed using visual estimation of the percentage of the smear surface area affected by deposition of amyloid, as recognized in polarized light: 0 - 4+. Grading the amount of amyloid in fat tissue helps to type amyloidosis with confidence: thus, in nearly all patients with grade 3+ and 4+ amyloid in fat tissue, immunochemical quantification reliably typed amyloid as AA, ATTR, AL-kappa, and AL-lambda. In contrast, the chance of reliably typing patients with grade 2+ amyloid is much lower (about 50%) and in only a minority of patients with grade 1+ (about 10%) is typing successful. More amyloid has been found in the fat tissue of women than of men; however, a satisfactory explanation for this increased deposition of all types of amyloid in the fat tissue of women is lacking. The amount of amyloid in subcutaneous fat tissue in systemic amyloidosis reflects the severity of disease in different groups of patients (5).

Of particular interest are the findings associated with amyloid deposits from the fat tissue of patients with a TTR-Val30Met mutation in transthyretin. Thus, amyloid fibrils that are formed exclusively from the full-length TTR protein were found to be associated with an early age of disease onset, the absence of cardiac involvement, and a strong affinity of the fibrils for the Congo red stain. In contrast, amyloid fibrils that are composed of TTR protein fragments are associated with the opposite clinical characteristics.

Proteomic analysis showed that, in patients with ATTR amyloidosis who had not undergone liver transplantation, the ratio of wild-type TTR to Val30Met TTR in amyloid fibrils was higher in older patients (>50 years) than in younger patients. Furthermore, the percentage of wild-type TTR in amyloid derived from fat tissue increased significantly (up to 90-100%) after transplantation; this compares to pre-transplantation values of 35-60%. It is known that, in pre-transplant patients, cardiac amyloid more easily incorporates wild-type TTR than does fat-tissue amyloid. This offers an explanation for the susceptibility of cardiac tissue for continued accumulation of amyloid after liver transplantation. In fat tissue, a rapid increase in the proportion of wild-type TTR after liver transplantation indicates a rapid turnover of the deposits (6).

If the amount of amyloid in fat tissue does indeed reflect disease severity, it may be interesting to study the effect of treatment on this. Thus, in patients with AL amyloidosis, for whom at least two different fat tissue aspirates were available for analysis, a significant decrease in amyloid deposition in fat tissue was seen after normalization of serum free light chains: a two-grade reduction of amyloid deposition in fat tissue was seen in 50% of these patients after 2.4 years and in 80% after 3.2 years. This rapid and significant regression of amyloid deposition in fat tissue was accompanied by stabilization or improvement of organ disease (7).

The results for questions on this topic posed during the meeting session were as follows: for fat biopsy, 63.9% of respondents used fine needle aspiration, while 15.1% used skin punch biopsy, 10.2% used surgical fat biopsy and 7.2% used all of the above. 3.6% used other biopsies (salivary gland, rectal?).

For fat biopsy, regardless of type, only 23.9% of respondents provided/received an “amyloid score”, i.e. a semi-quantitative estimate of the amyloid content.

FUTURE PROSPECTS – SCREENING, DIAGNOSIS AND TYPING

The structural typing of systemic amyloidoses by luminescent-conjugated polymer spectroscopy, and the use of oligothiophenes as fluorescent ligands for spectral assignment of protein aggregates are discussed elsewhere in this book.

ALTERNATIVES TO TISSUE BIOPSY:

While amyloid can be detected in various body fluids (urine, synovial fluid), the detection of unique urinary exosomes may be potentially applicable to screening for AL in the future (8, 9). For now, however, fat tissue continues to be the best choice for screening.

REPORTING

The assessment of organ involvement and response to therapy in AL has been in use for several years and has since undergone several modifications as well as validation. A similar process was initiated in Rome for ATTR amyloidosis and is under development for other types of amyloidosis as well (please see the reports from other consensus sessions held during this symposium). However, unlike the clinical organ-involvement definition, which is amyloid type dependent, the pathologic definition should preferably be applicable to all amyloid types, especially since the actual amyloid type is frequently unknown at the time of diagnosis.

For fat assessment, a scoring system has been in place for several years (please see above) and, currently, at least one fourth (23.9%) of respondents provided/received an “amyloid score”. For bone marrow biopsy in AL patients, a scoring system has been used for the purposes of mobilization of stem cells, bone marrow reconstitution, etc (10). In this system, a 1+ score is assigned if amyloid is present in vessels only, while interstitial amyloid is assigned a score of 2+ or 3+ if amyloid involves <2/high-power field or >2/hpf, respectively. However, for universal, i.e. amyloid type-independent, bone marrow biopsy reporting, a distinction should be made between stromal (interstitial) marrow versus vascular-only versus involvement of only peri-osseous structures. In such a “universal” bone marrow scoring procedure, only stromal amyloid would be subjected to scoring since it represents “true” marrow involvement. Thus far, this issue has not been addressed and, therefore, currently, no universal, i.e. amyloid type-independent, criteria for bone marrow involvement are in use. At the consensus session, for amyloid reporting, 83.3% of respondents requested the inclusion of information that listed the structures involved, i.e. bone marrow itself (stroma) versus vessels-only and/or peri-osseous amyloid. For the involvement of other organs, such as kidney, heart and liver, a *simple* and reproducible scoring system needs to be developed and implemented for general use. For kidney amyloidosis, one proposal has been published, but has not been widely adopted or validated (11).

For the diagnosis of amyloid in general, 82% of respondents required information regarding the method used to diagnose amyloid (Congo red stain versus other stains) and amyloid distribution (vascular, stromal).

Interestingly, almost all respondents (97.1%) voted for the inclusion of a semi-quantitative estimate of the amount of amyloid (“amyloid score”) for all specimens (36.5%) or, individually, for either fat, bone marrow or liver biopsies, or in various combinations (60.6%).

In general, it is important to distinguish between stroma/interstitial amyloid versus vascular only. For gastrointestinal biopsies, only interstitial amyloid constitutes true pathologic organ involvement, while vascular-limited amyloid is insufficient. A diagnosis of amyloidosis is based on biopsy of an affected organ *or* biopsy at an

alternate site. The latter typically includes abdominal fat and/or biopsy of the minor salivary glands, rectum, or gingiva. However, for gastrointestinal tract, lungs, skin and muscle, direct biopsy verification is required, if symptoms are present.

Based on the response from the audience, fat and kidney biopsies were most often diagnostic (36.1 and 34.7% respectively) while cardiac, gastrointestinal and other sites were diagnostic in 7.6%, 6.3% and 15.3% of cases, respectively. Tissue diagnosis of amyloid was made by the pathologist in 78.1% and by the clinician in 16.8% of cases, and in 5.2% by other. The main impediment to the early diagnosis of amyloidosis was the lack of clinical suspicion (86.7% of cases), while the inexperience of the pathologist was responsible in 6.1% of cases, with late biopsy, insensitive stain and other being responsible in 2.8, 2.8 and 1.7%, respectively.

RECOMMENDATIONS FOR EARLY DIAGNOSIS AND SCREENING IN PATHOLOGY

(i) the use of methods that increase the sensitivity of screening for amyloid, such as Congo red-fluorescence and Thioflavin stains, is encouraged although Congo red stain/polarization continues to be considered the “gold standard” for the diagnosis of amyloid,
(ii) an increase in the frequency of screening by fat biopsy,
(iii) an increase in the frequency of amyloid investigation through the examination of native kidney biopsies, native cardiac biopsies, bone marrow biopsies, peripheral nerve biopsies, gastrointestinal biopsies and, possibly, also through carpal tunnel procedures,
(iv) an engagement in efforts to introduce and clinically validate new and emerging methods for the diagnosis of amyloidosis

RECOMMENDATIONS FOR REPORTING IN PATHOLOGY

The following information should be included in the pathology report:
(i) anatomic site (if known),
(ii) histologic structure(s) (if known, list *all*),
(iii) distinction between vascular-limited versus stromal; distinctive patterns should be also described (glomerular versus extraglomerular, sinusoidal versus portal, interstitial versus endocardial, etc),
(iv) scoring should be provided for fat, according to established criteria (scoring for bone marrow, liver, kidney is currently under discussion/development),
(v) method (stain) by which amyloid was diagnosed

REFERENCES

1. Westermark P. Methods Mol Biol 2012;849:363-71.
2. Linke RP. Virchows Arch 2000;436:439-48
3. Picken MM. In: Amyloid and related disorders in surgical pathology and clinical correlations. Ed: MM Picken, A Dogan, GA Herrera, Springer, 2012, pp 209-217
4. Biancalana M, Koide S. Biochim Biophys Acta 2010 Jul;1804(7):1405-12
5. Bijzet J, van Gameren II, Hazenberg BP. In: Picken MM, Dogan A, Herrera GA, Amyloid and Related Disorders: Surgical Pathology and Clinical Correlations. New York: Springer, 2012:191-207.

6. Ihse E, Suhr OB, Hellman U, Westermark P. J Mol Med. 2011;89:171-180.
7. van Gameren II, van Rijswijk MH, Bijzet J, Vellenga E, Hazenberg BP. Haematologia. 2009;94:1094-1100.
8. Picken MM. Diagnosis of amyloid in urine cytology specimens. XIIIth Int Symposium on Amyloidosis
9. Ramirez-Alvarado M, Ward CJ, Huang BQ, Gong X, Hogan MC, Madden BJ, Charlesworth MC, Leung N. PLos One, 2012;7(6):e38061. Epub 2012 Jun 18
10. Cowan AJ, Seldin DC, Skinner M, Quillen K, Doros G, Tan J, O'Hara C, Finn KT, Sanchorawala V. Biol Blood Marrow Transpant 2012 Jul 27 [Epub ahead of print]
11. Sen S, Sarsik B. Arch Pathol Lab Med 2010;134:532-44.

Looking for Consensus: Organ Involvement and Response Criteria in AL

M.A Gertz[1], A. Wechalekar[2], G. Palladini[3]

Division of Hematology, Mayo Clinic[1], Centre for Amyloidosis and Acute Phase Proteins, University College London Medical School, UK[2], Amyloidosis Research and Treatment Center Foundation "Istituto di Ricovero e Cura a Carattere Scientifico (IRCCS) San Matteo" Pavia[3]

NEW CRITERIA FOR RESPONSE TO TREATMENT IN AL AMYLOIDOSIS: IMPACT ON SURVIVAL OUTCOMES

On the occasion of the 12th International Symposium on Amyloidosis (Rome, 2010) the Consensus Panel of the International Society of Amyloidosis initiated a study to establish the criteria for hematologic and cardiac response to treatment in AL amyloidosis based on survival outcomes. The criteria were identified on a testing population of 816 patients retrospectively collected from the database of 7 referral centers in the European Union and in the United States and then validated on an independent series of 374 patients diagnosed at the Pavia Amyloidosis Research and Treatment Center. The impact on survival of the response criteria was assessed in a landmark analysis.

The validated criteria for hematologic response are reported in Table 1. The criteria are based on the difference between the involved (amyloidogenic) and uninvolved circulating free light chain (dFLC). A new category, very good partial response (VGPR) was introduced, based on the absolute value of dFLC reached after treatment. VGPR confers a distinct significant survival advantage over PR, emphasizing the direct link between the concentration of the amyloidogenic precursor and patients' outcome. The adopted criterion for VGPR discriminated better patients with a good outcome compared to other criteria based on dFLC percent reduction.

Table 1. Hematologic response criteria

New response criteria	Definition	Estimated 2-year survival (6-month landmark)	P
Complete response	Negative serum and urine immunofixation and normal FLC κ/λ ratio	95%	-
Very good partial response	dFLC <40 mg/L	85%	0.01
Partial response	dFLC decrease >50%	60%	<0.001
No response	All other patients	35%	<0.001

dFLC, difference between the involved (amyloidogenic) and uninvolved circulating free light chain; FLC, circulating free light chain.

Decreases or increases in N-terminal pro-natriuretic peptide type-B (NT-proBNP) that were both >30% and >300 ng/L were significantly associated with survival, and were adopted as criteria for cardiac response and progression, respectively. Other criteria of cardiac response and progression were identified and validated (Table 2). Interestingly, there was no survival advantage for patients who achieved a 2 mm or more reduction in interventricular wall thickness at echocardiography (P=0.800), which historically was considered a criterion of cardiac response to treatment.

Table 2. Cardiac response and progression criteria

New criteria	Definition	Estimated 2-year survival (6-month landmark)	P
NT-proBNP response	>30% and >300 ng/L decrease if baseline NT-proBNP ≥650 ng/L	90%	<0.001
NT-proBNP progression	>30% and >300 ng/L increase	35%	<0.001
cTn progression	≥33% increase	60%	<0.001
NYHA class response	≥2 class decrease if baseline NYHA class 3 or 4	35%	0.001
EF progression	≥10% decrease	50%	0.007

cTn, cardiac troponin; NT-proBNP, N-terminal pro-natriuretic peptide type-B; NYHA, New York Heart Association.

This study provides for the first time a prognostic correlation of the criteria of hematologic and cardiac responses in AL amyloidosis in a large international population. Our data support the use of early response measures that can be obtained with simple and readily available techniques, as the primary validated surrogate endpoint for clinical trials in newly diagnosed patients with AL amyloidosis, allowing for simpler study designs and enabling clinical trials to be completed more quickly.

DISEASE STAGING IN AL AMYLOIDOSIS – A MOVING TARGET

A number of staging systems have been reported in AL amyloidosis (Table 3). A simple system using the level of N-terminal fragment of brain natriuretic peptide (NT-proBNP) and cardiac troponin-T or I (TNT or TNI) has been widely used since 2004 (1) - patients with both biomarkers abnormal had a median survival of just three months and consequently have been excluded from prospective trials. Recently, a high troponin assay (hs-TNT) has become available and is likely to be adopted by most laboratories. An hs-TNT cut-off of >0.05 µg/L has the same prognostic significance as a standard troponin cut-off of >0.03 ng/ml (2). This new threshold should be used to define “abnormal” troponin in context of AL staging if the hs-TNT assay is used. Hs-TNT levels are also independently prognostic in AL (3). In patients with stage III AL, a very high NT-proBNP level and a low systolic blood pressure, at presentation, defines a very poor prognostic subgroup with median survival of 3 months – benefits of chemotherapy remain uncertain in this high risk subgroup (4) although other stage III patients with none or one of high risk features appear to benefit from chemotherapy if they can achieve an excellent hematological response (CR or VGPR).

It has become increasing apparent that the FLC level is important in determining the disease outcome. A revised classification using a combination of presenting dFLC, NT-proBNP and TNT stratifies AL into four stages and provides a more accurate disease classification (5). However, the threshold of biomarkers is different from the previous reports. The genetic abnormalities in plasma cells are also of significance and presence of 1q gain is an independent marker of poorer outcomes (6).

In summary, we have tools for better prognostic disease classification of AL amyloidosis based on the disease related organ involvement, the level of free light chains and the biology of plasma cells. The prognostic markers for relapsed patients remain to be defined. An integrated data set will be developed with a view to validating these markers and moving a new and unified method of disease stratification.

Table 3. Staging systems in AL amyloidosis

Staging system	Stages	Median survival
Standard "Mayo" Staging (1) (NT-proBNP >332 ng/L and TNT >0.03 ng/ml)	Stage I (both < threshold)	26 months
	Stage II (either > threshold)	10 months
	Stage III (both > threshold)	3.5 months
Revised Mayo Staging (5) (dFLC 18mg/L, NT-proBNP >1800 pg/ml, TNT >0.025ng/ml)	Stage I (all below threshold)	94 months
	Stage II (any one > threshold)	40 months
	Stage III (any two > threshold)	14 months
	Stage IV (all three > threshold)	5.8 months
NT-proBNP and SBP in stage III (4) (NTproBNP >8000 ng/L; SBP <100 mm of Hg)	No risk factors	26 months
	One risk factor	6 months
	Two risk factors	3 months
Hs-Troponin only (2) (<14 ng/ml, >14 but <54ng/ml; >54 ng/ml)	Stage I (hs-TNT low)	71 months
	Stage II (hs- TNT intermediate)	43 months
	Stage III (Hs TNT high)	6 months
Chr 1q gain (6)	Present	12.5 months
	Absent	38 months

There are no criteria that will allow one to distinguish localized from systemic pulmonary amyloid. Other than obtaining a lung biopsy that shows amyloid deposits, mechanisms that quantify systemic pulmonary amyloid have not been defined by the amyloidosis community. Criteria for soft tissue involvement, including purpura, arthropathy, claudication, tongue involvement, and myopathy are all clinical criteria, and no consensus exists as to when one of these organs are involved. The amyloidosis community will remain challenged until uniform criteria are established.

As studies of amyloid move forward, understanding what constitutes response and progression is essential. The neurologic criteria that were used for trials in familial amyloid polyneuropathy may or may not be acceptable in the treatment of light chain amyloidosis and neuropathy. The role of EMG is not defined in assessing response and progression in the small non-myelinated fiber neuropathy seen in amyloid. It is unclear whether or not soft tissue amyloid, pulmonary amyloid or GI amyloid improves the way cardiac, hepatic, and renal involvement improves. It is unclear whether this is due to an inability to measure organ response.

REFERENCES

1. Dispenzieri A, Gertz MA, Kyle RA, et al. Journal of clinical oncology. 2004 Sep 15;22(18):3751-7.
2. Palladini G, Barassi A, Klersy C, et al. Blood. 2010 Nov 4;116(18):3426-30.
3. Dispenzieri A, Gertz MA, Saenger AK, et al. ASH Annual Meeting Abstracts. No 18, 2011;118(21):2887.
4. Wechalekar A, Schonland SO, Kastritis E, et al. ASH Annual Meeting Abstracts. Nov 18, 2011;118(21):995.
5. Kumar S, Dispenzieri A, Lacy MQ, et al. Journal of clinical oncology. 2012 Mar 20;30(9):989-95.

6. Bochtler T, Hegenbart U, Benner A, et al. ASH Annual Meeting Abstracts. Nov18, 2011;118(21):3946

Organ involvement and response criteria in non-AL amyloidosis: with special attention to peripheral neuropathies and cardiomyopathy in ATTR amyloidosis

Ingemar S.J. Merkies[1], Laura Obici[2], and Ole B Suhr[3]

[1]Department of Neurology, Maastricht University Medical Centre, Maastricht and Spaarne Hospital, Hoofddorp, the Netherlands
[2]Amyloidosis Research and Treatment Centre, IRCCS Fondazione Policlinico San Matteo, Pavia, Italy
[3]Department of Public Health and Clinical Medicine, Umeå University, Umeå, Sweden.

INTRODUCTION

Of the non-AL amyloid diseases, transthyretin amyloidosis (ATTR) is the most common. Clinical manifestations in the hereditary forms are predominantly those of neuropathy and/or cardiomyopathy, whereas cardiomyopathy dominates the clinical picture of wild-type ATTR. Since new therapeutic interventions are emerging, high quality outcome measures are needed to monitor the effectiveness of these interventions. In the following, we will recapture the essential topics of the consensus panel discussion on organ involvement and response criteria in non-AL amyloidosis.

NEUROPATHY

Peripheral neurological disorders such as neuropathic ATTR cause impairments (weakness and/or sensory deficits), which lead to problems in daily life and social functioning with decrement in quality of life expectations (1-3). Choosing proper outcome measures should therefore be considered as one of the most important, fundamental parts of preparing clinical studies in neuropathic ATTR. However, selection of outcome measures is not only dependent on the proposed research purposes, but also, and perhaps more importantly, on the fulfilment of the scientific needs by these measures (4). A thorough and comprehensive evaluation of an outcome measure is needed to determine its simplicity, communicability, validity and reliability before it is used as an outcome measure (4-6). Moreover, outcome measures should be unambiguously constructed and represent only one of the outcome levels according to World Health Organisation international classification of Functioning, Disability and Health (ICF) and quality of life concept (7).

Various neurological outcome measures have been proposed in ATTR studies, but no systematic evaluation has been conducted to determine the scientific soundness of these scales in this condition. The Neuropathy Impairment Scale (NIS), has gained particular interest and has been used in a recent trial in hereditary (V30M) ATTR (8). However, the NIS, a neurological composite measure capturing the findings as part of neurological examination, is an ordinal measure based on the classical test theory (CTT) with many disadvantages despite

its worldwide recognition as a 'proper' neurological scale (9).

Outcome measures based on classical test theory

Outcome measures like NIS fulfil the complete spectrum of clinimetric needs (4,9). However, DeVellis has published a comprehensive review highlighting the pros and cons of CTT based outcome measures and the reader of this abstract is kindly requested to appraise this paper (9). In brief, CTT based outcome measures like the NIS, have been constructed by arbitrarily recruitment of items, which seem logical, but without examining the impact (weight or significance) of each of the items being part of the scale. In addition, each item has Likert-based response options (e.g., for muscle strength examination: 0: normal, 1: 25% weakness, 2: 50% weakness, 3: 75% weakness, 3, 25: move against gravity, 3.5: movement eliminating gravity, 3,75: muscle flicker, 4: paralysis) assuming a 'true' numerical distance in the ordinal setting of the scale, which is highly unlikely. In other words, a 1 point change from 0 to 1 is considered equivalent to a 1 point change from 2 to 3, which is incorrect, since the scale is ordinal based and not at the interval or linear level. In addition, a sum score is generally computed from the obtained values for each item, assuming a linear setting and subjecting these scores to parametric analyses, which is also incorrect. The interpretation of sum scores in ordinal based measures, like in the NIS, suggests that the whole may not equal the sum of its parts (10). These limitations hamper accurate measurement of differences in scores and changes over time and proper comparison between for example two arms of treatment (9).

Shifting from a classic to a modern clinimetric approach

The NIS has never been subjected to modern clinimetric analyses, like the Rasch methodology (11, 12). The Rasch model enables the transformation of ordinal obtained scores into interval/linear measures that are scale independent and suitably accurate for individual patient assessment. The Rasch method, although seemingly mathematically complex, is simply based on the following logical assumption: individuals with high levels of whatever is being measured (for example: "the ability to accomplish daily activities") should have an increased probability, relative to individuals with low levels of ability, of getting a better score on any items. In other words, item response patterns of individuals are compared to the entire sample examined to estimate person ability and item difficulty and places item estimates as well as person estimates on the same logit figure (see figure 1). Rasch has many clinical benefits, since it gives a true reflection of disease impact, differences between both individuals and groups, and treatment effects. These constructed measures are considered, after having fulfilled all model's expectations, more proper for parametric analyses in chronic conditions like ATTR.

Finally, to date no scale has been constructed at any level for ATTR using modern clinimetric approach. With all attention directed towards potential new therapeutic agents, the lack of attention by neurologists for proper development of outcome measures for this illness, as seen in almost all other neurological chronic conditions, has been highly neglected. Therefore, the ATTR and neurology communities are persuaded to act fast and to develop proper measures for the assessment of the neurological consequences and possible therapeutic effects of new agents. The Rasch method can be used to accomplish this, and perhaps as part of a consensus meeting on outcome measures in FAP.

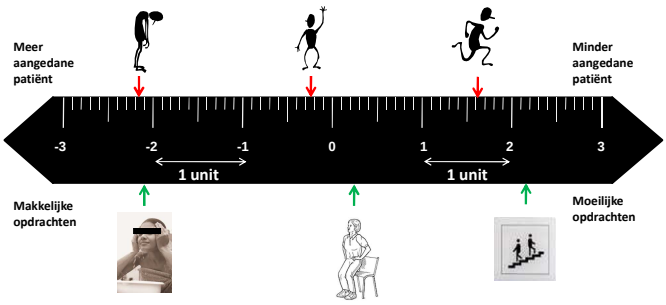

Figure 1. Using linear measures instead of ordinal scores would give a true reflection of disease impact, differences between individuals and groups, and treatment effects. The corresponding weights ("location") of the items and patients are also calculated by the model depending on the interaction between the items and patients and placed on one ruler (see also reference 15 and its supplemental material explaining in a simplistic way the Rasch method to neurologist, which is also suitable for every medical doctor; this reference shows the construction of a Rasch-built overall disability scale in inflammatory neuropathies and the same procedure can be done for the ATTR patients).

CARDIOMYOPATHY

Cardiac biomarkers

Although most centers routinely use cardiac biomarkers NT-proBNP, BNP and troponin I or T in patients with ATTR, limited studies are available on their diagnostic and prognostic significance. In patients with ATTR, BNP and NT-proBNP levels tend to be less elevated compared to AL, in spite of higher mean LV wall thickness and LV mass, suggesting different mechanisms of heart damage. Moreover, there is variability among TTR variants.

In one study, the diagnostic performance of BNP in detecting ATTR heart involvement was 93% when defined as a mean left ventricular wall thickness of 12 mm or more, and 81% in patients with abnormal basal septal strain (13). NT-proBNP detected amyloid heart disease in 80 % ATTR patients in another series (14). The prognostic significance of these biomarkers in ATTR remains to be elucidated. In a recent study of 60 patients carrying the Ala60 variant, NT-proBNP concentration at diagnosis was an independent predictor of survival (15). In another study of 84 patients with ATTR associated with 18 different TTR mutations, progression of NT-proBNP at 6 months, defined as ≥30% and ≥300 ng/L changes, was an independent predictor of survival, irrespective of the underlying TTR variant (14).

Overall, natriuretic peptides do not seem to detect ATTR heart involvement at an early stage as in AL amyloidosis. However, NT-proBNP could be a valuable prognostic marker. Differently from AL, no diagnostic and prognostic relevance has been found to date for cardiac troponins in ATTR (13, 14). In light of upcoming treatments there is a huge need for a novel, non-invasive gold-standard method to predict survival and/or

development of symptomatic heart disease in ATTR amyloidosis. Large cohort studies should be undertaken to further characterize and validate the diagnostic and prognostic significance of cardiac biomarkers and novel imaging techniques in ATTR.

Imaging techniques

Cardiovascular magnetic resonance examination of the heart with late gadolinium enhancement has been utilised for detection cardiac amyloid disease, though the reported number of patients with ATTR and follow-up examinations are too low to make any solid conclusions on its usefulness for follow-up of ATTR patients (16, 17). In addition, the relatively high percentage of patients with pacemaker implants limits its use and may limit its usefulness in follow-up studies.

Echocardiography is an easily available method for heart examination, but even though several findings, such as highly sparkling echoes can suggest the presence of amyloid heart disease, the findings are not specific. In addition, the measurements of heart dimensions, such as inter-ventricular septal thickness are examiner dependent, and for follow-up purposes, reading of the individual patient's echoes by one investigator is mandatory to achieve reliable measures. However, since new computerised imaging techniques, such as left ventricular global strain rate measurements are less observer dependent they appear promising tools for follow-up purposes (18).

Scintigraphic heart examination, utilising 99mTc-diphosphono-propanodicarboxylic acid (99mTc-DPD) or Tc-99m pyrophosphate has demonstrated excellent results. The examination is readily available, and DPD-scintigraphy has demonstrated high sensitivity and specificity for ATTR (19, 20). It should have potential for follow-up purposes, but this has bot been demonstrated in any study so far.

The consensus from the audience suggested MR and computerised echocardiographic examinations to be used in clinical trials of ATTR cardiomyopathy.

CONCLUSIONS

It appears to be of vital importance to construct a proper outcome measure for neurological impairment in ATTR, an outcome measure that preferable is based on linear measures constructed by the Rasch method instead of ordinal scores. For cardiomyopathy, the data available so far are too scarce to recommend any method. However NT.-pro BNP together with newly developed computerised echo analysis such as global strain measurements and MR examination with late gadolinium enhancement appeared to be the most acceptable methods based on currently available data.

REFERENCES

1. Merkies IS, Lauria G. 131st ENMC international workshop: selection of outcome measures for peripheral neuropathy clinical trials 10-12 December 2004, Naarden, The Netherlands. Neuromuscul Disord. 2006;16(2):149-56. Epub 2006/01/25.
2. Merkies IS, Schmitz PI, van der Meche FG, Samijn JP, van Doorn PA. Quality of life complements traditional outcome measures in immune-mediated polyneuropathies. Neurology. 2002;59(1):84-91.
3. Merkies IS, Schmitz PI, van der Meche FG, Samijn JP, van Doorn PA. Connecting impairment, disability,

and handicap in immune mediated polyneuropathies. J Neurol Neurosurg Psychiatry. 2003;74(1):99-104.

4. Streiner DL, Norman GR. Health measurement scales. A practical guide to their development and use. New York: Oxford University Press; 1995.
5. Feinstein AR. Clinimetrics. New Haven and London: Yale University Press; 1987.
6. Liang MH. Evaluating measurement responsiveness. J Rheumatol. 1995;22(6):1191-2.
7. Organisation WH. International classification of impairments, disabilities, and handicaps. . Geneva 2001.
8. Coelho T, Maia LF, Martins da Silva A, Waddington Cruz M, Plante-Bordeneuve V, Lozeron P, et al. Tafamidis for transthyretin familial amyloid polyneuropathy: A randomized, controlled trial. Neurology. 2012;79(8):785-92..
9. DeVellis RF. Classical test theory. Med Care. 2006;44(11 Suppl 3):S50-9.
10. Stucki G, Daltroy L, Katz JN, Johannesson M, Liang MH. Interpretation of change scores in ordinal clinical scales and health status measures: the whole may not equal the sum of the parts. J Clin Epidemiol. 1996;49(7):711-7.
11. Rasch G. Probabilistic models for some intelligence and attainment tests. Chicago: University of Chicago Press; 1960.
12. Tennant A, Conaghan PG. The Rasch measurement model in rheumatology: what is it and why use it? When should it be applied, and what should one look for in a Rasch paper? Arthritis Rheum. 2007;57(8):1358-62.
13. Suhr OB, Anan I, Backman C, Karlsson A, Lindqvist P, Morner S, et al. Do troponin and B-natriuretic peptide detect cardiomyopathy in transthyretin amyloidosis? J Intern Med. 2008;263(3):294-301.
14. Obici L, Palladini G, Perlini S, Musca F, Salinaro F, Russo P, et al. NT-proBNP is a novel and powerful prognostic marker for transthyretin amyloidosis (abstract). Amyloid 2010;17, suppl 1.:P 65.
15. Sattianayagam PT, Hahn AF, Whelan CJ, Gibbs SD, Pinney JH, Stangou AJ, et al. Cardiac phenotype and clinical outcome of familial amyloid polyneuropathy associated with transthyretin alanine 60 variant. Eur Heart J. 2012;33(9):1120-7.
16. Perugini E, Rapezzi C, Piva T, Leone O, Bacchi-Reggiani L, Riva L, et al. Non-invasive evaluation of the myocardial substrate of cardiac amyloidosis by gadolinium cardiac magnetic resonance. Heart. 2006;92(3):343-9.
17. Maceira AM, Prasad SK, Hawkins PN, Roughton M, Pennell DJ. Cardiovascular magnetic resonance and prognosis in cardiac amyloidosis. J Cardiovasc Magn Reson. 2008;10(1):54. Epub 2008/11/27.
18. Gustafsson S, Ihse E, Henein MY, Westermark P, Lindqvist P, Suhr OB. Amyloid Fibril Composition as a Predictor of Development of Cardiomyopathy After Liver Transplantation for Hereditary Transthyretin Amyloidosis. Transplantation. 2012. Epub 2012/03/08.
19. Perugini E, Guidalotti PL, Salvi F, Cooke RM, Pettinato C, Riva L, et al. Noninvasive etiologic diagnosis of cardiac amyloidosis using 99mTc-3,3-diphosphono-1,2-propanodicarboxylic acid scintigraphy. Journal of the American College of Cardiology. 2005;46(6):1076-84.
20. Rapezzi C, Quarta CC, Guidalotti PL, Pettinato C, Fanti S, Leone O et al. Role of (99m)Tc-DPD scintigraphy in diagnosis and prognosis of hereditary transthyretin-related cardiac amyloidosis. JACC Cardiovasc Imaging 2011;4: 659-70.

SECTION X

AMYLOIDOSIS DIAGNOSIS AND RESEARCH WORKSHOP

(SPONSORED BY SPECTRAL IMAGING)


Thursday

Overview and Applications of Spectral-Imaging Microscopy with a Focus on Analysis of LCP-Coupled Amyloid Deposits

Per Hammarström[1], Peter Nilsson[1], Chanan Sluszny[2] (on behalf of the LUPAS consortium)

[1]IFM-Department of Chemistry, Linkoping University, Sweden and [2]Applied Spectral Imaging, Migdal HaEmek, Israel

NOVEL AGENTS & METHODS FOR DIAGNOSTIC IMAGING OF AMYLOID

The LUPAS project (Luminescent conjugated Polymers for in vivo Amyloid Signatures) develops novel agents and methods for diagnostic imaging of amyloid deposits. The project is funded through the EU FP-7 – Health program and entails six partner sites from Academia and two from industry with participants from France, Germany, Israel, Norway, Sweden and Switzerland (1).

The novel imaging tools and reporter molecules, used in this research project, are focused on luminescent conjugated probes (LCPs) based on oligo-thiophenes. Please see separate chapter by Nilsson for a description of this class of molecules.

It is well established that LCPs can bind effectively to animal and human amyloid deposits with striking fluorescence contrast (2, 3). In addition the binding results in structural alterations of the LCP, which cause the probe to respond optically, providing an optical fingerprint that, can be readily recognized. Several hyperspectral imaging technologies could be used to record LCP fluorescence bound to amyloid deposits in tissue sections. Within LUPAS we have chosen to predominately record the spectral output using the SpectraView® system from ASI. Hence the spectral output, as recorded by the SpectraView® system (Figure 1), works as a surrogate marker of the aggregated protein structure. This feature is a rather direct way of identifying amyloid structure heterogeneities within the same tissue and even to enable classification of distinct amyloid deposits between individuals.

SPECTRAL IMAGING – ADDRESSING THE NEEDS IN MICROSCOPY & CELL BIOLOGY

Why use hyperspectral imaging? Spectral imaging combines imaging and spectroscopy, providing complete spectrum at every location (pixel) of the image (Figure 2). Image 1 represents the difference between typical imaging and spectral imaging. In the first case (typical imaging), each pixel in the image represents the intensity (i.e, fluorescence, transmittance, etc) related with the specific acquired image. In the second case (spectral imaging), information inside each pixel provides a complete spectrum for the VIS to NIR range (Figure 2). This latter information can be used for a variety of applications, which provides chemical and spatial information related with LCP-labeled amyloid deposits.

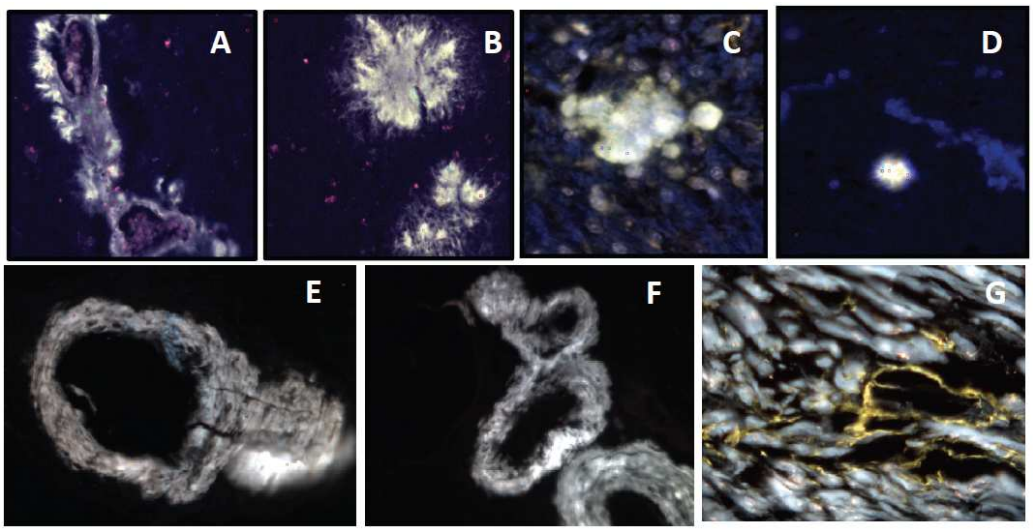

Figure 1. *Hyper spectral images from an ASI SpectraView® system of LCP stained A) Cerebrovascular amyloid angiopathy (Aβ) B) Alzheimer senile plaque (Aβ) C) Chronic wasting disease (APrP) and D) BSE (APrP), in transgenic mouse models. E) Liver amyloisosis (AL), F) Kidney amyloid (AA), G) Cardiac amyloid (ATTR).*

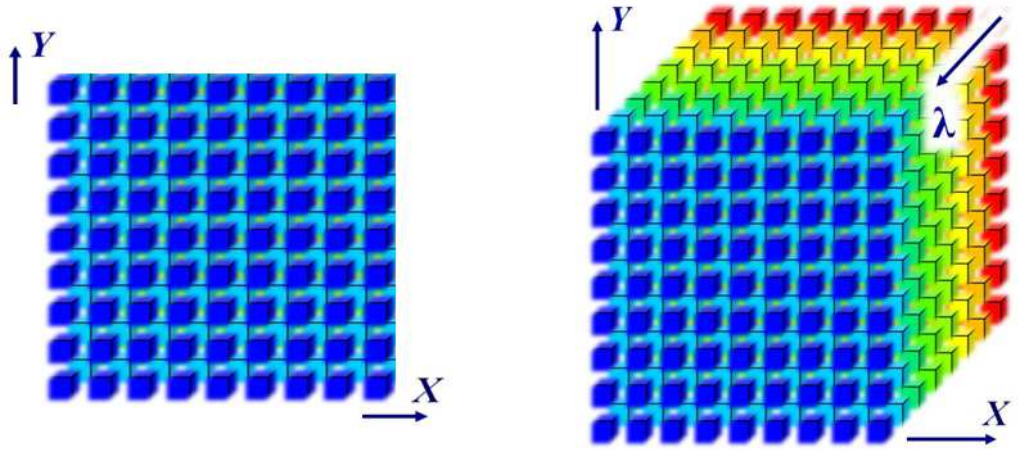

Typical Imaging: Intensity @ each pixel *Hyperspectral Imaging: Spectrum @ each pixel*

Figure 2. Typical imaging vs. spectral imaging

FOURIER-BASED SPECTROSCOPY

How does it work? Schematics of the spectral imaging setup of ASI is shown in figure 3. The system is based on common-path Sagnac interferometry.

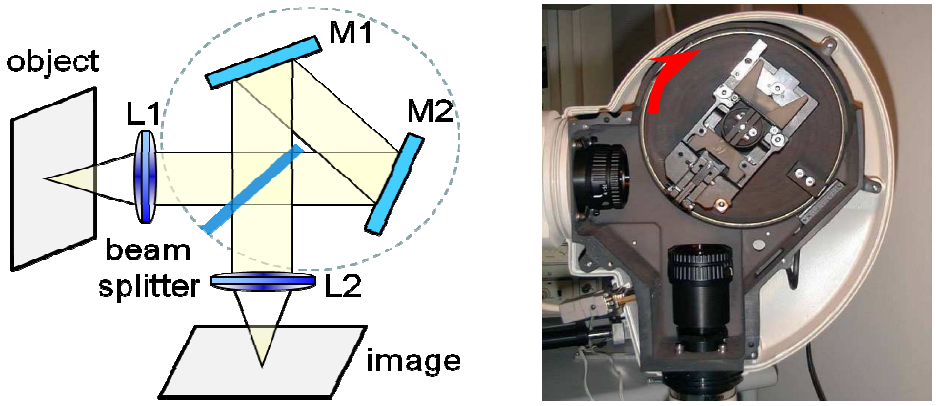

Figure 3. Sagnac Fourier-based spectroscopy.

ADVANTAGES OF THE FOURIER-BASED INTERFEROMETER

The Fourier-based interferometer with the Sagnac configuration provides various advantages, including:

- Wide spectral range: 400-1000 nm
- High spectral resolution: 5 nm @ 400 nm
- Transmission efficiency >80% @ 450-800nm
- Flat spectral response (dependent on CCD response)
- No polarization effects
- High dynamic range: 16bit spectral data representation
- Supports brightfield, fluorescence and reflectance applications
- Direct view available (with all spectral content)

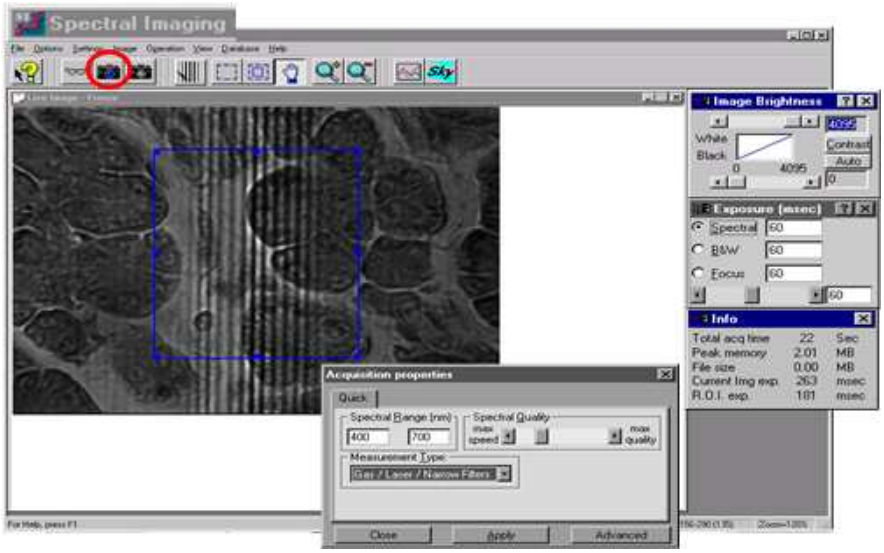

Figure 4. Acquisition of a spectral image

ACQUISITION AND ANALYSIS OF A SPECTRAL IMAGE

Acquisition of a spectral image is performed as shown below in figure 4. Parameters related with spectral resolution, ROI and various other parameters can easily be modified according to the specific application of each user.

SOFTWARE FOR ANALYSIS OF SPECTRAL IMAGES

Hyperspectral images recorded by the system can be analyzed using the SpectraView software. A specific software tutorial for LCP stained sections have been developed within the LUPAS project to facilitate analysis of such specimens (Figures 5-6).

FEATURES

Spectra View includes a variety of analysis features, including:

- Viewing spectra from different locations within plaques at high spatial resolution (CCD dependent) ~ 0.6μm with 10X magnification for the typical CCD (6 μm pixel size)
- Spectral Un-mixing algorithm (SUN) to identify and separate into layers variations in LCP distribution in plaques according to spectral features
- Dynamic color-settings to observe defined layers
- Classification algorithm for direct observation of spectral differences within plaques
- Ability to view intensity variations, within plaques, for a defined spectral range
- Target (regions) segmentation & quantitative information related with content of LCP's

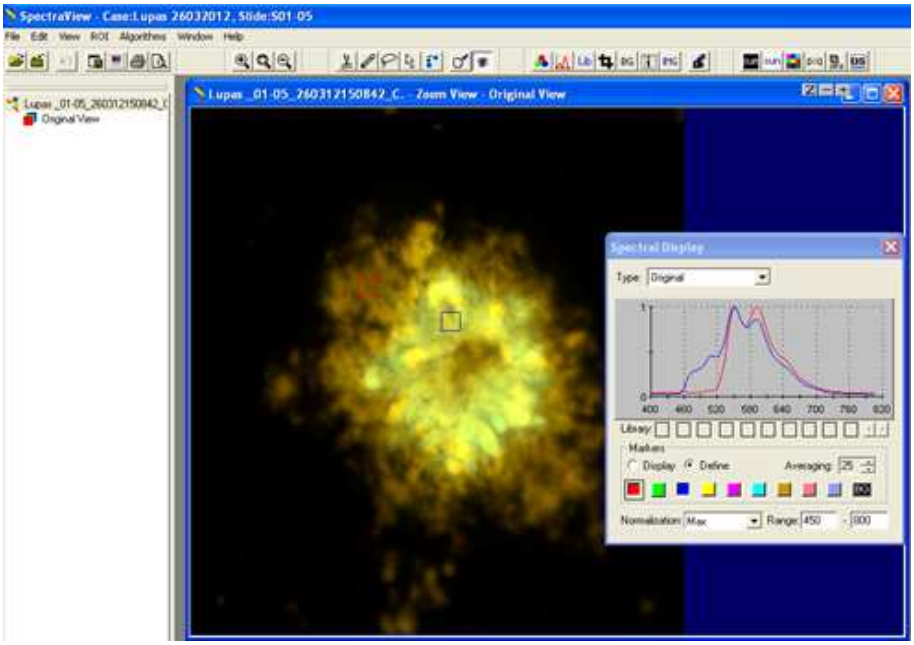

Figure 5. Spectra View software demonstrating spectral features from various locations within an amyloid plaque (Aβ) stained with LCPs.

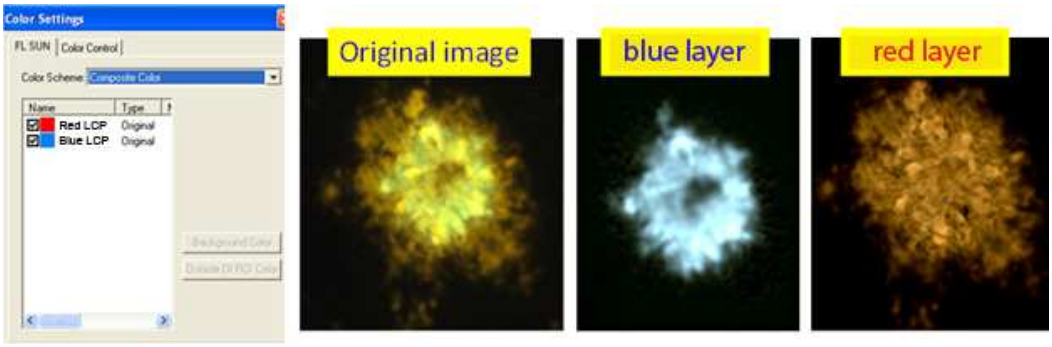

Figure 6. An amyloid plaque (Aβ) labeled with two different LCPs, one blue shifted and one red shifted LCP, can easily be divided into various components, based on differences in spectral features. In this example the sample was analyzed by spectral un-mixing which provides accurate spacial separation of distinct components within the amyloid plaque.

CONCLUSION

The LCP staining technology used in parallel with the SpectraView® system provides a new way of analyzing amyloid deposits within a variety of specimens. Structural variations within and between specimens can be readily analyzed.

ACKNOWLEDGEMENTS

This work was supported by the EU-FP7-Health project LUPAS. We are grateful to all participants of the LUPAS project in particular to Sofie Nyström and Daniel Sjölander for sharing images used in this paper.

REFERENCES

1. www.lupas-amyloid.eu
2. Nilsson KPR, Hammarström P, Ahlgren F, Herland A, Schnell EA, Lindgren M, Westermark GT, Inganäs O. Conjugated polyelectrolytes - Conformation-sensitive optical probes for staining and characterization of amyloid deposits. *Chembiochem.* 2006;7:1096-1104.
3. Nilsson KPR, Ikenberg K, Åslund Å, Fransson S, Konradsson P, Röcken C, Moch H, Aguzzi A. Structural typing of systemic amyloidoses by luminescent-conjugated polymer spectroscopy. *Am. J. Pathol.* 2010;176:563-574.

The use of luminescent conjugated polythiophene (LCP) probes for classification of amyloid deposits

K.P.R. Nilsson

IFM, Department of Chemistry, Linköping University, SE-581 83 Linköping, Sweden.

Molecular probes for selective identification of amyloid deposits are important to advance our understanding of the molecular pathogenesis underlying protein aggregation diseases. The most common small amyloid ligands are derivatives of Congo red or Thioflavins and these dyes are rather selective for protein aggregates having an extensive cross β-pleated sheet conformation and sufficient structural regularity. However, a drawback of many conventional probes is that only a subset of aggregates that roughly correspond to histologically identifiable amyloid deposits can be identified, whereas it is becoming more evident that several diverse types of protein aggregates are involved in protein misfolding diseases. In this regard, a novel class of amyloid imaging agents, luminescent conjugated polythiophenes (LCPs), consisting of a repetitive thiophene backbone (Fig. 1A) has been developed. LCPs provide a direct connection between the geometry of the thiophene backbone and the fluorescence being emitted (2-6). Hence, one molecule can emit blue, green or red light depending and when binding to protein aggregates, the conformation of the backbone is dictated by the protein, which results in conformation-sensitive spectral signatures from the LCP.

HISTOLOGICAL CHARACTERIZATION OF AMYLOID DEPOSITS IN TISSUE SAMPLES

Recent studies have shown that LCPs can be used as amyloid specific dyes for histological staining of tissue sections and that LCPs appear to provide additional information regarding the pathological events of proteinopathies, compared to conventional techniques (1-5). In 2006, Nilsson et al. exhibited the proof of concept of by utilizing the LCPs as amyloid specific dyes in tissue samples (2). Under alkaline (pH 10) conditions the anionic LCP, polythiophene acetic acid (PTAA, Fig. 1A), were shown to selectively stain a plethora of amyloid deposits in formalin fixed tissue sections. Furthermore, some results indicated that PTAA emits light of different colors upon binding to different amyloid subtypes and that smaller protein deposits that were undetected with conventional dyes was visualized by PTAA. The latter was verified by Nilsson et al in 2010 (4) when it was shown that PTAA could be utilized for spectral assignment of distinct amyloid subtypes (Fig. 1D and 1E). In addition, the LCP technique has been extremely useful for assessing heterogenic protein aggregates observed in the infectious prion diseases. Prions can occur as different strains and the prion strain phenomenon is believed to be encoded in the tertiary or quaternary structure of the prion aggregates. This belief was also verified when protein aggregates in brain sections from mice infected with distinct prion strains were

being stained by LCPs (3). The LCPs bound specifically to the prion deposits and different prion strains could be separated since PTAA emitted light of different wavelengths when bound to protein deposits associated with a distinct prion strain (Fig. 1B and 1C). Furthermore, the LCP technique was recently used for specific spectral identification of protein deposits seen for a de novo generated prion strain (5). These protein deposits were not stained by any of the conventional amyloid ligands, ThT and Congo red, indicating that LCPs could be used to identify a subset of protein deposits normally undetectable by conventional methods. Whether this observation was due to an increased sensitivity of the LCPs compared to other amyloid ligands or if LCPs identify a broader range of structurally diverse protein deposits compared to conventional amyloid dyes has yet to be clarified.

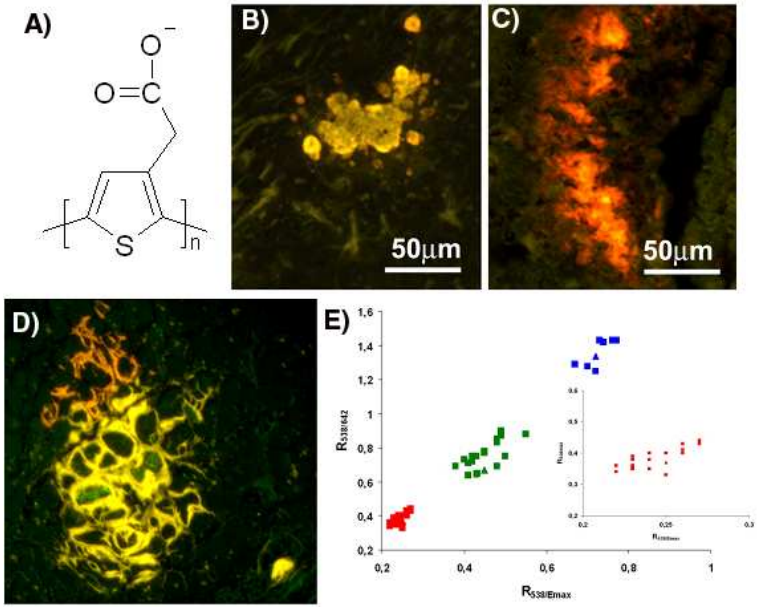

Figure 1. A) Chemical structure of the anionic LCP, polythiophene acetic acid (PTAA). Fluorescence images of prion deposits, murine CWD (B) and murine sheep scrapie (C) stained by PTAA. D) Fluorescence image of AA deposits in a heart tissue stained by PTAA. E) Correlation plot showing the separation of different cases of systemic amyloidoses, AA (blue), AL (green) and ATTR (red) by using the emission properties of PTAA.

NOVEL THIOPHENE BASED SCAFFOLDS FOR IN VIVO IMAGING OF AMYLOID DEPOSITS

In 2009, Åslund et al improved the LCP concept and presented defined pentameric structures termed luminescent conjugated oligothiophenes (LCOs) that could be utilized for *in vivo* imaging of protein aggregates (6). The anionic pentameric LCO, p-FTAA (Fig. 2A) could also be utilized for staining of Aβ aggregates in brain sections from transgenic *Drosophilia* model (Fig. 2B and 2C) and was also shown to detect non-thioflavinophilic pre-fibrillar Aβ species preceding the formation of amyloid fibrils during *in vitro* fibrillation of recombinant Aβ peptide (Fig. 2D9 (6, 7). In addition, p-FTAA crossed the blood-brain barrier and offered the possibility to perform real time optical imaging of Aβ aggregates in a transgenic mouse model with Alzheimer´s disease (AD) like pathology through a cranial window (Fig. 2E). The dye could also be utilized for visualization of other

amyloid deposits, such as AA-amyloid in the spleen (Fig. 2F). Hence, the addition of LCOs to the toolkit of fluorescent amyloid ligands will be important for studying the underlying molecular events of protein aggregation disease and for obtaining sensitive diagnostic tools for these diseases.

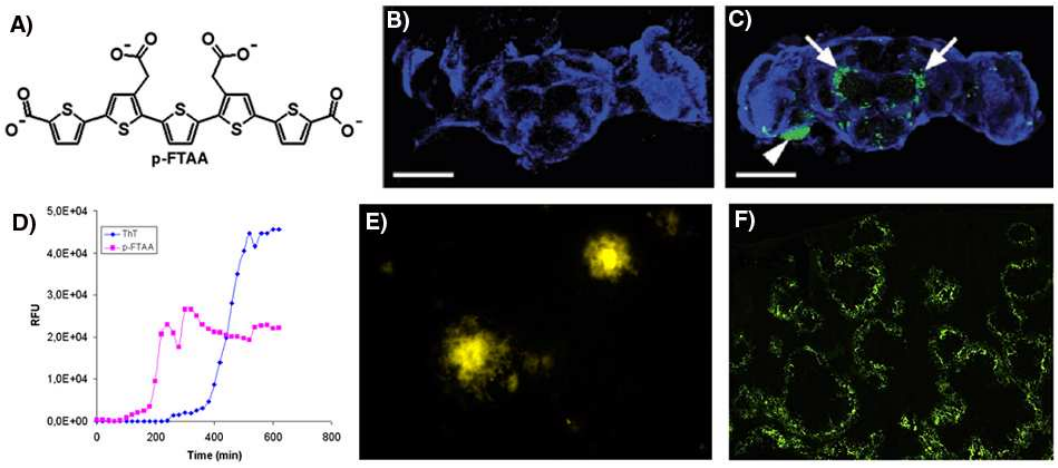

Figure 2. A) Chemical structure of the anionic LCO, p-FTAA. Fluorescence images of p-FTAA stained brain sections from a normal *Drosophilia* (B) and a transgenic *Drosophilia* having Aβ deposits (C). D) In vitro fibrillation kinetics of recombinant Aβ peptide monitored with p-FTAA and thioflavin T (ThT). E) Fluorescence image of p-FTAA labeled Aβ deposits in the brain of a transgenic mouse model with AD-like pathology. F) Fluorescence image of p-FTAA labeled AA deposits in the spleen from a mouse model for AA-amyloidosis.

REFERENCES

1. Nilsson KPR, Herland A, Hammarström P, Inganäs O. Conjugated polyelectrolytes – conformation sensitive optical probes for detection of amyloid fibril formation. *Biochemistry* 2005;44:3718-3724.
2. Nilsson KPR, Hammarström P, Ahlgren F, Herland A, Schnell EA, Lindgren M, Westermark GT, Inganäs O. Conjugated polyelectrolytes - Conformation-sensitive optical probes for staining and characterization of amyloid deposits. *Chembiochem.* 2006;7:1096-1104.
3. Sigurdson CJ, Nilsson KPR., Hornemann S, Manco G, Polymenidou M, Schwarz P, Leclerc M, Hammarström P, Wüthrich K, Aguzzi A. Prion strain discrimination using luminescent conjugated polymers. *Nature Methods* 2007;12:1023-1030.
4. Nilsson KPR, Ikenberg K, Åslund Å, Fransson S, Konradsson P, Röcken C, Moch H, Aguzzi A. Structural typing of systemic amyloidoses by luminescent-conjugated polymer spectroscopy. *Am. J. Pathol.* 2010;176:563-574.
5. Sigurdson C J, Nilsson KPR, Hornemann S, Heikenwalder M, Manco G, Schwarz P, Ott D, Rülicke T, Liberski PP, Julius C, Falsig J, Stitz L, Wüthrich K, Aguzzi A. De novo generation of a transmissible spongiform encephalopathy by mouse transgenesis. *Proc. Natl. Acad. Sci. USA* 2009;106:304-309.

6. Åslund A, Sigurdson CJ, Klingstedt T, Grathwohl S, Bolmont T, Dickstein DL, Glimsdal E, Prokop S, Lindgren M, Konradsson P, Holtzman DM, Hof PR, Heppner FL, Gandy S, Jucker M, Aguzzi A, Hammarström P, Nilsson KPR. Novel pentameric thiophene derivatives for in vitro and in vivo optical imaging of a plethora of protein aggregates in cerebral amyloidoses. *ACS Chem. Biol.* 2009;4:673-684.
7. Berg I, Nilsson KPR, Thor S, Hammarström P. Efficient imaging of amyloid deposits in Drosophila models of human amyloidoses. *Nature Protocols* 2010;5:935-944.

Organizing Committee and Faculty

International Members

Bouke P.C. Hazenberg, Host XIIIth International Symposium on Amyloidosis, Groningen, The Netherlands
Robert A. Kyle, Past President ISA, Rochester, USA
Giampaolo Merlini, Immediate Past President ISA, Pavia, Italy
Martha Skinner, President ISA, Boston, USA
Merrill D. Benson, VP and President-Elect ISA, Indianapolis, USA
Laura Obici, Secretary ISA, Pavia, Italy
Angela Dispenzieri, Treasurer ISA, Rochester, USA
Per Westermark, Editor-in-Chief of AMYLOID, Uppsala, Sweden
Giovanni Palladini, Member-at-Large ISA, Pavia, Italy
David C. Seldin, Member-at-Large ISA, Boston, USA

Yukio Ando, Kumamoto, Japan
Vittorio Bellotti, Pavia, Italy
John L. Berk, Boston, MA, USA
Joel N. Buxbaum, San Diego, USA
Ray L. Comenzo, Boston, SA
Ahmet Dogan, Rochester, USA
Marcus Fändrich, Halle, Germany
Morie A. Gertz, Rochester, USA
Gilles Grateau, Paris, France
Erik Gruys, Utrecht, The Netherlands
Philip N. Hawkins, London, UK
Shu-Ichi Ikeda, Matsumoto, Japan
Jeff Kelly, San Diego, CA, USA
Robert Kisilevsky, Ontario, Canada
Barbara Kluve-Beckerman, Indianapolis, USA
Helen J. Lachmann, London, UK
Reinhold P. Linke, Martinsried, Germany
Avi Livneh, Tel-Hashomer, Israel
Maria M. Picken, Chicago, USA
Martin H. van Rijswijk, Amsterdam, The Netherlands
Chris Röcken, Kiel, Germany
Maria J. Saraiva, Porto, Portugal
Stefan Schönland, Heidelberg, Germany
Ole B. Suhr, Umeå, Sweden
Jonathan S. Wall, Knoxville, USA
Ashutosh D. Wechalekar, London, UK
Gunilla T. Westermark, Linköping, Sweden
Steven R. Zeldenrust, Rochester, USA

National Members

Johan Bijzet, Groningen
Ingrid I. van Gameren, Groningen
Maarten P. van den Berg, Groningen
Sandra Croockewit, Nijmegen
Andor W.J.M. Glaudemans, Groningen
Elisabeth B. Haagsma, Groningen
Philip M. Kluin, Groningen
Jan B. Kuks, Groningen
Pieter C. Limburg, Groningen
Paul G. Luiten, Groningen
Ingemar S.J. Merkies, Maastricht
Monique C. Minnema, Utrecht
Edo Vellenga, Groningen

Author Index

E

F

G

H

I

J

K

L

M

N

O

P

Q

R

S

T

U

V

W

Y

Z

Subject Index

A

B

C

D

E

F

G

H

I

K

L

M

N

O

P

Q

R

S

T

U

V

Y

XIIIth International Symposium on Amyloidosis

Edited by
Bouke P. C. Hazenberg & Johan Bijzet

In 1967 Professor Enno Mandema hosted the first International Symposium on Amyloidosis in Groningen and, almost 45 years later, Groningen was again the venue of the XIIIth Symposium.

This Symposium focussed on basic and translational research in the systemic amyloidoses. The systemic amyloidoses are rare diseases caused by clonal immunoglobulin light chains, mutant and wild type transthyretin proteins, serum amyloid A protein, and β2microglobulin that cause disease in all organ systems but most frequently in kidney, heart, gastrointestinal tract and nervous system.

The systemic amyloidoses also include diseases caused by a number of inherited mutant proteins, that lead to late onset amyloid fibril deposition in renal, gastrointestinal, and neurologic systems, including the proteins: apolipoprotein AI, apolipoprotein AII, fibrinogen, lysozyme, LECT2 and gelsolin.

This book harbours many oral and poster presentations of the different topics of the scientific program:

- Mechanisms of amyloid formation
- Animal models and cell culture systems
- Pathogenesis of organ dysfunction
- Improving diagnosis and amyloid typing
- Imaging
- Clinical evaluation and prognosis
- Monitoring of response to treatment
- Gene therapy and innovative drug trials

GUARD
Groningen Unit for Amyloidosis
Research & Development
The Netherlands

e-book ISBN number
978-90-821593-1-8